Late quaternary palaeoclimatic reconstructions in Patagonia using chironomid analysis

Gilchrist , Sarah Josephine Louise

DECLARATION

I declare that all of the work in this thesis has been carried out by myself, unless otherwise stated, whilst studying for a PhD at the Institute of Geography, University of Edinburgh.

Sarah J L Gilchrist

Dec 2004

PAGE NUMBERING AS ORIGINAL

ABSTRACT

This thesis investigates Late Quaternary palaeoclimate in Patagonia to increase our understanding of the nature and timing of climate change in the mid-latitude regions of the Southern Hemisphere. Palaeoenvironmental reconstructions are presented which date back to the Last Glacial Interglacial Transition (> *c.* 13.5 cal ka BP) from two lakes in Chilean Patagonia: Laguna Boal in the Chonos Archipelago (44° 39'S, 73° 39'W) and Laguna Leta in the Chilean Lake District (41° 33'S, 73° 10'W). The investigation focuses principally on the analysis of sub-fossil Chironomidae (Insecta: Diptera) to infer palaeoenvironmental conditions. Combined ^{14}C dating and tephrochronology provide the chronological framework for the records. As ecological information about the modern Patagonian Chironomidae fauna is scarce, faunal assemblages at 78 lakes were analysed in conjunction with potentially controlling environmental variables in order to aid the ecological interpretation of sub-fossil assemblages.

Analysis of the modern data raised taxonomic issues related to identification of sub-fossil larval specimens, highlighting the need for more Neotropical taxonomic studies. Multivariate analysis of relationships between the modern day fauna and environmental variables indicated that the relationships present were not strong enough to produce a transfer function for the region. The environmental factors that varied most with the taxonomic assemblages were the organic content of substrate, lake depth, altitude, latitude and longitude. Water temperature, which has previously been demonstrated to have a strong effect on Chironomidae distribution, was not significantly correlated with the Patagonian faunal assemblages. These results indicate that the fauna encountered in this study may be more eurytopic than that studied in previous Holarctic investigations. Although the strength of environmental - taxonomic relationships was insufficient to warrant production of a transfer function, the investigation allowed qualitative interpretations of the down-core record to be made in conjunction with previously published data on Holarctic midge ecology.

The records from Laguna Leta and Laguna Boal both indicate that climate oscillated during the transition from glacial to interglacial conditions, as fluctuations in lake depths are

suggested by changes in both the chironomid assemblages and sediment properties. Results are generally equivocal in terms of determining whether such changes were precipitation or temperature driven. Nonetheless, such inferred changes add valuable evidence to the assertion that climatic instability prevailed throughout this time period in Patagonia – an argument that has been refuted by previous palynological work. Climatic interpretation of the Laguna Boal Holocene record is somewhat equivocal, but indicates that local, basin specific changes may have determined the assemblage versus palaeoclimatic controls. However, at a Laguna Leta a drop in lake levels during the early Holocene may have been followed by a notable rise in water level at c. 7.8 cal yr BP. This latter record supports previous palynological work in the region indicative of a concomitant rise in effective precipitation. The results of this pioneering study suggest that the use of chironomid analysis as a palaeoclimatic technique for this area is promising, but that more information on the midges' modern distribution in Patagonia is required to improve its application in future studies.

ACKNOWLEDGEMENTS

This thesis was conducted whilst in receipt of a NERC studentship. Additional funding was provided by the Quaternary Research Association, who contributed funds towards field assistance for my second field season and presentation of results at the 9th International Paleolimnology Conference. The Graduate and Alumni Fund of the University of Edinburgh also funded fast-stream ^{14}C dating to allow chronological constraint of the findings presented at this aforementioned conference. Other ^{14}C dates were funded by NERC (Allocations 1016.0303 and 952.1201). Many thanks to the staff that have given me supervision over my studies Prof David Sugden, Prof Sarah Metcalfe, Dr Bob McCulloch, Dr Mike Kaplan and Steve Brooks.

Analysis of my second core, Laguna Boal, was only made possible through the generosity of Prof Keith Bennett. Many thanks to his colleagues at Uppsala for helping me during my stay and adding to the enjoyment of the visit. Dr Peter Hill and Dr Anthony Newton have provided useful advice back in Edinburgh regarding EMPA. Chuck Stern provided added expert insight to allow these results to be effectively placed in a Patagonian context. Klaus Brodersen also provided enthusiasm and insight into how best to conduct TWINSPAN analysis. Kelly Holmes, Zoe Adams and Raleigh International are thanked for collecting samples from the Chonos, Park de Rafael and the Chacabuco Valley. Pat Haynes mounted samples from Chonos sites and also spent several days teaching me how to process and mount chironomid samples.

My lasting memories of my PhD will be my times in Chile and Argentina. My fieldwork in Patagonia was made both memorable and possible by the help of the following individuals. In addition to supervision in the first year of my PhD, Bob McCulloch also provided invaluable logistical insight into Patagonian field work, guidance and assistance during my first fieldtrip. Javier Corripio has been a companion through UGrad and PGrad study – his Spanish skills were pivotal to ensuring that our field-equipment shipments made it through customs at Santiago. Julietta Massaferro co-ordinated and lead fieldwork in the Bariloche area. Many thanks also go to Lindsey and Sarah Steele for field assistance in 2001 and to Andrea and Mauro for their hospitality for two weeks in San Carlos de Bariloche. Roberto Urrutia not only made open his labs for chemical analysis and provided loan of equipment, but also provided accommodation during my stay in Concepcion. Thanks also to all the staff at EULA for making me feel so at home, despite my rudimentary Spanish. My 2003 field season would have been impossible if Darcey Gillie had not offered her help and enthusiasm for 2 weeks. Many thanks.

Penultimately thanks to all of the friends that have supported me during my last 4 years. My family too have always been there to aid and support me – without the gift of a laptop completion of this thesis would have been very difficult. Thanks for this and your thoughts and consolations when times were tough.

Last but not least, I must thank Steve Brooks at the Natural History Museum. His dedication and passion to my supervision has been truly outstanding. I feel very lucky and honoured to have received supervision from an academic who is not only outstanding in his field, but incredibly generous in spirit and always optimistic in outlook. From inspiring

the subject of this thesis, to field trips to test equipment to excellent coaching in taxonomy to prompt and thorough reading of draughts, his support has been unwavering. Thank you Steve!

TABLE OF CONTENTS

Acknowledgements 1
Table of contents.....3
List of Figures.....8
List of Tables.....16
Glossary.....19

1 INTRODUCTION 23

1.1 AIM AND SPECIFIC OBJECTIVES.....23
1.2 WHY STUDY CLIMATIC CHANGE?.....24
1.3 THE VALUE OF PALAEOECOLOGICAL STUDIES.....24
1.4 PATAGONIA AS A LOCATION TO STUDY CLIMATE CHANGE.....26
1.4.1 The importance of Patagonia within Palaeoclimatic studies 26
1.4.2 Present day Patagonia – Geography, climate and vegetation 27
1.4.2.1 Geography and geology of Patagonia.....27
1.4.2.2 Climate 30
1.4.2.3 Vegetation 33
1.5 THESIS STRUCTURE 33

2 LATE PLEISTOCENE CLIMATE CHANGE: A GLOBAL AND PATAGONIAN PERSPECTIVE..... 36

2.1 THE CHANGING NATURE OF OUR UNDERSTANDING OF LATE PLEISTOCENE PALAEOCLIMATE.....36
2.1.1 A note on nomenclature and terminology regarding LGIT palaeoclimatology..... 39
2.2 CURRENT HYPOTHESES DEBATING THE SYNCHRONEITY OF LGIT CLIMATE CHANGE ...41
2.2.1 Hypothesis 1: Globally synchronous LGIT climate change.....41
2.2.1.1 Evidence.....41
2.2.1.2 Forcing mechanism and modes of teleconnection 44
2.2.2 Hypothesis 2: Northern Hemisphere changes lead those in the Southern Hemisphere or are not global in extent.....45
2.2.2.1 Evidence.....45
2.2.2.2 Forcing mechanism and modes of teleconnection 47
2.2.3 Hypothesis 3: Southern Hemisphere leading Northern Hemisphere changes 48
2.2.3.1 Evidence.....48
2.2.3.2 Mechanisms 52
2.3 MILLENNIAL SCALE HOLOCENE CLIMATE FLUCTUATIONS.....53
2.4 LGIT AND HOLOCENE PALAEOENVIRONMENTAL EVIDENCE FROM PATAGONIA 58
2.4.1 LGIT evidence.....59
2.4.1.1 Sedimentary and geomorphology evidence 59
2.4.1.2 Modelling Former Icesheets 63
2.4.1.3 Pollen Studies 64
2.4.1.4 Coleopteran Studies.....74
2.4.1.5 Ocean cores 74
2.4.2 Holocene Change.....76
2.4.2.1 Evidence for Neoglaciations in Patagonia.....76

2.4.2.2 Palaeolake levels in the Pampas 77
2.4.2.3 Pollen Analysis and Ocean Cores 80
2.5 SUMMARY 82

3 CHIRONOMIDS AND THEIR APPLICATION AS A PALAEOECOLOGICAL PROXY 84

3.1 INTRODUCTION 84
3.2 THE BIOLOGY AND ECOLOGY OF CHIRONOMIDAE 84
3.2.1 Egg : oviposition to eclosion 86
3.2.2 Larva : eclosion to final ecdysis 86
3.2.3 Pupa: final ecdysis to emergence 87
3.2.4 Imago: emergence to oviposition 87
3.3 CHIRONOMID SYSTEMATICS AND TAXONOMIC DIVERSITY AND GENERAL FAUNAL BIOGEOGRAPHIC TERMS 88
3.4 CHIRONOMIDS AS BIOINDICATORS OF THE TROPHIC STATUS OF LIMNIC SYSTEMS 90
3.5 CHIRONOMIDS AS A PROXY IN PALAEOLIMNOLOGY 92
3.5.1 Chironomids : Qualitative reconstructions 93
3.5.2 Chironomids and temperature: qualitative to quantitative postdictions 94
3.5.3 Issues facing the quantitative use of chironomids 101
3.5.4 Other quantitative reconstructions 104
3.6 APPLICATIONS OF CHIRONOMID ANALYSIS IN PATAGONIA 108
3.7 SUMMARY 112

4 METHODS 113

4.1 INTRODUCTION 113
4.2 METHODS IN THE FIELD 113
4.2.1 Modern chironomid ecological sampling 113
4.2.1.1 Site selection 113
4.2.1.2 Surface sampling 113
4.2.1.3 Environmental variables 114
4.2.2 Long cores 116
4.2.2.1 Laguna Leta 116
4.2.2.2 Laguna Boal 116
4.3 METHODS IN THE LABORATORY 117
4.3.1 Water chemistry 117
4.3.2 Sediment description 118
4.3.3 Loss on ignition 118
4.3.4 X-ray analysis 118
4.3.5 Tephra analysis 119
4.3.6 Radiocarbon dating 121
4.3.7 Magnetic Susceptibility 124
4.3.8 Chironomid analysis 124
4.3.9 Taxonomic notes 127
4.4 MODERN DATA ANALYSIS, MANIPULATION AND PRESENTATION 129
4.4.1.1 Data normalisation and simplification 133
4.4.2 Modern chironomid data analysis 133
4.4.2.1 Cluster analysis 133
4.4.2.2 Ordination 134
4.4.2.2.1 Unconstrained ordination 134
4.4.2.2.2 Constrained Ordination 138

4.5 PALEOECOLOGICAL DATA ANALYSIS AND PRESENTATION 139
4.6 SUMMARY 140

5 MODERN CHIRONOMID ECOLOGY AND TRANSFER FUNCTION ANALYSIS 141

5.1 INTRODUCTION 141
5.2 MODERN DATA SET: INITIAL RESULTS 141
5.2.1 Environmental data 141
5.2.1.1 Trends within the environmental variables and water chemistry data 144
5.2.2 Chironomid data 147
5.2.2.1 Exclusion of rare taxa 149
5.3 TWINSPAN CLASSIFICATION 149
5.3.1 TWINSPAN results 150
5.3.1.1 TWINSPAN classification of sites 150
5.3.1.2 TWINSPAN Classification of taxa 156
5.3.1.3 Discussion of TWINSPAN results 158
5.4 TRANSFER FUNCTION PRODUCTION: REGRESSION STAGE 160
5.4.1 Unconstrained ordination 160
5.4.1.1 Minimising Noise in the taxonomic data set 160
5.4.1.2 DCA and gradient length 160
5.5 CONSTRAINED ORDINATION 162
5.5.1.1 Inclusion of Cation data 170
5.5.1.2 Inclusion of nutrient data 173
5.6 PRELIMINARY ASSESSMENT OF ORDINATION RESULTS 175
5.6.1 Water Temperature 175
5.6.2 Altitude 181
5.6.3 pH 182
5.6.4 Biogeographical Effects 184
5.6.5 Strong relationships of water chemistry and faunal assemblage 186
5.7 FURTHER INVESTIGATION AFTER LIMITING THE pH RANGE 188
5.7.1.1 Summary of Ordination 193

6 LAGUNA LETA 195

6.1 INTRODUCTION 195
6.2 SITE 195
6.2.1 Climate, Geology and Vegetation 199
6.3 RESULTS 199
6.3.1 Sediment analysis 199
6.4 TEPHRA GEOCHEMISTRIES 204
6.4.1 Geochronological data 207
6.4.2 Chironomid analysis 207
6.4.2.1 LET-1 (272 – 248.5cm) 209
6.4.2.2 LET-2 (248.5-239.5cm) 209
6.4.2.3 LET-3 (239.5-194cm) 209
6.4.2.4 LET-4 (194-150cm) 213
6.4.2.5 LET- 5 (150-0cm) 214
6.5 DEVELOPING A CHRONOLOGY 214
6.5.1 Tephrochronology 214
6.5.2 Combining tephrochronology with ^{14}C results 215

6.6 PALAEOENVIRONMENTAL INTERPRETATION 217
6.6.1 Sedimentary interpretation 217
6.6.2 Chironomid interpretation 218
6.6.2.1 LGIT environmental change 220
6.6.2.2 Holocene Palaeoenvironments 222
6.6.2.3 Change in the past c. 2000 years 226
6.6.3 Comparison of Laguna Leta with other palaeoenvironmental records from the area 227
6.7 CONCLUSIONS FROM LAGUNA LETA 230

7 LAGUNA BOAL 232

7.1 INTRODUCTION 232
7.2 SITE 232
7.3 RESULTS 236
7.3.1 Sedimentary data 236
7.3.2 Tephrochronology 239
7.3.3 Geochronological data 241
7.3.4 Chironomid Analysis 241
7.3.4.1 BOAL-1 (486-460cm) 241
7.3.4.2 BOAL-2 (431 – 391cm) 246
7.3.4.3 BOAL-3 (391-333cm) 246
7.3.4.4 BOAL-4 (332-310cm) 247
7.3.4.5 BOAL-5 (310-0cm) 247
7.4 DEVELOPING A GEOCHRONOLOGY 248
7.4.1 Tephrochronology 249
7.4.2 Addition of ^{14}C data 252
7.5 SEDIMENTARY INTERPRETATION 254
7.5.1 Chironomid interpretation 255
7.5.1.1 LGIT Palaeoenvironmental Change 258
7.5.1.2 Holocene Palaeoenvironmental Change 261
7.6 COMPARISONS OF LAGUNA BOAL WITH OTHER RECORDS FROM THE AREA 265
7.7 CONCLUSIONS 270

8 DISCUSSION 272

8.1 INTRODUCTION 272
8.2 MODERN DAY PATAGONIAN CHIRONOMIDAE FAUNA 272
8.2.1 Taxonomic Issues 273
8.2.2 Evidence of Vicariance Biogeographies 274
8.2.3 Taxonomic – Environmental relationships 276
8.2.3.1 Inter-regional differences in ecological niches 278
8.2.3.2 Poor correlation to environmental data 279
8.2.3.3 Improving environmental data 279
8.2.3.4 Modelling of temperature 279
8.3 DISCUSSION OF DOWN-CORE RECORDS 281
8.3.1 Chronology 281
8.3.2 Palaeoenvironmental records from Laguna Boal and Leta 281
8.3.3 Wider palaeoclimatic implications 283
8.4 CONTRIBUTION TO FUTURE CHIRONOMID STUDIES 286
8.5 CONCLUSIONS 287

9 REFERENCES 292

10 APPENDICES 320

LIST OF FIGURES

Figure 1.1: Map showing the present distributions of glaciers (left) and the main climatic features (right), (McCulloch *et al.*, 2000) 28

Figure 1.2: Map showing generalised tectonic, structural and topographic features of South America (Clapperton, 1993). 29

Figure 1.3: Map showing variations in precipitation and temperature across two Patagonian transects. The map shows the location of the two transects and the distribution of current meteorological stations (Villalba, 2003). 31

Figure 1.4: Map showing the (a) atmospheric pressure (sea level) patterns for January and July and (b) average airflow for January and July (Clapperton, 1933, 12).....32

Figure 1.5: Distribution of the seven major vegetation assemblages across Patagonia (Heusser *et al.* 1999) 34

Figure 2.1: Maps showing the locations of cores in (a) Antarctica and (b) Greenland. Maps based on images in Watanabe *et al.* (2003) and http://nicl.usgs.gov/green.htm.....37

Figure 2.2: Figure showing synchroneity between ice, land and marine records (Lowe and Walker, 1997) 38

Figure 2.3: GRIP $\delta^{18}O$ record (Dansgaard *et al.*, 1993) with the GRIP isotope event stratigraphy shown (Bjørk *et al.*,1998) 40

Figure 2.4: : Stable isotope profiles from Taylor Dome, GISP2, Byrd and Vostok. At the top, the estimated precision in the Taylor Dome age scale is shown. Boundaries of climate intervals, as defined in the GISP2 record, are shown by dashed vertical lines: Hol, Holocene; YD, Younger Dryas; B/A Bølling/ Allerød; LGM, Last Glacial Maximum, ACR is the Antarctic Cold Reversal as defined at Byrd after Blunier *et al.* (1997) and Steig *et al.* (1998). 43

Figure 2.5: Foraminiferal isotope analysis of core RC11-83 (41º36'S, 9º48'E) in the Southern Atlantic and comparison to ice core isotopic records (Charles *et al.*, 1996). (a) shows $\delta^{13}C$ of the benthic foraminifera relative to the Summit $\delta^{18}O$ record, (b) shows the $\delta^{18}O$ for two planktonic foraminifera species and the δD record from Vostok. 49

Figure 2.6: GRIP, Byrd and Vostok isotopic and CH4 records on a common time scale (GRIP timescale in years before 1989) showing asynchronous Late Glacial Interglacial Transition climate change (Blunier *et al.*, 1997). The numbers on the top of the GRIP isotopic record indicate the location of Dansgaard-Oeschger Events. The ACR shows the location of the Antarctic Cold Reversal. A1 and A2 refer to Antarctic warmings discussed in the text. 50

Figure 2.7: Diagram showing the Antarctic Cold Reversal (ACR) as recorded in $\delta^{18}O$ records from EPICA (European Project for Ice Drilling in Antarctica, Dome C), Vostok (Vk) and Dome Fuji (DF) (Based on Wanatabe, 2003). 51

Figure 2.8; :July mean temperate reconstructions from Toskaljavri (A) and Tsuolbmajavri (B) (Seppä and Birks, 2001) and the July solar radiation variations at 70°N since 10 000 cal yr BP (C) as calculated by Berger (1978) (Seppä and Birks, 2002).....55

Figure 2.9: Summary of glacier expansion phases in different areas of the world during the Holocene (Grove, 1988).....56

Figure 2.10 : Lake-Level status at (a)18000, (b) 6000 yr BP & (c) during modern times (Street Perrott and Harrison, 1985).....57

Figure 2.11:: Map showing the location of geomorphological studies and the timing of LGIT glacial advances. Each box refers to a different advance, as proposed by the referenced authors, within the relevant field area. All dates are given in ^{14}C (blue boxes) and calibrated ka BP (purple boxes),with the exception of Kaplan *et al.* (*in press*). 60

Figure 2.12: Map of Chilean Lake District showing location of pollen study sites discussed in this chapter.....65

Figure 2.13: Records of fossil beetles (redrawn from Hoganson and Ashworth, 1992) and pollen (summarised and redrawn with modification from Lowell *et al.*, 1995) representing regional full-glacial Subantartic Parkland and late-glacial North Patagonian Evergreen Forest. Subantarctic Parkland consisted of open comminities of herbs and shrubs (mostly Gramineae and Compositae) with stands of trees (*Nothofagus cf. betuloides*) until about 14000 yr BP; later, close comminities of North Patagonian Evergreen Forest developed, at first containing relatively thermophylic trees (Myrtaceae, *Lomatia, Maytenus, Nothofagus cf. Dombeyi*) and after 13000-12000 until 10000yr BP, species that are more cryophylic (*Podocarpus nubigena, Pseudopanax laetevirens*) (Heusser *et al.*, 1996, 181).....67

Figure 2.14: Map showing the location of Patagonian palynological investigations outside the Chilean Lake District 69

Figure 2.15: : Summary diagram drawn on a uniform timescale of *Nothofagus*/Gramineae ratios shown in relation to charcoal concentrations at Puerto del Hambre, Punta Arenas and Torres del Paine. Arrows indicate the horizons of ^{14}C dates (Heusser 1995, 21).....70

Figure 2.16 : (a) Diagram showing selected results of pollen analysis (Ericacae, Poaceae and *Nothofagus*) and δD of bog mosses from Puerto Harberton (after Pendall *et al.*, 2000).(b) δD of meteoric water, as inferred from δD of bog mosses, at Harberton plotted against isotopic records form Taylor Dome and Byrd. Methods of reconstructing temperature and humidity are explained in the reference, inferred precipitation is based on knowledge of modern relationship between vegetation and precipitation. 72

Figure 2.17 : Summary Pollen stratigraphy plotted against age (calibrated) below the water surface for each of four sequences of lake sediments in southern Chile. Black, pollen of trees; dark gray, pollen of herbs; light gray, spores of pteridophytes. Zonation schemes at right show chronozones, GRIP event stratigraphy and the ACR (Bennett *et al.*, 2000).....73

Figure 2.18: Reconstructed sea surface temperatures (Kim, *et al.*, 2002) and inferred shifts in the Westerlies (Lamy *et al.*,1991) based marine sediment cores from the continental slope off mid-latitude Chile (33ºS, 72ºW). 78

Figure 2.19: Schematic curve of lake level fluctuations of Lago Cardiel during the last 31,000 years. (Stine and Stine, 1990, 705 & 707). 79

Figure 3.1 : Diagram showing Chironomidae life cycle and associated information 85

Figure 3.2 : The Sclater and Wallace classification of faunal regions (after Smith (1983) in Hugget, 1998, 11) 89

Figure 3.3 : Ordination of chironomid taxa and environmental variables in Labrador, Canada (Walker *et al.*, 1991). 96

Figure 3.4 : Diagram showing development of the Canadian chironomid based temperature transfer function and its application to a constant data set from Splan Pond, New Brunswick (based on Walker *et al.*,1997). 98

Figure 3.5: Predicted chironomid-inferred mean July air temperatures using a 2 component WA-PLS model based on leave-one-out cross-validation plotted against observed mean July air temperature in 111 Norwegian lakes. The solid line shows a 1:1 relationship. (b) Residual (predicted - observed) temperatures plotted against observed mean July temperature. The thick solid line is a LOESS smoother (span = 0.35) (Cleveland, 1993) fit. The two 'outlying' lakes are labelled in plot (b) (Brooks and Birks, 2001, 1729).....102

Figure 3.6: Graph illustrating the relationship between standard deviation (SD) of temperatures inferred using different sizes of count sums in relation to the Root Mean Square Error of Prediction of the original sample (n = 212 - 717) (Heiri and Lotter, 2001, 347).....105

Figure 3.7: Chironomid percentage diagram, showing dominant taxa in the Late Quaternary sequence from Laguna Stibnite, southern Chile. Also shown are lithology, calibrated ^{14}C dates (modified after Lumley and Switsur, 1993) and calendar ages, based on a different ^{14}C chronology (after Bennett *et al.*, 2000), head capsule concentration and PCA sample scores for axes 1 and 2. Significant zones identified by BSTICK (Broken Stick technieque modelling) are shown as continuous lines, non-significant zones are shown as dotted lines (Massaferro and Brooks, 2000).....110

Figure 4.1 : Diagram of larval head capsules from (a) Chironomini, (b) Tanytarsini, (c) Tanypodinae, (d) Orthocladiinae and (e) Podonominae tribes. Major morphological features used in identification are annotated.....125

Figure 4.2 : Diagram showing drawings of the wide range in cephalic setae encountered within Procladiini and Macropelopiini tribes of Tanypodinae. Labelled diagrams of specimens in the left column are those taken from Rieradevall and Brooks (2001). The remaining nine illustrations are examples from the modern subfossil samples. Note the lack of consistent morphologies within the modern Patagonian samples which makes them both difficult to identify based on the Rieradevall and Brooks (2001) criteria or consistent arrangement within themselves. Drawings are not to scale. 130

Figure 4.3: Key showing the criteria on which Tanypodinae were identified 131

Figure 4.4: Species abundance patterns over long and short gradients. Short gradients tend to show linear patterns; long gradients may show non-linear patterns (Waite, 2000) 136

Figure 5.1: Map showing the location of the 78 lakes sampled in the Patagonian chironomid training set 142

Figure 5.2: Histograms showing the distribution of selected lake characteristic measurements, together with summary data (sample size, mean and standard deviation) 145

Figure 5.3: Diagram showing percentage data for chironomid assemblages at the 78 sites examined. Sites are ordered by altitude down the y axis. Grey shading indicates altitudes where sites were sampled. Numbers at the base of the diagram refer to the maximum (top) and mean (bottom) relative abundance with which they were encountered within the training set. 148

Figure 5.4: TWINSPAN two-way Table of showing ordination of Patagonian training set based on the taxa and sites. pseudo-species cut levels (1) = 0-1%, (2) = 2-4% (3) = 5-9%, (4) = 10-19%, (5) = 20 – 49% and (6) = 50-100%. 151

Figure 5.5 : Dendrogram showing TWINSPAN classification of sites based on modern taxa assemblages. Taxon names and numbers are the TWINSPAN indicator taxa with their pseudo-species cut levels (1) = 0-1%, (2) = 2-4% (3) = 5-9%, (4) = 10-19%, (5) = 20 - 49% and (6) = 50-100%. To the right of the dendrogram, the TWINSPAN classification groups and the site group numbers are given, together with the site membership 152

Figure 5.6: TWINSPAN classification of the surface sediment chironomid assemblages and mean abundance of major taxa within each group. The row order of taxa is in accordance with that produced through TWINSPAN classification of the samples. The dendrogram to the top indicates the levels at which groups were classified. 153

Figure 5.7 : Boxplots showing the range of major environmental variables within each lake group, as classified by TWINSPAN. Details of group membership is in Figure 5.5...154

Figure 5.8: Dendrogram showing TWINSPAN classification of taxa to four levels 157

Figure 5.9: Bi-plot of CA (a) taxa and (b) sites within training set. CA performed using down-weighting of rare taxa and square-root transformation of taxonomic data on MAJ_{incl}. See Appendix 5 for taxa codes. 161

Figure 5.10: Initial CCA Bi-plots of the four different CCAs run using EN1 and EN2 and both including and excluding Tanypodinae and Tanytarsini Undif (Majincl & MAJexcl). The graphs show the same major trends are brought out in all the analyses. Sites are shown on the top graphs, taxa on the lower graphs - taxa are not labelled due to close grouping. See Figure 5.11 for a more detailed example (EN2 vs MAJincl).The graphs show the same major trends are brought out in all the analyses correlated with LOI, and thus potentially lake productivity. 165

Figure 5.11: CCA Bi-plot of EN2 vs MAJincl. (a) shows variables plotted against sites, (b) shows the variables plotted against taxa. Note the different scales on the two graphs. Key for taxa is in Appendix 5.....168

Figure 5.12: CCA bi-plots showing the results when constrained ordination is conducted using (a) ENcat and (b) ENnut.Codes for taxa are given in Appendix 5.....172

Figure 5.13: Graph showing relationship between surface water temperatures (T_t) and basal water temperatures (T_b). 177

Figure 5.14: Correlation coefficients r^2 between the summer monthly mean air temperatures and the corresponding water temperatures measures adapt carious depths in the upper 20m of Zürichsee. Correlations are based on 54 years of data (1937-40 and 1946-95); significance levels are shown as dotted lines (Lotter and Livingstone, 1998, 194). 179

Figure 5.15: T_t-T_b plotted against summer days on which measurements were taken (calculated as the number of days elapsed since the 1st Nov) 180

Figure 5.16: Site scores on CCA axis 1 (using EN_2 vs MAJ_{incl}) plotted against site pH. Short dashed line is the 95% confidence limit for the regression line, long dashed line is the 95% prediction limit, based on the regression equation stated (shown in top right corner). 183

Figure 5.17: DCA of sites coded by (a) location to the West or the East of the Andes continental divide (b) field area location to explore possible biogeographical effects on faunal assemblages within the training set. (c) Map show the geographical divisions of sites by field area.....185

Figure 5.18: Simplified model of lake catchment processes and lacustrine sediments (modified after Edwards and Whittington, 2001). 189

Figure 5.19: (a) CCA and (b) RDA plots for lakes with pH between the mean average ± 1 s.d......149

Figure 6.1: Map of the Chilean Lake District and Isla de Chiloé showing the location of Laguna Leta, LGM ice limits and the direction of LGM piedmont lobe glacier flow based on Andersen *et al.* (1999).....196

Figure 6.2: Pictures of Laguna Leta taken facing nothwest (above) and west (below). Note the macrophyte growth in shallow regions of the lake. The lower picture shows the moraine ridge directly to the west of the basin and the domestic development on land to the west of the lake.....197

Figure 6.3: (a) Map showing the location of Laguna Leta within the geomorphic context. Geomorphological map and key taken from Andersen *et al.*, 1999 (accompanying plates to volume). Laguna Leta and the area included within the cross-section are marked.(b) Schematic diagram of the Bahía Huelmo composite cross-section which shows the position of Laguna Leta (site no. 58) (Andersen *et al.*, 1999). Note that the moraines and outwash plains are covered with pyroclastics flow sediments not shown in this diagram. Numbered sites refer to dates and sections described in Denton *et al.* (1999b.) 198

Figure 6.4: Average January and July isotherms and annual precipitation isohyets for the Southern Lake District and Isla Grande de Chiloé (based on Alemyda and Sáez (1958) cited in Heusser *et al.*, 1999).....200

Figure 6.5: Cross-section showing ecotone distributions over an altitudinal gradient in the Chilean Lake District and Isla de Chiloé (Heusser *et al.* 1999, 238). Red horizontal lines mark the approximate altitude of Laguna Leta.....201

Figure 6.6: Stratigraphy (established from visual examination and x-rays of cores) and organic content (% LOI) of Lago Leta core. Depths which were sampled for 14 C dating are indicated.....202

Figure 6.7: Photographs of the basal two segments of core taken from Laguna Leta. The arrow indicates the basal contact of the minerogenic horizon which was used to link the two cores. White hatching over the core indicates that this element of the core segment overlapped with another element and was therefore not subsampled.....203

Figure 6.8: Classification bi-plots of tephra shards analysed from Laguna Leta using Total alkali-silica (TAS) classification diagram annotated with subdivision of volcanic rocks into alkaline, transitional alkaline and subalkaline (tholeiitic) . Upper line after Irvine and Baragar (1971), lower line after Kuno (1966). All geochemical data were normalised before being plotted.....205

Figure 6.9: Tertiary plot showing unormalised electron microprobe analysis (EMPA) results of tephra shards analysed from 3 horizons in Laguna Leta. 206

Figure 6.10: Depth versus age diagram showing the results of 14C dating of the Laguna Boal core. Calibrated age ranges are shown using both one and two standard deviations. The core stratigraphy is shown in the insert on the left of the graph (for key see Figure 6.4). Further details are shown in Table 6.2. 208

Figure 6.11: Percentage diagram showing all taxa from Laguna Leta. Key to stratigraphy is in Fig. 6.6. Grey band is tephra horizon, which was not analysed for midges. All dates are in cal yrs BP.....210

Figure 6.12: Percentage diagram showing selected taxa from Laguna Leta. Key to stratigraphy is in Fig. 6.6. Grey band is tephra horizon, which was not analysed for midges. All dates are in cal yrs BP. 211

Figure 6.13 : Concentration diagram showing selected taxa from Laguna Leta. Key to stratigraphy is in Fig. 6.6. Grey band is tephra horizon, which was not analysed for midges. All dates are in cal yrs BP. All concentrations are given in head capsules per gram of wet sediment.....212

Figure 6.14 : Sedimentation curve for Laguna Leta. All ages are shown in calibrated ages (see Table 6.2 for further details) at 68% confidence (1sd). Chironomid zones are annotated on the left side of the graph. 216

Figure 6.15: Assemblages found in the down core Laguna Leta record as passive samples using the CCA ordination developed in Chapter 5. Different coloured lines represent different (sub) zones in the record. Grey crosses represent the location of modern day lakes plotted during CCA. Environmental variables used in the ordination are shown. 219

Figure 6.16 : Summary diagram showing the palaeolimnological changes inferred from sediment and chironomid analysis at Laguna Leta within the context of published palaeoclimatic reconstructions from the region. 228

Figure 7.1: Photograph of Laguna Boal taken looking east (K.D.Bennett). 233

Figure 7.2: Maps showing the location of Laguna Boal and other previously studied sites in the Chonos - Taitao region. 234

Figure 7.3: Montane vegetation survey exemplifying vegetation in the Chonos / Taitao region: summary diagram of forest composition along transect up Mount Optimist (Lumley, 1994). Y axis is height in metres a.s.l., the summit of the transect and peak being at 831m a.s.l.....235

Figure 7.4: Diagram summarising the results of sediment logging, Loss n Ignition (LOI), magnetic susceptibility and macrofossil content for Laguna Boal. ^{14}C date depths marked with an asterix indicate that plant macrofossils were subsampled for dating 237

Figure 7.5: Classification bi-plots of tephra shards analysed from Laguna Boal using total alkali-silica (TAS) classification diagram annotated with subdivision of volcanic rocks into alkaline, transitional alkaline and subalkaline (tholeiitic) . Upper line after Irvine and Baragar (1971), lower line after Kuno (1966). All geochemical data were normalised before being plotted. Note the similar geochemistries for samples from 356 and 423 cm. Results from other horizons are shown in grey to place the results in the context of the whole core. 240

Figure 7.6: Depth versus age diagram showing the results of ^{14}C dating of the Laguna Boal core. Calibrated age ranges are shown using both 1sd and 2sd errors 242

Figure 7.7: Percentage diagram of all taxa from Laguna Boal. Grey horizontal bands indicate where no sediment was collected. Key for stratigraphy is in Figure 7.4. Dates are calibrated using 2 s.d. 243

Figure 7.8: Percentage diagram of selected taxa from Laguna Boal. Grey horizontal bands indicate where no sediment was collected. Key for stratigraphy is in Figure 7.4. Dates are calibrated using 2 s.d. 244

Figure 7.9: Concentration diagram of selected taxa from Laguna Boal. Grey horizontal bands indicates depths where sediments was missing due to compression of core segments.....245

Figure 7.10: (a) Bi-plot showing the similar geochemical range of shards within samples 356 and 423 cm and (b) Schematic diagram showing how the three basal core segments were linked using these common geochemistries. In (a) Results from other horizons are shown in grey to place the results in the context of the whole core.correlation this horizon is used as a chronostratigraphic marker with a pooled mean age of 1690 ^{14}C yr BP, or 1560 cal yr BP.....250

Figure 7.11: Comparison of EMPA results from horizons in the Laguna Boal record and those published for Taitao 4 volcanic event in Haberle and Lumley (1998) 251

Figure 7.12: Sedimentation curve for Laguna Boal. All age ranges are shown in calibrated ages (see Table 1.1) at 68% confidence (1sd). Chironomid zones are annotated on the left side of the graph.....252

Figure 7.13: Approximate distribution of species of iron and manganese in relation to pH and redox potential Eh. Alkalinity is assumed to be equal to 2 meq litre^{-1}, Lines denote points at which the activities of soluble Fe are 10^{-5} mol litre^{-1} (Wetzels, 2001, based on Stumm and Lee, 1960 and Stumm and Morgan, 1996).....256

Figure 7.14: Assemblages found in the down core Laguna Boal record as passive samples using the CCA ordination developed in Chapter 5. Different coloured lines represent different (sub) zones in the record. Grey crosses represent the location of modern day lakes plotted during CCA. Environmental variables used during ordination are shown. 257

Figure 7.15: Diagram showing full LOI data, smoothed using a loess curve and relative abundance of Parapsectrocladius within Laguna Boal.....264

Figure 7.16 : Summary diagram showing the palaeolimnological changes inferred from sediment and chironomid analysis at Laguna Boal within the context of published palaeoclimatic reconstructions from the region. 266

Figure 8.1: Summary of generalised biogeographical tracks of the world (after Croizat, 1958). Solid tracks are boreal and austral (Cranston, 1991, 187). 275

Figure 8.2: Diagram showing suammary of Patagonian palaeoenvironmetnal reconstructions developed during this study within the context of other regional and global record of Late Quaternary change.....285

LIST OF TABLES

Table 1.1: Major taxa components and temperature and precipitation parameters for vegetation assemblages within Patagonia. Meteorological parameters taken from Heusser *et al.* (1999, 240). 33

Table 2.1 : The start and end of the four LGIT chronozones in ^{14}C and calibrated years. Calibrated ages were calculated by taking mid-points of 2 s.d. age ranges produced using CALIB 4.3 (Stuiver and Reimer, 1998).....39

Table 2.2. Summary of the major LGIT glacier advances identified in field areas south of the Chilean Lake District. *= Data from Stern 1990, cited in Marden (1997, 66). Data in italics comes from research where there is no cross-reference to the nomenclature for advances in the Magellan Straits and Torres del Paine field areas (shown in column 1). 63

Table 3.1: Lake classification based on the profundal chironomid fauna (from Brundin, 1949, 1958; Saether, 1975, Wiederholm, 1984a) (Lindegaard, 1995, 386).....91

Table 3.2 : Comparison of the performance statistics between different quantitative chironomid-based temperature transfer functions 100

Table 3.3 : Summary of the performance statistics of different quantitative chironomid-based transfer functions for environmental factors other than temperature 107

Table 4.1 : Table showing the months during which different field areas were sampled and notes on sampling methods used. 115

Table 4.2: Summary of water sampling strategy and sample treatment depending on the location at which water analysis was conducted. 115

Table 4.3: Table showing the location of water analyses for the sites where chironomid sampes were taken. Site abbreviations are detailed in Table 5.1. The analyses conducted are outlined below:.....117

Table 4.4 : Summary of the source, age and coverage of LGIT and Holocene Patagonian tephras that have been used in palaeoenvironmental investigations and associated references. Hudson is the source of $H_7 - H_1$ eruptions. 121

Table 4.5 : Summary of some of the major characteristics of the ordination techniques discussed. N.B. Unconstrained ordination can also be referred to as indirect ordination, and constrained ordination as direct.....134

Table 5.1: Summary table showing the location, field and water chemistry measurements of the lakes sampled. Summary statistics for each variable are shown at the base of the table, together with calculations used to determine whether data sets required normalisation (Birks, 1996) 143

Table 5.2 : Summary of the subsets of environmental data used during analysis, the number of lakes within each subset and the environmental measurements associated.

Notations used for both subsets and environmental variables within the study are also shown. 144

Table 5.3 : Correlation matrix between the major environmental variables. Because of missing data points, this was done using 4 different data sets (denoted by symbols: ‡=ENV1, ▫=ENV2, † = Cation, * =Nutrient) 146

Table 5.4: Summary statistics for DCA performed on whole data set, using non transformed and transformed taxonomic data sets. All analyses were detrended by segments with rare species downweighting. 160

Table 5.5: Table showing the results of CCA undertaken on both the TOT_{incl} and MAJ_{incl} taxonomic data sets against EN_1 162

Table 5.6 Comparison of DCA , CCA and RDA on all lakes using EN_1 and EN_2, MAJ_{incl}, MAJ_{excl}, TOT_{in} and TOT_{excl} 163

Table 5.7 : Results of forward selection using environmental data sets EN_1 and EN_2 and taxonomic sets MAJ_{INCL} and MAJ_{EXCL} 167

Table 5.8 : Lakes identified as outliers during CCA and the environmental variable and value upon which this classification was based. 169

Table 5.9: Results of DCCA using forward selection using MAJ_{incl} and EN_2 and results of DCCA λ /DCA $\lambda 2$ 170

Table 5.10 : Comparison of results of CCA and DCA using EN_1 and EN_{cat} dataset. n_i and n_v refer to the number of sites and variables included in analysis, respectively 171

Table 5.11: Percentage variance explained by each environmental variable and associated p-values and gradients in DCCA when that environmental variable was the sole constraining variable using ENV_{cat} dataset 173

Table 5.12 : Comparison of results of CCA and DCA using EN_1 and EN_{nut} environmental dataset and MAJ_{incl} taxonomic dataset. 174

Table 5.13: Percentage variance explained by each environmental variable and associated p-values and gradients in DCCA when that environmental variable was the sole constraining variable. 174

Table 5.14: Percentage of environmental variables range in ENV_1(*), ENV_2 (‡) and ENV_{cat}(†), captured in ENV_{nut} (TP, TN, Si and $N\text{-}NO_3$, Cl and SO_4 are not shown as they were only present in ENV_{nut}. Calculations made using logged environmental variables datasets. 187

Table 5.15: Results of DCA on MAJ_{ph} 190

Table 5.16: Percentage variance explained by each environmental variable and associated p-values and gradients in DCCA when that environmental variable was the sole constraining variable using ENV_{pH} dataset. 190

Table 6.1 : Mean percentage (shown with 1 standard deviation) of the 9 major oxides measured within tephra shards in minerogenic horizons in Laguna Leta 207

Table 6.2: Radiocarbon dates from Laguna Leta. All dates were achieved using AMS analysis of bulk sediment samples. Calibrated age estimates were achieved using 1standard deviations (s.d.) errors with CALIB 4.3 (Stuiver and Reimmer, 1993).....207

Table 6.3 : Calibrated age estimates bracketing each of the chironomid zones.....220

Table 7.1: Major oxide geochemistries, gained via Electron Microprobe Analysis, and standard deviation of the shard measurements. Sample sizes for all populations, n>10. 239

Table 7.2 : Table showing the results of ^{14}C dating of bulk sediment and plant macrofossils from Laguna Boal. Calibrations were performed using CALIB 4.3 (Stuiver and Reimmer, 1993). Sample descriptions: BS= Bulk sediment. PM = Plant Macrofossil ..239

Table 7.3: Table showing depths before and after correction for shrinkage within the top 3m of the Laguna Boal record.....249

Table 7.4: Calibrated age estimates bracketing each of the chironomid zones. Using the chronology produced in 7.4.2, bracketing ages can be assigned to each of the Laguna Boal chironomid zones and subzones discussed in 7.3.4.....258

Table 7.5 : Minimum age limits on deglaciation of sites in the Chonos – Taitao region from previously published work and this study. Data from Haberle and Bennett (*in press*), Bennett *et al.* (2000) and Lumley (1993). Sites are arranged from North to South.....267

Table 8.1 : Summary of the number of chironomid species found within different genera in this and other Patagonian studies 277

GLOSSARY

Allopatric – the biological species or speciation occurring in areas isolated geographically from one another

Antarctic Cold Reversal (ACR) - The temporary reversal in temperature increase at the end of the LGM seen in many Antarctic Ice-cores, spanning c. 13.9 – 12.6 cal ka BP.

Benthic - Associated with the lake floor

Botstrapping (boot) - a means of estimating the error of a model. The value of an environmental variable (x) is estimated by using a model with (n) samples in it, where n= the size of the training set. This can be done as the samples used to estimate x are selected at random and can be selected more than once each.

Canonical correspondence analysis (CCA) - an eigenvalue based ordination method which links taxon abundance to environmental measurements at the site, assuming a unimodal relationship between taxa and environmental gradients.

Correspondence analysis (CA) – an eigenvalue based ordination method assuming that taxa have unimodal relationships along environmental gradients

Detrended correspondence analysis (DCA) – correspondence analysis where the results are "detrended" along the second axis to minimise the arch effect that CA can impose on Axis 2 scores

Dissolved Organic Carbon (DOC) - is defined as all the organic carbon present in water that passes a 0.2 μm filter

Dissolved Oxygen (DO) – The concentration of oxygen dissolved in water - it is one proxy of water quality.

Downweighting – A technique to decrease the effects of rare species in statistical analysis.

Epilimnion - Area above the thermocline

Forward Selection (FS) – method to assess how much more statistically meaningful a relationship can be made by adding an additional environmental variable to the group of variables being used to produce the model

Inertia - a measure of the total amount of variance in a data set.

Jack-knifing (jack)- also known as 'leave-out-one cross validation'. The process of cross validating and assessing the errors involved in a training set by predicting the value of the variable being reconstructed at site x by running the model using the remaining training set sites. The error incurred in predicting the value at every individual site is then computed in this manner.

Last Glacial Interglacial Transition (LGIT) - The transition between the Last Glacial Maximum and the current interglacial (the Holocene)

Lentic - Relating to lake systems

Littoral Zone - Zone of contact between water and lake from just above the influence of saves and spray to depth of thermocline in the summer

Lotic - Relating to stream systems

Monte Carlo Tests – a method of assessing the chance that a relationship has occurred by chance (ie the Null Hypothesis) generated by the values for the environmental variables being reassigned to the values for the species data. The test is run multiple to times to assess what the statistical chance of the observed results being generated by random processes is.

Mutual Climatic Range (MCR) - Quantitative modelling technique where reconstructed value is calculated by the envelope of overlap of environmental tolerances for all of the taxa present within the assemblage found

Oxygen Isotope stage (OIS) / Marine Isotope Stage (MIS) – A period in time which has been determined by stacking and tuning (to Milankovitch cycles) many $\delta^{18}O$ records from the ocean. Changes in the $\delta^{18}O$ is, at a global scale, primarily driven by the changes in glacial ice present as this will lead to a depletion or enrichment of $\delta^{18}O$. This provides an overall framework of over 100 "stages" for the Quaternary. Stage 1 is the youngest – even numbers denote glacial periods, odd numbers interglacials.

Parsimonious model - The minimal adequate model

Principal Correspondence analysis (PCA) – an eigenvalue based ordination method assuming that taxa have linear relationships along environmental gradients

Profundal Zone - Zone of contact between water and lake depth of thermocline in the summer

Redundancy Analysis (RDA) – multivariate analysis in linking environmental measurements to taxonomic assemblages in which species are presumed to have linear relationships to environmental gradients

Root Mean Square Error of prediction (RMSEP) – A means of assessing the error of a model by squaring the mean average of the error between the calculated value of a datapoint and the actual value for the datapoint. A perfect relationship will give a value of 0.

Total Nitrogen - The total nitrogen in water is comprised of dissolved inorganic and organic nitrogen and particulate organic and inorganic nitrogen, minus N_2 gas

Total Phosphorous - A measure of all the forms of phosphorus, dissolved or particulate, that are found in a sample

Unimodal - a distribution with one mode. In environmental sciences this would mean one optimum per environmental condition

Vicariance- allopatric speciation which occurs when a formerly continuous population splits into two or more populations which are separated by barriers

Weighted Averaging Partial Least Squares (WA-PLS) – a commonly used method of to produce transfer functions using the assumption that taxa have a unimodal response to environmental variables.

Younger Dryas (YD) – in its strictest sense this is the chronozone between 11-10 ^{14}C ka BP. However the term is commonly used to describe the last and larges temporary reversal in temperature increase at the end of the LGM seen in many North Western Europe.

1 INTRODUCTION

1.1 Aim and specific objectives

This investigation seeks to improve our understanding of the manner in which global climate changed from the Last Glacial Maximum (LGM) to the present day. It focuses on palaeoecological evidence of the transition between glacial conditions and the Holocene, the current interglacial in which we live. By looking at Patagonia, it seeks to add a Southern Hemisphere perspective to the current debate regarding the mechanisms by which the Earth switches from glacial to interglacial conditions. In addition, investigation of how climate may have changed in the Holocene provides new information, as there are relatively few studies of how climate changed during the Holocene in southern South America.

Insect remains have been used as indicators of past climate, in particular temperature, in Europe and North America but the approach is yet to be fully exploited in investigations in the temperate regions in the Southern Hemisphere (Porch and Elias, 2000; Porinchu and MacDonald, 2003). Chironomidae, a family of non-biting midges, have come to the fore in palaeolimnological investigations, due their capacity to yield accurate and precise inference models that can be used to reconstruct palaeotemperature (Brooks and Birks, 2000a; Battarbee, 2000). Although one such model has been produced and applied in Australia (Dimitriadis and Cranston, 2001), no attempts have been made to reconstruct temperature in South America using this technique which has proven to be so powerful in the Northern Hemispere.

Thus, this thesis investigates the following questions:

- What is the current taxonomic distribution of Chironomidae taxa in Patagonia and which environmental variables control these distributions?
- How suitable are chironomids as a proxy for quantification of palaeoclimate, in particular palaeotemperature, change in Patagonia?
- How have chironomid faunal assemblages at specific Patagonian sites changed since the end of the LGM?

- What inferences can be made about Patagonian climate change from the results of chironomid analysis combined with other complementary analyses of the sequences investigated?
- How do these environmental reconstructions fit into the present research context, contribute to our understanding of late Quaternary climate change and address current controversies in the research field?

1.2 Why study climatic change?

Recent concerns over the climatic impact of anthropogenic activities have highlighted the need for a sound understanding of mechanisms of climate change (Hulme *et al.*, 1999). To provide a context for our understanding of recent climate change, it is vital that critical phenomena such as variability, periodicity, magnitude and the rate of climatic change under non-anthropogenic-forced conditions are understood (Moritz *et al.*, 2002; Crowley *et al.*, 2000).

It can be argued that application of our understanding of current climatic processes within the context of palaeoclimatic change allows more realistic predictions of future climate change to be made. Global Circulation Models (GCMs) are one of the most important tools available to predict how climate may change and their output is fundamental to policy making on many environmental issues. Palaeoclimatic reconstructions provide an evidence-based framework for the construction, refinement and validation of GCMs and thus help to produce more realistic and representative predictions (Hoffert and Covey, 1992).

1.3 The value of palaeoecological studies

A palaeoecological approach to investigating past climate change has been argued to provide "the most effective and direct means we have at our disposal for reconstructing past environmental conditions" (Lowe and Walker, 1997a, 235). Such investigations provide key information as to how palaeoenvironments changed via reconstructions of past faunal and floral assemblages. By using the assumption that the environmental tolerances of species have remained constant (Rymer, 1978, cited in Lowe and Walker,

1997a, 162), analysis of micro or macrofossils can be used to infer changes in temperature, precipitation or secondary consequences of these primary forcing mechanisms, such as changes in lake pH or lake nutrients levels. Although such a qualitative approach is long established, recent advances in statistical techniques applicable to both ecological and palaeoecological data have allowed palaeoecological research to undergo a quantitative revolution. These new, powerful techniques support the production of quantitative models, or 'transfer functions' from datasets of modern analogues, collectively known as training sets. These can produce quantitative reconstructions of past environmental conditions such as temperature (e.g. Seppa and Birks, 2001), water pH (e.g. Fritz *et al.*, 1991) and conductivity (e.g. Davies *et al.*, 2002). The wide range of sub-fossil remains that can be analysed are, in turn, linked to a wealth of environmental variables that can be reconstructed, as different organisms show a particular sensitivity to specific environmental controls. Thus, the challenge for the palaeoecologist is to select the most appropriate archive, site and proxy for investigation in order to test the specific hypotheses underlying their research

Both qualitative and quantitative palaeoecological reconstructions can provide a powerful approach to complement other palaeoclimatic investigations. In Patagonia, many palaeoclimatic investigations to date have reconstructed former ice masses to infer associated past environmental conditions (e.g. McCulloch and Bentley, 1998; Denton *et al.*, 1999b). Although these studies contribute valuable information, an interpretation from such research is limited to reconstructing the combined effects of palaeotemperature and palaeoprecipitation. It is often difficult to disentangle the individual contribution of these two controlling variables on past ice masses. Moreover, evidence from such an approach is often chronologically restricted to periods of ice-limit maxima, during glacial advances or standstills. The advantage of biological fossil remains found in long records in a variety of archives such as lake, peat and marine sediments is that they offer continuous records of climate change. The study of lake records, or palaeolimnology, affords a wide variety of biological proxies for investigation and also lends itself to a large range of physical and chemical techniques (eg. Fritz *et al*, 1989). Additionally, the widespread location of lakes and the high stratigraphic resolution afforded by relatively rapid rates of accumulation make them excellent palaeoclimatic archives (Battarbee, 2000). Lake archives also allow environmental reconstructions at different spatial scales to be produced. Use of a proxy

such as diatoms will provide information directly related to the lentic system, analyses of the minerogenic component of the sediments provides information about the lake's catchment as a whole, whereas analysis of microfossils such as pollen can provide information on palaeovegetation at a micro – macro spatial scale. Thus paleolimnological studies are, arguably, at their strongest when a 'multi-proxy' approach is taken (eg. Birks *et al.*, 2000; Amman *et al.*, 2000).

1.4 Patagonia as a location to study climate change

1.4.1 The importance of Patagonia within Palaeoclimatic studies

Much late-Quaternary palaeoclimatic data has been obtained from studies in the Northern Hemisphere. By comparison there is a dearth of data from the South. Within the last twenty years, Patagonia has become increasingly important in palaeoclimatic research due to its unique geographic location (Denton *et al.*, 1999a, McCulloch *et al.*, 2000). The long and thin land mass acts as a 'finger' of land extending into the Southern Oceans which, outside Antarctica, is the most southerly protrusion of continental land.

Such a location is key within the context of trying to understand the reorganisation of climate during the transition between the Last Glacial Maximum (LGM) and Holocene period. As a land mass that lies perpendicular to the path of storm tracks, Patagonia also provides an ideal location in which to investigate how the southern Westerlies may have moved latitudinally during atmospheric reorganisations. Furthermore, as well as providing additional palaeoclimatic data from the Southern Hemisphere, Patagonian records provide reconstructions from a region with a similar climate and latitude to that of N.W. Europe, where climate change has been extensively investigated (Denton, 1999). This may aid North-South comparisons when trying to assess the extent of polar interhemispheric synchroneity.

Finally, the volcanically active nature of the region means that there are frequent deposits of tephra found within sedimentary sequences (Stern *et al.*, 1991; Tatur *et al.*, 2002). Such horizons can be used as time-parallel markers. This provides chronological constraints to be placed on individual sequences and also allows relative chronological correlation of cores using a method which complements ^{14}C dating. This is particularly advantageous

during the Last Glacial Interglacial Transition (LGIT), when errors associated with calibrating ^{14}C dates are known to be problematic (Lowe and Walker, 2000).

1.4.2 Present day Patagonia – Geography, climate and vegetation

1.4.2.1 Geography and geology of Patagonia

Patagonia is commonly taken to mean the land of Argentina and Chile that extends from 39°S to the southern tip of the continent at 55°S (McCulloch *et al.*, 1997). Working from West to East, the geography of the area can divided into three main regions. The western part is composed of a complex network of channels, islands and peninsulas that make up an extensive archipelago. These trace the arch of the continent's western coast and are remnants of a heavily glaciated landscape (Clapperton, 1993). Directly to the East of this zone lies the main axis of the Andes. Although Patagonian peaks do not rise as high as their contemporaries further north, their location close to the Pacific Coast often results in high local relief. Towards the south of the region, the mountain chain deviates from its overall N-S trend and sweeps eastwards, at which point the main axis of peaks become located within the archipelago region. In general summit altitudes become lower as one heads south. Despite relatively warm, mid latitude temperatures, the high levels of precipitation mean that the higher parts of the chain are able to support two ice fields and one major ice cap (Figure 1.1).

The continental scale geology of South America is shown in Figure 1.2. With respect to Patagonia, a major feature is the intrusion of Quaternary volcanic rocks into the surrounding Andean fold and thrust belt. To the east of these features the geology is composed of Palaeozoic-Mesozoic rocks and Pre-Cambrian basement (Clapperton, 1993). In effect, outside the peaks of the Andes, much of this bedrock geology is capped with Quaternary sediments from a variety of depositional processes, leading to thickness of deposits up to 3000m (Clapperton, 1993).

The Andes remain a volcanically active mountain range because of subduction of several oceanic plates under the western margin of the South American Plate (Futa and Stern, 1988). Within southern Chile there are two major zones or centres of volcanism: the Southern Volcanic Zone (SVZ, 33°-46°S) and the Austral Volcanic Zone (AVZ, 49° -54°) (Futa and Stern, 1988). This context has lead to several major explosive eruptions in

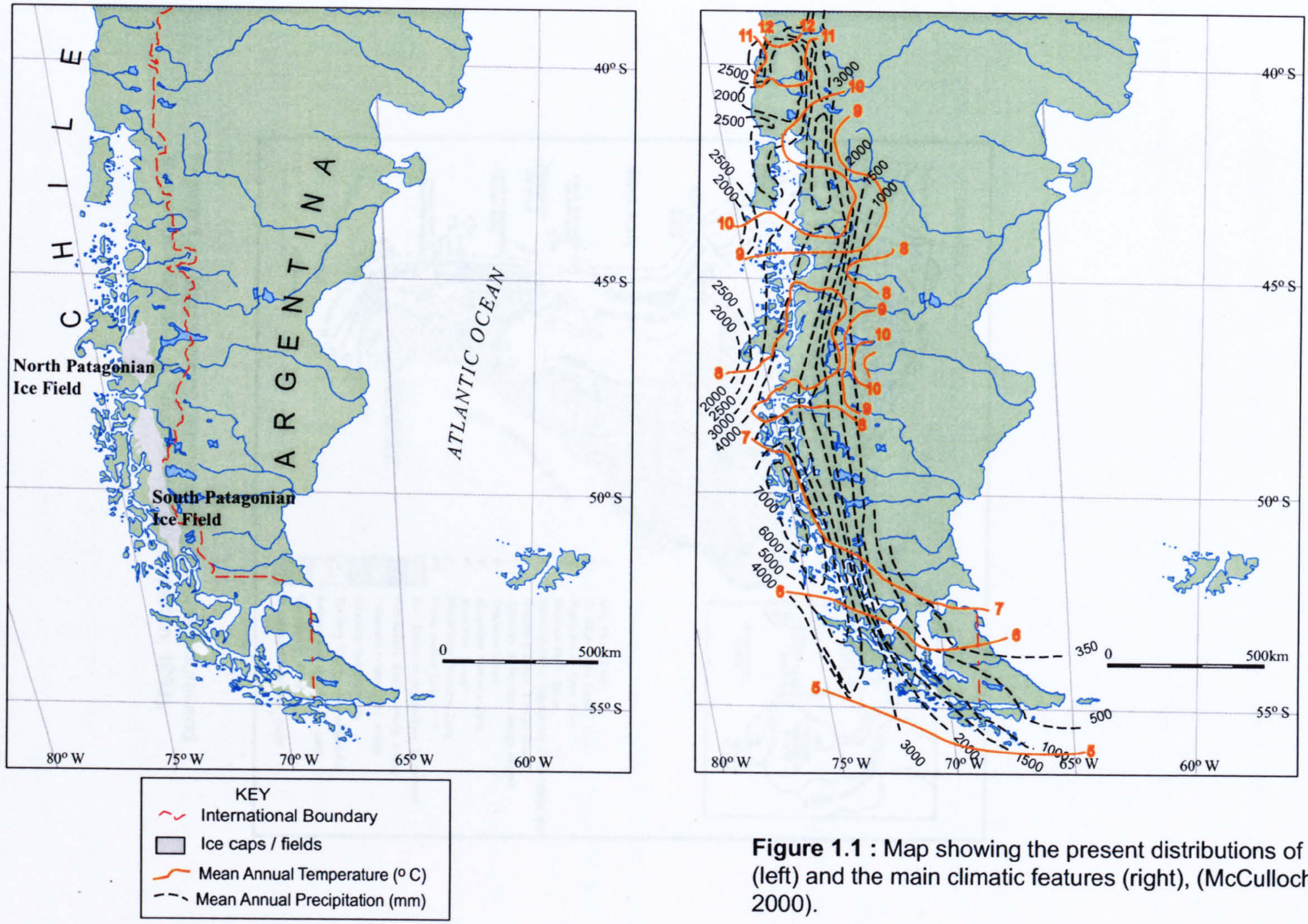

Figure 1.1 : Map showing the present distributions of glaciers (left) and the main climatic features (right), (McCulloch *et al.*, 2000).

Figure 1.2 : Map showing generalised tectonic, structural and topographic features of South America (Clapperton, 1993).

Patagonia during the LGIT and Holocene that have provided the basis for a late Pleistocene tephrochronological framework. Much of the initial research on Patagonian tephra deposits and their geochronology was conducted by Auer (1974, cited in Stern, 1990, 110 - 122). However, since this research, limited work has been undertaken on tephra in the area.

1.4.2.2 Climate

The presence of the Andes exerts a major control on the spatial variability of climate in Patagonia. This, combined with Patagonia's latitudinal range and the area's location in relation to the Westerly winds, determines modern day temperature and precipitation patterns. Unfortunately the density of instrumental meteorological data from Chile is low (Figure 1.3). However, the general trends in spatial climate variability are well understood and are summarised below. This overview is summarised by a climate map of Patagonia (Romero (1985) cited in McCulloch *et al*, 2000, 410) (Figure 1.1) and Figure 1.3 which shows biannual climate variability across two East-West transects.

The land mass lies perpendicular to the moisture-laden "Westerlies", that include winds that have crossed 10,000 km of the Pacific Ocean (Figure 1.4). Although at present the maximum annual precipitation brought by incoming frontal systems occurs at 50°S (Villagran, 1988), the latitudinal position of the saturated winds varies seasonally, partly in response to fluctuations in the extent of Antarctic sea-ice cover. Extended ice cover in the Austral winter causes an equatorward compression of the Southern Hemisphere circulation patterns, during which time the Westerlies shift by as much as *c.* 7° to 31°S (Miller, 1976). An acute orographic rainfall pattern across the region results from the location of the Andes so close to the western coast. This is exemplified by the fact that a location on the western flank of the Andes will receive three or four times as much rainfall as a location at the same altitude and latitude on the eastern side (Villalba, 2003). As the Westerlies and their associated storm tracks shed most of their moisture within the first 100 - 200 km of land crossed, the Patagonian Steppe experiences extremely arid conditions. Indeed, this rain shadow effect is so strong that distance from Andes explains 90% of the spatial variation in rainfall in the steppe (Jobbágy, 1995, cited in Villalba, 1995, 184).

As well as having a high influence on precipitation pattern, the Andes, together with latitude, are one of the major influences on temperature, with mean temperatures ranging from 12 - 6°C (Figure 1.1). Across Patagonia, mean temperatures range from 10-16°C in the

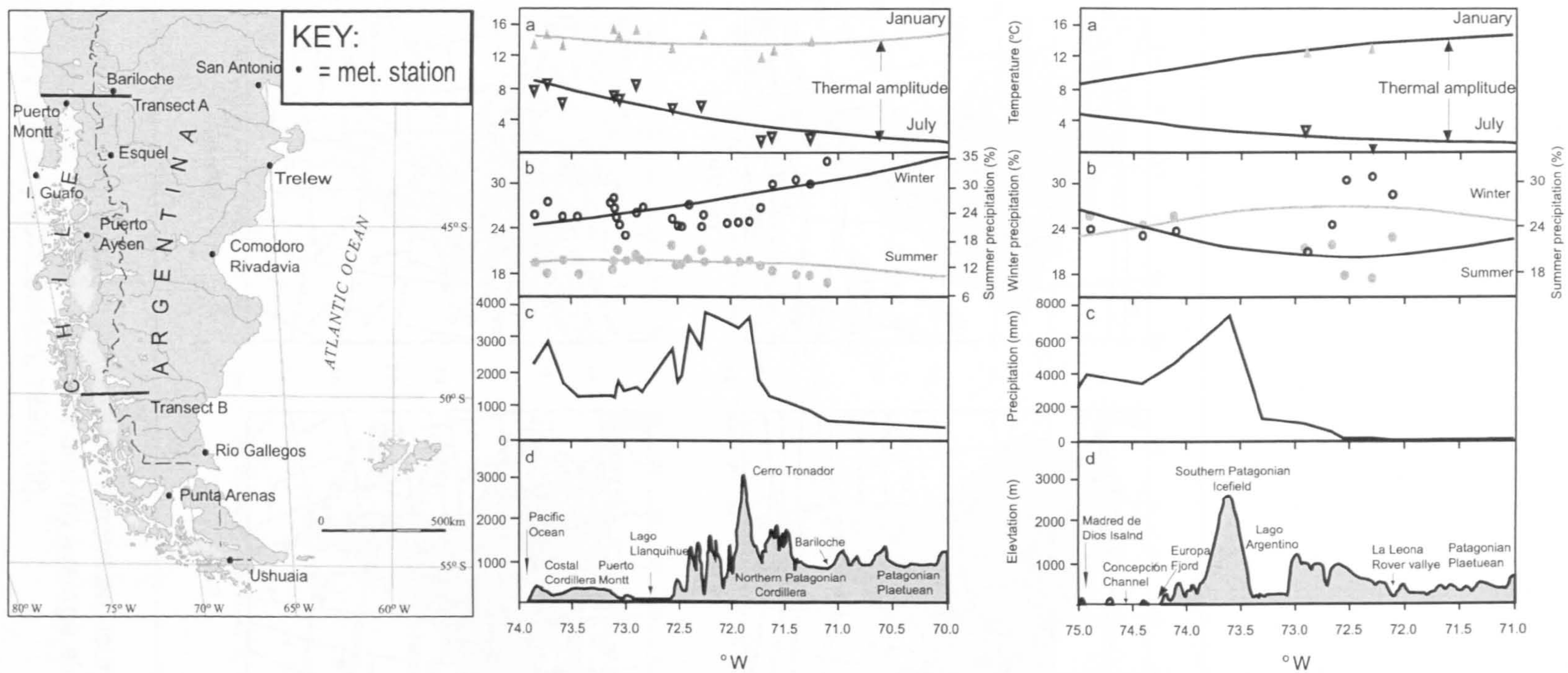

Figure 1.3 : Map showing variations in precipitation and temperature across two Patagonian transects. The map shows the location of the two transects and the distribution of current meteorological stations (Villalba, 2003).

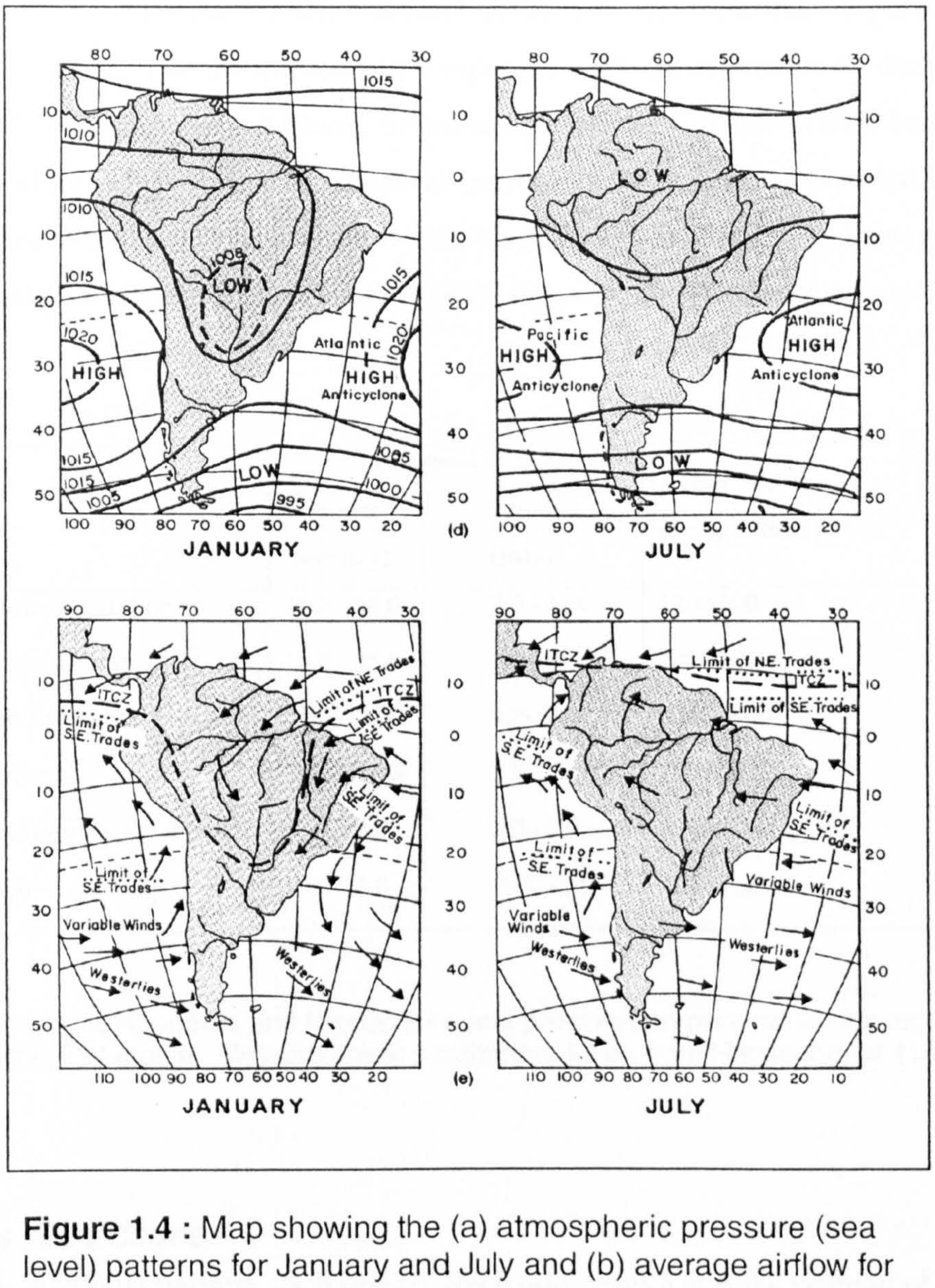

Figure 1.4 : Map showing the (a) atmospheric pressure (sea level) patterns for January and July and (b) average airflow for January and July (Clapperton, 1993, 12).

summer to 0-4°C in the winter, with seasonality being more marked in more continental steppe regions (Villalba, 2003). Minimum temperatures of less than -25°C have been recorded (Miller, 1976 and Prohaska, 1976, both cited in Villalba, 2003, 181).

1.4.2.3 Vegetation

The precipitation gradients caused by the Andes are responsible overall for the macro-scale vegetation patterns within Patagonia, as shown Figure 1.5. In general ecotones are fairly narrow and follow the orientation of the coast and the Andes. However this simple east-west model is complicated by the influence of temperature which, as previously discussed, is influenced by both altitude and latitude. Seven main vegetation ecotones have been distinguished and include species-rich, temperate rain forest, arid, grass-dominated steppe vegetation and the wet-tolerant taxa found within Magellanic Moorland. The average temperatures and precipitation values for each of these seven vegetational zones are listed in Table 1.1

Vegetation	Temperature (°C)		Average annual precipitation (mm)
	Summer (January)	Winter (July)	
Lowland Deciduous Beech Forest	15.0 – 18.0	7.0 – 8.0	1200-200
Valdivian Evergreen Forest	14.0 – 15.0	7.0 – 8.0	2000-3000
North Patagonian Evergreen Forest	12.0 -14.0	4.7 - 7.0	3000-5000
Magellanic Moorland	10.0 – 12.0	2.5- 5	1000-5000
Subantarctic Deciduous Beech Forest	8.0 – 11.0	3.0 - 5.0	1500-8000
Patagonian Steppe	5.0 – 15.0	-1.0 - 2.0	400-5000

Table 1.1: Major taxa components and temperature and precipitation parameters for vegetation assemblages within Patagonia. Meteorological parameters taken from Heusser *et al.* (1999, 240).

1.5 Thesis Structure

The thesis contains eight chapters, each one of which addresses a specific element of the investigation. This first chapter has provided a brief introduction to the context of the research and a summary of the regional, physical environment of Patagonia as a region. The contents and contribution of the following seven chapters are outlined below:

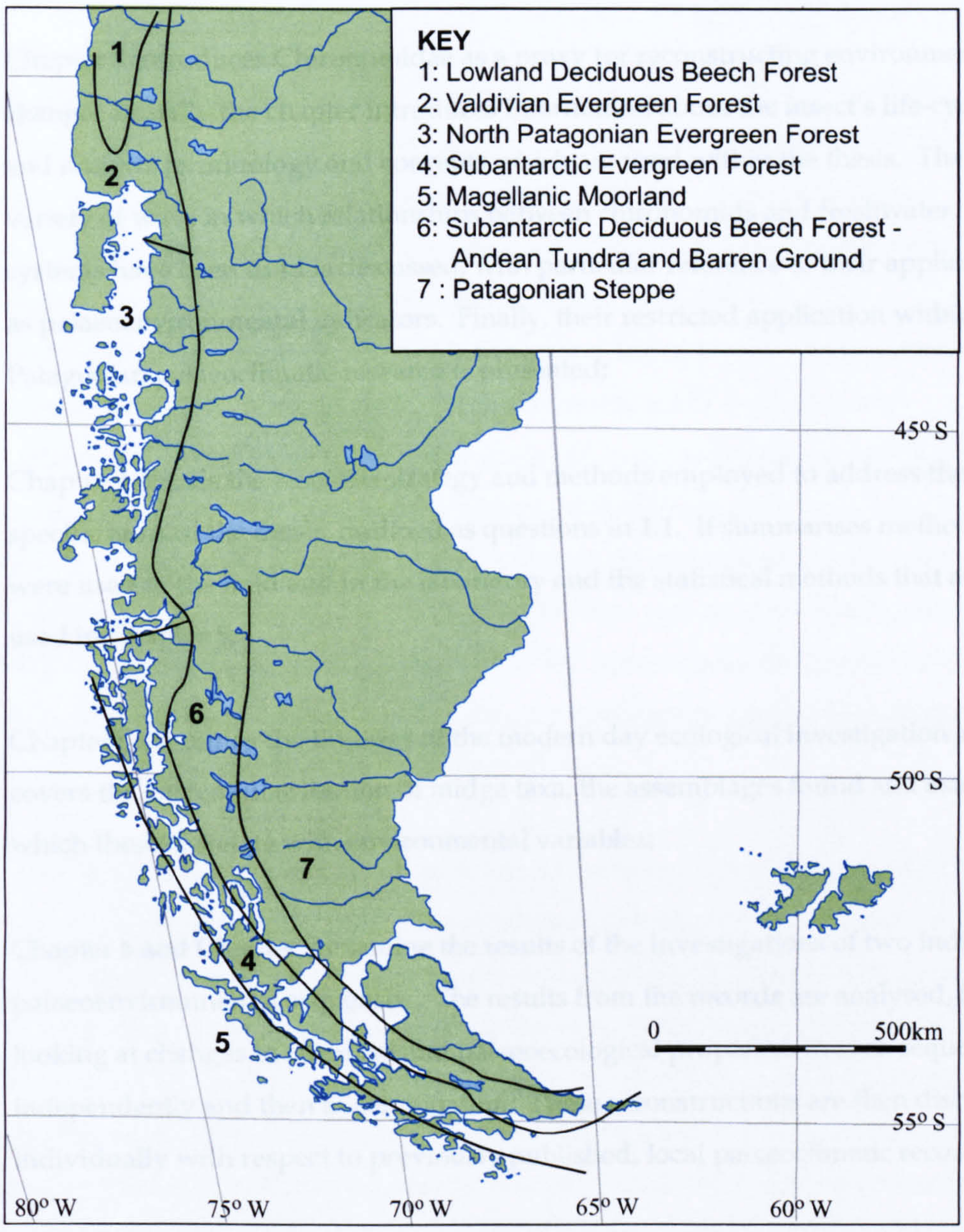

Figure 1.5 : Distribution of the seven major vegetation assemblages across Patagonia (Heusser *et al.*, 1999)

- Chapter 2 provides the palaeoclimatic context for this investigation. It sets the scene by discussing climate change during the late Quaternary at a global scale before focussing on the evidence from Patagonia;

- Chapter 3 introduces Chironomidae as a proxy for reconstructing environmental change. Initially the chapter introduces information about the insect's life-cycle and reviews terminology and concepts which are used within the thesis. The variety of ways in which relationships between chironomids and freshwater systems have been used is discussed, with particular reference to their application as palaeoenvironmental indicators. Finally, their restricted application within Patagonian palaeoclimatic research is presented;

- Chapter 4 details the research strategy and methods employed to address the specific aims of the thesis, outlined as questions in 1.1. It summarises methods that were used in the field and in the laboratory and the statistical methods that are used in Chapter 5;

- Chapter 5 examines the findings of the modern day ecological investigation and covers the current distribution of midge taxa, the assemblages found and extent to which these correlate with environmental variables;

- Chapter 6 and Chapter 7 examine the results of the investigations of two individual palaeoenvironmental sequences. The results from the records are analysed, first looking at changes in chemical and palaeoecological properties in each sequence independently and then in combination. These reconstructions are then discussed individually with respect to previously published, local palaeoclimatic records;

- Finally, Chapter 8 brings together the findings in a wider context. It assesses the success of the study with respect to its palaeoentomological research and the understanding of Patagonian climate change within a global context.

2 Late Pleistocene climate change: a global and Patagonian perspective

2.1 The changing nature of our understanding of late Pleistocene palaeoclimate

The transition into the Quaternary Period, 2.4 Ma BP, was marked by the initiation of cyclic, global changes between pronounced glacial and interglacial conditions occurring at frequencies of 19-21, 40 and 100 ka (Lowe and Walker, 1997). The presence of higher frequency, or 'sub-Milankovitch', climate flucuations has been discovered as the resolution of the palaeoenvironmental records and technical resources available to palaeoclimatologists have increased. Arguably, the most detailed records have been those retrieved from ice archives. Although these are mostly restricted to Antarctica and Greenland (Figure 2.1), other records have been retrieved from lower latitude and higher altitude sites more recently. As well as producing quantifiable reconstructions, ice-core records from Greenland hold the ability to produce relatively accurate and precise records due to the presence of annual layers for the last 14, 450 years with an error of ±70 years at 11,150 yr BP (Hammer *et al., in press*, Blunier *et al.*, 1998). Ice core records from across the globe can be correlated to this chronology by using the atmospheric composition of gas bubbles trapped within ice, such as methane concentration.

As the number of LGIT ice-core archives has increased, more records of this period of high frequency climate change have emerged. The reconstructions inferred from these ice-core data have been complemented by quantitative reconstructions from terrestrial and marine records and icesheet models (Birks, H. *et al.* 2000; Birks and Wright, 2000; Ammann *et al.*, 2000; Walker *et al.*, 1997; Purves and Hulton, 2000). Within the Northern Atlantic area, general agreement now exists concerning the overall timing and nature of climate change during the LGIT (Figure 2.2). However, results of work from outwith this area do not show such strong correlation to ice-core based reconstructions from Greenland. The presence of leads and lags are under debate due to the important implications they have for successfully establishing the driving mechanisms and modes of teleconnection of sub-Milankovitch climate change (White and Steig, 1998)

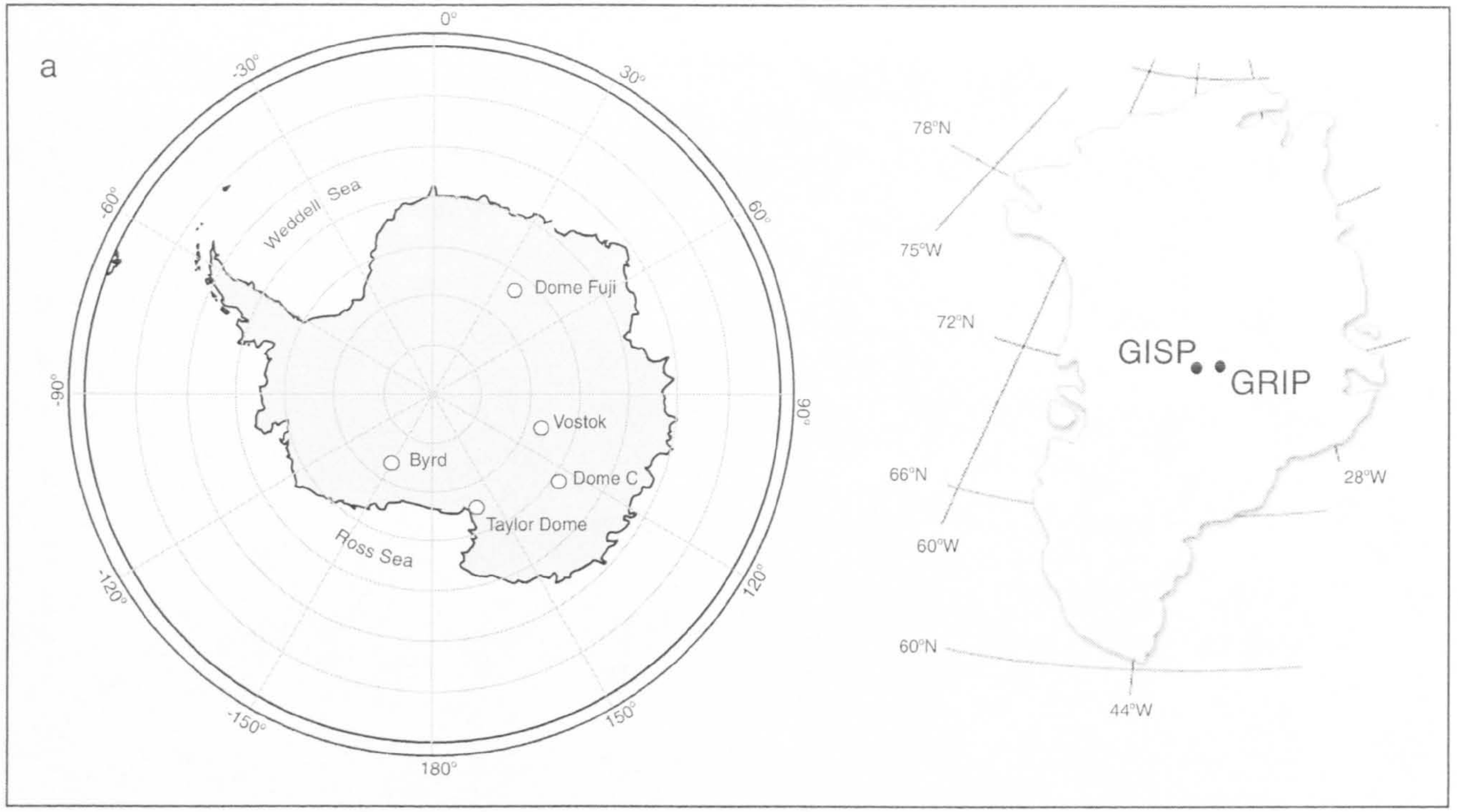

Figure 2.1 : Maps showing the locations of cores in (a) Antarctica and (b) Greenland. Maps based on images in Watanabe *et al.* (2003) and http://nicl.usgs.gov/green.htm

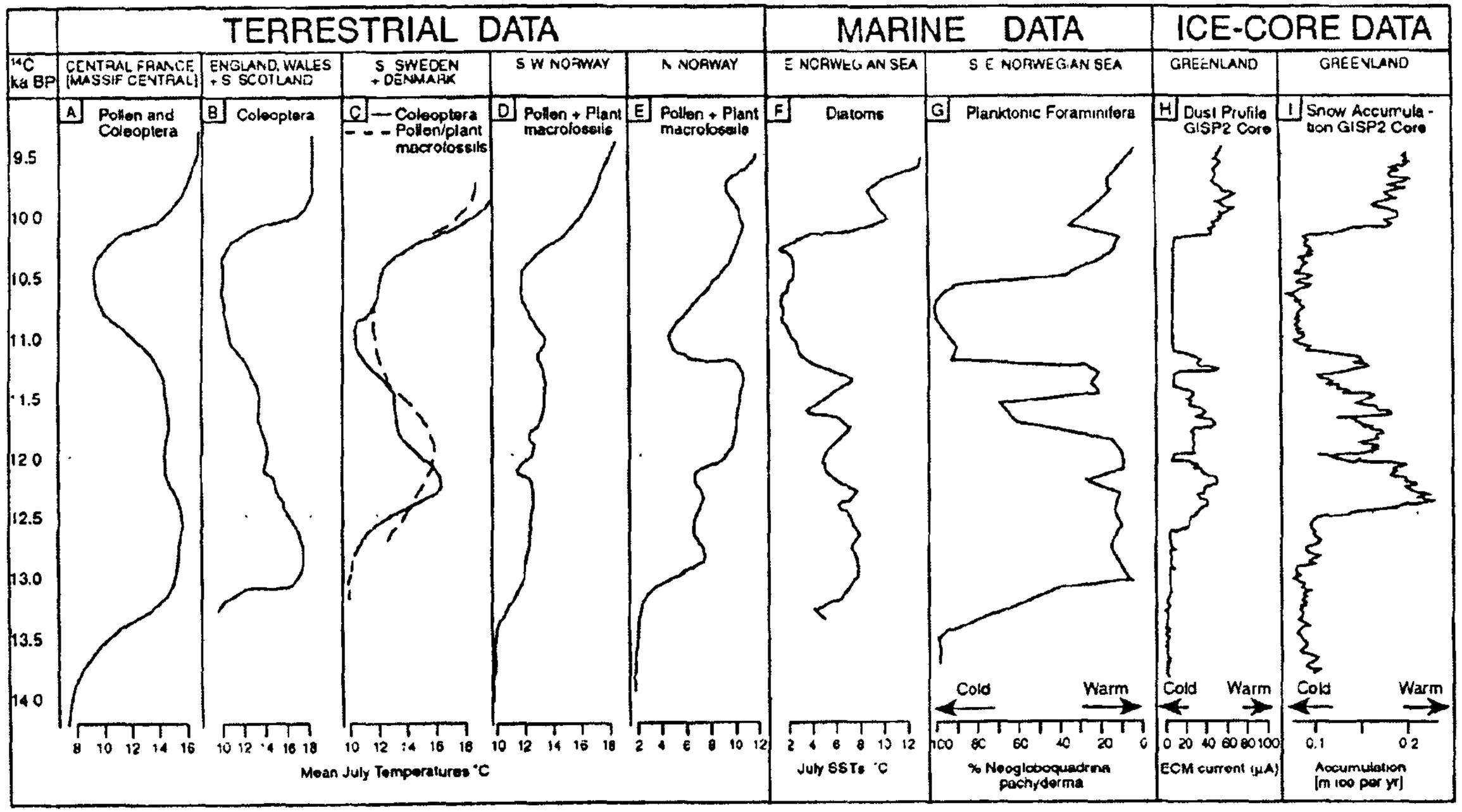

Figure 2.2: Figure showing synchroneity between ice, land and marine records (Lowe and Walker, 1997)

2.1.1 A note on nomenclature and terminology regarding LGIT palaeoclimatology

As the number and complexity of LGIT palaeoclimatological records have increased, so has the number of terms and names associated with the events. The original classification of the LGIT was formulated by Mangerud *et al.* (1974). Based on records from NW Europe, they divided the late-glacial into four chronozones, defined by a ^{14}C chronology (Table 2.1). Use of this system is somewhat problematic due to widespread, casual use of these terms outwith their strictest chronozonic sense (Bjørk *et al.*, 1998)

Chronozone	^{14}C ages		Calibrated ages	
	Start	End	Start	End
Bølling	13	12	15,631	14,484
Older Dryas	12	11.8	14,484	13,818
Allerød	11.8	11	13,818	12,912
Younger Dryas	11	10	12,912	11,583

Table 2.1 : The start and end of the four LGIT chronozones in ^{14}C and calibrated years. Calibrated ages were calculated by taking mid-points of 2 s.d. age ranges produced using CALIB 4.3 (Stuiver and Reimer, 1998)

Arguably one of the system's biggest flaws, if used in its traditional and strictest sense, is the system's implicit association with ^{14}C chronologies. Current palaeoclimatological studies place a large emphasis on correlating events through calibrated timescales because of constantly improving calibration data sets and the increasingly diverse range of archives exploited. Difficulties arise because of the ^{14}C plateaus known to have occurred during the LGIT. Bjørk *et al.* (1998) have, instead, advocated the use of an event stratigraphy based on the GRIP ice core (Figure 2.3). However, as the authors acknowledge, the applicability of this system is geographically limited to the extent of the constituent 'events'.

Therefore, in this review, reference to the event stratigraphy has been made where it appears appropriate and where the literature reviewed is not referring to a "chronozone" versus, for example, an event. Where present, ^{14}C dates are quoted directly from publications but have also been calibrated using INCAL 98 to aid correlation (Stuiver and Reimer, 1993). This results in a mixture of chronologies being presented in the following review, due to the different chronological methods used in different research. However, all

dates are appropriately assigned with terms to distinguish them as ages in ^{14}C, ice-core or calibrated years (cal yr BP) where specified in the original source.

2.2 Current hypotheses debating the synchroneity of LGIT climate change

A major debate to have emerged is the relative timing of LGIT sub-Milankovitch events as experienced in the Southern and Northern Hemispheres. Some published evidence supports the assertion that such changes were, essentially, globally synchronous. However, competing hypotheses propose that some events in the Southern Hemisphere lead or are out of phase with those in the Northern Hemisphere (White and Steig, 2002). The emergence of these hypotheses is predominantly the result of increasing amounts of palaeoclimatological investigations in the Southern Hemisphere. The following review discusses the key lines of evidence in favour of each hypothesis and explores the climatic mechanisms proposed to account for the competing theories.

2.2.1 Hypothesis 1: Globally synchronous LGIT climate change

2.2.1.1 Evidence

The argument that LGIT climate change was globally synchronous is still supported by a large body of data from ice core, sedimentary, geomorphological and palaeoecological investigations. Work by Denton and co-workers has underpinned much of the 'LGIT synchrony' hypothesis (Denton and Hendy, 1994, 1996; Denton *et al.*, 1999a, b; Lowell *et al*, 1995; Denton *et al.* 1999; Andersen *et al.*,1999; Moreno *et al*, 1999). Initial work focused on glacial chronologies based on evidence from the Franz Josef Glacier, South Island, New Zealand (Denton and Hendy, 1994). ^{14}C dates of wood embedded within confines of the Waiho Loop moraine were interpreted as dating the advance to 11.5 cal ka BP (10,050± 14 ^{14}C ka BP). Although only one other similar advance has been dated in New Zealand (Basher and McSaveney, 1989, cited in Denton and Hendy, 1994, 1437), Denton and Hendy (1994) argue that the synchronous behaviour of the Franz Josef glacier with other glaciers in New Zealand indicates a broad synchrony with climate. The authors argue that this cooling was synchronous with the initiation of the Younger Dryas. However, the interpretation of these ages has been criticised, with the earlier age of 13.3 cal ka BP (11,180

^{14}C yr BP) being proposed instead (Mabin, 1996). In summary, ^{14}C dated geomorphological evidence for a synchronous Younger Dryas in New Zealand is both limited spatially and controversial.

Cosmogenic exposure age dating in New Zealand has supported the proposals of Denton and Hendy (1994) (Ivy-Ochs *et al.*, 1999). ^{26}Al, ^{36}Cl and ^{10}Be dates produced an age of 11,720 ±320 cal yr BP for an ice advance (*c.*13.8 ^{14}C cal ka BP). This is taken to infer that an advance occurred during the Younger Dryas. These results seem to provide strong support for the case of a globally synchronous Younger Dryas cold reversal. Additionally, comparison to exposure ages on boulders on the outer Egesen moraine, Switzerland, accepted to represent a YD advance, showed a strong chronological correlation. Therefore, although the chronological technique is still in its infancy, initial results from cosmogenic chronologies in New Zealand seem to support the hypothesis of global synchrony.

Additional support of interhemispheric synchroneity has come from the Taylor Dome ice core in Antarctica (Figure 2.4). Taylor Dome reconstructions based on δD, broadly taken as a proxy for regional sea surface temperature (SST), have been correlated to those from GISP using measurement of atmospheric methane (CH_4) and the isotopic ratio of molecular oxygen ($\delta^{18}O_{atm}$) (Steig *et al*, 1998; Grootes *et al*, 2001. Figure 2.4 shows the strong correlation between GISP2 and Taylor dome δD records, with a post-LGM warming at Taylor Dome within 1000 years of the onset of a similar warming at GISP2. Further similarities exist between Taylor Dome and GISP during the LGIT, with the timing of the mid LGIT cooling events at both sites occurring within 500 years of each other. However, both of these sets of events, as recorded at Taylor Dome, lead the timing of comparable events in the other Antarctic ice core records at Byrd and Vostok by up to 2000 years (Steig *et al*, 2000). Grootes *et al.* (2001) argue that Taylor Dome's proximity to the sea, relative to other Antarctic ice cores, is responsible for these differences. A greater "North Atlantic character" is assigned to Taylor Dome because of the comparatively strong marine influence due to this location (Grootes *et al.*, 2001, 294). Furthermore, the magnitude of this influence would vary with the growth and retreat Ross Sheet sea ice, and thus the proximity of the sea to Taylor Dome site.

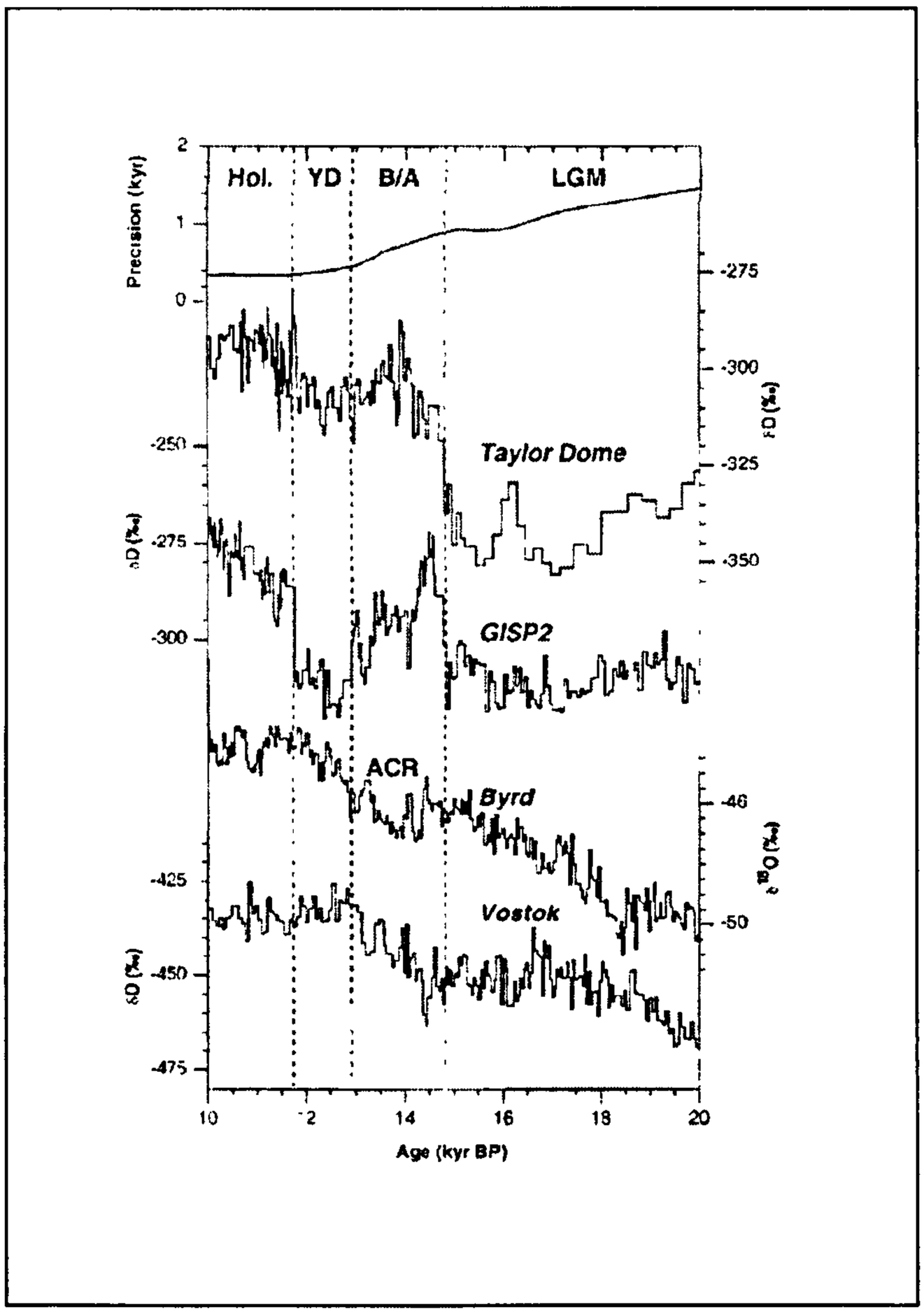

Figure 2.4: Stable isotope profiles from Taylor Dome, GISP2, Byrd and Vostok. At the top, the estimated precision in the Taylor Dome age scale is shown. Boundaries of climate intervals, as defined in the GISP2 record, are shown by dashed vertical lines: Hol, Holocene; YD, Younger Dryas; B/A Bølling/ Allerød; LGM, Last Glacial Maximum, ACR is the Antarctic Cold Reversal as defined at Byrd after Blunier *et al*. (1997) and Steig *et al.* (1998).

Tropical ice cores from the Andean Altiplano support a climatic cooling in the Southern Hemisphere which is synchronous and of similar magnitude to that evident in the Greenland ice cores (Thompson *et al.*, 1998). Sajama (18°06'S) and Hurascon (09°07'S) δ18 O ice-core records both indicate a cooling event that punctuated the gradual rise in temperatures during the LGIT, although it is a more extended signal than that recorded at GRIP and lasted c. 2500 years. Thompson *et al.* (1998) use this to argue that atmospheric telecommunications were responsible for dissemination of this LGIT cooling.

2.2.1.2 *Forcing mechanism and modes of teleconnection*

Proposing a mechanism that could result in virtually instantaneous global climate change is problematic. Any explanation through high-latitude insolation is unsatisfactory, unless some mechanism for rapid, global dissipation of the resultant signal can be established. One possibility is to accept traditional views that LGIT climate change was initiated by changes in the North Atlantic area and then find a suitable means for rapid dissipation of this event. A pivotal role of ice masses and global oceanic circulation is unlikely because of localised influence and slow response times, respectively (Lowell *et al.*, 1995). The major remaining candidate is atmospheric teleconnection. Results from Antiplano ice-cores, together with coeval evidence of shifts in global methane concentrations found in GISP (Severinghaus *et al.*, 1998), lead Thompson *et al.* (1998) to suggest an atmospheric method of transmission, potentially with the tropical hydrological systems as a forcing mechanism.

Denton *et al.*, (1999a) propose changes in greenhouse gases, and subsequent atmospheric teleconnections, as being the forcing mechanism for the changes. They argue that there are many sites which show that the warming step at the beginning of the Oldest Dryas c. 17.4 cal ka BP (c. 14,600 ^{14}C yr BP) started the end of the last glacialiation. They propose that this warming occurred due to changes in water vapour in the tropics, triggered by Milankovitch insolation changes in the Northern Hemisphere. This warming allowed the resumption of thermohaline circulation and a return to interglacial atmospheric water-vapour levels in the tropics. The warming, combined with the loss of extended and unstable marine-grounded ice sheets in the North Atlantic could have triggered Heinrich Event 1. The resultant massive influx of icebergs into the North Atlantic Ocean suppressed warming and the upwelling of warm water in this region, resulting in absence of the warming signal in this region and thus the cold signal recorded in the Greenland ice cores. Indeed, they argue that evidence of a rise in CH_4 in the Greenland ice cores, demonstrated

by Chappellaz *et al.* (1993), can be used to indicate an increase in temperature c. 17 ice-core ka BP. They proposed that the Younger Dryas cooling, argued to be a globally synchronous phenomenon, was initiated by further melting of ice in the N. Atlantic region, producing a 1000 year influx of freshwater which effectively shut down the thermohaline ocean circulation. "A link between thermohaline circulation and the tropical production of water vapour" is thought to be most likely for the atmospheric, rapid, teleconnection of this event at a global scale (Denton *et al.*, 1999a, 139).

The relevance of site-specific variations in determining mechanisms of climatic forcing and teleconnection is also discussed by Steig *et al.* (1998) in the discussion of their results from Taylor Dome. They argue that the non-synchrony between the Taylor Dome record and those from Vostok and Byrd is too great to be attributed to errors in the chronologies. Thus, Grootes *et al.* (2001) conclude that thermohaline circulation rapidly transports heat latitudinally at a global scale to produce synchronous climate change both on Milankovitch and sub-Milankovitch time scales.

2.2.2 Hypothesis 2: Northern Hemisphere changes lead those in the Southern Hemisphere or are not global in extent

2.2.2.1 Evidence

Evidence from the GISP ice-core caused Severinghaus and Brook (1999) to propose a North Atlantic lead during the LGIT, based on a lag between changes in CH_4 and $\delta^{18}O$ ice, when the two proxies are compared using a chronology based on thermal fractionation of N and Ar isotopes. These data indicate that climate change in the tropics, the principal global sink or source of CH_4, lagged the temperature rises experienced by Greenland at the termination of GS-2 by c.20 - 80 years. This indicates a N. Atlantic trigger as opposed to a tropical forcing mechanism. The resulting release of methane from the tropics meant that the effects of the event were felt at least a hemispheric level (Severinghaus *et al.*, 1998). The rapid dissipation of the event suggests atmospheric propagation (Severinghaus *et al.*, 1998, Severinghaus and Brook, 1999).

If LGIT sub-Milankovitch changes did originate in the Northern Hemisphere, an explanation for their absence in Southern Hemisphere records is that the events responsible were insufficiently large to force climate change on a global scale. This would result in absence of evidence of an equivalent event in the Southern Hemisphere.

Pollen records from South Island, New Zealand, have been used to argue that there was no significant change in climate during the LGIT apart from a gradual warming. This indicates a localised, North Atlantic forcing mechanism so minimal as to not influence deepwater formation, or alternatively a global event of a magnitude too small to be detected in the records investigated (Newnham *et al.*, 1989; Singer *et al.*, 1998). A similar conclusion is reached by McGlone (1995) from his review of geomorphic, sedimentary and palynological evidence from New Zealand. He proposed that changes in insolation, which was at its lowest in the Southern Hemisphere at approximately the same time as the Younger Dryas chronozone (Berger, 1978, cited in McGlone, 1995, 879), combined with increased cloud cover and precipitation, were responsible for the changes in LGIT palaeovegetation recorded.

Palynological records from three sites within 30km of the Waiho Loop in New Zealand lead Vandergoes and Fitzsimons (*in press*) to the same conclusion. The subtle changes in palaeovegetation could represent a small cooling between c. 12.9 -11.6 cal ka BP (c. 11-10 ^{14}C ka BP). However, attributing a drop in temperature as the cause is problematic due to possible insensitivity of the vegetation to changes in temperature as opposed to precipitation. They also cite increased cloud cover and precipitation as a possible cause of both vegetation change in these studies and the advance of the Franz Josef glacier during this period (2.2.1.1). Similar conclusions are drawn further North in South Island, where pollen records show no increase in cold-loving taxa during the Younger Dryas chronozone (Singer *et al.*, 1998). Instead the temporary replacement of *Halocarpus* by beech indicates a shift to wetter conditions during the deglacial period in New Zealand.

A speleothem record from South Island, New Zealand also supports the argument for palaeoprecipitation change in during the LGIT (Hellstrom *et al*, 1998). Changes in carbonate $\delta^{18}O$ correspond closely to periods of glacial advances in New Zealand. The speleothem record also correlates fairly well with changes in the GISP $\delta^{18}O$ record, with the most prominent isotopic excursion during the LGIT between 13,800 and 11,700 cal years BP. Although this window spans the GS-1 time frame, it also starts 1000 years earlier. Hellstrom *et al* (1998) concluded that their $\delta^{18}O$ record is more likely to reflect isotopic variations in the meteoric water sources during deposition as opposed to temperature

changes. Data from this record therefore also support the argument that there were no major, short-term temperature fluctuations in New Zealand during the LGIT.

2.2.2.2 Forcing mechanism and modes of teleconnection

There is good evidence to suggest that glacier response to climate change in the North Atlantic area can result in periodic, massive discharges of freshwater and that these in turn can affect climate in the North Atlantic region through changes in thermohaline Ocean Circulation. However, the extent of the geographical impact of these influxes of cold, fresh water is debated. Broecker and Denton (1990) argue that they could cause a reorganisation between modes of thermohaline circulation and cause climate to change on a global scale. Through a comparison of the Vostok and GISP ice core records between 100-49 k ice-core yr BP, Bender *et al.* (1994) suggested that sub-Milankovitch events during the last glacial could be explained by such a mechanism. Their evidence shows that when North Atlantic events were over 2000 years in duration, a coinciding event was recorded in the Vostok stratigraphy. The chronological control was insufficiently precise to establish whether the GISP excursion preceded that in Vostok, but the authors suggested that North Atlantic events may lead and, if big enough, would be propagated globally. As the nature of the Vostok excursions was less severe and more moderate in amplitude than the corresponding GISP excursions, the authors suggested an oceanic teleconnection that muted the severity of the North Atlantic signal.

Thus, evidence for this hypothesis comes from several camps. There are those records from the Southern Hemisphere where LGIT climate change is not recorded and those where it is recorded, but the change is attributed to forcing mechanisms other than temperature. A major difficulty in disproving the hypothesis related to the former is that absence of evidence is not evidence of absence. A "comparatively weak, short-term climate change" may not be shown up by certain proxies or at certain sites due to insufficient sensitivity of the individual organisms or assemblages present (Heusser, 1993; Heusser *et al.*, 1996, 182).

2.2.3 Hypothesis 3: Southern Hemisphere leading Northern Hemisphere changes

2.2.3.1 Evidence

Hays *et al.* (1976) proposed that warming in the Southern Ocean preceded that in the Northern Hemisphere. This research, and other supporting publications, used evidence based on marine micro- and macro-fossils. Charles *et al.*, (1996), produced a convincing argument from a South Atlantic core. They argued that $\delta^{13}C$ in benthic foraminifera acted as a proxy of NADW strength whereas $\delta^{18}O$ of planktonic foraminifera indicated the $\delta^{18}O$ of the Southern Ocean. Performing isotopic analysis of both types of organisms allowed a proxy of both the North and South Atlantic to be assessed and compared within the same depth in the stratigraphy. Figure 2.5 shows the results of these isotopic data together with the $\delta^{18}O$ Summit record and the δD record from Vostok, all on a common time scale. Phase relationship analysis of the data clearly suggests the lead of the Southern Atlantic over the North by an average of 1500 years.

Subsequent evidence that short, warm interstadials over the last 110 kaBP, termed Dansgaard Oeschger events, occurred in the Northern Hemisphere 2-3kyr later than those in the Southern Hemisphere during the last glacial period came from Antarctic ice cores (Blunier *et al.*, 1997, 1998). Comparison of $\delta^{18}O$ LGIT records from GRIP and Byrd indicated that GS-1, as recorded in GRIP, was preceded by a period of cooling, as represented by reduced $\delta^{18}O$ concentrations at Byrd, named the Antarctic Cold Reversal (ACR) (Figure 2.6). Analysis of ice-core records from Vostok, Dome Fuji and Dome C also report a similar cooling occurring at the same time (Blunier, 1998; Watanabe, 2003) (Figure 2.7). Blunier *et al.* (1998) argue that the fact that the rise in $\delta^{18}O$ in Byrd pre-empts the global rise in CH_4, recorded as synchronous in Byrd and GRIP, means that the changes in temperature at Byrd occurred before global changes in atmospheric methane levels. This leads to the conclusions that, firstly, warming occurred initially in the south and, secondly, that the oceans were the major mode of teleconnection of climate fluctuations of this scale. If atmospheric transportation was the major mode, this would cause synchronous rises in $\delta^{18}O$ (a proxy of Antarctic air temperature) and CH_4 (taken as a proxy of tropical climate change) at Byrd (Blunier, 1997).

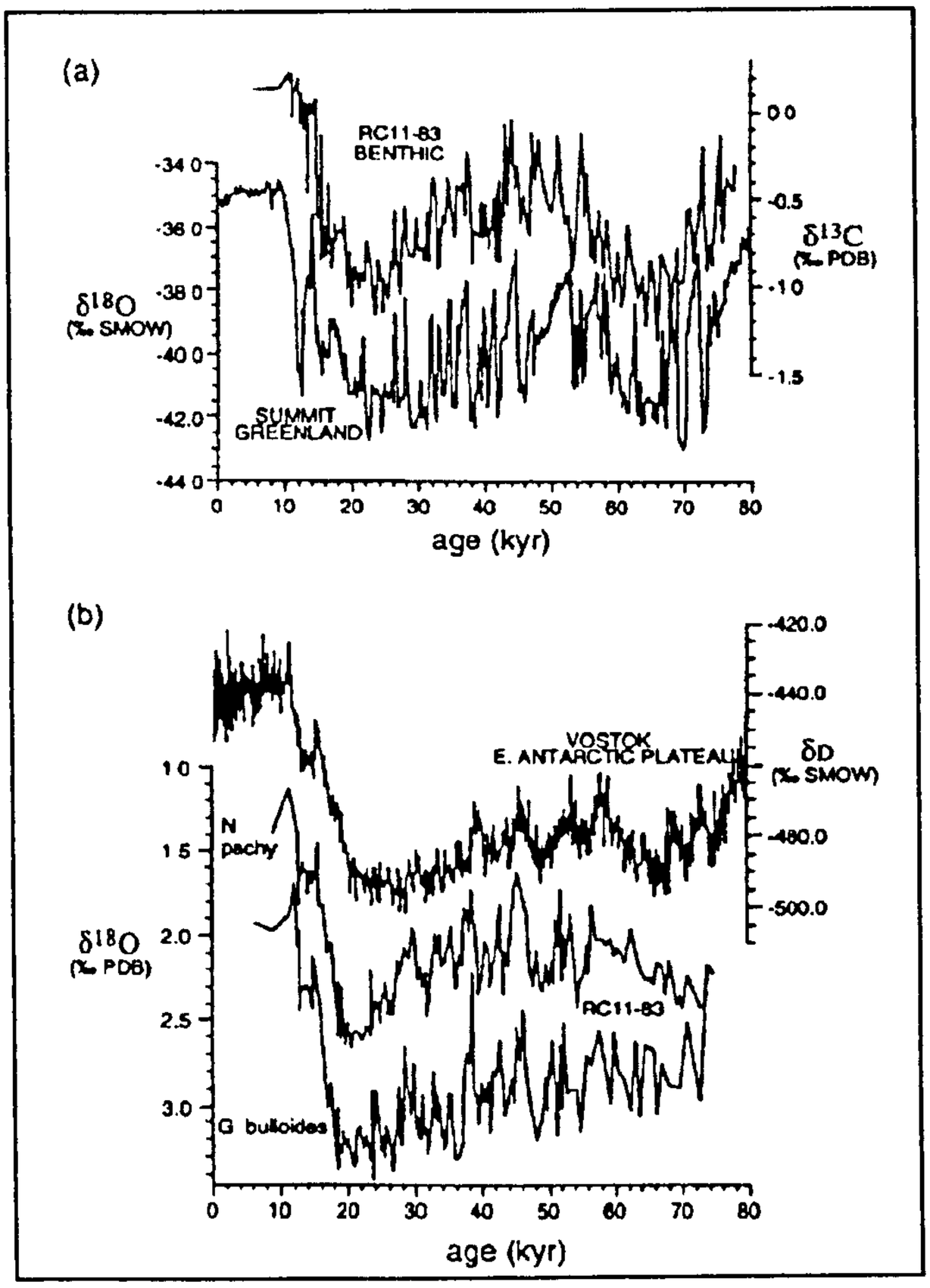

Figure 2.5: Foraminiferal isotope analysis of core RC11-83 (41°36'S, 9°48'E) in the Southern Atlantic and comparison to ice core isotopic records (Charles *et al.*, 1996). (a) shows $\delta^{13}C$ of the benthic foraminifera relative to the Summit $\delta^{18}O$ record, (b) shows the $\delta^{18}O$ for two planktonic foraminifera species and the δD record from Vostok.

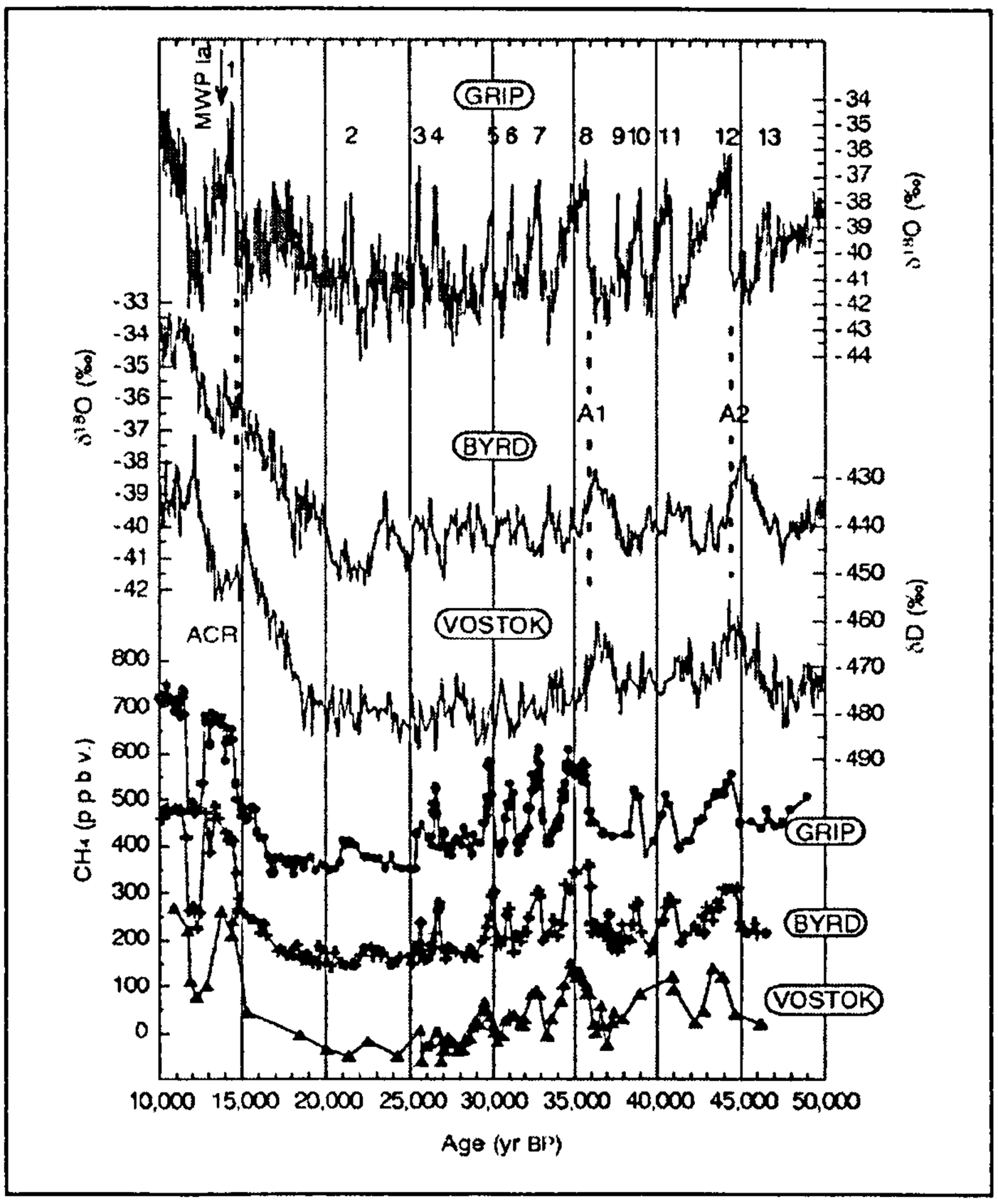

Figure 2.6: GRIP, Byrd and Vostok isotopic and CH_4 records on a common time scale (GRIP timescale in years before 1989) showing asynchronous Late Glacial Interglacial Transition climate change (Blunier *et al.*, 1998). The numbers on the top of the GRIP isotopic record indicate the location of Dansgaard-Oeschger Events. The ACR shows the location of the Antarctic Cold Reversal. A1 and A2 refer to Antarctic warmings discussed in the text.

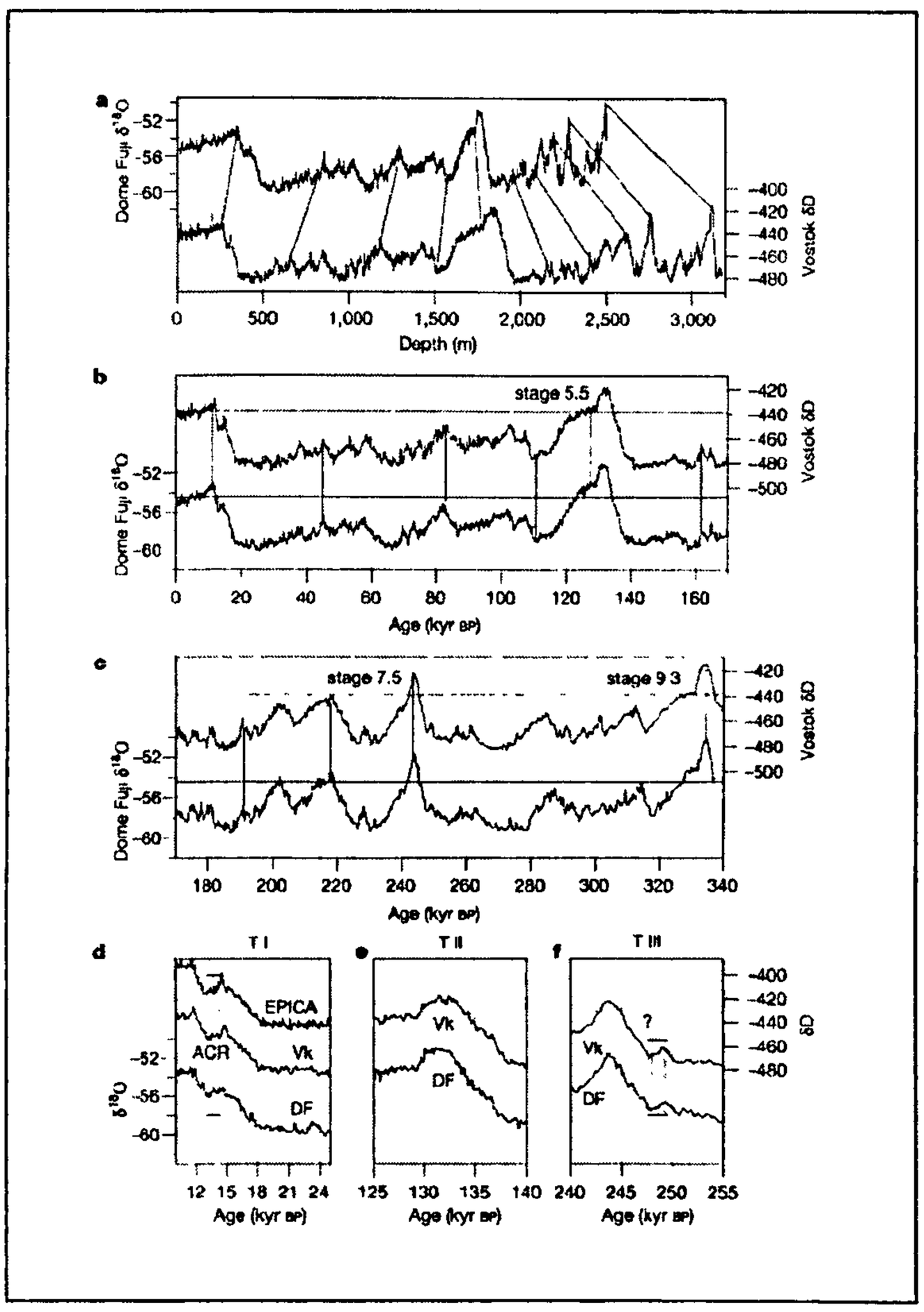

Figure 2.7 :Diagram showing the Antarctic Cold Reversal (ACR) as recorded in $\delta^{18}O$ records from EPICA (European Project for Ice Drilling in Antarctica, Dome C), Vostok (Vk) and Dome Fuji (DF) (Based on Wanatabe, 2003).

Sowers and Bender (1995) also argued that the rise in temperature at the end of the GS-2, as shown in the Greenland ice cores, actually happened 2000 – 4000 years after many records in the Southern Hemisphere. Using the same reasoning as Blunier *et al.*, (1997, 1998), a lag time of such magnitude leads to the conclusion that the method of teleconnection of these events must be ocean based. An alternative explanation is that the N. Atlantic was "buffered" from the effects of climatic warming on a global scale because of the location of the Polar Front, which did not migrate northwards until just before the start of the Bølling chronozone, 14.7 cal ka BP (11,800 – 12, 000 ^{14}C kaBP) (Keigwin *et al.*, 1991; Bard *et al.*, 1989 and Ruddiman and McIntyre, all cited in Sowers and Bender, 1995, 212). However, it should be noted that the authors argue, as do Denton *et al.* (1999), that records from Greenland ice-cores appear to be unrepresentative of some other Northern Hemisphere records, especially those south of 45° such as records from the Swiss Alps. Denton *et al.* (1999a) argue that a mass discharge of glacial melt water into the North Atlantic at the start of the Bolling would have depressed North Atlantic, and thus Greenland, temperatures – thus causing the warming to not be registered in such a prominent form as it is in more continental European sites.

Those opposing this hypothesis, that the Southern Hemisphere leads, have referred to the issue of the extent of regional versus site specific representivity of continental Antarctic ice core records (see Steig *et al.*, 2000). Additionally, it is argued that Antarctica is somewhat isolated from the rest of the Southern Hemisphere's climate, due to the strong circum polar currents that dominate atmospheric and surface ocean currents. Therefore, the extent to which Antarctic climate change is valid as a proxy of that of the Southern Hemisphere as a whole is arguable. However, evidence to support the relative timing and existence of the ACR preceding GS-1 has also emerged from terrestrial records outside Antarctica in Patagonia, most notably in the Magellan Straits (Sugden *et al.*, 2005). The findings from these investigations are discussed in 2.4.

2.2.3.2 Mechanisms

Two main mechanisms have been proposed to explain the antiphase character of sub-Milankovitch change between the northern and Southern Hemispheres (Steig and Alley, 2002). The first is the "seesaw" analogy, proposed by Broecker (1997). This is based on the logic that pulses of fresh, cold water coming into the N. Atlantic will shut down the North

Atlantic Deep Water (NADW), the formation of which is a major driving force in maintaining present ocean circulation at a global scale and the heat redistribution that accompanies it. A switching off or a slow down in this process, and the associated cooling in the Northern Hemisphere, would result in a warming in the Southern Hemisphere as heat was distributed differently. This theory is supported by box-model calculations and GCMs (Steig and Alley, 2002). However, by using deuterium excess measurements from Dome C as a proxy for sea surface temperature of the precipitation source area, in this case the Southern Indian Ocean, Stenni *et al.* (2001) indicated that temperatures in the sea surface temperature (SST) in the Southern Indian Ocean actually warmed 800 years after the start of the ACR. This finding suggests that the ocean-seesaw model is too simplistic to explain such palaeoclimatic change (Steig, 2001).

An alternative explanation is that climate change in the Southern Hemisphere actually leads that in the north due to a Southern Hemisphere forcing mechanism. One potential means is a change in the extent in sea ice due to changes in local Milankovitch cycles at periods such at the end of the last ice age (Kim *et al.*, 1998). Amplified by appropriate atmospheric CO_2 concentration feed back mechanisms, it is feasible that such events could affect the nature and timing of Milankovitch scale climate change by changing the outflow of Antarctic Bottom Water, which would then have a knock on effect on global ocean circulation and the North Atlantic (Kim *et al.*, 1998).

2.3 Millennial Scale Holocene climate fluctuations

Climate changes during the Holocene have been less dramatic than during the LGIT (Roberts, 1998; Mayewski *et al.*, 2004). However, there have been notable changes in climate during the last 11,500 cal yr as a result of complex interactions between the final effects and feedbacks of deglaciation following events such as the GS-1 (Figure 2.3), and changes in insolation due to orbital variations. These have produced both gradual changes in temperature, albeit on a smaller scale than that experienced during the LGIT, and latitudinal displacement of atmospheric circulation patterns. Superimposed on these changes are the effects of shorter term forcing mechanisms such as solar variance and volcanic activity (Bradley, 2003). However within this review, these latter mechanisms and their effects are not discussed as they occur at a higher resolution than concerns the Holocene investigation of this thesis.

Whereas the ice-core records from Greenland appear to be fairly sensitive to climate change during the LGIT, much of the Holocene climate variability is not as well mirrored in them, arguably because of the smaller scale of temperatures involved (Oldfield, 2003). However, the cores do appear to indicate a gradual cooling throughout the Holocene, following a warm early Holocene (Fisher and Koerner, 2003). Terrestrial and maritime records from temperate regions also support, in general, an early Holocene warming, especially in the Northern Hemisphere, prior to climatic deterioration in the latter half of the Holocene (Street Perrott- and Roberts, 1994).

The timing of the Holocene Thermal Maximum is thought to have varied spatially ranging from 11-7 cal ka BP (Kaufman *et al.*, 2004). For example, Figure 2.8 shows that, although maximum July insolation is calculated to have occurred at c. 12-10 cal ka BP, the post-LGIT warming in Northern Finland did not reach its maximum state till c. 7.5 cal ka BP. This, and other similar delays in warming in the Arctic area, are proposed to be due to the influence still exerted on such areas by the Northern Hemisphere ice-caps (Seppa and Birks, 2001; Kaufmann *et al.*, 2004). Evidence for an early Holocene thermal maximum is also indicated by raised treelines in N. Europe and N. America and shifts in ecotonal boundaries, both of which indicate that increases in insolation afforded longer growing seasons (Seppa and Birks, 2002; Dahl and Nesje, 1996). Deuterium data from bristle-cone pines from California also support such temperature trends, with a temperature maximum from 8000 – 6800 years BP (Feng and Epstein, 1995). At a global scale the dating of moraines deposited during the Holocene indicate that glacial advances were scarce during this period in comparison to the second half of the Holocene (Figure 2.9).

In tropical and subtropical archives, evidence of climate change in the first half of the Holocene predominantly reflects changes in effective precipitation as opposed to temperature patterns. This is due to the shifts in evaporation regimes due to changing insolation patterns and in turn changes in atmospheric circulation patterns. Comparisons of records from polar and tropical ice-core records indicate that fluctuations in climate were stronger in the lower latitudes than they were towards the poles (Fisher and Koerner, 2003). Figure 2.10 highlights these spatial trends, showing that sub-tropical and tropical lake levels in Africa and Asia were predominantly higher than present levels during the first half of the Holocene (Stager *et al.*, 2003; Gasse *et al*, 2000; deMenocal *et al*,. 2000). This

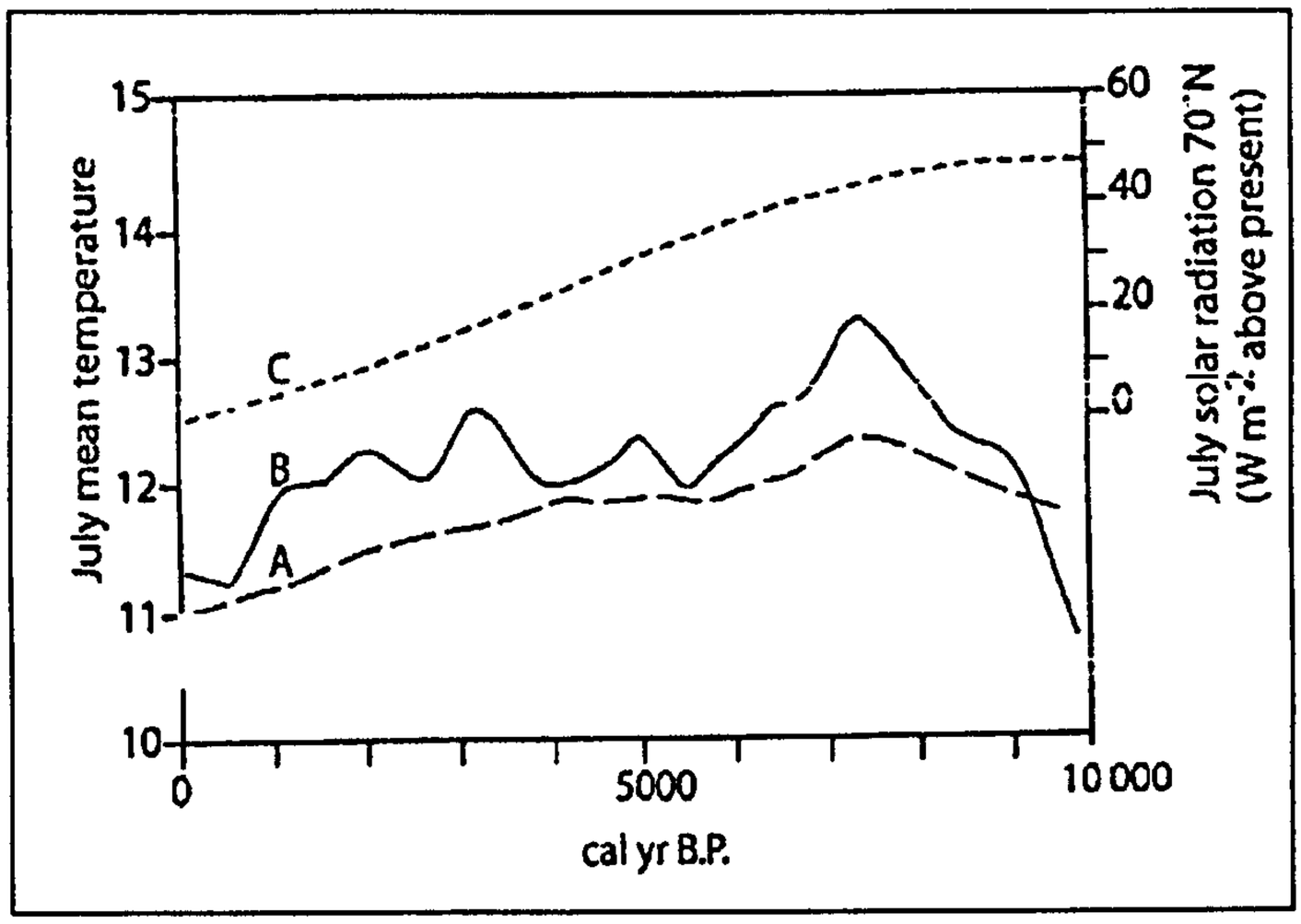

Figure 2.8: July mean temperate reconstructions from Toskaljavri (A) and Tsuolbmajavri (B) (Seppä and Birks, 2001) and the July solar radiation variations at 70°N since 10 000 cal yr BP (C) as calculated by Berger (1978) (Seppä and Birks, 2002)

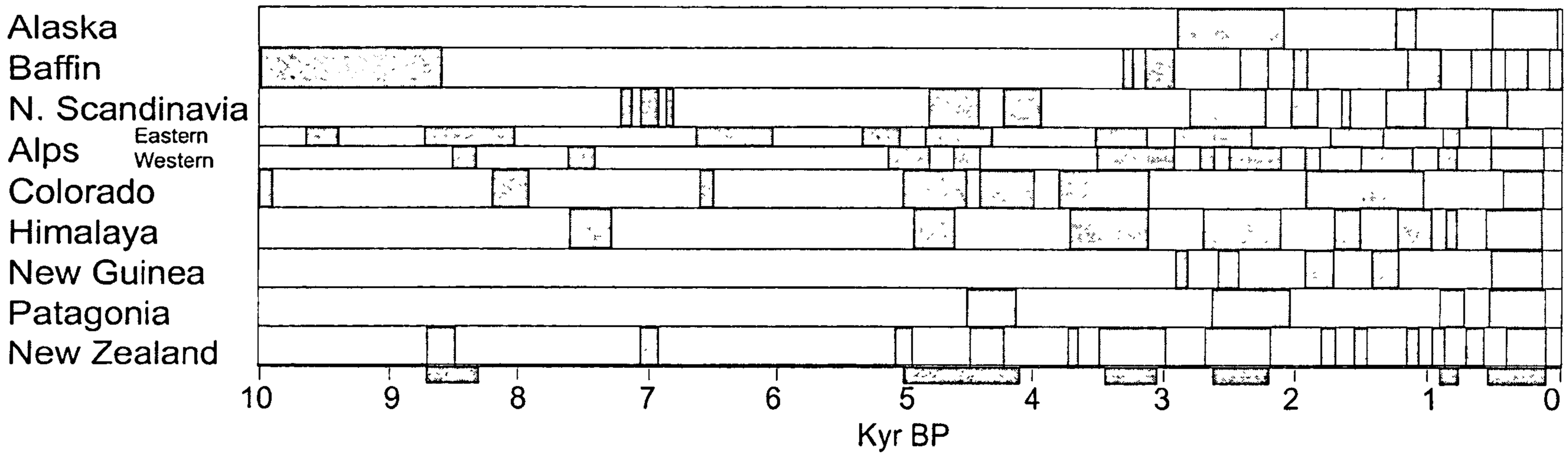

Figure 2.9 : Summary of glacier expansion phases in different areas of the world during the Holocene (Grove, 1988).

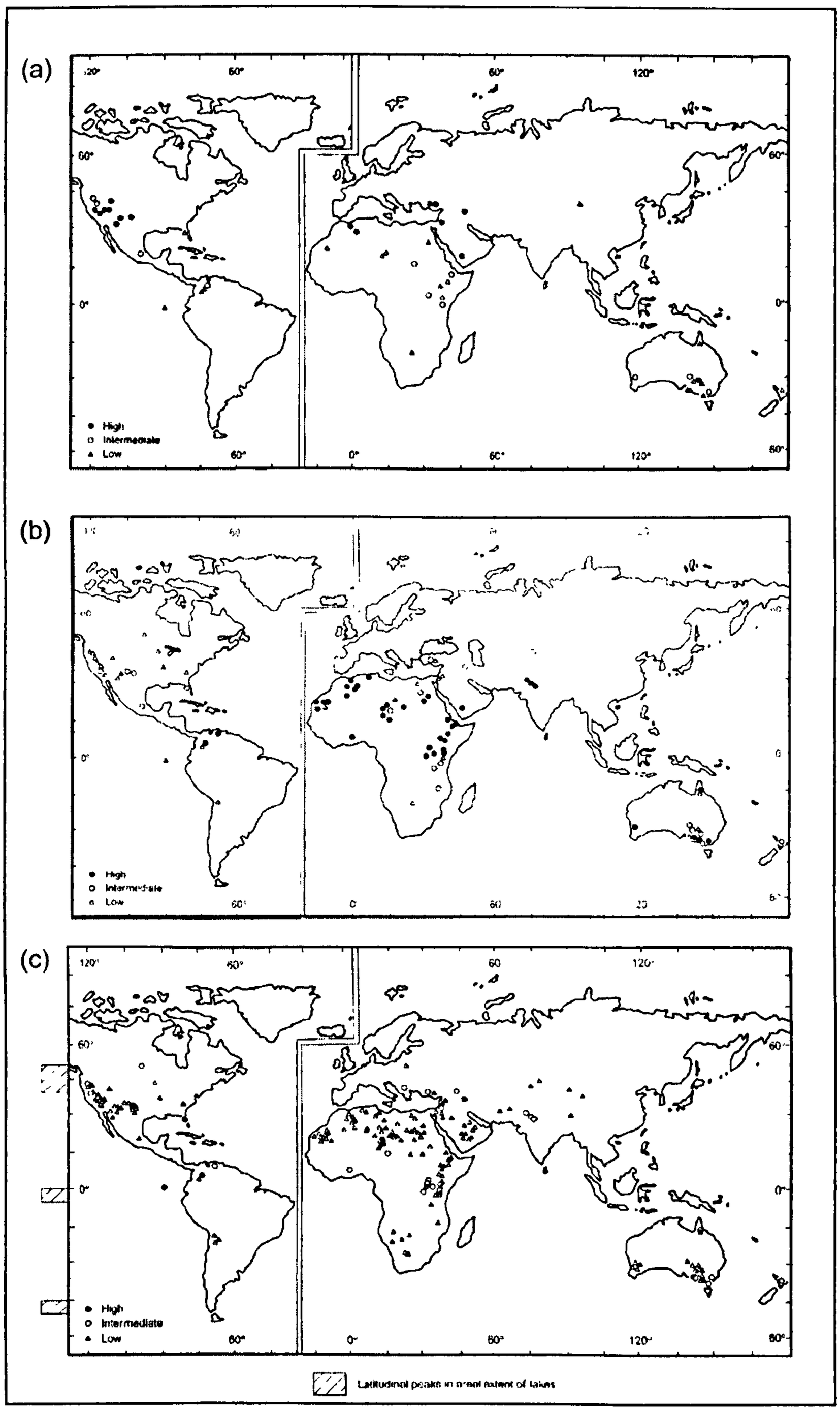

Figure 2.10 : Lake-Level status at (a)18000, (b) 6000 yr BP & (c) during modern times (Street Perrott and Harrison, 1985).

pattern is thought to be due to a displacement of the atmospheric cells and increased evaporation leading to an intensification of the monsoon. Conversely, lake levels on South American Antiplano were lower during this period (Abbott *et al.*, 1997, 2001). Local palynological and ice-core data support this hypothesis (Thompson *et al.*, 1998; Burbridge *et al*,. 2004), with changes in the location of atmospheric cells again being proposed as the mechanism. In this case orbitally driven January insolation minimum at 10-15° S would reduce the continental penetration of the ITCZ south of the equator and thus reduce the length of the summer rainy season (Burbridge *et al*, 1994).

During the latter Holocene climate became more similar to present conditions. As local insolation patterns changed to those more similar to today's, most of the characteristics associated with early Holocene climates became less severe or ceased over the last half of the Holocene. Cooling is noted to have occurred in the temperate northern latitudes, lake levels fell in the Asian and African tropics whilst the climate of subtropical South America became less xeric (Barker *et al.*, 2001; Seppä and Birks, 2001). On a global scale, glacial advances became more common, supported by the wetter and cooler conditions of the latter half of the Holocene (Figure 2.9).

Therefore, research showing Holocene millennial scale climatic variations have highlighted the importance of changes in insolation in influencing global climate systems. Whilst temperature changes in the early Holocene may be most prominent in the temperate Northern Latitudes, records from outwith this area have produced reconstructions with a more palaeoprecipitation focus.

2.4 LGIT and Holocene palaeoenvironmental evidence from Patagonia

The region of Patagonia has, within the last 20 – 30 years, assumed a major role within the debate surrounding the extent of LGIT and Holocene climate synchrony. As outlined in Chapter 1, the region holds a unique location which makes it a key source of new palaeoclimatic data. The approaches used within LGIT Patagonian palaeoclimatic research can be broadly categorised into three: glacial geomorphology and reconstructing former ice masses, pollen analysis and palaeovegetation reconstructions and other complementary palaeoecological techniques. As well as supplying much-needed evidence to the debates

regarding changes in temperature, these investigated have enhanced our understanding of LGIT and Holocene changes in precipitation regimes associated with proposed shifts in the latitudinal position of the Westerlies (Heusser, 1983, 1989, 2003; Markgraf, 1987, 1989). Some of these studies have also examined Holocene climate change, although this chronozone has generally received less attention that the preceding LGIT. In the following section, the key strands of previous investigations and their contribution to the research questions being posed by this study are discussed.

2.4.1 LGIT evidence

2.4.1.1 Sedimentary and geomorphology evidence

Non- palaeoecological Quaternary investigations in Patagonia mostly comprise of the mapping and analysis of glacial and fluvial glacial landforms, and to a lesser extent palaeolake features and deposits. These have often been chronologically constrained through ^{14}C dating of associated organic matter. However, more recent research has seen the implementation a wider range of chronological techniques. Following initial investigations by Mercer (1976) and Caldenius (1932), research to delimit past glacier fluctuations and produce a glacial chronology have focused mainly on the Chilean Lake District (Porter, 1981; Lowell *et al.*, 1995; Denton *et al.* 1999; Anderson *et al.*, 1995, 1999, the Straits of Magellan (Clapperton *et al.*, 1995, McCulloch and Bentley, 1995) and Torres del Paine (Marden, 1993, 1997; Clapperton *et al.*, 1995; Clapperton and Marden, 1995) (Figure 2.11). A smaller number of studies have investigated Neoglaciation in the region (Mercer, 1982; Clapperton and Sugden, 1988; Heusser, 1964). As well as stand-alone data, many of these geomorphological studies and minimum dates for deglaciation have been used to provide constraints for models of palaeoglaciation (Hulton *et al.*, 1994; Sugden and Hulton, 1997; Purves and Hulton, 2000; Hulton *et al.*, 2001).

Extensive mapping and dating of glacial and fluvioglacial features has produced a detailed history of glacial fluctuations in the Chilean Lake District (Andersen *et al.*, 1995, 1999; Denton *et al.*, 1999b, Lowell *et al.*, 1995). ^{14}C dated landforms indicate that moraines dating back as far as > 49 ^{14}C ka BP were formed during Marine Isotope Stage (MIS) 3. A complex series of moraine and outwash systems fringe the edge of Lagos Puyehue, Rupanco and Llanquihue, Seno Reloncavi and Golfo de Ancund delineating the extent of former glacial advances/standstills. Three major advances occurred prior to 20 ^{14}C kyr BP with a final

Figure 2.11: Map showing the location of geomorphological studies and the timing of LGIT glacial advances. Each box refers to a different advance, as proposed by the referenced authors, within the relevant field area. All dates are given in ^{14}C (blue boxes) and calibrated ka BP (purple boxes),with the exception of Kaplan *et al.* (in press).

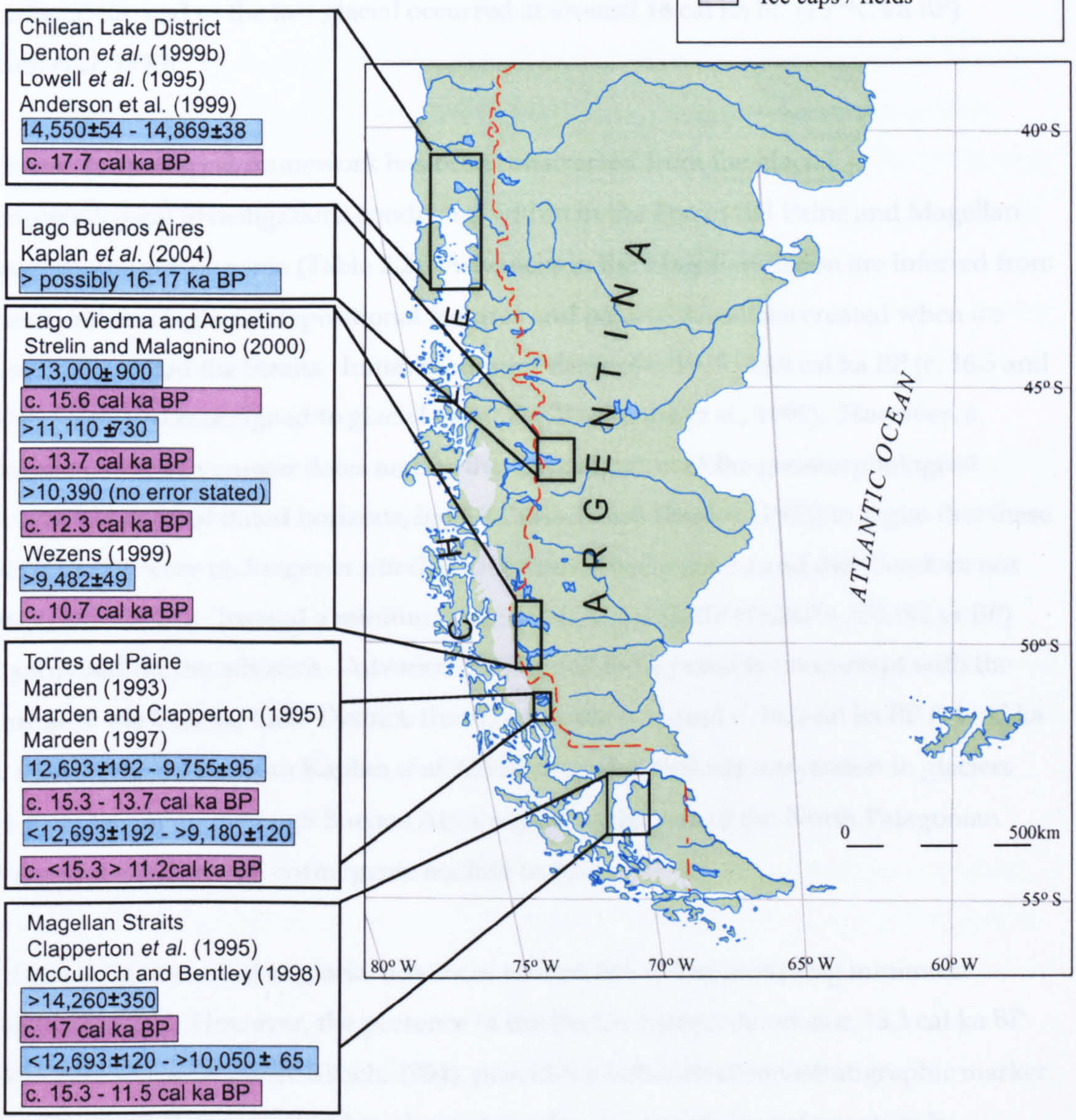

advance at c. 17.7 cal ka BP (14,805-14,869 ^{14}C yr BP). During this period snowlines are thought to have been c. 1000m lower than at present (Porter, 1981; Hubbard, 1997). There were spatial variations in terms of the extent of advances during these events. An event, c. 22 ^{14}C kyr BP, advanced furthes during the LGM in the north of the field area, whereas a later event at c. 18 cal ka BP (15 ^{14}C ka BP) advanced further during the LGM in the South. Retreat from this last major advance occurred rapidly and within 200 years of this last advance, glaciers were within 10 km of their present limits (Lowell *et al.*, 1995). In conjunction with the pollen records from the region, this indicates that the majority of the warming at the end of the last glacial occurred at around 18 cal ka BP (15 ^{14}C ka BP) (Lowell *et al*, 1995).

A similar chronological framework has been constructed from the glacial geomorphological investigations conducted within in the Torres del Paine and Magellan areas of southern Patagonia (Table 2.2). Advances in the Magellan region are inferred from a glacial and fluvioglacial depositional features and palaeo-shorelines created when ice damned lakes filled the Straits. Initial minimum dates of c. 19. 7 -18.9 cal ka BP (c. 16.5 and 15.8 ^{14}C ka BP) were assigned to glacial event D (Clapperton *et al.*, 1995). However, a subsequent suite of younger dates and further investigation of the geomorphological setting of the original dated horizons, led McCulloch and Bentley (1998) to argue that these initial deposits were no longer *in situ* due to tectonic displacement and did therefore not relate to Advance D. Instead a minimum age of >c. 17 cal ka BP (14,260 ± 350 ^{14}C yr BP) was proposed for the advance. Advance D is argued to be possibly concurrent with the advances in the Chilean Lake District, thought to have occurred c. 16.2 cal ka BP (14 ^{14}C ka BP). Cosmogenic data from Kaplan *et al.* (2004) may also indicate a recession in glaciers after 16-17 kyr BP in the Lago Buenos Aires region, to the east of the North Patagonian Icefield, as dated through cosmogenic nuclide techniques.

^{14}C chronological control of glacial advances is often limited to providing minimum constraining ages. However, the presence of the Reclús tephra, dated as c. 15.3 cal ka BP (12,693 ±192 ^{14}C yr BP) (McCulloch, 1994), provides a valuable chronostratigraphic marker within Southern Patagonia and has allowed maximum ages for glacial events to be established (Marden, 1997; McCulloch and Bentley, 1998). This allowed a window of c. 15.3 -11.5 cal ka BP (12,693 ±192 – 10,050 ±65 ^{14}C yr) BP to be established for advance E in the

Magellan Straits. This time window, during which glaciers extended c.100 km beyond their current position, correlates with timing of the ACR (14.7 -11.6GISP ice-core ka BP). Thus, McCulloch *et al.* (2000) argue that the two events may be related.

Event F is noted to have been major as it produced "large multiple moraines" and is interpreted to have been an advance as opposed to a standstill (Marden and Clapperton, 1995, 207). Marden and Clapperton (1995) interpret their results as an advance during the Younger Dryas chronozone.

Records from the Magellan Straits and Torres del Paine record contrast notably with those from the Chilean Lake District, where there is no evidence of an event coincident with Advance E (Marden, 1997, Marden and Clapperton, 1995). This, together with the fact that in the Straits ice extended far further beyond its modern limits 4000 years later than it did in the Chilean Lake District, has probable implications in terms of spatial variation in palaeoprecipitation and palaeotemperature over Patagonia (Marden and Clapperton, 1995; Hulton *et al.*, 1994). The importance of palaeoprecipitation is also highlighted by Singer *et al.*, (2000) and Kaplan *et al.*, (2000). They suggest that latitudinal fluctuations in the positions of the Westerlies may determine the latitudinal variation in the strength of glacial signals. Such an explanation may explain the geomorphological absence of advance F in the Chilean Lake District if one accepts that the winds were in a more southerly location than they had been during advances D and E. However, it is also worth acknowledging that the more equatorward position on the Chilean Lake District would mean that it would have become increasingly difficult for ice caps to form during the overall LGIT warming at these lower latitudes, relative to more southerly locations in Patagonia.

Further north, Wenzens (1999) argues that data from the West of the Patagonian icesheet correlates with Advance F as documented in Marden (1997) and Marden and Clapperton (1995) (Table 2.2). He also proposes that the advance occurred potentially in response to a global Younger Dryas cooling event. Evidence for a Younger Dryas age advance in the Lago Argentino area is also cited by Strelin and Malagnino (2000). The investigation also records two prior LGIT advances, at > c.15.6 and 13.7 cal ka BP (13,000 and 11,800 ^{14}C yr BP), although he does not correlate these events to those in Torres del Paine and the Straits of Magellan. However, it may be argued that the sole reliance on ^{14}C minimum dates for

deglaciaition in such an arid area, which may have been exacerbated when the hydroscopic ice sheet was larger than it currently is, may produce young dates due to slow rates of accumulation and low levels of organic material production.

		Magellan Straits		Torres del Paine	Lago Argentino	To East of South Patagonian Icefield
Paper		Clapperton *et al* (1995)	McCulloch and Bentley (1998)	Marden (1997)	Strelin and Malagnino (2000)	Wenzens (1999)
ADVANCE	D	>19.7 cal ka BP (>15,800 ±200 ^{14}C yr BP) > 18 9 cal ka BP (>16,590 ±320^{14}C yr BP)	> 17 cal ka BP (>14,260 ± 350 ^{14}C yr BP) ((possibly 18.7 – 18 7 cal ka BP) (15,700-14,800^{14}C yr BP))		*> 15 6 cal ka BP (>13, 000±900 ^{14}C yr BP)*	
	E	18.9 cal ka - 13 8 cal ka BP (16,590 ±320 – 11,880^{14}C yr BP) (tentative suggestion)	15 3 – 11.5 cal ka BP (12,693±192 – 10,050 ±65^{14}C yr BP)	<15.3 >11.2 cal ka BP (< *c.*12,693±192 >9,755±95 ^{14}C yr BP)	*>13.7 cal ka BP (>11,100 ± 730 ^{14}C yr BP)*	
					> 12 3 cal ka BP (>10,390 ^{14}C yr BP) *(no error stated))*	
	F			<15.3 cal ka BP (< 12,010 ^{14}C yr BP) >10.3 cal ka BP (> 9180 ± 120 * ^{14}C yr BP)		>10.7 cal ka BP (>9,482 ±49 ^{14}C yr BP) >10.5 cal ka BP (>9,310 ±50 ^{14}C yr BP)

Table 2.2. Summary of the major LGIT glacier advances identified in field areas south of the Chilean Lake District. *= Data from Stern 1990, cited in Marden (1997, 66). Data in italics comes from research where there is no cross-reference to the nomenclature for advances in the Magellan Straits and Torres del Paine field areas (shown in column 1). For information on advances D,E &F refer to text.

2.4.1.2 Modelling Former Icesheets

Hulton *et al.* (1994) produced the first model of the former Patagonian ice-sheet and used it as a means of inferring the past climates. Based on several assumptions, the authors argued that the combination of a relatively small decrease in temperature of 3°C and a c. 5°N equatorward shift of the Westerlies during the LGM could be sufficient to have caused ice sheet growth. Specifically, an increase in precipitation was required at c.42°S and a decrease at c.50°S.

Subsequent work by Hulton *et al.*, (2002) has refined the first model, to produce a coupled ice sheet / climate model, with climate affected by changes in the ice sheet's size, distribution and altitude, as it waxes and wanes. This model produced the best fit at the LGM if temperatures were 6°C colder than today. Such a temperature depression is similar to suggestions based on pollen studies in the Chilean Lake District (Denton *et al.*, 1999 Moreno *et al.*, 1999). When simulations of deglaciation were run, the modelled ice extent accorded well with the present understanding of the region's deglaciation history, albeit under a simplified simulation of deglaciation as a response to a single step warming. The Northernmost sector (40-45°S), between the North of the Chilean Lake District and the North of the Chonos archipelago, was most sensitive to warming, whereas the central latitudes between 53-43 °S survived intact for several thousand years under a simulated 7°C rise before separating into two.

2.4.1.3 Pollen Studies

Much of the Chilean Lake District's evidence has been produced by Calvin Huessser (Heusser, 1983, Heusser *et al.*, 1996, 1999), Villagran (1988, 1990a, b) and more recently Moreno (Moreno *et al.*, 1997, 1999, 2001; Moreno and Leon, *in press*). Many of the palaeoecological sites that have been studied were ice-free during MIS-3 & 2 advances and thus records often extend back to before the LGM (eg. Heusser *et al.*, 1999). However, this section focuses on the climatic interpretations of change since the LGM. Locations of these studies are shown in Figure 2.12.

Within the Chilean Lake District, the pollen data tells a fairly consistent story of climate change. During the LGM, vegetation in ice-free areas indicates the region received much more precipitation than at present (Villagran, 1990; Heusser, 1983; Heusser *et al.*, 1999; Moreno, 1997). Temperature reconstructions based on pollen indicate that temperatures may have been "as much as 8°C" cooler than present (Heusser *et al.*, 1999, 279). Following the retreat of the ice from its Llanquihue LGM advance position, *Nothofagus* woodland expanded across the region in a step-wise manner between c.19 – 16.5 cal ka BP (16.4 – 14 ^{14}C ka BP) (Moreno and Leon, *in press*). Heusser *et al.*, (1996) argued that during deglaciation after the coldest part of the glacial maximum, several sites show further cooling events at c. 20.8 – 19.2 and c.18.3 -17 cal ka BP (17.5 -16.1 and 15.3-14.4 ^{14}C ka BP), within the overall warming occurring from 21.4 - 16.5 cal ka BP (18-14 ^{14}C yr BP). These proposals are inferred by fluctuating *Nothofagus* / Gramineae ratios, as shown in Figure

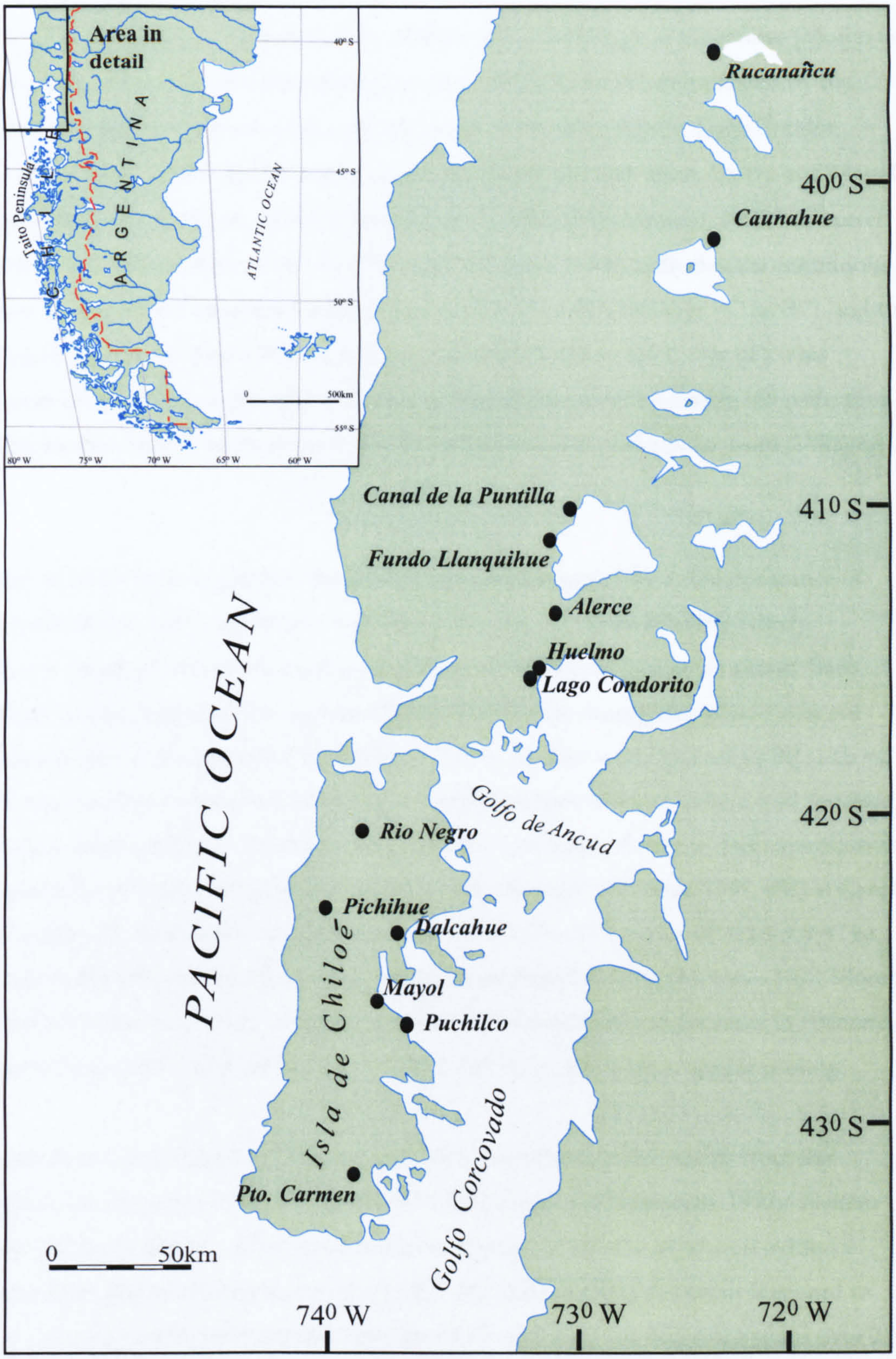

Figure 2.12 : Map of Chilean Lake District showing location of pollen study sites discussed in this chapter.

2.13. Similar fluctuations are indicated by shifts in the assemblage at other sites (Moreno *et al*, 1999). Climate remained wetter than present until 13 ^{14}C ka BP, as indicated by the presence of Magellanic Moorland taxa at sites such as Huelmo, Alerce, Lago Condor, Fundo Llanquihue, Canal de la Puntilla on the mainland and Dalcahue, Castro and Mayol on Chiloé (Moreno and Leon, *in press*; Heusser *et al.*, 1996, 1999; Moreno, 1997, Moreno *et al.*, 1999, 2001). Indeed, some work on Chiloé by Villagran (1988) indicates the continuous presence of Magellanic Moorland until at least c.21.4 cal ka BP (18000 yr ^{14}C ka BP), and the presence of certain moorland taxa until c. 8.0 cal ka BP (7,170 +- 120 C ^{14}yr BP). This increase in precipitation is thought to be due to the expansion and possible intensification of the Westerlies, due to an increase in sea ice and movement of the polar front (Villagran, 1990).

A switch to more xeric vegetation assemblage was accompanied by a disappearance of "high Andean Species" indicating a warming pulse at c. 13 ^{14}C yr BP, after which conditions remained consistent for the next 500 yrs (Moreno and Leon., *in press*). Both beetle and pollen data from the region indicate that climate during this period was not dissimilar to that of the present (Heusser *et al.*, 1996). At this point, 14.4 cal ka BP (12.5 ^{14}C ka BP), some authors argue that an expansion of *Podocarpus*, thought to be a cold resistant taxa, can be attributed to a climatic cooling (Moreno and Leon, *in press*). The expansion at "mid elevation of North Patagonian taxa with cool affinities" (Moreno, 1997, 498) at Canal de la Puntilla, Huelmo and Lago Condorito between 13.3 – 11.2 cal ka BP (11.4-9.8^{14}C ka BP) leads to the proposal of a second, Younger Dryas timed cooling (Moreno, 1997; Moreno *et al.*, 2001; Moreno and Leon, *in press*). Heusser (1984) associates an increase in *Podocarpus andinus* between 12.3 – 11.4 cal ka BP (10,440-10,000 ^{14}C yr BP) with a similar cooling.

The exception to this regional Chilean Lake District synthesis is the results from the Caunahue site (Heusser, 1981; Markgraf, 1991; Hoganson and Ashworth, 1992). Neither the two pollen studies nor the coleopteran investigation at the site produced evidence indicating any sort of cooling during the LGIT. If a LGIT cooling did occur it is hard to explain why it is not recorded at this site - the LGIT section of the sequence spans over 2 m, so there should be no issues due to a lack of resolution. It may be that the flora and fauna of the site was, for some reason, responding more to very local controls. However, the use of pollen as a proxy at Caunahue should have minimised such an effect.

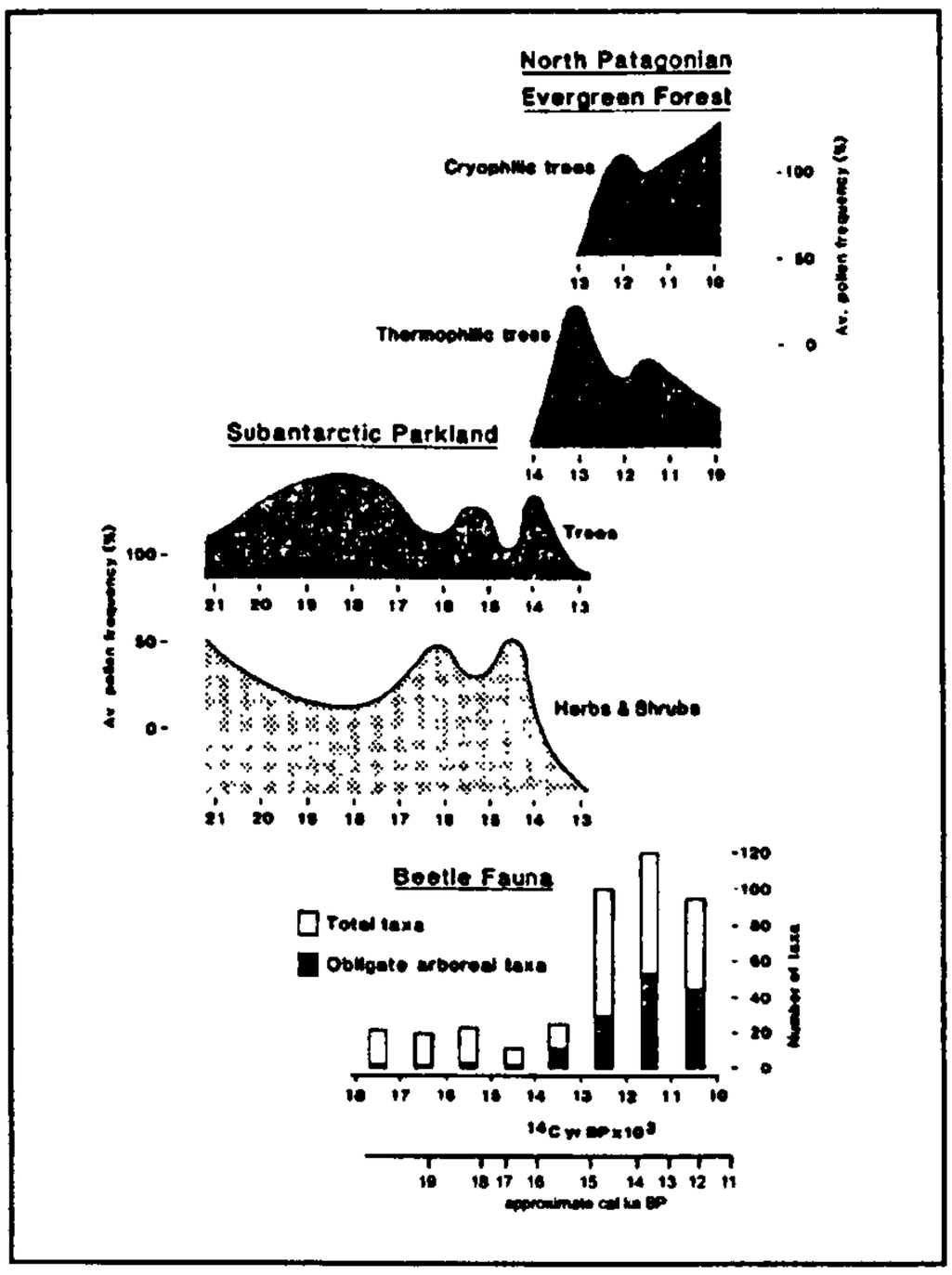

Figure 2.13: Records of fossil beetles (redrawn from Hoganson and Ashworth, 1992) and pollen (summarised and redrawn with modification from Lowell *et al.*, 1995) representing regional full-glacial Subantartic Parkland and late-glacial North Patagonian Evergreen Forest. Subantarctic Parkland consisted of open comminities of herbs and shrubs (mostly Gramineae and *Compositae)* with stands of trees (*Nothofagus* cf. *betuloides*) until about 14000 yr BP; later, close comminities of North Patagonian Evergreen Forest developed, at first containing relatively thermophylic trees (Myrtaceae, *Lomatia*, *Maytenus*, *Nothofagus* cf. *Dombeyi*) and after 13000-12000 until 10000yr BP, species that are more cryophylic (*Podocarpus nubigena*, *Pseudopanax laetevirens*) (Heusser *et al.*, 1996, 181).

N.B. Due to inherent difficulties associated with calibration ^{14}C ages into calibrated ages, dates on the calibrated age axis should just be taken as a guide.

The locations of other pollen studies in Patagonia, outside the Chilean Lake District, are show in Figure 2.14. The results of pollen analysis form one of the main lines of evidence in the multi-proxy study undertaken on cores from Lake Mascardi, Argentina (71°36W, 41°15S) (Ariztegui *et al.*, 1997). The investigation also incorporated particle grain size analysis, hydrogen index of the organic matter and chironomid analysis. Although the results of chironomid analysis were somewhat equivocal, the authors argued that the other lines of evidence inferred a cooling which started between 13.4-13.1 cal ka BP (11,500 and 11,200^{14}C yr BP) and ended at c. 13,450 - 11,550 cal yr BP (10,150 ± 80 ^{14}Cyr BP) (Ariztegui *et al.*, 1997; Hajdas *et al.*, 2003). The strongest line of evidence the authors use is the increase in particle size of the lake sediments, attributed to a glacial advance of the Tronador ice cap during this window. However, their evidence is unable to ascertain whether this is due to an increase in precipitation or a temperature cooling.

Pollen data from Fuego Patagonia has been predominantly undertaken by McCulloch (McCulloch, 1994; McCulloch and Davies, 2001), Heusser (1989, 1995, 1998; Heusser *et al.*, 2000) and Markgraf (1991, 1993; Pendall *et al.*, 2001). The site of Puerto del Hambre (53°36'21"S, 70° 55'53"W) has recently been investigated twice (Heusser *et al.*, 2000; McCulloch and Davies, 2001). Initial attempts to date deglaciation of the site were flawed because of the presence of reworked carbon in basal sediments (Heusser, 1999). Revised ages of *c.* 17.3 cal ka BP (>14, 455 ±115 or 14,470 ± 50 ^{14}C yr BP) for deglaciation of the site were later gained (dates from Heusser *et al*, 2000 and McCulloch and Davies, 2001, respectively). Both records show gradual warming up until *c.* 10.3 ka BP. McCulloch and Davies assess the climate to have been relatively humid between 17.3-15.3 cal ka BP (14.4 - 12.7 ^{14}C ka BP), indicated by an increase in wetland taxa. However, Heusser *et al.* (2000), infer an increase in aridity during this time frame from a lack of *Nothofagus* and an increase in *Empetrum*/Ericaceae presence (McCulloch and Davies, 2001). Between 15.3- 11.8 cal ka BP (12.8-10.3 ^{14}C ka BP) climate became cooler and drier. This time window correlates with a known glacial advance within the Straits of Magellan, to the west of the site. Heusser *et al.* (1999) argue that a return to a Gramineae-dominated assemblage between 12.9 -11.5 cal ka BP (11-10 ^{14}C ka BP) indicates a cooling, which he suggests was synchronous with the Younger Dryas. Heusser (1995) also suggests possible evidence for a Younger Dryas cooling shown as a slight increase in % Gramineae between 12.9 -11.5 cal ka BP at sites within Tierra del Fuego. Out of the three sites investigated to assess how the Steppe -

1. Lago Mascardi (Ariztegui *et al.*, 1997)
2. Puerto Harberton (Pendall *et al.*, 2001)
3. Puerto del Hambre (McCulloch and Davies, 2001, Heusser *et al.*, 2000)
4. Isla Dawson (McCulloch and Davies, 2001)
5. Puerto Eden, (Ashworth *et al.*, 1991)
6. Lapataia (Heusser and Rabassa, 1987; Heusser, 1998)
7. Punto Pinguinos (Heusser and Rabassa, 1987)
8. Chorillo Malo (Mancini, 2002)
9. La Mision (Markgraf, 1991)
10. Ushuiai (Heusser, 1998)
11. Coleta Robalo (Heusser, 1989)
12. Torres del Paine (Heusser, 1995)
13. Punta Arenas (Heusser, 1995)

Figure 2.14: Map showing the location of Patagonian palynological investigations outside the Chilean Lake District.

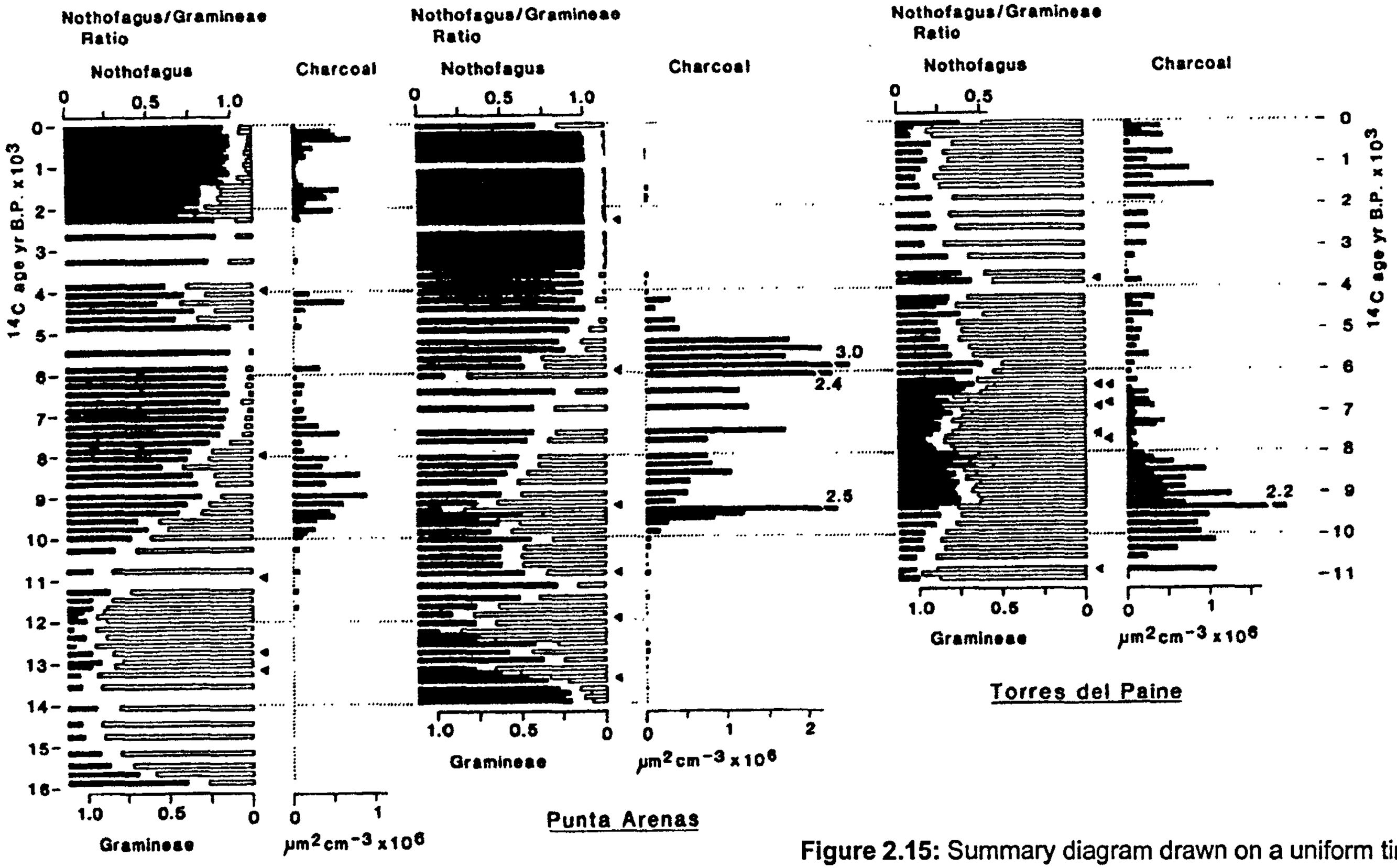

Figure 2.15: Summary diagram drawn on a uniform timescale of *Nothofagus*/Gramineae ratios shown in relation to charcoal concentrations at Puerto del Hambre, Punta Arenas and Torres del Paine. Arrows indicate the horizons of ^{14}C dates (Heusser 1995, 21).

deciduous forest ecotone boundary has shifted over time, this is best shown at the record from Punta Arenas (Figure 2.15) (Heusser, 1997).

Pendall *et al.,* (2001) augmented a 16 cal ka pollen record from Puerto Harberton in Fuego Patagonia (Markgraf 1993, 1991; Markgraf and Kenny, 1997) by reconstructing surface temperature and relative humidity through analysis of δD and $\delta^{13}C$ of cellulose of moss macrofossils, preserved within the peat archive. Figure 2.16 shows the main results of the investigation and comparisons against the δD records from the Taylor Dome and Byrd ice cores, Antarctica. Palaeovegetation and isotopic reconstructions mirrored each other well during the LGIT and mid Holocene, with periods of increased precipitation from c. 16-15 and 13-10.5 cal ka BP. These events were superimposed on an overall decrease in precipitation from the beginning of the record to present. When the δD record is compared against those from Antarctic ice-core records it shows greater accord with that from the more maritime record from Taylor Dome than the continental record from Byrd (Figure 2.16)

Long core analyses of 7 lake records from the Taitao Chonos region bear no evidence of a LGIT cooling event (Lumley, 1993; Lumley and Switsur, 1993; Bennett et al., 2000; Haberle and Bennett, in press; Massaferro et al., submitted). Figure 2.17 shows a typical pollen profile for the 4 cores that date back to the deglaciation of the sites. Minimum ^{14}C dates for glaciation of the sites yielded ages ranging from c.20.4 to 16.6 cal ka BP (17,205 ±185 to 13,820 ± 175 ^{14}C ka BP) after which the area was colonised by a "Empetrum heath-grassland mosaic" (Lumley, 1993, 229). Forest development began at or shortly after c. 16.5 cal ka BP (c.14 ^{14}C ka BP), featuring a succession from *N. Betuloides* and/or *N. Antarctica* assemblage to a more diverse *Nothofagus*, *Pilgerodendron uviferum* and Podocarpaceae forest composition. This succession is broadly similar to the modern latitudinal distribution. The taxa that currently extend furthest south, and are thus most tolerant of the cold, were the earliest to colonise the Taitao – Chonos region (Lumley, 1993). Within the Taitao-Chonos region, the area's vegetation was broadly similar to that of the present by the early Holocene (c. 9.5 ^{14}Cka BP). Throughout the LGIT there was no shift in taxa that can be interpreted as being representative of a climatic cooling, although the absence of charcoal and increase in *Pilgerodendron uviferum* in the record is interpreted to indicate more mesic conditions between c.14.5 - 11.9 cal ka BP.

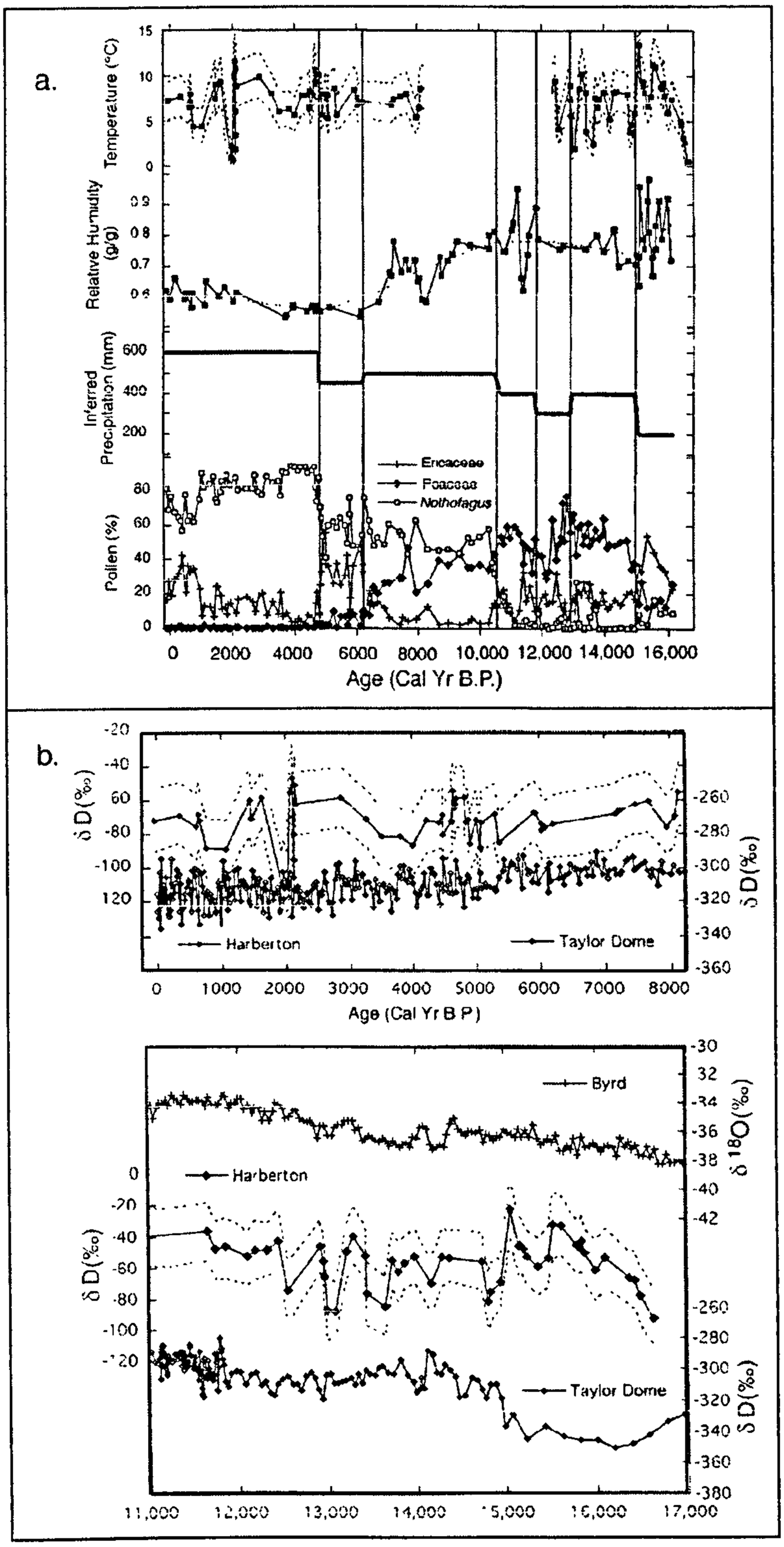

Figure 2.16: (a) Diagram showing selected results of pollen analysis (Ericaceae, Poaceae and *Nothofagus*) and δD of bog mosses from Puerto Harberton (after Pendall *et al.*, 2000).(b) δD of meteoric water, as inferred from δD of bog mosses, at Harberton plotted against isotopic records form Taylor Dome and Byrd. Methods of reconstructing temperature and humidity are explained in the reference, inferred precipitation is based on knowledge of modern relationship between vegetation and precipitation.

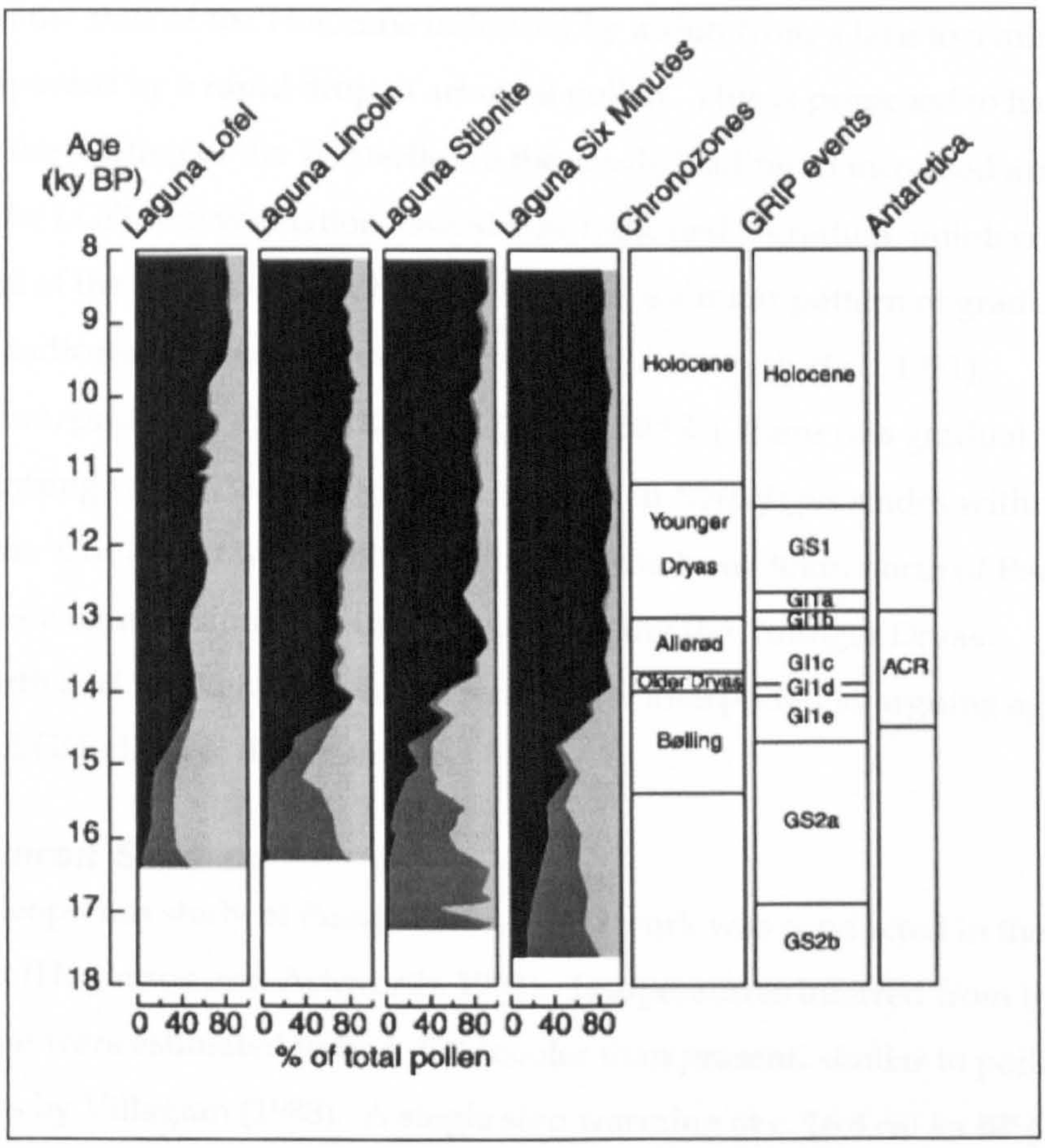

Figure 2.17 : Summary Pollen stratigraphy plotted against age (calibrated) below the water surface for each of four sequences of lake sediments in southern Chile. Black, pollen of trees; dark gray, pollen of herbs; light gray, spores of pteridophytes. Zonation schemes at right show chronozones, GRIP event stratigraphy and the ACR (Bennett *et al.*, 2000).

Between the Taitao and Fuego Patagonia, palaeoecological data are rather sparse (Figure 2.14). Studies at Cerro Atuad (Gilchrist, 2000) and Chorillo Malo (Mancini, 2002) used pollen data, whereas Ashworth *et al.* (1991) conducted a study combining pollen and coleoptera. The Cerro Ataud site lies to the West of the Andes, on one of the shorelines investigated by Turner (2002). The major signal highlighted at this site was a substantial increase in aridity at the start of the Holocene indicated by a shift from a lake to a mire environment accompanied by a rapid drop in arboreal pollen. This is proposed to have been in response to the shifting of the Westerlies to the south, leading to increased aridity at the site. During the LGIT, the vegetation assemblage indicated a gradual, uninterrupted warming. To the east of the Andes in the Chilean Channels, a similar pattern of gradual LGIT warming was indicated at records from Puerto Eden (Ashworth *et al.*, 1991). Following deglaciation, prior to c. 15.6 cal ka BP (12,960 ±150 ^{14}C), there was gradual and constant climate warming which caused a gradual increase in *Nothofagus* stades within the heathland vegetation. Combined with pollen and beetle data from 30km north of Puerto Eden, which indicates a climate similar to that of today during the Younger Dryas chronozone (Ashworth and Markgraf, 1989), the records are interpreted as arguing against the occurrence of an LGIT climatic deterioration.

2.4.1.4 Coleopteran Studies

In addition to the coleopteran study at Puerto Eden, beetle work was conducted in the Chilean Lake District (Hoganson and Ashworth, 1992). Temperatures inferred from the coleoptera assemblage were estimated to be 4 -5° C cooler than present, similar to pollen inferred temperatures by Villagran (1988). A single step warming at c. 16.8 cal ka BP (14 ^{14}C ka BP) meant that within 1500 years an open ground environment, similar to that currently found in Isla Chiloé, had been completely replaced by forest fauna. Between this step change and the beginning of the Holocene, there were no major shifts in the assemblage, leading the authors to infer that coleopteran evidence from the Chilean Lake District did not support the occurrence of a LGIT cooling. Unfortunately, the investigation of this site did not include analysis of Holocene deposits, thus no palaeoentomological data is available from environments post dating 10, 000 ± 280 14C yr BP.

2.4.1.5 Ocean cores

Alkenone sea-surface temperatures (SST's) reconstructions and terrigenous material analysis have been conducted on cores on the continental shelf, just off shore from

Valpariso (32°45'S, 72°02'W), approx 500km north of Puerto Montt (Kim *et al.*, 2002; Lamy *et al.*, 1999). During Oxygen Isotope Stage (OIS) 2/3 Kim *et al.* (2002) argue that artefacts of changes in ocean circulation caused by Heinrich Events were recorded in the cores, indicating the site's sensitivity to North Atlantic climatic events. Because the terrigenous mineral content and sediment characteristics at this site are inferred to act as a strong proxy of weathering and sediment provenance, they can be used to reconstruct palaeoprecipitation. Figure 2.18 illustrates the shifts in Westerlies, as inferred from these data, proposed by Lamy *et al.* (1999), combined with the SST reconstructions produced by Kim *et al.* (2002). Whilst the terrigenous sediment data shows a southerly shift in the Westerlies during the LGIT, alkenone results indicate the last termination occurred in 3 stages: 18.5-16.5, 15 and 13 cal kyr BP (Kim *et al.*, 2002). The start of the first warming was accompanied, and potentially partially driven, by a southward migration of the Westerlies, as inferred from the mineral content (Lamy *et al.* 1999). The authors argue that this correlates well with pollen evidence (Denton *et al.*, 1999a) and ice-core records (Thompson *et al.*, 1998) indicating the ocean and land are sensitive to the same forcings (Kim *et al*, 1999). The timing of second warming agrees with that of the Bølling / Allerød warming in the N. Atlantic and the most prominent warming within the Sajama ice core to the north in Bolivia (Thompson *et al.*, 1998). The authors found no event correlating to the third warming and thus inferred that it was a local, marine event. The record contains no LGIT cooling coeval with GS-1. However, a cooling event that started at 11 cal yr BP is recorded.

2.4.2 Holocene Change

2.4.2.1 Evidence for Neoglaciations in Patagonia

Mercer has conducted much of the work on neoglaciations in Patagonia (Aniya, 1995; Clapperton and Sugden, 1988). He proposed that evidence existed of three Patagonian neoglacial advances, reaching their maxima c. 4,600 – 4,200, 2,700 – 2,000 and the last during recent centuries (Mercer, 1984). Clapperton (1993) notes, however, that the chronology of these advances is based purely on minimum dates for events. Marden (1997) also notes the presence of at least two Holocene moraines in Torres del Paine, although no chronological constraints are placed on them. Several late Holocene (<3.6 ^{14}C kyr BP) advances have also been recorded in the area around current ice sheets (Anaya, 1995, 1996). However, work by Wenzens (1999) and Geyh and Röthlisberger (1986) suggests that

previous estimates have underestimated the number of Holocene glacial advances. They propose in excess of five advances. The lack of clarity in the current state of knowledge limits the palaeoclimatic inferences to be gained from Holocene glacial fluctuations.

2.4.2.2 Palaeolake levels in the Pampas

In Argentina, sedimentary and geomorphic evidence from Lago Cardiel (48.6°S 71.1°W) and Lake Cari Laufquen (41°35'S 69°25'W) have provided sound information on palaeoprecipitation regimes in Patagonia. At Lago Cardiel, the basin which the lake still fills, has beach ridges up to 60m above current shore lines. Dating of these, and associated deposits, has provided valuable palaeolake water level data. Figure 2.19 summarises the main fluctuations in lake levels of the last c. 30,000 years, constrained by ^{14}C dates. The most prominent finding being an early xeric Holocene dated to have begun between 11.5-8.8 cal ka BP (10 – 8,000 ^{14}ka BP), which is attributed to shifts in atmospheric circulation regimes associated with latitudinal movements of the Antarctic convergence position (Stine and Stine, 1990). However, in more recent research at the site this dry period was dated to have ended by 11.5 cal ka BP (Markgraf *et al.*, 2003). On the basis of the facies sedimentology and ostracod fauna, the record at Lake Cari Laufquen to the north of Cardiel indicates a shift from xeric to mesic conditions at c 13, 200 years (del Valle, 1991

cited in Whatley and Cuminsky, 1999, 236; Whatley and Cuminsky, 1999). These conditions persisted until some time during the Holocene period, when conditions became more arid causing a decrease in the size and diversity of the ostracod population and an increase in concentration of evaporite minerals. Whatley and Cuminsky (1999) argue that this is shows similar trends to pollen data from the site which indicate that mesic late-glacial conditions between 14.6 – 10.6 cal ka BP (12,500 – 9,500 ^{14}C yr BP) were followed by a dry early Holocene 10.6 – 7.4 cal ka BP (9,500 – 6,500 ^{14}C yr BP) (Garlef *et al.*, 1991 cited in Whatley and Cuminsky, 1999, 237). In the late Holocene, osctracods from the record indicate that a xeric environment continued, with aridity possibly increasing over this time period (Whatley and Cuminsky, 1999). This contrasts to evidence from Lago Cardiel, further south, where records indicate the climate from c. 10.6 - 6.9 cal ka BP (c. 9.5 – 6.1 ^{14}C ka BP) was wetter than the late LGIT (Markgraf *et al.*, 2003). Following this period, Markgraf *et al.*, (2003) argued for a drier late Holocene similar to that of today, with increased climate variability recorded from c. 5 cal ka BP to present. Evidence from both of

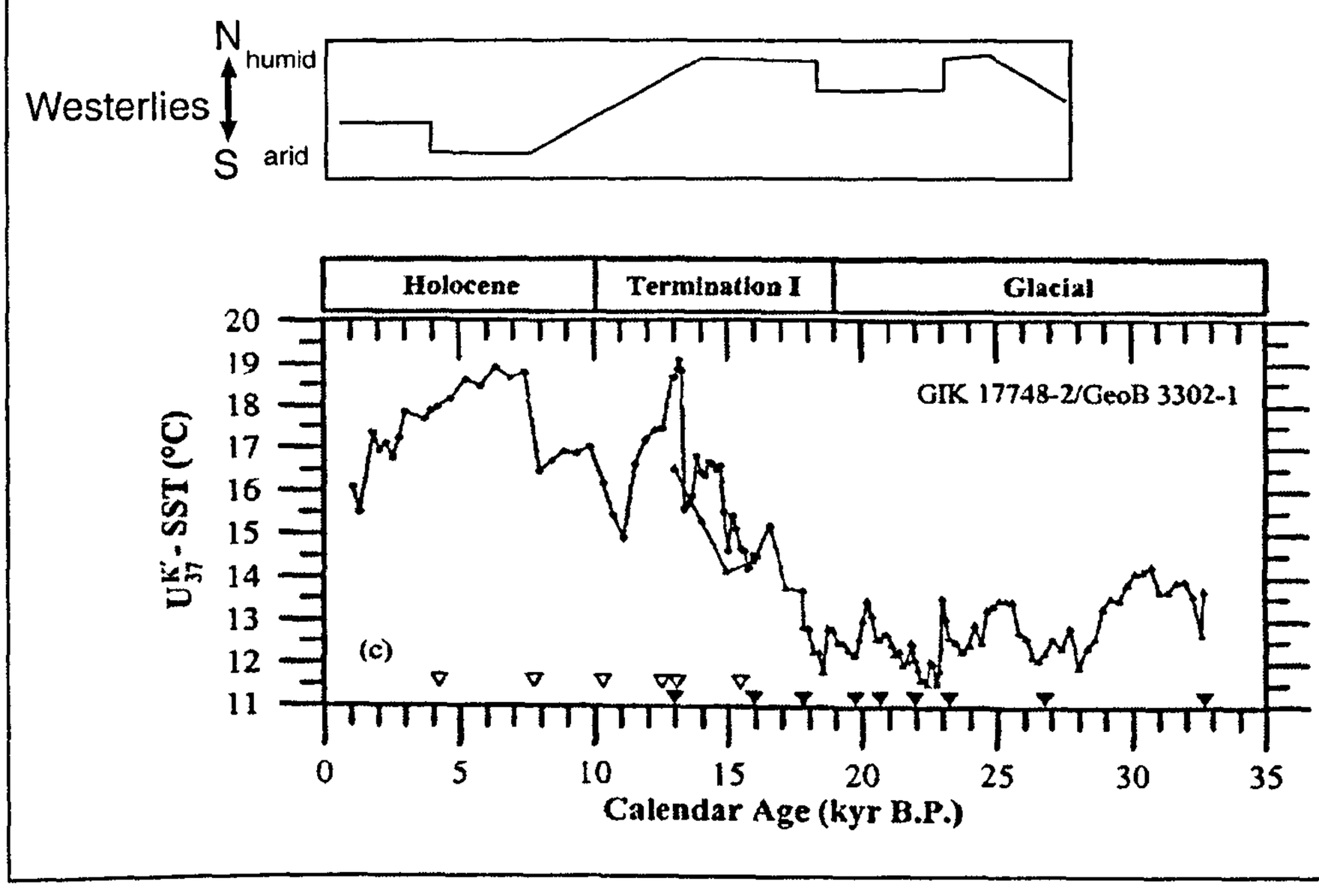

Figure 2.18: Reconstructed sea surface temperatures (Kim, *et al.*, 2002, 2089) and inferred shifts in the Westerlies (Lamy *et al.*, 1991, 91) based marine sediment cores from the continental slope off mid-latitude Chile (33°S, 72°W).

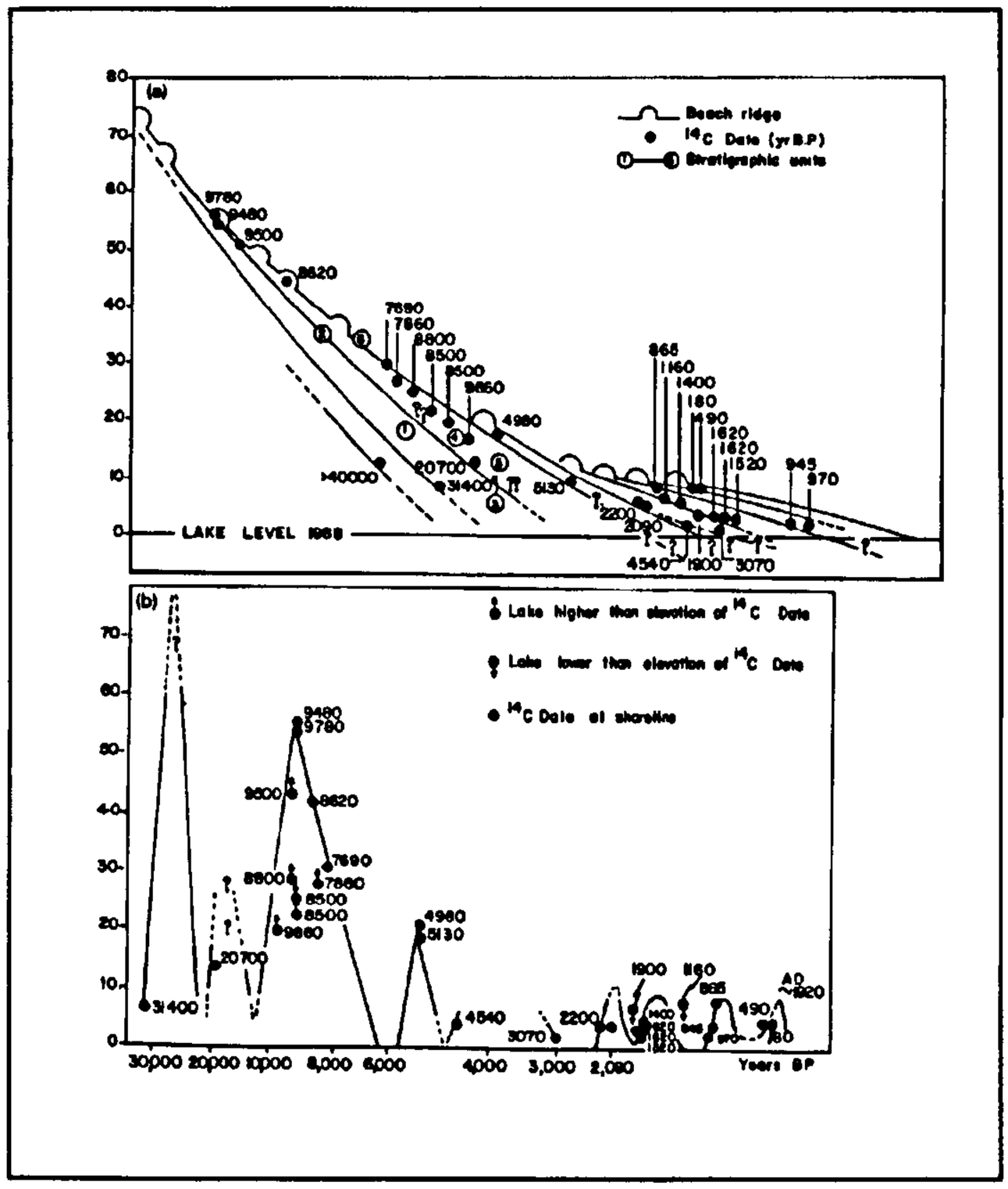

Figure 2.19 : Schematic curve of lake level fluctuations of Lago Cardiel during the last 31,000 years. (Stine and Stine, 1990, 705 & 707).

these lake records can be tied into the wider body of evidence suggesting that following a southerly shift in the Westerlies during the early Holocene, when both locations would become more xeric. However, whilst a more mesic late Holocene record at Cardiel fits with the hypothesis that the storm belts then returned north in the later Holocene, the ostracod data from Cari Laufquen seems to indicate that this atmospheric shift did not occur.

2.4.2.3 Pollen Analysis and Ocean Cores

Records from the Chilean Lake District indicate that the start of the Holocene saw substantial climatic re-organisations. Changes in the pollen assemblage indicate warming at 11.5 – 10.3 cal ka BP (10,000 and 9150 ^{14}C), and a shift from a gyttja to peats at 10.9 cal ka BP (9600^{14} C yr BP) at Huelmo indicates that precipitation decreased (Moreno and Leon, *in press*). Thermophylic taxa such as *N. obliqua* dominated the assemblage during the early Holocene until c.7.8 cal ka BP (6960 ± 120 ^{14}C yr BP), after which *N. Dombeyi* type dominates, peaking at c.3.4 cal ka BP (3,900 ± 140 ^{14}C yr BP), indicating cooler and wetter conditions which persisted to the present day (Heusser, 1984). These inferred climatic changes during the Holocene broadly correlate with composite interpretations from eight sites on Isla de Chiloé (Villagran, 1990; Abarzuá, 2004) which suggest that after becoming drier and warmer towards the mid-Holocene, levels of effective precipitation increased after c. 3,000BP. Heusser (1984) suggested that the cooler, more mesic late Holocene would provide conditions which could support glacial advances, as proposed by Mercer (1982, 1984) (2.4.2.1). Similar findings are found in sites in Argentina to the East of the Andes (Markgraf, 1983), with an increase in precipitation evident between 5,000 – 3,000 yr BP indicated by c. 90% arboreal pollen, after which Steppe taxa substantially increased indicating more xeric conditions.

At Puerto del Hambre in Fuego Patagonia the LGIT was followed by an extremely arid phase until 9.5 cal ka BP (8550 ^{14}C yr BP), at which point an increase in *Nothofagus* indicates an increase in moisture availability. This is due to a retreat in the size, and associated hydroscopic scouring of the ice-cap in the Andes to the west (McCulloch and Davies, 2001; Heusser *et al.*, 2000). Within the Holocene, there are further shifts in precipitation at various sites within Fuego Patagonia, although the timing of these shifts varies, possibly due to the variation in sites' proximities to the Atlantic Ocean and thus associated precipitation (Markgraf, 1993, 1991; Heusser, 1993, 1989). The major pattern seems to be that an early-

mid Holocene which was just wet enough to allow open arboreal growth prevailed. However, again precipitation increased in the mid Holocene, c. 4.5 – 5.7 cal ka BP (4-5 ^{14}C ka BP).

Within the Taitao - Chonos region, an arid early Holocene is indicated by the decrease in *Pilgerodendron uviferum* between c. 10 – 7 cal ka BP and an increase in charcoal accumulation rates (Haberle and Bennett, *in press*). Further palaeoenvironmental changes were proposed based on increased catchment erosion at sites on the Taitao during the later Holocene and a slight change in pollen that seems to be broadly synchronous with these events. Lumley (1993) proposes that an increase in aridity might be the driving factor. Although pollen records from the Chonos do not appear to support this hypothesis, with *Pilgerodendron uviferum* at higher relative abundances than the early Holocene, charcoal concentrations at Laguna Oprasa do increase slightly (Haberle and Lumley, *in press*). Thus records from the latter half of the Holocene may be recording both local and regional level palaeoenvironmental signals. The only stark disruption in the assemblage is during the Holocene, c.2.7 cal ka BP (c 2.6 ^{14}C yr BP), when *Pilgerodendron uviferum* virtually disappears from the record. The reasons for this switch in vegetation are unclear, although a plant pathogen or some link to the volcanic activity associated with a Hudson eruption (HW_6 – see Table 4.4) are possible reasons (Lumley, 1993). Chironomid analysis has subsequently been undertaken on two of the cores analysed for pollen within the studies mentioned above, Laguna Facil and Laguna Stibnite (Massaferro and Brooks, 2002, Massaferro *et al., submitted*). The results of these latter investigations are discussed in the next chapter.

To the west of the Andes at Puerto Eden, the climate was wetter than at present from c. 10.7-6.3 cal ka BP (9.5-5.5 ^{14}C ka BP), before becoming more arid between drier until 3.3 cal ka BP (3.0 ^{14}C ka BP). From 3.0ka BP the climate has been similar to that present today. To the East of the Andes at Cerro Attaud, early Holocene environments appeared xeric, with the site shifting from a lake to a mire and a sharp decrease in arboreal pollen. Arboreal pollen proportions do recover some time shortly before 7.5 cal ka BP, although ascertaining the exact timing of this decline and reestablishment of trees is difficult due to poor chronological control on the record. Another record to the West of the Andes from Chorillo Malo spans just the Holocene (Mancini, 2002). Climate at this site is interpreted to

have been wetter than at present during the beginning of the Holocene. At c. 9.5 cal ka BP (c.8.5 ka ^{14}C BP) there was a decrease in effective precipitation, followed by slight moistening in climate at c. 7.0 cal ka BP (c. 6.2 ^{14}C ka BP), with a further increase in effective precipitation from c. 3.8 – 0.9 cal ka BP (c.3.5 -1 ^{14}C ka BP). The author says that this latter pluvial phase may relate to neoglacial advances in the area (Mancini, 2002).

Ocean core evidence by Lamy *et al.* (1999) and Kim *et al.* (200) show a warming of 2°C at 10 cal ka BP, to temperatures similar to the present day and then a further warming pulse of 2.5°C at 8-7.5 cal ka BP. From this Holocene maximum, the temperature gradually declines to present day conditions.

2.5 Summary

This chapter has illustrated that Patagonia can play an important role in testing hypotheses relating to Late Quaternary climate change. Its location affords analysis which are key to understanding whether LGIT climate change was synchronous or if there was polar hemispheric asynchrony. However, evidence collected to date does not exclusively support one hypothesis. Following a widespread regional deglaciation at c. 17 cal ka BP, there is a substantial body of pollen and geomorphological evidence to suggest that some element of LGIT synchroneity with Northern Atlantic events exists, particularly in the northern parts of Patagonia (Deton *et al.*, 1999a, Moreno *et al.*, 2001). Further to the South, glacial advances also span the period of the ACR and thus indicate events may have been synchronous with the Antarctic region. Other investigations have shown no evidence of any sub-Milankovitch scale variability during this period (Ashworth and Hoganson, 1991; Bennett *et al.*, 2000). Unambiguous temperature inferences on the basis of glacial and pollen evidence is prohibited as precipitation associated with the location of the polar front and accompanying Westerlies is understood to have shifted latitudinally during the first half of the LGIT. Palaeoecological studies indicate that Holocene climate change has also been significantly effected by changes in the latitude of the Westerlies, particularly in the former half. Temperature may also have fluctuated during the Holocene. However, assessing to what extent records are documenting temperature versus these shifts in precipitation is difficult. Nonetheless, the combination of precipitation and temperature conditions contributed to several neoglacial advances in the latter half of the Holocene (Mercer, 1982).

Therefore, much scope still exists for improving our understanding of Late Quaternary climate in Chile. The complex interplay between precipitation and temperature in this region means that the capacity of reconstructions based on glacial fluctuations and pollen is stretched. Thus, the use of a complementary proxy such as chironomid analysis, which has been demonstrated to be able to deliver accurate quantitative temperature reconstructions, could be helpful.

3 Chironomids and their application as a palaeoecological proxy

3.1 Introduction

The family Chironomidae belongs to the order of two-winged flies, named Diptera, but members of the family are colloquially known as "non-biting midges". The life cycle of these insects is almost exclusively associated with water, as the vast majority of the insects' larvae live in aquatic biotopes. The larval stage inhabits marine, lentic, lotic and also, although less frequently, terrestrial environments. In addition to this range of habitats, the family has a wide geographical distribution due to its ability to survive extreme conditions in terms of salinity, temperature and water availability (Pinder, 1986; Cranston, 1995a).

This chapter reviews the biology, ecology and systematics of the family. This sets the context for discussing how chironomids have been used as bioindicators in the classification of lake trophic status. The application of chironomids as a palaeoecological proxy for assessing changes in trophic status is then reviewed. The development of the proxy and its use as an often quantitative palaeoenvironmental technique in reconstructions of both temperature and other palaeoenvironmental conditions is then discussed. Finally there is an examination of their use in Patagonian palaeoecological records, supplementing the regional palaeoenvironmental research discussed in Chapter 2.

3.2 The Biology and Ecology of Chironomidae

The life cycle of chironomids is holometabolous, in that during their life cycle each individual passes through 4 stages: egg, larva, pupa and imago (winged, sexually mature adult) (Figure 3.1). In temperate climates, the number of generations that occur per year, the voltinity, varies between one and four. However, there is evidence of a seven year life cycle from the *Chironomus* genus in Alaska, indicating that Nearctic taxa from high latitudes may have longer life cycles (Pinder, 1986). Such a negative correlation between habitat temperature and voltinity is often the case with aquatic insects (Ward, 1992).

EGG
Laid in egg mass, usually containing 20 - 30 eggs
Stage lasts for 2.5 - 6 days
170µm x70µm - 612µm -153µm

LARVA
4 instar stages occupied
Up to 30mm in length
Feed on algae, woody debris, detritus, macrophytes, invertebrates

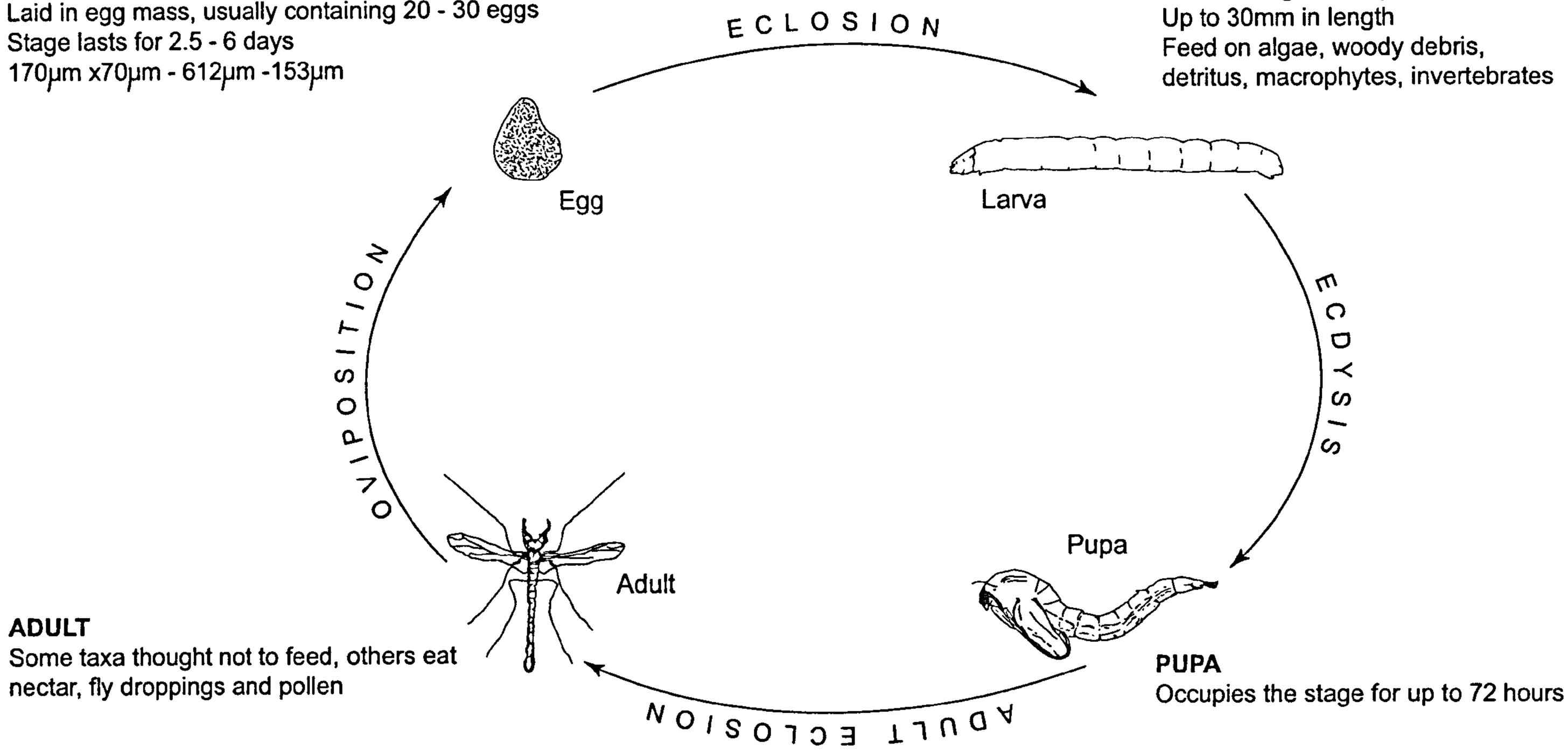

Figure 3.1: Diagram showing Chironomidae life cycle and associated information

3.2.1 Egg : oviposition to eclosion

Although they can be laid separately, the adult females usually lay eggs in egg-masses, containing between 20-3300 eggs (Pinder, 1995a). Sites suitable for oviposition vary from firm substrata close to water, to the water surface itself (Pinder, 1995a). The eggs, between 170µm and 612µm along their longest axis, are made of cytoplasm and deutoplasm, or yolk (Richards and Davies, 1977). As they are insects, chironomids are pokilotherms. That is to say their metabolic rate, and therefore the speed of growth and development, is related to ambient temperature (Speight *et al.*, 1999). Initial estimates of the duration of egg development of 2.5 - 6 days are thought to be have been an oversimplification and do not account for the strong positive effect of temperature on the rate of embryonic development (Pinder, 1995a).

3.2.2 Larva : eclosion to final ecdysis

When ready to hatch, the egg ruptures and the protolarva within the egg 'ecloses' to become a larva. The larval stage is particularly critical in the organism's development and survival as it occupies the vast majority of its life (Oliver, 1981). Within the larval stage, chironomids occupy 4 sub-stages, termed instars. As they develop, the larvae shed their cuticle and head capsules between each instar, in a process called ecdysis. Significant differences in morphology and behaviour of the first instar, relative to that of the latter three, has resulted in the first stage often being termed 'larvula' (Pinder, 1995a). Morphologically, major differences in the mentum, shape of the head capsule and antennae have been recorded in the first instar, and it is also believed that they often posses an enhanced ability to swim relative to later instars (Pinder, 1995a).

Chironomid larvae occupy a wide variety of habitats and exhibit a diverse range of feeding behaviour. Habitats vary from damp soils and films of water, to lakes and rivers, to intertidal and marine conditions. Although some chironomids live in the open, swimming in aquatic environments, research has indicated that most taxa, except carnivorous Tanypodinae, occupy tubes which they construct from material such as algae and leaf litter (Pinder, 1995b). This strategy is thought to minimise the likelihood of dislodgement of larvae by currents and decreases the risk of predation. It also aids respiration, especially during periods of reduced dissolved oxygen (DO) (Pinder, 1995b). In addition to these benefits, the shape of tubes is believed to be related to feeding techniques employed. For

example larvae constructing 'U' shaped tubes are often primarily filter feeders (Berg, 1995). The diet of larvae can encompass algae, detritus and associated organisms, macrophytes, woody debris and invertebrates (Pinder, 1986).

3.2.3 Pupa: final ecdysis to emergence

Relatively little is known about the pupal stage due to its short duration, usually less than 72 hours, and the opaque sheath within which the metamorphosis takes place during this period (Pinder, 1986). The pupal stage commences when the final instar sheds its larval suit during the final ecdysis phase. The fact that certain elements of the adult anatomy have already started to develop during the pupal stage is reflected in the fact that morphologically the pupa is more similar to the adult than the larva. When fully developed, the pupa rises to the surface of the water through a combination of enhanced levels of air absorption and pupal movement. In most cases the adult then emerges leaving the pupal exuviae on the water surface. However in certain taxa, parthenogenesis occasionally occurs. This involves the eclosion process halting when the pupal cephalothorax starts to split. The adult then lays eggs, which absorb water and swell to eventually cause the pupal cephalothorax to rupture. This effectively allows reproduction to take place underwater and without the need for fertilization of the eggs or for full eclosion of the adult that has laid them (Langton, 1995).

3.2.4 Imago: emergence to oviposition

The imago, or adult or reproductive, stage of the midge is also relatively short, lasting between a few days to a couple of weeks (Pinder, 1986). The actual timing of emergence appears not to be random; at a seasonal scale it is mainly affected by the ecological controls on the larvae. On a shorter temporal scale, there are also daily cycles controlled by light intensity and/or water temperature. Protandry, where males emerge just before females to enhance mating success, has also been observed (Armitage, 1995). Although initially doubted, it is now thought that adult chironomids do feed, selecting foods such as fresh fly droppings, pollen and nectar. In order to mate, the adult males usually swarm. Swarms can range in number less than 20 insects to hundreds and are usually almost exclusively composed of male insects, usually from one species. Having entered a swarm and been fertilized the female will then fly away and deposit the fertilized egg mass (Armitage, 1995).

3.3 Chironomid systematics and taxonomic diversity and general faunal biogeographic terms

According to nomenclature governed by International Commission of Zoolological Nomencalture (ICZN) (1985, cited in Cranston, 1995c, 32), biological classification within the family is as follows:

- Superfamily: Chironomoidea
- Family: Chironomidae
- Subfamily:Chironominae
- Tribe: Chironomini
- Genus: *Chironomus*
- Species: *Chironomus plumosus*

Within the family there are 10 subfamilies, with 355 proposed genera (Ashe, 1983 cited in Cranston, 1995b, 3) and estimates of between 10,000 and 15, 000 species (Cranston, 1995b, 2).

Zoologists have divided the world into six biogeographic regions based on the work of Sclater (1858) and Wallace (1880) (both cited in Huggett, 1998, 10). This system of spatial, biogeographic classification, shown Figure 3.2, is still in common use today. Although generally unsupported in terms of biogeographical evidence, proposed modifications that the Palaearctic and Nearctic were in fact one large realm, lead to the creation of the term 'Holarctic' to refer to the two realms collectively (Spellerberg and Sawyer, 1999). As is the case with much entomology, the majority of both ecological and palaeoecological research into Chironomid taxonomy (eg. Wiederholm, 1993; Rieradevall and Brooks, 2001) and distribution has been conducted within the Holarctic realms (Walker, 2001; Porinchu and McDonald, 2003). However, there are notable exceptions from this overall pattern. The work of Brundin (1966, 1988) made not only a great contribution to the knowledge of extra-Holarctic chironomid biogeography, but also provided valuable information supporting the principle of vicariance. Vicariance is the process by which biogeographical distribution over areas that are now disjunct, and thus separated by barriers such as seas, mountains or deserts, are explained using the rationale that the now disjunct areas were at one time linked (Briggs, 1987). Thus the theory does not cite dispersal as the primary driving force

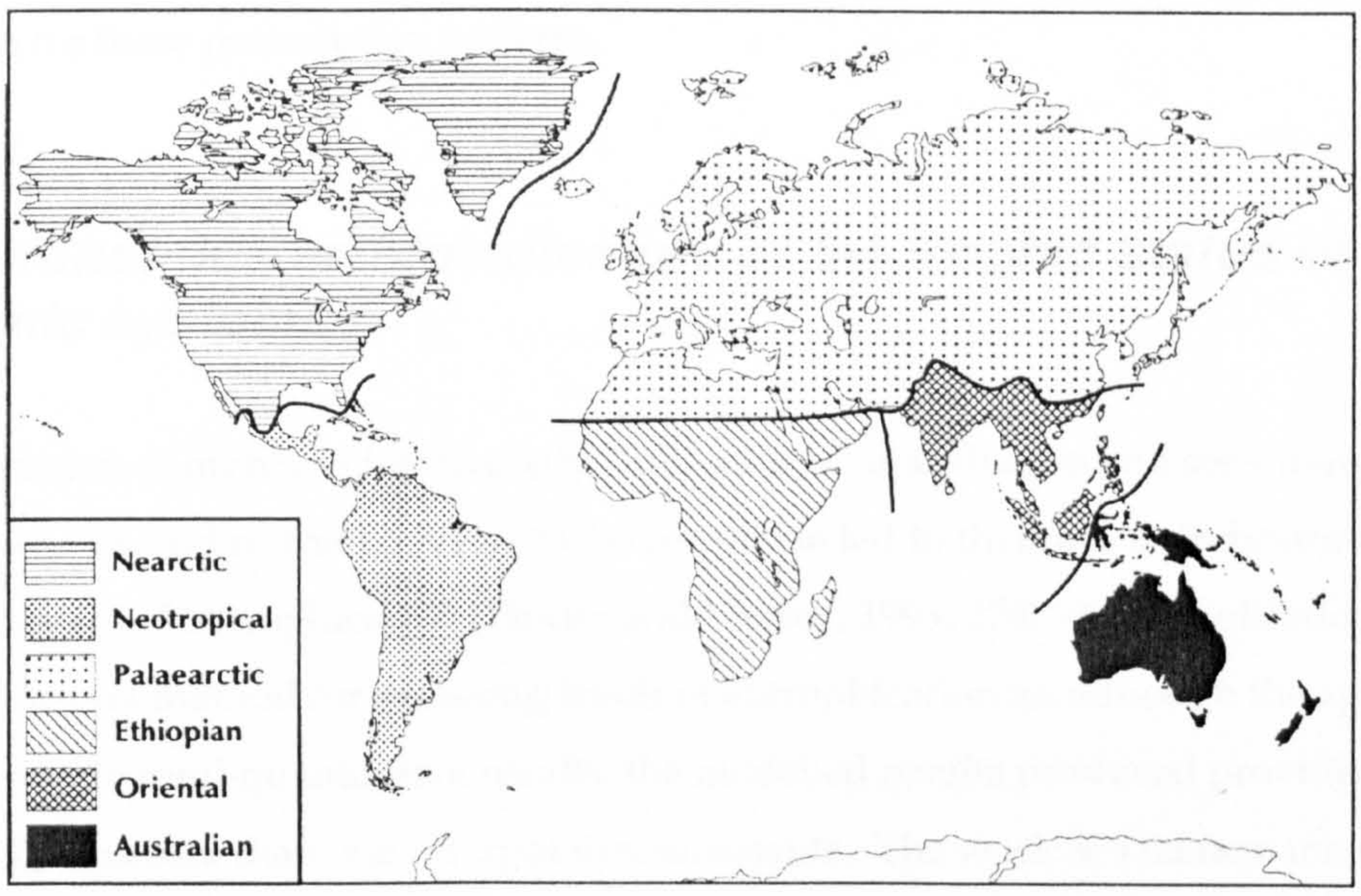

Figure 3.2 : The Sclater and Wallace classification of faunal regions (after Smith (1983) in Hugget, 1998, 11)

responsible for the creation of disjunct distributions. Brundin's record of different taxa almost exclusively within New Zealand, South America, South Africa and Australia showed how regions that are now separated by sizable biogeographic barriers held a common genetic heritage. He argued that these findings indicated a common population between the land masses when they were linked as Gondwana during the mid to later Jurassic, c. 188 – 120 my BP. Different levels of similarities between the now disjunct, or geographically separated, populations were argued to be due to populations becoming separated at different times as Gondwana broke up between 120-80 my BP to form the southern continents (Cranston, 1991). More recently, the work of Cranston (1997, 1999, 2000) in the Neotropical, Ethiopian and Australian regions has made notable contributions to furthering our knowledge of current taxonomic distribution and the cladistics responsible for these present-day patterns.

3.4 Chironomids as bioindicators of the trophic status of limnic systems

The combination of high species diversity, "ubiquitous" distribution and sensitivity to dissolved oxygen and nutrient levels of Chironomidae led to their use as indicators of lake quality and level of eutrophication (Pinder and Morley, 1995, 274). This application provided a useful method for assessing levels of eutrophication as, although the approach can only provide semi-quantitative results, the modelled results produced provided a more representative picture than one off, spot measurements. The work of Thienemann (1915, cited in Pinder and Morley 1995, 276), Brundin (1949, cited in Lindegaard, 1995, 386; 1958), Lundbeck (1936, cited in Ward, 1992, 92) and Saether (1979) produced a classification of lakes according to their trophic status using their chironomid population (see Pinder and Morley, 1995 and Ward, 1992 for reviews). This system was later expanded to allow the categorisation of limnic systems into one of 15 lake types (5 oligotrophic, 3 mesotrophic and 5 eutrophic) (Saether, 1979). A simplified version of these classifications is given in Table 3.1.

The system applies to stratified lakes, as it is based on the profundal element of the midge assemblage (Lindegaard, 1995). This is because, the hypolimnic oxygen availability which is influenced by nutrient availability, will be one of the main limiting factors on the

profundal taxa present. Therefore the assemblage is affected by the extent of hypolimnetic dissolved oxygen (DO), which then acts as a proxy of nutrient concentrations of the lake (Hofmann, 1988). Taxa found in the profundal, deoxygenated element of eutrophic lakes, such members of the *Chironomus* genus, are able to withstand relative anoxic conditions due to high levels of haemoglobin in their body fluids. The availability of food, which

Lake Type, trophic level	Indicator chironomids Europe	Indicator chironomids North America
Ultraoligotrophic	*Heterotrissocladius subpilosus* Brundin	*Heterotrissocladius oliveri* Saether
Oligotrophic	*Tanytarsus lugens* Kieffer with *Heterotrissocladius grimshawi* (Edwards) and *H. scutellatus* (Goetghebuer)	*Tanytarsus* sp. with: *Monodiamesa tuberculata* Saether and *Heterotrissocladius changi* Saether
Mesotrophic	*Stictochironomus rosenschoeldi* (Zetterstedt) and *Sergenita coracina* (Zetterstedt)	*Chironomus atritibia* Malloch and *Sergentia coracina*
Moderately eutrophic	*Chironomus anthracinus* Zetterstedt	*Chironomus decorus* Johannsen
Strongly eutrophic	*Chironomus plumosus* L.	*Chironomus plumosus*
Dystrophic	*Chironomus tenuistylus* Brundin with *Zalutschia zalutschicola* Lipina	*Chironomus* sp. *Zalutschia zalutschicola*

Table 3.1: Lake classification based on the profundal chironomid fauna (from Brundin, 1949, 1958; Saether, 1975, Wiederholm, 1984a) (Lindegaard, 1995, 386).

is also heavily affected by levels of primary productivity, is also believed to be a factor in determining the profundal assemblage (Warwick, 1980). In food rich, eutrophic systems larvae are often tube dwellers whereas relatively food-poor oligotrophic systems are often occupied by free swimming taxa such as *Procladius* that are able to be more proactive in seeking food (Lindegaard, 1995; Wiederholm, 1984). However, work by Schmäh (1993) highlights the contribution of sediment, and associated sub-fossil midge remains, from the littoral zone to sediment samples taken from beneath the hypolimnion, due to sediment focusing. Thus the subfossil midge content of sediment lying below the hypolimnion will also contain an element of littoral taxa. This latter study also indicated that a sample taken at a deep enough point may contain predominantly littoral assemblages, as anoxia above a critical level prohibits even the most anoxia-tolerant taxa.

Brundin (1958, 291) argued that, based on field work in the Chilean and Argentinean Lake Districts, the use of profundal chironomid fauna as bioindicators for lake trophic classification held "world-wide validity". However, within the context of this investigation, it is useful to note that application of this method of classification was problematic in Australia and New Zealand (Timms, 1978; Forsyth, 1978). Within the Northern Hemisphere, problems were also encountered applying it in Finland, partially because of the absence of a few of the key indicator species (Kansanen *et al.*, 1984). Some work has indicated that chironomids from littoral sediments may be useful as indicators of trophic status (Brodin, 1982). However the structure and ecological conditions of this environment and the associated taxonomic relationships are a lot more complex, and thus harder to predict (Lotter *et al.*, 1998). Therefore, at present, this approach still requires further development.

3.5 Chironomids as a proxy in palaeolimnology

Although chironomid analysis was used prior to the late 20th Century (eg. Stahl, 1969), it is only recently that the technique has gained prominent popularity as a palaeoecological technique. Within contemporary palaeolimnology, chironomid analysis is often thought to be one of the "promising biological" methods in palaeoecology (Battarbee, 2000, 107).

The attributes that make chironomids strong indicators of environmental change are outlined by Brooks (1995, 2003) as follows:

- Taxa are often stenotopic with narrow ecological tolerances and optima;
- Their larvae inhabit almost all aquatic systems;
- They are one of the most abundant benthic macroinvertebrates in freshwater systems;
- The heavily chitinized head capsules are well preserved in lake sediments and can be identified to genus, if not species level;
- A species-rich fauna means that the population should be sensitive to different types of changes in the environment;

- Chironomid larvae inhabit the lake and are therefore *in situ* indicators and truly reflect the limnic palaeoenvironment, as opposed to a proxy such as pollen which comes from outside the lake system;
- Rapid generation time and the adults' ability to fly means that they can migrate quickly in response to environmental forcing;

In c. 15-20 years of mainstream use, the use of chironomids has undergone a major revolution though, with an increased emphasis on the production of quantitative palaeoecological reconstructions from midge records.

3.5.1 Chironomids : Qualitative reconstructions

The traditional application of chironomids as bioindicators means that many of their qualitative applications have been as palaeoecological proxies to assess levels of eutrophication. Wiederholm and Eriksson (1979) demonstrated a link between the profundal midge fauna of a Swedish lake and eutrophication due to intensification in the land-use in the area. Taxa such as *Micropsectra* and *Phaenopsectra* were replaced by *Chironomus* as land cultivation increased, as did the local population. Ilyashuk and Ilyashuk (2001) argued that changes in the assemblage in a record from a high latitude lake in Russia showed evidence of heavy metal pollution, as well as eutrophication. They also argued that the most modern samples (post 1982 ± 2) possibly showed the impact of global warming through the decrease of cold indicator species, although such an interpretation must be viewed with caution as it was based only on the top two sub samples analysed. As well as changes in the taxonomic assemblage, factors such as decreasing concentration and deformities (Lami *et al.*, 1994; Nazarova, personal communication) of head capsules have been used as indicators of anthropogenic impacts on lake systems. However, 19th and 20th Century industrial activity is not the only impact to have left its mark in the chironomid record. Anthropogenic effects of earlier cultures, such as indigenous tribes in North America, were also indicated by faunal assemblages in the Bay of Quinte, Lake Ontario (Warwick, 1980) whilst chironomid assemblages from New England, USA, indicate that early settler agricultural practices changed the midge assemblage (Francis and Foster, 2001).

The potential of chironomids as bioindicators of acidification has been demonstrated by Brodin and Gransberg (1993). Changes in the fauna at the Round Loch of Glenhead, Scotland, were coeval with shifts in the diatom linked to changes in pH. However, in general it was the minor taxa that appeared to be sensitive to these changes, with none of the twelve most common taxa appearing to be sensitive to acidification. This lead the authors to conclude that, although midge assemblages are sensitive to shifts in pH, changes in trophic status may be more influential.

Hoffman (1998) has also indicated the potential of chironomids as indicators of palaeohydrology. Changes in the ratio of pelagic: littoral taxa in the cladoceran (water flea) and chironomid assemblage of cores were used to demonstrate that changes in water levels could be detected in the chironomid record. Chironomids have also been shown to indicate the influence of former drainage channels using multivariate analysis of the fossil assemblages to assess the relative influence of lentic and lotic taxa in the fauna preserved in the limnic record (Rück *et al.*, 1998). However, the findings of Walker and McDonald (1989b) should be born in mind, as his work across an altitudinal gradient indicated that the assemblage of an arctic, shallow lake may contain similar taxa to that found in a shallow arctic/alpine lake because of the cold conditions within the profundal element of the latter.

3.5.2 Chironomids and temperature: qualitative to quantitative postdictions

One of the periods of palaeoclimate that has received most attention from Quaternary entomologists investigating palaeotemperature is the LGIT. Before records from ice-cores elucidated the frequency and magnitude of temperature change during this transition, coleopteran studies which used mutual climatic range (MCR) methods had suggested that these rapid changes in temperature had occurred (Coope, 1977).

Many chironomid palaeoclimatic investigations have also focused on the LGIT. However, in the absence of quantitative, modern ecological knowledge of the insects' environments, the records produced can only be qualitative or semi-quantitative in nature. Nonetheless, records from Switzerland, Scotland, Western Canada and Norway have been confidently

interpreted using qualitative knowledge of modern ecology (Hofmann, 2001; Brooks, 1997; Brooks *et al.*, 1997a, 1997b). Semi quantitative methods such as classification of taxa as "cold", "warm" or exhibiting "weak thermal response" have been employed (Walker and Mathewes, 1987). Such interpretations appear to have been successful, within the confines of their semi-quantitative potential, with many detecting high frequency temperature change correlating to Northern Hemisphere ice core data. For example, regional climatic trends, such as the "Younger Dryas", were evident in four Swiss lake records analysed, despite evidence of other more local, site-specific controls, such as lake level fluctuations, indicated by changes in the faunal assemblage (Brooks, 2000, 276).

Much evidence suggests that temperature is one of the major controls over chironomid distribution (Rossaro, 1991). It was not until the 1990s that the extent to which this relationship could be exploited in palaeoclimatological studies was realised. As with many organisms, the extent of the influence of different environmental controls on chironomid assemblages seemed to be unclear. Substrate, DOC, salinity, pH and nutrients as well as temperature had all been proposed as at least partially controlling factors (see Pinder, 1986 for review).

The application of canonical correspondence analyses (CCA), allowed the extent of the effect of temperature on assemblages to be quantified and this relationship to then be exploited to reconstruct palaeotemperatures (ter Braak, 1986). The pioneering investigation of this type to use midges was based on a training set of 33 lakes from Labrador, Canada (Walker *et al.*, 1991). As indicated in Figure 3.3, the environmental variables of summer surface-water temperature and lake depth were most closely correlated to CCA axis 1 ($\lambda = 0.261$), with r values of 0.79 and 0.77, respectively. These quantitative results were further supported by a similar transition of species along an altitudinal gradient to that along the first axis when chironomid taxa within the training set were ordinated (Walker and Mathewes, 1989a). To test the apparent temperature - taxonomic assemblage relationship statistically, the model was used to predict the temperature of all the lakes within the training set, providing a root-mean-square-error of prediction (RMSEP) of 1.32°C and an $r^2_{(jack)}$ value of 0.79. This encouraging result indicated that the relationship between the midge taxa and temperature was sufficiently strong to use for reconstructing temperature.

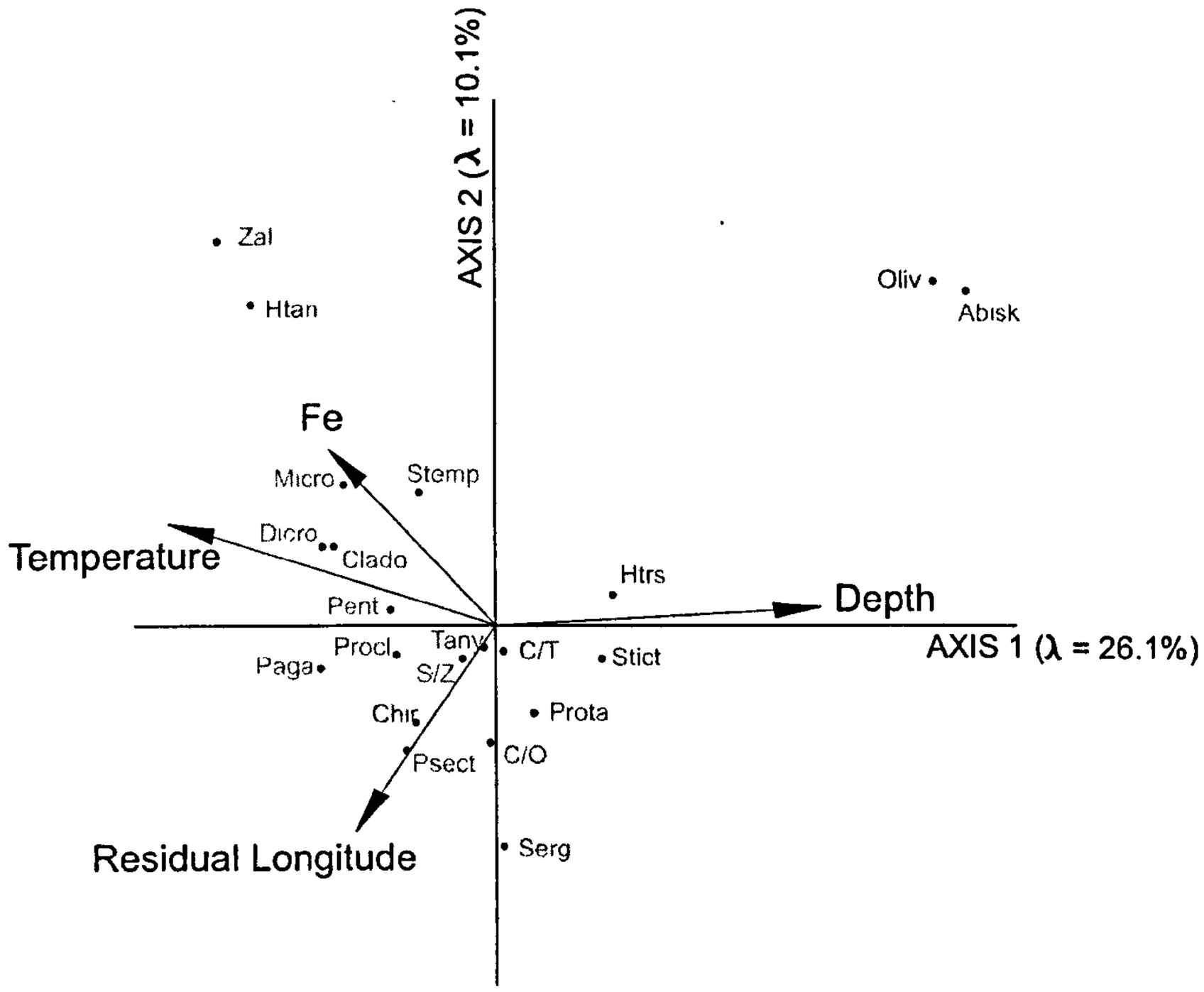

Abisk = *Abiskomyia*
Chir = *Chironomus*
C/O = *Cricotopus / Orthocladius*
C / T = *Corynoneura / Thienemanniella*
Clado = *Cladopelma*
Dicro = *Dicrotendipes*
Htan = *Heterotanytarsus*
Htrs = *Heterotrissocladius*
Micro = *Microtendipes*
Oliv = *Oliveridia*
Paga = *Pagastiella*
Petn = Tribe Pentaneurini
Procl = *Procladius*
Prota = *Protanypus*
Psect = *Psecrocladius*
S/Z = Stempellinella / Zalrelia
Serg = *Sergentia*
Stecit = *Stictochironomus*
Tany = *Tanytarsus* s. lat
Zal = *Zalutschia*

Figure 3.3 : Ordination of chironomid taxa and environmental variables in Labrador, Canada (Walker *et al.*, 1991).

This East Canadian model was subsequently augmented by adding further lakes to increase the temperature range of the training set and the use of more sophisticated statistical analysis of the modern data (Levesque *et al.*, 1993; Walker *et al.*, 1997). Figure 3.4 summarises the development of this transfer function over the 1990s. Reassessment of the model during expansion of the data set illustrates the importance of maximising the temperature gradient and the larger bias inherent during the initial versions of the model (Figure 3.4). This series of models has since been applied numerous times to records from the area to demonstrate the high frequency and amplitude of climate change along Eastern sea board Canada during the LGIT (eg. Mayle and Cwynar, 1995; Wilson *et al.*, 1993); the results of selected studies are included in Figure 3.4. Furthermore, it was argued that the precision of the reconstructions was sufficient to detect contemporary inter-site differences in temperature, leading to the detection of a north-south temperature gradient during stadials of the LGIT (Levesque *et al.*, 1996). More recent work has also been conducted within British Columbia, western Canada, to assess temperature change during the very end of the LGIT and the Holocene using a different training set (Palmer *et al.*, 2002) (Table 3.2). The authors noted a positive correlation between temperature and species richness at three sites. This association has also been indicated in other studies (Levesque *et al.* 1997; Brooks, 1997).

Encouraging results from the initial Canadian training set has lead to further quantitative investigations of temperature – chironomid relationships in other regions in the Northern Hemisphere: the Swiss Alps (Lotter *et al.*, 1997), Norway (Brooks and Birks, 2000a), Finland (Olander *et al.*, 1999) and Northern Sweden (Larocque *et al.*, 2001). Table 3.2 outlines the parameters and predictive power of the models produced from these investigations. In addition to these individual investigations, two independent training sets from Eastern Canada and Europe were combined to investigate the effect of merging training sets (Lotter *et al.*, 1999) (Table 3.2). The model from the combined data sets was similar to both of the original two in terms of its predictive power and results. However, when the Canadian transfer function was used to try and predict the temperature of European training set sites, and *vice versa*, the result was poorer than that produced by the combined transfer function. This suggests caution should be taken when assuming that modern ecological information data from one region is representative and transferable to another at a

Original **Walker *et al.* (1991) model**
Based on 24 original training set sites (red).
Estimates on 15 additional sites shown (purple).
Model uses classical deshrinking without tolerance down-weighting.

Wilson *et al.* (1993) model
Based on 34 training set sites (red).
Estimates on 5 additional sites shown (purple).
Model uses classical deshrinking without tolerance down-weighting.

Levesque *et al.* (1997) model
Based on 39 training set sites.
Model uses classical deshrinking and tolerance down-weighting.

Walker *et al.* (1997) model
Based on 39 training set sites.
2 component WA-PLS model uses classical deshrinking and tolerance down-weighting.
Model based on square-root transformed temperature data.

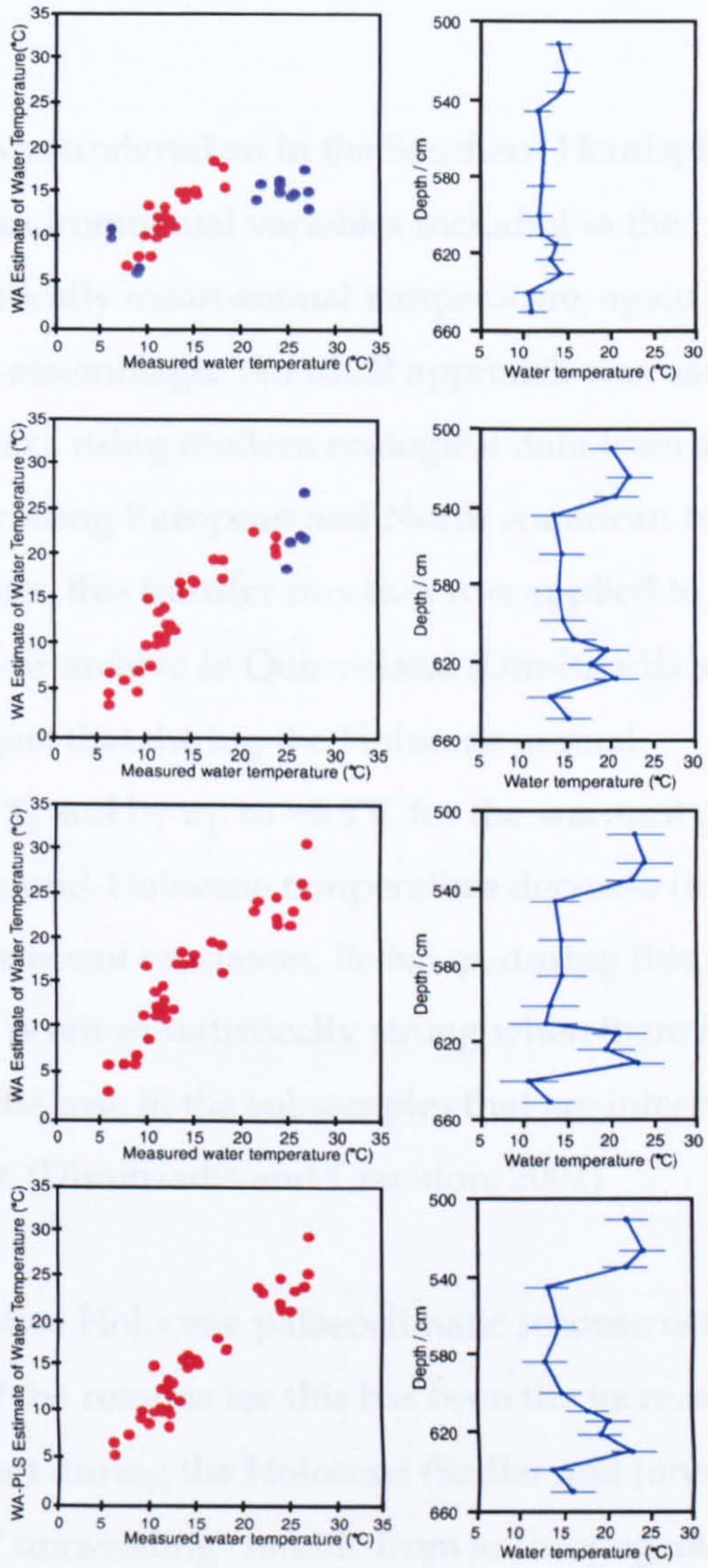

Figure 3.4 : Diagram showing development of the Canadian chironomid based temperature transfer function and its application to a constant data set from Splan Pond, New Brunswick (based on Walker *et al.*,1997).

The diagram summarises the parameters of the model, use of the model to predict water temperature of lakes within the training set (red) and application to samples collected after that version of the model was produced (purple). Temperature reconstructions are marked with model version specific standard errors.

biogeographic regional scale. Table 3.2 also demonstrates the improvements that have been made in the Norwegian training set. These refinements were produced by improving the methods by which sites' air temperatures were modelled and extending the temperature gradient to allow calculation of more accurate thermal optima for taxa at the periphery of the thermal range (Brooks and Birks, 2001).

Recently, the first investigation of this sort was undertaken in the Southern Hemisphere. In this Australian investigation, out of the 16 environmental variables included in the correspondence analysis, temperature, specifically mean annual temperature, again proved to be the most dominant in determining the assemblage. An MCR approach was used to ascertain the temperature tolerances of the taxa using modern ecological data from a variety of surveys. Whereas most of the preceding European and North American transfer functions had been applied to LGIT sequences, this transfer function was applied to a Holocene record from a tropical volcanic maar archive in Queensland (Dimitriadis and Cranston, 2001). These reconstructions suggest that during the Holocene annual temperatures fluctuated by as much as ~2.5°C and by up to ~6.6°C for the warmest quarter of the year. However, the magnitude of this mid-Holocene temperature decrease (to ~6.6°C) is predominantly driven by the presence of one taxon, *Rethia sp*, during this period. It is acknowledged that the MCR technique is not as statistically strong when there is a low abundance and low species diversity, as is the case in the subsamples that are interpreted to be colder due to the presence of *Rethia sp.* (Dimitriadis and Cranston, 2001).

Production of both qualitative and quantitative Holocene palaeoclimatic reconstructions using midges has been problematic. One of the reasons for this has been the increased impact of human activity on the environment during the Holocene (Sadler and Jones, 1995). A strategy to address the problem of unravelling climatic from anthropogenic signals has been to focus on lakes where human impact has been minimal, as Pellatt *et al.*, (1998) did in Canada. A further problem of poor early Holocene analogues was encountered by Rosén *et al.* (2001) within their study in northern Sweden. Indeed at this site and nearby site of Sjuodjijaure, sample-specific errors throughout the Holocene were higher in quantitative temperature reconstructions based on midges than those derived from diatom and pollen records from the same site (Rosén *et al.*, 2001; Bigler *et al.*, 2002).

Publication	Location	No of lakes	No. of taxa	Range of Temperature (°C)	Nature of temperature assessment	WA-PLS Components	RMSEP (°C)	R^2
Walker *et al.* (1991)	Eastern Canada	26	21	10.4	SSWT	1	1 32*	0.79*
Lotter *et al.* (1997)	Swiss Alps	50	58	6 4	SAT	1	1 370*	0.84*
Walker *et al.* (1997)	Eastern Canada	39	32	21	SSWT	2	2.26*	0.88*
Lotter *et al.* (1999)	Swiss Alps	51	40	13.4	July air temp	1	1.526*	0.832*
Lotter *et al.* (1999)	Eastern Canada	39	51	14	July air temp	3	1.599*	0.842*
Olander *et al.* (1999)	Finland	53	38	6 4	July air temp	2	0.497*	0.866*
Brooks and Birks (2000a)	Western Norway	44	32	11 4	July air temp	1	1 13*	0.69*
	Western Norway	44	32	8 3	SSWT	1	2 22*	0.30*
Brooks and Birks, 2001	Western Norway	109	119	12 1	July air temp	3	0.94	0.90
	Western Norway	111	119	22.7	SSWT	3	2.13*	0.86*
Hieri *et al.* (2003b)	Switzerland	81	76	11.5	July air temp	2	1.51*	0.81*
Palmer *et al* (2002)	Western Canada	51	NS	13 2	July air Temp	2	1.98*	0.70*
Korhola *et al* , 2002	Fennoscandia	62	52	5.9	July air Temp	NA	0.80	NA
Larocque *et al.* (2001)	Northern Sweden	100	48	7 7	July air temp	2	1.130*	0.64*
Lotter *et al.* (1999)	Swiss alps and Eastern Canada	90	57	16	July air temp	1	1.822*	0.792*

Table 3.2 : Comparison of the performance statistics between different quantitative chironomid-based temperature transfer functions

Number of lakes and taxa refer to numbers included in the transfer function after exclusion of rare taxa and outlying lakes from the initial training set

SSWT = summer surface water temperature, SAT= summer air temperature, NS = Not stated

Furthermore, Brooks (2004) and Rosén *et al.* (2003) have advised caution in the application of midges as a proxy for quantitative Holocene palaeotemperature reconstruction, simply because Holocene temperature changes themselves are small in magnitude relative to those reconstructed for the LGIT. Recent work by Korhola *et al.*, (2002) has attempted to address this issue by using a Bayesian modelling approach as opposed to the more routine Weighted Averaging Partial Least Squares (WAPLS) methods. Based on Root Mean Squared Error of Prediction (RMSEP) values, this produced a more accurate prediction, although reconstructions through the Holocene were consistently c. 1°C cooler using the Bayesian technique. As the authors point out, there is no absolute way to assess which is the more accurate of the models, but improved RMSEP results indicate that this may be a promising technique for future applications.

3.5.3 Issues facing the quantitative use of chironomids

The results displayed in **Table 3.2** highlight the issue of how temperature should be assessed and measured in order to obtain the most precise and accurate results when models are used for postdiction. Earlier investigations were generally conducted using measured water temperatures (Walker, 1991). However, as was highlighted by Hann *et al.* (1992), the use of such 'spot' measurements is problematic as it requires the assumption that these measurements are sufficiently representative of the lake temperature in general. Recent work has favoured the use of correlation with summer, often July, air temperatures. Indeed, investigations that have independently compared correspondence analysis of taxonomic data against Summer Surface Water Temperature (SSWT) and July air temperature have suggested the latter produces better predictions (Brooks and Birks, 2000a). Although this debate has been highly significant within the chironomid research community, it is also relevant to those using other techniques. There has been investigation to assess the viability of using organisms such as diatoms and cladocera as proxies of temperature (Lotter *et al.*, 1997). However, an essential distinction exists between these latter proxies and chironomids in that only three of the 4 four stages of chironomids' lives inhabit an aquatic environment where as, conversely, many other palaeolimnological proxies solely live in the lentic environment. Therefore air temperature may be more important in chironomid investigations as it directly affects the adult stage and thus their dispersal (Brooks and Birks, 2000a). However, in some conditions, particularly at high altitudes or latitudes, glacial fed lakes or lakes where ice cover persists for much of the year, there may be a marked discrepancy between the two measures. This issue is well exemplified by Birks and Brooks (2001), where two glacially fed lakes were outlying sites (Figure 3.5). Deletion of these sites from the July air temperature transfer function improved the RMSEP from 1.14 to 0.90 and r^2(jack) from 0.91 to 0.94.

Detailed research was conducted on the Swiss Plateau to assess the representivity of air temperature as a proxy for water temperature. A strong link was found between the air temperature and epilimnetic temperature to the extent that interannual variations in air temperature were reflected in surface water temperatures. However, theoretical analysis suggests that this coupling should decrease towards the poles as the limiting, minimum temperature of 0°C for lake water does not apply for air temperature (Straškraba, 1993).

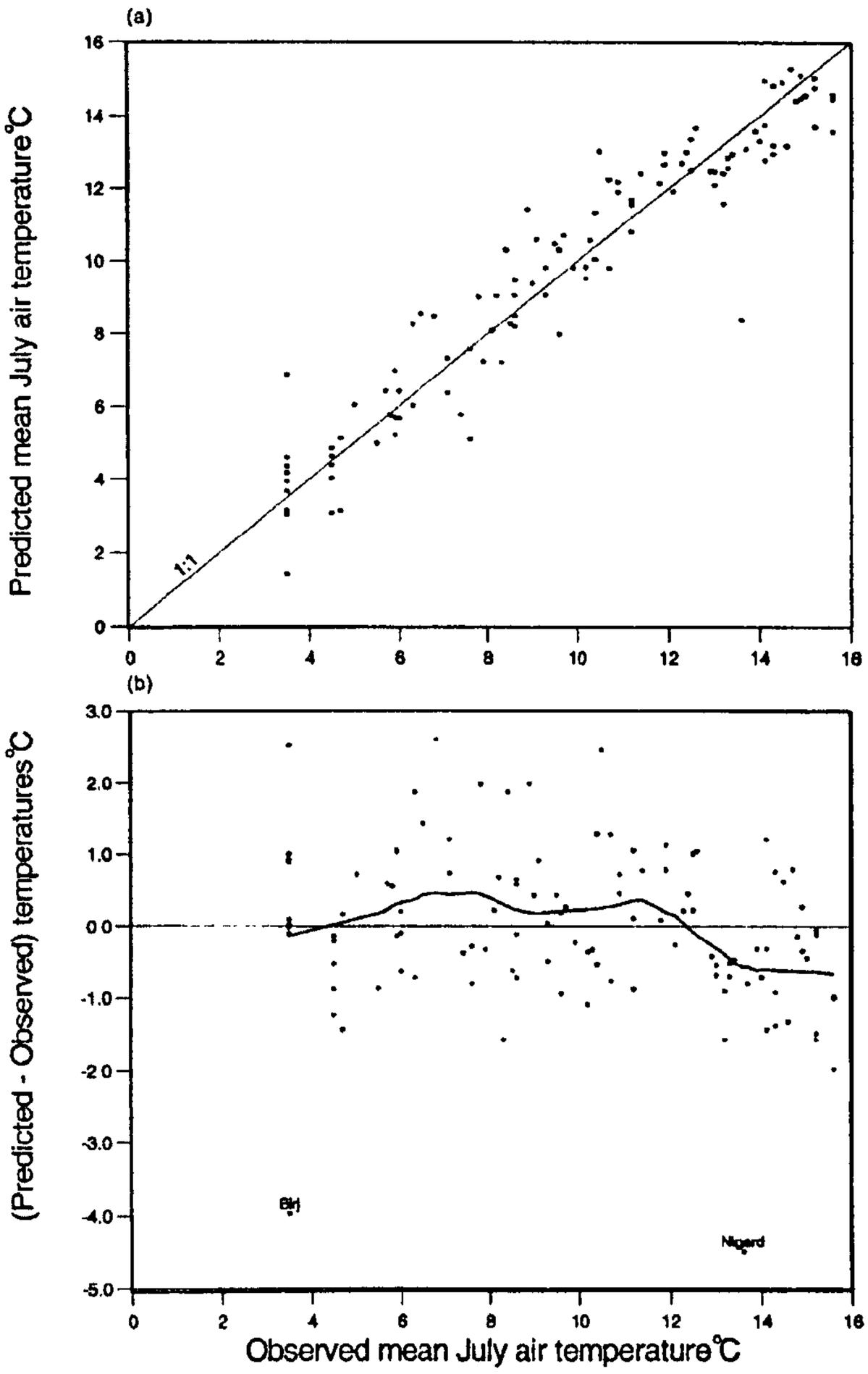

Figure 3.5 : Predicted chironomid-inferred mean July air temperatures using a 2 component WA-PLS model based on leave-one-out cross-validation plotted against observed mean July air temperature in 111 Norwegian lakes. The solid line shows a 1:1 relationship. (b) Residual (predicted - observed) temperatures plotted against observed mean July temperature. The thick solid line is a LOESS smoother (span = 0.35) (Cleveland, 1993) fit. The two 'outlying' lakes are labelled in plot (b) (Brooks and Birks, 2001, 1729)

Livingstone and Lotter (1998) concluded that temperatures derived from altitude-corrected air temperature models appear to be a more accurate assessment of water temperatures than would be achieved by one-off surface water measurements. Although not surprising, these findings have advantages and disadvantages for those wanting to produce of further chironomid training sets. Modelled air temperature is a variable which affects all four stages of development, as opposed to only the first three as is the case with water temperature, and therefore is arguably more appropriate. However, the modelling approach holds problems to those wanting to develop training sets in geographical regions where meteorological data are limited.

Although the often strong correlations found between temperature and midge assemblage has proved encouraging to palaeoclimatologists, Brodersen and Anderson (2002) advocate caution in the use of midges to reconstruct temperature without assessing the possible impact of correlated variables. Their study of 47 lakes from Greenland indicated that although the midge fauna found at sites was closely related to the temperatures, both datasets also correlated with nutrient data from the sites. Such a relationship can be responsible for the occurrence of taxa which are considered to be thermophylic in freshly deglaciated lakes (eg. Velle *submitted*, a) due to increased nutrient loading in the first few years of evolution (Engstrom *et al.*, 2000). This study is not the only one to highlight the potential issues caused by multicollinearity within environmental datasets (Birks, 1995). For example, Larocque *et al.* (2001) highlighted the need to compare temperature reconstructions with loss on ignition (LOI) measurements to try and assess if the latter control is driving faunal shifts. Such studies highlight the importance of a lake's catchment and the associated impact on the fauna, emphasising the idea that the lentic system cannot be considered in isolation from its surroundings (Velle *et al., submitted* a.; Kling, 2001).

Another issue to have recently received quantitative investigation is the minimum count number or 'cut level' suitable for temperature reconstructions using chironomids. Early research into palaeotemperatures using chironomids used a minimum count level of c. 40-50 head capsules (eg Hoffman, 1986; Walker *et al.*, 1984, 1991a), although counts in some investigations have often been much higher (eg. Brooks and Birks, 2001). In general, chironomid cut levels are much smaller than those used in pollen and diatom analysis, and this is partially justified by both the lower biodiversity and the long time involved in

chironomid sample preparation. The extent to which a sub-sample of subfossil head capsules is representative of the true assemblage increases as count sizes increase. A logical extension of this argument is that errors associated with reconstructed temperatures will decrease as the count size increases. However, within quantitative reconstructions, small down-core sample sizes appeared to produce reasonable results (Walker *et al.*, 1997). Recent statistical investigation of a suitable sub-fossil count level has indicated that, in the majority of cases, there is a minimum increase in precision gained when count levels exceed 50 (Figure 3.6) (Larocque, 2001; Heiri and Lotter, 2001; Quinlan and Smol, 2001). However, as even larger counts sizes produce greater consistency and repeatability, Larocque (2001) advocated using a cut level of 90 where head capsule concentration allowed. Additionally, application of these higher counts appears to reduce the issue of poor analogues for down-core assemblages in the modern day dataset (Heiri, *et al.*, 2003a; Rosén *et al.* 2003). Although such similar representivity issues exist within sub sampling of modern samples in training set production, the accuracy of the transfer functions produced can be statistically assessed using cross validation methods such as bootstrapping or jack-knifing (Heiri and Lotter, 2001).

The final issue that has received recent investigation is the possible over or underestimation of taxa resulting from counting all the head capsules found, irrespective of the instar involved. The chitinised head capsules from the first, second and third head instars are potentially stored in lake sediments, although those from the first and second instars may not be preserved due to insufficient levels of chitin (Brooks, 1995). Although they do sometime sink to the lake floor, fourth instar head capsules are sometimes retained by the pupal exuviae and frequently blown to shore (Brooks, *personal communication*). Carter (2001) investigated how results differed depending on whether only second, third and fourth instars, or all head capsules present, were counted. Her findings suggested that relative abundances of taxa were not affected by counting all the head capsules present. However if absolute deposition rates of head capsules is integral to the research questions being addressed, then distinction between different instar stages is necessary.

3.5.4 Other quantitative reconstructions

In addition to the production of the temperature transfer function outlined above, efforts have also been made to develop chironomid transfer functions for nutrients, specifically Total Phosphorous (TP) (Lotter *et al.* 1998; Brooks *et al.*, 2001), chlorophyll a (Brodersen and

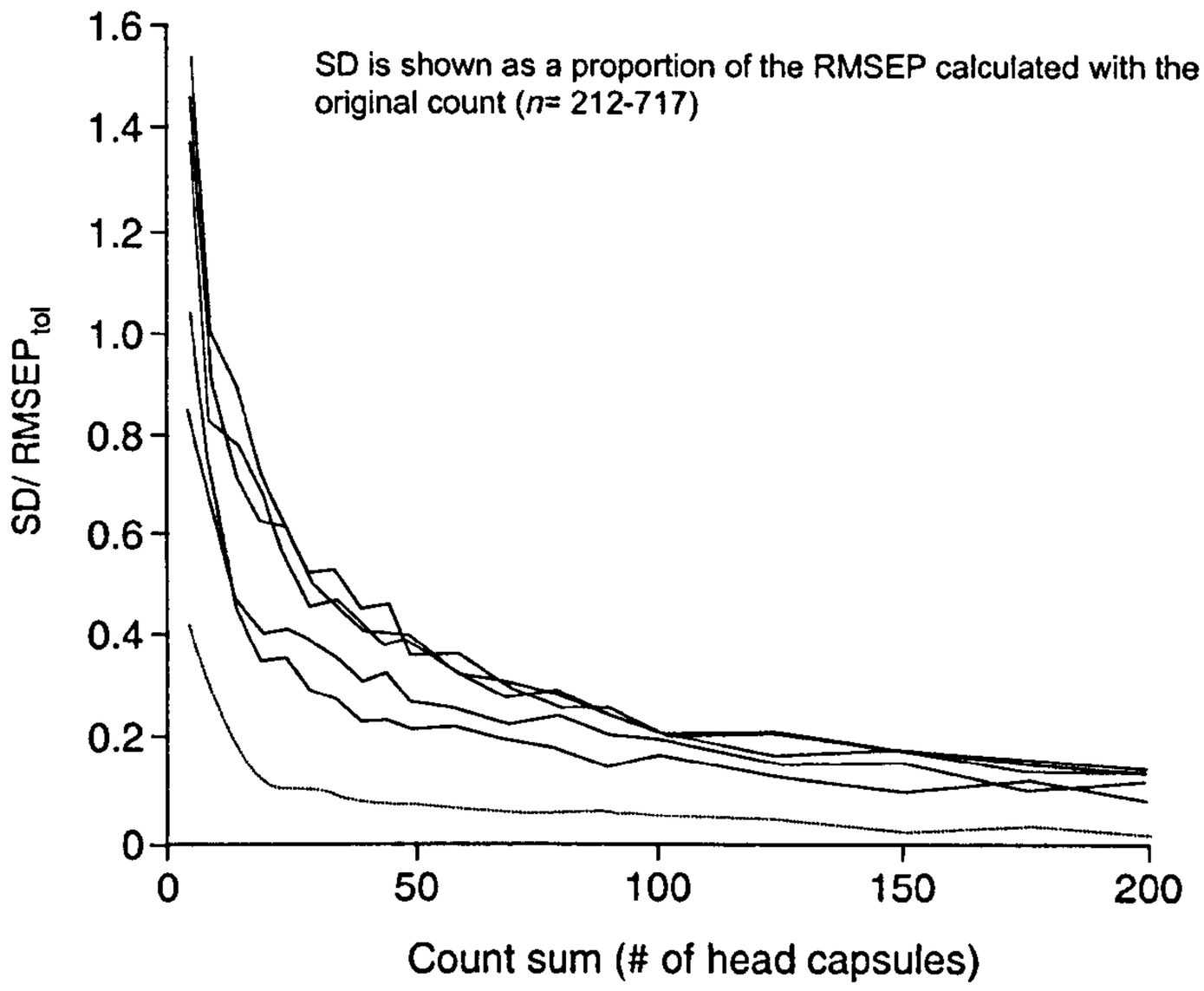

Figure 3.6: Graph illustrating the relationship between standard deviation (SD) of temperatures inferred using different sizes of count sums in relation to the Root Mean Square Error of Prediction of the original sample (*n* = 212 - 717) (Heiri and Lotter, 2001, 347).

Lindegaard, 1999), salinity (Walker *et al.*, 1995; Heinrichs *et al.*, 2001), hypolimnetic anoxia (Quinlan *et al.*, 1998; Little and Smol, 2001) and lake depth (Korhola *et al.*, 2000). **Table 3.3** outlines the main parameters of these studies.

The Swiss study assessing the nutrients - chironomid association was conducted in conjunction with the temperature investigation by Lotter *et al.* (1997). Despite the relatively long history of the use of midges as a means for assessing lake trophic status, log_{10} TP measured at sites only explained 11.4% of the variance in the chironomid data, compared to 18.4% explained by temperature. Performance of TP prediction of lakes within the training set was also poor, especially at the limits of the TP gradient measured, although this is partially due to the inherent bias weaknesses within the WA-PLS modelling method. Log_{10} TP also explained >10% of the taxonomic variance within a training set of 44 lakes from the UK (Brooks *et al.*, 2001). Although over half of the most frequently encountered taxa did not show any statistical relationship with Log_{10}TP, an r^2 of $0.60_{(jack)}$ was still present between observed and predicated Log_{10}TP within the training set. In order to allow chironomids to be used as a proxy for nutrient enrichment in both N and P limited lakes, Brodersen and Lindegaard (1999) have produced a transfer function for Chl a. An r^2 of 0.65 indicates that application of this model is a good way to quantify nutrient levels in the lakes that are too shallow to undergo stratification.

Greater levels of success were encountered when developing hypolimnetic anoxia transfer functions in North America (Little and Smol, 2001; Quinlan *et al.*, 1998). The development of such models has important applications; when making decisions on lake management it is important to know how climatic and morphological changes to the lake system have affected hypolimnic oxygen conditions in the past versus the possible effects of more recent anthropogenic activity on hypolimnetic anoxia. Although the manner in which hypolimnetic anoxia was assessed differed between the studies, both investigations came to the conclusion that changes in past levels of hypolimnetic anoxia could be quantified from chironomid records. In addition to this, Quinlan *et al.* (2001) discovered that the predictive power of the model was enhanced if littoral taxa were excluded. $R^2_{(boot)}$ values rose from 0.54 to 0.62 when littoral taxa were removed. This improvement may be due to the more complex nature of interaction of environmental variables in the littoral zone, as discussed above (3.4).

Walker *et al.* (1995) demonstrated the suitability of midges to act as palaeosalinity indicators, due to the dominance of groups such as *Cricotopus / Orthocladius* in saline lakes. Their log_{10} salinity transfer function produced an r^2 (adjusted) of 0.72. This training set was later augmented and reanalysed by Heinrichs *et al.* (2001) to produce a model which predicted log_{10} salinity (gl^{-1}) with an r_{jack} of 0.75. These models were applied to three cores from the area (Heinrichs *et al.*, 1999). Although the models produced high r^2 values, it should be noted that associated errors are are relatively large (range ~ 5.3 g/l) compared to the magnitude of change over the last $11^{14}C$ ka BP (range ~ $7.5gl^{-1}$). The potential application of midges to infer climate change in Africa has been pioneered by Verschuren (2003; Verschuren *et al.*, 2000a, b). Results of a chironomid based conductivity reconstruction at Lake Naivasha correlated well with that produced from the diatom record from the same lake. Ordination of modern data against environmental variables indicated that, as well as lake-water conductivity, the amount of papyrus-based swamp which fringed lakes also had a strong effect on the assemblage present.

Publication	Location	No. of lakes	Environmental variable being reconstructed	Type of inference model	RMSEP	R^2
Little and Smol (2001)	North Eastern N America	40	Avg DO(Summ))	WA-PLS 1		0.74(jack)
Quinlan *et al.* (1998)	Ontario, Canada	37	Annoxia factor	WA(tol)	0 64 (boot)	0.62(boot)
Heinrichs *et al.*, 2001	British Columbia, Canada	87	Log $_{10}$ Salinity (gl-1)	WA-PLS2	0.439 (jack)	0.76 (jack)
Walker *et al.* (1995)	British Columbia, Canada	86	Log $_{10}$ Salinity (gl-1)	WA(tol) inverse deshrinking	0.518 (boot)	0.72(adjusted)
Brooks *et al* (2001)	England	44	$TP_{log\ 10}$	WA	0.34 (jack)	0.60 (jack)
Brodersen and Lindegaard, 1999)	Denmark	54	Ln [Chl a]	WA- inv	0 65)	0.67 (jack)
Korhla *et al.* (2000)	Fennoscandia	53	Lake Depth (ln + 1)	WA-PLS2	0.49	0.70
Lotter *et al.* (1998)	Swiss Alps	51	TP	WA-PLS2	0.139 (jack)	0.679 (jack)

Table 3.3 : Summary of the performance statistics of different quantitative chironomid-based transfer functions for environmental factors other than temperature

Number of lakes and taxa refer to numbers included in the transfer function after exclusion of rare taxa and outlying lakes from the initial training set
Avg DO (Summ) = average end-of-summer hypolimnetic dissolved oxygen/ mg l^{-1}

Using multivariate statistics, investigations in Siberia, Russia and the Northern Territories, Canada have indicated that the position of the tree line may also act as an important

boundary for the insects (Porinchu and Cwynar, 2000; Walker and MacDonald, 1995). One study, by Korhola *et al.* (2000), has furthered the qualitative inferences that midges can be used as indicators of water depth (Hofmann, 1988 (3.5.1)). Depth was shown to account for 16.3% of the total explained variance in the training set of 53 lakes from Fennoscandia. This produced a transfer function with an r^2 of 0.7.

3.6 Applications of chironomid analysis in Patagonia

As is the case with other proxies, our current knowledge of chironomid palaeoecology in Patagonia is relatively limited. This is for a variety of reasons: fewer numbers of researchers working there, poorer logistical infrastructure and lower levels of taxonomic knowledge (Cranston, 1995a).

Results on investigations on four sites using midges have been published: two in the Taito Peninsula (Massaferro and Brooks, 2002, Massaferro *et al., submitted*) and the other two in the Argentinean Lake District (Bianchi *et al.*, 1997; Bianchi *et al.*, 1999; Ariztegui *et al.*, 1997). Although lack of modern ecological information makes interpretation of the chironomid record problematic, the situation has been aided in that all of these studies have implemented a multi-proxy approach. Therefore the chironomid data can be used in conjunction with these other techniques to improve data interpretation.

A study of the chironomid palaeofauna at Lago El Trébol, in the Neuquén province of Argentina (41°S 71°W), was conducted in combination with Total Carbon (TC) Total Nitrogen, (TN), biogenic silica ($BiSO_2$) and pollen analysis (Bianchi *et al.*, 1997). Although this investigation concentrated on the Pleistocene - Holocene boundary, its main focus was on the changes in lake productivity during this period versus changes in temperature. Therefore, only the midge head capsule concentration, as opposed to the faunal assemblage, was examined initially. Later interpretation of the changes in the chironomid fauna were argued to be related to the presence of tephra layers throughout the core (Bianchi *et al.*, 1999). Other than the response to the tephra deposits, the midge evidence correlated with variation in particle grain size which was inferred to indicate a change in the regional watershed following glacial retreat.

The investigation at Lago Mascardi was, again, multi-proxy: analysis of pollen, chironomid and particle size analysis was conducted as well as hydrogen index determination. The latter of these acts as an indicator of the hydrogen content of the organic matter. This can be used to indicate changes in the type of vegetation the hydrogen is derived from and, thus, changes in environmental conditions (Ariztegui *et al.*, 1997). With respect to interpretation of their chironomid records, one notable difference between the sequences from el Trébol and Mascardi is the nature of the systems in which they were deposited. Lago Trébol is 0.4 km^2 in size and 11 m depth max and although LGIT glacial fluctuations may have effected its catchment, it was not directly affected by glacial activity during this chronozone. Lago Mascardi is a palaeo proglacial lake, reaching up to 200m in depth, although the core analysed was taken at 12m depth. It is 30 km^2 and is located within the catchment of the south eastern flanks of the Mt Tronador ice-cap. This difference in environmental context and scale of the systems may have implications on the way in which chironomid data might be interpreted.

The most recent Patagonian records have been those compiled by Massaferro and Brooks (2002) and Masaferro *et al.* (*submitted*) (Figure 3.7). These records complement the LGIT and Holocene palaeovegetational investigations conducted in the Taito Peninsula and the Chonos Archipelago discussed in 2.4. Due to the acknowledged lack of ecological information about Patagonian midges, interpretations made from the record are tentative. However, changes in precipitation, trophic conditions and climate change are put forward as possible causes for the changes identified (Massaferro and Brooks, 2002). In contrast the Facil record seems to reflect more local changes.

At Laguna Stibnite, increases in trophic status or a lowering in lake level is inferred from increased percentages of the taxa *Limnophyes* between 12.8-11.6 cal ka BP (11.3 - 9.4 ^{14}C ka BP) and from 2.5 cal ka BP (2.4 ^{14}C ka BP) to the present. The first, trophic hypothesis is supported by the positive relationship between percentage *Limnophyes* and loss on ignition (LOI) values, indicating that *Limnophyes* was more dominant when lake productivity was at its highest. Changes in precipitation are another possible cause of changes in the relative abundance of the taxa, as *Limnophyes* has repeatedly been documented as inhabiting littoral habitats in the Holarctic (Hofmann, 1998). A precipitation-based interpretation is also supported by the pollen record (Lumley and Switsur, 1993). Periods of high percentages of

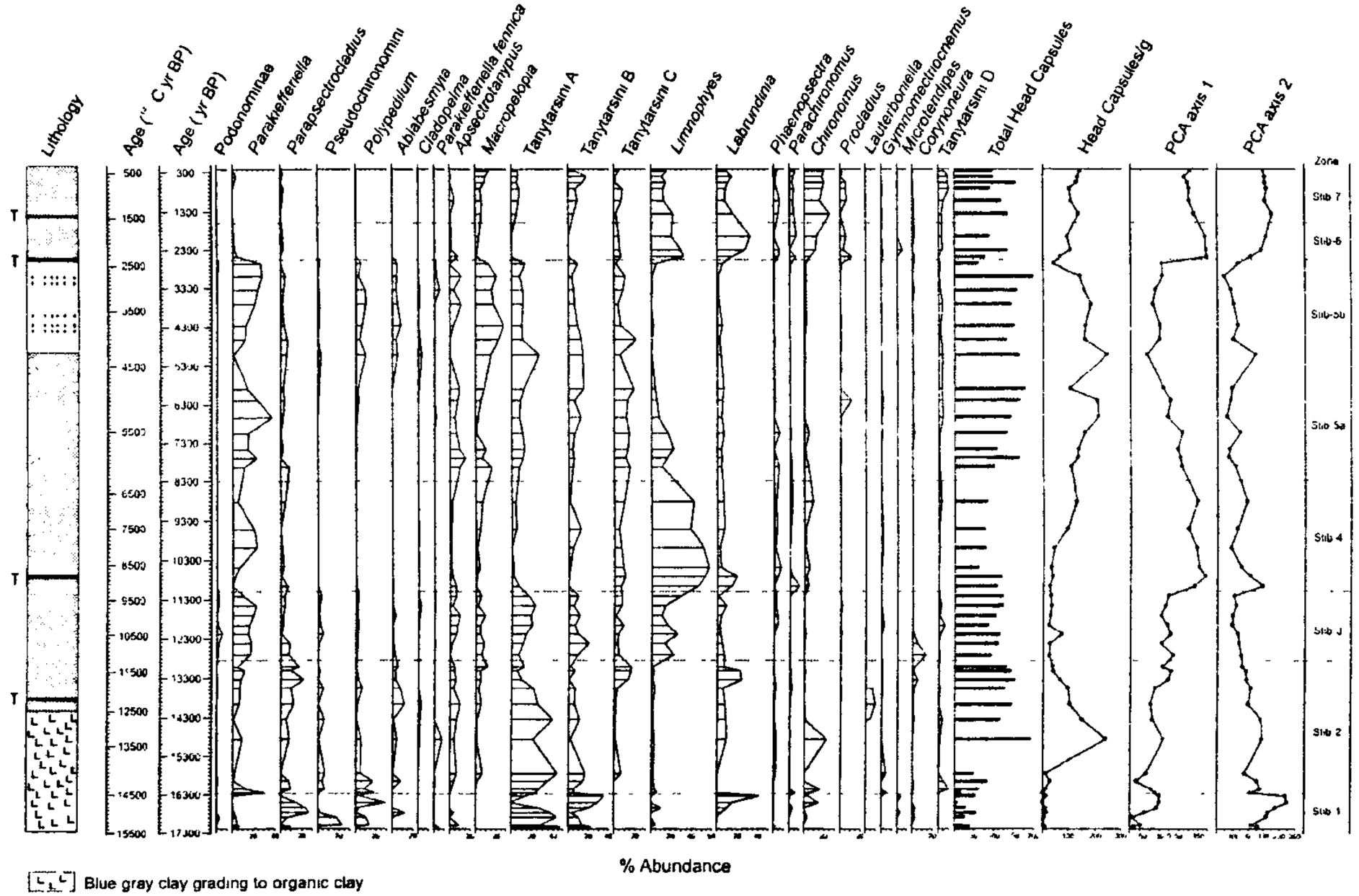

Figure 3.7 : Chironomid percentage diagram, showing dominant taxa in the Late Quaternary sequence from Laguna Stibnite, southern Chile. Also shown are lithology, calibrated ^{14}C dates (modified after Lumley and Switsur, 1993) and calendar ages, based on a different ^{14}C chronology (after Bennett *et al.*, 2000), head capsule concentration and PCA sample scores for axes 1 and 2. Significant zones identified by BSTICK (Broken Stick technieque modelling) are shown as continuous lines, non-significant zones are shown as dotted lines (Massaferro and Brooks, 2000).

Limnophyes are accompanied by low relative abundance of *Pilgerodendron uviferum* which is found in moist or marshy ground (Massaferro and Brooks, 2002; McCulloch *et al.*, 2000). Therefore the second interpretation of changes in percentage *Limnophyes* would be supported by changes in palaeoprecipitation as indicated by the pollen record. Within a regional context, this adds weight to the argument of latitudinal shifts by the Westerlies during the last 15 ^{14}C ka, as periods of increased precipitation at Laguna Stibnite are out of phase with those indicated by beetle and pollen data from Puerto Edén, 330 km to the south (Ashworth *et al.*, 1991). In addition to changes in precipitation, the record also provides possible evidence of a mid LGIT cooling between 11.3 – 9.4 ^{14}C ka BP (12.8-11.6 cal ka BP) due to a small peak in percentage Podonominae during this period. This sub-family is known to inhabit glacier-fed lakes (Brundin, 1988). In conjunction with low head capsule concentration indicating low productivity, this taxon's occurrence is interpreted to infer a possible climatic cooling (Massaferro and Brooks, 2002).

The more recent midge study on another core from the Chonos and Taitao region by Massaferro *et al.* (*submitted*) gives different results. This record, from Laguna Facil, indicates that the midge assemblage appears to be strongly influenced by changes in the catchments vegetation rather than the direct effect of climate change. This is based on the fact that the first two of the three midge-zone boundaries in the record both occur soon after significant changes in the vegetational assemblage. The final midge zone boundary, at c. 7.2 cal ka BP, slightly precedes that of the pollen. Thus, in this last case the authors argue that both the chironomids and pollen are responding to climatic change at this point, but that this change is registered first in the midge assemblage and that there is a slight lag in the vegetational shift. The record at this site shows no obvious presence of a LGIT climatic cooling. Overall, the results from this record highlight the fact that a lake's midge fauna is sensitive to local, catchment scale controls as well as broader climatic influences.

Therefore, although Patagonian palaeoenvironmental investigations using chironomids have been limited, some records appear to indicate that changes have occurred in faunas during the LGIT and Holocene. At present, interpretation of these records has been tentative, often relying on other proxies from the same record to guide or support the explanation of the midge record. This state of play highlights the potential of records from the area, but also the importance of conducting modern ecological work.

3.7 Summary

As one of the most ubiquitous insects inhabiting aquatic systems, chironomids serve as excellent biomonitors of their habitat. Studies have shown that the assemblage present is affected by several different environmental variables, including pH, salinity, trophic status and associated variations in hypolimnetic anoxia. Recent quantitative analysis of their modern ecology has also highlighted the importance of temperature in determining the fauna assemblage present. By exploiting these quantified relationships between temperature and taxa, high resolution, accurate palaeotemperature reconstructions have been produced. However, current lack of knowledge regarding ecology of the insects in the Southern Hemisphere has meant that such studies have almost exclusively been undertaken in just Europe and North America.

Although chironomid records have been used to make qualitative inferences about palaeoenvironments in Patagonia, there is a paucity of palaeorecords and modern ecological data. Existing studies indicate that the Patagonian palaeoenvironment was subject to notable change during the LGIT and Holocene, highlighting the importance of the development of quantitative reconstructions.

4 METHODS

4.1 Introduction

This chapter discusses the methods employed in this study, under three main headings: methods in the field, techniques in the laboratory and methods of data analysis, manipulation and presentation. It also justifies the techniques used.

4.2 Methods in the field

4.2.1 Modern chironomid ecological sampling

4.2.1.1 Site selection

As it was intended that the training set would be used to reconstruct temperature, the modern data set was selected to gain the maximum range of temperature (Wilson *et al*, 1993; Walker *et al*, 1997; Brooks and Birks, 2001a). Ideally this is achieved by collecting samples from lakes over a large range in altitude and latitude. To allow sound reconstructions to be calculated, the training set would need to span the range of temperatures that occurred during the LGIT and early Holocene, based on estimates of palaeotemperatures in the region (Chapter 2). Due to poor rural infrastructure in Patagonia, achieving a full range in both altitude and latitude proved difficult, as the vast majority of lakes at higher altitude were not accessible by vehicle. Thus, it was deemed more effective to focus on a latitudinal range to provide the range in temperature desired.

4.2.1.2 Surface sampling

In each lake, 1 cm samples of the sediment at the sediment / water interface were taken using a mini-Renberg corer. The boat was anchored during coring. Wherever possible, samples were taken from the deepest point in the lake, as indicated by echosounder measurements. Theoretically, this would mean that the head capsules in the sediment collected would represent fauna from all habitats within the lake, both profundal and littoral (Schmäh, 1993). Such samples would also be the most comparable to the sediments laid down in the limnic, down-core palaeorecords from Laguna Leta and Laguna Boal. However, this ideal was not achieved at all lakes for two reasons. Firstly, some lakes were

deeper than 20m, the maximum depth at which the Renberg coring system could operate with the rope available. In such cases samples were taken at depths just less than 20m. Wind was the second factor which prevented the deepest part of the lake being cored. When wind strengths were high we let the boat out on a rope fastened to the shore, so that we would be able to return safely.

The position of all lakes sampled was recorded using a GPS and the altitude recorded using an altimeter. Taking altitudinal measurements in Patagonia using instruments operating on changes in barometric pressure is often problematic due to the rapidity with which different atmospheric systems move in off the Pacific Ocean on the Westerlies. In an attempt to minimise inaccuracies due to this, the altimeter was calibrated, as near to the lake as possible, at locations of known altitude before and after the lake reading was taken. Where possible, lake altitude readings were also cross referenced against surveyed spot heights as marked on maps.

In addition to the samples collected by the author, additional surface samples (collected by Steve Brooks, co-workers and Raleigh International venturers) were also made available for analysis and inclusion in the transfer function development. Not all of these samples had been collected using a coring mechanism due to restrictions of sampling equipment. For example, sediment from the ten lakes from the Chacabuco valley were sampled using a grab, as indicated in Table 4.1. In summary 77 samples were retrieved from a range of altitudes of 1- 1466m a.s.l. and spanning latitudes 40-55°S.

4.2.1.3 Environmental variables

A range of environmental variables that could potentially affect the lake's chironomid ecology were measured at each lake. These were depth of lake, secchi depth, temperature (basal and surface), pH, conductivity and water chemistry. Dissolved Oxygen (D.O) and Chlorophyll *a* were not measured as the equipment required to measure such variables was not available.

Temperature was measured using a Metler Toledo pH meter MP120 both at the surface of the lake and at the bottom. Both measurements were taken so that the water temperature above and below any thermocline would be recorded. As discussed in section 3.5.2,

previous chironomid transfer functions have reconstructed climate using both surface and basal water temperatures. Profundal water temperatures were taken in water that was either collected at the lake bottom using a spring loaded water sampler or in the water that was collected at the water / sediment interface when sediment samples were taken. In order to increase the consistency and comparability within the temperature data set, all measurements were taken during the Austral summer in the months indicated in Table 4.1.

Region	Field season duration	Notes
Bariloche Lakes	March 2001	
Puerto Montt – Cochrane	Feb 2001	
Fuego Patagonia	Feb 2002	
Chonos Archipelago	Feb 2002	
Chacabuco Valley	March – April 2001	Sampled using a grab
Neff	Nov 2002	

Table 4.1 : Table showing the months during which different field areas were sampled and notes on sampling methods used.

pH and conductivity were measured at the surface of the lake using Toledo pH meter MP120 and Metler Toledo conductivity meter MC126 probes, respectively. The maximum depth of the lake, or the deepest point at which they could be sampled (see above) was recorded using an echosounder. To assess the turbidity of the lake water secchi depth readings were also taken.

Analysis location and year of field season	Bottle 1	Bottle 2	Bottle 3
Palanza (2001)	Refrigerated	-	-
Conception (2002)	Nitric Acid	Refrigerated	
Conception and Valdivia (2001)	Mercury Chloride	Sulphuric Acid	Nitric Acid
Natural History Museum (2001-2)	Refrigerated	Nitric Acid	-

Table 4.2: Summary of water sampling strategy and sample treatment depending on the location at which water analysis was conducted.

Water samples for chemical analysis were taken in 1l Nalgene bottles at the surface. As the samples were collected by different field parties, the number of samples collected and

treatment of samples varied between lakes (Table 4.2). Samples were stabilised using the chemicals outlined in Table 4.2, this would minimise the change in water chemistry between sampling and analysis in the lab.

The extent of macrophytic vegetation and human impact in the direct catchment were also recorded and a photograph of the site was taken for future reference.

4.2.2 Long cores

4.2.2.1 Laguna Leta

Cores were taken from a raft using a 5cm diameter, 50cm Russian corer (Jowsey, 1966). Cores were taken from the deepest part of the basin, as sediment focusing would mean that the highest resolution record should be located there (Davis *et al.*, 1984; Lehman, 1975). This point was found using an echosounder. In order to maximise the probability of sampling a complete record, twin cores were taken with 10cm overlap. Cores were placed in plastic guttering and wrapped in layflat and, on return to the UK, were stored at 4°C to minimise fungal growth.

4.2.2.2 Laguna Boal

Cores were collected from the deepest part of the lake to 4.70m below the water/sediment interface using a 1m long, 5.0cm diameter Livingston corer by Bennett, co-workers and Raleigh International venturers in 1996. Core segments overlapped by 50cm. Cores were wrapped in cling film and aluminium foil and stored in plastic guttering. Although the cores were stored at 4°C during the majority of storage, a brief fault in the cold store thermostat meant that temperatures temporarily dropped to below 0°C. This caused limited freeze-thaw damage to the cores. However, the stratigraphic integrity of the cores was maintained. Within the upper half of the core, there were several areas where there was no sediment available for analysis presumably due to enhanced shrinkage during this period due to higher water content. Such areas are all highlighted within the presentation of results.

4.3 Methods in the Laboratory

4.3.1 Water chemistry

Complete water chemistry analyses were conducted on a subset of the lakes sampled sediment samples. Analyses were carried out at three establishments: University of Concepcion, Chile, University of Palanza, Italy and the Natural History Museum, UK. At each institution, methods standard to that laboratory were used. All anion and cation concentrations were measured in parts per million (ppm) before converting them to milliequivalents (μeq l^{-1}) to allow comparisons. Table 4.3 shows the location of water

SITE	Lab. where analysed	SITE	Lab. where analysed	SITE	Lab. where analysed	SITE	Lab. where analysed
PIR	P	FUT	C_1	PRI	C_2	COM	NHM*
BW	P	LAR	-	bro	C_2	ERI	NHM
TBL	P	GUA	-	BNA	C_2	CON	NHM
ESC	P	ESM	-	MRG	C_2	HEN	NHM
MOR	P	ATR	-	LNF	C_2	ADE	NHM
VER	P	LOB	C_1	MOA	C_2	CHE	NHM
FON	P	LET	C_1	LAV	C_2	II	NHM
HES	P	BLC	C_1	TOL	C_2	III	NHM
MOS	P	CAS	C_1	VICI	NHM	IV	NHM
GAL	P	TAM	C_1	DII	NHM	V	NHM
PAT	P	FOI	-	PIII	NHM	VIN	NHM
ANG	P	RIS	C_1	GIV	NHM	VII	NHM
HUL	P	TRE	C_1	VV	NHM	VIII	NHM
LEZ	P	MAN	-	QVI	NHM	IX	NHM
RED	P	CIS	-	QVII	NHM	X	NHM
MER	P	EI	-	QVIII	NHM	XI	NHM
LGA	-	ENV	-	EII	NHM	XII	NHM
COF	-	TWI	C_2	ALD	NHM	XIII	NHM
X-667	-	AVE	C_2	MEC	NHM		
PIG	C_1	FLO	C_2	NOR	NHM		

Table 4.3: Table showing the location of water analyses for the sites where chironomid sampes were taken. Site abbreviations are detailed in Table 5.1. The analyses conducted are outlined below:

Palanza (P)= Na, Ca, K, Mg, TP, TN, Si, N-NO_3, SO_4 and Cl

Concepcion (C_1)= Na, Ca, K and Mg

(C_1)= Na, Ca, K, Mg, TP, TN, Si, N-NO_3, SO_4 and Cl

Natural History Museum (NHM) = Na, Ca, K, Mg, SO_4 and Cl *

* = results discarded due to contamination

- = no water chemistry data available

chemistry analysis for each site, and the specific analyses conducted. A more complete water chemistry dataset could not be achieved due to logistical issues transporting water samples for analysis.

4.3.2 Sediment description

Cores were described by logging the colour, texture and organic content of the sediment. Where visible, features such as macrofossil presence and particle grain sizes were recorded.

Macrofossils were frequently encountered within the Laguna Boal core, especially towards the base. Assessing the extent of macrofossil presence across the whole core was difficult due to the friable nature of some of the core segments. However, as the core segment spanning 3.48 – 3.98m was still moist, a semi-quantitative assessment of macrofossils remains content was conducted. Every 2cm, the sediment was given a score ranging from complete macrofossil absence (a score of 0) and high presence of macrofossils (score = 5). This allowed a quick assessment of how dense the macrofossil content was.

4.3.3 Loss on ignition

Loss on Ignition (LOI) was conducted to assess the amount of organic carbon in sediment (Bengtsson and Enell, 1986; Heiri *et al.*, 2001). LOI values can be taken as an approximate proxy of site productivity and minerogenic input into a lacustrine system (Battarbee *et al.*, 2002; Lowe and Walker, 1997a). LOI was conducted on sediment subsamples from both modern and downcore sediment samples. Within the cores, subsampling was undertaken every 2 cm. After drying at 105°C overnight, all samples were burned at 550°C for 5 hours.

4.3.4 X-ray analysis

X-ray analysis has been illustrated to be a powerful, non-destructive technique to assess the relative minerogenic content of sediments (Oldfield, 1999). This capability is particularly valuable when attempting to detect very fine bands of minerogenic material that are not visible with the naked eye, such as tephra (Dugmore and Newton, 1992). Laguna Leta segments were x-rayed for 2 minutes at 42kV and 2Ma at the X-ray facility at British Geological Survey, Edinburgh. The results were used to locate the depths horizons that might prove useful when correlating between core segments or providing chronological control through tephrochronology. Since the Laguna Boal core was stored at the University of Uppsala, Sweden, it was not possible to x-ray this record.

4.3.5 Tephra analysis

The last 20 years have seen a growing exploitation in the use of tephra horizons as chronostratigraphic markers (eg. Dugmore *et al.*, 1996; Lowe, 2001). The method, tephrochronology, is based on the principle that a volcanic eruption is a discrete event in geological time during which pyroclastics of a unique geochemistry are produced and deposited. Within the context of palaeolimnological investigations, the amount of time that tephra spends in atmosphere prior to deposition is an order of magnitude less than that which fine particles will stay suspended within a lake. This means that within such contexts tephra horizons can be assumed to be "instantaneous time-parallel 'marker' horizons" (Turney and Lowe, 2001, 454). Ash deposits can be divided into those that are visible to the naked eye, "macro-tephras", and finer deposits that cannot be detected with the naked eye, "micro-tephras". The latter deposits can be detected using a variety of methods, such as X-raying of the core as discussed above, although both detection and separation of volcanic material from the surrounding matrix is more challenging when the shards are deposited within highly minerogenic sediments (Turney, 1988).

An important strength of tephrochronology is that the finer fractions of the pyroclastics expelled can be transported thousands of kilometres before being deposited (Einarsson, 1986). This, together with an eruption's unique, geochemical "fingerprint", facilitates the cross correlation between intra or inter regional archives based on both major and trace element geochemistry of the volcanic deposits. In addition, dating of the volcanic deposits or the surrounding sediments, using techniques such as ^{14}C dating, allows the horizon to act as a known point in time when identified in other records.

In this investigation, the detection of tephra is used to constrain the chronologies of the limnic records and augment the extent of the region's known tephrochronology. On discovering minerogenic layers within the core, potential tephra horizons were visually inspected under a microscope. Samples were then prepared for Electron Microprobe Analysis (EMPA) using acid digestion (Dugmore and Newton, 1995). Samples were analysed at the NERC facility at the Grant Institute, University of Edinburgh. Due to a change in the Electron Microprobe being operated at the facility, samples were analysed on a combination of the Cambridge Instruments Microscan Mk5 (Laguna Leta) and Cameca

Camebax Microbeam (Laguna Boal). Operating conditions along with all raw data from these analyses are listed in Appendix 1.

Both microprobes were programmed to measure Na ions at both the beginning and end of each analysis due to the highly mobile nature of this oxide (Frogatt, 1992). This procedure allowed Na to be measured first, before potential loss of this more volatile oxide during measurements of other oxides. It also allowed the comparison of Na readings at the beginning and end of analyses to assess loss during the procedure (Hunt and Hill, 1993). To minimise the time that the shard was exposed to the electron beam, the latter was blocked (Cambridge Instruments Microscan Mk5) or moved off the crystal (Cameca Camebax Microbeam) during the drive time. The accuracy of the probe was monitored regularly between shard analyses by analyses of anhydrite, a crystalline standard of known geochemistry (Newton and Metclalfe, 1999). EMPA results were not normalised to 100% and analyses with totals <95% were discarded, as advocated by Hunt and Hill (1993).

Major oxide geochemistry data were first used to classify the volcanic shards using the total alkalis-silica method (Rollinson, 1993). This classification required normalisation of the data (Rollinson, 1993). As well as allowing the shards' petrologies to be classified, it offers a visual examination of the spread of the data. In this study the unormalised results from EMPA were plotted using both bi-plots and ternary plots to assess correlation both within the horizons analysed and between the results from this investigation and previously published geochemistries.

Some of the major tephra horizons that have been found in Patagonia are indicated in Table 4.4. Although other eruptions and associated deposits have been identified (Stern, 1990 and Stern, unpublished data, cited in Stern, 1992, 140), only those that have been encountered in and are relevant to palaeoenvironmental investigations are included in this summary. Deposits from Burney, Reclús and Hudson as well as unidentified volcanic sources are readily found in macro-tephra deposits within the region. Recent work by Tatur *et al.* (2002) and Gogorza *et al*, (2002) in the Argentinian Lake District, has discussed the high number of tephra bands present in lake sediments. The challenge remains to establish whether all layers actually relate to a single eruption or if they are volcanic shards from earlier eruptions reworked within the lake catchment. Nonetheless, published data

Eruption / Source	Date (^{14}C yr BP)	Known distribution	Associated References
Unknown	*c.* 9.6 - 9.4 ka BP	41-42°30'S	Moreno and Leon (*in press*) Moreno (1999) Heusser (1995)
Unknown	*c.*6.4 ka BP	*c.*47°30'	Turner (2003) Gilchrist (2000)
HW_1	*c.*12,440 ± 120	44°30'– 44° 60'S	Haberle and Lumley (1998)
HW_2	*c.*11,190 ± 120	44°30'– 44° 60'S	Haberle and Lumley (1998)
HW_3	*c.*9,950 ± 80	44°30'– 44° 60'S	Haberle and Lumley (1998)
HW_6	*c.*2,580 ± 60	44°30'– 44° 60'S	Haberle and Lumley (1998)
HW_7	*c.*1,690 ± 60	44°30'– 44° 60'S	Haberle and Lumley (1998)
Hudson	c. 6,725	45-47° S	Naranjo and Stern (1998) Haberle and Lumley (1998) (HW_4)
Hudson	c. 3,570	45-47° S	Naranjo and Stern (1998) Haberle and Lumley (1998) (HW_5)
Burney	3,860± 50	45-55° S	Stern (1992)
Reclús	12,693 ± 192	52-56° S	McCulloch (1994) McCulloch and Bentley (1994) Stern(1990) McCulloch and Davies (2001)

Table 4.4 : Summary of the source, age and coverage of LGIT and Holocene Patagonian tephras that have been used in palaeoenvironmental investigations and associated references. Hudson is the source of $H_7 - H_1$ eruptions.

provide a reasonably well dated Patagonian, tephrochronological framework within which to work, as well as sound geochemical data pertaining to specific eruptions.

4.3.6 Radiocarbon dating

Radiocarbon (^{14}C) dating was used as an absolute method for dating sediments from Laguna Boal and Laguna Leta. This chronological method is based on the assumption that ^{14}C, a cosmogenically produced radio-isotope of carbon, forms within the atmosphere at a constant rate over time. In general, isotopic composition of carbon in the atmosphere will be in equilibrium with contemporary organisms through photosynthesis or ingestion. However, when an organism dies this interchange with the atmosphere responsible for maintaining the C equilibrium ceases. The organism's existing ^{14}C content undergoes radioactive decay, thus reducing the ^{14}C concentration, or δ^{14}C. As the half life of ^{14}C is

known, the $\delta^{14}C$ of organic material therefore acts as a proxy for the age since organism's death.

Measurement of $\delta^{14}C$ can, therefore, produce a radiocarbon age estimate, expressed in years before present (yr BP). However, there is not an exact accordance between ^{14}C years and sidereal years. Thus, the former need to be calibrated before they can be compared to chronologies produced via other geochronological techniques. This is done through cross referencing the ^{14}C age estimates against records that are dated using both ^{14}C and a complementary method to produced a 'calibrated' age in calibrated (cal) yr BP (Bradley, 1999).

The use of ^{14}C dating is complicated by two major issues. Firstly the assumptions which underlie the method do not always hold true (Bradley, 1999). Secondly, there can be issues with the chronological representivity of the sample dated (Walker *et al.*, 2001). The major complication pertaining to the first point is that it is now known that ^{14}C production rates have not been constant over time. This causes the presence of ^{14}C plateaus in the calibration curves due to the fact that at certain points in the curve a specific $\delta^{14}C$ can be representative of more than one sideral ages. This issue is known to be particularly problematic during the LGIT, with plateaus centring on 12.7-12.6, 11.4-11.3, 11.0 -10.9, 10.4-10.3 and 10 – 9.9 ^{14}C ka BP (Lowe and Walker, 2000).

In terms of sample representivity, the major issue within limnic archives is the reworking of old carbon in the form of carbonate lithologies, organic soils and sediments within the catchment or nearby carbonaceous / carboniferous deposits. Problems of 'old carbon' from the reworking of fossilised carbon deposits have caused problems before in palaeoecological studies in Patagonia (Heusser, 1999). However, location on *in situ* or reworked metamorphic or igneous petrologies at both Laguna Leta and Laguna Boal meant that there was negligible risk of such contamination. This igneous lithology also reduces the risk of ^{14}C:^{12}C dissolution due to reworking of surrounding carbonate deposits. Nonetheless, there is still the possibility of reworking of sediments within the catchment. This problem may be particularly acute in age estimates associated with deglaciation in the presence of glacial rock flour (Sutherland, 1980). With the development of AMS methods of ^{14}C measurement the dating of terrestrial plant-macrofossils has come to the fore as a

method to avoid ^{14}C:^{12}C dissolution through the processes summarised above (Trumbore, 2000; Lowe and Walker, 2000). Although it has been argued that a plant-macrofossil age estimate will give a more accurate date for a horizon, this assumes that the macrofossils themselves have not undergone reworking which may not always be the case. Several studies have investigated the use of coleopteran (Walker *et al.*, 2001) and chironomid head capsules as samples for dating (Jones *et al.*, 1993; Snyder *et al.*, 1994; Fallu *et al.*, 2004). The use of the latter is particularly attractive when dating lakes in harsh environmental regions, where the presence of plant macro-fossils may be scarce or absent. Dating of the chitinous material appears to consistently yield dates that are younger than both macrofossil and bulk ages, although the mechanisms responsible for this are not totally clear.

Putting the issue of sediment reworking to one side, it must also be appreciated exactly what a sample represents. A bulk sediment sample taken from a 0.5cm thick horizon in the sequence may represent tens to hundreds of years of sediment deposition. Thus the date associated with this will be a weighted mean of all the different organic components within the sample. However, the large size and composited nature of the sample mean that it is likely to be representative of the time period it was deposited. Conversely, whilst dating of plant macrofossils may provide more precise dates, the age estimate is reliant on the stratagraphic integrity of a sole specimen.

10 and 11 samples from the Laguna Boal and Laguna Leta cores, respectively, were taken for ^{14}C dating. There were no plant macrofossils within the Laguna Leta sequence and thus bulk samples were submitted for every horizon dated. Laguna Boal, however, contained macro-fossil rich horizons towards the base of the core. Therefore, an overall chronology throughout the sequence was obtained, based on eight bulk samples and with two additional plant-macrofossil from the bottom metre of the core. The criteria for selection of horizons for ^{14}C dating were based on the following criteria:

1. A depth of palaeoecological change, as indicated by chironomid analysis;
2. A depth of change in sedimentary and depositional environment, as indicated by changes in physical properties of the sediment;
3. The depth at which a tephra was located.

To allow correlations between sequences analysed in this study and archives dated using non ^{14}C dating methods, dates were calibrated using INTCAL 98 (Stuiver and Reimer, 1993).

4.3.7 Magnetic Susceptibility

As x-ray analysis could not be conducted on the Laguna Boal core, magnetic susceptibility was conducted to identify the position of minerogenic horizons which could be tephra deposits (Oldfield, 1999). The iron-rich nature of volcanic glass, relative to the surrounding organic, mud matrix, means that this technique is a useful, non-destructive method to locate micro-horizons. In-wash of allochthonous material will also result in high magnetic susceptibility readings, also allowing inwash and associated periods of slope instability to be reconstructed (Dearing, 1986, Erikkson and Sandgren, 1999). Magnetic susceptibility was measured using an MS2E/1 Logging Sensor connected to the MS2 Barrington Metre on the two core segments that had not been affected by freeze-thawing (2-3m and 3.5-4.5m). Cores were mounted on a Tamiscan-TS1 automated platform, allowing measurements to be taken at 2mm intervals.

4.3.8 Chironomid analysis

The highly chitinised nature of the chironomid larva's head capsule allows it to be preserved in sediments, long after the rest of the body has disintegrated. It is therefore the morphological characteristics of the head that are used for taxonomic identification.

The major morphological features of the larval head capsule are illustrated in Figure 4.1. The features used for identification are mostly located on the ventromental side (the front side of the head) and include the mandibles, the ventromental plates, the antennae, post occipital plate, premandibles and ligulae. Identification to subfamily and tribe level can be made initially by inspection of the ventromental plates, if present. Chironominae ventromental plates are striated; within the family there is a clear morphological difference between Chironomini, whose plates are 'fan' shaped, and Tanytarsini, where the plate is 'sausage' shaped. The ventromental plates of Orthocladiinae and Podonominae are narrow and less prominent, where as within Tanypodinae they are not present.

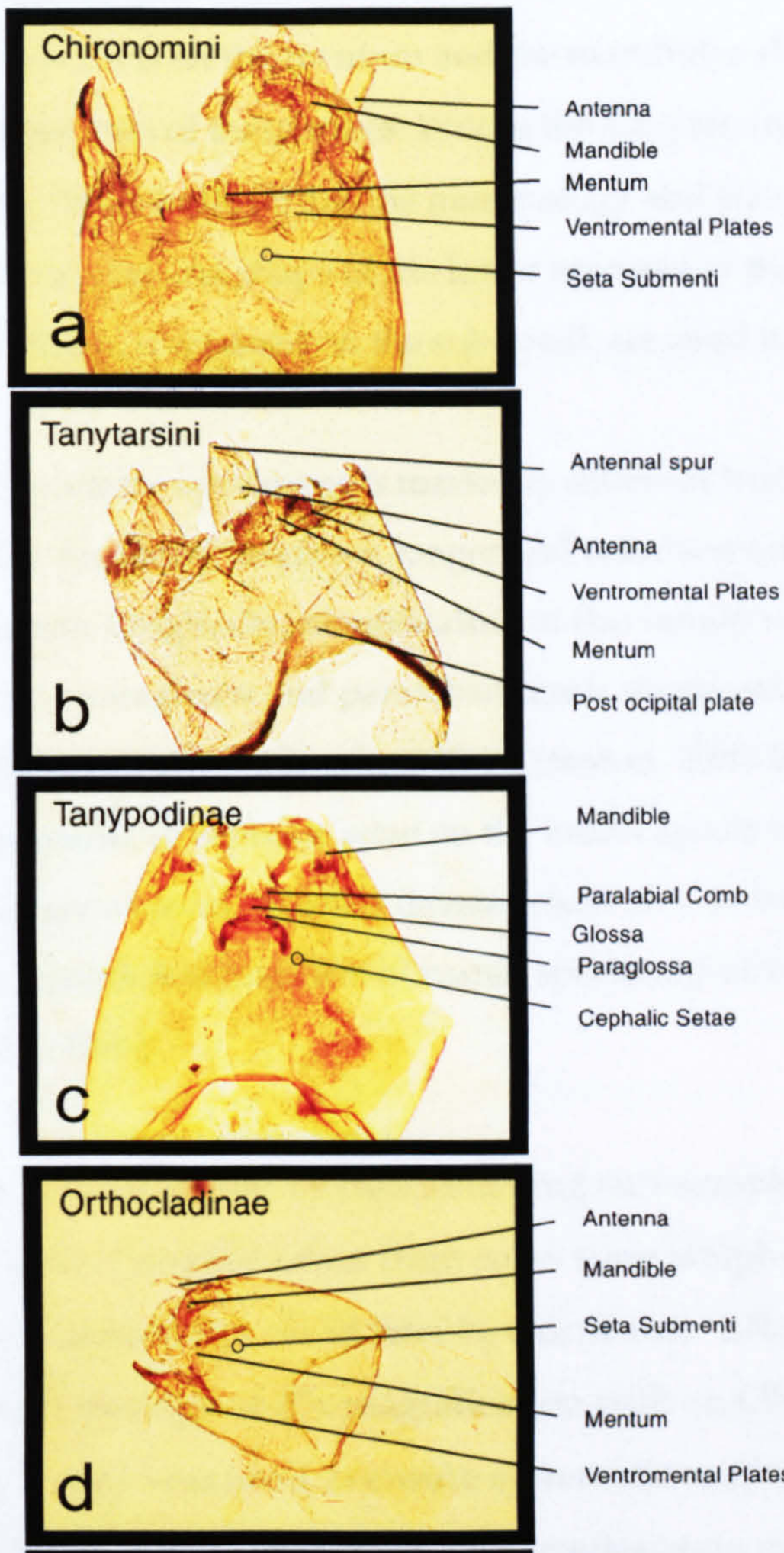

Figure 4.1 : Diagram of larval head capsules from (a) Chironomini, (b) Tanytarsini, (c) Tanypodinae, (d) Orthocladiinae and (e) Podonominae tribes. Major morphological features used in identification are annotated.

The mentum, arguably the most striking characteristic of the head capsule, is present in Chironominae, Podonominae and Orthocladiinae. The number, arrangement and shape of the teeth shaped structures on both the mentum and the mandibles allow identification to genus or lower level in first two of these tribes. Within the Tanytarsini differences in these characteristics are subtle. Thus in this tribe, the morphology and size or absence of the post-occipital plate and the size and shape of the lower segment of the antennae and the morphology of premandibles, if retained on the sub-fossil, are used to aid identification.

The appearance of Tanypodinae specimens is markedly different from those of the other subfamilies (Figure 4.1c): the larval heads are longer and narrower and the mentum teeth are replaced with the ligula. Originally, identification of this family was based on the morphology of the glossa, paraglossa and paralabial comb, if present. However, recent identification guides (Rieradevall and Brooks, 2001; Cranston, 2000-2002) have highlighted the usefulness of the positions of cephalic setae on the head capsule in enhancing taxonomic resolution to genus level. Further development of keys based on setation has been hampered due to insufficient numbers of reared specimens of reliable identification (Rieradevall and Brooks, 2001).

Chironomid samples were prepared by deflocculating sub-samples in 10% NaOH, before using a 90µm sieve. Samples taken from cores were weighed first so that concentrations of head capsules g^{-1} could later be calculated. After sieving, the coarse fraction was then sorted through at 40x magnification with an Olympus SZ40 microscope. A Bogorov tray was used to ensure systematic sorting and head capsules were removed and placed in 80% alcohol. Head capsules were subsequently dehydrated, by transferral into 100% alcohol, before being finally transferred into Euperal essence. Capsules were mounted in Euperal under 6mm diameter coverslips, 2 – 6 capsules per coverslip.

Identification was undertaken at 400x magnification using an Olympus BX40 microscope. Wiederholm (1983), Walker (2000), Rieradevall and Brooks (2001) and Cranston (1997) were used as taxonomic keys. Although these texts provided a sound base for identification, their mainly Holarctic focus meant that sometimes they were

inadequate. In such cases, taxa were keyed out into morphological groups based on consistent features.

Although care was taken during preparation to minimise mechanical damage to the head capsules, broken head capsules were often encountered. Such breakages were predominantly along the vertical axis of the ventral side, thus producing two mirror-image halves. If less than half a head capsule was encountered, it was not included but if portions of more than a half head were seen they were picked out and classed as a whole capsule during the identification process. Symmetrical breakages along the vertical axis, leaving exact half head capsules, were more prevalent amongst Chironomini and Orthocladiinae. In order to avoid over or under representation of taxa where breakages were common, it was noted whether the half identified was from the left or right hand side of the head capsule by using the plane of focus that the ventromental plate was in, relative to that of the teeth. Left and right halves were then taken into account accordingly when overall counts for the sample were calculated. In this study, the guidelines advocated by Larocque (2001) of 90 head capsules as standard, dropping to 50 if concentration was prohibitively low, were followed.

Sub sampling of the cores was initially conducted at 8cm during the LGIT / Early Holocene section of the core, and 16 cm within more recent sediments. Key depths were then revisited later on and analysed at a higher resolution of 1cm.

4.3.9 Taxonomic notes

Figures of taxa identified are listed in Appendix 2. Existing keys provided a fairly comprehensive summary of taxa within the Chironominae and Orthocladiinae sub-families, although some genus had to be grouped together due to uncertainties as to whether they could be accurately and consistently separated. This applied to the following genera:

- *Corynoneura / Thienemanniella*
- *Cricotopus / Orthocladius*
- *Tventia / Eukiefferiella*
- *Limnophyes / Paralimnophyes*

Although the head capsules of the last two genera were not distinguishable from each other, it appeared to be possible to categorise specimens depending on the location of the seta submenti relative to the base of the ventromental plate. Additionally, two morphotypes of *Micropsectra* were also found. Examples of *Paralimnophyes / Limnophyes* Taxon A and *Paralimnophyes / Limnophyes* Taxon B and *Micropsectra* Taxon A and *Micropsectra* Taxon B shown in Appendix 2.

Within the Tanytarsini tribe, Tanytarsini A, B, C and D were identified using the features described in Massaferro and Brooks (2002). Additionally a further morphotype was identified and classified as follows:

Tanytarsini taxon E: broad, antennal pedestal with a medium length spur, rounded apically, premandible with 3 teeth, mandible with 3 inner teeth and 1 medium lengthened tooth, 1 dorsal tooth, 0 surficial teeth. The ventromental plate is very prominent and large, often with a scalloped-shaped base. Tanytarsini B may represent and early instar of Tanytarsini Taxon E, as early instars often do not posses the ventromental plate that a later instar will (Brooks, *personal communication*). However, the two morphotypes were kept separate during identification.

Previous work within the Tanypodinae subfamily has suggested that identification using the arrangement of cephalic setae is a sound way to distinguish between taxa (Rieradeverall and Brooks, 2001). Within this study, this method and the taxonomy outlined in Rieradevall and Brooks (2001) was successful in identifying *Labrundinia, Clinotanypus* and *Ablabesmyia* within Patagonian samples. However a detailed survey of individual setae arrangement within Macropelopiini and Procladiini indicated that these characteristics were ineffective. One consistent morphological characteristic within the survey was that specimens which had a ligula with a median tooth that was equal in length, or longer, than the 2 lateral teeth, always had paired paraligula. In specimens where the ligula's median tooth was the shortest of all 5 teeth, paraligula could be either branched or paired. Initially it appeared that, when the median ligula tooth was short, allocation of an either 'branched' or 'paired' morphology of the paraligula could be used to split this group into two morphotypes. However, it was later decided that identification using this characteristic was not sufficiently consistent. It appeared that whether a paraligula was deemed to be 'branched' or 'paired' was partially determined by the angle

from which it was being viewed. Additionally, the characteristic was particularly hard to identify on smaller specimens. The arrangement of setae within Tanypodinae with combs ranged across those depicted for *Djalmabatista, Macropelopia, Procladius* and *Apsectrotanypus* within Rieradevall and Brooks (2001) (Figure 4.2). However, there were no clear distinctions between the different arrangements of setae and individual head capsules often seemed to possess setal arrangement that indicated one taxon on their dorsal side and another based on their ventral side.

Therefore, to summarise, specimens within the Tanypodinae genera were identified as (a) either *Labrundinia, Clinotanypus* or *Ablabesmyia*, on the arrangement of their cephalic setae, (b) Tanypodinae Taxon C or Tanypodinae Taxon B, based on the morphology of the ligula, or (c) Tanypodinae Taxon A if the ligula was absent and identification could not be made from the setal arrangement. This decision making process is outlined in the key in Figure 4.3. Although such a system leads to taphonomic influence on the assemblage recorded, any such effects should be consistent across samples in a given study.

4.4 Modern Data analysis, manipulation and presentation

Modern chironomid assemblage data were analysed using both classification and ordination approaches. Classification of the data through cluster analysis seeks to subdivide datasets based on either the similarities or differences within them. Essentially, ordination simplifies multivariate data sets by ordering the taxa along either theoretical or environmentally constrained gradients.

4.4.1.1 Data normalisation and simplification

Environmental and taxonomic data were normalised for two reasons. Firstly, normalisation reduces statistical noise, especially within the taxonomic dataset where otherwise a few high abundance scores can skew the results of data analysis if datasets are not normalised (ter Braak, 1986). Secondly, many of the statistical techniques are based on assumptions that data are normally distributed (Legendre and Legendre, 1998). This often conflicts with environmental data sets, which are frequently positively skewed (Birks, 1995, 1998). Data within the environmental dataset were normalised using log transformation. Guidelines by Birks (1996) were used to assess when normalisation was required. These indicate there are two scenarios when normalisation is required:

Rieradevall and Brooks (2001)	This study		
Djalmabatista 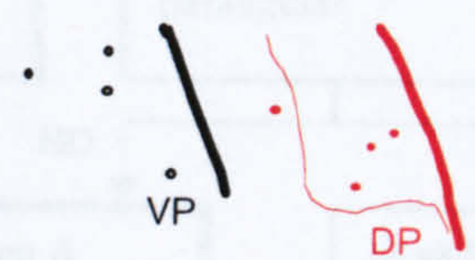	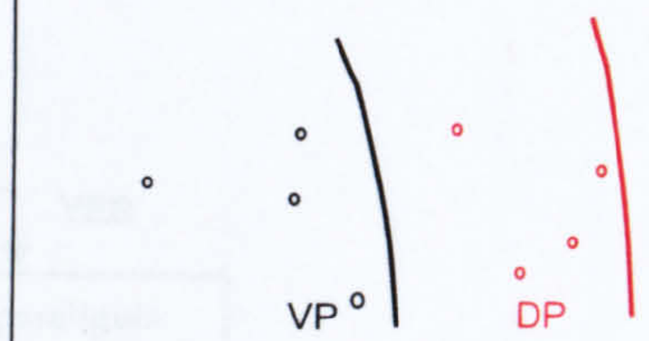		
Apsectrotanypus 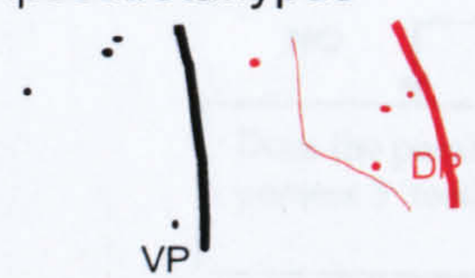	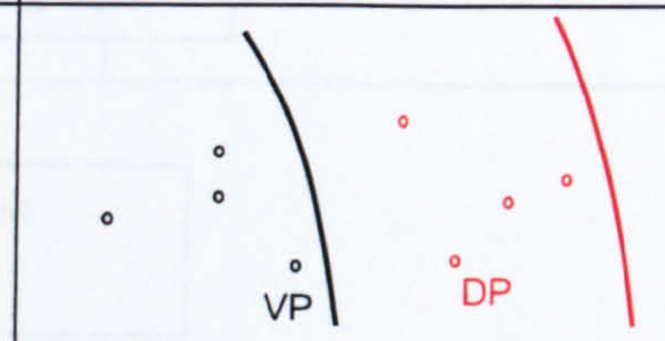		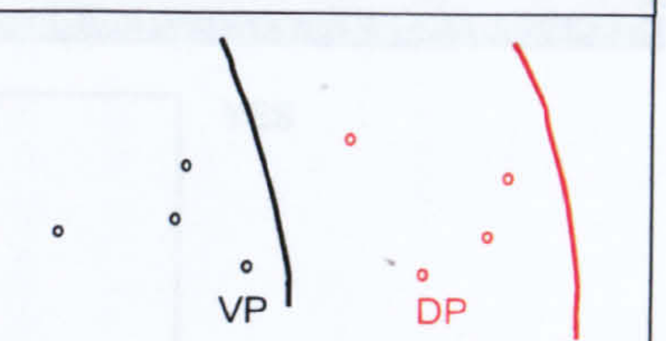
Macropelopia 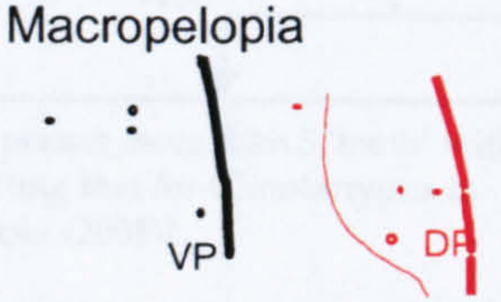	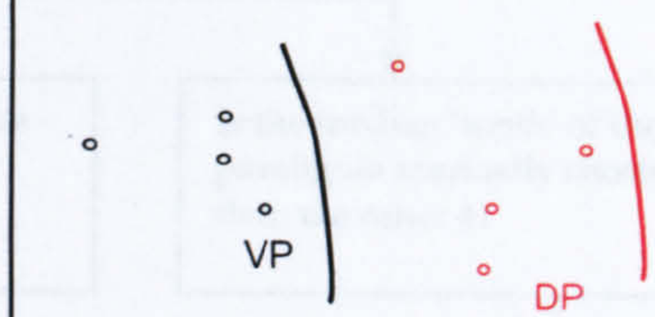	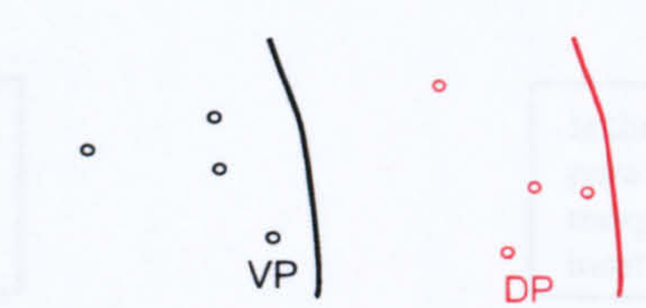	

Figure 4.2 : Diagram showing drawings of the wide range in cephalic setae encountered within Procladiini and Macropelopiini tribes of Tanypodinae. VP = Ventral Pores, DP = Dorsal Pores. Labelled diagrams of specimens in the left column are those taken from Rieradevall and Brooks (2001). The remaining nine illustrations are examples from the modern subfossil samples. Note the lack of consistent morphologies within the modern Patagonian samples which makes them both difficult to identify based on the Rieradevall and Brooks (2001) criteria or consistent arrangement within themselves. Drawings are not to scale.

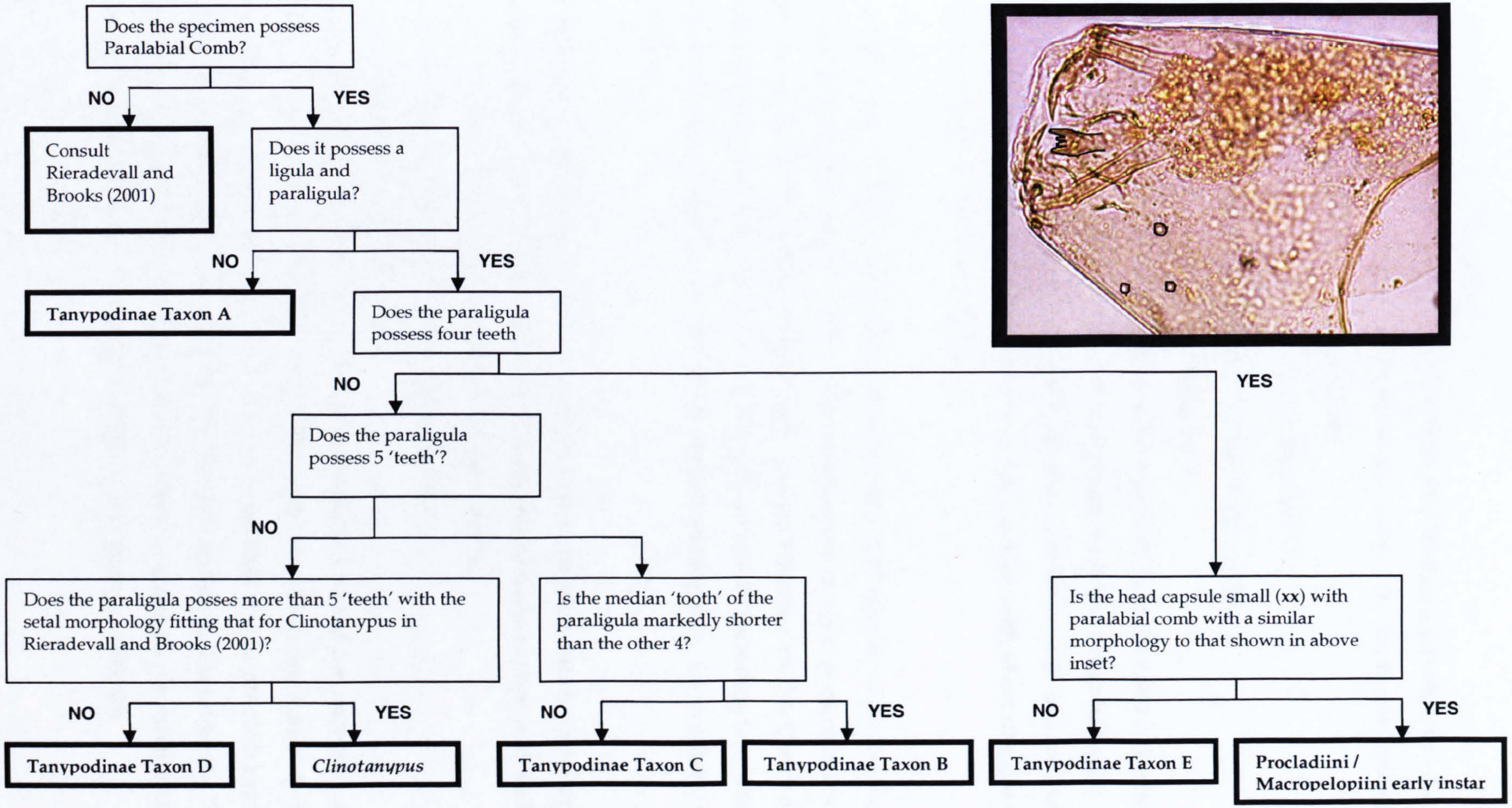

Figure 4.3: Key showing the criteria on which Tanypodinae were identified

1. When 1. s.d. > than the mean

2. When the data set minimum value multiplied by 20 equals less than the maximum.

When the environmental datasets contained zero values, the log transformation prescribed by Jager and Looman, (1995, 21) was applied:

$$Y^*_{ki} = \log_e (Y_{ki}+1)$$

Where Y_{ki} = value of the *k*-th response variable in the *i*-th site

And Y^*_{ki} is the replacement value for Y_{ki}

Within taxonomic datasets, abundance data were initially normalised using both square-root and log transformation as both are recognised methods of normalisation. Total inertia, a term measuring variance in a dataset, from these two techniques was compared against that of the non-transformed data, and the transformation method resulting in the least total inertia was selected for subsequent use.

Taxa that are rare, both in abundance and the number of sites at which they occur, are often omitted from training sets to reduce noise and increase models' performances. Through work based on their Canadian hypolimnetic oxygen inference model, Quinlan and Smol (2001) indicate that the use of the common protocol of only including taxa which occur at >2% in > 2 lakes is suitable for use in chironomid training sets. These criteria were used in this study.

Within ecological data matrices it is common to have missing data for a variety of reasons. Legendre and Legendre (1998, 48) suggest three mechanisms to cope with such scenarios:

- Deleting rows or columns from the data matrix;
- Accommodate algorithms to missing data;
- Estimating missing values.

As it was unclear whether the environmental variables would correlate with either each other or with the taxonomic assemblage, the estimation of missing values seemed unsound. The second option of allowing certain data to be omitted was impractical since prescribed methods within CANOCO were to be used for data analyses. Therefore the "simplest, yet the most costly" method of deleting rows (i.e. sites) or columns (i.e. environmental variables) from datasets was used (Legendre and Legendre, 1998, 48).

4.4.1.2 Descriptive statistics

Basic descriptive statistics were conducted on each of the environmental variables and graphically presented using Minitab 13.1. This was mainly done to visually assess the distribution of values within each environmental variable. If distributions were highly skewed then normalisation of the data might be necessary to increase the performance of ordination analysis, and thus the model produced (4.4.1.1). Environmental variable data were correlated against each other to assess whether there was multicollinearity (Birks, 1998).

4.4.2 Modern chironomid data analysis

4.4.2.1 Cluster analysis

Taxonomic data classification provides a powerful tool to superimpose categorisation on a large, detailed and continuous data sets. Its application in this study highlights lakes that, based on their taxonomic assemblage, are similar. It additionally allows the assignment of indicator taxa to certain lake 'types', as the technique specifies which taxa are characteristic of each subset of lakes at each stage of division.

Cluster analysis of modern data sets was undertaken using TWINSPAN (two-way indicator species analysis) (Hill, 1979; Gauch and Whitaker, 1981). This is a divisive form of classification analysis whereby categories are created by splitting the data set in between the sites where the largest taxonomic differences occur when the sites are ordinated along a Correspondence Analysis (CA) axis 1 (Kovach, 1995; Waite, 2000). This is repeatedly performed so a hierarchical form of site classification is obtained. It is then the analyst's decision to decide at which stage such divisions become predominantly statistical and ceases to be ecologically 'meaningful'. It is also the decision of the analyst at what level pseudospecies cut levels are set. Pseudospecies are created by dividing all taxa into subgroups based on categories of abundance. Abundance category divisions, or pseudospecies cut levels, are determined by the analyst and are uniform across all taxa. This modification of data is required as TWINSPAN uses the presence or absence of a taxa as the criteria to assign sites to the negative (*0) or positive (*1) side of each division; thus the process cannot use ratio data. The translation of abundance data into pseudospecies form converts the results from ratio to nominal data, from which presence or absence at each pseudospecies level can be assessed (van Tongeren, 1995). TWINSPAN was used, as

opposed to cluster analysis, on the recommendation that divisive methods, of which TWINSPAN is one of the strongest and most established, are recommended over the agglomerative one (Waite, 2000; Gauch, 1994).

4.4.2.2 Ordination

Ordination holds a key stage in analysis of the modern chironomid data set: in addition to its role in exploring the relationships within the data set it acts as the basis for production of a model for palaeoreconstructions. A variety of ordination techniques are available to

Type of Ordination analysis	Acronym	Type of response curve	Type of ordination
Principal components analysis	PCA	Linear	Unconstrained
Correspondence analysis	CA	Unimodal	Unconstrained
Detrended correspondence analysis	DCA	Unimodal	Unconstrained
Redundancy Analysis	RDA	Linear	Constrained
Canonical correspondence analysis	CCA	Unimodal	Constrained

Table 4.5 : Summary of some of the major characteristics of the ordination techniques discussed. N.B. Unconstrained ordination can also be referred to as indirect ordination, and constrained ordination as direct.

the palaeoecologist. The selection of the most suitable methods depends on the nature of the taxonomic dataset, and whether or not analysis of this is to be linked to the associated environmental variables measured. The techniques used in this investigation are summarised in Table 4.5. All ordination was conducted using CANOCO 4.0 (ter Braak and Šmilauer, 1998). During all ordination, downweighting of rare taxa was selected to minimize the influence of such taxa (ter Braak, 1995). This is because any relationship between rare taxa and ordination gradients is going to have relativlely low statistical significance so it is desirable to minimise the influence of such relationships.

4.4.2.2.1 Unconstrained ordination

The first type of ordination performed was detrended correspondence analysis (DCA), a statistical method that looks for theoretical axes of change within the taxonomic dataset. The technique is based on correspondence analysis (CA). The primary use of DCA within this study was to indicate whether linear or unimodal statistics were most suitable for investigating the taxonomic datasets. Although DCA is often more useful in ecological

investigations, the following summary of both techniques discusses CA first, as DCA builds on the CA method.

CA is based on the assumption that taxa have a Gaussian unimodal response to changing environmental conditions and, as is the case with all the unimodal methods discussed, it uses weighted averaging to estimate the environmental optimum for each taxon (ter Braak and Prentice, 1988; Birks, 1995). Although it is acknowledged that real ecological response curves are more complex than depicted by the Gaussian standard curve (Birks, 1995; Lepš and Šmilauer, 2003), the model serves as a "convenient and robust approximation for the analysis of biological data that span gradients in excess of 2 s.d. units (of biological turnover)" (Birks, 1995, 175) (Figure 4.4). CA analysis uses the taxonomic assemblages recorded at different sites to statistically determine theoretical "axes" that best explain the spread of the taxa across the dataset. To determine which of the infinite number of axes is the *most* influential, taxa are given values on each of these theoretical gradients depending upon the position of their optima on the axis. These values are known as their "species scores". The gradient that has the largest range in species scores is theoretically the most influential in determining their occurrence, as it has the greatest ability to spread out the taxa. The extent to which this axis explains the distribution of the taxa is indicated by the size of the assigned eigenvalue (λ), which equals the range of species scores along that axis. The range of the species score along each gradient, expressed in standard deviation units of biological turnover, is termed the "gradient length" (Hill and Gauch, 1980, cited in Birks, 1995, 174). CANOCO generates both λ and gradient lengths for axes 1-4 by default, as the majority of total inertia will be explained within these first four axes.

In addition to determining the primary gradient (axis 1), CA is repeated on the data to find the second and further most influential gradients. As the second axis aims to explain as much of the remaining data variation, ie. that which is totally unexplained by CA axis 1, it is forced to be totally uncorrelated to it. The sum of all the eigenvalues from all the axes produced during CA on one data set ≤ 1.

CA possesses two main weaknesses (Kovach, 1995, ter Braak, 1995, Digby and Kempton, 1987):

a) it tends to compact values at the ends of axis 1 relative to those in the centre.

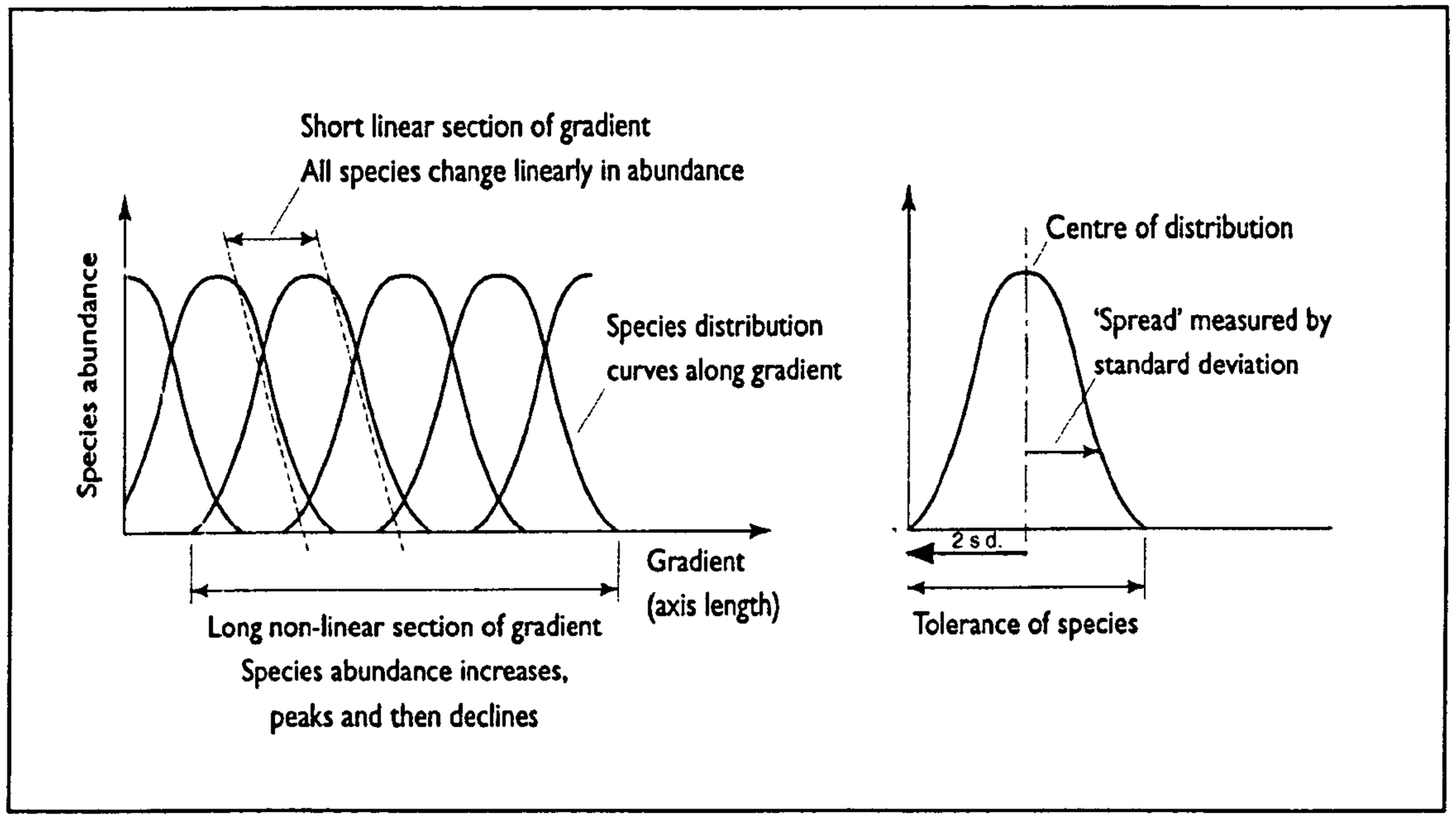

Figure 4.4 : Species abundance patterns over long and short gradients. Short gradients tend to show linear patterns; long gradients may show non-linear patterns (Waite, 2000)

b) it also often induces a quadratic relationship between axis 1 and 2, which is indicated by and arcuate arrangement of site data on ordination diagrams; hence the phenomenon is often referred to as the "arch" effect.

Detrended Correspondence Analysis (DCA) addresses the latter of these flaws by "detrending" CA results to minimise the arch. If detrending by segments is selected, as is always the case in this study, this is done by dividing axis 1 into sections and then adjusting the species scores on axis 2 by subtracting the mean axis 2 score from that section. This results in the average species score in axis 2 for each section being similar. Although it holds certain disadvantages, detrending by segments was selected since it allows the estimation of the length of gradient of species turnover (Legendre and Legendre, 1998). Although this extra step means that DCA holds advantages over CA for the ordination of data, the detrending can be over-zealous and lead to the masking of meaningful relationships within the data set (ter Braak, 1995; Palmer, 1993, Legendre and Legendre, 1998, Kovach, 1995). Therefore, graphical results of CA and DCA should be examined (Kovach, 1995). Within this study, if little or no arch was prominent when CA results were plotted, detrending was not carried out.

DCA results were used initially to assess which sort of data transformation was most effective by comparing total inertia results after square root, logarithmic transformation results and results when now transformation was performed (4.4.1.1). As total inertia is a measure of the total (both unexplained and explained) variation in the dataset, the higher the total inertia, the more noise there is within the dataset. Moreover, DCA results were used to indicate whether taxa within the data sets were responding to theoretical gradients in a unimodal or linear manner.

Although it is almost always the case that the relationship between taxa and environmental conditions is unimodal, the full range of this Gaussian response may not be detected during ordination if the range of the environmental variable measured is not large enough. If the data set range is not large enough, the relationship will appear closer to a linear correlation than a unimodal one. In theory, the whole Gaussian curve occurs over 4 s.d. of biological turnover on the ordination axis. Therefore, if the gradient length >2s.d., a unimodal method of ordination is recommended (Birks, 1995) (Figure 4.4). If the gradient length <2s.d., within the range of the training set, the taxa are essentially responding in a linear manner within the scope of the analysis (1995). Although the value of 2s.d. is

advocated as a cut-off by Birks (1995) it should be noted that other authors indicate that a cut off of 3-4s.d. may be more appropriate (Lepš and Šmilauer, 2003). Therefore, when gradient lengths of 2-3 s.d. were discovered in this investigation, both linear and unimodal techniques were investigated to see which performed best. If linear relationships appear present, the use of Principal Components Analysis (PCA) is appropriate to investigate unconstrained ordination. This technique effectively works in the same manner as CA, but assumes a linear correlation between environmental variables and taxonomic variation.

4.4.2.2.2 Constrained Ordination

Constrained ordination using either Canonical Correspondence Analysis (CCA) or Redundancy Analysis (RDA) was used to determine the environmental variables that were important in determining the assemblage. Whereas the preceding methods of CA, DCA and PCA are solely concerned with theoretical gradients gained solely from analysis of taxonomic data, CCA and RDA pull out axes that can be "best explained by the observed environmental variables" (ter Braak, 1995, 137). The technique therefore combines the ordination of species data and analysis of its relationship to environmental variables in one step (ter Braak, 1986). CCA assumes a unimodal response, whereas RDA works using linear regression. Therefore, as is the case with unconstrained ordination, the most appropriate method was selected by examining the gradient length produced for axis 1 and 2 during DCA.

CCA works by selecting the best linear combination of environmental variables to maximise species scores along axis 1. This axis is therefore essentially a hybrid combination of the environmental variables included in the analysis. As orientation of the axis is tied to environmental variables, and is therefore more restricted than indirect ordination, the range of species scores, and therefore λ, tends to be lower (ter Braak, 1985). However, the more environmental variables used, the less restricted the analysis becomes due to more permutations available to produce axis 1. Therefore, the more environmental variables included, the greater the likelihood that the CCA axis 1 λ approaching that achieved via DCA/ CA. As CCA is a permutation of CA, RDA uses the same underlying mechanics as PCA but, like CCA, the axes produced are constrained by the environmental variables.

Comparison of the results of unconstrained and constrained ordination results can be used to indicate the extent to which the environmental variables measured are determining the taxonomic assemblages (ter Braak, 1996; Lepš and Šmilauer, 2003). Similar results between CA, based on the unconstrained optimum, and CCA, where formulation of axes is constrained by those environmental variables measured, suggests that the variables important in determining the assemblage are included in constrained analysis. Another useful application of constrained ordination is conducting Detrended Canonical Correspondence Analysis when the environmental variables used are constrained to a single variable that one wishes to investigate in more detail. This provides the gradient length in standard deviations of that specific variable. This can then be compared to DCA Axis 2, to indicate the ability of the variable in question to maximise the spread of the taxon scores, thus indicating the strength of the variable *verus* all other controls on determining taxon scores (ter Braak & Juggins, 1993).

CANOCO also offers the opportunity to test the statistical significance of an environmental variable - taxonomic relationship by using a Monte Carlo permutation test within forward selection. This generates p-values associated with taxonomic - environmental relationships via comparison to the null hypothesis of there being no taxonomic - environmental correlation present (Crowley, 1992; Lepš and Šmilauer, 2003).

4.5 Paleoecological data analysis and presentation

Downcore chironomid data were compiled and converted into percentage data using TILIA 2.0 (Grimm, 1991-93). These data were presented using TILIAGRAPH 2.0.b.5 (Grimm, 1991) and constrained cluster analysis (CONISS, Grimm, 1987) was used as an agglomerative form of zonation. The broken-stick model (Bennett, 1996) was used to determine the number of statistically significant zones. However, the zonation of a record is not only important in showing which levels are statistically most similar, but also aids description of results and interpretation of the dataset (Bennett, 1996; Birks, 1986). Thus, additional sub-zones were also added, using CONISS as a guide to the depths at which they should be placed.

4.6 Summary

This chapter has provided an overview of the methods selected and justified their suitability for the investigation. Overall the study comprises two major strands of investigation: (a) an exploration of relationships between the modern fauna and environmental variables and (b) the production of palaeoenvironmental records from limnic sequences. The combination of physical, chemical and biological data relating to the region's modern chironomid fauna provides a sound framework for analysis of down core material. Use of the statistical methods outlined allows robust and quantitative inferences to be made about any relationships found between the fauna and their environmental record. Within the palaeoenvironmental, down-core record, inferences made from the midge assemblage data are complemented by sediment description and analysis to provide information on the associated sedimentary processes. The application of ^{14}C dating in conjunction with tephrochronology affords chronological control on these records.

5 MODERN CHIRONOMID ECOLOGY AND TRANSFER FUNCTION ANALYSIS

5.1 Introduction

Chironomid analysis formed the backbone of the palaeoenvironmental studies in this investigation. In order to make accurate interpretations of the down-core data, a sound understanding of the ecological preferences of the modern day fauna is required. At present, knowledge of Patagonian midge ecology is scarce. The following chapter investigates relationships between midge faunal assemblages and environmental variables using a variety of statistical methods. The aim was to ascertain whether the link between any environmental variables – taxonomic distribution were strong enough to allow production of a transfer function. The results of the following analyses form the basis for subsequent palaeo-environmental interpretations.

5.2 Modern data set: initial results

78 lakes were sampled for surface sediments to produce the Patagonian training set. The location of these lakes is shown in Figure 5.1. The lakes range over a latitudinal gradient of > 15°. A more even distribution of lakes was not possible due to logistical constraints and the region's geography. For example, in the steppe to the east of both icecaps, lakes are uncommon due to the arid climate and relatively flat relief. The locations of all lakes sampled, together with associated environmental variables and water chemistry data are given in Table 1. During collation of data it transpired that one site, Laguna Edita, had been unintentionally sampled twice on two different field trips, once by the student and then independently by the Raleigh International field trip. As both sediment samples had been analysed prior to discovering this, they were both kept in the training set as they would provide a valuable independent check (EI and EII).

5.2.1 Environmental data

Environmental data, along with variable specific maxima, minima and means, are shown in Table 5.1. At the base of the table are data regarding the statistical distribution of the data set, which were used in assessing whether data required logarithmic transformation for use

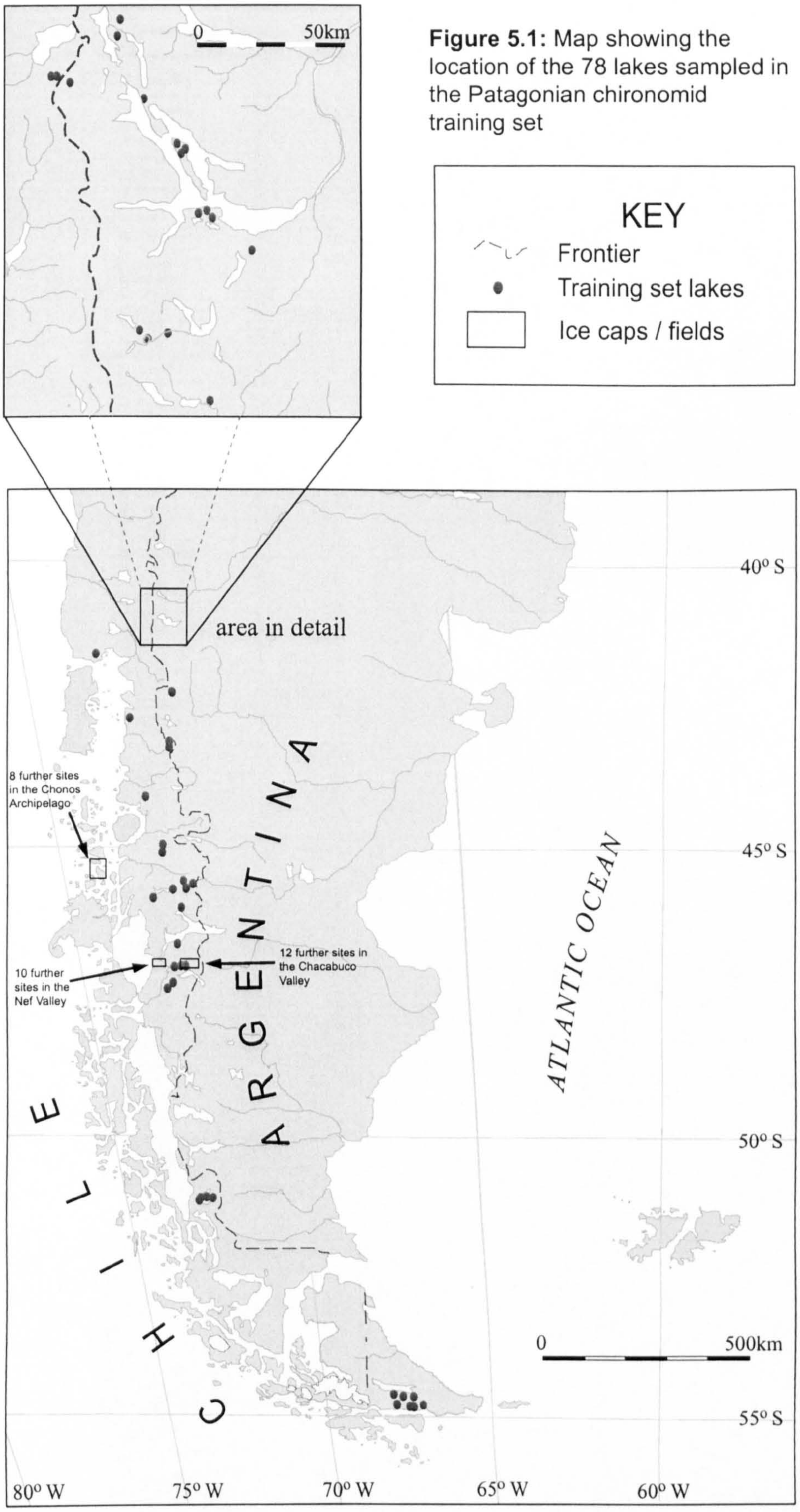

Figure 5.1: Map showing the location of the 78 lakes sampled in the Patagonian chironomid training set

Number in figures	Name	Code	FIELD									WATER CHEMISTRY											
			Decimal long (° N)	Decimal Lat (°E)	Altitude (m)	Depth (m)	Secchi Dept (m)	pH	Conductivity (µs)	Surface temperature °C	Basal temperature °C	LOI (%)	TP µg l-1	TN mg l-1	Si mg l-1	N-NH4 µeq l-1	Ca µeq l-1	Mg µeq l-1	Na µeq l-1	K µeq l-1	T.Alc. µeq l-1	Cl µeq l-1	SO4 µeq l-1	N-NO3 µeq l-1
1	Pire	PIR	71.807	40.789	738	20	6.2	5.93	36.4	16.1	14	0.12	4	0.06	7.33	0.52	365.77	602.82	318.71	187.50	7330.00	206.71	152.61	0.52
2	Bailey Willis	BW	71.705	40.700	799	8.9	2.8	4.05	0.14	20.5	17.9	0.26	6	0.23	17.17	2.57	287.42	164.48	179.14	40.93	617.00	30.46	3.33	0.00
3	Trebol	TBL	71.441	41.164	760	10.5	3.8	7.75	92.4	18.3	18.5	0.28	5	0.4	5.45	1.78	420.66	258.23	179.14	13.56	766.00	46.25	58.92	0.00
4	Escondido	ESC	71.441	41.164	754	7.2	5.18	7.53	63.8	19.3	18.3	0.24	5	0.29	7.33	1.50	352.29	150.50	128.27	11.77	579.00	29.33	19.57	0.00
5	Morenito	MOR	71.521	41.136	754	8.5	4.8	7.67	78	18.6	18.5	0.22	7	0.27	5.21	2.93	402.19	199.84	145.66	14.07	601.00	35.81	120.76	0.00
6	Verde	VER	71.717	40.694	1466	1.5	0.92	7.48	34.1	15.5	15.4	0.08	18	0.29	0.84	0.86	136.73	97.04	83.05	10.49	303.00	8.18	2.29	0.00
7	Fonck	FON	71.299	41.356	750	17.5	6.1	7.66	7.66	17.6	12	0.28	5	0.14	6.5	2.50	164.67	86.35	93.92	12.79	324.00	16.36	7.08	0.00
8	Hess	HES	70.736	41.372	730	8.3	8.3	7.39	45.9	17.7	17.7	0.09	4	0.13	5.2	2.57	295.91	88.82	69.13	10.49	382.00	10.72	56.84	0.00
9	Moscos	MOS	71.618	41.494	803	20	7.6	7.56	53.7	18.4	17.4	0.09	7	0.17	4.94	2.71	296.91	86.35	63.05	10.23	378.00	10.15	66.00	0.00
10	Gallinas	GAL	71.618	41.497	998	8.5	6	7.02	32	13.3	15.2	0.14	8	0.08	7.74	1.00	108.78	79.77	99.13	11.77	273.00	29.33	9.37	0.57
11	Patos	PAT	71.004	40.761	973	7.2	5.1	6.97	33.1	16.1	15.1	0.24	4	0.08	8.04	0.64	110.78	79.77	100.87	11.77	280.00	27.64	8.12	0.14
12	Angustura	ANG	71.659	40.864	768	5.5	2	7.55	17.5	19.4	19.7	0.24	19	0.24	19.54	3.57	368.26	361.86	208.70	27.11	885.00	36.38	46.85	0.00
13	Huala Hue	HUL	71.509	41.644	828	6.7	6.7	8.85	126.6	14.3	17.7	0.47	8	0.1	5.83	0.86	878.24	209.71	93.92	7.16	1117.00	2.82	80.78	0.00
14	Lezana	LEZ	71.463	40.987	679	7	7	8.48	103.6	19.1	17.5	0.29	12	0.14	3.17	0.64	409.18	246.72	286.97	29.42	915.00	35.81	22.49	0.00
15	Redonda	RED	71.563	40.989	840	7.6	1.9	7.04	63.3	16.4	15.8	0.22	10	0.05	16.2	3.14	209.58	142.28	200.01	30.70	555.00	29.61	2.08	0.00
16	Mercedes	MER	71.573	41.003	818	20	5.2	7.29	48.9	18.3	9.2	0.30	31	0.17	7.28	1.29	134.73	127.47	182.62	24.30	425.00	40.33	2.08	0.00
17	Larga	LGA	71.570	40.041	830	17	5.5	7.42	48.8	17.4	16.5	0.06	-	-	-	-	-	-	-	-	-	-	-	-
18	Cofre	COF	72.742	46.214	560	17.5	7	7.38	38.7	12.8	12.8	0.06	-	-	-	-	-	-	-	-	-	-	-	-
19	X-667	X-667	71.907	45.833	718	9.5	3.3	7.82	72.5	12.9	12.8	0.20	-	-	-	-	-	-	-	-	-	-	-	-
20	Pedro Aguirre Cerda	PIG	72.115	45.147	274	16	7.1	7.23	31.4	12.8	12.2	0.16	-	-	-	-	203.59	30.74	81.84	10.98	-	-	-	-
21	Futalafú	FUT	71.860	43.186	324	10	4.7	7.52	50.3	16.2	14.6	0.30	-	-	-	-	342.31	56.79	93.81	22.46	-	-	-	-
22	Larga	LAR	72.803	47.478	270	17.3	9.6	7.8	68.3	13.5	13.2	0.15	-	-	-	-	-	-	-	-	-	-	-	-
23	Guanaco	GUA	72.396	47.106	440	7.15	4	8.58	496	14.8	14.8	0.59	-	-	-	-	-	-	-	-	-	-	-	-
24	Esmereida	ESM	72.596	47.425	291	17	6.3	8.09	98	15.1	15	0.10	-	-	-	-	-	-	-	-	-	-	-	-
25	Atraversado	ATR	72.219	45.786	368	10.5	3.3	7.78	71.3	14.3	14	0.22	-	-	-	-	-	-	-	-	-	-	-	-
26	Lobo	LOB	72.328	44.772	230	7	5.65	6.38	19.75	14	11.7	0.26	-	-	-	-	86.83	16.37	65.87	2.99	-	-	-	-
27	Leta	LET	73.165	41.578	72.4	2.5	2.05	6.01	19.7	19	18.8	0.56	-	-	-	-	58.88	22.36	131.74	13.47	-	-	-	-
28	Blanco	BLC	72.607	42.753	98	29	4.82	6.73	18.1	14.2	12.7	0.33	-	-	-	-	92.81	27.74	93.81	13.97	-	-	-	-
29	Castor	CAS	71.808	45.672	690	8.5	8.5	7.99	88.7	12.2	12.1	0.24	-	-	-	-	458.08	127.00	414.17	51.90	-	-	-	-
30	Tamango	TAM	71.902	43.344	415	5	4.4	6.91	53.5	12.6	12.3	0.36	-	-	-	-	350.30	60.78	111.78	17.96	-	-	-	-
31	Foitzick	FOI	72.089	45.636	276	4.6	2.6	8.09	22	16.3	15.3	0.33	-	-	-	-	-	-	-	-	-	-	-	-
32	Risaptrón	RIS	72.513	44.378	142	17	6.1	7.22	32.2	13.5	12.5	0.12	-	-	-	-	211.58	35.63	77.84	20.46	-	-	-	-
33	Tres Hermanos	TRE	72.483	46.844	266	11.9	1.5	8.17	309	17.6	17.4	0.17	-	-	-	-	2000.99	366.77	698.60	174.15	-	-	-	-
34	Mañiguales	MAN	72.146	43.300	130	19.5	3.6	6.84	12.88	15	14.9	0.28	-	-	-	-	-	-	-	-	-	-	-	-
35	Cisnes	CIS	72.604	47.281	436	6	5.5	8.64	507	14.6	14.5	0.25	-	-	-	-	-	-	-	-	-	-	-	-
36	Edita I	EI	72.429	47.244	572	7.75	4.1	8.31	136.7	13.6	13.7	0.13	-	-	-	-	-	-	-	-	-	-	-	-
37	Envidia	ENV	72.016	46.200	463	5	1.5	7.89	224	13.4	13.1	0.21	-	-	-	-	-	-	-	-	-	-	-	-
38	Mallinanez	TWI	72.963	51.181	93	8.6	1.6	8.2	530	11.1	11.3	0.16	-	-	-	-	-	-	-	-	-	-	-	-
39	Ave	AVE	72.924	51.106	117	10.5	1	8.68	449	12.6	12.3	0.43	0.028	0.69	7.1	-	2095.80	3009.98	2217.48	127.90	-	1034.94	1124.28	-
40	Flores	FLO	72.833	51.178	116	19	2.2	8.52	457	12.1	11.9	0.33	0.028	1.02	8.1	-	1896.20	287.84	3347.96	43.49	-	411.72	366.43	-
41	Primero	PRI	72.804	51.039	290	9	1.3	9.04	1503	11.3	9.3	0.29	0.019	0.63	10.6	-	2495.00	222.05	2391.40	63.95	-	566.82	1149.26	-
42	Brown	bro	67.498	54.994	5	4	0.9	8.51	114	13.3	11.4	0.48	0.038	1.22	12	-	2345.30	518.11	7956.84	716.24	-	1325.40	3416.56	-
43	Blanco	BNA	67.248	54.758	221	2.8	1.4	7.31	46.1	11.8	11.9	0.69	0.023	0.47	6.8	-	1546.90	139.81	913.08	30.70	-	908.04	237.35	-
44	Margeritta	MRG	67.247	54.756	120	14	4.3	8.05	150	12.3	12.3	0.08	0.013	0.45	0.07	-	139.72	600.35	304.36	20.46	-	211.50	25.14	-
45	Nothofagus	LNF	67.194	54.992	32	7	0.7	7.41	192	11.3	11.2	0.37	0.007	0.1	2.5	-	1347.30	0.58	260.88	7.67	-	141.00	520.50	-
46	Moat	MOA	66.793	55.042	17	3.7	0.65	7.04	184.1	9.5	8.6	0.53	0.027	0.57	0.6	-	648.70	1537.89	1087.00	25.58	-	1136.46	5.21	-
47	Lavendera	LAV	66.947	54.978	34	3.2	1.35	8.32	242	10.6	10.2	0.34	0.028	0.89	0.33	-	379.24	213.82	1130.48	23.02	-	1142.10	5.21	-
48	Verde	TOL	67.192	54.683	32	3.2	3.2	7.6	104.6	12.3	11.1	0.47	0.017	0.39	0.42	-	1946.10	337.18	695.68	17.91	-	479.40	624.60	-
49	Lake 1	Vicl	74.114	45.318	6	5.8	3	5.775	108	23.7		0.23	0.011	0.31	0.6	-	798.40	1110.24	304.36	15.35	-	183.30	210.28	-
50	Lake 2	DII	74.216	45.327	83	4.91	3	6.1	42	22.7	14.7	0.22	-	-	-	-	373.06	48.94	165.24	6.00	-	138.90	14.02	-
51	Lake 3	PIII	74.071	45.387	18	1.61	1.29	6	61	20.8	20.4	0.38	-	-	-	-	0.65	38.47	131.24	3.82	-	95.36	6.63	-
52	Lake 4	GIV	73.812	45.446	43	3.31	1.74	6.2	61	16.3	12.7	0.42	-	-	-	-	403.78	52.59	173.33	6.69	-	117.67	13.05	-
53	Lake 5	VV	74.082	45.483	48	7.66	3.32	6.4	61	16.8	13.5	0.28	-	-	-	-	496.24	41.54	114.37	4.67	-	63.31	17.44	-
54	Lake 6	QVI	73.926	45.515	31	4.31	1.1	5.2	73	15.3	9.1	0.48	-	-	-	-	479.79	36.17	120.04	6.58	-	83.07	136.70	-
55	Lake 7	QVII	73.846	45.383	63	2.57	1.22	3.9	132	22.4	15.4	0.52	-	-	-	-	0.87	57.86	143.85	5.69	-	89.67	23.19	-
56	Lake 8	QVIII	73.854	45.413	1	1.36	1.4	4.5	73	17.7	13.6	0.44	-	-	-	-	0.61	44.42	144.09	8.48	-	102.49	11.56	-
57	Edita II	EII	72.431	47.244	572	8.40	4.1	7.8	144	9	-	0.12	-	-	-	-	474.09	55.68	191.73	6.53	-	120.71	11.13	-
58	Al-Dabhan	ALD	72.481	47.272	989	4	4	7.6		10	-	0.11	-	-	-	-	928.45	314.66	210.80	15.82	-	29.95	59.26	-
59	Meche	MEC	72.486	47.150	980	14.00	10	7.7	108	8	-	0.21	-	-	-	-	876.47	86.27	92.63	24.77	-	23.64	103.63	-
60	Norita	NOR	72.500	47.164	1070	-	7	7.5	100	9.5	-	0.10	-	-	-	-	926.68	286.24	223.61	30.54	-	26.45	110.89	-
61	Compeanos	COM	72.503	47.272	1070	-	3	7.7	30	11	-	0.26	-	-	-	-	820.99	81.03	66.24	17.89	-	13.15	127.34	-
62	Erica	ERI	72.419	47.133	579	14.10	5.15	7.3	152	11	-	0.20	-	-	-	-	-	-	-	-	-	22.58	-	-
63	Condor	CON	72.392	47.875	583	7.90	4.25	6.9	139	15	-	0.14	-	-	-	-	1013.89	320.38	237.59	32.00	-	41.45	62.92	-
64	Henley	HEN	72.383	47.133	700	14.30	4	7.3	157	10	-	0.07	-	-	-	-	1235.26	480.66	214.57	27.11	-	42.32	68.60	-
65	Adelita	ADE	72.367	47.217	623	13.20	10.25	7.1	194	10.5	-	0.18	-	-	-	-	1060.32	396.01	203.37	20.05	-	41.87	85.59	-
66	Chela	CHE	72.419	47.214	608	29.40	8	7.4	290	8	-	0.17	-	-	-	-	153.72	49.01	98.44	14.79	-	44.94	120.79	-
67	Lake 2	II	72.820	47.225	383	15.24	5.05	7.248	46	13.42	11.4	0.50	-	-	-	-	1430.02	1133.60	420.64	40.17	-	70.37	65.71	-
68	Lake 3	III	72.754	47.184	955	3.11	3.109	7.82	46	9	8.7	0.60	-	-	-	-	390.43	78.34	58.67	7.21	-	14.30	3.99	-
69	Lake 4	IV	72.752	47.271	963	4.11	4.1148	7.07	15	10.1	8.9	0.34	-	-	-	-	330.03	91.31	58.05	4.87	-	9.57	25.14	-
70	Lake 5	V	72.766	47.327	1195	1.25	1.2497	7.07	5	8.1	7.3	0.17	-	-	-	-	140.38	27.41	46.08	4.11	-	11.68	15.69	-
71	Lake 6	VI	72.776	47.294	1103	8.50	6.71	7.14	8	7.1	6.45	0.32	-	-	-	-	78.72	8.37	20.74	2.85	-	7.69	16.22	-
72	Lake 7	VII	72.740	47.334	1038	8.81	7.62	7.07	2	7.58	7.8	0.46	-	-	-	-	105.50	13.77	32.08	2.62	-	8.10	47.81	-
73	Lake 8	VIII	72.750	47.209	728	27.43	7.01	7.07	21	8.2	7.7	0.05	-	-	-	-	0.67	14.23	29.62	2.31	-	7.43	7.65	-
74	Lake 9	IX	72.731	47.187	866	6.40	-	7.07	71	8.6	8.2	0.31	-	-	-	-	178.65	31.29	37.47	3.86	-	8.63	28.90	-
75	Lake 10	X	73.024	47.244	341	14.63	3.15	7.05	39	14.7	6.8	0.59	-	-	-	-	333.66	36.60	45.92	2.49	-	6.36	11.13	-
76	Lake 11	XI	73.171	47.114	748	6.04	6.035	7.01	2	15.4	12.2	0.65	-	-	-	-	276.11	100.42	45.51	5.10	-	12.00	17.75	-
77	Lake 12	XII	73.173	47.114	740	9.20	7.04	7	4	13.5	9.1	0.58	-	-	-	-	35.27	10.00	28.52	3.29	-	11.51	1.09	-
78	Lake 13	XIII	72.839	47.246	414	17.16	7.02	7.01	54	16.7	7.3	0.36	-	-	-	-	0.51	10.22	29.57	4.25	-	10.78	1.41	-
													-	-	-	-	425.56	121.34	61.38	4.16	-	13.97	25.49	-
Summary statistics																								
MAX			74.22	55.04	1466.00	29.40	10.25	9.04	1503.00	23.72	20.35	0.69	31.00	1.22	19.54	3.57	2495.00	3009.98	7956.84	716.24	7330.00	1325.40	3416.56	0.57
MEAN			71.98	46.11	512.07	9.93	4.33	7.28	122.93	14.14	13.10	0.29	5.68	0.35	6.55	1.82	574.72	242.63	434.72	33.74	983.13	165.38	171.16	0.08
MEDIAN			72.42	46.53	566.00	8.45	4.10	7.39	63.30	13.80	12.80	0.26	4.00	0.27	6.50	1.64	365.77	88.82	131.74	13.56	567.00	35.81	25.32	0.00
MIN			66.79	40.04	1.00	1.25	0.65	3.90	0.14	7.10	6.45	0.05	0.01	0.05	0.07	0.52	0.51	0.58	20.74	2.31	273.00	2.82	1.09	0.00
RANGE			7.42	15.00	1465.00	28.15	9.60	5.14	1502.86	16.62	13.90	0.64	30.99	1.17	19.47	3.05	2494.49	3009.41	7936.10	713.93	7057.00	1322.58	3415.47	0.57
Values pertaining to wheter data need normalisation (see text for explaination)																								
Minimum x 20			148.47	300.02	29300.00	563.01	192.00	102.80	30057.20	332.44	278.04	12.76	619.86	23.40	389.40	60.92	49889.82	60188.17	158721.96	14278.52	141140.00	26451.60	68309.37	11.42
Standard deviation			1.69	3.92	365.19	6.49	2.46	0.97	199.95	3.82	3.45	0.16	7.35	0.31	5.14	1.03	621.18	447.28	1109.08	92.46	1711.21	318.09	498.65	0.19
Transform on the basis that 1sd > mean									LOG				LOG				LOG	LOG	LOG	LOG	LOG	LOG	LOG	LOG
Transform on the basis that the maximum value > 20 x the																								

Figure 5.1: Summary Table showing the location, field and water chemistry measurements of the lakes sampled. Summary statistics for each variable are shown at the base of the table together with calculations to determine whether data sets required normalisation

in subsequent analysis. Assessment according to Birks (1996) indicated that 14 variables had skewed distribution (marked in Table 5.1), and were thus normalised for ordination techniques using the methods described in 4.4.2.2. The full data set, after appropriate environmental variables values were normalised, is given in Appendix 3. Histograms showing distributions for selected environmental variables in more detail are presented in Figure 5.2.

Bearing in mind that some lakes were without measured basal water temperatures and also that water chemistry data was incomplete the whole data set was subdivided into 4 subsets. This allowed analysis on separate sets to maximise the use of the data available. Table 5.2 outlines the environmental variables covered within each subset, the number of lakes they contain, as well as notations used for subsets and environmental variables during the subsequent statistical analyses.

Notation used	Number of lakes	Dec long	Dec Lat	Altitude	Depth	Secchi D	pH	Conductivity	Top water temperature	Basal water temperature	LOI	Ca	Mg	Na	K	Total Phosphorous	Total Nitrogen	Si	SO_4	Cl	$N\text{-}NO_3$
	n_t	Long	Lat	Alt	Depth	Secchi	pH	Cond	Tt	Tb	LOI	Ca	Mg	Na	K	TP	TN	Si	SO_4	Cl	$N\text{-}NO_3$
Environmental dataset																					
EN_1	78	√	√	√	√	√	√	√	√		√										
EN_2	68	√	√	√	√	√	√	√	√	√	√										
EN_{cat}	65	√	√	√	√	√	√	√	√		√	√	√	√	√						
EN_{nut}	27	√	√	√	√	√	√	√	√	√	√	√	√	√	√	√	√	√	√	√	√

Table 5.2 : Summary of the subsets of environmental data used during analysis, the number of lakes within each subset and the environmental measurements associated. Notations used for both subsets and environmental variables within the study are also shown.

EN_1 = All lakes
EN_2 = All lakes where basal water temperature was measured
EN_{cat} = All lakes where water cation data was measured
EN_{nut} = All lakes where water nutrient levels were measured

5.2.1.1 Trends within the environmental variables and water chemistry data

The results of regression analysis between environmental variables for all sites are shown in Table 5.3. The analyses conducted on each subset vary due to inclusion of different variables in different sub-sets. Three relationships showed an $r^2 > 0.75$ and a further nine had an $r^2 > 0.5$.

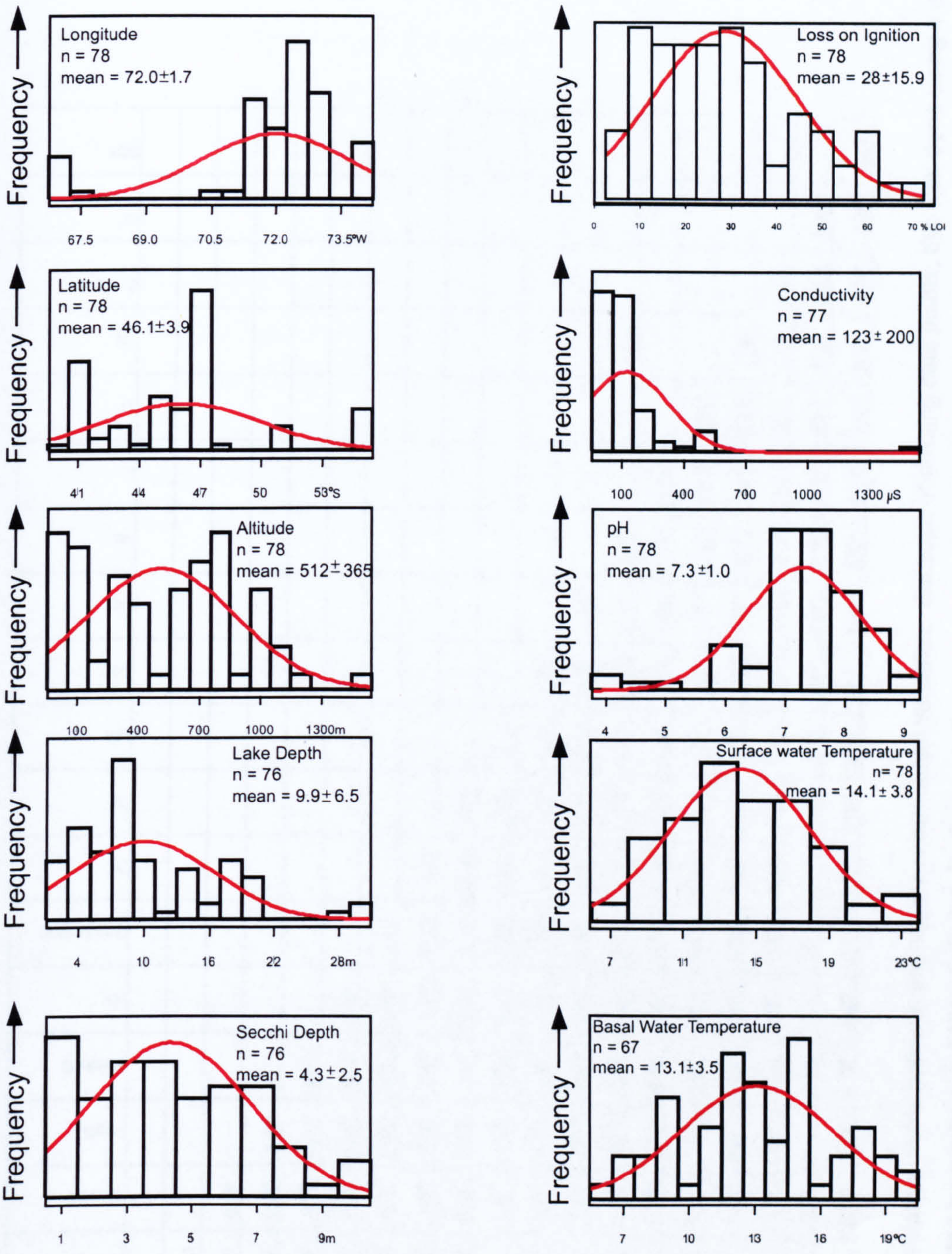

Figure 5.2: Histograms showing the distribution of selected lake characteristic measurements, together with summary data (sample size, mean and standard deviation)

	Dec long	Dec Lat	Altitude	Depth	Secchi D	pH	Conductivity	Tt	Tb	LOI	Ca	Mg	Na	K	TP	TN	Si	Cl	SO4
Dec Lat	-0.22‡																		
Altitude	0.02‡	-0.19‡																	
Depth	0.01‡	-0.02‡	0.15‡																
Secchi D	0.03‡	-0.09‡	0.27‡	0.36‡															
pH	-0.10‡	0.09‡	0.10‡	0.07‡	0.02‡														
Cond	-0.02‡	0.15‡	-0 07‡	0 00‡	-0.03‡	0.23‡													
Tt	0 05‡	-0.30‡	-0.05‡	-0.02‡	-0.03‡	-0.16‡	-0.01‡												
Tb	0.00▪	-0.30▪	0 00▪	0.00▪	0 00▪	0 00▪	0 00▪	0.55▪											
LOI	-0 01‡	0.09‡	-0.11‡	0.18‡	-0.11‡	-0.02‡	-0 01‡	0.00‡	-0.07▪										
Ca	-0.09†	0.05†	0.00†	0.04†	-0.01†	0.27†	0.26†	0 04†	-0.13*	-0.10†									
Mg	-0.06†	0 02†	0.00†	0.01†	-0.04†	0.08†	0 24†	0 00†	-0.02*	0.00†	0.23†								
Na	-0.11†	0.21†	-0.16†	0 00†	-0 21†	0.12†	0.47†	0.00†	-0.42*	0.00†	0.26†	0 40†							
K	-0 05†	0.01†	0.00†	0 07†	-0.03†	0.12†	0 25†	0.00†	-0.15*	-0.07†	0.27†	0.46†	0 65†						
TP	0.32*	-0 95*	0.73*	0 05*	0.36*	-0.13*	-0.30*	0.73*	0.51*	-0.24*	-0.48*	-0.02*	-0.54*	-0.08*					
TN	-0.02*	0.40*	-0.34*	-0 07*	-0.47*	0.13*	0 21*	-0.25*	-0 21*	0.23*	-0.39*	0.20*	0.57*	0.13*	-0.39*				
Si	0.58*	-0.34*	0.20*	0.37*	0.10*	0.00*	-0 04*	0.28*	0.17*	-0.26*	0.00*	-0.02*	0.00*	0.07*	0.24*	-0.09*			
Cl	-0 14	0 69	-0 64	-0.01	-0.47	0 05	0.37	-0.53	-0.55	0.16	0 39	0.13*	0.80*	0.39*	-0.70*	0.47*	-0.08*		
SO_4	0.00	0.23	-0.15	0.02	-0.02	0.34	0.44	-0.19	-0 06	0.00	0.90	0.01*	0.34*	0.20*	-0.34*	0.17*	0.01*	0.24*	
$N\text{-}NO_3$	-0.09*	0.37*	-0.25*	0.00*	-0.17*	0.00*	0.14*	-0.50*	-0.69*	0 06*	0.07*	0.10*	0.32*	0.13*	-0.38*	0.13*	-0.01*	0.50*	0.03*

Table 5.3 : Correlation matrix between the major environmental variables. Because of missing data points, this was done using 4 different data sets (denoted by symbols: ‡=ENV1, ▪=ENV2, † = Cation, * =Nutrient)

Total Phosphorous (TP) showed a strong correlation with other variables; $r^2 > 0.5$ when it was correlated against T_t, T_b, Alt, Lat and Na. However, it is important to note that the 27 samples in EN_{nut} upon which regression analysis was conducted only reflect two study areas within Patagonia: Bariloche and Tierra del Fuego (areas are annotated Figure 5.17c). Therefore, strong correlations within EN_{nut} may be driven by the strong contrasts in natural environment and levels of human impact between these two areas. TP concentrations are likely to be much higher in the Bariloche area than southern Patagonia, due to the more intensive land-use and higher population density (Stumm and Baccini, 1978). Strong correlations between Na and TP, and Na and TN, may again be a result of high Na values within the more concentrated waters of saline lakes (ENV, TWI, FLO, PRI and MAL) in Torres del Paine, where anthropogenic nutrient loading is low. Ascertaining a direct cause and effect relationships which would produce a high level of correlation between N-NO3 and Tb is difficult. However, the relationship may again be due to differing temperatures between the two aforementioned field areas analysed, due to the latitudinal, and thus thermal, difference between the two. Table 5.3 supports this, showing a weak negative relationship between both temperature datasets and latitude ($r^2 = -0.3$). Therefore, it is probably the case that some of the high r^2 gained through correlation using ENV_{nut} are not due to cause and effect between the variables measured. Rather independent differences in nutrient enrichment and climatic and geographic factors between the two areas are responsible.

A similarly strong gradient exists within the water Cl values measured at the 27 sites in the Bariloche and Tierra del Fuego areas. This difference in Cl is probably driven by higher aridity and/or maritime locations of the sites in Tierra del Fuego, relative to those near to Bariloche. Thus high correlations between Cl and Lat, Tt, Tb and TP are attributed to sampling distribution reasons similar to those discussed above with reference to TP.

5.2.2 Chironomid data

Within the whole training set, 46 chironomid taxa are encountered. These taxa covered less than the 50 genera which have been encountered in modern surveys to date in Patagonia, but also includes taxa that are have previously not been documented in such surveys of the area, such as *Microtendipes* and *Pseudochironomus* (Spies, *pers comm.*; Cranston, 2000; Cranston and Edwards, 1999; Brooks and Jackson, 2002). Head count sample sizes from surface samples range from 90– 293, with a mean of 138 head capsules examined per site. Figure 5.3 shows percentage data for all the lakes, with lakes ordered

along the y axis according to altitude. The complete, raw data set is presented in Appendix 4. The numbers at the base of Figure 5.3 indicate the maximum and mean percentage occurrence of each taxon within the data set, and also the number of lakes at which it is encountered. Visual examination of these results shows that assemblages are dominated by Orthocladiinae and Tanytarsini, with *Parapsectrocladius* and Tanytarsini Taxon E and Taxon B being particularly prominent. Certain taxa, such as *Polypedilum*, *Dicrotendipes*, *Pseudochironomus* and *Parakiefferiella* and Podonominae, have relatively low mean occurrences, but were particularly dominant in a few, specific lakes. The diagram indicates that there is no strong relationship apparent between taxon occurrence and changes in altitude. However, it appears that taxa to the left of the figure do tend to be present in lower abundances at higher altitudes, with the exception of altitudes between c. 600 and 900m. This trend suggests that altitude may be correlated to site assemblages, but that another variable or other variables may also be determining taxon distribution.

5.2.2.1 Exclusion of rare taxa

When the screening using the criteria proposed by Quinlan and Smol (2001) was conducted to detect rare taxa, the following taxa classified as "minor":

Chironomini Undif	Orthocladius Undif	*Procladius*
Cryptochironomus	Orthocladiinae (Cranston)	Orthocladiinae Taxon B
Stenochironomus	*Paratanytarsus*	Orthocladiinae Taxon A
Microtendipes Taxon A	*Clinotanypus*	*Gymnometriocnemus*
Orthocladiinae Taxon D	Orthocladiinae Taxon C	

Any taxonomic data set subsequently referred to as "major", or coded MAJ_{xxx}, meant that the above taxa are excluded from it. This brought the number of taxa within modern samples down to 34. Although this may sound low, such a value is similar to other transfer functions that have successfully used chironomids, eg. 38 Quinlan *et al* (1998), 32 (Brooks and Birks, 2000a) and 48 (Larocque *et al*, 2001).

5.3 TWINSPAN classification

TWINSPAN pseudospecies cut levels were set at 0, 2, 5, 10, 20 and 50%. These levels were selected so as to allow changes in minor taxon abundance to effect the classification, but still take into account the fact that 6 lakes (VER, PRI, VicI, NOR, COM, IX) were dominated by > 50% of a single taxon. The category for lowest abundances (0-2%) was downweighted to carry half the weight of the other categories.

5.3.1 TWINSPAN results

5.3.1.1 TWINSPAN classification of sites

To accompany the discussion of site classification, TWINSPAN classification results of modern samples are presented in several different ways. Figure 5.4 shows the raw TWINSPAN matrix produced during computer analysis. Figure 5.5 shows the hierarchical TWINSPAN classification in the form of a dendrogram, the lake group number assigned to each group classified and the site membership. Figure 5.6 indicates the mean taxonomic assemblage for each lake group. Figure 5.7 is a series of boxplots which show the range and mean of major environmental variables associated with each lake group.

Following five levels of classification, the 78 sites are classified into 17 groups (Figure 5.5). A major feature conveyed in Figure 5.5 is the difference in the sizes of site groups produced after five levels of TWINSPAN classification. At the third level of division, the midge assemblage at certain sites, such as VI, PIII and QVI, is so unique and distinct that these lakes are classified into individual groups on their own. Conversely, Group 9 contains 24 members, even at the fifth level of classification, indicating a statistically similar assemblage across all these sites. It is of interest that the two samples from Laguna Edita taken on different field trips (EI and EII), are classified into separate categories, even at the first level of classification: EI is placed on the positive of the primary sample dichotomy (*1), whereas EII is placed within *0, probably because of high levels of *Parapsectrocladius* in EII vs EI. EII was one of the samples collected with the grab, therefore this may be a possible explaination as to why there is such a discrepancy between the samples.

Mean taxonomic assemblages associated with groups and the manner in which they vary across the classifications is illustrated in Figure 5.6. Care must be taken to take into account the size of the groups when interpreting these averaged results, as group membership size varies from 1-24. Results substantiate those presented in Figure 5.3, in showing the ability of certain taxa to dominate certain site groups, in particular Tanytarsini Taxon E, Tanytarsini Taxon B, *Ablabesmyia*, *Parakiefferiella* and *Parapsectrocladius*. The graph also indicates that these taxa occur across a large range of lake groups, especially *Parapsectrocladius* which is encountered in all but one of the TWINSPAN groups, Group 17, which contains only one site.

Groups 1-5 (*01) are characterised by high levels of *Parapsectrocladius* and groups 6-9 (*010) by Tanytarsini Taxon E and B (Figure 5.4 and Figure 5.5). Groups 10-13 (*011), contain a

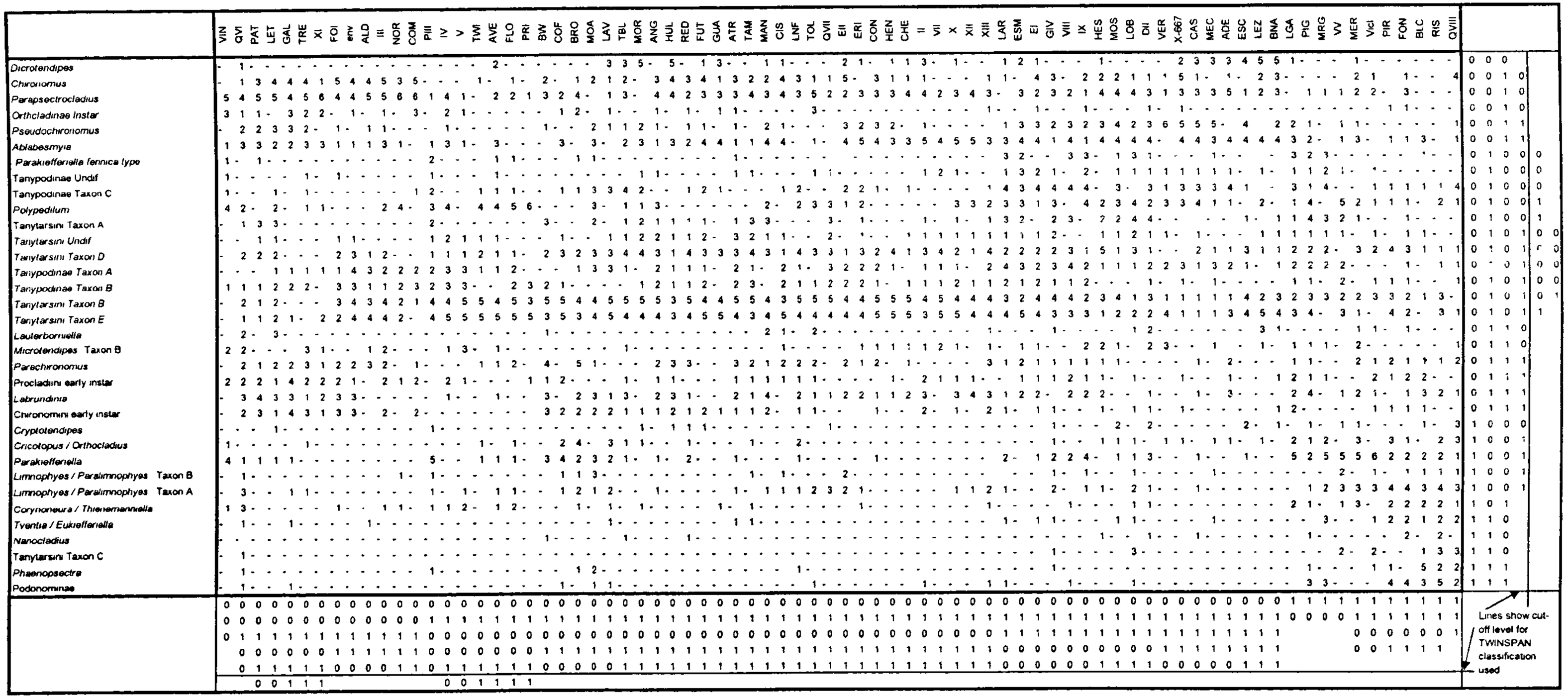

Figure 5.4 : TWINSPAN two-way Table of showing ordination of Patagonian training set based on the taxa and sites. pseudo-species cut levels (1) = 0-1%, (2) = 2-4% (3) = 5-9%, (4) = 10-19%, (5) = 20 – 49% and (6) = 50-100%

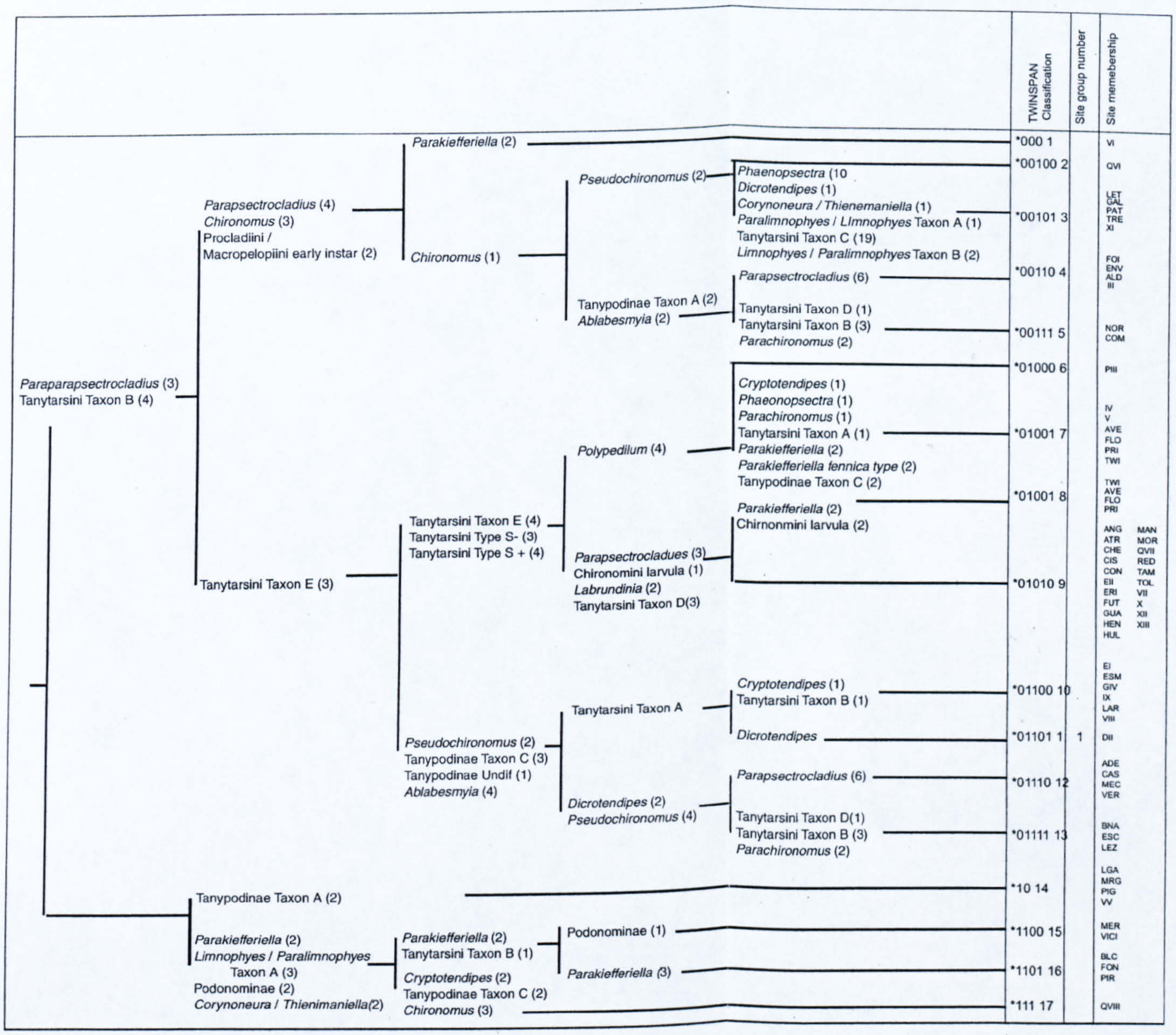

Figure 5.5 : Dendrogram showing TWINSPAN classification of sites based on modern taxa assemblages. Taxon names and numbers are the TWINSPAN indicator taxa with their pseudo-species cut levels (1) = 0-1%, (2) = 2-4% (3) = 5-9%, (4) = 10-19%, (5) = 20 - 49% and (6) = 50-100%. To the right of the dendrogram, the TWINSPAN classification groups and the site group numbers are given, together with the site membership

KEY
+ 0-1%
+ 1-3%
o 3-5%
• 5-10%
● 10-20%
● 20-50%
● >50%

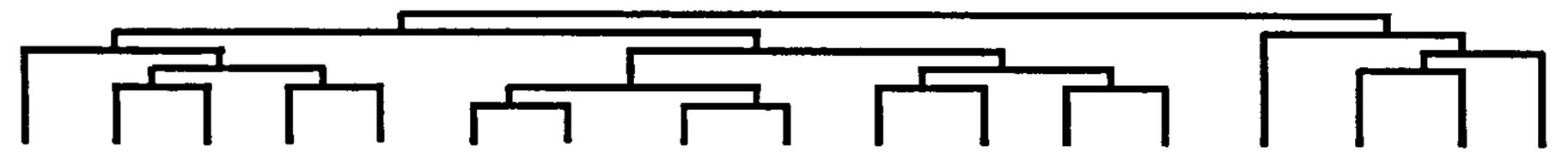

	1	2	3	4	5	6	7	8	9	10	11	12	13	14	15	16	17
Number of lakes in group →	1	1	5	4	2	1	6	5	24	6	4	5	3	4	2	4	1
Dicrotendipes		+					+	+	o	+	+	•	●	+	+		
Chironomus		+	•	●	●		+	+	o	o	+	•	o		o	+	●
Parapsectrocladius	●	•	●	●	●	+	o	•	•	o	●	●	o	+	o	o	
Orthocladini early instar	•	+	o	+	o		+	+	+	+	+	+				+	
Pseudochironomus		o	o	+			+	+	+	o	•	●	•	+	+		+
Ablabesmyia	+	•	•	+	+	+	+	o	●	•	●	●	●	o	o	o	+
Parakeifferiella fennica type	+		+			o	+	+		o	+	+		o		+	
Tanypodinae Undif	+		+	+		+			+	o	+	+	+	+	+		
Tanypodinae Taxon C	+		+		+	o		o	+	●	o	•	+	•	+	+	●
Polypedilum	●	•	+	+	•	•	●	+	+	•	•	•	+	•	o	+	+
Tanytarsini Taxon A		+	o			o		+	+	o	•		+	•	+	+	
Tanytarsini Undif		o	+	+		+	+	+	+	+	+	+	+	+	+	+	
Tanytarsini Taxon D			+	o		+	+	•	•	+	•	+	o	o	o	•	+
Tanypodinae Taxon A			+	•	+	o	+	o	+	•	o	•	+	o		+	+
Tanypodinae Taxon D	+	+	+	o	•	o	o	+	+	+	+	+		+	+	+	+
Tanytarsini Taxon B		o	+	●	+	●	●	●	●	•	•	+	•	o	•	•	
Tanytarsini Taxon E		+	+	●	+	●	●	•	●	●	o	•	●	•	+	•	+
Lauterborniella		o	+					+	+	+	+		o		+	+	
Microtendipes Taxon B	o	o	+	+			+		+	+	+	+	+	+	o		+
Parachironomus		o	o	o	+		+	•	o	+	+	+		+	+	+	o
Procladiini / Macropelopiini early instar	o	o	o	+	o		+	+	+	+	+	+	+	+	o	o	
Labrundinia		•	•	o			+	o	o	o	+	+		o	o	o	+
Chironomini early instar		o	•	o	+			+	+	+	+	+	+	+	+	+	
Cryptotedipes			+			+			+	+	+		+	+	+	+	•
Cricotopus / Orthocladius	+		+				+	o	+	+	+	+	+	o	o	o	•
Parakiefferiella	●	+	+			●	+	•	+	•	o	+	+	●	●	o	+
Limnophyes / Paralimnophyes Taxon B		+			+	+		+	+	+	+	+		+	+	+	+
Limnophyes / Paralimnophyes Taxon A		•	+			+	+	+	+	+	+	+		o	•	●	•
Corynoneura / Thienimanniella	+	•		+	+	+	+	o	+	+	+			+	o	o	+
Tvenitia / Eukiefferiella		+	+	+				+	+	+	+	+		+	+	o	o
Nanocladius								+	+		+	+		+		+	
Tanytarsini Taxon C		+								+	o			+	+	+	•
Phaenopsectra		+				+		+	+	+				+	+	●	o
Podonominae		+	+					+	+	+	+			o		●	o

Figure 5.6 : TWINSPAN classification of the surface sediment chironomid assemblages and mean abundance of major taxa within each group. The row order of taxa is in accordance with that produced through TWINSPAN classification of the samples. The dendrogram to the top indicates the levels at which groups were classified.

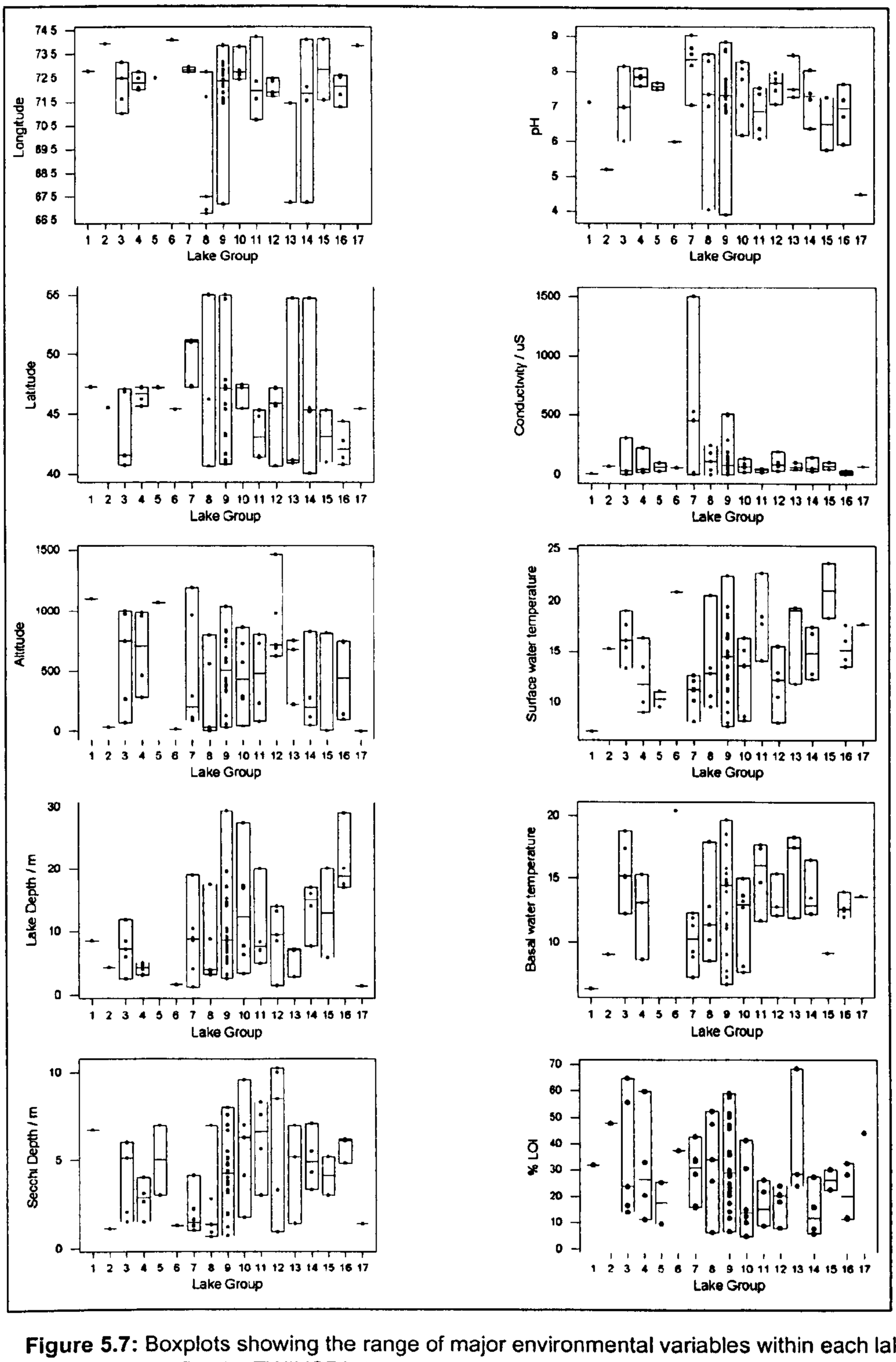

Figure 5.7: Boxplots showing the range of major environmental variables within each lake group, as classified by TWINSPAN. Details of group membership is in Figure 5.5.

larger range in the composition than their negative counterpart, *010. Within groups 10-15, there are mean levels of > 5% of *Parapsectrocladius, Ablabesmyia* and Tanytarsini Taxon E. Lakes in groups 14-17 have high levels for *Parakiefferiella* and *Paralimnophyes / Limnophyes* Taxon A, relative to other taxa within the groups.

In general taxa are fairly well distributed across all the groups (Figure 5.6). The absence of a taxon from a lake group is often accompanied by low group membership, indicating the potential statistical influence of low sample numbers on the mean taxonomic assemblage values. However, certain taxa are absent from lake groups which have larger sample sizes. For example, 10 of the major 34 taxa are not present in Group 7 (n=6). Furthermore, even with 24 members, the morphotaxon Tanytarsini Taxon C is not encountered within Group 9.

Figure 5.7 shows that a large range in environmental variable values is often associated with each lake group. Groups where the ranges are smaller are often coincidental with small membership. For example, in Group 5, where n=2, the small ranges in environmental variables such as pH and conductivity associated with the group may be due to a small size. Although environmental variable ranges are usually large, some TWINSPAN site groups seem to be represented by certain environmental characteristics. Group 16 only contains lakes >15 m deep, with generally large Secchi depths and low conductivity. Conversely, Group 4 is dominated by shallow lakes, less than 5.0 m deep, all of which had a pH of between 7.6 and 8.09.

It is interesting to note that groups with single lake membership are often associated with extreme values in one or more environmental variables (Figure 5.7). The three, sole lakes in groups 2, 6 and 17 are all from the far west of the training set in the Chonos – Taitao region and together span only 2° latitude (QVI, PIII and QVIII). These lakes are all from the Chonos region. Lake PIII (Group 6) also has the highest temperature (24°C), is located at the low altitude of 18m a.s.l and is the fourth shallowest lake sampled (1.6m). Group 2 and group 17's sole members are also located at the very low altitudes of 31m (QVI) and 1 m a.s.l (QVIII), respectively. Additionally, relatively acidic conditions were also recorded at QVIII (pH = 4.5). Lakes from higher elevation were often also grouped into individual or small groups via TWINSPAN. VIN, the sole member of Group 1, was at high elevation (1103m a.s.l.) and had cold Tb and Tt (7.1°C and 6.5°C). Group 5 contained two lakes,

located close together in the Chacabuco Valley (COM, NOR) which were both at a high altitude of 1070m. Thus there does appear to be a negative relationship between TWINSPAN group size and the amount that environmental variables values associated with group's sites deviate from mean averages associated with the respective variable.

5.3.1.2 TWINSPAN Classification of taxa

Figure 5.8 shows the hierarchical classification of major taxa within the Patagonian training set after four levels of division. The TWINSPAN split at the first level places 11 taxa in the*1 group and the remaining 23 in *0. In general, *1 members are Tanytarsini, Tanypodinae and Chironomini, whereas *0 is predominantly composed of Orthocladiinae and contains no Tanypodinae. The only Tanytarsini morphotaxon present within *0 is Tanytarsini Taxon C.

Taxa to the negative side of the primary sample dichotomy (i.e. those within *00, *0010, *0011) are taxa that have a high level of presence across the training set (Figure 5.4). Abundances are often high, with the exception of Orthocladiinae early instar, which registers no pseudospecies scores > 3 (>10% relative abundance). Occurrences of taxa within *0100 are less frequent across the training set and tend to be at lower pseudospecies levels than those within *00. However within *0100, Tanypodinae Taxon C occurs at pseudospecies level 4 (>20%) on eight occasions, and *Polypedilum* is present at levels 6 and 5 in one and two sites, respectively. Group *0101 contains taxa that are present in the majority of the samples across the whole training set. Within this class, the most ubiquitous taxa are Tanytarsini Taxa B and E, which occur in 73 and 72 of the 78 lakes, respectively. Additionally, pseudospecies levels of taxa within this TWINSPAN group are generally high (Figure 5.4). As well as having the presence in the highest number of lakes, the aforementioned Tanytarsini are regularly present at pseudospecies levels of 4 and 5, as is Tanytarsini Taxon D too. Groups *0110 and *011 are totally composed of Tanypodinae and Chironomini. Pseudospecies levels of taxa within *0110 and *0111 are generally lower (1-4). Levels of presence within this class are similar to those in *0100, although these taxa occur in lakes that are positioned closest to the negative end of the primary sample dichotomy (*0) as apposed to those in the positive side (*1).

In general, taxa within *1 are present in fewer lakes than those within *0; taxa within *0 are, on average, present in 68% of training set sites where as for taxa within *1 this drops to taxa being present in a mean average of 28% of samples. Generally, within the *1 classes, taxa do not tend to be present in such high pseudospecies levels, with the exception of

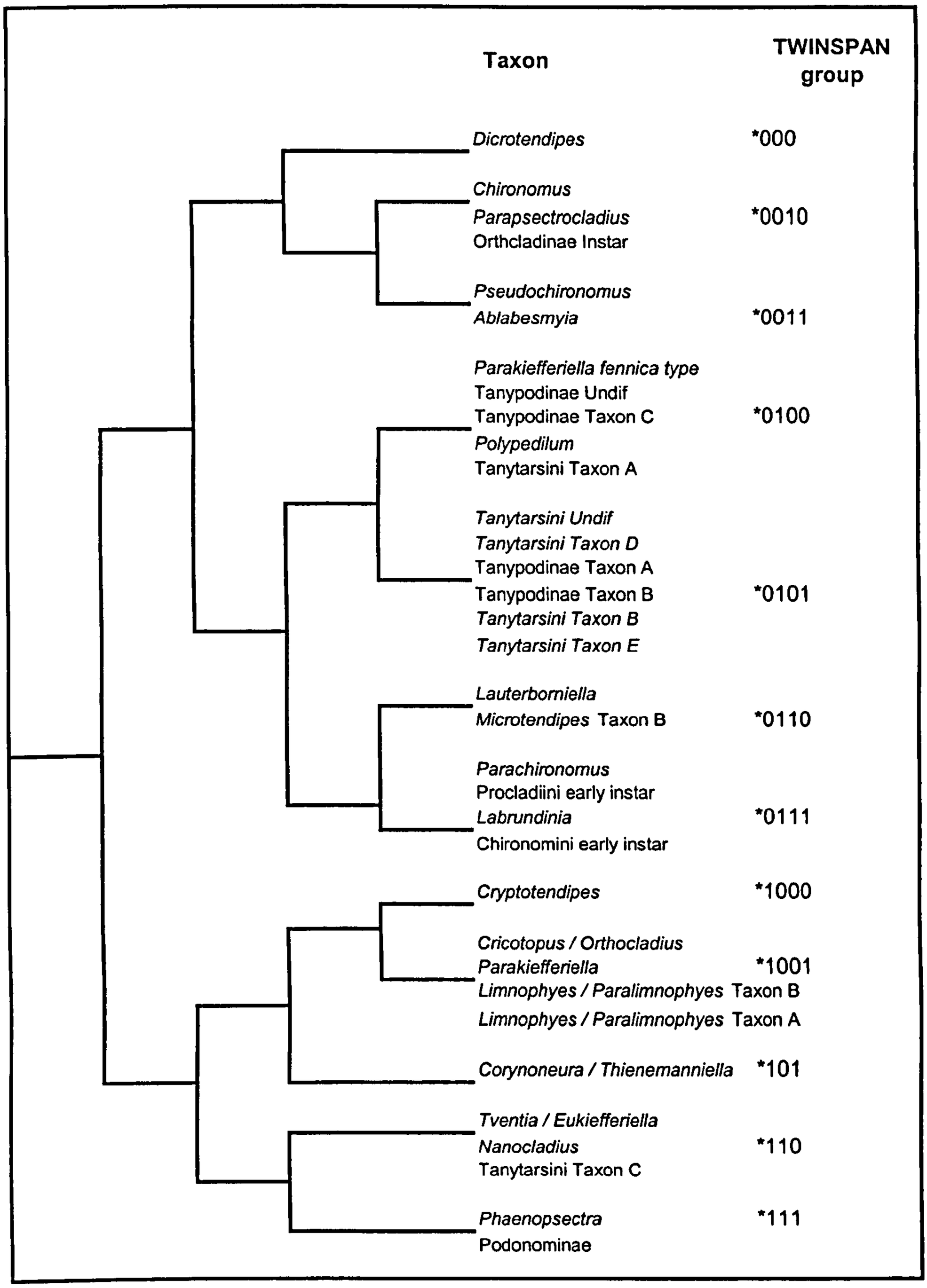

Figure 5.8: Dendrogram showing TWINSPAN classification of taxa to four levels.

Parakiefferiella. This taxon, and others within *1001 and *100 sub-groups, tend to have a more diverse range of occurrences, whereas occurrences of taxa within *110 and *111 are more restricted to the negatively classified sites. *Phaenopsectra* and Podonominae, the only taxa within *111, both occur in higher abundances than taxa within *110, with pseudospecies levels of both of these taxa reaching 5.

5.3.1.3 Discussion of TWINSPAN results

Examination of results obtained from TWINSPAN provides valuable insight into the Patagonian midge dataset. The first finding worthy of discussion is the variety in group sizes classified using the technique. The large number of sites within certain lake groups, such as Group 9, can be explained by three hypotheses. One possibility is that the taxa present in these lakes are cosmopolitan, with wide tolerances, thus resulting in their ability to colonise a wide range of lentic environments. Alternatively, the taxonomy used in this study may be insufficiently detailed or precise to have sufficiently distinguished between different taxa. This results in the grouping of individual taxa into larger taxonomic groups, which collectively may exhibit a larger environmental tolerance with an associated weighted mean average optima based on the individual taxon's optima. The final possible hypothesis is that that the identification is sufficiently precise, and that the taxa have a tolerance range that is not unusually wide, but that the lakes sampled are all similar in terms of their ecological systems, and therefore all determine the presence of a similar faunal assemblage. This explanation is weakened by the large range of environmental variables associated with the large groups such as Group 9 (see Figure 5.7). The fact that taxa such as Tanytarsini E, B and D occur across so many groups, often in high proportions (Figure 5.3 and Figure 5.6), may be interpreted as favouring the first two explanations, as a large range in the environmental variables measured were covered by the training set in general. However, it may be that the midges are responding to another environmental variable, not included measured in this study, and that this variable is determining the differences in group sizes.

The lack of particularly tight grouping of any one environmental variable associated with TWINSPAN lake groups, indicates that there does not appear to be a strong correlation between the lake groups, as determined by the faunal assemblages, and any single environmental variable. Moreover, the large range in many of the environmental variables associated with most groups, illustrated in Figure 5.7, suggests further that the environmental variables measured may not be particularly well correlated with the

assemblages on the whole. Alternatively, the spot measurements, associated with many of the environmental variables, may have produced unrepresentative results, obscuring relationships which may in reality exist. However the small ranges, and thus consistent environmental characteristics, in pH and conductivity (Group 4) and lake depth (Groups 16 and 4) suggest that, in certain circumstances, these factors may be partially controlling the assemblage present at these sites. Furthermore, the extreme environmental variables measurements associated with the occurrence of these more unusual taxonomic assemblages, and the resultant small TWINSPAN group size (Figure 5.6 and Figure 5.7), indicates that in extreme conditions environmental factors are exerting some control on sites' fauna to a certain extent. This may be because the combination of environmental conditions at such sites is relatively unique, when compared to the training set as a whole, resulting in the presence of the unusual assemblage.

In general, a broad scale correlation between tribe and TWINSPAN classification was indicated. Tanytarsini and Chironomini were prevalent in *0, as were Tanypodinae, although to a lesser extent; Orthocladiinae were found within both *0 and *1, whilst members of Podonominae were much more common in *1. This indicates that generalised statements about evidence of environmental preferences at tribe level discussed in Walker (1987) and Walker and MacDonald (1995) may hold true in the Neotropical region. It is interesting to note that, with the exception of Tanytarsini Taxon C, TWINSPAN classified all Tanytarsini together within the first two levels (*01). This indicates that the majority of Tanytarsini morphotaxa encountered tolerate similar sorts of environments and, therefore, will colonise the same sites.

The main findings of TWINSPAN can therefore be summarised in the following points:

- In general, TWINSPAN groups tend not to be characterised by a small ranges in environmental variables;
- The exception to this is in very extreme environments, although the significance of these 'groups' is hard to assess due to small group size;
- The Patagonian fauna may be responding in a fairly cosmopolitan manner or, alternatively, the taxonomy of this study has not been able to split taxa to a level so as to reveal specific environmental optimum conditions and tolerances;
- There seems to be some correlation between the composition of assemblages present (at tribe level) and TWINSPAN groups.

5.4 TRANSFER FUNCTION PRODUCTION: REGRESSION STAGE

5.4.1 Unconstrained ordination

5.4.1.1 Minimising Noise in the taxonomic data set

Table 5.4 shows the results of DCA when taxonomic datasets underwent log and square root transformations, in addition to results when the analysis was conducted using the untransformed data set. In this, and all subsequent ordinations, detrending was by segments and rare taxa were downweighted. Results indicate that square-root transformation was most appropriate. This method results in the highest percentage variance explained by axis 1 and 2, and also has the lowest total inertia. Therefore,

		Cumulative Variance		Eigenvalue		Grad / S.D.		Total Inertia
		Axis 1	Axis 2	Axis 1	Axis 2	Axis 1	Axis 2	
TOT_{incl}	No log	15.0	24.5	0.361	0.230	2.737	2.519	2.410
	Sqrt	16.4	25.7	0.225	0.126	2.199	2.024	1.370
	Log	15.1	24.8	0.341	0.218	2.589	2.417	2.253
MAJ_{incl}	No log	15.5	25.5	0.356	0.231	2.713	2.472	2.309
	Sqrt	18.6	29.3	0.218	0.127	2.110	2.034	1.240
	Log	15.7	25.5	0.337	0.212	2.601	2.442	2.150

Table 5.4: Summary statistics for DCA performed on whole data set, using non transformed and transformed taxonomic data sets. All analyses were detrended by segments with rare species downweighting.

taxonomic data were square root transformed in all subsequent analyses. Comparisons of DCA analyses of both full (TOT_{incl}) and major (MAJ_{incl}) taxonomic data sets indicates that there was less noise when minor taxa were excluded.

Examination of the CA plots indicates that some elements of a curve appear to be present in the ordination (Figure 5.9). This indicates that detrended ordination techniques are most appropriate.

5.4.1.2 DCA and gradient length

DCA results of both MAJ_{incl} and TOT_{incl} taxonomic datasets are shown in Table 5.4. In all analyses Axis 1 is > 2 s.d., indicating that taxa are likely to be responding in a unimodal manner to environmental controls (Birks, 1995) and, thus, that unimodal ordination and

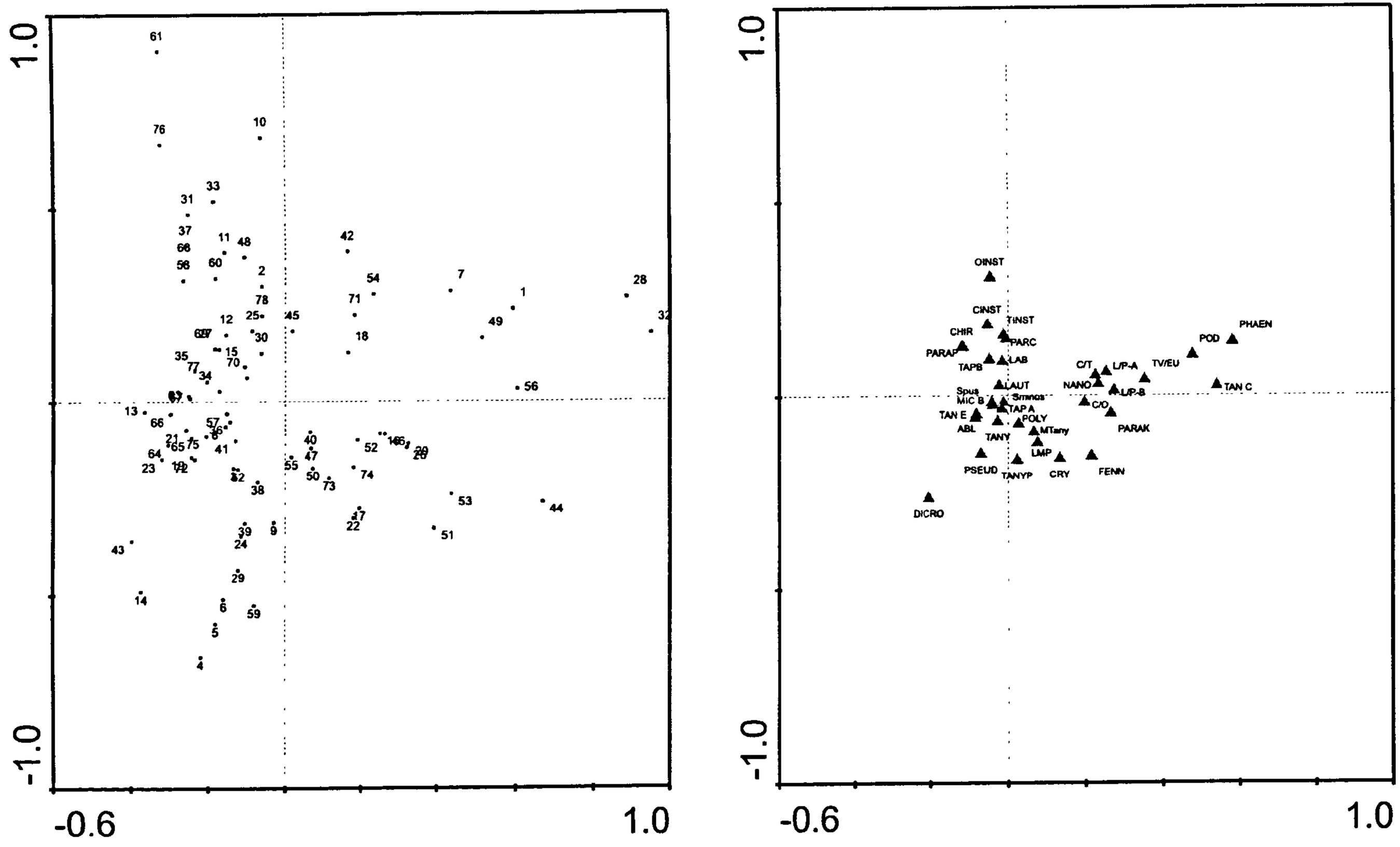

Figure 5.9 : Bi-plot of CA (a) taxa and (b) sites within training set. CA performed using down-weighting of rare taxa and square-root transformation of taxonomic data on MAJincl. See Appendix 5 for taxa codes.

calibration methods would be most appropriate. However, as these gradients are so close to 2, investigating statistical techniques based on linear responses may still be valuable (Birks, 1995; Lepš and Šmilauer, 2003; see 4.4.2.2).

The percentages of variance in the taxonomic data sets were fairly low (< 30% for axis 1 and 2 combined). However, a high result is not to be expected due to the high number of zero values in the taxonomic data (Jongman *et al.*, 1995). The percentage of variance explained was higher when data sets containing only major taxa were used. This correlates with the accompanying reduction in total inertia discussed in 5.4.1.1.

A potential reason for such low percentage variance explained DCA scores being produced is that up to 7% of the assemblage at some sites contained taxa only identified to tribe level (Chapter 3). It may be expected that this, which effectively results in unintentional taxonomic harmonisation, might result in a loss of precision as different taxa, with a range of different environmental optima, are amalgamated together (Birks, 1994; Velle *et al.*, *in press*). To try to assess the impact of this, taxonomic percentages were recalculated, omitting these results, to form the taxonomic datasets MAJ_{excl} and TOT_{excl}. Recalculated results are shown in Table 5.6 relative to comparable results before the exclusion of Tanytarsini and Tanypodinae Undif. Although the results show some improvements, they are minimal.

5.5 Constrained Ordination

	Parameter			TOT_{incl}	MAJ_{incl}
CCA	Cumulative percentage variance	of species data	Axis 1	9.9	11.5
			Axis 2	13.9	15.4
		of species-environment relation	Axis 1	37.4	41.0
			Axis 2	52.5	55.0

Table 5.5: Table showing the results of CCA undertaken on both the TOT_{incl} and MAJ_{incl} taxonomic data sets against EN_1.

As DCA produced gradient lengths that were close to 2, both CCA and RDA were conducted to investigate both unimodal (CCA) and linear (RDA) taxonomic response to variations in environmental variables (Birks, 1995). CCA consistently outperforms RDA, in that larger percentage variances are explained by variables in the former (Table 5.6). This underlines the results from DCA (5.4.1.2) that many of the taxa in the training set are responding unimodally to the environmental gradients. As was the case with DCA, the

				Including Unidentified Tanypodinae and Tanytarsini				Excluding Unidentified Tanypodinae and Tanytarsini			
				EN_1		EN_2		EN_1		EN_2	
				TOT_{incl}	MAJ_{incl}	TOT_{incl}	MAJ_{incl}	TOT_{excl}	MAJ_{excl}	TOT_{excl}	MAJ_{excl}
Initial No of sites				78	78	68	68	78	78	68	68
Initial No of taxa				53	34	53	34	52	32	52	32
Initial no of environmental variables				9	9	10	10	9	9	10	10
Analysis	Parameter										
DCA	Cumulative Variance		Axis 1	16.4	18.6			16.9	18.6		
			Axis 2	25.7	29.3			25.5	29.3		
	Eigenvalue		Axis 1	0.225	0.218			0.233	0.218		
			Axis 2	0.126	0.127			0.118	0.127		
	Grad		Axis 1	2.199	2.110			2.32	2.110		
			Axis 2	2.024	2.034			1.69	2.034		
	Total Inertia			1.370	1.240			1.377	1.176		
CCA	Eigenvalue		Axis 1		0.134		0.146		0.136		0.148
			Axis 2		0.046		0.055		0.046		0.056
	Cumulative percentage variance	of species data	Axis 1		11.5		12.4		11.8		10.9
			Axis 2		15.4		17.1		15.8		14.8
		of species-environment relation	Axis 1		41.0		39.8		41.6		39.6
			Axis 2		55.1		54.9		55.7		53.7
	Species-environment correlations		Axis 1		0.815		0.838		0.811		0.799
			Axis 2		0.750		0.777		0.745		0.739
RDA	Eigenvalue		Axis 1		0.101		0.113		0.105		0.112
			Axis 2		0.048		0.052		0.048		0.051
	Cumulative percentage variance	of species data	Axis 1		10.1		11.3		10.3		11.2
			Axis 2		14.9		16.5		15.1		16.3
		of species-environment relation	Axis 1		37.6		37.9		38.0		38.2
			Axis 2		55.2		55.5		55.7		55.5
	Species-environment correlations		Axis 1		0.800		0.833		0.799		0.828
			Axis 2		0.722		0.745		0.721		0.743

Table 5.6: Comparison of DCA , CCA and RDA on all lakes using EN_1 and EN_2, MAJ_{incl}, MAJ_{excl}, TOT_{incl} and TOT_{excl}

analysis performs marginally better when Tanytarsini and Tanypodinae Undif (MAJ_{incl}) were retained in the taxonomic dataset (Table 5.5).

Variance inflation factors (VIF's) generated during forward selection are all <20, thus it is not necessary to exclude any of them from future analyses to reduce autocorrelation within the data set (Brooks *et al.*, 2001). Comparisons of the CCA and DCA axes indicate that the length of CCA axes are notably shorter than those gained during DCA (Table 5.6 and Table 5.5). In line with this, eigenvalues produced during constrained ordination are also notably smaller. Both of these characteristics indicate that a significant proportion of the total taxonomic variance in the datasets cannot be explained by the environmental variables measured.

When CCA bi-plots produced using both EN_1 and EN_2 and MAJ_{incl} and MAJ_{excl} are plotted it can be seen that pH and altitude consistently plot close to CCA axis 1 (Figure 5.10). This indicates that out of the environmental variables measured, they vary most closely with the axis of maximum turnover in the faunal assemblage. When EN_2 is used, depth plots in almost the opposite direction from these two variables (Figure 5.10). This inverse relationship may be explained by the existence of shallower, more saline lakes being present towards the steppe region of Patagonia, where local relief is and precipitation values are lower. Although not tightly grouped, there is a general agreement in terms of the direction in which LOI, temperature measurements and Secchi depth increase. These are encouraging results, since these factors would be expected to increases with temperature in general. The position of sites and taxa, relative to each other and the environmental variables within the ordination, are similar on all four of the bi-plots in Figure 5.10. The graphs consistently show taxa with optima to the left of axis 1, i.e. axis 1 scores < 0, being more closely grouped than those with scores > 0. This could be either because the optima for these taxa may be similar or it may be that an inadequate range of lakes has been sampled in this part of the environmental gradient to allow a more accurate estimation of taxon optima. The sample, or site, ordination scores plot over a much larger range than those of the taxa. These bi-plots indicate that many of the taxa, especially those grouped around the origin, have calculated optima close to average environmental variable values within the dataset.

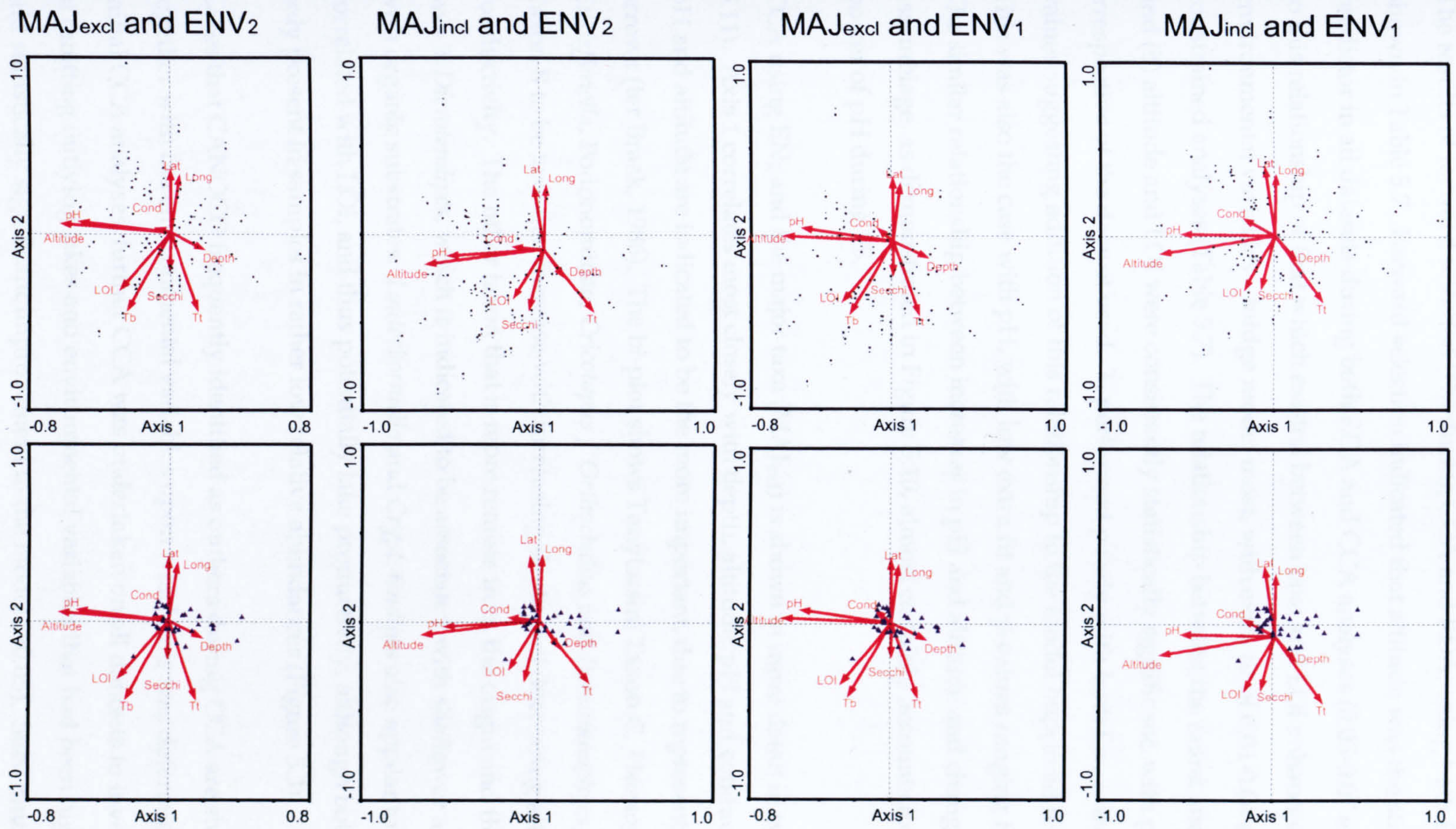

Figure 5.10 : Initial CCA Bi-plots of the four different CCAs run using EN_1 and EN_2 and both including and excluding Tanypodinae and Tanytarsini Undif (Maj_{incl} & MAJ_{excl}). The graphs show the same major trends are brought out in all the analyses. Sites are shown on the top graphs, taxa on the lower graphs - taxa are not labelled due to close grouping. See Figure 5.11 for a more detailed example (EN_2 vs MAJ_{incl}).The graphs show the same major trends are brought out in all the analyses.

The results of forward selection (FS) during CCA and RDA, using both EN_1 and EN_2, are shown in Table 5.7. Forward selection indicated that altitude was the strongest sole predictor in all datasets during both RDA and CCA analyses (0.05-0.07 extra fit). Addition to this relationship of that which existed between taxa and LOI enhanced the environmental variables – midge model most, with extra fit of 0.04-0.06 across all constrained analyses (Table 5.7). The relationship between the fauna and (a) just altitude and (b) altitude and LOI were consistently statistically significant, with p values < 0.005 irrespective of the dataset used. T_t performed poorly with both low extra fit values and p-values suggesting addition of this relationship to the model improved it little (0.003-0.385). This was also the case with pH, with low extra fit and p-values ranging from 0.014-0.82. The similar relationship between increases in pH and altitude and changes in the faunal assemblage, as demonstrated in Figure 5.10, almost certainly accounts for the poor additive power of pH during FS.

CCA using EN_2 and the major taxa (MAJ_{incl}) is shown in more detail in two bi-plots (Figure 5.11). Axis 1 correlates most closely with depth, altitude, pH and conductivity. Of these, pH and altitude are indicated to be the more important, due to representation by longer arrows (ter Braak, 1986). The bi-plot shows Tanytarsini Taxon C, *Phaenopsectra, Tventia / Eukiefferiella*, Podonominae, *Cricotopus / Orthocladius* and *Paralimnophyes/ Limnophyes* Taxon B to be taxa that increase with increasing depth and decreasing altitude and conductivity. The other taxon that is more remote from the origin and the main group of taxa is *Dicrotendipes*, which is indicated to be associated with shallower and warmer lakes with organic substrates. *Lauterborniella* and *Cryptotendipes* also appear to be positively correlated with LOI, and thus potentially lake productivity, although both of these taxa are only present in samples in rather low relative abundances (Figure 5.3)

Lakes that CANOCO frequently identified as outliers during CCA are shown in Table 5.8, together with the environmental variables upon which this was determined. Following initial CCA analyses, further CCA was undertaken on all datasets to investigate the effect of omitting outlying lakes and environmental variables that had been highlighted to not add statistically significant improvement to the model (>0.05). Such omission did not improve the extent to which the dominant environmental variables explained the variation in taxonomic assemblage.

	Including Tanytarsini and Tanypodinae Undif						Excluding Tanytarsini and Tanypodinae Udnif					
	All lakes (CCA:73 lakes, 34 taxa)			Lakes with bottom temperatures (CCA :66 lakes 34 taxa RDA :67 lakes 34 taxa)			All lakes (CCA: 73 lakes, 32 taxa)			Lakes with bottom temperatures (CCA : 67 lakes 32 taxa)		
CCA	Environmental variable	Extra Fit	p Value	Environmental variable	Extra Fit	p Value	Environmental variable	Extra Fit	p Value	Environmental variable	Extra Fit	p Value
	Alt	0.07	0.002	Alt	0.07	0.0020	Altitude	0.07	0.0020	Altitude	0.07	0.0020
	LOI	0.05	0.002	LOI	0.06	0.0020	LOI	0.05	0.0020	LOI	0.06	0.0020
	Cond	0.05	0.002	Cond	0.04	0.0020	Cond	0.05	0.0020	Cond	0.04	0.004
	Depth	0.04	0.004	Depth	0.04	0.0020	Depth	0.04	0.0020	Depth	0.04	0.0020
	Dec Lat	0.03	0.004	Dec Lat	0.03	0.004	Dec Lat	0.03	0.0020	Dec Lat	0.04	0.0040
	Long	0.04	0.002	Long	0.04	0.0040	Dec long	0.03	0.0020	Dec Long	0.04	0.0020
	Secchi	0.03	0.006	T_t	0.02	0.0580	Secchi	0.03	0.0080	T_t	0.02	0.0420
	T_t	0.02	0.0320	Secchi	0.02	0.0580	T_t	0.02	0.0420	Secchi D	0.02	0.0580
	pH	0.01	0.900	T_b	0.02	0.214	pH	0.01	0.8820	T_b	0.02	0.1740
				pH	0.01	0.5600				pH	0.01	0.4960
RDA	Environmental variable	Extra Fit	p Value	Environmental variable	Extra Fit	p Value	Environmental variable	Extra Fit	P Value	Environmental variable	Extra Fit	p Value
	Alt	0.05	0.0020	Alt	0.05	0.0020	Altitude	0.05	0.0020	Altitude	0.05	0.0020
	LOI	0.05	0.0020	LOI	0.06	0.0020	LOI	0.04	0.0020	LOI	0.06	0.0020
	Cond	0.04	0.0020	Secchi	0.04	0.0040	Cond	0.04	0.0020	Secchi	0.04	0.0040
	Secchi	0.04	0.0040	Cond	0.03	0.0020	Secchi	0.04	0.0040	Cond	0.03	0.0020
	Depth	0.03	0.160	lat	0.02	0.0040	Depth	0.03	0.0160	Depth	0.02	0.0440
	lat	0.02	0.032	Long	0.03	0.0060	Lat	0.02	0.0340	Lat	0.02	0.0440
	Long	0.03	0.0020	Depth	0.02	0.0018	Long	0.03	0.0020	Long	0.03	0.0040
	T_t	0.01	0.3180	T_b	0.02	0.2580	T_t	0.01	0.3340	T_t	0.01	0.2860
	pH	0.01	0.8100	pH	0.01	0.4260	pH	0.01	0.7760	Top	0.01	0.3540
				T_t	0.01	0.3580				T_b	0.01	0.5780

Table 5.7 : Results of forward selection using environmental data sets EN1 and EN2 and taxonomic sets MAJ_{INCL} and MAJ_{EXCL}.

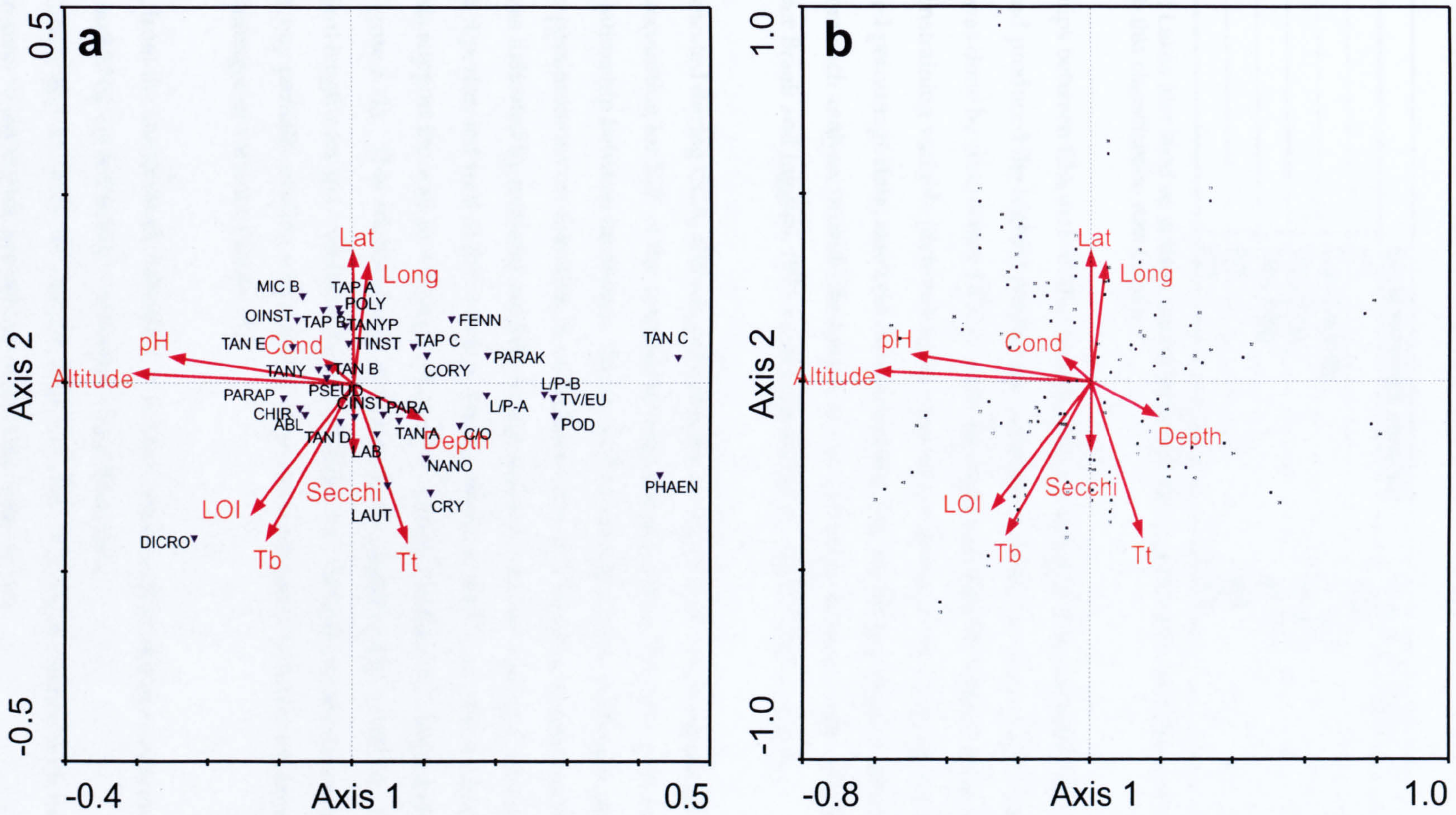

Figure 5.11: CCA Bi-plot of EN_2 vs $MAJ_{incl.}$ (a) shows variables plotted against sites, (b) shows the variables plotted against taxa. Note the different scales on the two graphs. Key for taxa is in Appendix 5.

Lake	Environmental variable	Value of outlier
BW	pH	4.05
BW	Conductivity	0.14µS
MOA	Dec long	66.8 °S
LAV	Dec long	67.0 °S
QVII	pH	3.9
QVIII	pH	4.5

Table 5.8 : Lakes identified as outliers during CCA and the environmental variable and value upon which this classification was based.

Relationships between EN_2 and MAJ_{incl} were further analysed as this combination of datasets had produced the highest percentage variance explained scores in CCA (Table 5.5). This was done by conducting DCCA, with the environmental variable of interest, *x*, as the sole constraining variable (detrending by segments, non-linear rescaling, square root transformed percentage data, rare taxa downweighted) (ter Braak and Juggins, 1993). Results from such analysis provide the length of *x* in S.D. units, in terms of the DCCA axis gradient (ter Braak and Juggins, 1993, cited in Brooks *et al.*, 2001, 517) (Table 5.9)

As was indicated during CCA, altitude performs the strongest in terms of explained variance, accounting for 55% of the variance identified during DCA. Results again indicate that the relationship between taxonomic change and LOI is significant. Although pH adds little to the parsimonious combination of variables with which midge response could be modelled, as indicated by minimal extra fit during and low p-values during FS in CCA (Table 5.7), it performed well in this analysis. Strong results of DCCA λ1 / DCA λ2 (45%) in this analysis support the way in which pH plots close to axis 1 on the CCA bi-plot (Figure 5.10 and Figure 5.11). This relationship is also statistically significant ($p = 0.0020$). The long gradient lengths for pH, conductivity and altitude over the training set sites sampled (Table 5.1) may partially explain why some of these environmental variables explained larger percentages of variance (Table 5.9)

Therefore, from the constrained ordination of the taxonomic and principal environmental data (EN_1 and EN_2) the following conclusions could be drawn:

- Altitude appears to be the variable which is most strongly associated with the turnover in taxonomic assemblage within the training set;
- pH also appears to be another relatively strongly correlated factor. Like altitude, it is closely related to axis-1 when CCA results are plotted. The variable also performs well when its influence is assessed using DCCA λ1 /DCA λ2. However, p-values derived from forward selection during CCA indicate that it adds little

		DCCA			DCCA λ1 /DCA λ2
	Gradient Length	Variance	P-value	λ1	
Alt	1.131	5.8%	0.0020	0.068	0.55
LOI	0.795	3.5%	0.0040	0.041	0.33
Cond	0.980	2.5%	0.0520	0.03	0.24
Depth	0.693	2.4%	0.0600	0.028	0.23
T_b	1.010	2.9%	0.0280	0.034	0.28
Dec Lat	0.534	1.9%	0.0280	0.022	0.18
Long	0.615	2.1%	0.1520	0.024	0.20
Secchi	0.619	2.4%	0.0400	0.028	0.23
T_t	0.778	2.7%	0.0280	0.032	0.26
pH	1.083	4.7%	0.0020	0.055	0.45

Table 5.9: Results of DCCA using forward selection using MAJ_{incl} and EN_2 and results of DCCA λ /DCA λ2

unique contribution to producing a simplified model between environmental variables and taxonomic assemblages when altitude is already included in the model;

- Bottom temperature measurements perform similarly to those taken from the top of the lake, both in the extra fit during CCA FS, DCCA λ 1/DCA λ 2 and related p-values;
- Although the gradient length within the taxonomic dataset, as calculated in DCA, is close to 2s.d., unimodal responses appear to be present within the data, as inferred from higher percentage variance explanations in CCA than RDA.

As additional environmental data had been obtained from some of the lakes, two further sets of ordination investigations were conducted, using subsets with additional cation and nutrient information.

5.5.1.1 Inclusion of Cation data

The 65 lakes in ENV_{cat} have environmental measurements from the previously discussed dataset, EN_1 and EN_2 (excluding T_b), and information on lake-water Na, Ca, K and Mg concentration. Table 5.10 shows results of DCA and CCA on this dataset alongside those gained from the equivalent analyses against all lakes (using EN_1 and MAJ_{incl}). Results of DCA analysis were similar to those gained when using EN_1 and EN_2.

Analysis	Parameter			All Lakes n_i=73 n_v=9	Cation Lakes n_i=65 n_v=14
DCA	Cumulative Variance		Axis 1	18.6	18.1
			Axis 2	29.3	27.8
	Eigenvalue		Axis 1	0.218	0.222
			Axis 2	0.127	0.119
	Grad		Axis 1	2.110	2.088
			Axis 2	2.034	1.776
	Total Inertia			1.240	1.226
CCA	Eigenvalue		Axis 1	0.134	0.172
			Axis 2	0.026	0.062
	Cumulative percentage variance	of species data	11.5	10.8	14.1
			15.4	14.7	19.2
		of species-environment relation	41.0	39.6	36.7
			55.1	54.8	49.9

Table 5.10 : Comparison of results of CCA and DCA using EN_1 and EN_{cat} dataset. n_i and n_v refer to the number of sites and variables included in analysis, respectively.

CCA of the data set produced eigenvalues of 0.172 and 0.062, for axes 1 and 2, respectively. These axes explained cumulative percentages of 14.1% and 19.2% of the variance in the species data. These are slightly higher than the control data set of EN_1, as shown as Table 5.10. However, this is not surprising, as results of CCA approach that of CA as n_i and n_v converge (ter Braak, 1995). As DCA results for both data sets were similar to begin with, a higher CCA for the cation dataset would be expected, due to the smaller n_v of ENV_{cat}. Examination of the CCA bi-plot in Figure 5.12 shows environmental variables included in EN_1 plot in a similar orientation to previous ordinations (Figure 5.10), with long arrows for altitude and pH plotting close to axis 1. In terms of the additional cation data, Mg has a rapid rate of change and is likely to be a significant environmental variable, as indicated by its long arrow length (ter Braak, 1986). Conversely, K, Na and Ca are all represented by short arrows. All of the cations correlate positively with increasing pH to a greater or lesser extent.

When DCCA restricted to one variable is conducted (Table 5.11), Mg explains 54% of the variance ($p=0.002$), although altitude was still a more strongly correlated variable, explaining 65% of the variance in the data set's fauna ($p=0.002$). pH, cond, Tt, Na and K all held statistically significant relationships ($p=<0.05$).

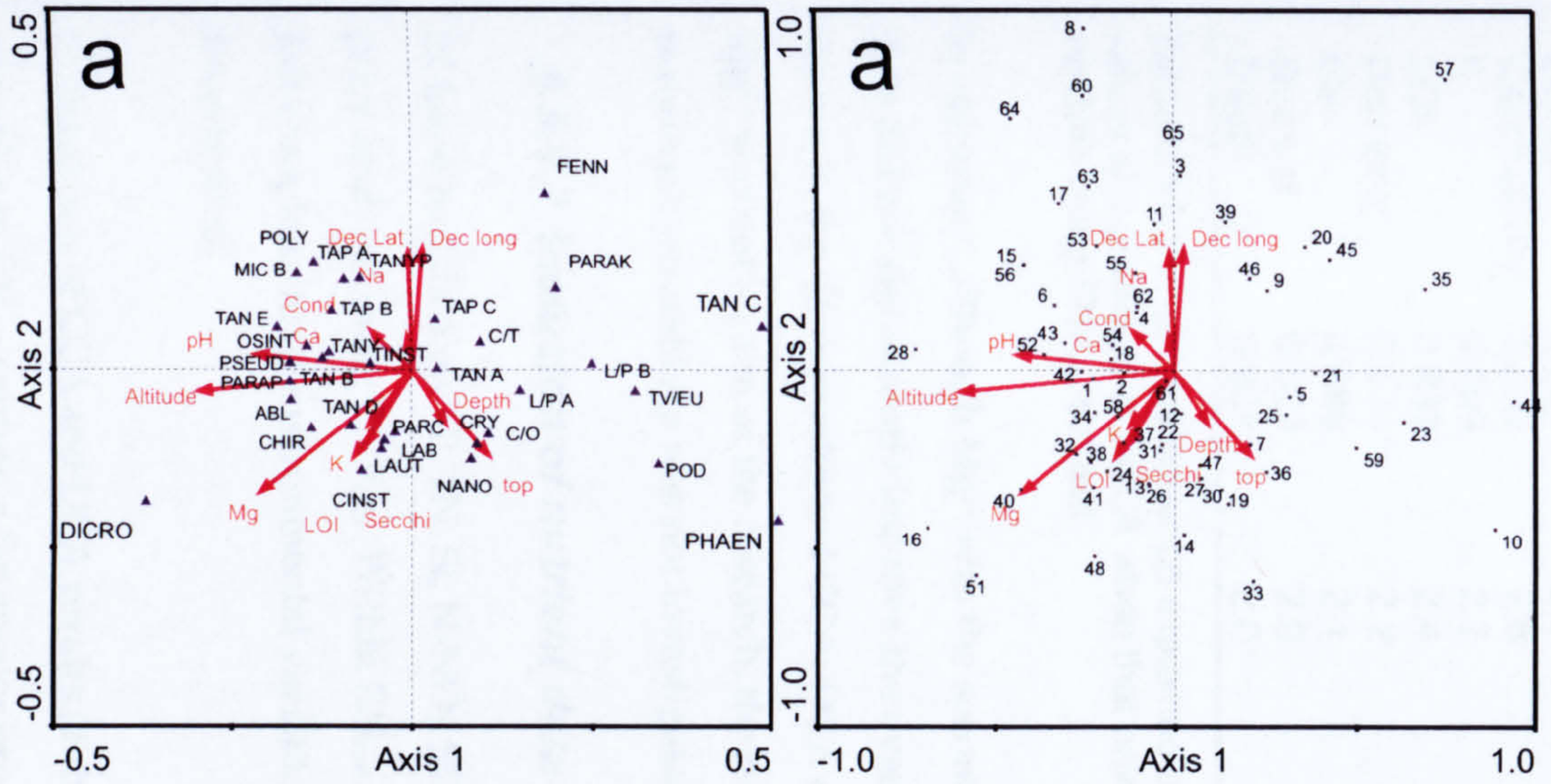

Figure 5.12 : CCA bi-plots showing the results when constrained ordination is conducted using (a) EN_{cat} and (b) EN_{nut}.Codes for taxa are given in Appendix 5

N.B. the environmental variable arrows are shown at 50% of actual size in taxonomic bi-plot using EN_{cat}

	Gradient Length	Variance of species data explained	P-value	DCCA λ1	DCCA λ1 /DCA λ2
Altitude	1.195	6.5	0.0020	0.079	66%
Mg	0.666	5.3	0.0020	0.064	54%
pH	1.083	4.3	0.0020	0.052	44%
top	0.739	3.3	0.0120	0.041	34%
Na	0.984	3.0	0.0360	0.036	30%
Secchi D	0.687	2.9	0.0440	0.035	29%
Conductivity	1.039	2.8	0.0480	0.034	29%
K	0.690	2.7	0.0560	0.033	28%
LOI	0.682	2.4	0.0980	0.029	24%
Dec long	0.624	2.2	0.1460	0.027	23%
Ca	0.686	2.1	0.1860	0.026	22%
Dec Lat	0.523	2.0	0.2180	0.025	21%
Depth	0.638	2.0	0.1960	0.025	21%

Table 5.11: Percentage variance explained by each environmental variable and associated p-values and gradients in DCCA when that environmental variable was the sole constraining variable using ENV_{cat} dataset

In summary, although Mg^{2+} was the second most influential variable, inclusion of cation data did not significantly improve the overall ordination performance of the training set, as shown in the CCA results and CCA: DCA eigenvalues (**Table 5.10**). As reconstructing Mg^{2+} was not an aim of the research, the relationships solely between cation data and the taxonomic assemblage was not investigated further.

5.5.1.2 Inclusion of nutrient data

27 lakes had data on TP, TN, Si, N-NO_3, SO_4 and Cl as well as the 4 cations included in the prior analyses using ENV_{cat}. Within EN_{nut}, T_b had been recorded at all the lake, allowing a full complement of environmental variables and their relationship to the fauna to be investigated.

Comparison of CCA and DCA results (Table 5.12) highlight that the environmental variables in EN_{nut} capture a far greater proportion of the overall variance within the taxonomic dataset. Again, this could be partially attributed to the smaller sample size. During FS within CCA, significant levels of autocorrelation were highlighted with 5 environmental variables with VIF > 20 (long , lat, alt, T_t, T_b, TP, Na, Cl and Ca). These high levels are in line with the higher r^2 gained during environmental data analysis in 5.2.1.1 and Table 5.3. Furthermore, these inter-variable relationships are displayed graphically in

Analysis	Parameter			EN_1 n_i=73 n_v=9	EN_{nut} n_i=27 n_v=20
DCA	Cumulative Variance		Axis 1	18.6	19.7
			Axis 2	29.3	31.4
	Eigenvalue		Axis 1	0.218	0.230
			Axis 2	0.127	0.137
	Grad		Axis 1	2.110	1.978
			Axis 2	2.034	2.214
	Total Inertia			1.240	1.166
CCA	Eigenvalue		Axis 1	0.134	0.222
			Axis 2	0.026	0.163
	Cumulative percentage variance	of species data	11.5	10.8	19.0
			15.4	14.7	33.0
		of species-environment relation	41.0	39.6	21.7
			55.1	54.8	37.8

Table 5.12 : Comparison of results of CCA and DCA using EN_1 and EN_{nut} environmental dataset and MAJ_{incl} taxonomic dataset.

	Gradient Length	Variance of species data explained	P-value	DCCA λ /DCA λ2
Na	1.420	10.1	0.0020	86%
K	1.726	10.0	0.0040	85%
Mg	1.906	9.3	0.0040	80%
Cl	1.115	8.3	0.002	71%
Ca	0.998	7.9	0.0040	67%
TN	1.099	7.5	0.0220	64%
Conductivity	1.503	7.4	0.0140	63%
bottom	0.795	7.1	0.0180	61%
SO_4	0.996	6.1	0.542	53%
Altitude	0.993	6.0	0.0660	51%
Secchi D	0.814	5.8	0.0880	49%
Depth	0.984	5.5	0.1240	47%
pH	1.318	6.5	0.1500	47%
LOI	0.935	5.3	0.1580	45%
TP	0.686	5.2	0.1440	44%
top	0.827	4.9	0.1600	42%
Dec Lat	0.554	4.8	0.1940	41%
$N\text{-}NO_3$	0.910	4.6	0.2240	39%
Dec long	0.662	4.3	0.3220	36%
Si	0.778	3.1	0.6640	22%

Table 5.13: Percentage variance explained by each environmental variable and associated p-values and gradients in DCCA when that environmental variable was the sole constraining variable.

the CCA bi-plot (Figure 5.12), with environmental variables arrows often clustered in similar directions, eg. Lat and Cl, Ca and Na. In contrast to previous analyses, environmental gradients were often highly correlated with axis 2 on the ordination diagram (Figure 5.12).

DCCA using a sole constraining environmental variable further highlighted the relative strength of the midge - cations relationship. All cations explained high proportions of the variance (67-86%) with statistically significant relationships ($p<0.01$). Cl (71% total variance explained), TN (64%), Alt (51%), Tb (61%) and Cond (63%) also produced statistically significant results ($p=0.01$-0.05). To summarise, constrained ordination indicated a high level of autocorrelation between the environmental variables measured in ENV_{nut}. As was the case with ENV_{cat}, cations again appeared to be correlated with changes in assemblage composition. The combination of such a small sample size and high levels of autocorrelation within the environmental dataset makes it difficult to determine which environmental variables are most likely to be driving the species assemblage.

5.6 Preliminary assessment of ordination results

Having supplemented results from constrained ordination of the base datasets, EN_1 and EN_2, with those gained using additional cation and nutrient data (EN_{cat}, EN_{nut}), several points have arisen from the ordination analysis of the Patagonian chironomid training set. These findings are discussed individually in more detail in the following sections, together with their impact on the objective of producing a transfer function from the training set.

5.6.1 Water Temperature

Constrained ordination consistently implies that the water temperature measurements do not correlate strongly with the faunal assemblage. Furthermore, the percentage variance in the faunal assemblages across all sites that was explained by temperature was low (*c.* 2.5-2.7%) (Table 5.9). Although some past studies have also not found temperature to be a major control on midge assemblages (Porinchu and Cwynar, 2000), this result is potentially unexpected within the context of past quantitative midge studies (see section 3.5.2). However, there are various reasons as to why a stronger relationship was not found.

One possibility is that an insufficiently large temperature gradient was sampled within the Patagonian training set. However, this appears unlikely as a temperature range within this study, of 16°C (T_t) and 14°C (T_b), is comparable with or exceeds ranges in previous published work, with the exception of Walker *et al.*, (1997) and Brooks and Birks (2001a), whose training sets both had a range of 21°C (Table 3.2).

A more realistic issue is the reliance on spot measurements. The integrity of the temperature data might be questioned as CCA biplots show that the variable shows no correlation with altitude. This spurious relationship is also displayed in the preliminary environmental dataset analysis (Table 5.3). The potential unrepresentivity of temperature data is further highlighted at Laguna Edita where the two T_t measurements recorded on different occasions for this lake were 13.6°C and 9°C, in association with EI and EII, respectively. Basal measurements at the site cannot be compared as they were not taken in conjunction with sample EII. Brooks and Birks (2000a) argue that the unrepresentivity of one-off measurements may be more severe in maritime regions such as Norway and, therefore, also Chile. Lotter *et al.* (1997, 415), who address the issues of spot measurement unrepresentivity raised by Hann (1992) by using "mean summer air temperatures" computed through a GIS for their Swiss climate transfer function, advocate their approach as a possible way to counteract such problems. However, such climatic averages are potentially reliant on a high density of meteorological data being available.

Nevertheless, previous transfer functions based on one-off water temperature measurements have resulted in accurate models, with high r^2 and low RMSEPs (Walker *et al.* 1997) (3.5.2). Furthermore, some research indicates that in shallow lakes, and in deeper lakes during summer, surface temperatures should provide a good proxy for air temperature (T_a) (Arai, 1981). Livingstone and Lotter (1998, 184) support this proposal, arguing there can be a "high degree of correlation between the two (temperatures)". Their research on this phenomenon at sites on the Swiss Plateau indicated that during the summer T_t mirrored average T_a well.

The similar performance of T_t and T_b in the current study reflects the results of correlation between the two variables. An r^2 0f 0.56 (Table 5.3) indicates that the two temperature measurements are reasonably well correlated, with a large number of lakes where there is very good accordance between the two data sets (Figure 5.13). However, the overall correlation is weakened by a notable proportion where $T_b<T_t$. Conversely, occurrence of T_t greatly exceeding T_b is rare: only 2 lakes had $T_b-T_t>1$°C. Livingstone and Lotter (1998) also

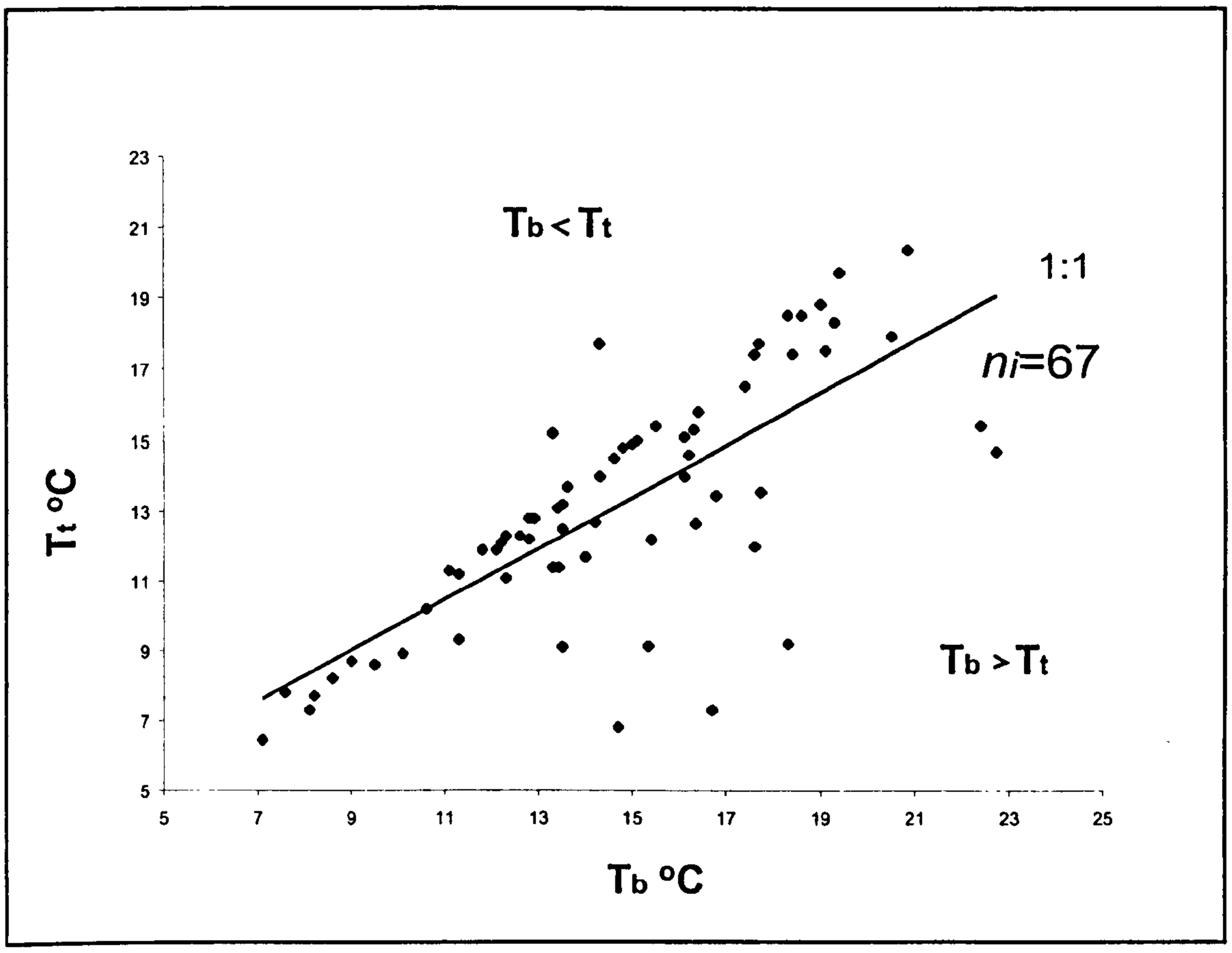

Figure 5.13 : Graph showing relationship between surface water temperatures (Tt) and basal water temperatures (Tb).

investigated the relationships between T_t and T_b in their Swiss study. Deeper water temperatures, taken from 5-5.5m below the surface, showed trends of a gradual, absolute, warming over the summer. During June and July, air temperatures usually fell between water temperature measured at 0 and 5m water depth. However by August, T_a would normally drop to lower than both of these water temperature measurements (Figure 5.14). Within the Austral context of this study this would translate to an expectation that T_a would correlate with water temperatures in January and February, but would be cooler than lake measurements during March. As discussed in Chapter 4, much of the sampling was conducted in February and March.

To assess whether there appeared to be any intra-annual variation in the relationship between surface and basal water temperatures, $T_t - T_b$, was plotted against summer days calculated as the number of days elapsed since the 1st Nov. To examine the possible influence of depth on this relationship, lakes were categorised into five categories by depth (see Figure 5.15). The graph shows no overall trends; although regression lines are sometimes steep, they are often being significantly affected by one or two data points towards the low end of the *x* axis. Thus, it is important to note that small sample sizes and the uneven distribution of data points along the *x* axis mean that this is not a particularly strong dataset with which to assess this relationship.

Another issue is, irrespective of accuracy and representivity of measurements versus air modelled temperatures, which of water temperature and air-temperature is actually the most influential on determining the midge assemblage. As the majority of the insects life is spent in its larval stage, and thus within a lake, it could be argued that water temperature exerts the strongest control. Conversely, the air temperatures will control the dispersive adult stages and thus will control the areas in which oviposition occurs (Brooks and Birks, 2000a). The different thermal capacities of air and water mean that the adult stage may be more vulnerable to effect high magnitude, low frequency thermal anomalies, due to the inability of the atmosphere to buffer and absorb such changes to the same extent as a lake can. Superimposed on this issue is the argument that, irrespective of the most important control on the midge assemblage, reconstruction of air temperatures is, arguably, preferable over water temperatures within the remit of palaeoecological studies (Lotter *et al.*, 1997).

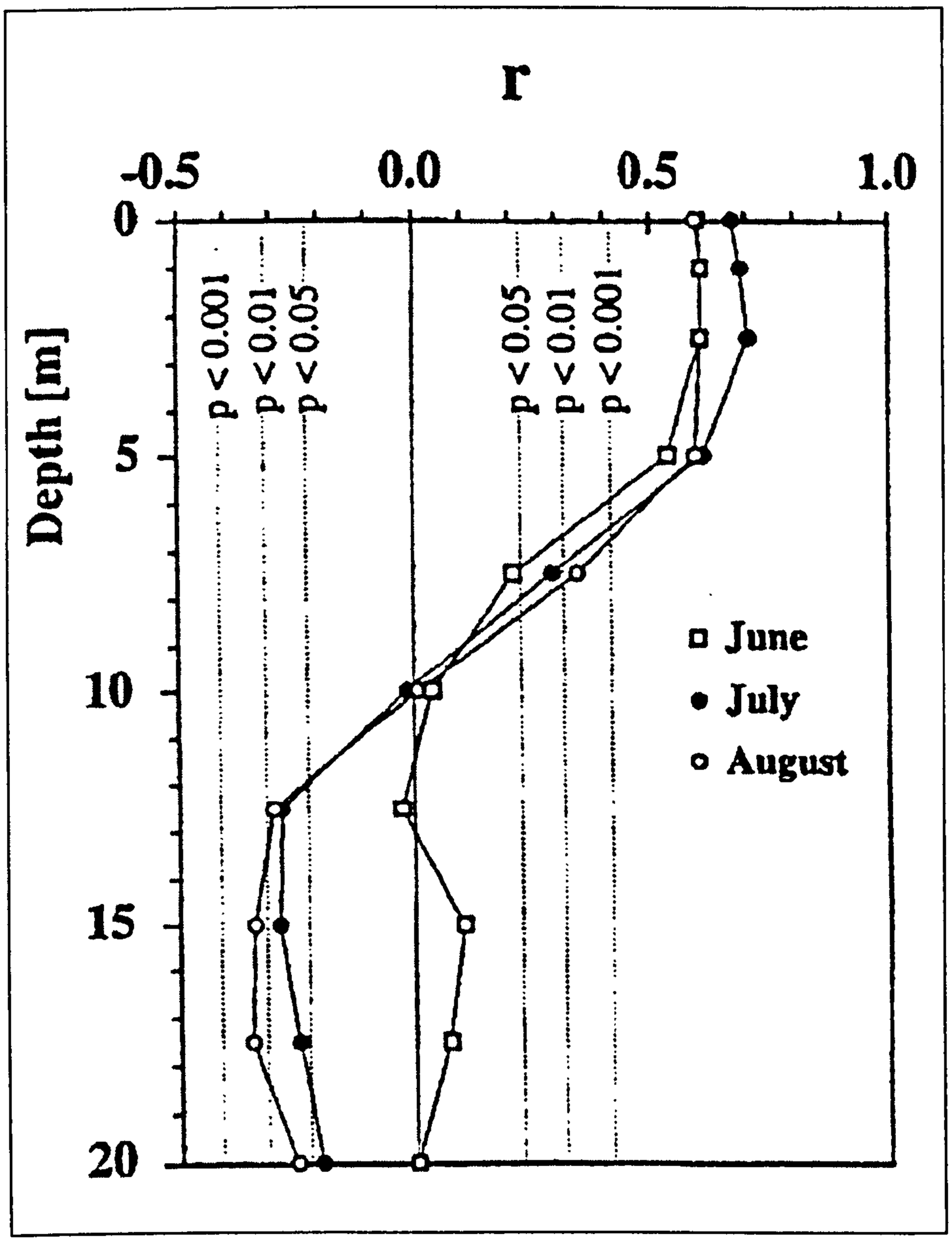

Figure 5.14 : Correlation coefficients r^2 between the summer monthly mean air temperatures and the corresponding water temperatures measures across various depths in the upper 20m of Zürichsee. Correlations are based on 54 years of data (1937-40 and 1946-95); significance levels are shown as dotted lines (Lotter and Livingstone, 1998, 194).

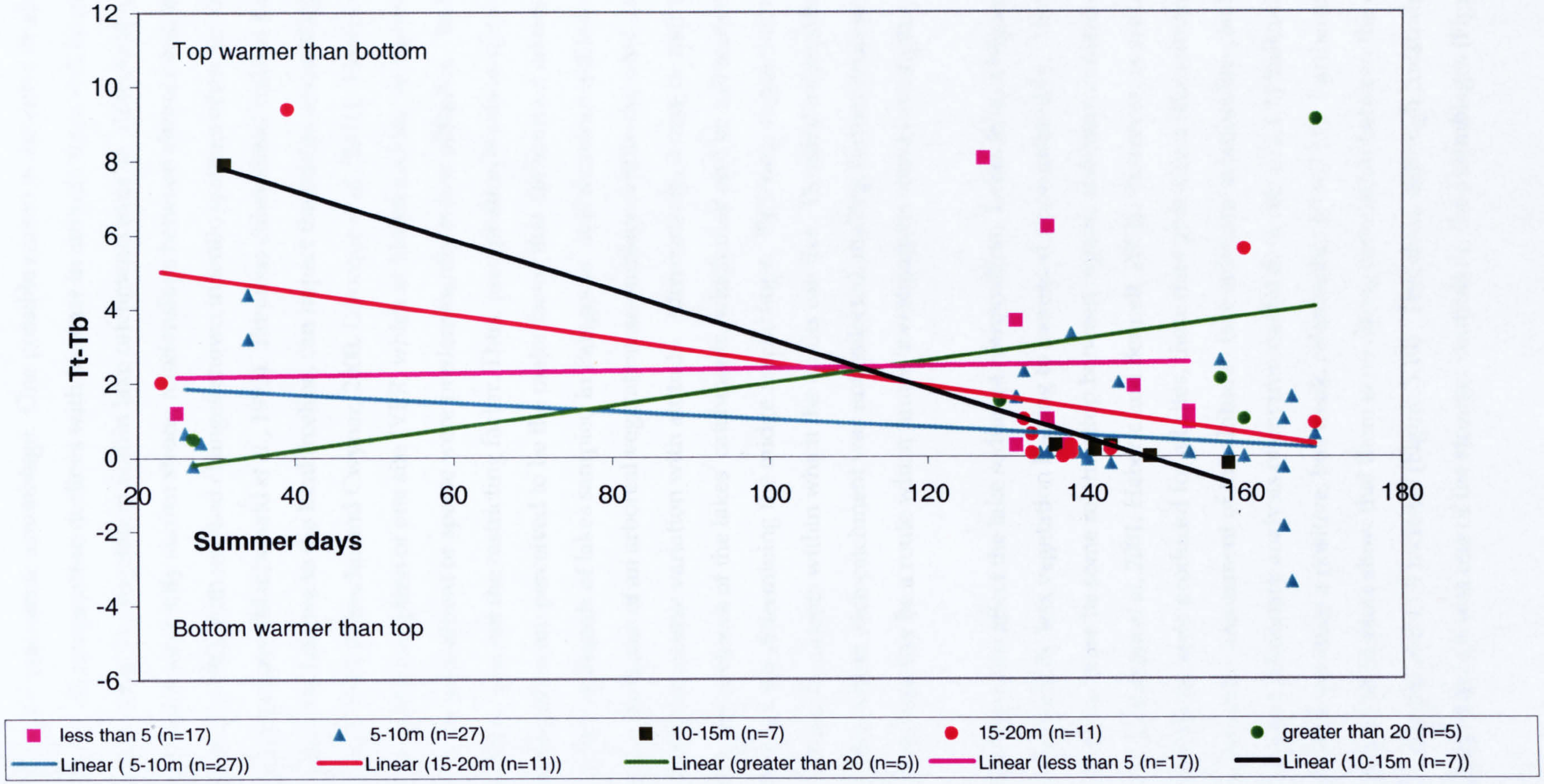

Figure 5.15 : Tt-Tb plotted against summer days on which measurements were taken (calculated as the number of days elapsed since the 1st Nov).

5.6.2 Altitude

Altitude was consistently the highest performing environmental variable in terms of explaining the taxonomic assemblage. One possible reason is the effect of altitude on vegetation. As temperature declines with increase in attitude there will be gradual and threshold changes in vegetation within lake catchments over an altitudinal gradient. Studies have consistently shown strong relationships between altitude and treeline (Lowe and Walker, 1994), with marked changes shown in lentic systems often accompanying the ecotonal boundary (MacDonald *et al.*, 1993). Previous chironomid studies have indicated a lake's position, relative to the local treeline, can impact the midge assemblage (Walker and McDonald, 1995; Porinchu and Cwynar, 2000, Larocque *et al.*, 2001). However in this study, with the exception of one site (VER, which at 1466m a.s.l lay on the treeline), sites where trees were absent or sparse were predominantly at low altitudes – indicating that temperature was not the restricting factor. Thus, precipitation levels as opposed to altitude and temperature are perceived to be the major factor that determined arboreal distribution within the catchments of lakes sampled in Patagonia. It is therefore unlikely that the absence or presence of an arboreal vegetation assemblage within the sites' catchments can explain the taxonomic variation with altitude. Alternatively, it may be that changes in vegetational ecotones of the lakes' catchments, which may also be influenced by altitude, may be partially determining the midge assemblages. Differing vegetation will provide different environments within which the adults can live. Detailed information on the vegetation within each catchment was not collected, making further analysis difficult. However, this may be a route which future investigations could investigate.

Altitude may also affect the lake sediment composition. Lakes from a higher altitude may be surrounded by less vegetation leading to increased slope instability. Therefore it may be expected that there be some relationship between organic sediment content (LOI) and altitude (Larocque *et al*, 2001; Haberle and Bennett, 2002). However, as sediment LOI measurements were produced for all sites, these data give direct lake substrate composition measurements. Assessment of the altitude - lake substrate relationship can be gained by referring to preliminary analysis of environmental data sets (5.2.1.1) indicating that LOI and altitude produce a positive, but weak, relationship ($r^2 = 0.11$). Furthermore, many of the ordination bi-plots show that there is no strong correlation between the direction in which altitude and LOI increase (Figure 5.10). Therefore, although constrained ordination indicated that LOI was one of the stronger controls on the assemblages (Figure 5.10), it is

unlikely that changes in LOI with altitude are driving the change in the fauna associated with the altitudinal range.

5.6.3 pH

pH was repeatedly shown to be one of the environmental variables which covaried most with the taxonomic assemblage (Table 5.9 and **Table 5.11**). Whilst there are no published chironomid pH training sets, Walker, (1995, 2001) and Hoffman (1988) both indicate that shifts in down-core midge records accompany late 20th Century lake acidification. Acidification can affect aquatic insects through direct effects on their physiology, increasing the release of metals to toxic levels and indirect effect on the lake ecosystem in general, thus affecting food availability, competition and predation (Hall *et al.*, 1980). Therefore, it is not unexpected that a relationship between pH and the taxonomic turnover should exist. A possible reason for this relationship not having been quantitatively harnessed in previous studies is that pH has been intentionally limited, as in training set studies it is effective not only to maximise the gradient of the variable in which one is interested, but to also minimise others when composing training sets (Brooks and Birks, 2001a). For example, in order to reduce the large pH range in the Swiss training set, Lotter *et al.* (1997) specifically avoided more alkaline lakes on calcareous bedrocks, allowing the pH range to be limited to 8-9. Furthermore, it could be argued that there is less attraction to develop chironomids as a proxy for pH due to the highly successful application of diatom analysis in lake pH reconstructions (eg, Fritz, 1991).

The relatively strong results gained through ordination indicated that the pH - taxonomic relationship warranted further investigation. pH was plotted against CCA axis 1 sample scores to examine the covariation existing between these values (Figure 5.16). This relationship produces an r^2 of 16%. This low r^2 was emphasised by the wide 95% prediction level bands (shown as dashed lines). Examination of the data point spread indicates that sites which were given CCA axis 1 scores from -1 - 0 often fall within a relatively broad window of pH 7 - 8.5. This range of pH values, over which the training set site density is at its highest, associated with a relatively narrow range of CCA scores increases the uncertainty with which the intercept of the linear regression equation or line of best fit can be best estimated. Figure 5.16 also highlights the influence of a small proportion of sites at the periphery of the pH gradient sampled, in particular the more acidic sites, which are the predominant control on determining the gradient of the regression line. Therefore although 45% of the overall variance in the dataset was explained

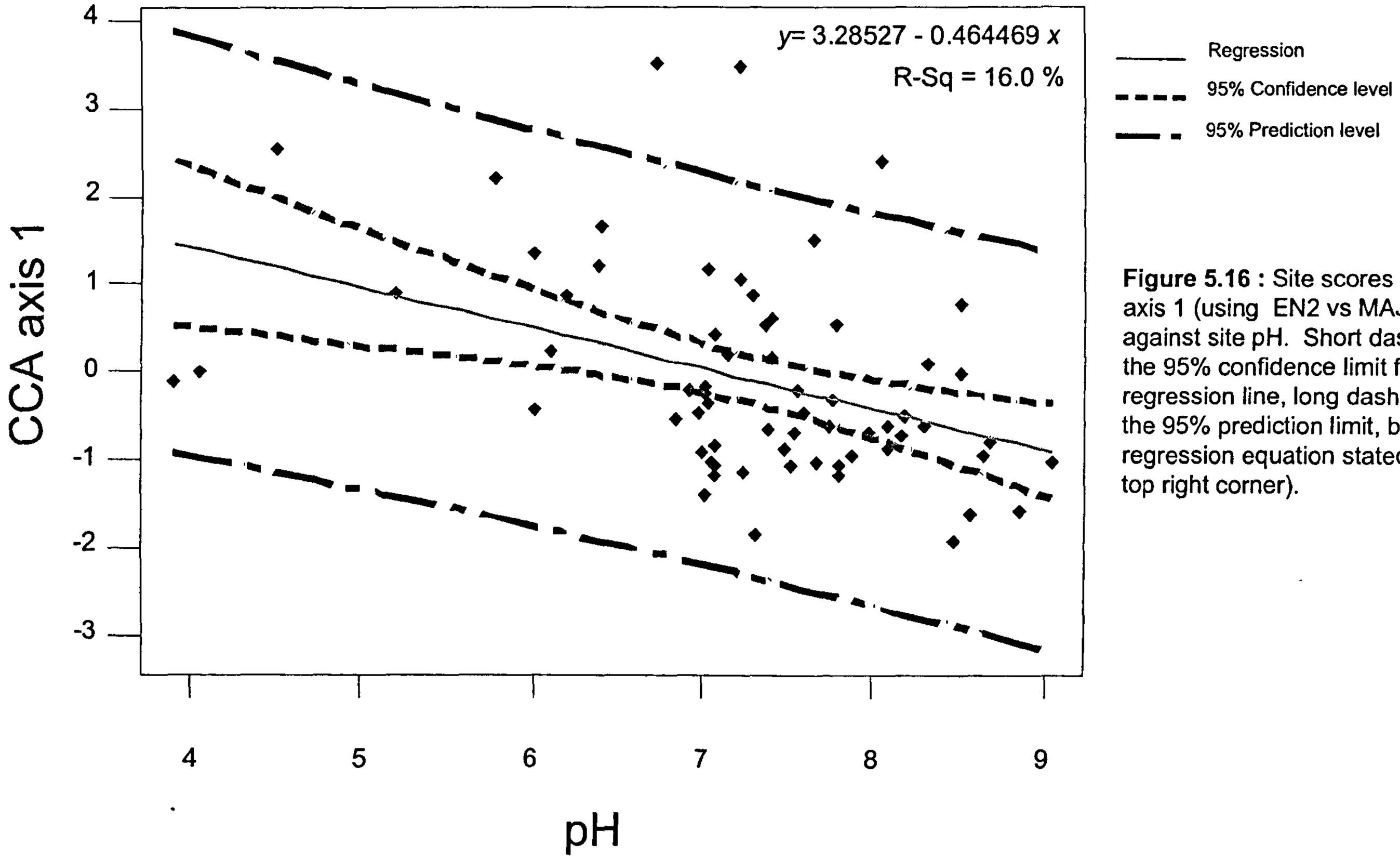

Figure 5.16 : Site scores on CCA axis 1 (using EN2 vs MAJincl) plotted against site pH. Short dashed line is the 95% confidence limit for the regression line, long dashed line is the 95% prediction limit, based on the regression equation stated (shown in top right corner).

by pH, the rather low r^2 and graphical presentation of results in Figure 5.16 indicate that whilst the Patagonian midge fauna does appear to be sensitive to lake acidity, the training set does not allow an accurate or precise quantification of this relationship to be extrapolated. Therefore the overall pH- taxonomic relationship is not deemed sufficiently robust to warrant production of a transfer function.

5.6.4 Biogeographical Effects

One potential reason for there being no outstanding variables in the analyses controlling the assemblage is because of biogeographic controls. It may be that, in such a large field area, samples have been taken from what are essentially disjunct, biogeographic populations between which there is little migration or exchange in genetics. If this has been the case for a sufficient length of time, taxa may have evolved to occupy different niches within the different communities. This would result in both different real, and calculated, environmental variable optima for the relevant, individual taxa in each population.

The possible impact of this was explored using two different methods. Figure 5.19 shows a DCA bi-plot, conducted using MAJ_{incl} only, on which sites are coloured according to their geographic location. Sites were classified, both in terms of (a) the field area from which they came and (b) whether they lay to the Pacific or Atlantic side of the Andes, as this geographic feature may act as a biogeographical barrier. The former set of spatial divisions is shown geographically on the accompanying map (Figure 5.17c). Secondly, the relationships between latitude and longitude and the TWINSPAN groupings produced in 5.3.1.1 (Figure 5.7) were assessed in terms of geographic trends.

DCA bi-plots indicate that samples do not tend to fall into discrete groups depending on their field area. It could be argued that faunal assemblages from certain areas, such as the Chonos and Taitao, plot in close proximity (Figure 5.17a). However, they do not plot distinctly from the rest of the samples. Additionally, a certain amount of grouping is to be expected, irrespective of any biogeographical effects, as a site's geographical location will partially determine environmental conditions such as temperature and pH, which may, in turn, impact the fauna present. Assessment of the relationships between longitude and latitude and the TWINSPAN groups was problematic due to the uneven geographical distribution of the sites. The only group that was tightly grouped both in terms of longitude and latitude, thus indicating the lakes were geographically clustered, was group

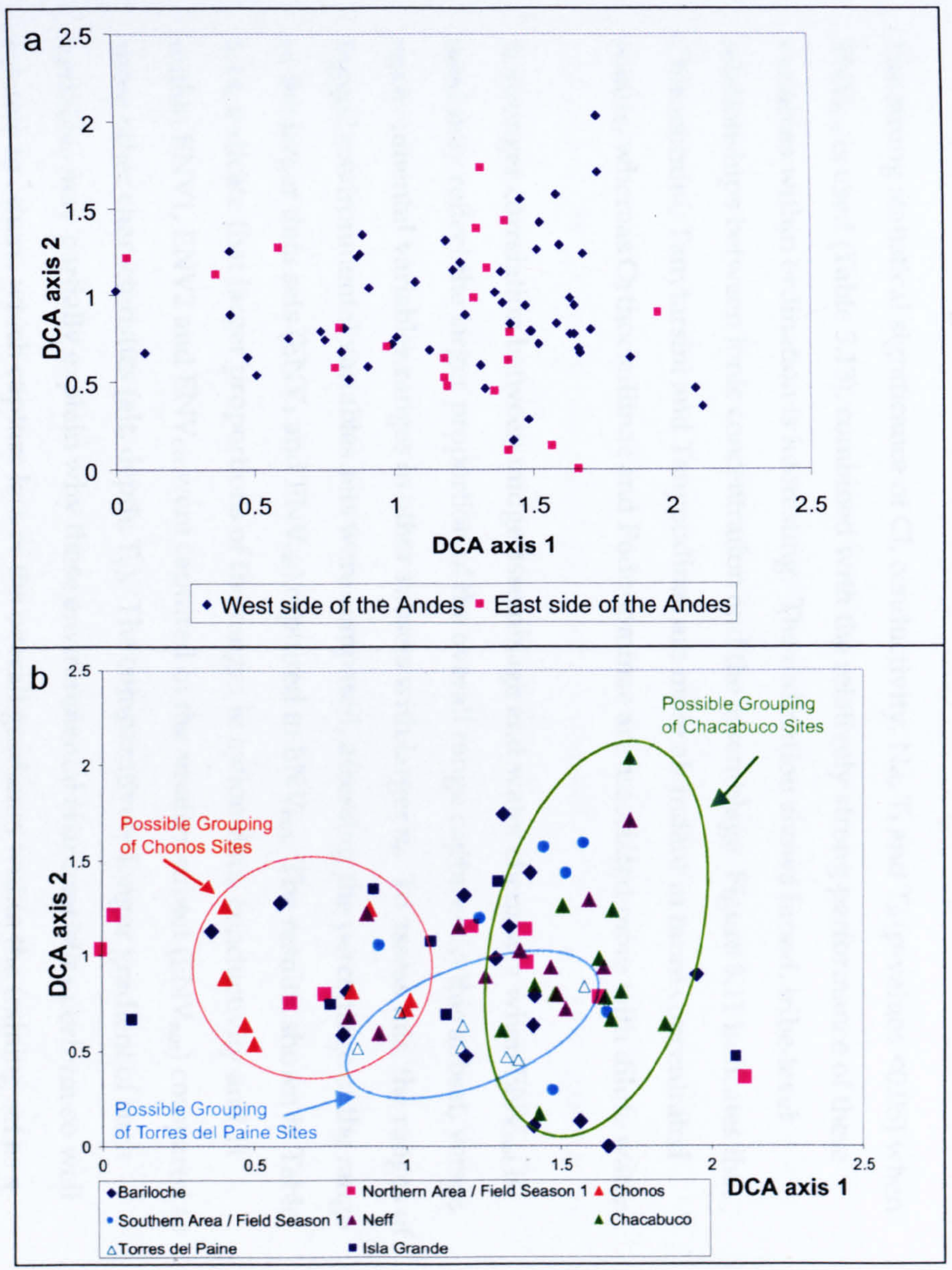

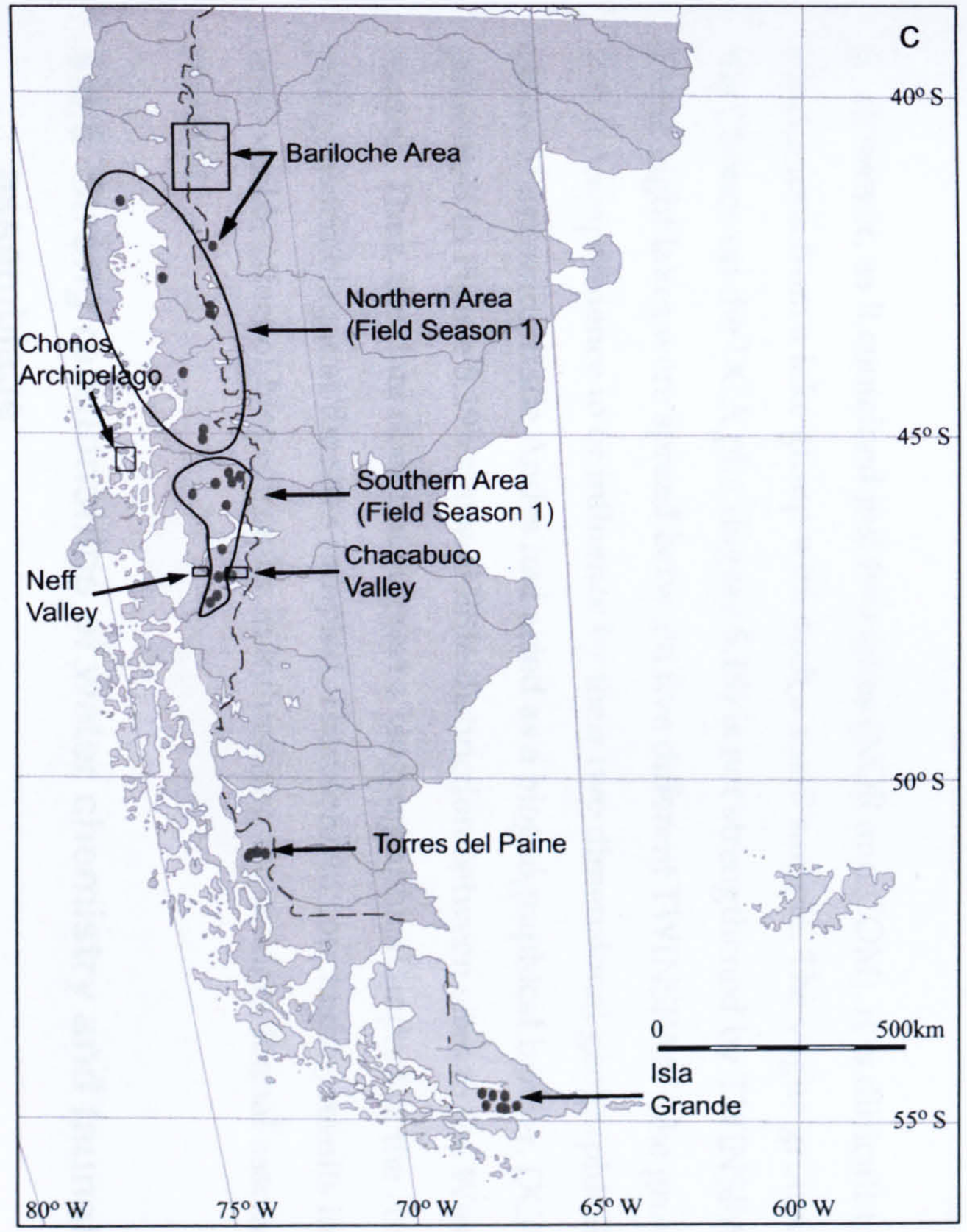

Figure 5.17: DCA of sites coded by (a) location to the West or the East of the Andes continental divide (b) field area location to explore possible biogeographical effects on faunal assemblages within the training set. (c) Map show the geographical divisions of sites by field area.

5. However, as it contained just two lakes (NOR and COM), it is difficult to draw firm conclusions from a lake group with such a small sample. The vague grouping of sites from the Chonos on the DCA plot (Figure 5.19) is not strengthened by TWINSPAN results. These eight lakes were spread between five different TWINSPAN lake groups, indicating little correspondence to or influence by their two dimensional geographical position. In terms of assessing if the Andes had acted as a biogeographical barrier, DCA scores presented in Figure 5.19b showed little distinction between sites to the West and East of the Andes. Thus, the data does not suggest a biogeographical impact of the Andes on the midge assemblages at the sites sampled. Therefore, in conclusion, results indicate that there is no visible effect of biogeography in influencing the modern faunal assemblages at sites sampled.

5.6.5 Strong relationships of water chemistry and faunal assemblage

The strong statistical significance of Cl, conductivity, Na, T_t and T_b (p-values <0.05) when ENV_{nut} is used (Table 5.13), combined with the relatively strong performance of these variables within ordination is interesting. The ordination shows broad, tribe-level relationships between ionic concentration and the assemblage. Figure 5.11 indicates that Chironomini, Tanytarsini and Tanypodinae are more abundant in more concentrated waters, whereas Orthocladiinae and Podonominae are associated more with dilute waters.

A stronger correlation between midge assemblage and water chemistry when ENV_{nut} is used may reflect the larger proportion of the overall range captured in this subset, versus environmental variables ranges in other subsets with larger n_i. To assess this, the ranges of logged environmental variables sets were compared, assessing the percentage of the range of the larger data sets (ENV_1 and ENV_{cat}) captured in ENV_{nut}. The results, shown in Table 5.14, indicate that larger proportions of the ranges in cation data, conductivity and Tt within ENV1, ENV2 and ENV_{cat} were captured in the smaller subset (ENV_{nut}) compared to some other characteristics (alt, depth, T_b). The comparatively longer gradient of such variables may partially explain why these environmental characteristics perform so well relative to others, which capture less of the overall gradients within the training set as a whole. Ca is a good example of this, as when ENVcat was analysed the variable only explained 22% of the variance (Table 5.11), but this grew to 67% when ENV_{nut} was used (Table 5.13).

Environmental Variable	Percentage of range captured in ENV_{nut}
Dec long*	100%
pH*	100%
Ca†	100%
Mg†	100%
K†	100%
Dec Lat*	95%
LOI*	95%
Na†	94%
Conductivity*	91%
T_t*	91%
Secchi Depth*	80%
Altitude*	73%
Depth*	65%
T_b‡	58%

Table 5.14: Percentage of environmental variables range in ENV_1(*), ENV_2 (‡) and ENV_{cat}(†), captured in ENV_{nut} (TP, TN, Si and N-NO_3, Cl and SO_4. are not shown as they were only present in ENV_{nut}). Calculations made using logged environmental variables datasets.

Correlations between ionic water composition and midge fauna have been found in other studies (Nyman *et al., submitted*). Furthermore, Velle *et al* (*submitted*, a) also found conductivity to be correlated with the fauna, which is itself a proxy of the concentration of ionic concentration of water. Within the training set used in their study, the inter-set correlation of conductivity with CCA axes 1 and 2 were 0.28 and 0.22, respectively, indicating that conductivity played a notable role in species turnover. Brodersen and Anderson (2002) found that conductivity held a statistically significant relationship with taxonomic variance ($p = 0.014$), explaining 13.6 % of the variance in taxa. However, in their study from Greenland, separating the influence of conductivity and temperature in this study was problematic as the warmer lakes in the study were also more saline. Additionally, Nyman *et al.* (*submitted*) demonstrate that in Finnish lakes Ca, which is itself correlated to pH, ALK, Na and Mg within the dataset, shows a good correlation with taxonomic richness.

The total sum of concentration of all ionic constituents in waters is termed salinity (Wetzel, 2001). According to Wetzel (2001) there are three major controls on freshwater-salinity: rock dominance, atmospheric precipitation and the evaporation-precipitation budget. Establishing exactly the extent to which these mechanisms would affect lakes in the Patagonian training set is problematic without detailed geological and hydrological information. Assuming all the above variables to be constant, changes in cation concentration could be related to the levels of erosion in the catchment. The concentration

of cation concentration in lake sediments is recognised to act as a proxy of landscape stability (Mackereth, 1965; Lowe and Walker, 1986, Walker *et al.*, 2003, Engstrom and Wright, 1984; Doner, 2003). However, limnic sediment metallic content can be delivered to the lake in both solution or in the sediment influx (Figure 5.18). Therefore establishing to what extent cations in solution are reflecting erosion rates versus temperature may be problematic. One possible approach is to compare LOI, which may act as a proxy of inwash of allochthonous material, with the lake-water cation concentrations. Examination of these data in Table 5.3 shows there is little correlation; thus it may be that within this dataset the range in cation concentration in the training set is not representing differing levels of erosion but different physical and geochemical settings/locations of the lakes, relating to the above processes suggested by Wetzel (2001).

Assessing the cause and effect relationship between varying ion concentration and the midge assemblage is difficult. Organisms, such as cyanobacteria, are known to have different levels at which they are able to regulate ions such as Na and K (Wetzel, 2001). Therefore, changes in the midge assemblage may be due to the influence of these cations on lower levels within the food chain, as opposed to the midges themselves. Alternatively, it may be that the turnover in taxa is reflecting a general increase in salinity in line with increasing cation concentrations. Certain Chironomidae taxa are sensitive to salinity levels in Africa (Verschuren, 1997; Verschuren *et al.*, 2000b), N. America (Walker *et al.*, 1995; Heinrichs *et al.*, 1999, 2001) and Australia (Edward, 1986; cited in Pinder, 1995b, 131). Therefore, as stressed in Ward (1992), separating the effects and forcings of changes in pH and total ionic content is difficult. Thus from the data presented here, limited inferences can be made from the datasets.

5.7 Further investigation after limiting the pH range

The preceding constrained ordinations consistently highlighted pH as one environmental variables which correlates best with the turnover in the faunal assemblage. As discussed in 5.6.3, the magnitude of this correlation may be artificially high due to the large range in pH sampled in this study (5.14 pH units). This may be undesirable if it is not the variable that is wanted to be reconstructed.

In contrast to studies such as Lotter *et al.* (1997), the large pH range within the Patagonian training set may not only pull out the effect of pH, but mask possible effects of temperature

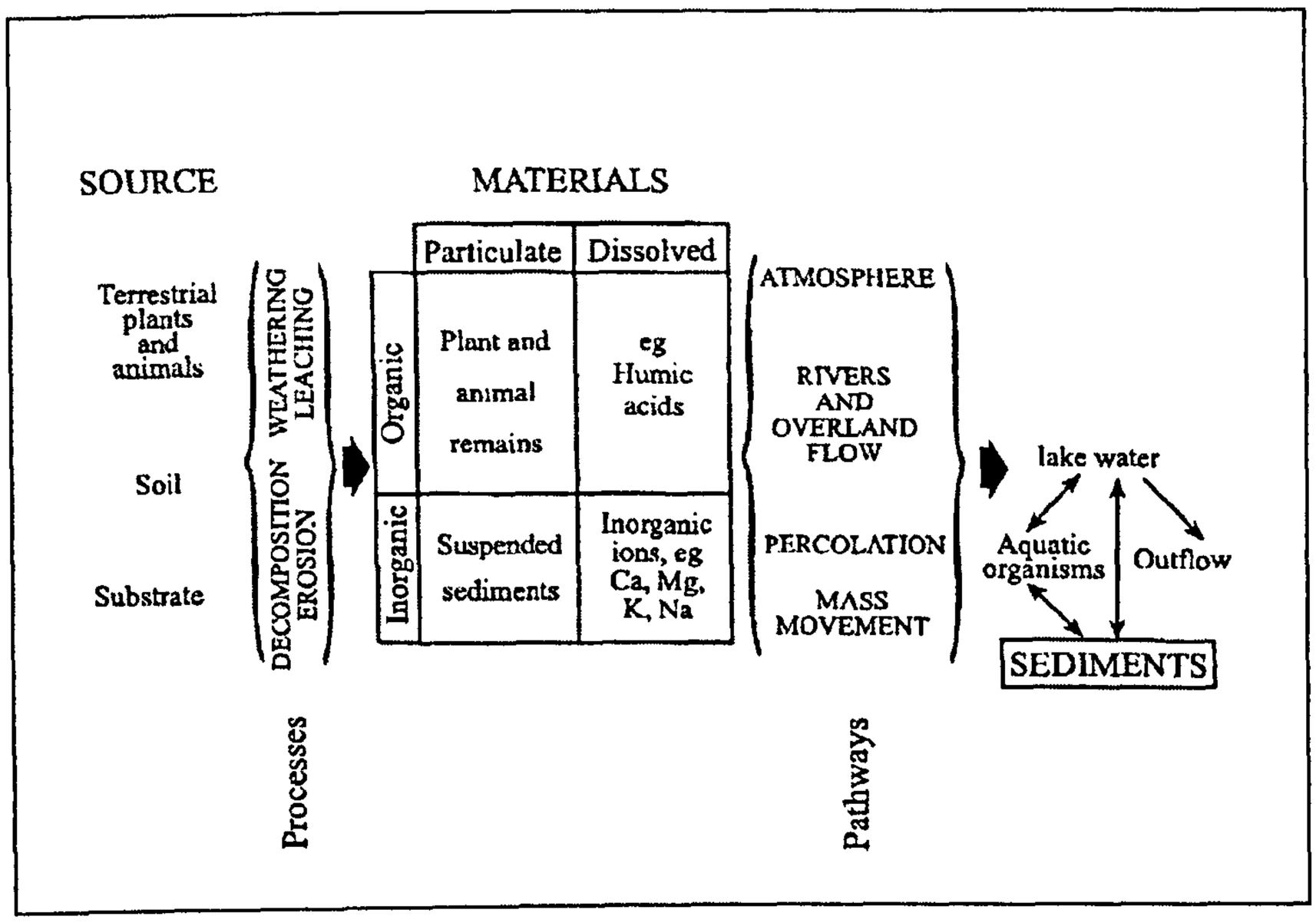

Figure 5.18: Simplified model of lake catchment processes and lacustrine sediments (modified after Edwards and Whittington, 2001).

and correlated variables. However, the choice of lakes that was logistically feasible to sample in Chile and Argentina were limited, and therefore data was collected from every lake that was accessible.

In order to assess whether the large range in acidity of lakes sampled was masking the importance of other variables in determining the assemblage, the range was reduced. This was done by investigating lakes within a subset, named EN_{pH}, whose pH ranged from the mean value by ± 1s.d (based on all 78 lakes). This reduced the pH range from 9.04-3.90 (range= 5.14) to 6.73-8.32 (range = 1.59). When lakes that did not include all the variables present in EN_1 were excluded, the subset contained 58 lakes.

Axes	1	2	3	4	
Eigenvalues	0.209	0.114	0.077	0.049	
Lengths of gradient	2.350	1.544	1.796	1.567	
Cumulative percentage variance of species data	18.7	28.9	35.8	40.2	
Total inertia					1.118

Table 5.15: Results of DCA on MAJ_{ph}.

		DCCA			DCCA λ1 /DCA λ2
	Gradient Length	Variance	P-value	λ1	
Depth	1.030	4.8	0.0040	0.052	0.46
Alt	0.855	4.3	0.0120	0.046	0.40
LOI	0.771	3.5	0.0320	0.038	0.33
pH	0.715	3.4	0.140	0.037	0.32
Secchi	0.744	3.4	0.0360	0.037	0.32
Cond	0.897	3.0	0.0700	0.033	0.29
Long	0.578	2.5	0.1440	0.027	0.24
T_t	0.545	2.2	0.2520	0.024	0.21
Dec Lat	0.499	1.8	0.4640	0.020	0.18

Table 5.16: Percentage variance explained by each environmental variable and associated p-values and gradients in DCCA when that environmental variable was the sole constraining variable using ENV_{pH} dataset.

Gradient lengths calculated with DCA again suggested that it was worth exploring the dataset using both RDA and CCA. Results of both of these ordinations are shown in Figure 5.19. Both diagrams show that pH continues to plot with a long arrow, indicating a fast rate of change (ter Braak., 1986); however, in comparison to the diagrams in Figure 5.11 based on previous analyses, both pH and conductivity now plot closer to axis 2, indicating that the relative extent to which they correlate with the assemblage has decreased. The

importance of depth appears to be strengthened in these analyses, as indicated by its representation with a longer arrow plotting closer to axis 1. These relationships were further investigated using DCCA Axis 1 / DCA Axis 2 (Table 5.16). The results further highlight the importance of depth, with the variable explaining 58% of the total variance within the taxonomic dataset.

A relationship between the chironomid fauna and depth accords with previous quantitative work in which depth has been shown as a controlling factor (Walker *et al.*, 1991a Walker and McDonald; Quinlan *et al.*, 1998; Olander *et al.*, 1999; Korhola *et al.*, 2000,Larocque *et al.*, 2001; Porinchu *et al.*, 2002). Changes in depth could affect the assemblage present through combinations of the following factors:

- affecting the temperature at the bottom of the lake (Walker, 1991)
- altering the oxygen available at the lake / sediment interface (Walker *et al.*, 1990)
- changing the ratio of littoral to benthic areas within the lake (Hofmann, 1998 Larocque *et al.*, 2001).

Assessing which of these factors is predominant is difficult, and it is likely that a hybrid of the three is responsible for the assemblage present. The position of certain taxa relative to depth in constrained ordination bi-plots indicates that there may be a thermal element in driving a change in taxonomic assemblage with depth, similar to that noted in Walker *et al.* (1990). Previous work has indicated taxa from the subfamily Podonominae, which in this study were indicated to be correlated with the depth axis during ordination especially when RDA is used (Figure 5.19), to be indicators of cold conditions (Brundin, 1988). This correlation supports the hypothesis that changes in basal water temperatures decreases with increasing lake depth; in deeper lakes, water may stay cold right throughout the year, if protected and capped by a sufficiently stable hypolimnion (Walker and McDonald, 1995). However, the position of environmental variables on ordination bi-plots (Figure 5.10) and relationships displayed in the correlation matrix (Table 5.3) do not corroborate this as they indicate that there is minimal correlation between depth and T_b. This again might indicate issues due to unrepresentivity of the temperature measurements.

With relation to depth, some taxa plot in positions which contradict the findings of previous Holarctic ecological research. The increase of % *Tventia / Eukiefferiella* and *Limnophyes / Paralimnophyes* along the depth axis is possibly unexpected. Previous Holarctic work has indicated these taxa to be lotic (*Tventia / Eukiefferiella* (Pinder and Reiss, 1983)) and littoral (*Limnophyes / Paralimnophyes* (Cranston *et al.*, 1983)). Furthermore,

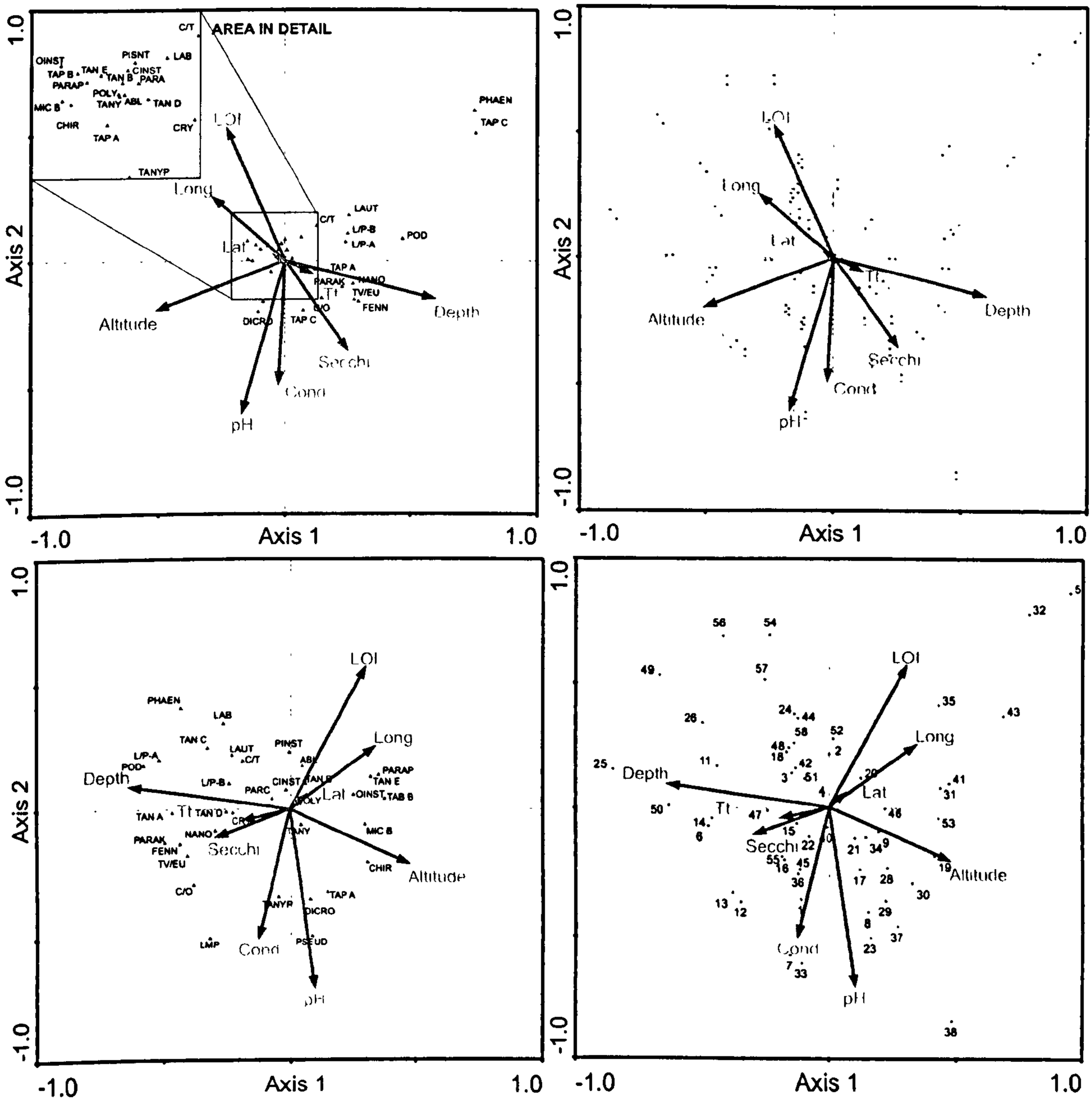

Figure 5.19: (a) CCA and (b) RDA plots for lakes with pH between the mean average ± 1 s.d..

Massaferro and Brooks (2002) use *Limnophyes* as a key indicator for changes in water level and thus palaoeprecipitation in their interpretation of the Laguna Stibnite record based on this Holarctic relationship. In addition to these taxa, others such as *Corynoneura / Thienemanniella* and *Lauterborniella* are plotted closer to the deeper lakes than those that are shallow, which is unexpected as they are usually associated with running water (*Corynoneura / Thienemanniella* ((Cranston *et al.*, 1983; Walker, 1988 cited in Rück *et al.*, 1998, 69) or littoral environments (*Lauterborniella* (Pinder and Reiss, 1983)). Thus, it would be expected that abundance of these taxa would decrease with increasing lake depth, and thus an increase in the area beneath the hypolimnion. Such contrast with the results of previous Holarctic descriptions could be due to differing ecological preferences of these taxa in the Neotropics to those previously recorded, predominantly in Holarctic regions. Alternatively it could indicate the taxonomic optima calculated using weighted averaging of the training set data is inaccurate. However, there do seem to be some similarities with previously described, Holarctic habitats. For example, the shallower environmental conditions inferred for taxa such as *Chironomus* and *Microtendipes* accord with previously published data (Pinder and Reiss, 1983; Walker *et al.*, 1991a), athough it should be noted that certain species of Chironomus are profundal dwellers partially due to their ability to withstand prolonged periods of hypolimnoxia (Kansanen, 1985)

5.7.1.1 Summary of Ordination

Results and interpretation of the ordination analysis have indicate that temperature cannot be reconstructed by using a temperature-based transfer function. Within the training set, pH seems to be one of the most promising environmental variables to reconstruct. However, the robustness of the taxonomic – pH relationship is weakened by a low concentration of sites within the more acidic element of the pH gradient. The strength of the relationship between taxonomic turnover and altitude is also inviting. However, establishing the way in which altitude effects taxonomy is challenging, due to the correlation of pH and altitude during ordination and the potentially poor representivity of temperature measurements. Initial comparisons between results of constrained and unconstrained analysis suggest that between a third and half of total variance within the dataset is not captured when ordination is constrained. It may therefore be that there are environmental variables which are important controls on the midge assemblage that have not been measured in this study, such as DO and density of macrophyte growth around the lake.

Although work has been published where similar DCA and CCA results have been used to infer a significant relationship strong enough to produce a transfer function (eg. Larsen *et al.*, 1996), the relationships displayed in this chapter are insufficiently strong to produce a transfer function. Any palaeoenvironmental reconstructions made at Laguna Leta and Laguna Boal cannot be quantitative. This finding in itself is interesting when put in the context of other attempts to quantify climate change in the region. Calibration sets produced using pollen in the area have had relatively limited results (Heusser, 1983; Markgraf *et al.*, 2002). Using a calibration set to reconstruct climate change since the LGIT, Markgraf *et al.* (2002) reconstructed that temperatures prior to 17 cal ka BP were 1°C warmer than those at present. This is totally incongruent with the rest of the data from the area, indicating the model is flawed. When the modern climatic dataset used to produce these constructions is examined, there are limited data points from the coolest end of the spectrum, which may account for accuracies during periods of what are believed to be cold temperatures. Such difficulties in reliably being able to quantify palaeorecords from Patagonia may also indicate that the meteorlogical data used by Hoganson and Ashworth (1992) was too poor to allow them to detect LGIT fluctuations in temperature in the Chilean Lake District, even though many other records indicate there was climatic change.

However, within this study, sufficiently strong relationships exist to allow the modern ecological – taxonomic relationships to guide interpretations. This is argued to particularly be the case in terms of depth, which accounted for almost 50% of the total taxonomic variance, after pH gradient reduction. Inferences regarding LOI, potentially acting as a proxy for lake productivity, are also justifiable. By using the relationships demonstrated between these environmental variables and the taxonomic assemblages, hypotheses regarding Late-Quaternary climate change at the sites investigated in this study can be investigated.

6 LAGUNA LETA

6.1 Introduction

This chapter presents and discusses the results of palaeoenvironmental analysis of the record Laguna Leta. Following a brief summary of the site and the present day environment, results from the sedimentary and chironomid analyses are presented in conjunction with geochronological data. These results are then interpreted to produce a synthesis of palaeoenvironmental change at Laguna Leta and its wider regional significance.

6.2 Site

Laguna Leta lies *c.* 10 km to the West of Seno Reloncavi, the northernmost bay of the marine element of the Valle Central, a structural trough that separates the Cordillera de la Coasta and Isla Grande de Chile from the Cordillera de los Andes (Figure 6.1). Laguna Leta (41°33'10"S, 73°09'53"W) is a small lake measuring *c.* 100 by 100 m (Figure 6.2). It is located at 74 m a.s.l. and is situated on what has been described as "hummocky moraine topography" within Llanquihue drift deposits which skirt Seno Reloncavi (Anderson *et al.*, 1999; Denton *et al.* 1999b). Within the drift complex, there are suites of moraines which fringe the coast (Figure 6.3), relating to different advances over the last *c.* 30 000 ^{14}C yr BP. The lake is drained by a stream to the NW of the basin (Anderson *et al.*, 1999 (see accompanying plates)).

Geomorphological mapping and ^{14}C dating of the area indicate that Laguna Leta lies on the outermost complex of moraine ridges (Figure 6.3). The glacial advance responsible for their deposition has three associated minimum ages of 20.480 +325-315, 21,230±169 and 22,680+415-395 ^{14}yr BP (Denton *et al.*, 1999b). This chronology is based on basal dates from mires occupying hollows on the hummocky moraine. Denton *et al.*'s research in the 1990s sampled the Laguna Leta basin, which is bounded to the NW and SE by moraine ridges. ^{14}C dating of the basal sediments within the part of the basin infilled by a mire yielded an age of 18,655+ 515-485 ^{14}C yr BP (A-8264) (Figure 6.3) (Denton *et al.*, 1999b).

Echosounder transects of the lake showed the maximum water depth to be 2.5m. There were no obvious streams flowing into the lake. Presently the lake is probably influenced

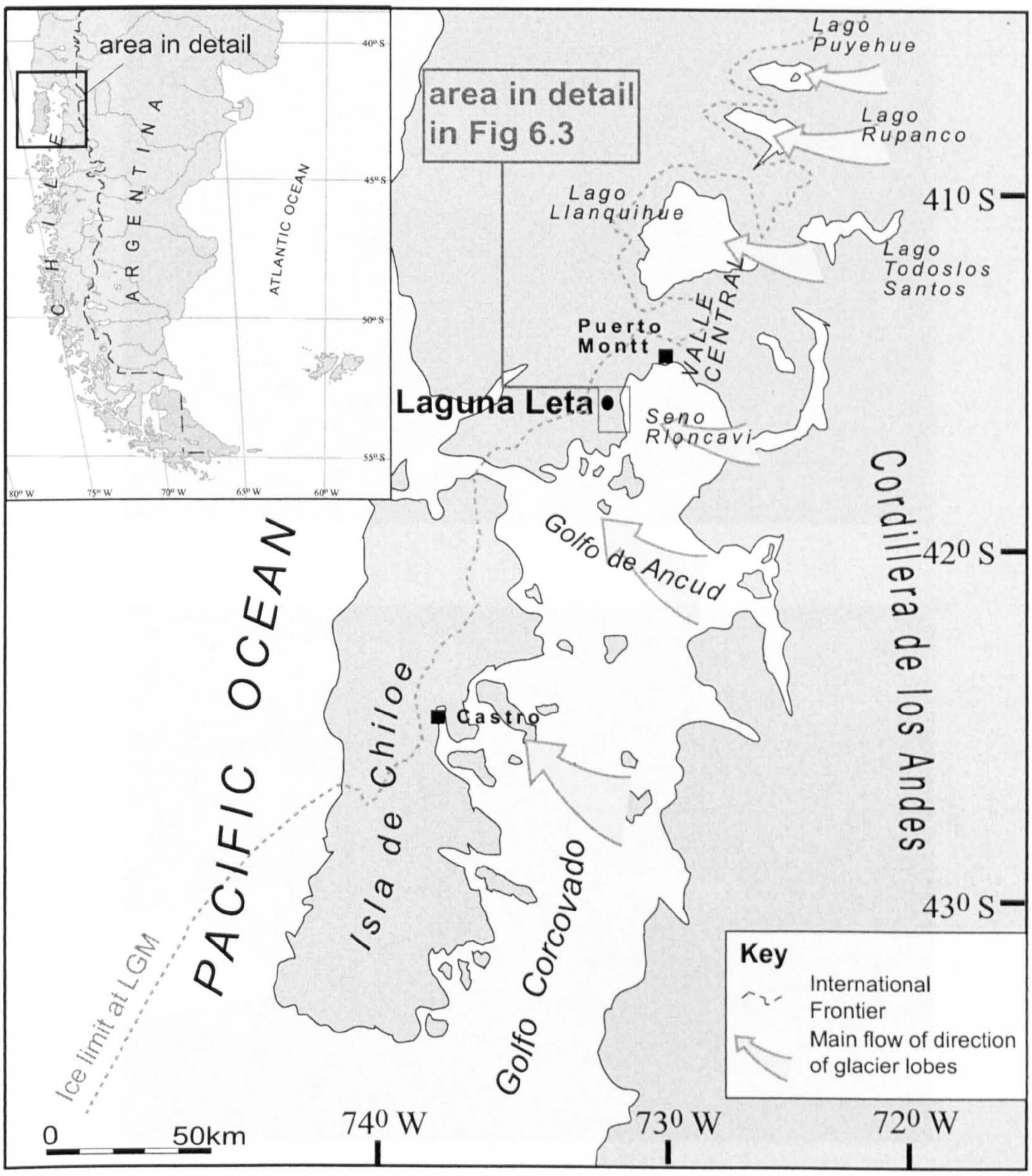

Figure 6.1: Map of the Chilean Lake District and Isla de Chiloé showing the location of Laguna Leta, LGM ice limits and the direction of LGM piedmont lobe glacier flow based on Andersen *et al*. (1999).

Figure 6.2 : Pictures of Laguna Leta taken facing nothwest (above) and west (below). Note the macrophyte growth in shallow regions of the lake. The lower picture shows the moraine ridge directly to the west of the basin and the domestic development on land to the west of the lake.

(a)

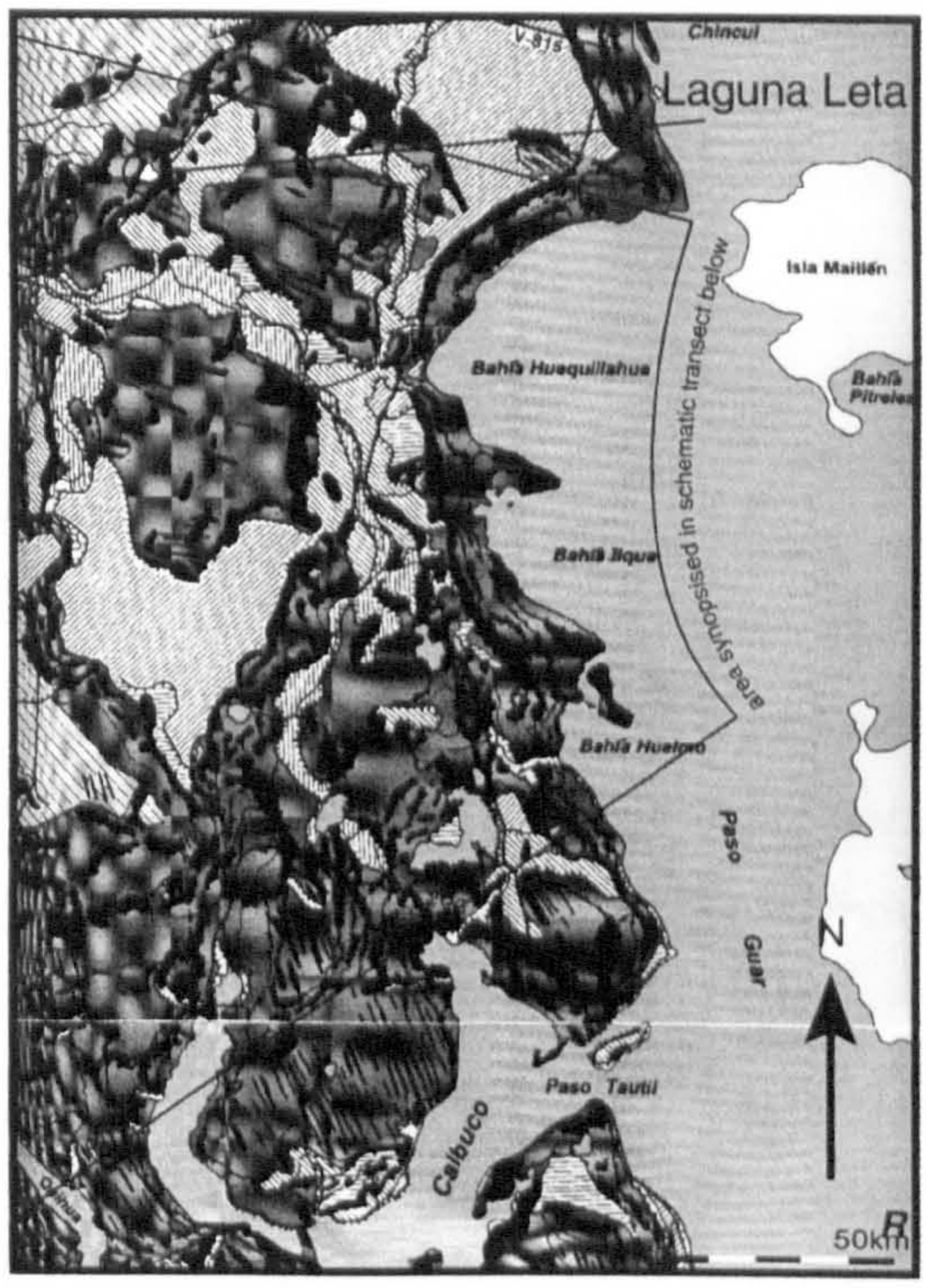

(b)

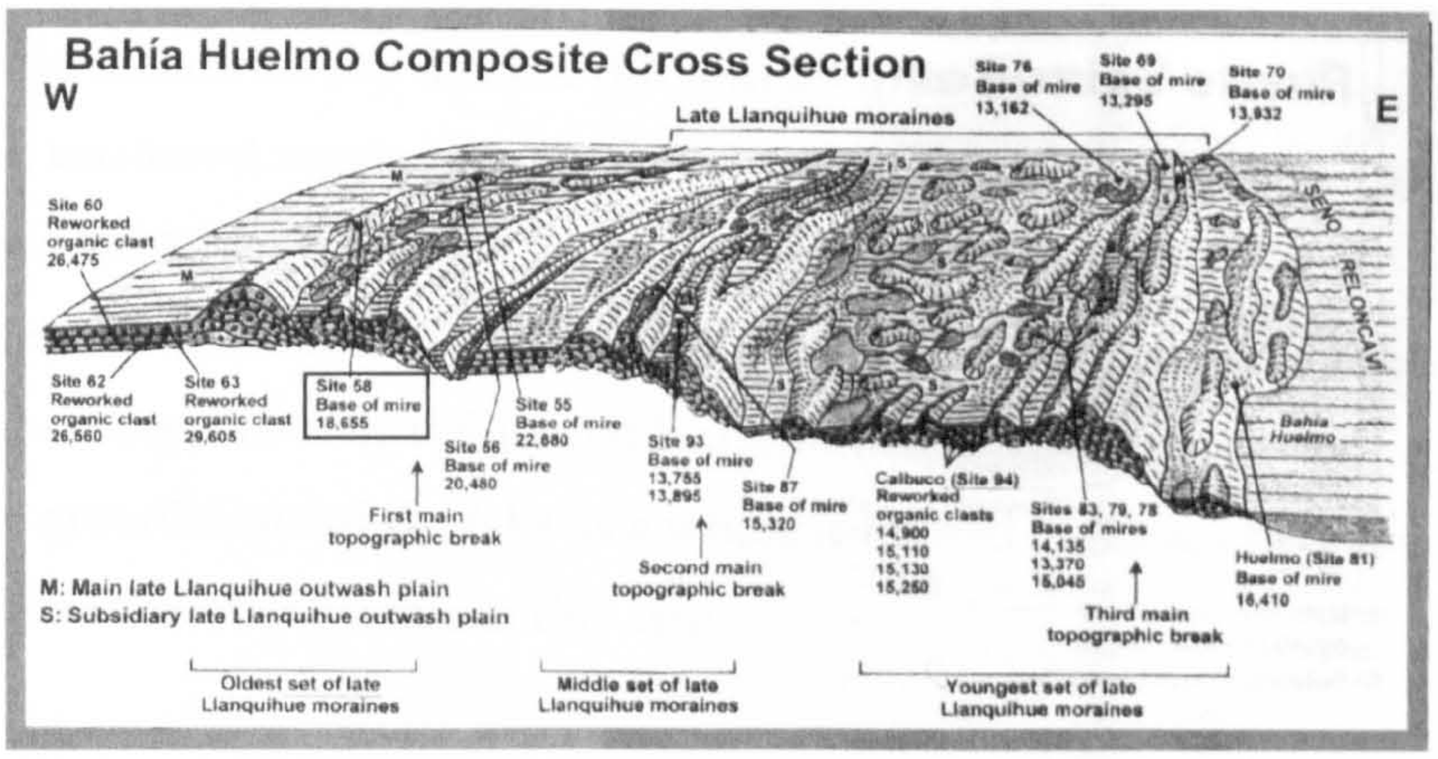

Figure 6.3: (a) Map showing the location of Laguna Leta within the geomorphic context. Geomorphological map and key taken from Andersen *et al.*, 1999 (accompanying plates to volume). Laguna Leta and the area included within the cross-section are marked

(b) Schematic diagram of the Bahía Huelmo composite cross-section which shows the position of Laguna Leta (site no. 58) (Andersen *et al.*, 1999). Note that the moraines and outwash plains are covered with pyroclastics flow sediments not shown in this diagram. Numbered sites refer to dates and sections described in Denton *et al.* (1999b.)

by anthropogenic influences, since a house is located at the south west end of the lake and the main road from Puerto Monte to Pargua / Isla de Chiloé (Route 5) runs to the east of the site (Figure 6.3).

6.2.1 Climate, Geology and Vegetation

As with everywhere to the west of the Andes in Patagonia, the precipitation regime of the Chilean Lake District is determined by the Westerlies. During the austral winter the westerly storm tracks can move as far north as 31°S. This means that the Chilean Lake District experiences a wetter winter than summer. Mean annual precipitation at Puerto Montt (41°28'S, 72°57'W, 5m a.s.l), which is *c.* 30km to the NE of Lago Leta, is 2341mm (Moreno *et al.*, 1999,). Mean temperatures in Puerto Montt range from 15.1°C in the summer to 7.7°C in the winter, with an annual mean of 11.2°C (Figure 6.4) (Moreno *et al.*, 1999). Porter (1981) estimates that the modern snowline in this area is approximately 1900m a.s.l.. Outcrops of pre-Quaternary, bedrock lithologies are extremely rare due to the high sedimentation in the region over the last 2.4 my. Quaternary glacial, volcanic, aeolian, alluvial and colluvial sediments cap most of the bedrock geology in the area (Heusser, 1999). The natural, unaltered vegetation of the Chilean Lake District would be Valdivian Rainforest (Heusser, 1999; Moreno, 1999) (Figure 6.5). However, this vegetation assemblage has been dramatically altered by human interference. Current vegetation surrounding Laguna Leta is heavily influenced by clearance to leave grassland or grazing areas. Macrophyte growth around the lake as a whole is limited to the south and west of the lake. Reeds are thick and extensive in this area.

6.3 Results

6.3.1 Sediment analysis

272 cm of sediment was retrieved from the centre of the lake using a Russian corer operated from a raft platform. Results of LOI and sediment description are displayed in Figure 6.6 (LOI results are given in App 6). The sediment comprises of organic-rich muds which are more minerogenic towards the base. Overall, there is a strong correlation between the stratigraphy of the Laguna Leta record and LOI results. The sequence shows an overall pattern of increasing organic content from the bottom to half way up the core, above which the carbon content stabilises. Photographs of the basal two core segments are shown in Figure 6.7.

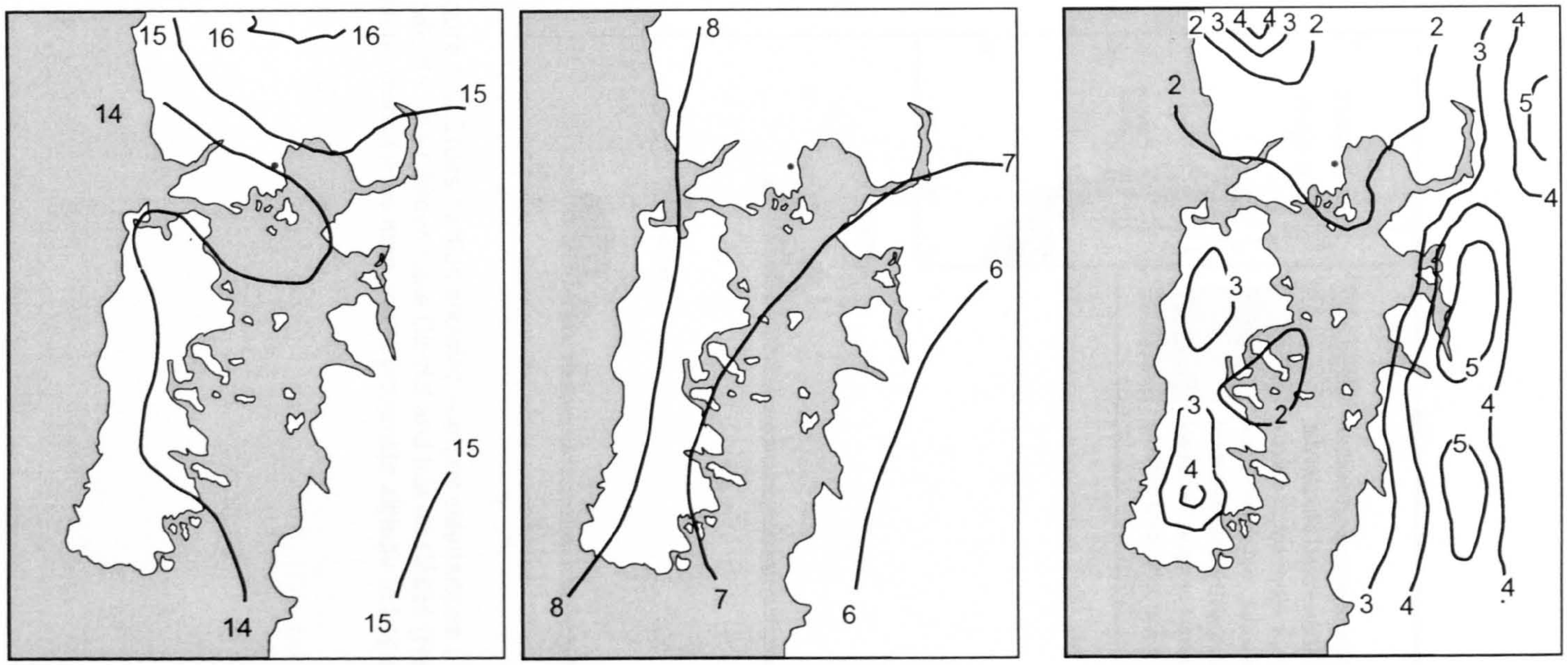

Average January Temperature (°C) Average July Temperature (°C) Average Annual Precipitation (mm x 10^3)

Figure 6.4 : Average January and July isotherms and annual precipitation isohyets for the Southern Lake District and Isla Grande de Chiloé (based on Alemyda and Sáez (1958) cited in Heusser *et al.*, 1999). Red circle marks the location of Laguna Leta.

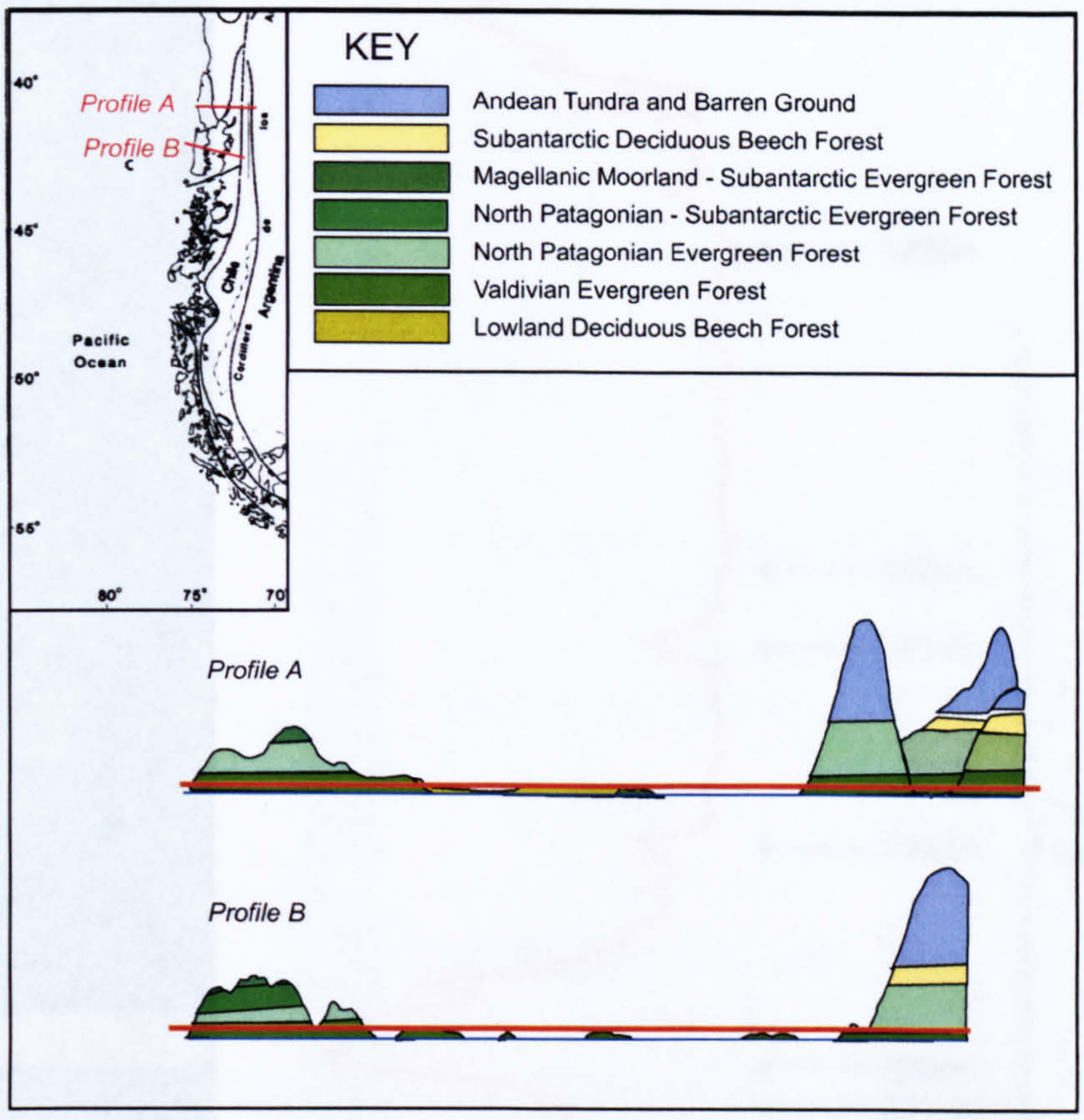

Figure 6.5: Cross-section showing ecotone distributions over an altitudinal gradient in the Chilean Lake District and Isla de Chiloé (Heusser *et al*. 1999, 238). Red horizontal lines mark the approximate altitude of Laguna Leta.

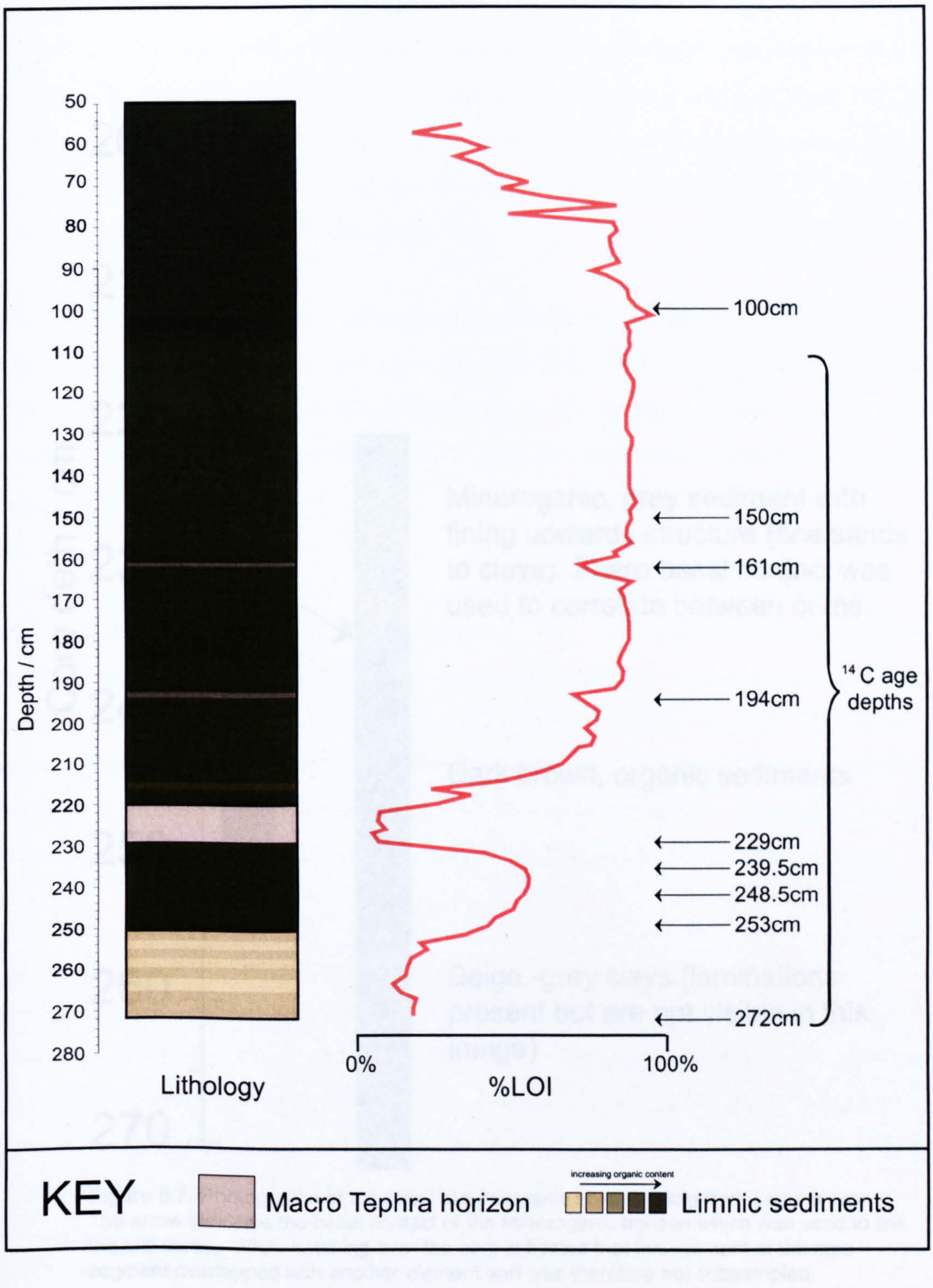

Figure 6.6 : Stratigraphy (established from visual examination and x-rays of cores) and organic content (% LOI) of Lago Leta core. Depths which were sampled for ^{14}C dating are indicated.

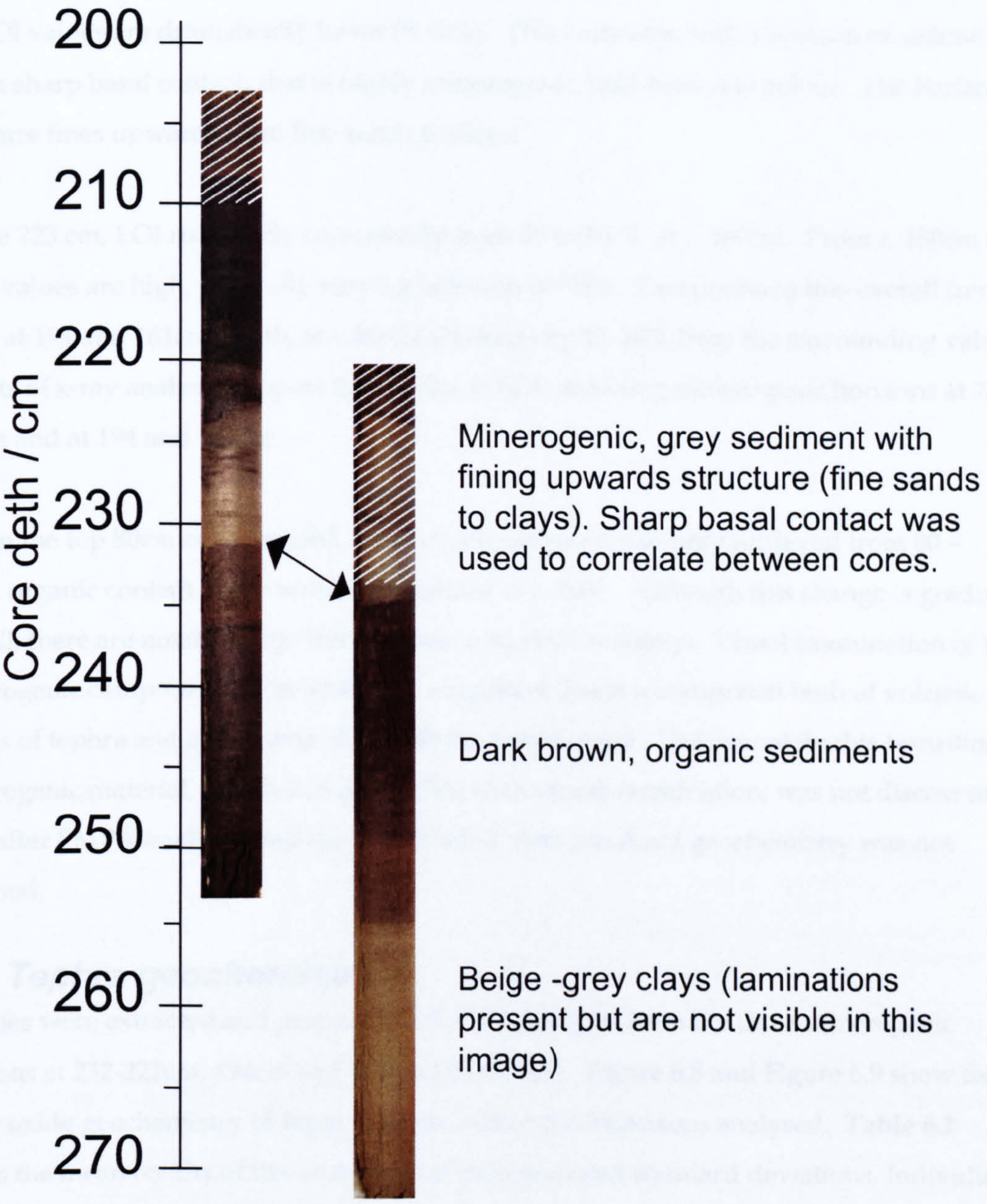

Figure 6.7: Photographs of the basal two segments of core taken from Laguna Leta. The arrow indicates the basal contact of the minerogenic horizon which was used to link the two cores. White hatching over the core indicates that this element of the core segment overlapped with another element and was therefore not subsampled.

Percentage organic carbon shows a gradual rise from low levels of 12-19% to 55% in the basal 43 cm of the core. Within this basal section the more minerogenic deposits between 266-253 cm display laminations which are beige and mid-brown in colour. From 230-223 cm LOI values are dramatically lower (8-10%). This coincides with a horizon of sediment, with a sharp basal contact, that is highly minerogenic, mid-brown in colour. The horizon's structure fines upwards from fine sands to clays.

Above 223 cm, LOI rises fairly consistently from 60 to 90 %, at *c.* 180cm. From *c.* 180cm to *c.* 90cm values are high, generally varying between 80-95%. Exceptions to this overall trend occur at 194 and 161cm depth, at which LOI drops by 15-20% from the surrounding values. Results of x-ray analysis support the results of LOI, detecting minerogenic horizons at 232-221cm and at 194 and 161cm.

Within the top 80cm of the record, from which sediment was only retrieved from 80 – 50cm, organic content of the sediment declines to *c.* 30%. Although this change is gradual overall, there are notably large fluctuations in the LOI readings. Visual examination of the minerogenic component of the sediment suggested that it is comprised both of volcanic shards of tephra and also grains of non-shard morphology. Unfortunately this transition to minerogenic material, which was not visible with visual examination, was not discovered until after EMPA analyses had been conducted; thus the shard geochemistry was not analysed.

6.4 Tephra geochemistries

Samples were extracted and prepared for EMPA analysis from the three minerogenic horizons at 232-221cm, 194cm and 161cm (**Table 6.1**). Figure 6.8 and Figure 6.9 show the major oxide geochemistry of tephra shards within the 3 horizons analysed. **Table 6.1** shows the mean results of the analyses and the associated standard deviations. Individual shard results are illustrated in biplots and ternary plots and results are detailed in Appendix 1.

Figure 6.8 shows that the tephra shards are mostly dacitic and rhyolitic in nature. The analyses from the thicker horizon 221-232cm show that the geochemistry of the rhyolitic shard are tightly grouped. Although generally silicic in nature, the shards from the other levels have a less consistent geochemistry. This is indicated by larger standard deviations within the population and looser groupings on the diagram.

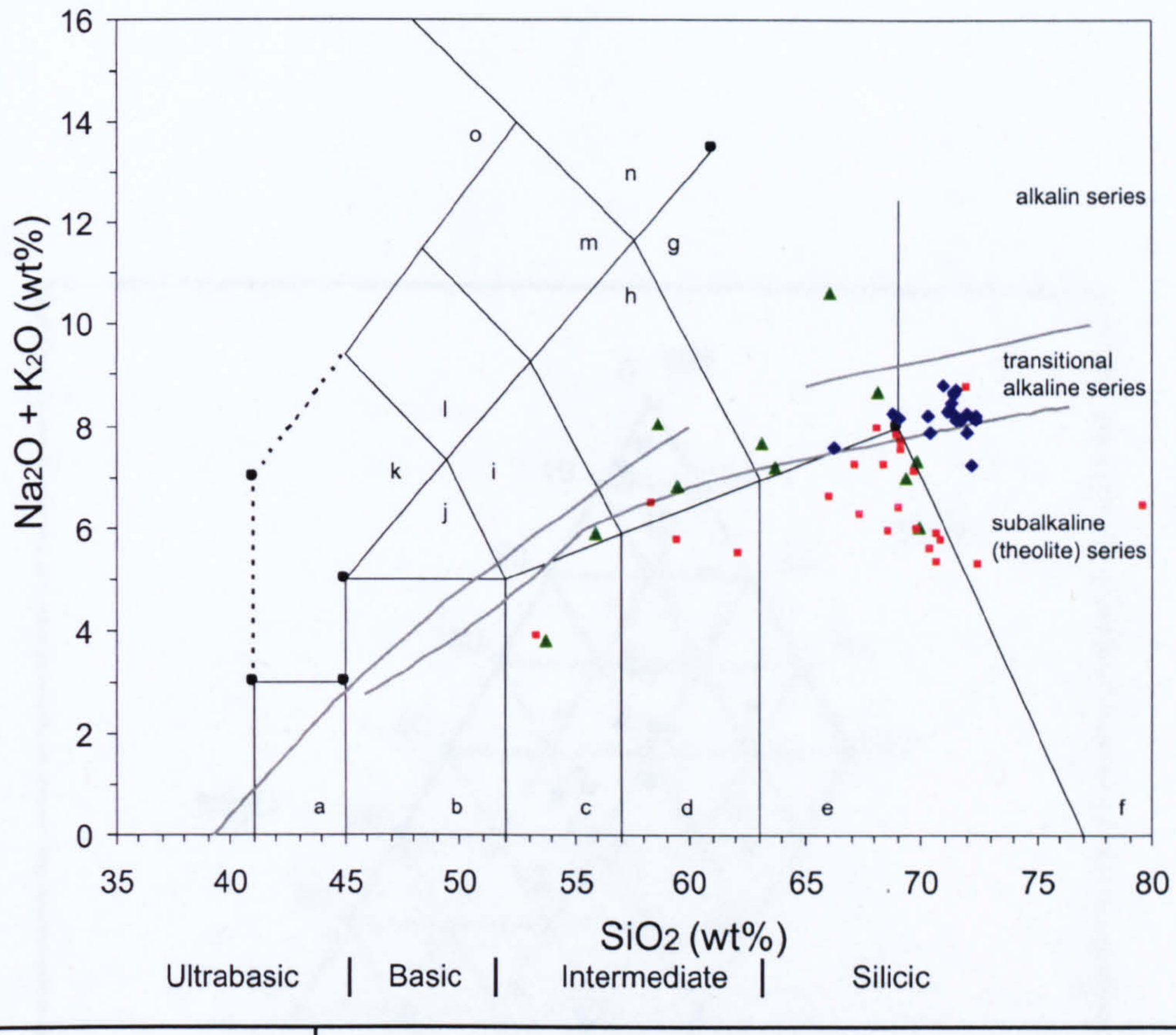

KEY	Chemical classification and nomenclature of volcanic rocks (Le Maitre *et al.*, 1989): a = Picrobasalt; b = Basalt; c = Basaltic andesite; d = Andesite; e = Dacite; f = Rhyolite; g = Trachyte (normative quartz <20%) or Trachydacite (normative quartz >20%); h = Trachyandesite; i = Basaltictrachyandesite; j = Trachybasalt; k = Tephrite (normative olivine <10%) or Basanite (normative olivine >10%); l = Phonotephrite; m = Tephriphonolite; n = Phonolite; o = Foidite.
▲ 161cm ▪ 194 cm ◆ 221-232 cm	

Figure 6.8: Classification bi-plots of tephra shards analysed from Laguna Leta using Total alkali-silica (TAS) classification diagram annotated with subdivision of volcanic rocks into alkaline, transitional alkaline and subalkaline (tholeiitic) . Upper line after Irvine and Baragar (1971), lower line after Kuno (1966). All geochemical data were normalised to 100% before being plotted.

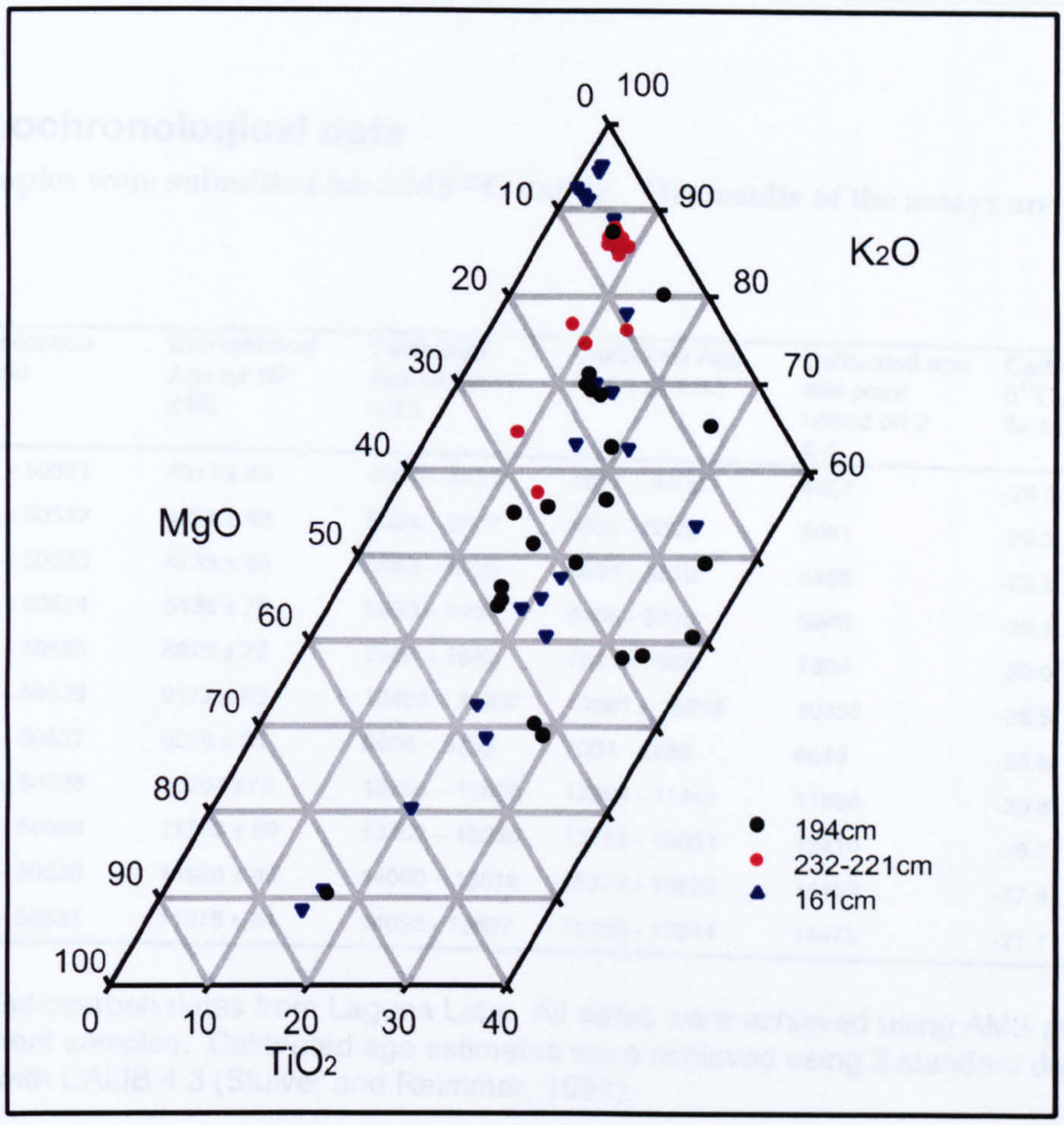

Figure 6.9: Tertiary plot showing unormalised electron microprobe analysis (EMPA) results of tephra shards analysed from 3 horizons in Laguna Leta.

Table 6.1 : Mean percentage (shown with 1 standard deviation) of the 9 major oxides measured within tephra shards in minerogenic horizons in Laguna Leta

Depth (cm)	SiO_2	TiO_2	Al_2O_3	FeO	MnO	MgO	CaO	Na_sO	K_2O
161	65.73 ± 6.55	0.65 ± 0.49	15.69± 1.85	3.99± 2.26	0.12 ± 0.05	1.24 ± 1.36	3.18 ± 2.71	4.28±1. 10	2.47 ± 0.84
194	65.71 ± 5.04	0.77 ± 0.42	15.26 ± 1.66	4.00 ± 2.21	0.12 ± 0.05	1.04 ± 1.11	3.56 ± 2.07	4.31 ± 0.53	1.88 ± 0.84
212-232	68.55 ± 1.37	0.37 ± 0.11	13.82 ± 0.28	3.67 ± 0.49	0.14 ± 0.02	0.41 ± 0.35	1.66 ± 0.54	4.46 ± 0.31	3.42 ± 0.23

6.4.1 Geochronological data

11 bulk samples were submitted for AMS ^{14}C dating. The results of the assays are given in Table 6.2.

Sample depth /cm	Publication Code	Conventional Age (yr BP ±1б)	Calibrated Age range (1 s.d.)	Calibrated Age range (2 s.d.)	Calibrated age mid point based on 2 s.d	Carbon $\delta^{13}C_{-PDB}$ ‰ ± 0.1
100	AA – 50521	4011 ± 48	4564 – 4417	4507 – 4406	4457	-29 3
150	AA – 50522	4764 ± 49	5334 – 5597	5597 - 5325	5461	-29 2
161	AA – 50523	4735 ± 49	5583 – 5329	5591 - 5320	5456	-29.2
189	AA – 50524	5135 ± 70	5933 – 5754	6166 - 5725	5946	-29 1
194	AA – 50525	6970 ± 72	7923 – 7686	7941 - 7666	7804	-29.0
208	AA – 50526	9172 ± 63	10486 – 10237	10501 – 10215	10358	-28.5
232	AA – 50527	6018 ± 55	6906 – 6755	7001 - 6688	6845	-28.8
239.5	AA – 50528	10204 ±73	12284 – 11695	12354 - 11441	11898	-30.8
248.5	AA – 50529	11353 ± 80	13452 – 13260	13788 - 13031	13410	-28.7
253	AA – 50530	11926 ± 83	14080 – 13819	15278 - 13625	14452	-27 8
272	AA – 50531	11975 ± 84	14098 - 13827	15306 - 13644	14475	-21.1

Table 6.2: Radiocarbon dates from Laguna Leta. All dates were achieved using AMS analysis of bulk sediment samples. Calibrated age estimates were achieved using 2 standard deviations (s.d.) errors with CALIB 4.3 (Stuiver and Reimmer, 1993).

Figure 6.10 shows these results plotted against depth in the core. These results indicate that the core dates back to 11975 ± 84 ^{14}C yr BP, which produces a basal calibrated age range of 15306 – 13644 cal yr BP, based on calibration using 2 s.d.. With the exception of the ^{14}C date from just below the most prominent minerogenic layer at 232cm (AA-50527), all the dates lie in stratigraphic order.

6.4.2 Chironomid analysis

The full chironomid record analysed from Laguna Leta is displayed in Figure 6.11. Using the broken stick method and optimal partitioning, four zones were identified as being statistically significant. In addition to this, sub-zones were added, where appropriate, to

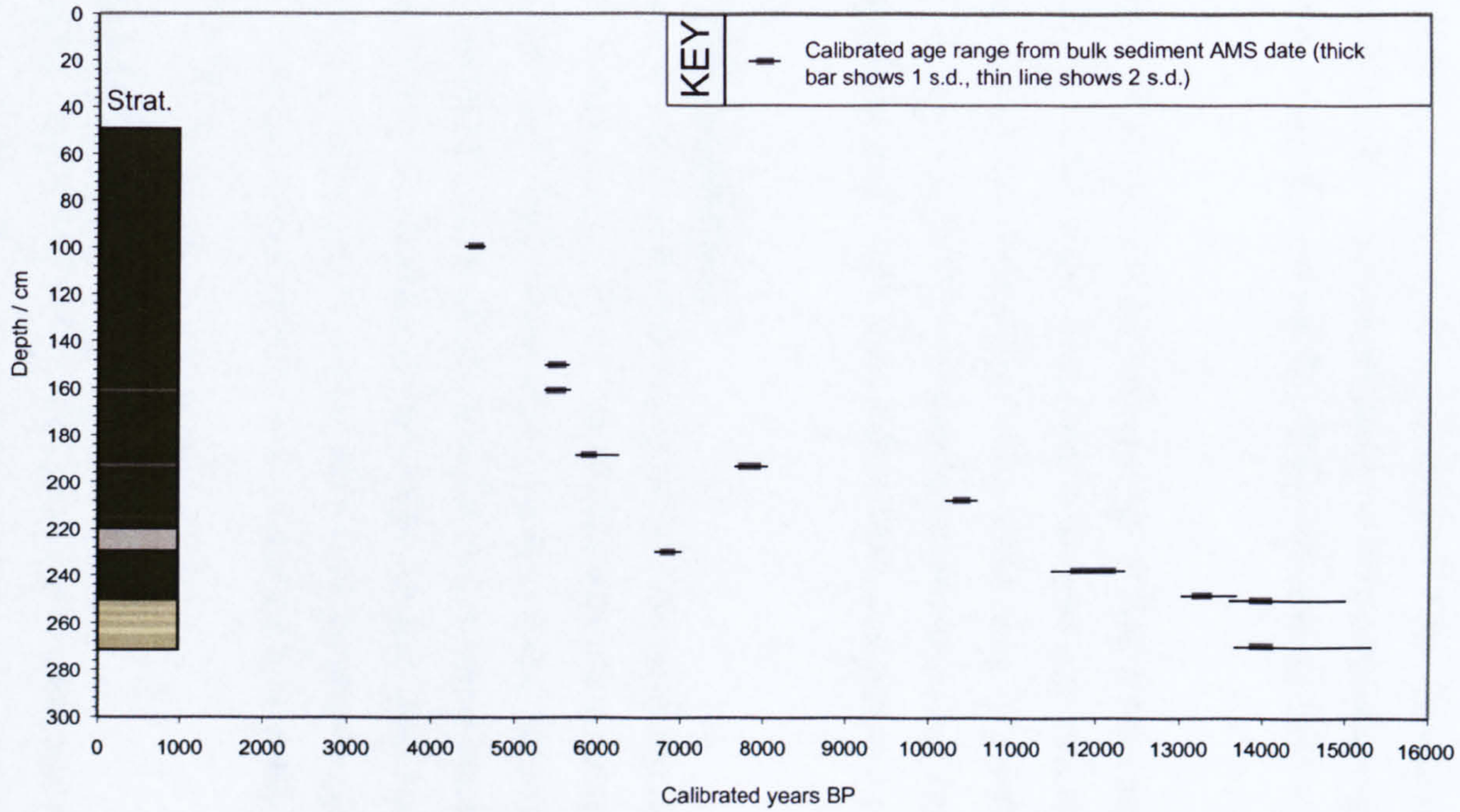

Figure 6.10 : Depth versus age diagram showing the results of ^{14}C dating of the Laguna Boal core. Calibrated age ranges are shown using both one and two standard deviations. The core stratigraphy is shown in the insert on the left of the graph (for key see Figure 6.4). Further details are shown in Table 6.2.

aid description of the record. These zones and the chironomid concentrations in head capsules g^{-1} (wet sediment) are shown on the diagram. These data are summarised, along with LOI data, in Figure 6.12. Taxon-specific concentration data are shown in Figure 6.13.

6.4.2.1 LET-1 (272 – 248.5cm)

LET-1 spans the basal 25cm of the sequence. Within the zone there is quite a high degree of variability in the assemblage. This is mainly a function of low counts, especially in the lowest two samples, due to low concentrations (< *c.* 150 head capsules per gram). For this reason, these lower two samples were assigned the sub-zone of LET-1a, leaving 255-248.5 as LET-1b.

Pseudochironomus and *Polypedilum*, along with a range of Tanytarsini, are all present in the LET-1a. Within LET-1b, where sample sizes exceed 50 head capsules, the fauna is quite diverse with similar a percentage abundance of *Lauterborniella*, *Polypedilum*, *Parakiefferiella*, Tanytarsini Taxa E, A, D and B, *Ablabesmyia* and Macropelopiini and Procladiini, all <25%. In this sub-zone, concentrations start to rise, with a sub-zonal mean of *c.* 80 head capsules per gram.

6.4.2.2 LET-2 (248.5-239.5cm)

Tanytarsini A is the dominant taxon in LET-2 (17-43%). There are also high percentages of *Ablabesmyia* (3-14%), Tanytarsini E (13 – 18%) and *Parakiefferiella* (6-18%). Within the zone, Tanytarsini Taxa D and B are also present, as are *Lauterborniella*, *Polypedilum* and *Paralimnophyes/ Limnophyes* Taxon A, although in lower concentrations than the surrounding zones. There is also a sharp decline in the relative abundance of *Pseudochironomus*, due to a decrease in concentration from zonal averages of 5 – 3 head capsules per gram. Concentrations within the zone are highly variable, ranging from 90–380 head capsules per gram.

6.4.2.3 LET-3 (239.5-194cm)

Although Chironomini, Tanytarsini and Tanypodinae are the dominant tribes and family within LET-3, there is a distinct difference in the taxonomic assemblage above and below the minerogenic horizon (221-232cm). Therefore the zone was divided into LET-3a below the horizon (239.5-232 cm) and LET-3b above (221-194cm).

The seven levels within LET-3a have a high percentage of Tanytarsini Taxon E (8-25%), *Lauterborniella* (1-16%) and *Ablabesmyia* (3-23%). Although found in high abundance at the

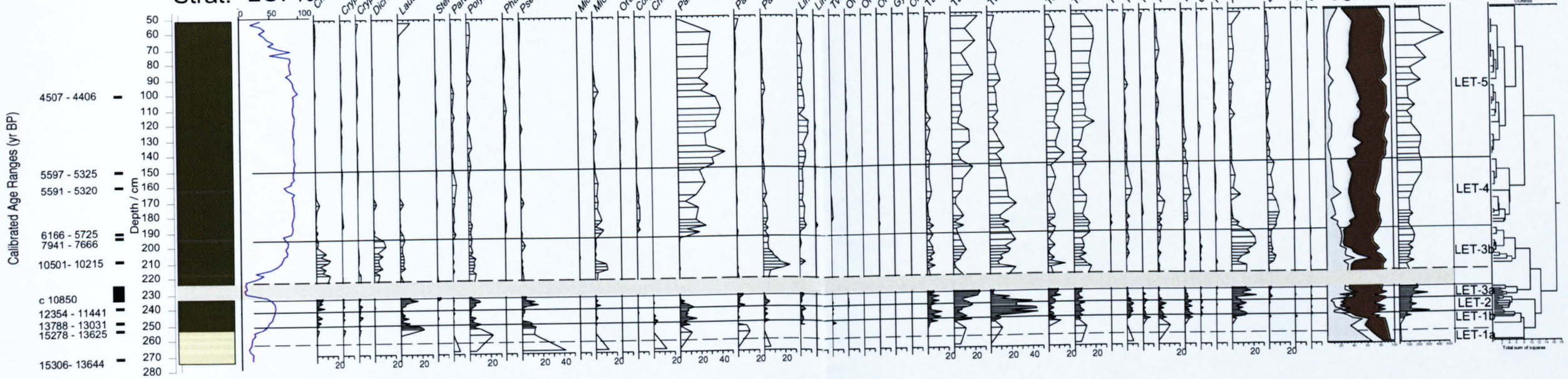

Figure 6.11 : Percentage diagram showing all taxa from Laguna Leta. Key to stratigraphy is in Fig. 6.6. Grey band is tephra horizon, which was not analysed for midges. All dates are in cal yrs BP.

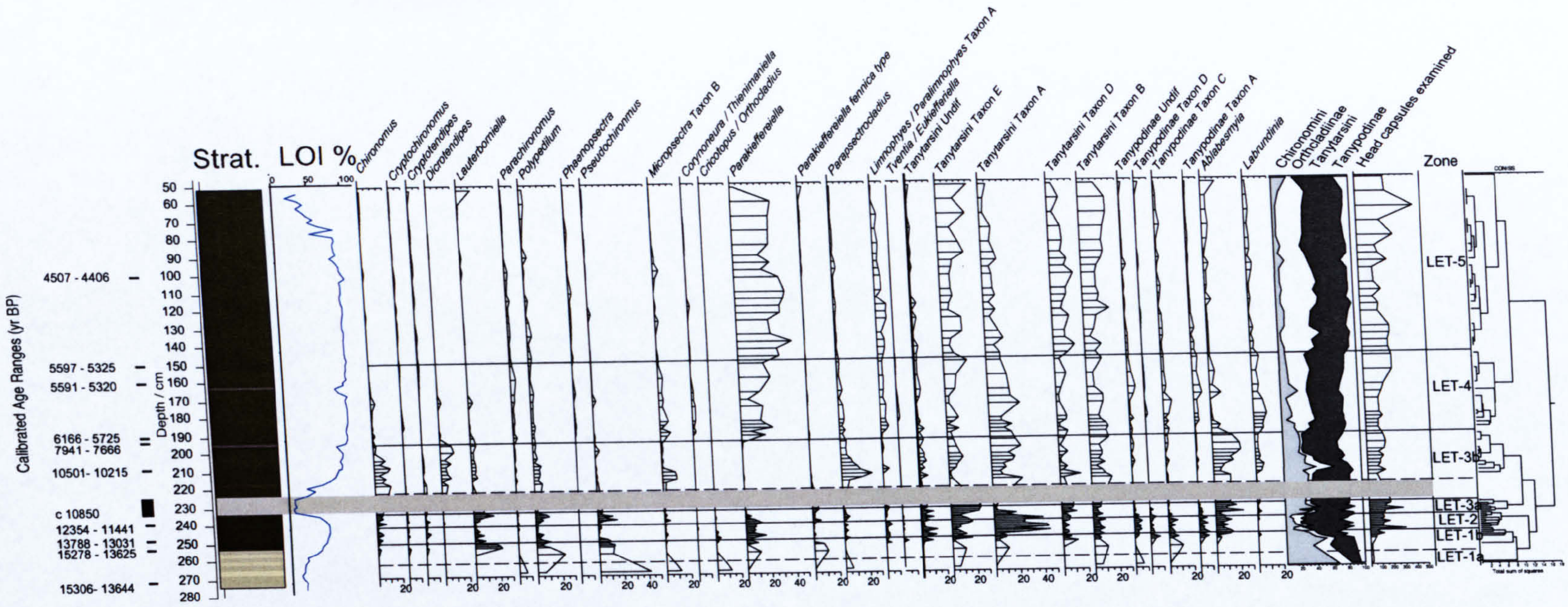

Figure 6.12 : Percentage diagram showing selected taxa from Laguna Leta. Key to stratigraphy is in Fig. 6.6. Grey band is tephra horizon, which was not analysed for midges. All dates are in cal yrs BP.

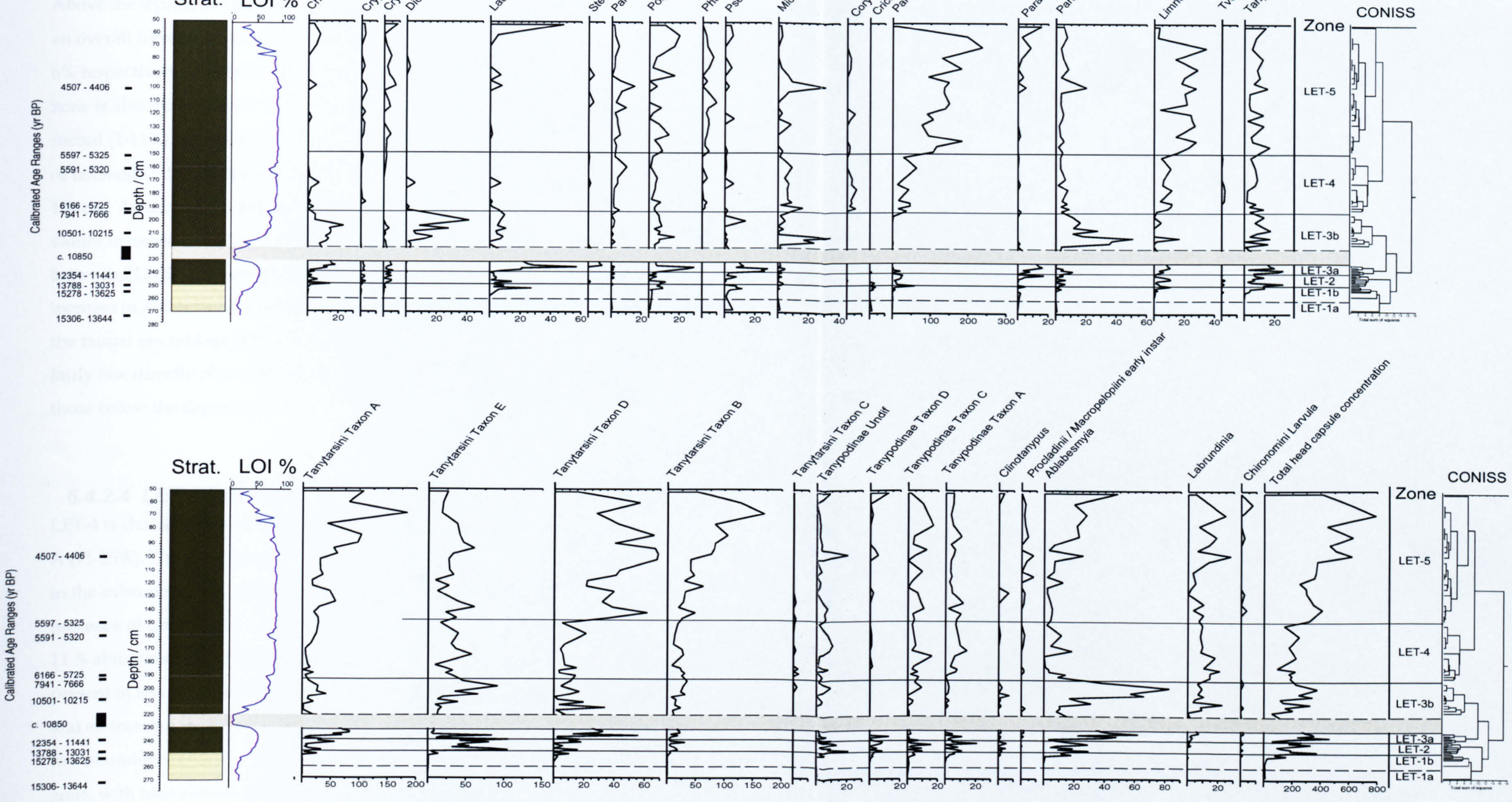

Figure 6.13 : Concentration diagram showing selected taxa from Laguna Leta. Key to stratigraphy is in Fig. 6.6. Grey band is tephra horizon, which was not analysed for midges. All dates are in cal yrs BP. All concentrations are given in head capsules per gram of wet sediment.

base of the zone (39%), Tanytarsini Taxon A quickly drops down to levels as low as 1%. Percentages of Tanytarsini Taxas D and B remain generally remain steady, with values of 1-16%. *Chironomus, Pseudochironomus* and *Polypedilum* are present throughout the zone (< 20%). Head capsule concentration is generally quite high, averaging *c.* 270 head capsules per gram.

Above the tephra, in LET-3b, the percentages of Tanytarsini Taxon E are lower, and there is an overall increase in abundance of *Chironomus* and *Labrundinia,* ranging from 1-13% and 0-6% respectively. *Parakiefferiella* is almost exclusively absent from the sub-zone. This sub-zone is also the only time when *Dicrotendipes* is notably present in the fauna within the record (1-11%). In addition to these major differences from LET-3a, there is also a sequence of taxonomic dominance through a succession of several different taxa between 221 and 194 cm. An increase in the concentration of *Parapsectrocladius* and *Micropsectra* Taxon B to values in excess of *c.*50 and *c.*30 head capsules per gram causes a peak in their abundance between 212-216 cm, rising to 12 and 15%, respectively. This is then followed by an increase in *Ablabesmyia* to concentrations of 60 – 80 head capsules per gram and > 17% of the faunal assemblage between 200 and 206cm. Total head capsule concentrations are fairly low directly above the minerogenic horizon but increase to levels comparable with those below the deposit at 206cm.

6.4.2.4 LET-4 (194-150cm)

LET-4 is characterised by high percentage of *Parakiefferiella* (6-26%) and Tanytarsini Taxon A (11-25%). The presence of the former is particularly notable, as it only occurs in one level in the subzone below, at an abundance of <1%. In addition to these taxa, there is a constant presence of *Labrundinia* and *Limnophyes / Paralimnophyes* Taxon A at levels of between 3 and 11 % abundance. Although *Parachironomus, Micropsectra* Taxon B and *Polypedilum* are often present in low percentages (< 8%), there is an overall low representation of Chironomini and an increase in Orthocladiinae within the zone. *Parapsectrocladius* remains, although in low abundance (< 5 %). Macropelopiini / Procladiini are also well represented within the zone, with total percentage abundance for this group of 2-9 %. Although fairly consistent, concentration levels (*c.* 100 – 250) are often lower than those in zones above and below LET-4.

6.4.2.5 LET- 5 (150-0cm)

LET-5 is also dominated by high abundance of *Parakiefferiella* and Tanytarsini. There is also a persistent presence of *Paralimnophyes/ Limnophyes* Taxon A throughout the zone (0.5-9%). There are two major changes within the zone. Firstly there is a marked drop in the concentration of head capsules in the upper two levels above 60cm. Until this point there is a fairly constant increase in concentration of head capsules throughout the zone. When compared with other zones, LET-5 has the highest chironomid concentrations at *c.* 450 head capsules wet g^{-1}. The second major change is the increase in Tanytarsini Taxon E, *Lauterborniella* and *Ablabesmyia* in the uppermost sub-sample. Examination of the concentration data show that although concentration of these taxa does increase, the increase in abundance is primarily driven by the sharp drop in concentration in *Parakiefferiella* from levels averaging *c.* 140 throughout the zone to 10 head capsules per gram in the uppermost level.

6.5 Developing a chronology

6.5.1 Tephrochronology

When EMPA results of tephra shards from the 3 horizons were analysed the data suggests that only one of the horizons marked the deposition of an individual volcanic event. The wide range of values within the horizons at 161 and 194cm (Figure 6.8 and Figure 6.9) indicates that these deposits contain a composite of several different eruptions. A possible mechanism for their deposition is inwash events due erosion in the catchment, possibly due to an increase in precipiation.

Conversely, the tightly grouped results of EMPA analysis of the minerogenic horizon between 221 and 232cm (Figure 6.8 and Figure 6.9), together with its consistent colour and upwards grading indicates that it is the result of a single eruption. Work by Heusser and Moreno has documented the wide-spread distribution of an early Holocene tephra within the Chilean Lake District and Chiloé region (Heusser *et al.*, 1995; Moreno *et al.*, 1999). Dating of this horizon at three sites on Isla de Chiloé has provided maximum constraining dates of 9500 ± 110, 9200 ± 80 and 9760 ± 90 ^{14}C yr BP at the sites of Mayol, Estero Huitanque and Puchilo, respectively (Heusser *et al.*, 1995). However, no geochemical data on the horizons are available. Based on the assumption that the horizon at Laguna Leta was derived from the same eruption, a mean of these dates could be used to aid constraint of the the site's chronology. Following calibration of the individual dates using errors at 2

standard deviations, a mean age range of 11026 - 10477 cal yr BP was estimated for the eruption.

6.5.2 Combining tephrochronology with ^{14}C results

Results of ^{14}C dating of sediment from Laguna Leta were used as the framework for a chronology at the site. These ^{14}C age-estimates are augmented by the inclusion of the mean value of the age range derived from the presence of the tephra layer at 232-221 cm of c. 10751 cal yr BP (6.5.1).

The validity of the ^{14}C age estimate of 232cm depth (AA – 50527), located just below the macro-tephra, is questionable. It lies out of stratigraphic order with the other ^{14}C results and disagrees with the results of dating of this eruption within other sites (6.5.1). Two hypotheses could explain this apparent contradiction: either the two different sets of results actually refer to two different volcanic events, or the date from Laguna Leta is inaccurate. The former hypothesis was rejected based on the following arguments:

a) the thickness of the deposit suggests it is unlikely to be localised,
b) the early Holocene deposit dated in Heusser *et al.* (1995) has been found both to the South and the North of Laguna Leta and is therefore likely to be present,
c) the anomalous age of the layer at 232cm lay out of sequence with other dates from the site.

For these reasons AA – 50527 is eliminated from further discussion of the age-estimates constraining Laguna Leta's chronology.

A sedimentation curve was constructed using the 11 chronologically constrained depths discussed above (Figure 6.14). To produce a more realistic representation of the sedimentation processes, it was assumed that the deposition of the early Holocene macro-tephra was a geologically 'instantaneous' event (*sensu* Turney and Lowe, 2001). Therefore, depths from 221–232 cm were all assigned the same age. The sedimentation curve is based on calibrated ages as opposed to ^{14}C ages. This was deemed more suitable as substantial ^{14}C plateaus, known to exist during the LGIT, mean that the use of uncalibrated age estimates result in a sedimentation rate influenced by artificial fluctuations in the ^{14}C concentrations (Hughen, 1998). The production of a calibrated chronology also affords easier comparisons with records dated using methods other than ^{14}C, such as the ice-cores.

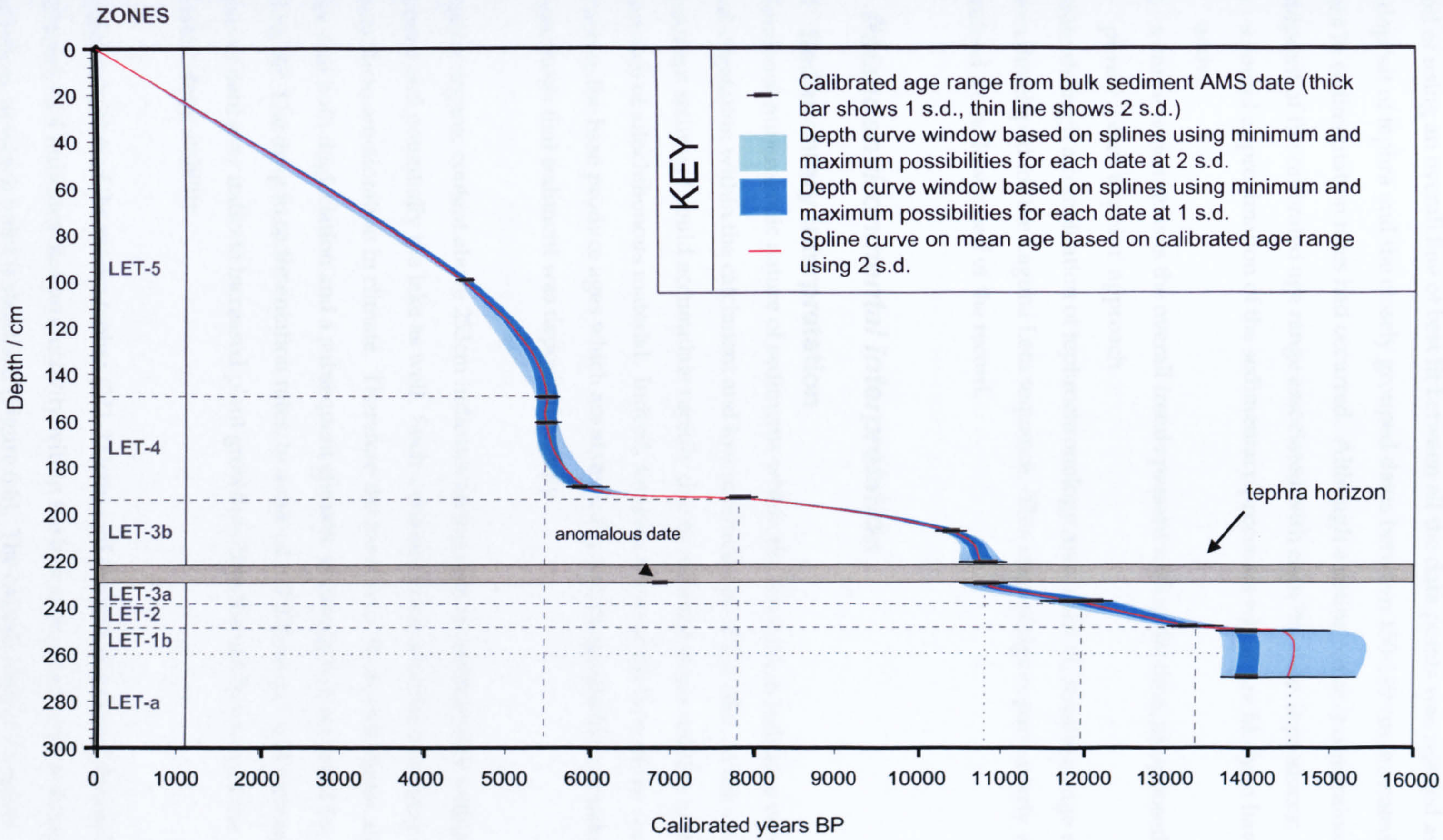

Figure 6.14: Sedimentation curve for Laguna Leta. All age ranges are shown in calibrated ages (see Table 6.2 for further details) at 68% confidence (1sd). Chironomid zones are annotated on the left side of the graph.

A spline curve was used to reconstruct the record's sedimentation rate. The alternative method of using an overall line of best fit between all the data points was rejected as the mass-deposit of tephra and the closely grouped dates between 150-189 cm indicated that changes in sedimentation rates had occurred. Although a spline curve is constrained by the midpoint of the calibrated age range associated with each ^{14}C date, it produces:

a) a sound approximation of the sedimentary processes which are likely to have been active
b) a curve which reflects the overall trends present within the data, as opposed to a purely 'point to point' approach.

Therefore through a combination of tephrochronology and AMS ^{14}C results an age model has been developed for the Laguna Leta sequence. This chronology is particularly well constrained in the lower half of the record.

6.6 Palaeoenvironmental interpretation

6.6.1 Sedimentary interpretation

The dominant minerogenic nature of sediments within the basal 20cm indicates very limited vegetation within the catchment and low productivity of the lake. Within such an environment sediment could accumulate rapidly due to minimal slope stability and thus high inwash of allochthonous material. Indeed, samples taken at the base of the core and 20cm above the base produce ages which are statistically indistinguishable, consistent with the hypothesis that sediment was deposited rapidly.

Increasing organic content above 253cm indicates an increase in productivity within the catchment and potentially the lake as well. Such a change in bio-environment may be attributable to amelioration in climate. Therefore the basal two ^{14}C age estimates allows us to infer that both deglaciation and a subsequent climatic warming had occurred by *c.* 13.8-14 cal ka BP. The drop in sedimentation rates, to a rate of *c.* 0.006cm yr^{-1} and increasing organic content may indicate increased plant growth within the catchment and the associated slope stability.

With the exception of the macro-tephra (221-232cm) and the proposed inwash bands (161 and 194cm), LOI indicates that productivity within the lake continued to increase until about 190cm, at which point it stabilised (Figure 6.6). The overall high LOI results throughout the upper 140cm of the sediment may indicate that the lake's catchment was

highly productive over the last *c.* 7000 cal yr BP. Within this period there are several notable changes in sedimentation rates which increased to probably > 0.8 cm yr^{-1}, before decreasing to < 0.05cm yr^{-1}. These latter rates are still faster than in the early Holocene. Unfortunately, ascertaining an accurate date for of this latter deceleration in the sedimentation regime is difficult due to a lower density of ^{14}C assays, but the change probably occurred some time after c. 5.5 cal ka BP.

It is difficult to ascertain what caused the increasing minerogenic content of the core between 80– 50 cm without further analysis of the geochemistry of this part of the core. Sediment analysis of the record from Rucañancu, Isla de Chiloé, shows the presence of two late Holocene layers of tephra, both of which were deposited some time after 3,900 ± 140 ^{14}C ka BP (Heusser, 1984). However, since no geochemical data on these horizons are available it is problematic to say with certainty that the two deposits result from two separate eruptions. Within the Laguna Leta record, the gradual decline in LOI between 50-80cm is uncharacteristic a trend that would be expected as the result of a single volcanic eruption. Such an event would be characterised by a sharp drop in LOI followed by a gradual recovery, as is the case with the macro-tephra encountered between 232-221cm in the Laguna Leta record. Therefore, it may be that during the Late Holocene at Laguna Leta there was increased inwash of allochthonous material into the basin due to a change in environmental conditions, and that tephra eruptions were responsible for pulses of minerogenic input, as is indicated by the higher frequency fluctuations in the LOI results.

6.6.2 Chironomid interpretation

The chironomid zones described in 6.4.2 can be chronologically constrained by the bracketing ages as given in Table 6.3.

The assemblages found throughout the core were also plotted on the CCA ordination bi-plot developed in Chapter 5 (Figure 6.15) to assess how they relate to the statistically significant environmental variables ($p>0.05$) (altitude, longitude, latitude, LOI, lake depth and conductivity). The position of the modern day sites on which the ordination was based are also shown to indicate the overlap of the palaeorecords with modern day assemblages. The assemblage represented by the modern day sample from Laguna Leta is highlighted. The diagram shows that, in general, the down-core results plots in a similar area to these of modern day sites, indicating that taxonomic assemblages similar to those

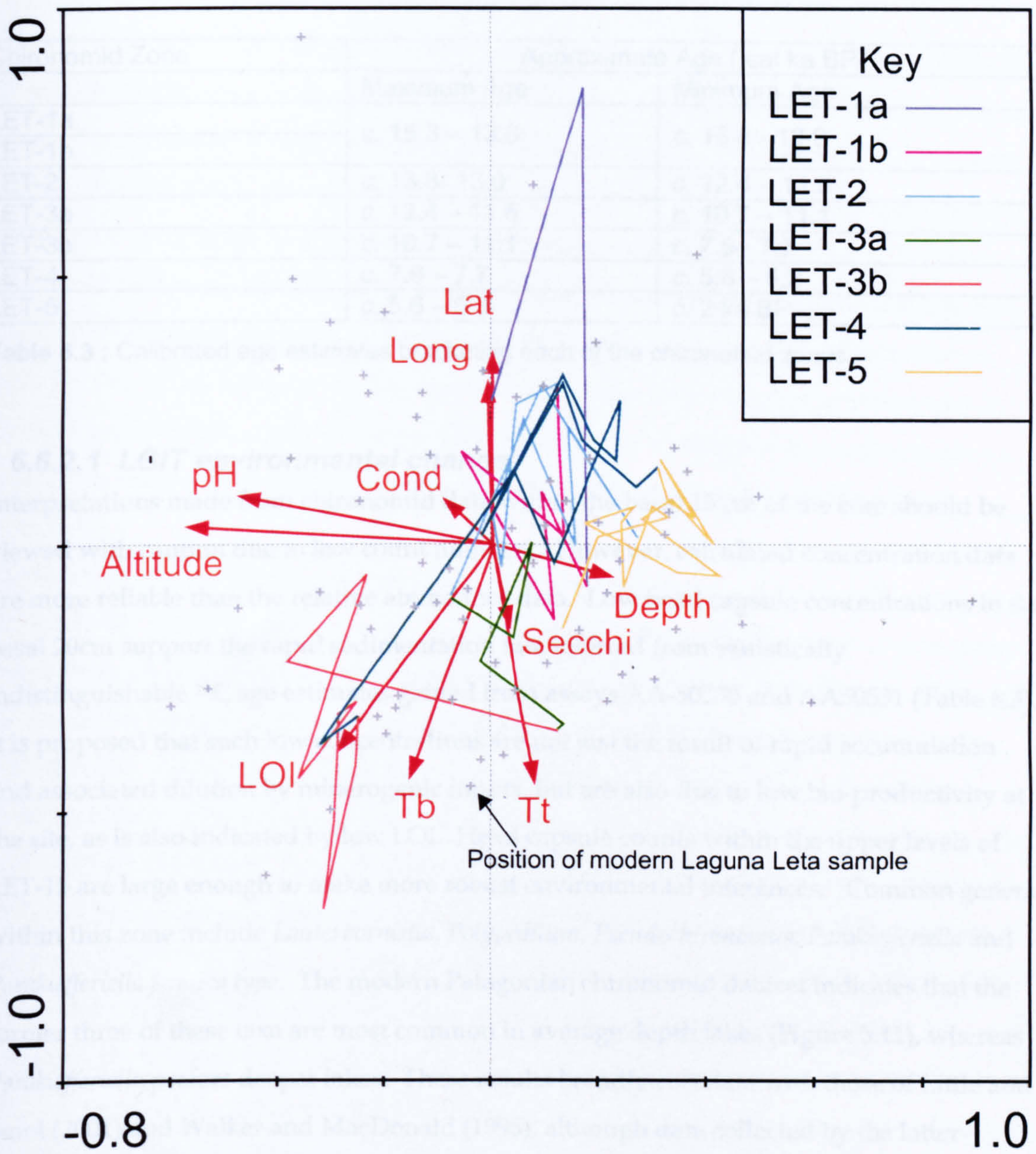

Figure 6.15: Assemblages found in the down core Laguna Leta record as passive samples using the CCA ordination developed in Chapter 5. Different coloured lines represent different (sub) zones in the record. Grey crosses represent the location of modern day lakes plotted during CCA. Environmental variables used in the ordination are shown.

encountered in the modern day sites existed in the past and should, thus, have good analogues in the modern training set.

Chironomid Zone	Approximate Age (cal ka BP)	
	Maximum Age	Minimum Age
LET-1a LET-1b	*c.* 15.3 – 13.6	*c.* 13.8 - 13.0
LET-2	*c.* 13.8- 13.0	*c.* 12.4 – 11.5
LET-3a	*c.* 12.4 – 11.5	*c.* 10.7 – 11.1
LET-3b	*c.* 10.7 – 11.1	*c.* 7.9– 7.7
LET-4	*c.* 7.9 – 7.7	*c.* 5.6 – 5.3
LET-5	*c.* 5.6 – 5.3	*c.* 2 ka BP

Table 6.3 : Calibrated age estimates bracketing each of the chironomid zones.

6.6.2.1 LGIT environmental change

Interpretations made from chironomid data within the basal 15 cm of the core should be viewed with caution due to low count numbers. However, calculated concentration data are more reliable than the relative abundance data. Low head capsule concentrations in the basal 20cm support the rapid sedimentation rate inferred from statistically indistinguishable ^{14}C age estimates gained from assays AA-50530 and AA50531 (Table 6.3). It is proposed that such low concentrations are not just the result of rapid accumulation and associated dilution by minerogenic inputs, but are also due to low bio-productivity at the site, as is also indicated by low LOI. Head capsule counts within the upper levels of LET-1b are large enough to make more robust environmental inferences. Common genera within this zone include *Lauterborniella, Polypedilum, Pseudochironomus, Parakiefferiella* and *Parakiefferiella fennica type.* The modern Patagonian chironomid dataset indicates that the former three of these taxa are most common in average depth lakes (Figure 5.11), whereas *Parakiefferiella* prefers deeper lakes. These results broadly correlate with those of Little and Smol (2001) and Walker and MacDonald (1995), although data collected by the latter suggested that *Polypedilum* prefers shallower lakes. Pinder and Reiss (1983) state that *Lauterborniella* is common in small bodies of water and is often associated with macrophytes and that *Polypedilum* is a highly cosmopolitan taxon. In contrast to these taxa, *Parakiefferiella fennica type* is indicated by Walker and McDonald (1989, 1995) to be an indicator of cold and oligotrophic conditions as opposed to being particularly linked to lake depth. However, the modern Patagonian training set did not indicate this latter taxon to be indicative of particularly deep waters but to be more associated with low LOI, indicating low bio-productivity of these lakes. Therefore the interpretation of the down-core midge assemblage from post deglaciation lake formation up until *c.* 13.4 cal ka BP is

not conclusive. However, the data suggest that the lake was a medium-depth body of water, potentially with macrophyte growth but with rather low productivity.

The marked increase in both concentration and percentages of *Parakiefferiella* at *c.* 13.4 cal ka BP possibly indicates a deepening of the lake. The genus *Parakiefferiella* is associated with a range of environmental conditions (Walker and MacDonald, 1989, 1995; Lotter *et al*, 1998, Little and Smol, 2001). However, based on the Patagonian modern ecological information, the increase of *Parakiefferiella* at Laguna Leta strongly indicates a deepening of the lake which endured from *c.*13.4 - 12.0 cal ka BP. Such a deepening seems a plausible scenario when viewed in conjunction with the increase in Tanytarsini Taxon A and reduction in more littoral, Chironomini taxa., The major candidate for such a change is an increase in effective precipitation. Such a change could be via either an increase in precipitation or a decrease in temperature and a consequential decrease in evaporation of lake waters.

A reversal to an assemblage more similar to that present before *c.* 13.4 cal yr BP occurs at *c.* 12.0 cal yr BP. There is an increase of *Lauterborniella* and *Polypedilum* in both concentration and percentage abundance, concomitant with a sharp decrease in *Parakiefferiella*. This could indicate either a return to the combination of environmental conditions present prior to 13.4 cal yr BP. Alternatively, there may have been a change to another permutation of environmental conditions which resulted in the lake supporting the same assemblage. The increase of *Lauterborniella, Polypedilum* and *Chironomus* potentially indicates an increase in trophic status, as all these taxa have been found to thrive in more nutrient rich conditions (Little and Smol, 1995; Brundin, 1958). *Pseudochironomus* also increases at the LET-2 / LET-3a boundary, both in concentration and percentage occurrence. Although there is no overriding preference of this genus within the Patagonian training set, Lotter *et al.*, (1997, 1998) indicate that the taxon may be positively related to temperature and nutrient levels in their Swiss training set. *Ablabesmyia* also increases markedly during this period, both in percentage abundance and in concentration. Holarctic references indicate a range of environments support *Ablabesmyia* including eutrophic, acidic and oligotrophic conditions (Brundin, 1949; Brodin, 1986; Brooks *et al.*, 2001 and Lotter *et al*, 1998). Furthermore, Fittkau and Roback (1983, 40) describe the genus as "eurytopic and cosmopolitan". Results from Patagonia indicate *Ablabesmyia* to be more common in shallower lakes with higher conductivities (Figure 5.11). Widespread occurrence of the taxon across the TWINSPAN-classified lake groups (5.3), indicate that it may also be a cosmopolitan taxa with a wide tolerance within Patagonia. Thus, a tentative suggestion of a shallowing and increase in

productivity of the lake system can possibly be proposed, mainly based on the increase in Chironomini. Although taxonomic succession within the ecosystem cannot be dismissed as the cause of this change in assemblage, an increase in temperature during this period could cause both a lowering lake level and an increase in productivity. Thus, a possible climatic change could have occurred between *c.* 11.9 and 10.9 cal yr BP.

6.6.2.2 Holocene Palaeoenvironments

The deposition of the 11cm of tephra at *c.* 10,850 cal yr BP caused increased sedimentation rates at the site in the early Holocene due to primary deposition of tephra fallout in the lake and subsequent reworking of the deposit within the lake's catchment. This event is likely to be the major reason for the decrease in midge concentration at the base of LET-3b, rather than changes in bio-productivity at the site.

Following this deposition of tephra, *Micropsectra* Taxon B and *Parapsectrocladius* seem to be the first taxa to recover, as indicated by concentration data. Modern day data indicates that *Micropsectra* Taxon B is common in sites with minerogenic substrates such as the lakes TRE, V and VER, potentially due to habitat requirements or feeding techniques adopted by the taxon. Thus the increase in this taxon may be due to the increase in allochthonous input into the lake as opposed to a climatic mechanism. Although the early Holocene rise and fall in percentage of *Parapsectrocladius* is more prolonged than that of *Micropsectra* Taxon B, examination of the concentration data (Figure 6.13) indicates that these percentage results may be a facet of the varying concentrations of other taxa, such as the decline of *Micropsectra* Taxon B prior to that of *Parapsectrocladius*. This indicates that a relationship may also exist between the increase in *Parapsectrocladius* and tephra input into the system. As the genus has only been recently described and is believed to be exclusive to Patagonia and Southern Chile (Cranston, 2000), there is only limited knowledge about its ecological preferences. One species of the genus has been collected from running waters. Specimens found in lotic environments range from low altitude to glacial lakes (Cranston, 2000). Within the constrained ordination of modern day data, *Parapsectrocladius* is associated with lakes which have higher conductivity and LOI values, although this relationship is indicated to not be that strong, as *Parapsectrocladius* plots close to the origin (Figure 5.11). This plot location indicates either a narrow tolerance close to average environmental conditions or the cosmopolitan nature of the taxa. The widespread occurrence of the taxa and its presence within many lake groups, as classified by TWINSPAN (4.4.2.1), indicate

the latter to be likely. This corroborates the wide range of environments in which the taxa has been previously recorded (Cranston, 2000).

Tephra input into lentic systems has been shown to have an impact on the diatom of flora of lakes, with phosphorous limitation and silica loading being proposed as possible mechanisms (Barker, 2000). However, identifying whether shifts in taxonomic assemblages are due to the direct effect of tephra input into the limnic system, the indirect effect of catchment disturbance as a result of the tephra deposition or to contemporary climate change can be problematic (Metcalfe, 1995; Lotter and Birks, 1993; Bennett *et al*,. 1992). It is also uncertain how long the effects of the tephra may last. The diatom study by Hickman and Reasoner (1994) suggested that the effect could persist for several hundred years, as did that by Barsdate and Dugdale (1972), whereas Lotter and Birks (1993) suggest the effect lasts for 2-20 years.

Following the increase of *Micropsectra* Taxon B and *Parapsectrocladius*, it appears that a productive, organic system prevailed during the early Holocene from *c.* 10.9 - 7.8. *Dicrotendipes*, which is associated with the highest temperatures and LOI values within the study of modern Patagonian fauna, is at its maximum relative abundance and concentration within the core during this period. Studies of the environmental preferences of this taxon in the Holarctic region also highlight preference for such habitats and, additionally, often indicated that the genus is common in de-oxygenated, nutrient rich waters with macrophyte presence (Little and Smol, 1999; Walker *et al.*, 1995; Hoffmann, 1984, Brodin, 1986). The coincidental increases in percentage abundance of both Tanytarsini Taxon E and *Ablabesmyia* fit well with the modern data, since ordination indicates that these two taxa have similar environmental optima (Figure 5.11). The presence of *Labrundinia* and *Chironomus* may also indicate a warmer and more productive lake, as certain groups within these genera are associated with warm, eutrophic conditions (Brooks *et al*, 1997b, Lotter *et al.*, 1997, 1998; Brooks *et al.*, 2001).

Constrained ordination indicates that the relative abundance of *Ablabesmyia, Chironomus* and Tanytarsini Taxon E all correlate positively with conductivity (Figure 5.11). Percentage abundance of all of these taxa increases in the early Holocene. This may indicate that there is still enhanced lake-water ionic conductivity following the deposition of the tephra. Alternatively it may be an increase in the lakes salinity as a result of warming or a decrease in precipitation, or a combination of the two. When viewed in conjunction with the

concomitant decrease in *Parakiefferiella* and increase in Chironomini in general, these taxa may indicate a shallowing of the lake. However, interpretations based on results of CCA of the modern fauna must be made cautiously since the results of the core samples plotted on constrained ordination also indicate that this period of the core should be characterised by high LOI. However, the measured LOI (Figure 6.6) does not reflect the values inferred from the ordination plot (Figure 6.15). It may have been that the lake was very productive, but that this is not reflected in the LOI content because of the input of minerogenic tephra diluting the organic content. Thus the chironomid assemblage between 10.9 – 7.9 ka cal BP is interpreted to have been driven by both the input of tephra into the system and climatic warming.

The marked shift to LET-4's *Parakiefferiella* and Tanytarsini dominated assemblage at *c.* 7.9 ka BP suggests a major change in environmental conditions at the site. This could be either climatically driven or due to a waning effect of the tephra. Tephra might be interpreted to be the responsible factor, as LOI essentially recovers at the same depth as the taxonomic shift at the base of LET-4 (Figure 6.12). However, levels of LOI are not just determined by tephra inwash into the lake, but also by changes in productivity. Furthermore, this taxonomic shift is interpreted to have occurred c. 2800 cal yr after the tephra deposition. In the light of past research, it seems unlikely that the tephra deposits would exert an effect on the fauna for such a length of time (Hickman and Reasoner, 1994; Barsdate and Dugdale, 1972; Lotter and Birks, 1993). If the assemblage profile is examined, it can be seen that the increase in *Parakiefferiella* occurs at the same time as *Chironomus*, *Dicrotendipes* and *Ablabesmyia* decrease. Additionally, there are synchronous, smaller increases in *Labrundinia* and *Limnophyes / Paralimnophyes* Taxon A. Comparison of the similar trends in individual taxa concentration data (Figure 6.13) to the percentage abundance data (Figure 6.12) indicates that this shift in assemblage is not being driven by the increase or decrease in the presence of a specific, individual taxa but a change in the taxonomic composition overall. When these results are put in the context of the modern data and plotted on the CCA bi-plot (Figure 6.15), a decrease in conductivity or an increase in the water depth are potential explanations for this shift in assemblage. This would imply an increase in precipitation or a decrease in temperature are the potetial climatic forcing mechanisms.

It is interesting to compare these inferences with shifts in inferred sedimentation rates. ^{14}C data indicates slow sedimentation rates of 0.03 cm yr^{-1} for the first *c.* 2000 years after 7.9 ka, followed by very rapid accumulation between *c.* 5.8 - 5.4cal ka BP. The midge subsample

within the sediment deposited during this latter period of rapid deposition (152cm), yielded concentration results approximately half of those of samples taken from above and below. LOI shows no marked change to that from sediment deposited during the early Holocene, even though the interpretation of the taxa using ordination might indicate a decrease in organic content might be expected. Together this information suggests that it is not a relative increase in the allochthonous element of sedimentation that was responsible for the increase in the sedimentation rate during this period. Taxonomic changes correlating to the LET 4-5 transition are minor, with Tanytarsini Taxon E and *Parakiefferiella* increasing slightly as sedimentation rates increase at *c.* 5.4 cal ka BP. In summary, neither published ecological information nor that from the modern study within this investigation provides a clear explanation to why an increase in these particular taxa might accompany this shift in accumulation rates.

The upper 140cm of the core appears to have been deposited between *c.* 5.4 ka BP and the late Holocene. Based on the extrapolated sedimentation rate shown in Figure 6.14, the additional, missing upper 50cm of the core may correlate with approximately the last 1.5 ka BP. During the latter half of the Holocene, the assemblage is characterised by a slight and gradual increase in *Parakiefferiella*, which absolute data indicate is the result of increasing concentration of the taxon (Figure 6.13). Tanytarsini D and *Limnophyes / Paralimnophyes* Taxon A also undergo a marked increase over the zone boundary between LET-4 and LET-5 at *c.* 5.4 cal yr BP, both in relative abundance and in concentration. Examination of the CCA bi-plot of modern data gives no pronounced indication as to what the shifts in the abundances of these latter two taxa indicate. When the LET-5 assemblage is compared to that of LET-4, there is also a small but notable increase in concentration of *Cryptotendipes*, a taxon which was also indicated to be associated with deeper lakes within the modern ecology of Patagonian midges (Figure 5.12). The fluctuations in the percentage occurrence of Chironomini taxa vary between total absence and *c.* 1%. This may not be due to specific environmental fluctuations but, rather, statistical noise as a function of the sample size and low percentage abundance occurrence. When plotted on the CCA bi-plot of modern data, the assemblages within LET-5 plot to the far right, with high CCA axis one scores. Such a location is associated with deep water conditions. The plot of the assemblages here is probably being driven by the high abundance of *Parakiefferiella* within the zone's assemblages. Thus, in general, the strongest proposal that can be put forward for late-Holocene environmental change is that at *c.* 5.4 cal ka BP there was a further increase in

effective precipitation in the Chilean Lake District area which deepened the lake. This could be a result of either an increase in precipitation or a decrease in temperature.

6.6.2.3 Change in the past c. 2000 years

The sharp decline in both percentage and concentration of *Parakiefferiella* in the uppermost sub-sample analysed is interesting. This may pertain to a drop in water levels c. 2000 - 1500 cal yr BP. However, more conclusive interpretation is problematic due to poor chronological control and this taxonomic change being restricted to only one sub-sample. As stated in 6.3.1, the upper 50 cm of the record at Laguna Leta could not be retrieved as the sediments were not sufficiently cohesive. However, it is interesting to compare the uppermost analysis of the down-core record (54cm) with the modern day taxa.

When the data are plotted on the CCA ordination bi-plot of modern data, the present-day assemblage at Laguna Leta is notably different from that of LET-5, deposited between *c.* 5.4-1.5 cal ka BP (Figure 6.13). Based on the midge assemblages the bi-plot suggests that the lake, is currently more productive than the assemblages of LET-5 suggest, as LOI as inferred from the bi-plot is higher in the modern sample than those from the downcore samples. When this inference is compared to the measured data these results are problematic as the modern sample from Laguna Leta had LOI of 56% whereas the mean for LET-5 was 77%. However, this difference may not be as acute as mean zonal values indicate, as towards the top of LET- 5, LOI is approaching levels measured in the surficial sediments; LOI at 54 cm is 38%. However, this again highlights the issues of difficulties in interpreting taxonomic assemblage shifts, highlighted by inferred LOI during LET-3a, directly following the tephra deposition.

Without more chronological control towards the top of the core or knowledge of the intermediate fauna between 54cm and the current sediment surface of Laguna Leta, it is impossible to ascertain the timing or rate of this change in assemblage. However, possible candidates for causing the change can be suggested. These could include:

- Building of the road (Route 5) causing an increase in erosion and associated ionic nutrient enrichment of the lake;
- Nutrient loading of the system due to waste from of house on the edge of the lake
- Infilling of the lake due to natural and / or anthropogenic processes such as building the road or house, leading to reduction in lake water depth;
- Late Holocene climatic change;

The location of the modern Laguna Leta assemblage on the ordination diagram suggests that today, LET is one of most productive lakes, as indicated by being located close to the arrow head on the axis along which LOI increases. Examination of data in Table 5.1 shows that Laguna Leta had the sixth highest LOI results (56%) and the ninth highest T_t (19.0°)(n= 78). It is also one of the shallowest sampled; its depth, of 2.5m, is not only substantially less than the mean depth within the training set (9.9m± 6.5) but also falls outside the 1s.d. distribution of those sampled.

6.6.3 Comparison of Laguna Leta with other palaeoenvironmental records from the area

Figure 6.16 shows a summary of the palaeolimnological and palaeoclimatic changes inferred from the Laguna Leta core within the context of previously published data from the Chilean Lake District and Isla de Chiloé.

The minimum date for lake formation, *c.* 13.9 cal ka BP, coincides well with the general pattern of deglaciation inferred within the Chilean Lake District region. The final stage of deglaciation in the Chilean Lake District region has been proposed to occur between 15.6 and 14.3 cal ka BP (Heusser, 1993; Moreno *et al*, 1999, Hoganson and Ashworth, 1992). Palaeovegetation data from Chiloé indicates a concomitant change from an open-ground vegetation assemblage to a forest assemblage (Villagran, 1990b). The slightly younger date gained at Laguna Leta, versus dates of *c.* 18.7 cal ka BP gained by Denton *et al.* (1999), still fits well within this regional chronology as this basal date acts as a *minimum* date for initiation of a limnic system at a site where the basin is thought to have been a kettle hole. Ice may have remained in the kettle hole for several hundred years after the main ice lobe had retreated (Lowe and Walker, 1980). Thus this younger age fits the regional pattern.

Tentative suggestions of a lake level rise at Laguna Leta during the Late-glacial can be made from the Laguna Leta midge record. Potential climatic forcing mechanisms of a climatic cooling or an increase in precipitation are proposed, either or both of which would result in an increase in effective precipitation. Regional palynological and sedimentological data indicates LGIT cooling events between 14 – 11.7 cal ka BP, although beetle data did not support this (Moreno and Leon, *in press*; Moreno, 1997; Moreno *et al.*, 1999, 2001; Heusser, 1993, 1996; Hoganson and Ashworth, 1992; Hajdas *et al.*, 2003). It is possible that such coolings caused the potentially rising water levels suggested by the Laguna Leta

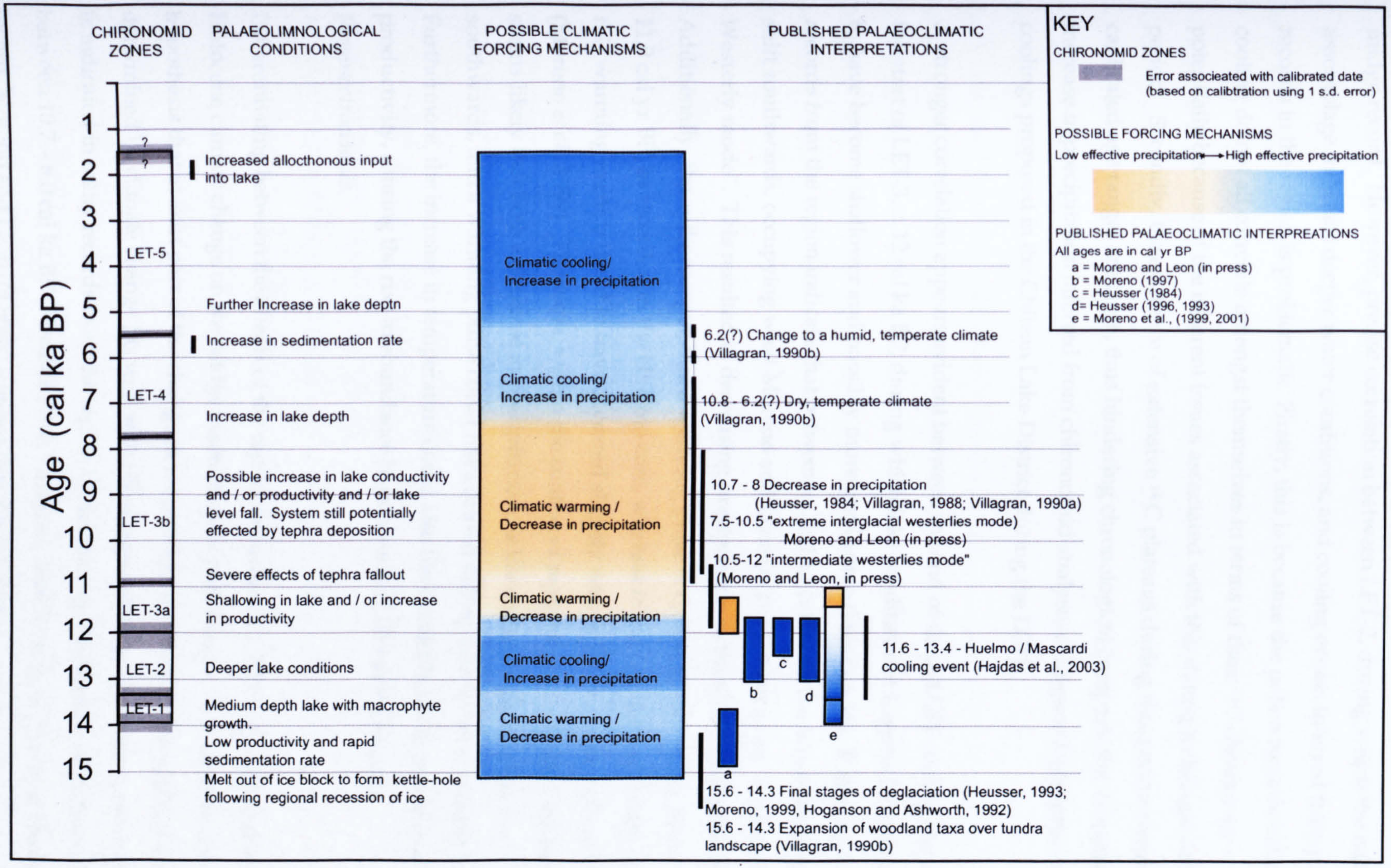

Figure 6.16 : Summary diagram showing the palaeolimnological changes inferred from sediment and chironomid analysis at Laguna Leta within the context of published palaeoclimatic reconstructions from the region.

midge record. However, precise correlation between LET-2, during which the midge assemblage indicates deeper water conditions, and cooling events inferred from pollen records in the region is problematic. Firstly, this is because the pollen records indicating cooling do not all correlate amongst themselves in terms of their ^{14}C chronology - potentially because of the inherent issues associated with this dating technique during this period. Secondly, the existence of extensive ^{14}C plateaus during this period means that calibrated age ranges are large, thus hindering chronological comparisons. Nonetheless, the increase in precipitation inferred from chironomid analysis of Laguna Leta agrees with the coolings proposed in the Chilean Lake District during the LGIT.

A stronger correlation appears evident between the end of these LGIT cooling events and the start of LET-3, *c.* 12 cal ka BP, during which lake conditions at Laguna Leta are inferred to have become shallower and possibly more productive (Figure 6.16). Palynological records from the region indicate that between c. 12-10.5 cal ka BP the Westerlies began to shift southwards, occupying what Moreno and Leon (*in press*) term as an "intermediate Westerly mode". This resulted in decreasing precipitation in the CLD and Chiloé region. Additionally, the authors argue that a warming pulse occurred at 10.2 ^{14}C ka BP (*c.* 11.75-11.9 cal yr BP) as recorded in the Huelmo core, whereas in the Canal de la Puntilla record, this warming event is dated to have occurred slightly later at 9.8 ^{14}C ka (*c.* 11.2 cal ka BP) (Moreno *et al.*, 1999). Therefore, within the context of regional palynological studies, it seems likely that both a decrease in precipitation, as Westerlies began to migrate southwards, and a warming pulse could have caused falling lake levels at Laguna Leta. Furthermore, the increase in temperature could also have contributed to an increase in lake productivity, causing the rise in abundance in taxa such as *Dicrotendipes* and *Parapsectrocladius*.

Differentiating between the effects of the tephra deposited at *c.* 10.9 cal ka BP and early Holocene climate change on the midge assemblage is problematic. Nonetheless, the hypothesis that at least part of the change in assemblage seen in the early Holocene is determined by climate change fits well with other regional data. Decreasing precipitation is indicated in many records from the region by decreasing abundances of hydrophilic taxa between 10.7 – 8.0 cal ka BP (Heusser 1984; Villagran, 1988, 1990a). From their Huelmo record, Moreno and Leon (*in press*) suggest that the Westerlies were in an "extreme interglacial" mode between 10.7 – 8.0 cal ka BP and that a second warming pulse occurred at *c.* 10.2 cal yr BP. Thus, it could be argued that the continual absence of *Parakiefferiella*, a

taxon interpreted to be indicative of deep water conditions at Laguna Leta until 7.8 cal yr BP, was the consequence of shallower water depths due to this southerly migration of the Westerlies, possibly intensified by an increase in temperature.

As discussed in Chapter 2 there is limited data available for climate change in the CLD during the late Holocene. However, the palynological data from Rucañancu (Heusser, 1984) indicates an increase in humidity and decreasing temperature during the middle and latter part of the Holocene, especially after 6960 ^{14}C ka BP. This coincides with the marked increase in *Parakiefferiella* at 6970 ^{14}C ka BP (*c.* 7.8 cal yr BP) seen in the record from Laguna Leta. Villagran (1988, 1990b,) also documents the increase in hydrophilic, cushion-bog taxa during the latter part of the Holocene. Unfortunately poor chronological control of this switch limits the event to a date sometime after 7,170±120 ^{14}C ka BP (< *c.* 7.9 cal ka BP) (Villagran, 1988). Both Villagran (1990a) and Heusser, (1984) draw links between this, more humid late Holocene and the Patagonian Neoglacial advances presented by Mercer (1982, 1984).

6.7 Conclusions from Laguna Leta

From the preceding results and interpretations, the following major conclusions can be drawn from the analysis of the Laguna Leta record:

- The assemblages preserved within the Laguna Leta core have good analogues with the modern training set;
- The minimum age for the formation of a lake at Laguna Leta at *c.* 13.9 cal ka BP fits well with the final stage in the regional pattern of deglaciation and palaeoclimatic change in the CLD and Isla de Chiloé;
- The inferred deepening of Laguna Leta between *c.* 13.3-12 cal yr BP may correlate with the late LGIT cooling events inferred from pollen records in the region;
- A decrease in lake depth at *c.* 12.0 cal ka BP may relate to late LGIT / early Holocene southerly migration of the Westerlies and warming proposed by Moreno and Leon (*in press*) and Moreno *et al.*, (1999a, b);
- The sharp rise and subsequent fall in *Parapsectrocladius* and Micropsectra Taxon B indicates the deposition of tephra from the volcanic eruption at 10.9 cal ka BP yr BP may have had strong effect on the site's taxonomic assemblage;
- The further change, after *c.* 10.9 cal ka BP, to an assemblage dominated by *Ablabesmyia*, Tanytarsini, *Chironomus* and *Dicrotendipes* may indicate a further

decrease in lake level and increase in productivity. This is possibly related to further latitudinal shifts in the Westerlies and increasing temperatures. However, a sound interpretation of the changes in the midge assemblage may be complicated by the potential, residual effects of the 11 cm deposit of tephra at the same time;

- The marked change to a *Parakiefferiella* dominated assemblage at *c.* 7.8 cal ka BP may represent a deepening in the lake. This could be caused by an increase in effective precipitation which correlates with cooler and wetter climates, higher humidity and the Holocene neoglaciations proposed by Mercer;
- Lake deepening continues after 5.0 ka but may shallow at core top.

7 LAGUNA BOAL

7.1 Introduction

The results and interpretation of chironomid stratigraphy from Laguna Boal, the second lake investigated in this study, are presented within this chapter. A description of the modern vegetation and climate of the local area provides a context within which to view the palaeoenvironmental record. Results of ^{14}C dating and chironomid analyses are combined to produce a palaeoenvironmental reconstruction of the site in the Chonos – Taitao region.

7.2 Site

Laguna Boal (44°39'02"S, 73°39'03"W) is a small lake of *c.* 100 x 200 m diameter and 4m depth which is located 400m a.s.l (Figure 7.1,Figure 7.2 and Figure 7.3). The lake occupies a bedrock hollow on a ridge on Isla Caputa, one of the eastern islands within the Chonos Archipelago, and is drained by an outlet stream to the northwest. As is evident in Figure 7.1, the site is surrounded by thick vegetation. *Pilgodendron* and *Tepulia* are both abundant, with *Nothofagus nitida, Podocarpus* and *Weinmannia trichosperma* also present in the catchment. A field-based estimate suggested 25% canopy cover within the lake's catchment (Haberle and Bennett, 2001).

The Chonos Archipelago and the Taitao Peninsula, which lies to the south, are a complex, emerged artefact of a region which has undergone repeated glacial erosion, most recently at the LGM during OIS 2 (Clapperton, 1993). The actual timing of deglaciation of Laguna Boal is unclear. Nearby sites in the Chonos & Taitao have yielded minum dates for deglaciation of between 20.5 – 15.9 cal ka BP, however these dates are all from sites at lower altitudes (<50m a.s.l) (Haberle and Bennett, in press; Bennett et al., 2000; Lumely, 1993). Therefore it is likely that Laguna Boal would have become deglaciated at a later date during the LGIT. The Taitao Peninsula itself is the onshore expression of the subduction of the Chile rise, the divergent boundary between the Antarctic and Nazca Plate, under the South American plate (Clapperton, 1993). The area's geology is dominated by metamorphic rocks from the Palaeozoic and Cretaceous granites (Haberle and Lumley, 1998).

Figure 7.1: Photograph of Laguna Boal taken looking east (K.D.Bennett).

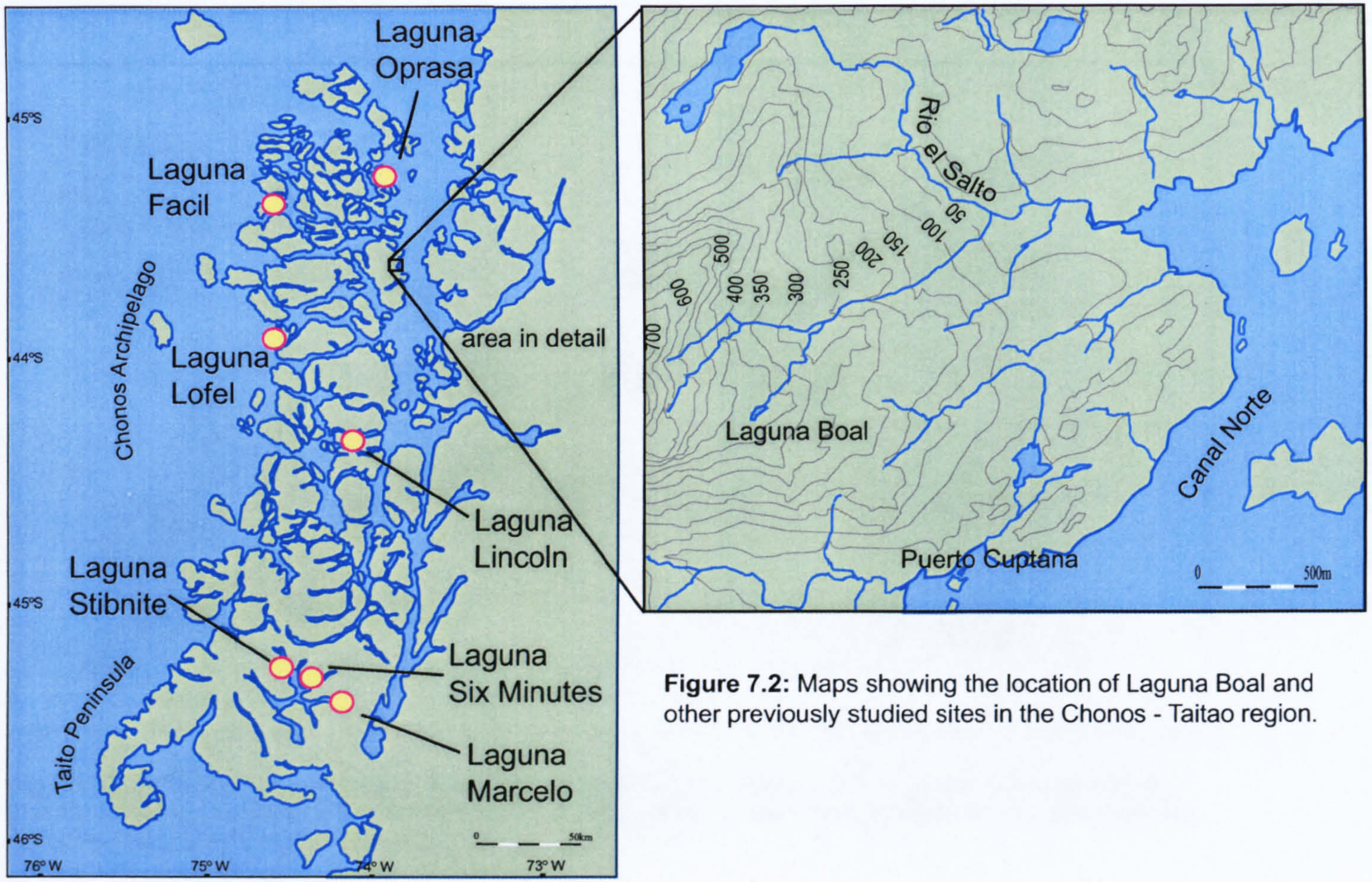

Figure 7.2: Maps showing the location of Laguna Boal and other previously studied sites in the Chonos - Taitao region.

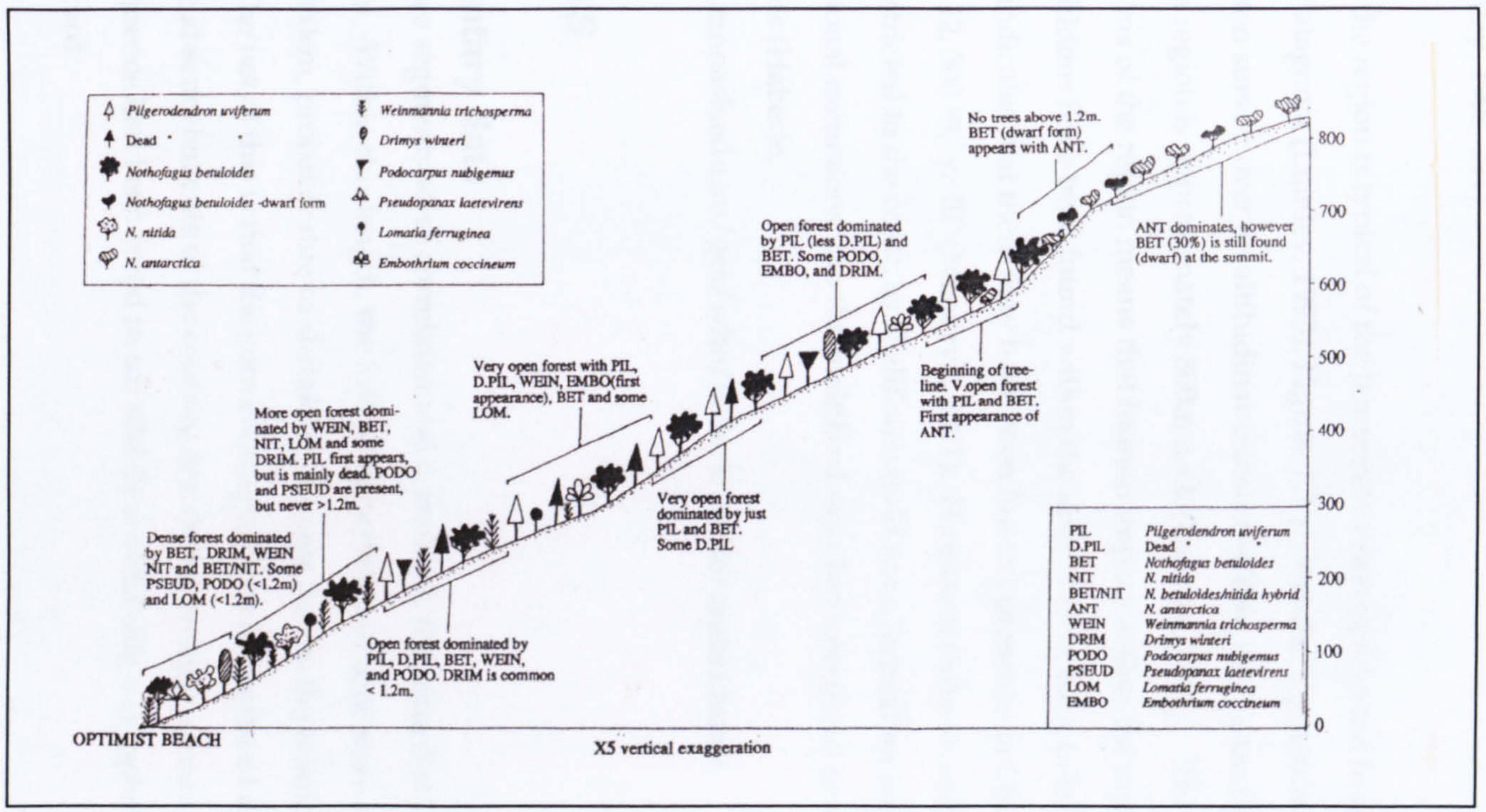

Figure 7.3: Montane vegetation survey exemplifying vegetation in the Chonos / Taitao region: summary diagram of forest composition along transect up Mount Optimist (Lumley, 1994). Y axis is height in metres a.s.l., the summit of the transect and peak being at 831m a.s.l.

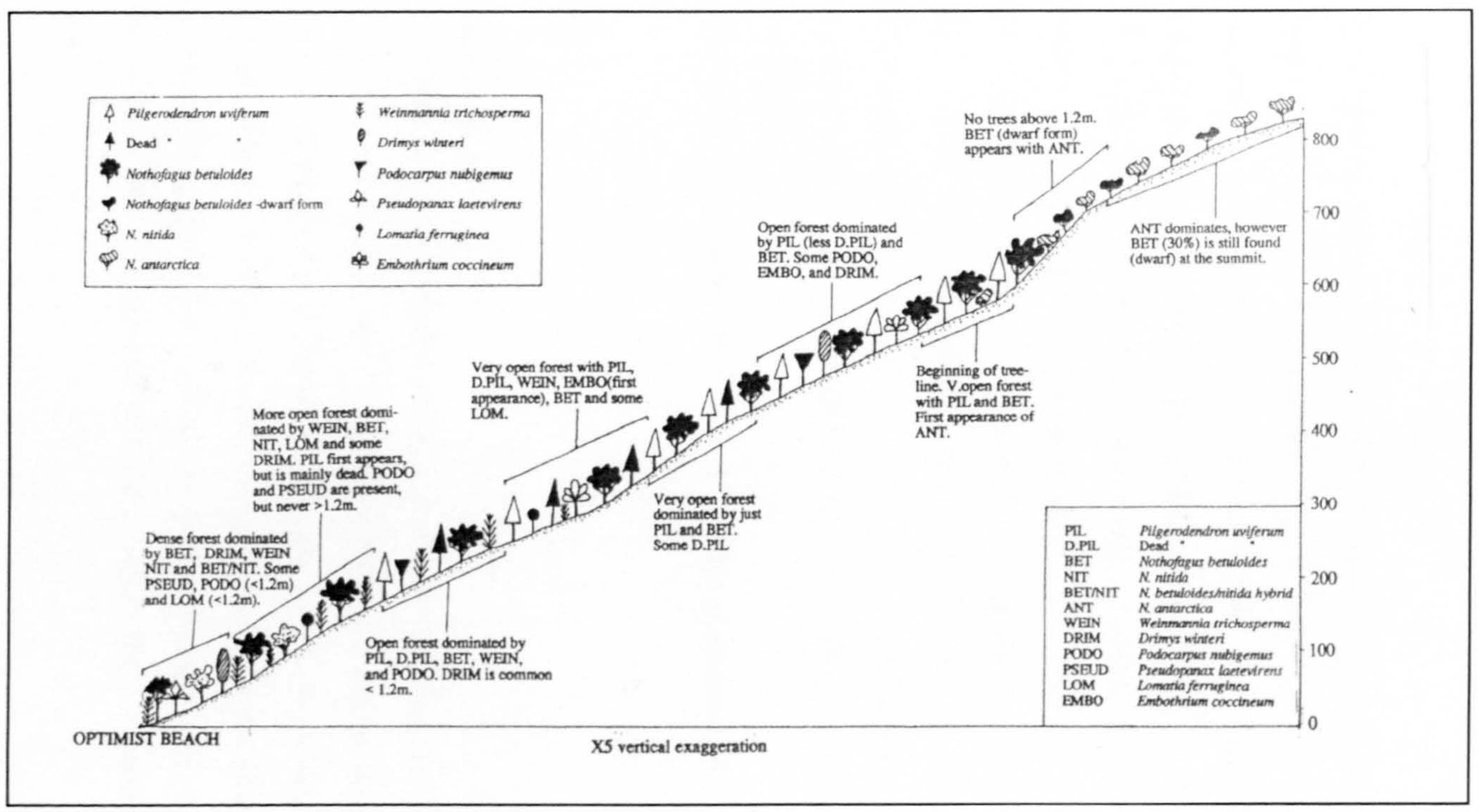

Figure 7.3: Montane vegetation survey exemplifying vegetation in the Chonos / Taitao region: summary diagram of forest composition along transect up Mount Optimist (Lumley, 1994). Y axis is height in metres a.s.l., the summit of the transect and peak being at 831m a.s.l.

The area's location within the influence of the Westerlies means that precipitation levels are very high. Totals of up to 3000mm yr^{-1} have been recorded at sea level (Haberle and Lumley, 1998, 241). As altitude increases so does rainfall to levels in excess of 10,000mm yr^{1} (Hablerle and Lumley, 1998, 241). Mean annual temperatures are between 8 and 10°C (Haberle and Lumley, 1998, 241).

The vegetation of the region is typical of the temperate rainforest found in maritime regions of North Patagonia (Lumley, 1993). Figure 7.3 shows the vegetation encountered through a vegetation survey over an altitudinal transect within the Taitao Peninsula. The treeline within the region is approximately 800m a.s.l. (Lumley, 1993). The isolated nature and harsh conditions of the region means that human impact within the region has been minimal. Shell middens have been found within the area, dating back to before 2,500 ka. Certain evidence indicates that there may have been human presence in Chonos-Taitao region as early as 12, 500 ^{14}C yr BP (Mandryk, 2001). Human activity would have been predominantly restricted to the coast, as shellfish would have formed an important element of the diet. Occasional excursions into the mainland may have occurred to search for wood and plant resources (Haberle,
http://www.arts.monash.edu.au/ges/who/haberle/chile/tephra.html).

7.3 RESULTS

7.3.1 Sedimentary data

When separate core segments were correlated and combined, the record at Laguna Boal extended to 4.70 m. Within this length, the following sections of core were absent: 69-100, 190-200 and 296-300cm, probably due to shrinking of cores due to the temporary freezing (See chapter 5). The net of this is that the core is complete but is displaced in the upper half of the core. These absent elements of the core are annotated on appropriate diagrams. Below 3m, the sequence had been cored in parallel thus obtaining a complete, uninterrupted record.

The results of stratigraphic analysis are shown in Figure 7.4. In general, the core comprises of dark brown limnic muds which appear to be organic-rich. Towards the base, the core sediments become more minerogenic, indicated by changes in colour occurring at 446cm (dark brown to mid brown), 457cm (mid brown grey - light brown grey) and 462cm (light brown grey - fawn / beige).

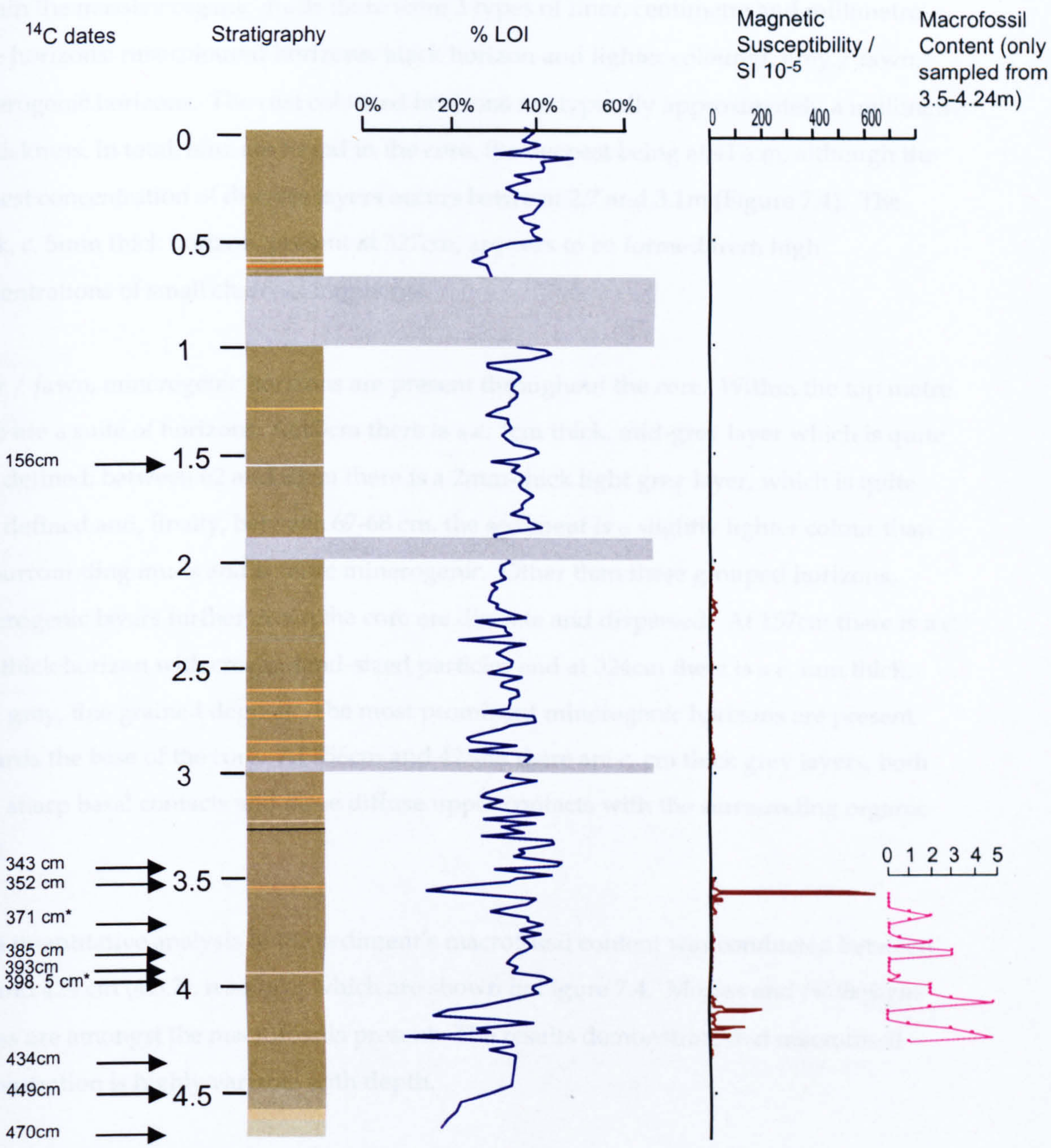

Figure 7.4 : Diagram summarising the results of sediment logging, Loss on Ignition (LOI), magnetic susceptibility and macrofossil content for Laguna Boal. ^{14}C date depths marked with an asterix indicate that plant macrofossils were subsampled for dating.

Within the massive organic muds there were 3 types of finer, centimetre and millimetre-scale horizons: rust coloured horizons, black horizon and lighter coloured, grey / fawn, minerogenic horizons. The rust coloured horizons are typically approximately a millimetre in thickness. In total, nine are found in the core, the deepest being at 412cm, although the highest concentration of discrete layers occurs between 2.7 and 3.1m (Figure 7.4). The black, *c.* 5mm thick horizon, present at 327cm, appears to be formed from high concentrations of small charcoal fragments.

Grey / fawn, minerogenic horizons are present throughout the core. Within the top metre there are a suite of horizons. At 60cm there is a *c.* 1cm thick, mid-grey layer which is quite well defined; between 62 and 63cm there is a 2mm-thick light grey layer, which is quite well defined and, finally, between 67-68 cm, the sediment is a slightly lighter colour than the surrounding muds and is more minerogenic. Other than these grouped horizons, minerogenic layers further down the core are discrete and dispersed. At 157cm there is a *c.* mm thick horizon with cream, sand-sized particles and at 324cm there is a *c.* mm thick, light grey, fine grained deposit. The most prominent minerogenic horizons are present towards the base of the core. At 356cm and 423cm there are *c.* cm thick grey layers, both with sharp basal contacts and more diffuse upper contacts with the surrounding organic mud.

Semi-quantitative analysis of the sediment's macrofossil content was conducted between 350 and 424 cm (4.3.2), results of which are shown in Figure 7.4. Mosses and *Nothofagus* leaves are amongst the macrofossils present. The results demonstrate that macrofossil concentration is highly variable with depth.

Overall, LOI results from Laguna Boal lie between 30 – 45% throughout the core. However in the bottom 20cm of the core, LOI decreases from *c.* 34% to *c.*16% at the base. These overall trends are punctuated by high frequency changes in LOI, with levels fluctuating by as much as 27% over 2cm. The largest rapid fluctuations in LOI are broadly coincident with the grey horizons noted in the stratigraphy discussed above (Figure 7.4). However, LOI identified additional low concentrations of organic content in zones that had not been detected by visual examination of the core (Figure 7.4)

7.3.2 Tephrochronology

EMPA analysis was conducted on 22 horizons from within Laguna Boal that appeared to be possible tephra deposits. Ten of these gave satisfactory results in terms of sufficient data yield, i.e. $n > 10$. An overview of these results is given in Table 7.1 and Figure 7.5. Full datasets are appended in Appendix 1. Both graphical and numerical presentation of

Depth (cm)	SiO_2	TiO_2	Al_2O_3	FeO	MnO	MgO	CaO	Na_2O	K_2O
59cm	55 27 ± 1.60	1.454 ± 1.21	15.52 ± 1.99	7.73 ± 0.98	0.18 ± 0.05	3.93 ± 1.24	7.00 ± 1.17	4.41 ± 0.42	1.51 ± 0.33
62cm	62.41 ± 5.12	0.95 ± 0.34	15.06 ± 0.24	4.72 ± 2.00	0.15 ± 0.04	1.86 ± 1.44	3.6 ± 2.36	4.95 ± 0.36	2.65 ± 0.78
67cm	57.94 ± 3.52	1.40 ± 0.39	15.03 ± 2.13	4.74 ± 2.30	0.20 ± 0.08	3.1 ± 2.70	5.33 ± 2.17	4.55 ± 0.58	1.76 ± 0.61
157cm	52.14 ± 0.52	1.33 ± 0.07	15.80 ± 0.88	9.39 ± 0.46	0.19 ± 0.05	4.96 ± 0.63	8.64 ± 0.38	3.60 ± 0.27	0.7 ± 0.09
356cm (upper core segment)	56 60 ± 4.58	1.76 ± 0.79	14.28 ± 1.46	8.31 ± 2.59	0.27 ± 0.30	3.10 ± 1.77	6.13 ± 2.37	3.88 ± 0.45	1.89 ± 0.80
356cm (lower core segment)	56.63 ± 5.32	1.60 ± 0.63	14.73 ± 1.24	8.36 ± 2.55	0.20 ± 0.05	3.13 ± 1.85	6.49 ± 2.52	3.95 ± 0.52	1.83 ± 0.82
374cm	62.47 ± 4.81	0.93 ± 0.12	16.07 ± 0.41	4.15 ± 2.13	0.14 ± 0.22	1.71 ± 1.67	3.02 ± 2.43	5.17 ± 0.74	2.62 ± 0.80
411cm	55.13 ± 5.67	1 90 ± 0.63	15.09 ± 1.21	8.24 ± 2.65	0.19 ± 0.07	3.08 ± 1.38	6.62 ± 2.68	4.55 ± 0.44	1.74 ± 0.78
423cm (upper core segment)	63.48 ± 1.62	0.69 ± 1.34	16.07 ± 1.40	4.72 ± 0.98	0.12 ± 0.29	1.09 ± 0.65	3.85 ± 0.79	5.33 ± 0.44	1.91 ± 0.37
423 cm (lower core segment)	64.33 ± 1.27	0.87 ± 0.11	14.52 ± 1.25	8.07 ± 0.82	0.14 ± 0.04	1.08 ± 0.52	3.09 ± 0.65	4.43 ± 0.36	2.27 ± 0.30

Table 7.1: Major oxide geochemistries, gained via Electron Microprobe Analysis, and standard deviation of the shard measurements. Sample sizes for all populations, n>10.

results, with standard deviation, show that the spread in major oxide geochemistries within most of these horizons is large. Almost all the analyses show shards to be intermediate or silicic in geochemistry with most of the shards falling within the transitional alkaline series / subalkaline (theolitic) series (Figure 7.5). Although most of the populations fall within the same broad geochemistries, few of the horizons appeared to contain shards from the same population. The exception to this was analyses from horizons at 356cm and 423cm. Both of these horizons had been taken from two, overlapping core segments and thus each had been analysed in two, individual samples. The similar range of geochemistries shown in these horizons is highlighted in Figure 7.5.

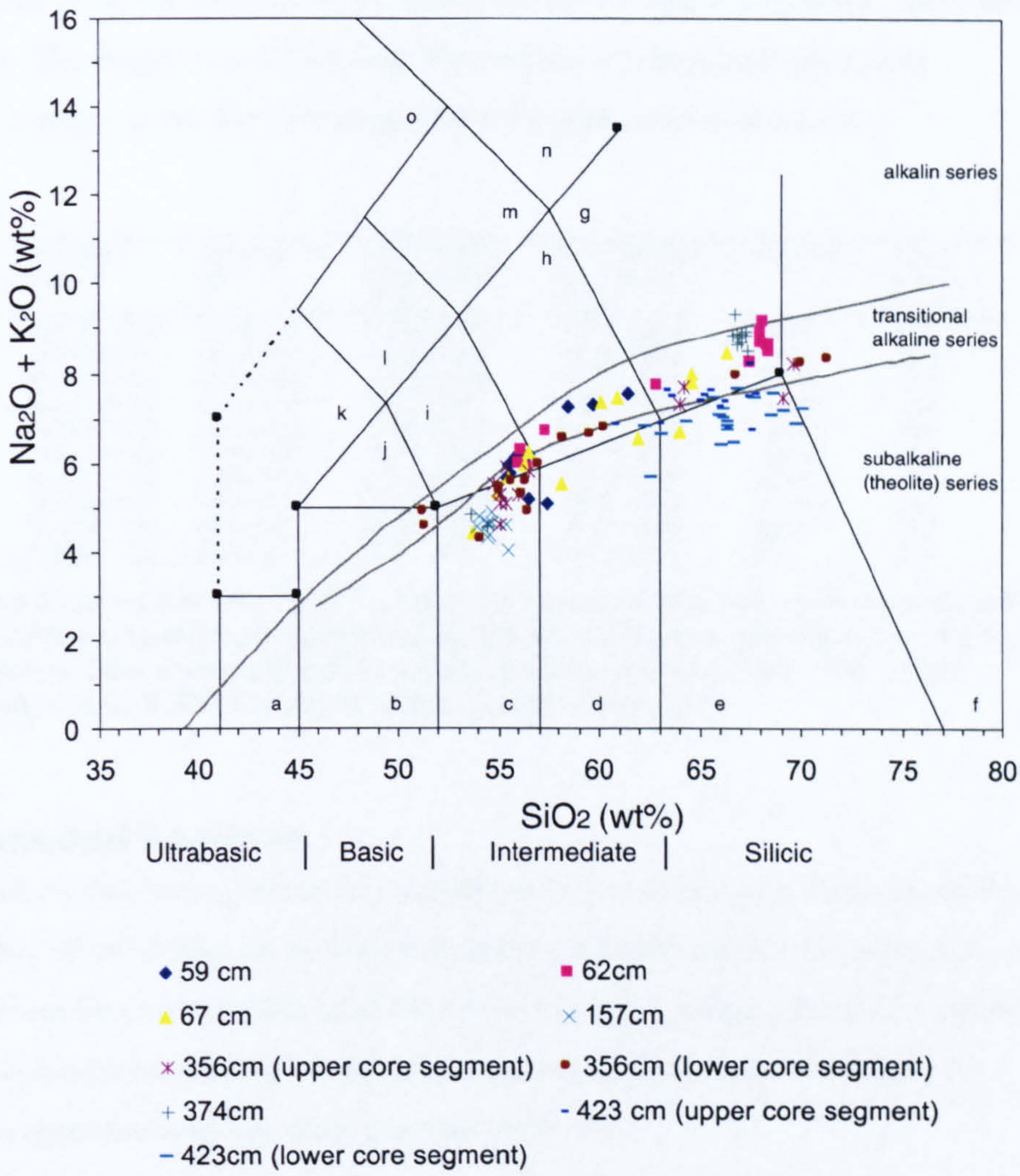

Figure 7.5 : Classification bi-plots of tephra shards analysed from Laguna Leta using total alkali-silica (TAS) classification diagram annotated with subdivision of volcanic rocks into alkaline, transitional alkaline and subalkaline (tholeiitic) . Upper line after Irvine and Baragar (1971), lower line after Kuno (1966). All geochemical data were normalised before being plotted. Note the similar geochemistries for samples from 356 and 423 cm. Results from other horizons are shown in grey to place the results in the context of the whole core

7.3.3 Geochronological data

Eight bulk samples and two macrofossils were submitted for ^{14}C dating. The results of these analyses are presented in Table 7.2. Figure 7.6 illustrates that the ages plotted against depth. The core stratigraphy is shown in the insert on the left of the graph (for key see Figure 7.6). Further details are shown in Table 7.2. The estimates gained from assays at 352cm and 393cm lie out of order with the rest of the dates which, otherwise, increase in age with depth. The diagram also indicates that both macrofossil samples yield systematically younger dates than those gained from bulk sediment assays.

Depth (cm)	Sample description	Publication Code	Conventional Age	Calibrated Age range (using ± 1S.D.)	Calibrated Age range (using ± 2S D)	Mid point	Carbon $\delta^{13}C_{PDB}$ ‰ ± 0 1
470	BS	SUERC-1752	14175 ± 86	17255-16740	17531- 16497	17014	-25 2
449	BS	SUERC-1753	13658 ± 84	16646-16157	16905-15923	16414	-28.8
434	BS	SUERC-1754	13215 ± 83	16126-15649	16375-14831	15603	-29 0
398.5	PM	Beta -180729	11570 ± 60	13801-13437	13839-13190	13514 5	-28 2
393	BS	SUERC-1755	10568 ± 56	12789-12365	12931-12178	12554.5	-29 4
385	BS	SUERC-1757	11491 ± 61	13782-13330	13813-13164	13488 5	-29.7
371	BS	SUERC-1758	10378 ± 59	12610-11965	12820-11784	12302	-29 3
352	PM	Beta-180731	9320 ± 50	10634-10427	10673-10288	10480 5	-34 8
343	BS	SUERC-1759	9525 ± 48	11066 – 10692	11092-10600	10846	-29 7
156	BS	SUERC-1763	4768 ± 33	5586 - 5471	5591-5331	5461	-25.8

Table 7.2 : Table showing the results of ^{14}C dating of bulk sediment and plant macrofossils from Laguna Boal. Calibrations were performed using CALIB 4.3 (Stuiver and Reimmer, 1993). Sample descriptions: BS= Bulk sediment (analysed at Beta Analytic, USA). PM = Plant Macrofossil (Analysed at NERC Facility at SURC, East Kilbride, UK)

7.3.4 Chironomid Analysis

The broken stick model distinguishes five significant zones within the Boal record, three of which are further divided into up to three sub-zones. All chironomid abundance results and total head capsule concentrations (in the form of head capsules g dry sed^{-1}) are shown in Figure 7.7, with a summary of percentage data of the dominant taxa in Figure 7.8. Individual taxa concentrations are presented in Figure 7.9.

7.3.4.1 BOAL-1 (486-460cm)

BOAL-1, between 486 and 431cm, is dominated by 4 major taxa: *Polypedilum*, *Parakiefferiella*, *Parapsectrocladius* and Podonominae. Within the whole zone, all of these taxa reach relative abundances of > 10%. However, the zone can further be divided into BOAL-1a (486-460cm) and BOAL-1-b (460-431cm), with higher percentages of *Parakiefferiella*, Podonominae and *Microtendipes* Taxon B in the 2 basal levels of analysis within BOAL-1a. Within BOAL-1b, *Pseudochironomus*, *Corynoneura / Thienemanniella*, *Cricotopus/ Orthocladius* and *Paralimnophyes / Limnophyes* Taxon A become more prominent. Although not totally absent, occurrences of Tanytarsini and Tanypodinae are very low, with totals for the tribe

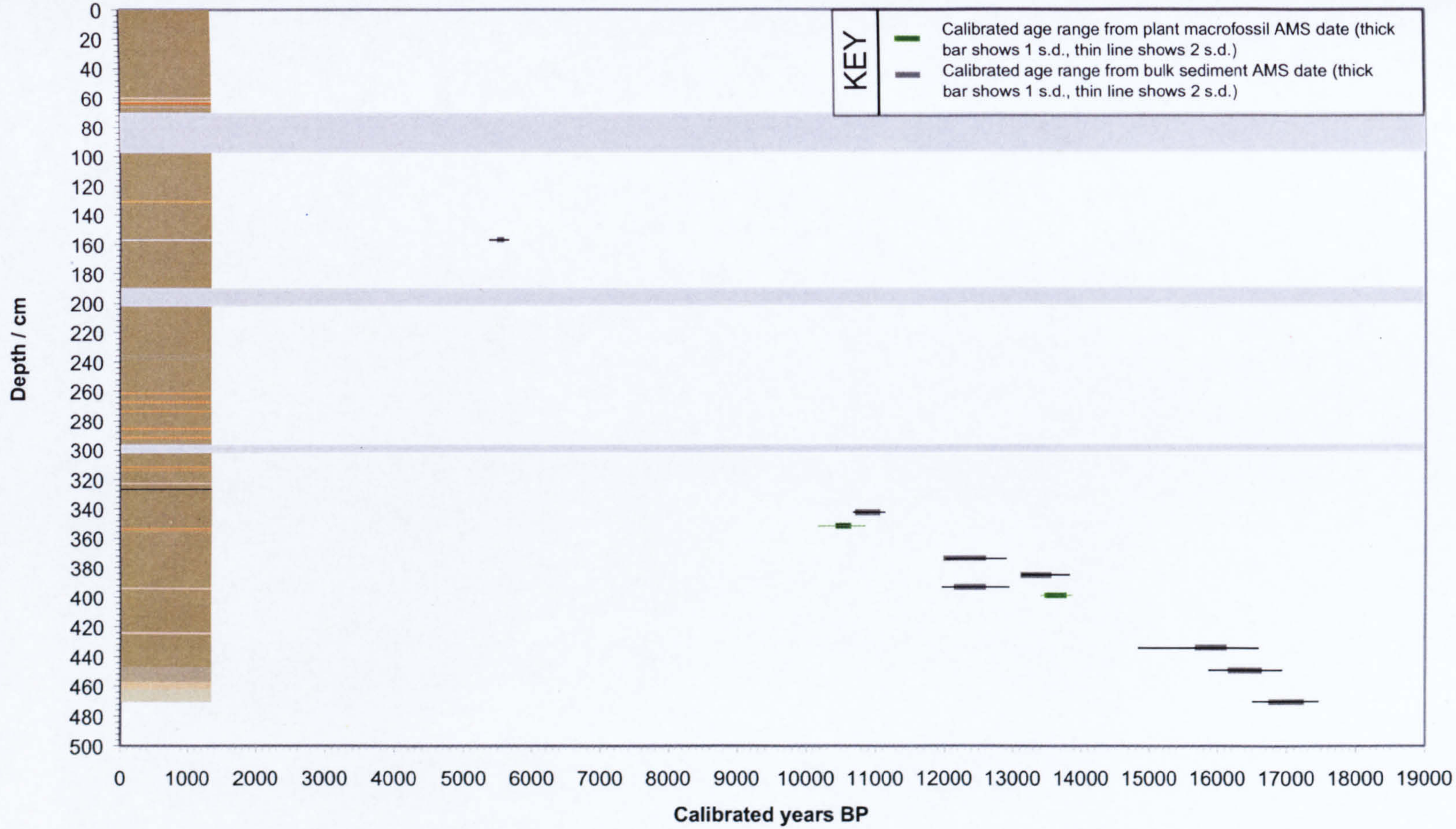

Figure 7.6: Depth versus age diagram showing the results of ^{14}C dating of the Laguna Boal core. Calibrated age ranges are shown using both 1sd and 2sd errors. The core stratigraphy is shown in the insert on the left of the graph (for key see Figure 7.6). Further details are shown in Table 7.2

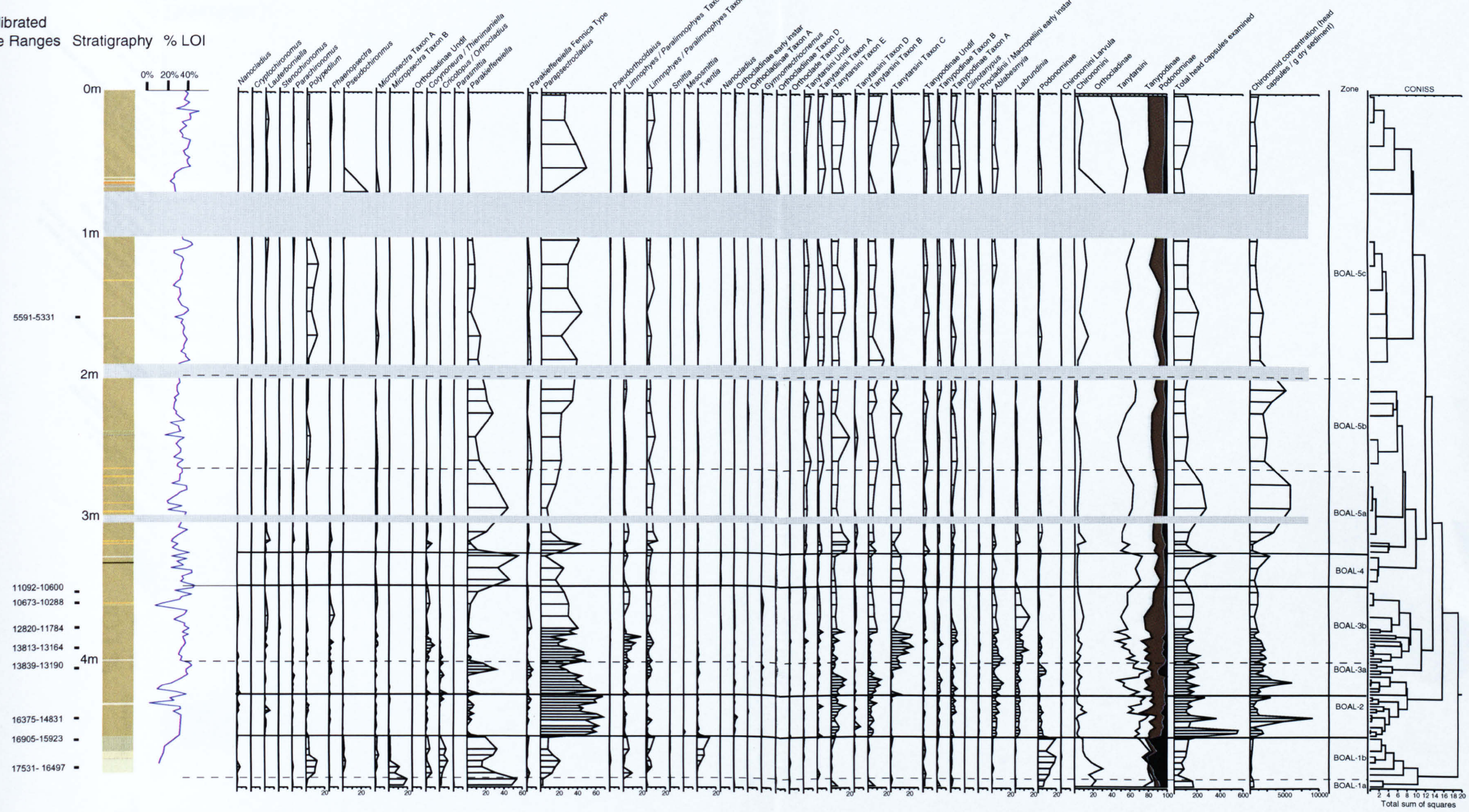

Figure 7.7: Percentage diagram of all taxa from Laguna Boal. Grey horizontal bands indicate where no sediment was collected. Key for stratigraphy is in Figure 7.4. Dates are calibrated using 2 s.d.

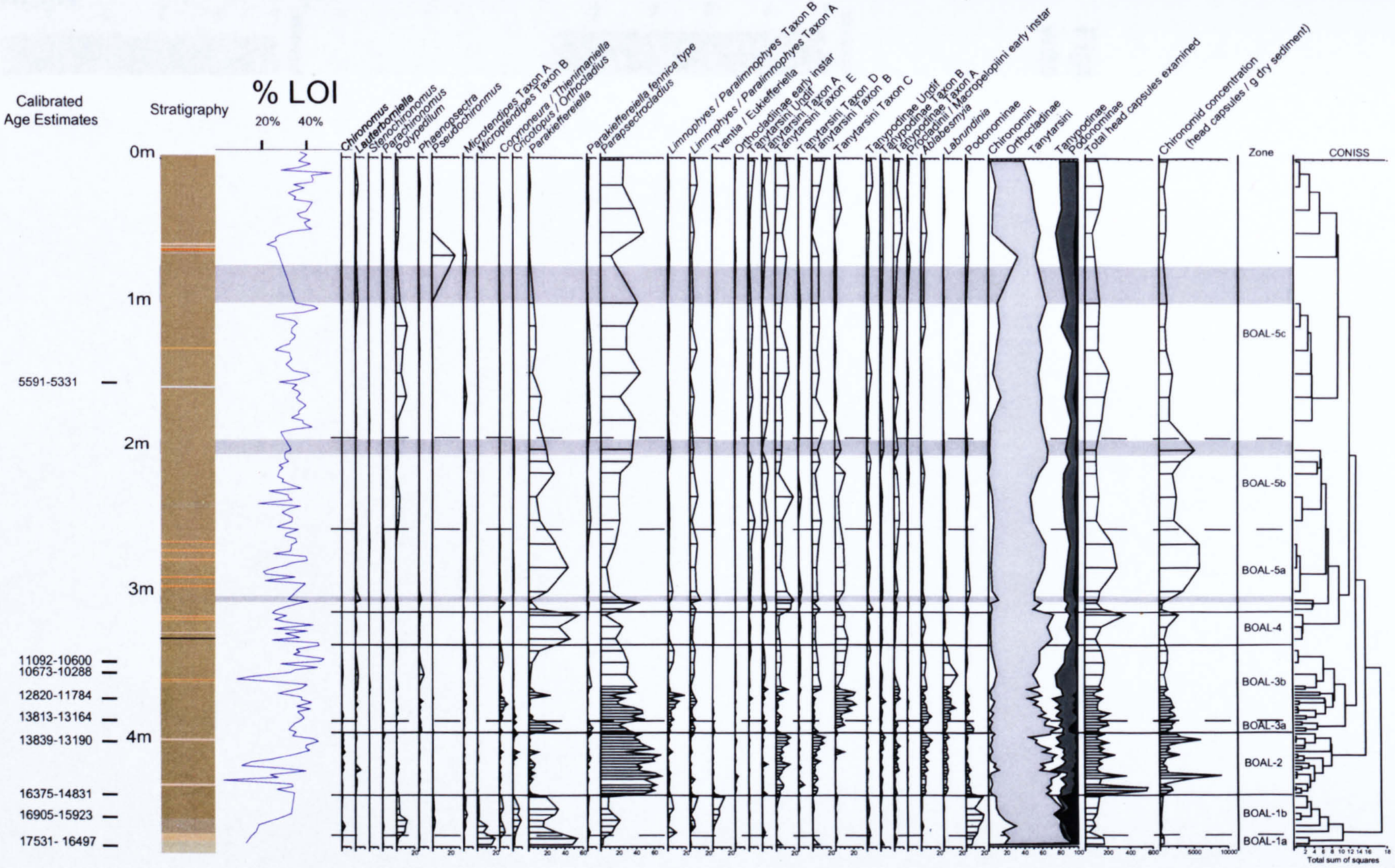

Figure 7.8: Percentage diagram of selected taxa from Laguna Boal. Grey horizontal bands indicate where no sediment was collected. Key for stratigraphy is in Figure 7.4. Dates are calibrated using 2 s.d.

Figure 7.9 : Concentration diagram of selected taxa from Laguna Boal. Grey horizontal bands indicates depths where sediments was missing due to compression of core segments . Key for stratigraphy is in Figure 7.4. Dates are calibrated using 2 s.d.

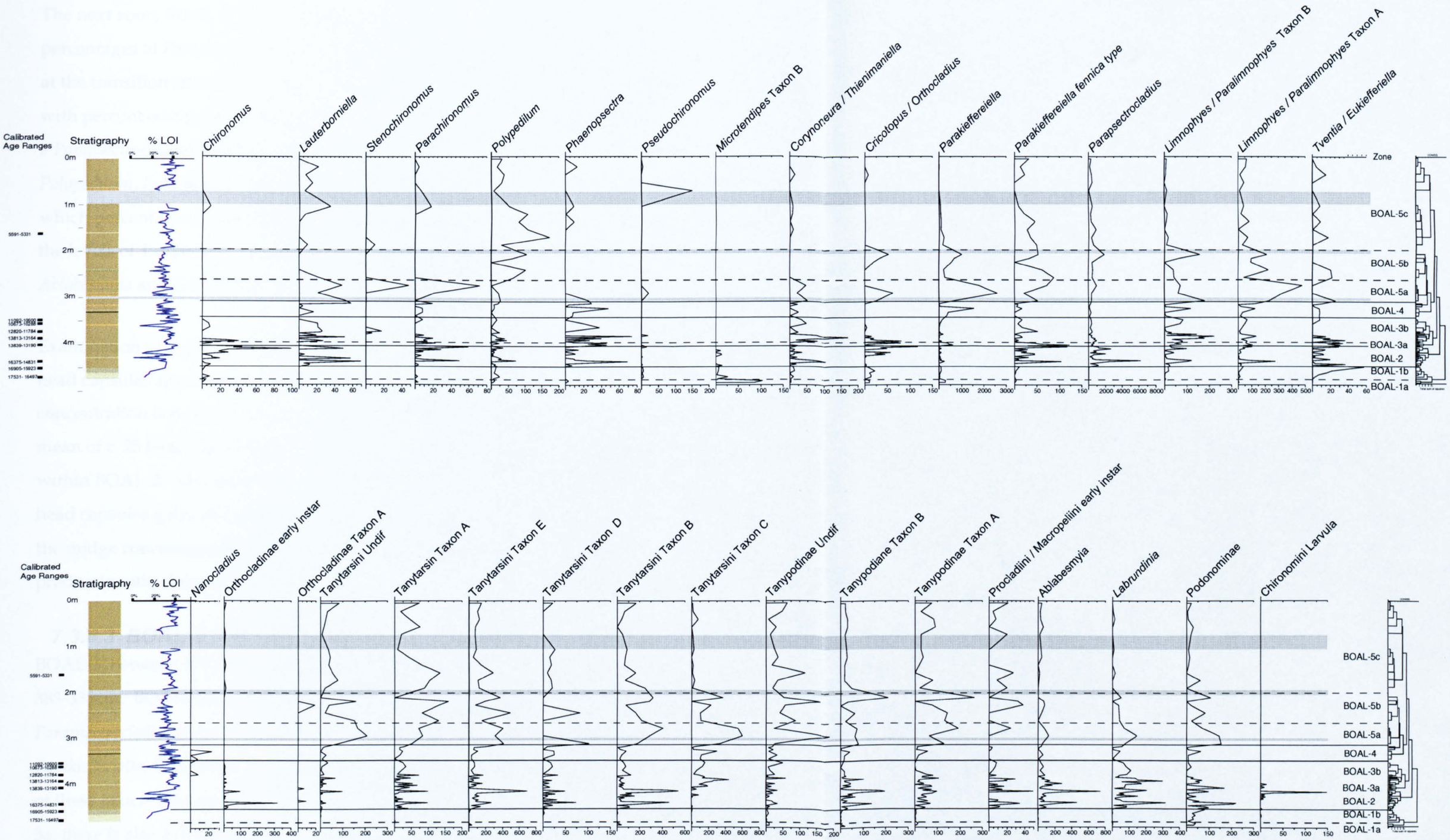

and subfamily, respectively, not exceeding 15% for any level analysed. Concentrations of head capsules remain low throughout the whole of BOAL-1 (<1000 head capsules g dry sed^{-1}), although concentrations are slightly higher within BOAL-1a (*c.* 500 head capsules g dry sed^{-1}). Within the two samples in BOAL-1a, concentrations of *Parakiefferiella* and *Microtendipes* Taxon B, are higher than they are in BOAL-1b.

7.3.4.2 BOAL-2 (431 – 391cm)

The next zone, BOAL-2, lies between 431– 391 cm. This zone is characterised by a high percentages of *Parapsectrocladius* (25- 68%). The change in relative abundance of this taxon at the transition from BOAL-1 to BOAL-2 is the sharpest in any taxon within the record, with percent occurrence jumping from 11% at 430cm to 57% at 432cm. This marked shift to a *Parapsectrocladius* dominated assemblage is accompanied by a drop in levels in *Polypedilum*, *Eukiefferiella / Tventia*, Podonominae and, most notably, *Parakiefferiella* for which percentages drop from 25 – 2%. Within the zone there is also a gradual increases in the levels of Tanytarsini, in particular taxon E and taxon B, and in Tanypodinae, especially *Ablabesmyia* and *Labrundinia*.

Examination of Figure 7.9 at the BOAL-1 / 2 boundary shows that the concentration of head capsules approximately doubles over the zone boundary. This change in overall concentration is mirrored by a specific jump in concentration of *Parapsectrocladius*, from a mean of *c.* 25 head capsules g dry sed^{-1} in BOAL-1 to *c.* 1250 head capsules g dry sed^{-1} within BOAL-2. Overall, head capsule concentration is higher in BOAL-2 (mean = *c.* 2,400 head capsules g dry sed^{-1}) than in BOAL-1. Within BOAL-2, there are two notable peaks in the midge concentrations at 420-422cm and 396-398cm; these increases in concentration are predominantly driven by increases in *Parapsectrocladius* and *Ablabesmyia*.

7.3.4.3 BOAL-3 (391-333cm)

BOAL-3, between 391– 333 cm, is further divided into BOAL-3a, 391-383cm, and BOAL-3b, 383-333cm. BOAL-3a is characterised by a dip in the percentage occurrence of *Parapsectrocladius* to 19-34%. This is accompanied by increases in relative abundance of *Parakiefferiella*, *Parakiefferiella fennica type*, and *Podonominae*. The increased abundance of all of these taxa is sustained over the four levels analysed within the sub-zone. Within BOAL-3a, there is also a decrease in Tanytarsini B, to levels <6 % and an increase in Tanytarsini C, for which values drop from *c.* 3% to 0% at the top of BOAL–3a. Head capsule concentrations within BOAL-3a are fairly low (835-2241 head capsules g dry sed^{1}).

Parakiefferiella, *Parakiefferiella fennica* type and Podonominae, all taxa which rise in percentage occurrence, peak in concentration during the zone. However, the concentration of many other taxa, such as *Chironomus*, *Parachironomus*, all Tanypodinae, Tanytarsini Taxa E and B and *Cricotopus / Orthocladius*, decreases notably.

With the transition from BOAL-3a to BOAL- 3b (383 - 332cm), there is a change to a more diverse faunal assemblage. The fauna returns to being dominated by *Parapsectrocladius* (9-49%), although there is an overall decrease in percentage occurrence of the taxa over the duration of the sub-zone. *Lauterborniella*, *Corynoneura*, *Paralimnophyes*, Tanytarsini A, B and C, Tanypodinae Taxon D, Tanypodinae Taxon A, *Ablabesmyia* and *Labrundinia* are also present throughout much of the zone. Whereas Podonominae is better represented towards the base of the zone, *Lauterborniella*, *Phaenopsectra* and Tanytarsini Taxon B are found in higher abundances in the upper half of the zone. There is a small but significant deviation from the overall trends between 376-366 cm, where percentage occurrences of *Parakiefferiella* and *Paralimnophyes/ Limnophyes* rise rapidly, accompanied by a drop in percentage abundance of *Parapsectrocladius*. Individual taxonomic data reveals that this is due to decreases in concentrations of Tanytarsini taxa B and E, *Parapsectrocladius* and members of the Tanypodinae and Chironomini, whereas concentrations of *Paralimnophyes / Limnophyes* Taxon A, *Corynoneura / Thienemanniella* and *Parakiefferiella* increase. Within the zone as a whole, concentrations of head capsules remain fairly stable, ranging from *c.* 600 – *c.* 2400 head capsules g dry sed^{-1}. There is a large peak in the concentration of *Limnophyes / Paralimnophyes* Taxon B within the bottom 14cm of the zone.

7.3.4.4 BOAL-4 (332-310cm)

BOAL-4 extends between 332- 310cm and is characterised by a rise and fall in *Parakiefferiella* from levels of 11%, above and below BOAL-4, to up to 55% occurrence within the zone. Tanytarsini Taxa E, B and C and *Paralimnophyes / Limnophyes* Taxon A are all present in lower percentages (<10%). Percentages of *Parapsectrocladius* continue to decrease, dropping from 16%, at the base of the zone, to 4% at the top. Head capsule concentrations rise fairly steeply towards the top of the zone, to levels of *c.* 2800 head capsules per g dry sed^{-1}.

7.3.4.5 BOAL-5 (310-0cm)

BOAL- 5, is further divided into BOAL-5a (310–252cm), BOAL-5b (252-190cm) and BOAL-5c (190-0cm). Within BOAL-5a, there is a sharp peak in levels of *Parapsectrocladius* (23-43%) and Tanytarsini Taxon E (13-19%), accompanied by a drop in the occurrence of *Parakiefferiella* to levels of less than 12%. Although of a much smaller magnitude, there are

notable increases in percentage abundance of *Polypedilum* and Tanytarsini Taxon A in the sub-zone. BOAL–5b shows a return to *Parapsectrocladius* as the dominant taxon, with the sub-zone being characterised by relative abundances of the taxon, gradually rising from *c.* 20% at the base of the sub-zone, to *c.* 35% at the top. Tanytarsini Taxa A, E, B and C are present throughout most of the sub-zone in abundances ranging from 0-19%, as is *Limnophyes / Paralimnophyes* Taxon A. *Polypedilum* also returns to the assemblage during BOAL–5b and is present in all but one of the samples; although relative abundance remains low (0-4%), concentration data shows a substantial decrease from the concentrations present in BOAL-5b. Throughout BOAL-5c, the relative abundance of *Parakiefferiella* declines from *c.* 10% at the base of the sub-zone to a mean value of 1% within the upper metre of the core. Concentration data in Figure 7.9 indicate that this is driven by falling concentrations of the taxon, versus the rise in concentration of another taxon. Percentages of *Parapsectrocladius* stay relatively high at 11-48%. Tanytarsini Taxon A, E and B are well represented within the sub-zone, as are Tanypodinae taxa in general. Above 120cm, there is a constant presence of *Ablabesmyia* (2-5%). In line with the overall lower head capsule concentration values, the concentrations of most taxa are lower in BOAL-5c than BOAL-5b, with the exception of *Polypedilum*. The major change responsible for the zonal division between 68 and 100cm is the high levels of *Pseudochironomus* (26%) at 68cm. The concentration data show this is due to a sharp increase in the concentration of *Polypedilum* solely at that sub-sample level. However, within the zone this taxon only occurs only in this level of analysis.

7.4 Developing a Geochronology

Due to the sediment compaction that had occurred in the top 3m of the record, it was decided that a better geochronology would be produced if the record from the three relevant cores segments were expanded. This would mean that records from these segments would again represent 1m versus, for example, 69cm in the segment spanning 0-1m. The shrinkage was corrected uniformly over each core segment. Although this may result in an oversimplification of the effect of the compression, no data was available to help constrain a more detailed approach.

Table 7.3 shows key depths in the record both before and after the depths had been calibrated. As the shrinkage only occurred between 0 - 3m, no depths greater than 3m were affected by this correction. All depths less than 3m in the rest of the chapter are corrected, and indicated with the suffix 'cor'.

Former Depth (cm)	Corrected depth(cm_{cor})	Significance
156	162	Horizon dated for ^{14}C assay SUERC-1763. Date gained = 5261 cal ka BP
252	254	Base of BOAL-5b
190	200	Base of BOAL-5c
60	87	Mid grey, minerogenic horizon
62-63	90-91	Light grey, minerogenic horizon
67-68	97-98.5	More minerogenic horizon

Table 7.3: Table showing depths before and after correction for shrinkage within the top 3m of the Laguna Boal record.

7.4.1 Tephrochronology

Results of EMPA analysis were used firstly to aid correlation between core segments. This was applicable within the bottom 1.2m of the records, where the three deepest core segments taken from the site were thought to overlap to produce a complete sequence. The common geochemical ranges from the two individual subsamples at c. 356cm from different core segments (Figure 7.10), combined with the similar depth of these horizons relative to the water/sediment interface, allow precise correlation between these core segments (see Figure 7.10). A similar correlation was also possible at c. 423 cm. Therefore, the presence of these two, volcanic chronostratigraphic makers allowed a continuous record for the basal 1.7 m to be produced (Figure 7.10).

Secondly, the results of EMPA analysis were compared to published data on eruptions of known ages to see if any horizons could be linked into the regions tephrochronological context. The generally large spread of most of the horizons' geochemistries meant that there was little significant correlation to major oxide geochemistries of previously analysed and dated tephra horizons from the Chonos - Taitao (Haberle and Lumley, 1998). The exception to this was the group of minerogenic horizons between 87 and 99 cm_{cor}. Figure 7.11 shows the results of analyses of these horizons compared to data published in Haberle and Lumley (1998). Two ^{14}C ages for this event have been published, dating it to 1830±75 (AA10296) and 1605±75 ^{14}C yr BP (AA10300) (Haberle and Lumley, 1998).. Although tightly grouped, analyses from the horizon at 162 cm_{cor} showed no geochemical correlation with results from the Taitao region. Discussions with Charles Stern (*pers. comm.*) lead to the suggestion that the major element geochemistry of this population indicated deposits possibly originating from the mafic basaltic eruption of Melimoyu < 2.7 ka BP.

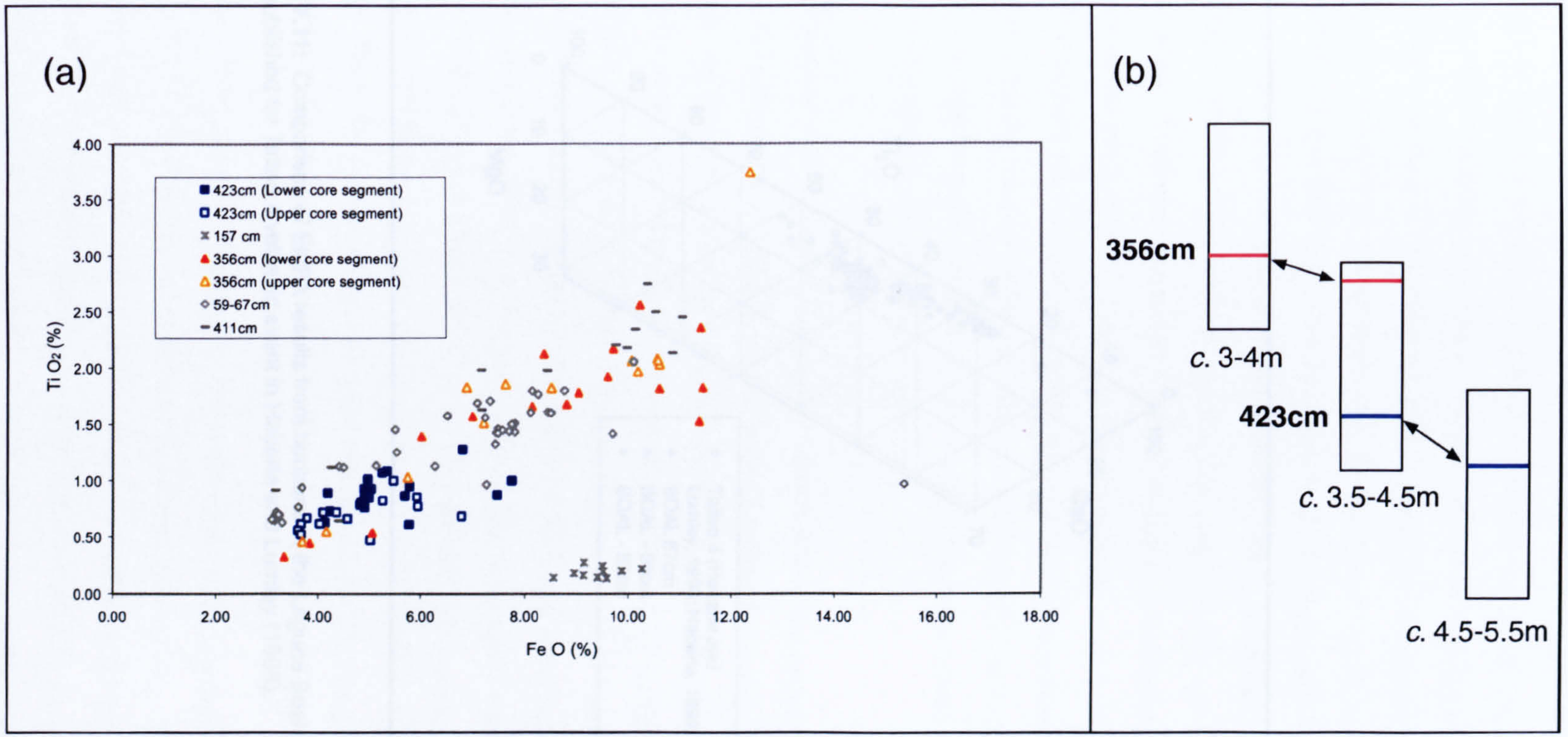

Figure 7.10: (a) Bi-plot showing the similar geochemical range of shards within samples 356 and 423 cm and (b) Schematic diagram showing how the three basal core segments were linked using these common geochemistries. In (a) Results from other horizons are shown in grey to place the results in the context of the whole core.

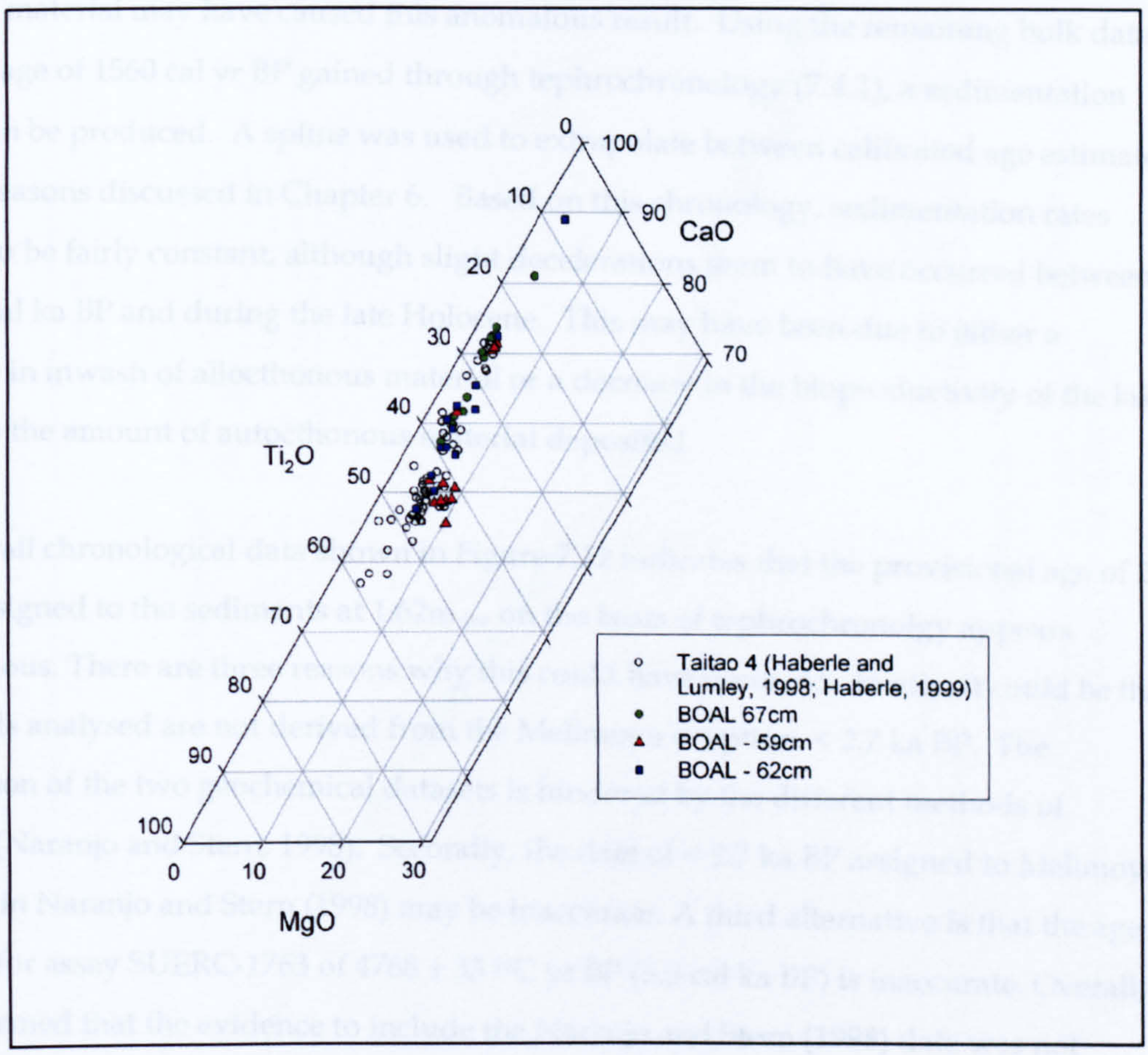

Figure 7.11: Comparison of EMPA results from horizons in the Laguna Boal record and those published for Taitao 4 volcanic event in Haberle and Lumley (1998).

7.4.2 Addition of ^{14}C data

The ^{14}C results presented in 7.3.3 were added to the tephrochronological framework established in 7.4.1 to produce a sedimentation curve for the sequence. Figure 7.12 shows these data and the sedimentation curve produced using corrected age depths where appropriate. Within the bulk AMS samples (shown in grey) the sample from 393cm (SUERC-1755) lies out of sequence. Since the rest of the bulk analyses lie in chronological sequence, it was deemed that this result should be omitted. Contamination by younger or modern material may have caused this anomalous result. Using the remaining bulk dates, and the age of 1560 cal yr BP gained through tephrochronology (7.4.1), a sedimentation curve can be produced. A spline was used to extrapolate between calibrated age estimates for the reasons discussed in Chapter 6. Based on this chronology, sedimentation rates appear to be fairly constant, although slight decelerations seem to have occurred between *c.*11-13 cal ka BP and during the late Holocene. This may have been due to either a decrease in inwash of allocthonous material or a decrease in the bioproductivity of the lake and thus the amount of autocthonous material deposited.

The overall chronological data shown in Figure 7.12 indicates that the provisional age of 2.6 ka BP assigned to the sediments at 1.62m $_{cor}$ on the basis of tephrochronolgy appears incongruous. There are three reasons why this could have occurred. Firstly, it could be that the shards analysed are not derived from the Melimoyu eruption, < 2.7 ka BP. The comparison of the two geochemical datasets is hindered by the different methods of analysis (Naranjo and Stern, 1998). Secondly, the date of < 2.7 ka BP assigned to Melimoyu eruption in Naranjo and Stern (1998) may be inaccurate. A third alternative is that the age estimate for assay SUERC-1763 of 4768 ± 33 ^{14}C yr BP (5.3 cal ka BP) is inaccurate. Overall, it was deemed that the evidence to include the Naranjo and Stern (1998) date was not sufficiently strong. Thus, the potential chronological constraint of <2.7 ^{14}Cka BP provided via the possible Melimoyu origin of the shards at 1.62m cor was not used any further.

Age estimates gained from plant-macrofossil assays were consistently younger than the extrapolated age gained from the bulk age spline curve – based chronology. Following calibration of all dates, age estimates were c. 600 cal yr (Beta -180729) and 700 cal yr (Beta - 180731) younger than the extrapolated age proposed for the same depths. The production of younger plant macrofossil ages is in keeping with research at other sites. For example, Walker *et al.* (2001) propose that the true ^{14}C age of sediment at their site, St Bees in the UK, was likely to lie between age estimates gained from analysis of plant

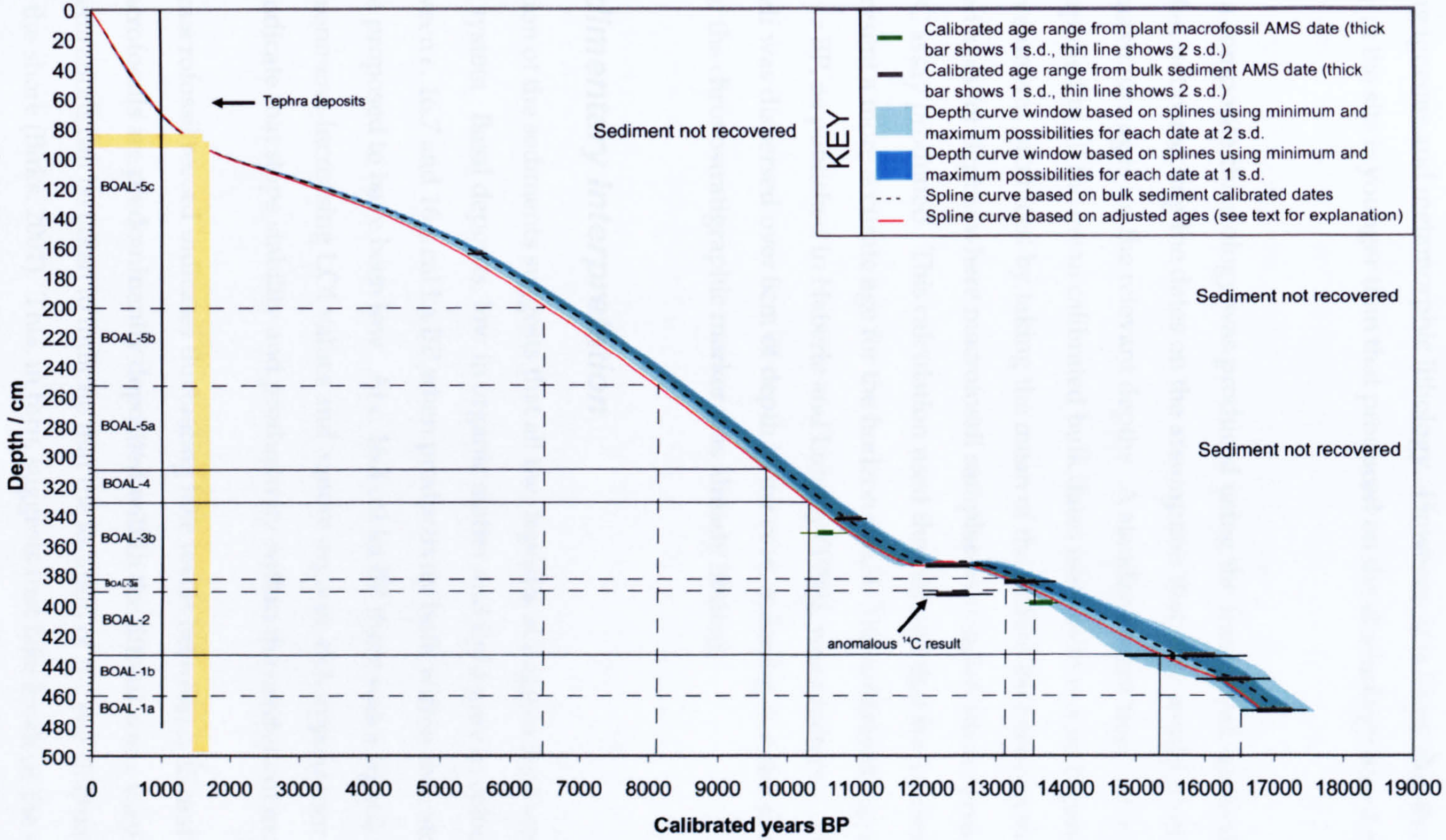

Figure 7.12: Sedimentation curve for Laguna Boal. All age ranges are shown in calibrated ages (see Table 1.1) at 68% confidence (1sd). Chironomid zones are annotated on the left side of the graph.

macrofossils and the humic content of the sediment, acting as minimum and maximum bracketing ages, respectively. The effects of contamination via reworking of old carbon or hard water at Laguna Boal are likely to be minimal, due to the relatively young age of the surrounding igneous and metamorphic lithology. However, it is likely that the true chronology at the site is younger than that produced on the chronology based on bulk dates.

Therefore, a composite chronology was produced using the framework derived from the bulk samples, but correcting the dates on the assumption that they would probably represent maximum ages for the relevant depths. A standard correction factor of -650 cal years was applied to all the mean calibrated bulk dates (shown in red on Figure 7.12). The correction value was produced by taking the mean of the difference between the extrapolated ages for depths where macrofossil samples were taken from versus the result the AMS ^{14}C assay produded. This calculation used the rational that the macrofossil dates would represent a more accurate age for the horizon dated. The calibrated age of the tephra at 1560 cal yr BP, as published in Haberle and Lumley (1998), was unaltered. The tephra deposit itself was dispersed over 8cm of depth in the core, meaning that the stratigraphic precision of the chronostratigraphic marker was already limited.

7.5 Sedimentary Interpretation

Interpretation of the sediments suggests that all the deposits at Laguna Boal were formed in a limnic system. Basal deposits, low in organic matter and light grey in colour, were laid down between *c.* 16.7 and 16.4 cal ka BP when productivity both within the catchment and the lake are proposed to have been low. At *c.* 16.4 cal ka BP there was a significant change in the environment. Increasing LOI values and a more organic-rich appearance of the sediment indicate that slope stability and productivity within the catchment increased.

The plant macrofossil record indicates fluctuating lake levels between *c.* 15 and *c.*10.8 cal ka BP. As macrofossils are predominantly deposited within the littoral zone, varying macrofossil concentrations can be taken to indicate that the location of the site fluctuated in relation to the shore (Birks, 2001). This, in turn, suggests that lake levels at the site fluctuated. The presence of *Nothofagus* leaves among these macrofossils indicates that the genus was growing in either its shrub or arboreal form within the catchment. This indicates climatic amelioration from the prior low productivity to allow shrub and/or arboreal vegetation growth on Isla Cuptana.

A productive limnic system prevails throughout the record to the present day. This is indicated by relatively high LOI values and the dark brown, organic-rich colour of the sediments. The high variability of the shard geochemistries of the minerogenic horizons suggests that such deposits are the results of inwash events in the catchment rather than single volcanic events. The significance of palaeoenvironmental interpretations that can be drawn from such bands is limited as they could have been caused by some sort of internal landscape instability or excessively high rainfall in a geologically, very short space of time. The high concentration of charcoal at 327cm indicates local fire activity during the early Holocene, c. 10.2 cal ka BP. This might be interpreted to mean that relatively xeric conditions were present, although the possibility of anthropogenically induced burning should not be excluded (7.2).

The repeated occurrence of oxidised ferric material in the core is interesting and allows suggestions to be made about the palaeolimnic environment. Iron exists in aqueous solution as either Fe^{2+} (ferrous state) or Fe^{3+} (ferric state). In certain conditions iron in its ferric state (Fe^{3+}) combines with OH^- to form $FeOH_3$. The amount of iron present as $FeOH_3$ is dependent on lake pH and redox potential (E_h), which is a measurement of the electron availability within the lake water (Wetzel, 2001). In freshwaters, $FeOH_3$ is found in alkaline conditions (Sivan *et al.*, 1998; Langmuir, 1997; Wetzel, 2001; Dodds, 2002). The proportion of iron in the Fe^{3+} state will also increase with the amount of dissolved oxygen in lake water, as this will increase the system's redox potential (Wetzel, 2001). These relationships are illustrated in Figure 7.13. The presence of $FeOH_3$ deposits in the Laguna Boal sequence therefore means that water was either sufficiently alkaline or was well enough oxygenated to allow iron in its $FeOH_3$ state to survive both deposition and burial without undergoing reduction. However, the conditions required for $FeOH_3$ to form would also depend on the extent to which the lake water was saturated with iron, a variable which cannot be ascertained from the analyses conducted within this study. Although interesting, little inference can be made about pH and redox potential of the lake in the past

7.5.1 Chironomid interpretation

When the assemblages encountered in the Boal record are plotted on the CCA ordination based on the modern Patagonian data it can be seen that there is limited overlap (Figure 7.14). In general, down-core samples have higher axis 1 scores than the modern samples. Using inferences gained from CCA, this would indicate that Laguna Boal was deeper, more alkaline and at a lower altitude than the lakes sampled in the training set. However, the

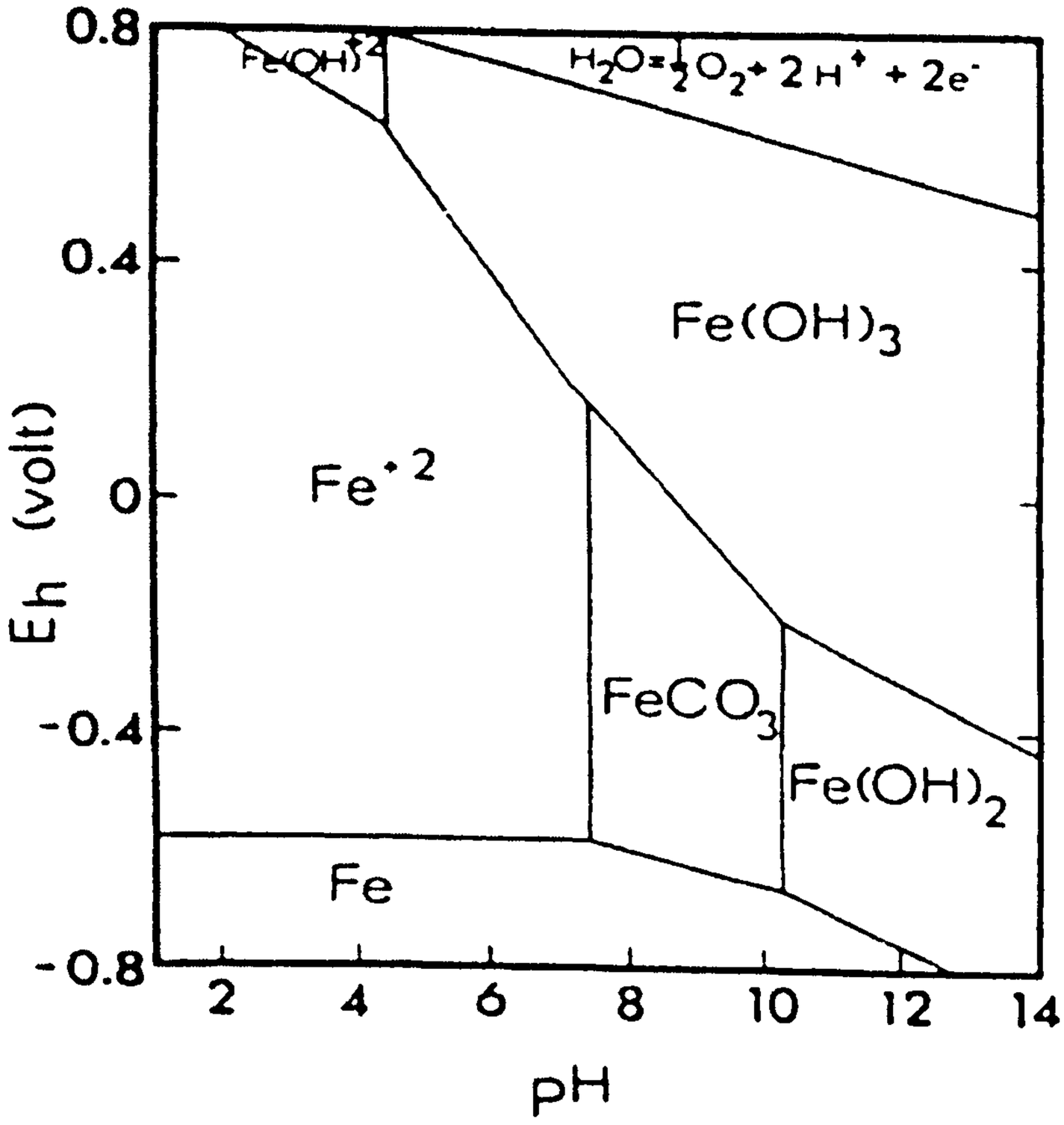

Figure 7.13: Approximate distribution of species of iron and manganese in relation to pH and redox potential Eh. Alkalinity is assumed to be equal to 2 meq litre^{-1}, Lines denote points at which the activities of soluble Fe are 10^{-5} mol litre-1 (Wetzels, 2001, based on Stumm and Lee, 1960 and Stumm and Morgan, 1996)

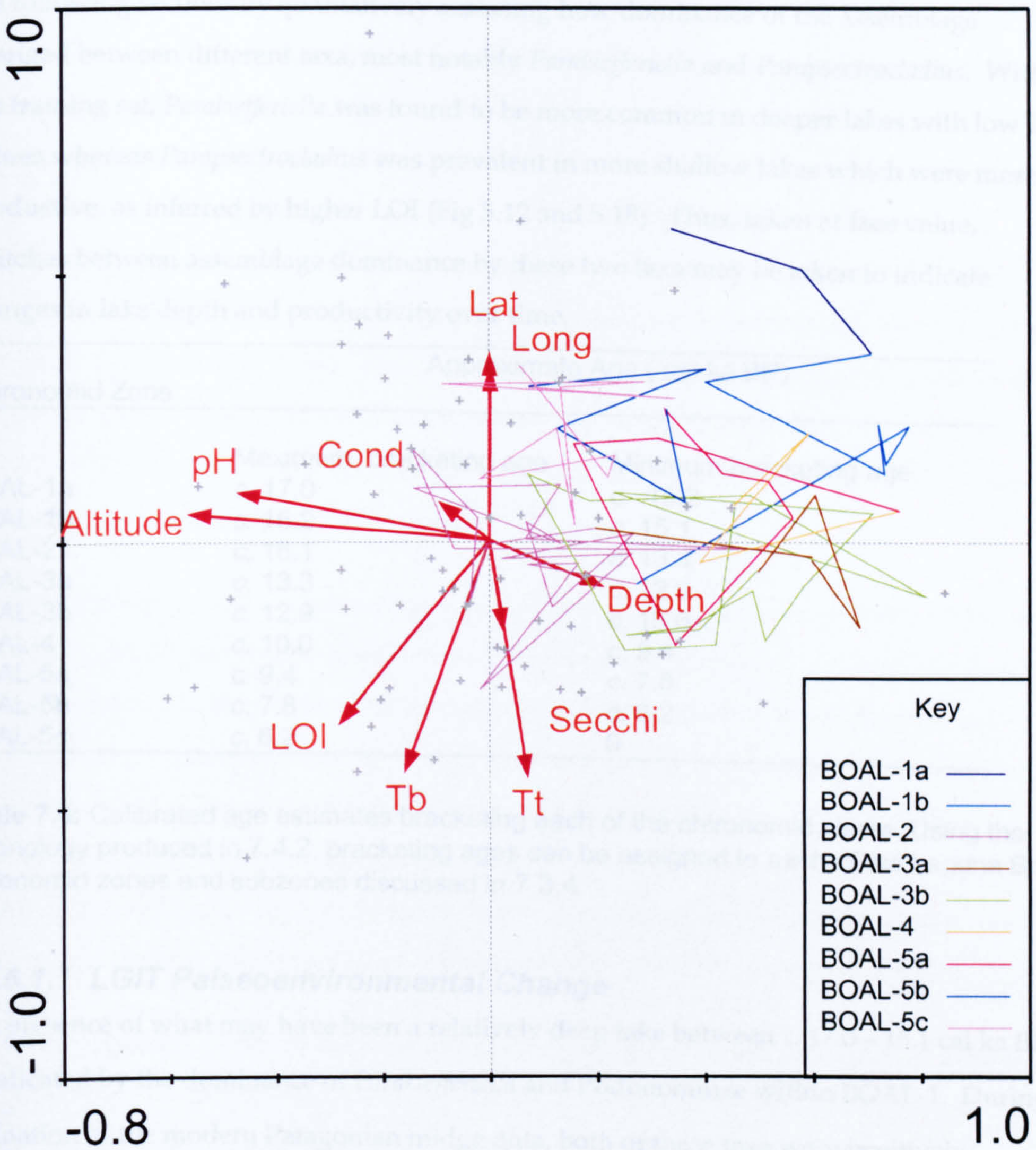

Figure 7.14: Assemblages found in the down core Laguna Boal record as passive samples using the CCA ordination developed in Chapter 5. Different coloured lines represent different (sub) zones in the record. Grey crosses represent the location of modern day lakes plotted during CCA. Environmental variables used during ordination are shown.

no-analogue issue is less severe in several parts of the core (BOAL-5c, BOAL-3b and BOAL-2), where samples plot closer to both the origin and modern day samples. Because of the 'no analogue' issue, the changes in taxonomic assemblage are predominantly interpreted in the following sections by qualitatively assessing how dominance of the assemblage changed between different taxa, most notably *Parakiefferiella* and *Parapsectrocladius*. Within the training set, *Parakiefferiella* was found to be more common in deeper lakes with low LOI values whereas *Parapsectrocladius* was prevalent in more shallow lakes which were more productive, as inferred by higher LOI (Fig 5.12 and 5.18). Thus, taken at face value, switches between assemblage dominance by these two taxa may be taken to indicate changes in lake depth and productivity over time.

Chironomid Zone	Approximate Age (cal ka BP)	
	Maximum bracketing age	Minimum bracketing age
BOAL-1a	*c.* 17.0	*c.* 16.2
BOAL-1b	*c.* 16.2	*c.* 15.1
BOAL-2	*c.* 15.1	*c.* 13.3
BOAL-3a	*c.* 13.3	*c.* 12.9
BOAL-3b	*c.* 12.9	*c.* 10.0
BOAL-4	*c.* 10.0	*c.* 9.4
BOAL-5a	*c.* 9.4	*c.* 7.8
BOAL-5b	*c.* 7.8	*c.* 6.2
BOAL-5c	*c.* 6.2	0

Table 7.4: Calibrated age estimates bracketing each of the chironomid zones. Using the chronology produced in 7.4.2, bracketing ages can be assigned to each of the Laguna Boal chironomid zones and subzones discussed in 7.3.4

7.5.1.1 LGIT Palaeoenvironmental Change

The presence of what may have been a relatively deep lake between *c.* 17.0 – 15.1 cal ka BP is indicated by the dominance of *Parakiefferiella* and Podonominae within BOAL-1. During ordination of the modern Patagonian midge data, both of these taxa were positively correlated to depth (Figure 5.10). Changes in the assemblage between 16.3-15.8 cal ka BP indicate a climatic amelioration and increase in site bioproductivity. The increase in relative abundance of *Parapsectrocladius* is caused by the decrease in concentrations of *Parakiefferiella* and *Microtendipes* Taxon B as opposed to increase in concentration of the former taxon (Figure 7.9). Such shifts in concentration could be driven by two mechanisms. Either (1) *Parakiefferiella* and *Microtendipes* Taxon B abundances at the site stayed the same, whilst sedimentation rates and occurrence of other taxa increased or (2) occurrence of other taxa and the sedimentation rate could have remained constant whilst

the concentration of *Parakiefferiella* and *Microtendipes* Taxon B decreased. It seems reasonable to propose that climate amelioration occurred following deglaciation given that rising LOI indicates that higher levels of productivity existed either in the catchment or the lake itself. This would facilitate an increase in the relative abundance, and potentially concentration, of *Parapsectrocladius*, a taxon which CCA of the modern Patagonian dataset indicated was correlated with higher LOI values than those of *Parakiefferiella* and *Microtendipes* Taxon B (Figure 5.11). Such a proposal is supported by a concomitant increase in the concentration and relative abundance of *Polypedilum*. Although the ordination of Patagonian taxa does not indicate *Polypedilum* to be a particularly stenotopic taxon, Holarctic studies have suggested that it is indicative of nutrient rich habitats (Little and Smol, 1995; Brundin, 1958). Therefore, the overall changes in taxonomic assemblage between *c.* 16.3-15.8 cal ka BP can be interpreted to indicate that productivity at the site increased. This change in environmental conditions to a more nutrient rich system may have been the result of climatic warming.

Towards the top of BOAL-1, percentages of *Parapsectrocladius* and *Polypedilum* decrease, as concentration and percentage abundance of *Parakiefferiella* increase. *Tventia / Eukiefferiella* also increases at the same time. The modern dataset indicates that *Parakiefferiella* and *Tventia / Eukiefferiella* were found in deeper lakes with lower LOI, as is *Parakiefferiella fennica* type (Figure 5.11). Therefore, these assemblage changes may be due either to falling nutrient levels or a deepening in the lake. The fact that the LOI records do not support the former hypothesis may add weight to the latter. If so, a short-lived (c. 700 cal years) period in increased effective precipitation may be indicated by the brief changes in species.

It is worth explaining the implications of the mismatch between the assemblages during this first period of colonisation (BOAL-1) and the training set. The extent of the mismatch is indicated in the CCA diagram by the location of the BOAL-1 data in the far corner of the top right quadrant and minimal overlap with modern sites (Figure 7.14). Although limiting, this is not surprising, as no lakes from recently deglaciated terrain were included in the training set. The problem of poor understanding of these early stages of lake development and processes following deglaciation is recognised to be a common problem (Engstrom *et al.*, 1991). Therefore, although the assemblage may indicate that Laguna Boal was deep during the first 1,500 cal yrs of the limnic system, it might alternatively be proposed that the assemblage actually represents cold conditions. Although such conditions are not directly indicated via comparisons of the fossil record and ordination of

the modern data, the lack of reconstructions indicating a cold climate might be explained by potentially unrepresentative temperature data in the modern day study (Chapter 5). Thus, using the observation that cold taxa are found in deep lakes, even when air and surface temperatures appear warmer than their tolorence (Walker and Matthews, 1989a) and that Podonominae, which is one of the major taxa during these first 1,500 years, is a cold indicator (Brundin, 1966, 1988), the BOAL-1 assemblage may well be recording cold conditions.

The pronounced change in taxonomic assemblage at *c.* 15.4 cal ka BP indicates a change in the system, which appears to be driven by climatic warming. The taxa that dominate during BOAL-2, Tanytarsini E and B, *Parapsectrocladius* and *Ablabesmyia*, are indicated by TWINSPAN analysis to be potentially fairly cosmopolitan taxa. However, within the training set as a whole, the optima of these taxa are generally in shallow lakes (Figure 5.11). These lakes are also often more bio-productive, as indicated by high LOI and low Secchi depth (Figure 5.11). Although LOI fluctuates repeatedly during BOAL-2, this may have been due to frequent in-wash events that interrupt a record of what is, otherwise, a period of higher bio-productivity than before *c.* 15.3 cal ka BP. Alternatively, some of the fluctuations in LOI may be due to the variation in presence of plant macrofossils (Figure 7.4). An increase in bioproductivity would also explain the increase in concentration of head-capsules during BOAL-2 (Figure 7.9), although such an increase could also be partly a consequence of the decreased sedimentation rates (Figure 7.12). This latter decrease might be a result of an increase in slope stability as vegetation cover increases as temperature ameliorates. Thus, the overall combination of sedimentary and taxonomic data during this period suggests climatic warming occurred at the site. This would induce an increase in bioproductivity within the lake and catchment and a decrease in lake depth, through increased evaporation or a decline in rainfall. Both these consequences of climatic warming would result in the observed decrease in relative abundance of *Parakiefferiella* and Podonominae, taxa which are more indicative of deeper lakes, and the increase of Tanytarsini, *Parapsectrocladius* and *Ablabesmyia* (Figure 5.11). Alternatively it may be that this lake shallowing is purely been driven by the basin infilling.

The sharp change in midge fauna for the *c.* 400 hundred years between 13.5 and 13.1 cal ka BP may indicate an increase in lake depth. The concomitant increase in concentrations of *Pliaenopsectra*, *Parakiefferiella*, Podonominae and, additionally, Tanytarsini Taxon C (within the last 3 cm of BOAL-3a) shows a switch to an assemblage dominated by taxa shown by

CCA to be correlated with increasing depth (Figure 5.11). Additionally, Podonominae are proposed by Brundin (1966, 1988) to be indicative of cold conditions. The associated decrease in Tanytarsini E and B, *Ablabesmyia* and *Chironomus* in the record supports this proposal, as CCA also indicated these were indicative of productive lakes (Figure 5.11). In Holarctic studies *Chironomus* has often been associated with shallow conditions, although it can inhabit profundal habitats (Korhola *et al.*, 2000), and Chironomini, in general, are proposed by Walker (1987, 37) to be generally "warm-adapted" taxa. Low macrofossil presence during these depths also supports the hypothesis of rising lake levels. An increase in precipitation or decrease in temperature could raise lake levels and increase the distance between the shore and the core site.

Following this apparent, short duration of lake level rise from 13.3 to 12.9 cal ka BP, an increase in macrofossil abundance indicates that lake levels started to drop. However, the shallowing was only minimal. This is because, although the assemblage reverts to one characteristic of *c.* 15.1 - 13.3 ka BP (BOAL-2), there is a consistent presence of Tanytarsini Taxon C throughout the sub-zone. This taxon is indicative of deeper lakes within the Patagonian training set (Figure 5.11). These lower lake levels are inferred to persist for c. 300 cal years.

Notable increases in both percentage and concentration of *Parakiefferiella* between 12.3-11.1 ka BP, concomitant with a decrease in LOI, and a further subsequent rise in the relative abundance of *Parakiefferiella* at *c.* 10.7cal ka BP indicates that there were fluctuations in the lentic system during the BOAL-3b (12.9-10.0 cal ka BP). An increase in effective precipitation, either through an increase in precipitation or decrease in temperature, may have caused lake levels to rise and thus concentrations of *Parakiefferiella* to rise. It may be argued that a decrease in temperature may be the most likely of these scenarios, as this could also account for the associated decrease in bioproductivity at the site. This would result in a decrease in LOI and accumulation rates, as less organic material would have been produced in the catchment and lake, and thus the slight decrease in head capsule concentration, all of which is coeval with the relative and absolute increase in *Parakiefferiella*.

7.5.1.2 Holocene Palaeoenvironmental Change

The decrease in percentages and concentration of *Parakiefferiella*, after 12.9 cal ka BP, suggests a return to shallower conditions similar to those present between 12.9 and 12.4 cal ka BP. Following this c. 1,600 cal year-long period during which the assemblage is

dominated by *Parapsectrocladius*, there is a gradual rise in percentages of *Parakiefferiella* at *c.* 9.4 ka cal BP. The rise and fall in abundance of *Parakiefferiella* between *c.* 9.4 and *c.* 7.8 ka cal BP is accompanied by increases in concentration of taxa indicative of deeper lakes with less organic substrates (*Phaenopsectra, Limnophyes / Paralimnophyes* Taxon A and B, *Parakiefferiella fennica* type). It is also interesting to note that the rise in *Parakiefferiella* between c. 9.4 – 7.8 cal ka BP occurs during the depths where rust-coloured deposits are present in the core. This is also the case within the earlier peak of relative abundance in *Parakiefferiella* between 10.0 -9.4 cal ka BP. Within the modern dataset, *Parakiefferiella* was shown often to be present in the more acidic lakes sampled, such as VicI and PIII (see Figure 5.11). Thus, the concomitant occurrence of relatively high abundances of *Parakiefferiella* and the presence of $FeOH_3$ deposits might indicate periods of increased dissolved oxygen levels in the lake as opposed to high pH. Such a proposal is strengthened by the observation that *Parakiefferiella* is present in higher abundances in lakes with relatively low LOI. Low values of LOI indicating low productivity could allow DO levels to remain undepleted. Alternatively the low LOI may be due to increased slope stability and an increased in wash of minerogenic sediment from the catchment.

Using the combination of palaeo midge assemblage and sediment characteristics, two simplified hypotheses can be proposed. It may be that temperature dropped, thus reducing bioproductivity, as represented by a drop in LOI in the record, and that this lead to an increase in dissolved oxygen due to lower levels of respiration within the limnic system. Alternatively, if precipitation in the region increased due to a shift in the position of the Westerlies, it is likely that an increase in windiness would have accompanied this change. Invigorated physical mixing of the lake would cause an elevated supply of dissolved oxygen to the system and a lowering or eradication of a hypolimnion, if present (Wetzel, 2001). Therefore, it may be that another increase in precipitation can be linked with the lake level rises proposed to have occurred at 9.4-7.8 cal ka BP.

The strong decrease in midge head capsule concentration in conjunction with a rise in LOI between 310 -300 cm (c. 9.4 – 9.1 cal ka BP) may indicate a short-lived increase in sedimentation rates. Although this is not indicated in the sedimentation curve (Figure 7.12), an explanation might be that the resolution of ^{14}C dates throughout the Holocene is too coarse to detect such a change. Following this there appears to be a great increase in lake productivity, or a decrease in sedimentation rates, as the increase in the concentration of head capsules is dramatic and remains elevated until *c.* 7.8 cal ka BP.

The contemporary switch to a *Parapsectrocladius* dominated assemblage appears to be the result of decreasing *Parakiefferiella* concentrations (Figure 7.9). The coincident rise in concentration and percentage abundance of Tanytarsini Taxon E may indicate an increase in productivity of the lake, as CCA indicated that this taxon was indicative of shallow lakes with higher LOI (Figure 5.11). LOI between 300-310cm is higher than that during BOAL-4. A climatic warming could have produced both a shallowing of the lake and the associated decrease in *Parakiefferiella* and also an increase in productivity at the site, leading to increases in *Parapsectrocladius*, Tanytarsini Taxon E, LOI and overall head capsule concentration. This period appears to have been followed by a cooling or an increase in precipitation leading to an increase in taxa indicative of deeper and less productive conditions (*Parakiefferiella, Limnophyes / Paralimnophyes* Taxon A, and Tanytarsini Taxon C) which starts at 9.3 cal ka BP and continues until 8.3 cal ka BP.

At c. 7.8 cal ka BP, when the abundance of *Parakiefferiella* and other taxa associated with deeper conditions begins to decrease, *Polypedilum*, thought in the Holarctic to be an indicator of littoral conditions (Walker and MacDonald, 1995), increases dramatically in concentration, although less noticeably in relative abundance. A continual decline in both percentages and concentrations of *Parakiefferiella* until c. 1.5 cal ka BP might be interpreted to indicate a shallowing in lake depth. However, as the present level of Laguna Boal is determined by the basin's lowest drainage point, absolute lake levels cannot have fallen during the Holocene unless significant erosion of the drainage point has occurred. Thus, one explanation is that the lake's drainage route has been eroded away leading to a lower, absolute water level. Alternatively, a relative decrease in lake depth could be explained by basin infilling, as c. 2.5m sediment has accumulated during this time. At least a partial influence on the fauna of a relative decrease in water depth during the mid to late Holocene may be indicated during this period by the decrease in Tanytarsini Taxon C, which is coincidental with a further increase in the relative abundance of *Polypedilum* c. 6 cal ka BP. Tanytarsini Taxon C plotted towards deeper lake conditions during ordination of the modern fauna (Figure 5.11). A different approach is to attribute the rise in relative abundance of *Parapsectrocladius* at the expense of *Parakiefferiella* to an increase in bio-productivity unrelated to lake depth. Figure 7.15 shows a smoothed LOI curve for Laguna Boal plotted next to the relative abundance of *Parapsectrocladius* throughout the core. Although the initial increase in LOI lags behind the increase in percentage of Parapsectrocladius at the base of the curve, there is a general agreement in the shape of the

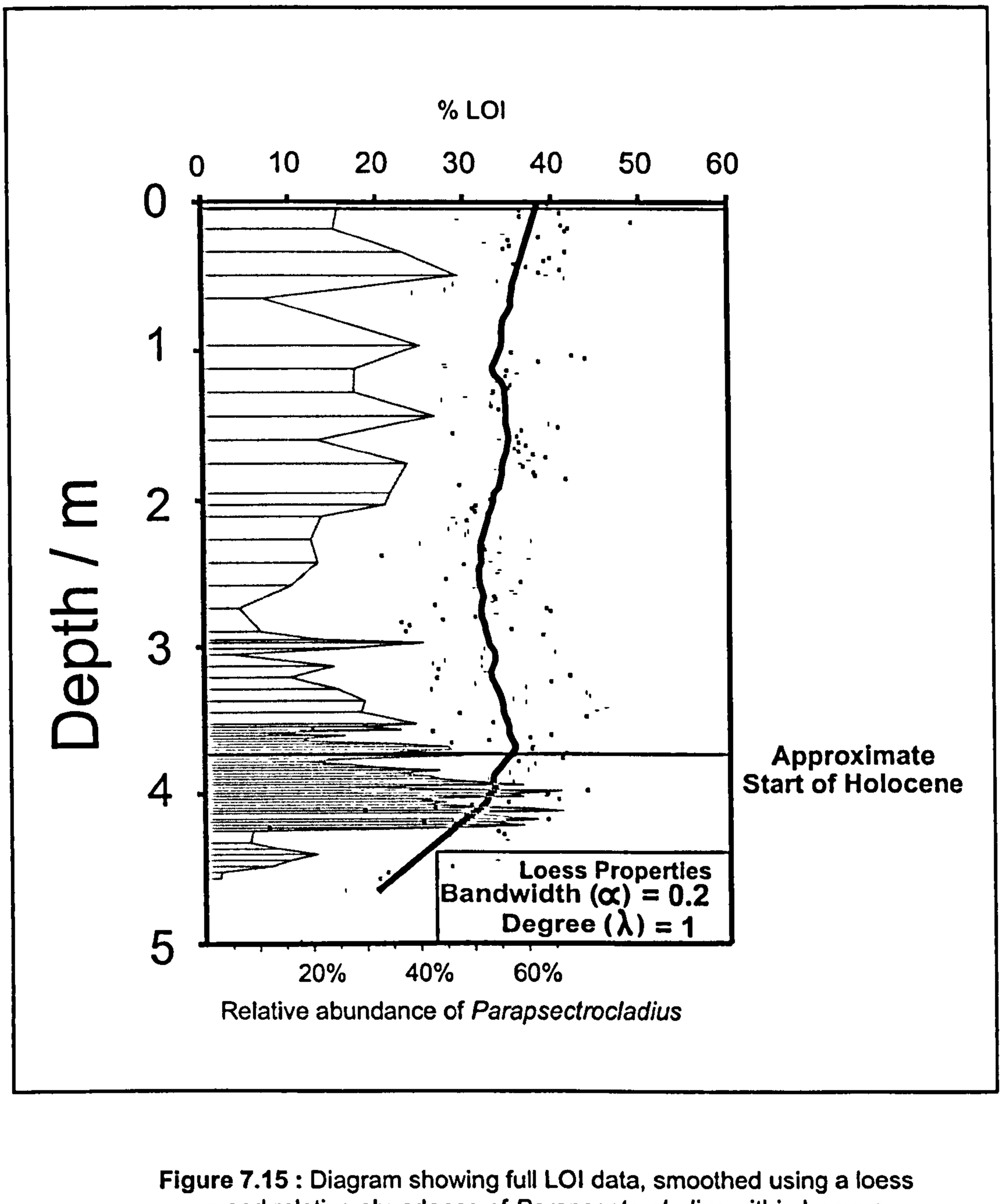

Figure 7.15 : Diagram showing full LOI data, smoothed using a loess curve and relative abundance of *Parapsectrocladius* within Laguna Boal.

curves overall. Within the Holocene, it can be seen that the two datasets accord well, suggesting that catchment productivity may be influencing the assemblage during this period. A possible forcing mechanism for this increase in bioproductivity may have been a rise in temperature. Thus, to summarise, the Holocene midge record is somewhat equivocal. Although interpretations of decreasing water depth can be made, the extent to which this can be linked to climate is limited when the lake's current hydrology is taken into account. Whilst LOI values do not rise dramatically, increased productivity might have supported the rise and subsequent dominance of *Parapsectrocladius* during this period.

The high relative abundance and concentration of *Pseudochironomus* at *c.* 1.5 cal ka BP may be directly determined by the input of tephra horizons between at *c.* 1560 cal yr BP. High percentage occurrence of the taxon is limited to just one level of analysis and is at the level of the tephra horizons. Additionally, within the modern fauna investigated the abundance of *Pseudochironomus* was highest in VER, a lake with a minerogenic, grainy substrate which produced low LOI (8%) when analysed. This inferred Patagonian ecological niche is corroborated by Pinder and Reiss (1983) who indicate the taxon's preference for habitats with sandy substrate.

7.6 Comparisons of Laguna Boal with other records from the area

There are fewer palaeoenvironmental records with which to compare the midge record from Laguna Boal to than is the case with Laguna Leta. However, palynological studies on seven cores have been conducted (Six Minutes, Facil, Stibnite, Marcelo, Lincoln, Lofel and Oprasa) (Lumley 1993, Lumley and Switsur, 1993; Bennett *et al.*, 2000, Haberle and Bennett, *in press*; Massaferro *et al.*, *submitted*) (Figure 7.2). All of these records date back to the LGIT, with the exception of Marcelo, which only spans the latter half of the Holocene (Lumley, 1993). Massaferro *et al.* (*submitted*) argue that the long-distance transport of pollen and regional dominance of similar arboreal species mean that an event stratigraphy approach based on the existing pollen records is valid for the region. Two of the records on which pollen analysis has been conducted (Facil and Stibnite) have also been analysed using chironomids (Massaferro and Brooks, 2002; Massaferro *et al.*, *submitted*) (See chapter 2). Additionally, *c.* 400km to the South a sequence spanning from >13,000^{14}C to present was analysed at Puerto Eden using beetle and pollen analysis (Ashworth *et al*, 1991; Ashworth and Markgraf, 1989). The results of these studies in relation to the interpretations of the Laguna Boal record are shown Figure 7.16.

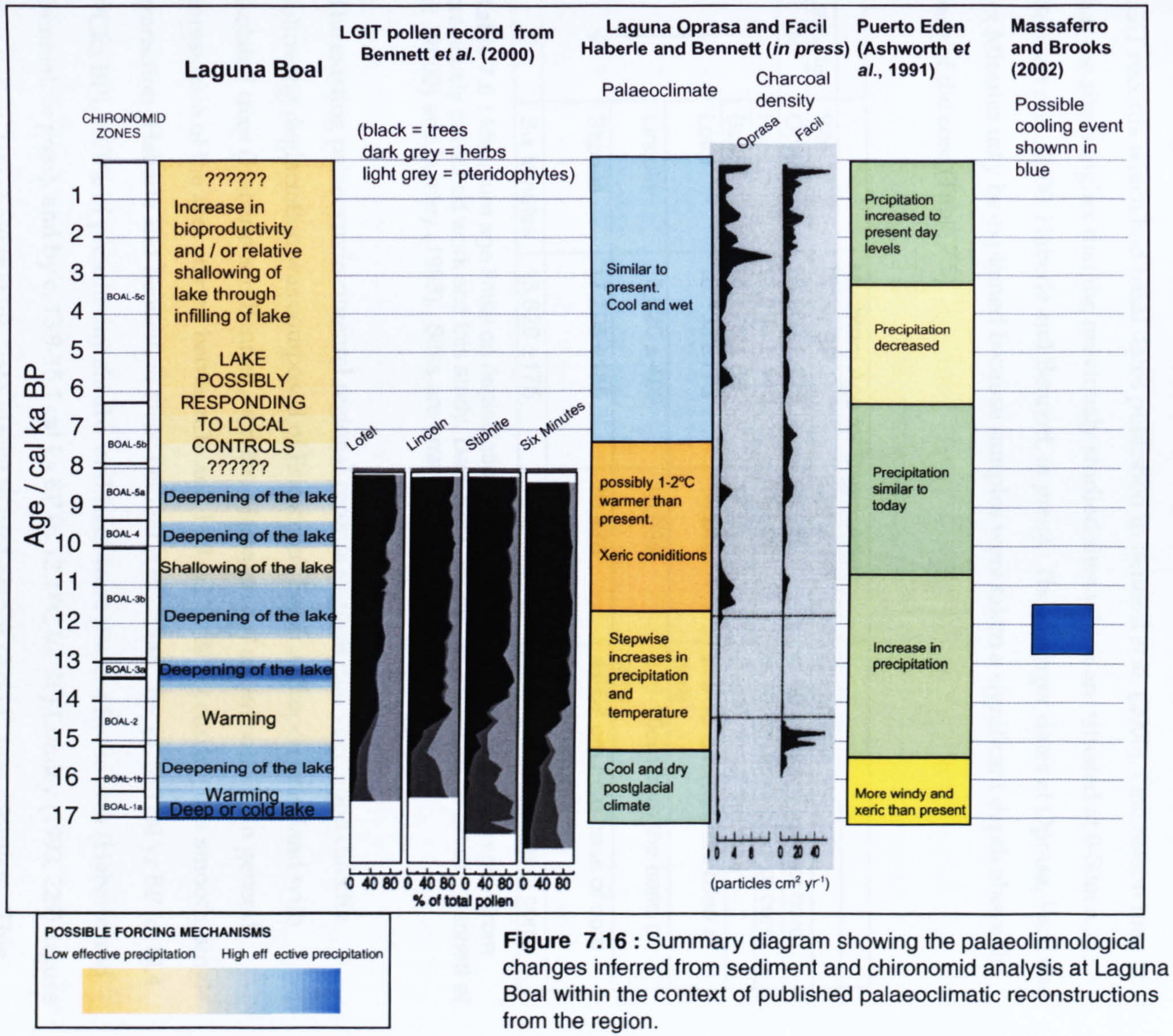

Figure 7.16 : Summary diagram showing the palaeolimnological changes inferred from sediment and chironomid analysis at Laguna Boal within the context of published palaeoclimatic reconstructions from the region.

When compared to other LGIT records from Taitao – Chonos region, the minimum date from Laguna Boal of 17 cal ka BP (14175 ± 86 ^{14}C cal ka BP) fits in well with the regional pattern of deglaciation (Table 7.5). The date is younger than those from three of the four LGIT records which had basal dates published in Bennett *et al.* (2000). One reason may be that the site is higher that the previously studied sites which are situated at 0-50m a.s.l. (Bennett *et al.*, 2000; Haberle and Bennett, *in press*). The younger dates at Oprasa, Facil and Six Minutes may be explained because samples were taken a significant depth above the base of the core (Table 7.5)

		Minimum Age for Deglaciation		
Latitude	Site	^{14}C yr BP	Cal yr BP	Comment
N	Oprasa	13,560 ± 125	16,280	c. 40 cm from base of core
↓	Facil	13,230 ± 140	15,900	c. 15 cm from base of core
	Boal	14,175 ± 86	17,014	Basal cm of the core
	Lofel	16,135 ±175	19,245	c. 5-15 cm from the base of core
	Lincoln	15,920 ± 400	18,999	c. 5-10cm from the base of core
	Stibnite	17,205 ±185	20,478	47-67 cm from base of core
S	Six Minutes	13,820 ±175	16,582	c. 60 cm from base of core

Table 7.5 : Minimum age limits on deglaciation of sites in the Chonos – Taitao region from previously published work and this study. Data from Haberle and Bennett (*in press*), Bennett *et al.* (2000) and Lumley (1993). Sites are arranged from North to South

The existing palaeoenvironmental regional records suggest that vegetation directly following deglaciation was composed of Ericaceous heath and open grassland with isolated trees (Haberle and Bennett, *in press*; Massaferro *et al.*, *submitted*). In general, forestation of the area started between 16 and 14.9 cal ka BP, occurring in a smooth, single transition (Haberle and Bennett, *in press*; Bennett *et al.*, 2000). By 14, 560 cal yr BP (c. 12.4 ^{14}Cka BP), c. 70% of present day shrubs and trees were present in the area (Haberle and Bennett, *in press*), and by c. 13.9-15.1 cal ka BP (c. 12.1^{14}C ka BP) Lumley (1993, 229) argues that pollen data show that the "late-glacial to post-glacial period" was complete. This regional pattern fits well with the possible warming between 16.5-16 cal ka BP indicated by the midge record and the subsequent warming inferred from the sudden increase in productivity indicated by the increase in LOI and percentage abundance of *Parapsectrocladius*, which occurred at c. 15.1 cal ka BP.

Deviations from this overall LGIT vegetational shift from heath to *Nothofagus-Pilgerodendron-Podocarpus* forest are thought to be minor (Bennett *et al.*, 2000; Haberele and Bennett, *in press*; Lumley, 1993). Additionally these changes are not correlated with ages corresponding to the Younger Dryas, GS-1 or the ACR (Figure 2.17). Both pollen and coleopteran evidence from the Chilean Channels also fail to indicate any notable LGIT climatic deteriorations (Ashworth *et al.*, 1991). Thus, these records have been argued to show no evidence of LGIT sub-Milankovitch change (Bennett *et al.*, 2000; Haberle and Bennett, *in press*; Ashworth *et al.*, 1991; Ashworth and Markgraf, 1989). In contrast to pollen and beetle evidence, chironomid records from the Taitao region have indicated LGIT environments to be more fluctuating. The presence of Podonominae between 12.8-11.6 cal ka BP, coeval with the Younger Dryas Chronozone, at Laguna Stibnite is inferred to indicate a climatic cooling (Massaferro and Brooks, 2002). It is possible that the cooling at Stibnite is related to the two stage cooling indicated by midge and sedimentary data at Boal between 13.3-12.9 cal ka BP and 12.3-11.1 cal ka BP. Ascertaining the synchrony of these two events is particularly problematic due to the presence of a ^{14}C plateau, highlighted by the large calibrated age ranges associated with SUERC-1758, relative to the standard deviations associated with the actual ^{14}C error (±59 ^{14}C years). It might be argued that the lack of evidence for this deterioration in local pollen records may be due to an insensitivity of pollen as a proxy for such subtle climatic change in this region. This may be accentuated by varying pollen production rates: *Nothofagus dombeyi* type, *Tepulia* and *Podocarpus* are all recognised to be over-represented in pollen spectra, whilst taxa such as *Maytenus* and *Desfontainia* are under-represented (Haberle and Bennett, 2001). Alternatively the periods of increased water depths and reduced bioproductivity at Boal may be related to the "step-wise" manner in which Haberle and Bennett (*in press*) indicate that the overall LGIT warming may have occurred.

Although pollen and beetle records show no evidence for temperature fluctuations during the LGIT, they all indicate that there were shifts in palaeoprecipitation patterns during this period (Figure 7.16). Massaferro *et al.* (*submitted*) suggest that a rapid increase in *Pilgerodendron*, a tree which favours damp soils, coincident with a decrease in charcoal concentration at *c.* 14.9 cal ka BP is indicative of an increase in precipitation in the area. The record from the Puerto Eden in the Chilean Channels also indicates an increase in

effective precipitation driven from *c.* 15.5 cal ka BP (Ashworth *et al.*, 1991). In contrast, the midge record from Laguna Boal does not strongly indicate a mesic LGIT climate. However, the trend towards general domination of the assemblage by *Parapsectrocladius* in the early LGIT is proposed to be temperature, as opposed to a precipitation driven. Thus it may be that a decrease in *Parapsectrocladius* in response to increasing precipitation was compensated for by an increase in bioproductivity which allowed the taxon to dominate, even though water depths were not at an optimum for the taxa. Nonetheless, the extent to which the midge assemblage corroborates the inference of mesic conditions is debatable.

From 10,600-10,000 cal yr BP, Haberle and Bennett (*in press*) and Massaferro *et al.* (*submitted*), suggest that pollen data and an increase in the concentration of charcoal indicate that a warmer climate prevailed. Although the presence of charcoal must be interpreted with caution due to possible occupation of the area by humans by this time, a drier climate could have allowed or enhanced burning by anthropogenic or environmental mechanisms. Such events may coincide with the sole charcoal horizon visible in the Boal core at 327 cm which is thought to have taken place *c.* 10.0 cal ka BP. The midge data, however, from Laguna Boal do not indicate a change to more xeric conditions. At this point the inferences from changes in the midge assemblage suggest that there was either a lake level increase or a decrease in site bio-productivity.

A change from a dry early Holocene to a wet latter half is seen in several pollen cores. By c. 7.2 cal and 6.8 cal ka BP the climate is inferred to have become cooler at Oprasa and Facil, respectively. The polar front, and thus the Westerlies, are inferred to be in a similar position to that of today (Haberle and Bennett, *in press*), indicated by an increase of hydrophilic *Pilgerodendron*, which persists till the end of the Holocene at Facil (Massaferro *et al, submitted*). A similar change from dry, early Holocene conditions to a wet latter half is also seen at sites on the Taitao peninsula, although to a lesser extent, potentially because Taitao lay closer to the centre of the Westerlies course, and was thus less sensitive to a latitudinal movement during the Holocene (Lumley and Switsur, 1993). This change in precipitation is further supported by changes in the chironomid assemblage record at Laguna Stibnite during the Holocene which are interpreted to infer changes in precipitation (Massaferro and Brooks, 2002).

Integration of the data from Laguna Boal into this Holocene regional synthesis is problematic as data from the upper part of the core appears somewhat equivocal in terms

of climatic reconstruction (7.5.1.2). The possibility of an increase in bioproductivity caused by increasing temperatures in the early Holocene does not seem to be supported by pollen data. It could be that possible nutrient enrichment at Boal is paralleled by the increase in lake productivity, indicated by higher biogenic silica content, in the Stibnite and Six Minute records from Taitao (Lumley, 1993). At these sites, this increase in productivity was often correlated with a decrease in LOI indicating increased catchment erosion. However, the Boal LOI record does not indicate increased erosion of minerogenic material in the catchment during the Holocene, as is seen at Stibnite and Six Minutes. Thus, it may be sensible to suggest that the record at Boal during the mid and late Holocene is not representing a response to climatic trends. Unfortunately, as pollen analysis has not been conducted on this core, the benefits of direct comparisons between vegetational and chironomid changes afforded at Facil and Stibnite, are not possible. In terms of catchment specific changes that could account for the changes seen at Boal, it may be that nutrient enrichment of the system occurred, favouring the presence of *Parapsectrocladius* occurred during the Holocene. Ascertaining exactly what could be determining such a change in catchment productivity at such a local scale is not possible from the data produced in this study. However, it seems fair to suggest that during this period, the midge fauna from Boal may not be responding directly to climatic forcing mechanisms.

7.7 Conclusions

When placed in a regional palaeoclimatic context, the preceding combination of chironomid, sedimentary and geochronological data from Laguna Boal can be interpreted to draw the following conclusions:

- When compared to modern sites investigated in Chapter 5, some of the midge assemblages present in Laguna Boal have suitable analogues, however some do not. The problem of no analogue assemblage is most acute in samples from c. 17-15.3 & 13.5-13.1 cal ka BP;
- A minimum date for deglaciation of 14175 ± 86 (17531- 16497 cal years, using 2 s.d.) fits well within the context of previously published minimum dates from the region;

- A climatic warming dated at 15.3 cal ka BP is inferred from the rapid increase in *Parapsectrocladius* concomitant with a drop in *Parakiefferiella* and Podonominae. This is broadly coeval with regional warming indicated by arboreal colonisation of the area;
- Contrary to pollen data from the area, the chironomid record at Boal suggests the LGIT was environmentally unstable. Two notable increases in *Parakiefferiella* and decreases in LOI suggest that two events, possibly caused by increases in precipitation or decreases in temperature, punctuated the LGIT. The latter of these appears to slightly pre-date cooling inferred from midge data from Laguna Stibnite (Massaferro and Brooks, 2002) proposed to be coeval with the Younger Dryas chronozone;
- Comparisons of the Holocene reconstruction with other studies indicates that changes in the midge fauna during the Holocene are likely to have been caused by catchment specific environmental changes. Establishing a mechanism which would explain the switch from regional scale to more local, catchment based influences is problematic;
- A previously undocumented volcanic eruption is dated to have occurred 4768 ± 33 ^{14}C ka BP (5591-5331 cal yr BP). This eruption produced the deposition of a basaltic andesitic, cream-coloured tephra;

8 DISCUSSION

8.1 Introduction

This study has investigated the use of chironomids as a proxy for Late Quaternary climate change in Patagonia, by specifically addressing the following research questions:

- What is the current taxonomic distribution of Chironomidae taxa in Patagonia and which environmental variables control these distributions?
- How suitable are chironomids as a proxy for quantification of palaeoclimatic, in particular palaeotemperature, change in Patagonia?
- How have chironomid faunal assemblages changed at specific Patagonian sites since the end of the LGM?
- What inferences can be made about Patagonian climate change from the results of chironomid analysis and other complementary analyses of these sequences?
- How do these environmental reconstructions fit into the present research context and contribute to our understanding of late Quaternary climate change?

Past results of similar investigations in other regions, such as Brooks and Birks (2001) and Walker *et al.*(1997), indicated that the study might allow quantified temperature reconstructions to be produced at the two Patagonian sites investigated. The results presented in Chapter 5 indicated that the chironomid fauna encountered did not display a strong enough relationship to temperature, or any of the other environmental variables, to warrant the production of a transfer function and, thus, quantitative reconstructions. Nonetheless it has been possible to reach qualitative-based conclusions from down-core analysis as is commonly done in other palaeoecological studies (eg Massaferro and Brooks, 2002). The wider implication of these findings form the basis for this chapter.

8.2 Modern Day Patagonian Chironomidae Fauna

The collection of quantitative, modern ecological and distributional data of the current chironomid fauna of Patagonia is new. Analysis of these data has provided information on modern ecological relationships as well as assessing the suitability of the organisms for environmental reconstructions, both qualitative and quantitative. The results of these investigations have highlighted a number of points worthy of discussion.

8.2.1 Taxonomic Issues

This study has produced interesting findings with respect to the taxonomic identification of both modern and sub-fossil, down-core head capsule specimens. With regard to Tanypodinae, the fact that the cephalic setation arrangement could not be used as a characteristic to distinguish between members of the Procladiini and Macropelopiini tribes is a significant conclusion. Within the scope of this study, this reduced precision in taxonomic identification may have hindered the extent to which relationships between taxa and environmental variables could be determined. As is demonstrated with data from Regenmoos, Switzerland, biostratigraphic information is lost when taxa are not distinguished to below sub-family level (Rieradevall and Brooks, 2001). Thus the ability to separate members of these tribes to genus level in this study would have proved advantageous.

This finding provides direction for further research. The results of this study have indicated that cephalic setation of Patagonia fauna may be different from that of equivalent taxa from the Holarctic, as keyed out by Rieradevall and Brooks (2001). Furthermore, the lack of consistency in setal arrangement encountered in Patagonian specimens possibly indicates that this attribute may not be suitable as a trait for classification in the Neotropics. Alternatively, it may be that consistent patterns are present but that they have not been recognised within the scope of this study. Further work to build up a good collection of specimens from which to establish such patterns may resolve this issue and permit future classification. Ultimately, a similar process to that achieved by Rieradevall and Brooks (2001) is desirable, with analysis of reared taxa affording direct reference to the imago stage to produce a robust key.

More taxonomic work using reared specimens would also allow some morphotypes, as identified using larval sub-fossil head capsules specimens, to be taxonomically identified to a lower taxonomic level. This is particularly the case for Tanytarsini, where such an approach would facilitate taxonomic identification to genus level of the morphotypes encountered in Patagonian chironomid studies. Additionally, there is scope to build on the discovery of previously unpublished morphotaxons, such as Orthcladiinae A, B and C, which were only rarely encountered in this study. Further taxonomic research of these rarer taxa in their larval stage would increase the potential to advance taxonomic, ecological and distributional information from our current understanding of imago midge

habitats and biogoegraphies. This knowledge could then be applied to down-core records which might aid palaeoenvironmental reconstructions.

8.2.2 Evidence of Vicariance Biogeographies

The discovery of head capsules that can be identified as Orthoclade and SO4, both taxa which have only been identified within S. America by Cranston (1997), further corroborates biogeographical links as the result of vicariance biogeography mechanisms. Although *Gymnometriocnemus* has been recorded in the Holarctic (Cranston *et al*, 1983), the Holarctic larval mentum morphology illustrated in this key is entirely different to that encountered in Patagonian samples. Conversely, strong similarities exist between the *Gymnometriocnemus* mentum morphology of Australian specimens illustrated in Cranston (1997) and what appear to be Patagonian specimens of this taxon, found within this study. Such links to specimens found in Australian keys, yet not in those from the Holarctic, support the assertion that current Chironomidae distributions are the result of vicariance as well as dispersal mechanisms.

This finding is in line with the conclusions of Brundin (1966) based on his study of several chironomid genera (Chapter 3). The existence of general biogeographical tracks through which taxa, across a wide range of organisms, could be linked across biogeographic barriers, was published by Croizat (1958, cited in Cranston and Naumann, 1991, 187) (Figure 8.1). Indeed, these links are so strong that some authors have argued the case for the splitting of the Neotropics into two biogeographic regions, the southern temperate area and northern tropical region, due to the hybrid nature of the origin of the continent's biota (Humphries and Parenti, 1989; Crisci *et al.*, 1991). The concept is an important one as it refutes the claim that dispersal is preponderantly responsible for creating the distributions evident today, an idea central to Darwin's theories (Briggs, 1987).

More recent work investigating vicariance with specific examination of Orthocladiinae studies in the Southern Hemisphere has been undertaken by Cranston (1999, 2000). Cranston (1995a, 1999) suggested that biogeographic links between Australasian and Patagonian taxa are most common within cool stenothermic taxa, such as Aphroteninae, Podonominae, Diamesinae and Orthocladiinae. Such a relationship is not explicitly supported by the findings of this study. However, regional level endemism and the occurrence of geographically disjunct populations may be present to a lesser extent than

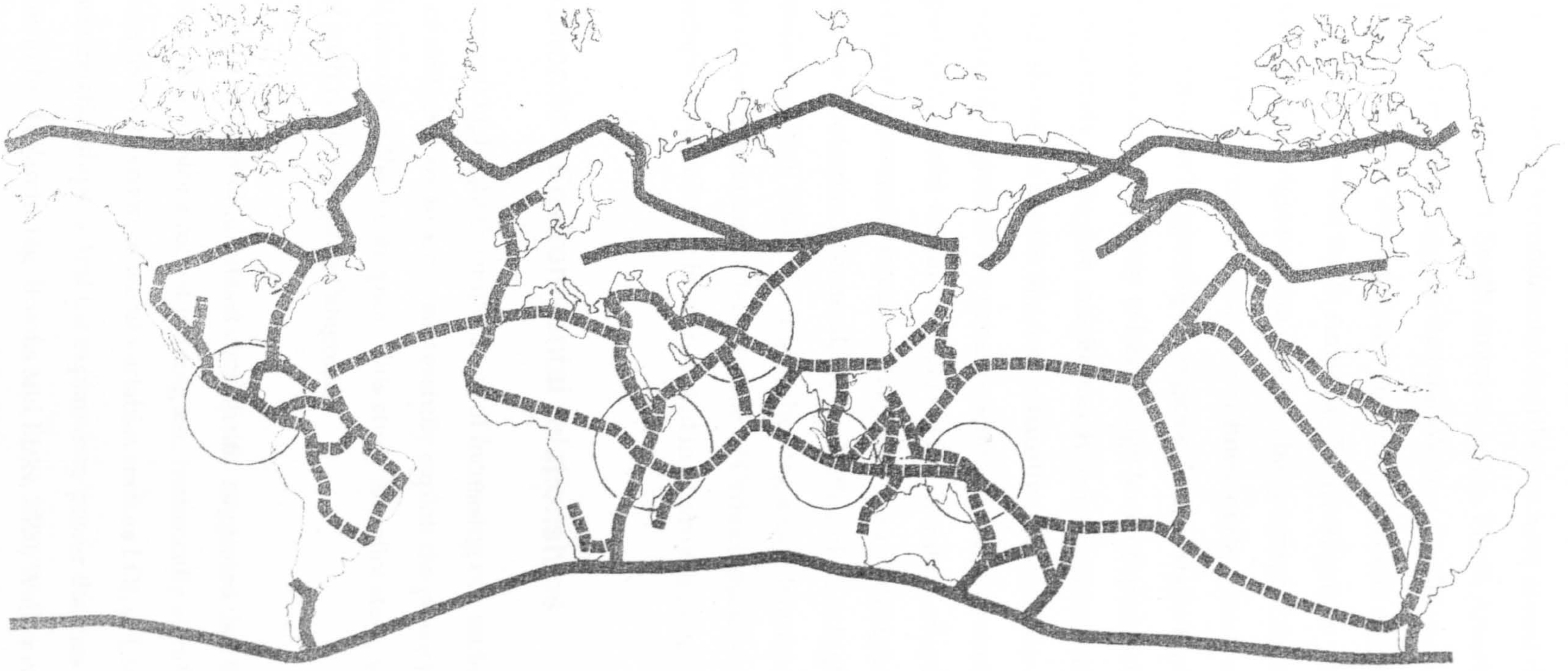

Figure 8.1: Summary of generalised biogeographical tracks of the world (after Croizat, 1958). Solid tracks are boreal and austral (Cranston, 1991, 187).

often proposed, due to inexhaustive sampling and taxonomic issues (Cranston and Oliver, 1987; Saether, 2000).

Over time, changes in relative continental distribution have meant that organisms have been able to exchange between South America, Africa, North America and Antarctica (Briggs, 1987). Saether (2000) suggests that the Western Cordilleras have served as a route for a track allowing the migration of some primarily Holarctic chironomid taxa, including *Limnophyes*, down into western South America. To investigate to what extent the Patagonian fauna might originate from different biogeographic regions, a small-scale survey was undertaken to assess the species richness of the genera encountered in Patagonia relative to other biogeographic regions. Theory states that in general, evolutionary centres are more likely to have a high level of species diversity (Briggs, 1987). Therefore, such a study might give insight into the origin of taxa within the Patagonian fauna. Table 8.1 shows the results of a non-exhaustive search of the species richness in several biogeographic regions of the genera encountered in this study and others recorded by Martin Spies (*pers. comm*) within Patagonia. High numbers of species of *Parochlus* and Podonominae have been encountered in Patagonia. Taxa with high diversity in both Patagonia, and the Neotropics in general, are typically linked to high diversity in regions such as Australia and New Zealand – thus indicating a Gondwanan ancestry. Improvement of better taxonomic identification of Orthocladiinae A, B & C would allow such relationships to be looked at in more detail in future research.

8.2.3 Taxonomic – Environmental relationships

Velle *et al.*, (*in press*) highlight the importance of increasing our understanding of modern day ecology of midges if we to are to successfully exploit the proxy in palaeoecology. Such a lack of data is acute in the Neotropics. This study is a pilot study in assessing the extent and nature of such relationships in Patagonia.

Statistical analysis of the midge dataset consistently suggested that there was insufficient data upon which to produce a robust training set. Statistically significant relationships were demonstrated with environmental variables such as LOI, pH, lake depth and altitude. However, these relationships lacked the explanatory power that has been demonstrated in similar studies in the Holarctic (eg. Brooks and Birks, 2000; Walker *et al*,. 1997). This could

Subfamily	Genus	Recorded by / Collated by	No of Species	Encountered in this sudy	Neotropics	Asia	Palaearctic	Nearctic	Africa	New Zealand	Australia
Aphtotenıinae	Paraphrotenia	MS	2								
Chilenomyiinae	Chirlenomyia	MS	1								
Chironomiae	Camposimyia	MS	1		-	-	-	-	-	-	-
	Chironomus	MS	2	x	12	x	x	11, 13	16	6, 1	10
	Crytopchironomus	*SJLG*		x	x	x	30		6	x	x
	Cryptotendipes	*SJLG*		x	-	-	4	3, 5	-	-	-
	Dicrotendipes	MS	3	x	10	x	30		9	x	12
	Megacentron	MS	1		-	-	-	-	-	-	-
	Microtendipes	*SJLG*	2*	x	-	-	17		<13, 6	1	3
	Lauterborniella (Zavriella)	*SJLG*	-	x	1 of L (9 of Z)	-	1		-	-	3
	Nimbocera (Tanytarsini)	MS	1		1	-	-	y	-	-	-
	Parachironomus	MS	2	x	12	x	>30		5	1	5
	Paratanytarsus	MS	1	x	-	-	20	x	-	1	5
	Phaenopsectra	MS	2	x	-	-	3	9?	-	-	-
	Polypedilum	MS	1								
		KH & SJB	2	x	51	x	>100		36	12	18
	Pseudochironomus	SJLG	-	x	>5	-	1-2	11		-	10
	Rheotanytarsus	MS	2		1	x	14		8	x	7
	Riethia	MS	1							1	
	Tanytarsus	MS	6	x	9	x	>85		8	5	10
	Stenochironomus	MS	1	x	14	-	c.7	c.11	7	-	1
Diamesinae	Heptagya	MS	1				-	-			
	Limaya	MS	1				-	-			
	Mapucheptagyia	MS	1				-	-			
	Parapheptagyia	MS	4				-	-			at least 2
	Reissia	MS	3				-	-			
Orthocaldiinae	Austrocladius	MS	1				-	-			
	Botryocladius	PSC & DDE	2				-	-			
	Bryophaenocladius	MS	2		1		x		3		x
	Clunio (marine larvae)	MS	2		1	-	18	-	1	1?	x
	Corynoneura	MS	1	x?	x	x	x	x	3	2?	x
		MS	?								
	Cricotopus	KH & SJB	4*	x?			c.60	>20	12	6	11
	Edwardsidia	MS	1								-
	Eukieffenella	KH & SJB	1	x?			25		1	3/ 4?	1
	Gymnometrocnemus	*SJLG*		x	-	-	-	-		1	2
	Limnophyes	MS	3	x?	x	x	x	x	2	1	at least 1
	Nanocladius	*SJLG*	-	x	2				4		
	Paratrissocladius	MS	1				4	x	x		
	Parakiefferiella	*SJLG*	-	x	1	x	9	c. 9	x	-	-
	Parakiefferiella fennica type	*SJLG*	-	x							-
	Paralimnophyes	*SJLG*	-	x?	-	-	2	-	-	-	2
	Physoneura	MS	1		-	-	-	-	-	-	-
	Pseudosmittia	MS	1	x	-	-	least	-	-	-	at least 1
		KH & SJB	2*		-	-	-	-	-	-	-
	Rhinocladius	MS	2		-	-	-	-	-	-	-
	Smittia	MS	1	x	x	x	x	x	3	1	at least 1
	Stictocladius	MS	2	x	-	-	-	-	-	2	-
	SO4 appears similar to Stitocladius (Cranson, 1997)										
	Symbiocladius	MS	2		-	-	2		-	-	-
	Parapsectrocladius	PSC			-	-	-	-	-	-	-
	Orthocladius	*SJLG*		*x?*	*x*	*x*	*>100*		*3*	*2*	*x*
	Thienimaniella	*SJLG*		*x?*					3		
	Tventia								1		
Podonominae	Parochlus	MS	21	x	30	-	-	1	-	#####	4
	Podochlus	MS	15								
	Podonomopsis	MS	3							4	
	Podonomus	MS	23							4	
	Rheochlus	MS	1								
Prodiamesinae	Monodiamesa	MS	1								
Tanypodinae	Ablabesmyia	MS	2	x	-	-	4	13	5	1	> 2
	Coelotanypus	MS			>20	-	-	5	1	-	1
	Clinotanypus	*SJLG*	-	x	1/2	20-27	1	-	4, 1	-	1
	Djalmabatista				6						
	Pentaneura	MS	2		2	-	-	2	-	-	>6 genus
	Psectrotanypus	KH & SJB	1		-	-	1	2	-	-	-
	Procladius	SJLG	x						6		5
	Labrundinia	*SJLG*	-	x	numerous	-	1	6	-	-	-
		KH & SJB	1								
	Macropelopia			?					1	4	
	Tanypus	MS	1		4	-	4	11	1	2	-
Telmatogetoninae	Halirytus	MS	1		-	-	-	-		-	-
	Telmatogeton (marine larvae)	MS	2		3	x	5		2	2	2

Table 8:1 : Summary of the number of chironomid species found within different genera in this and other Patagonian studies

The second column indicates how many taxa were recorded by Spies, M (pers comm.) Crantson (2000), Cranston and Edwards (1999) Brooks and Jackson (2002). If the taxa was not recorded in these studies but was encountered in this study, SJLG is entered. Throughout the whole table "?" means possibly encountered and "x" means that the genus was encountered but number of species was not determined.

Information was gained from Wiederlholm (1983), Cranston (2001), Makarchenko et al., (2000) Boothroyd and Forsyth (no date stated) and Mendes (date not stated).

either be due to the use of poor quality environmental variable measurements or, alternatively, a eurytopic nature of the Patagonian fauna or a combination of the two.

8.2.3.1 Inter-regional differences in ecological niches

It is interesting that environmental optima, produced during constrained ordinations, agreed with those gained in Holarctic studies to different degrees. Whereas taxa such as *Dicrotendipes* and *Pseudochironomus* were assigned environmental optima which compared well with those proposed from Northern Hemisphere studies, others did not. An acute example of this latter scenario is the *Paralimnophyes/Limnophyes*. In this study, deep lakes with low LOI appeared to be favoured by the taxon, whereas in Holarctic studies such as Cranston *et al.*, (1983), Kansanen (1985) and Hoffman (1998) argued that the taxa is common in more littoral environments.

Several hypotheses can be proposed to explain such discrepancies. The first is that environmental optima of these taxa in Patagonia actually deviate markedly from European and Northern American optima. The second is that the optima calculated in this study are inaccurate. Data that may support the latter hypothesis are the strong inverse relationship between *Limnophyes* and *Pilgerodendron* at Laguna Stibnite (Massaferro and Brooks, 2004). If the midge fauna in this record was responding to palaeoprecipitation changes and the changes in arboreal pollen are taken to represent fluctuations in precipitation, then the European data indicating that *Limnophyes* is common in shallow conditions corroborates this pollen data. Additionally, it could be argued that although a statistically significant relationship has been demonstrated to exist between depth and the Patagonian midge fauna in this thesis, it is not as strong as faunal – depth relationships that have been found in other studies which have indicated *Limnophyes* to be a littoral taxa (Kansanen, 1985; Hoffman, 1998). Alternatively it may be that in the lakes where *Paralimnophyes/Limnophyes* dominate the assemblage, there are negligible amounts of profundal taxa able to exist due to anoxic conditions, resulting in high relative abundances of littoral taxa such as *Limnophyes* within the sediments. This would mean that the midge remains of a mainly littoral assemblage would be preserved, even in a deep lake. Further studies of modern midge ecology in Patagonia may further clarify and potentially resolve this issue.

8.2.3.2 Poor correlation to environmental data

Although there is certainly scope to improve the quality of environmental data used in the species - ecology relationships investigation undertaken in this study, the presence of a more eurytopic Patagonian chironomid fauna still remains both a strong possibility and an interesting hypothesis for future testing. Within this study such proposals can only be based on the data already discussed, which is based mainly on spot measurements. Nonetheless, large ranges in environmental variables associated with individual TWINSPAN groups, as discussed in Chapter 5, indicate that the existence of a more eurytopic midge fauna in Patagonia than that found in N. America and Europe is a real possibility. Rearing of specimens within controlled environments or further collection of modern environmental data would help resolve such an issue.

8.2.3.3 Improving environmental data

A possible explanation for identification of an apparent eurytopic fauna is that the quality of the spot environmental data measured and used in statistical analysis was not sufficiently representative to identify environmental - taxonomic relationships that actually exist. Alternatively, it may be that an insufficient number of environmental variables were measured in this study and that those measured were not the most appropriate. In this study, the variables measured together routinely explained c. 60-70% of the total taxonomic variance. A future study might increase this percentage by measurement of additional variables such as dissolved oxygen. Indeed, strong links discussed in Chapter 3 between midge assemblages and lake trophic state indicates that DO may exert a control on the taxa present (eg. Quinlan *et al.*, 1988). Additionally, more relationships may be discovered by undertaking a more comprehensive water chemistry study. Where the full range of water chemistry measurements had been made within this study, statistically significant relationships were indicated (Chapter 5). Further studies may wish to build on this relationship, both in terms of constraining the nature of the correlation which exists and undertaking further work to try and assess the mechanisms responsible for the relationship. With respect to the quality of the data collected in this study, the representivity of some of the data collected in this study, such as temperature, appears arguable. Environmental variables measurements based on larger temporal sample sizes at each site would be desirable.

8.2.3.4 Modelling of temperature

The lack of response of the midge assemblage to temperature meant that a desirable potential outcome of this study, to produce a chironomid temperature training set for

Patagonia, could not be achieved. Possible reasons for a lack of correlation between temperature and the faunal assemblage have been discussed in 5.6, with two hypotheses being presented. Either the quality of temperature data was insufficiently accurate to allow an existing trend to be detected or there is not a strong taxonomic response to a thermal gradient within Patagonian Chironomidae.

Attempts to reject the first of these hypotheses could be made by collection of more field data. Although possible, this would be a time consuming and financially expensive process, as is discussed in Walker (1989c). A more attractive alternative may be the production of modelled air temperatures for the sites sampled, an approach taken by Lotter *et al.*, (1997) and Brooks and Birks (2000). At the most rudimentary level this could be done using the assumption that continentality, latitude and altitude are the three variables that dictate air temperature. Initial attempts to model these relationships were made; however predicted results differentiated too substantially (>4 °C) from empirical data of average temperatures recorded at major towns to justify inclusion of modelled temperature in ordination analysis and, thus, have not been reported. Alternatively, use of modelling software such as BIOCLIM, used during the production of the MCR model by Dimitriadis and Cranston (2001), is an alternative approach. However, the paucity of modern Patagonian data means that such models will never be able to be tested with the rigour of those from more developed and populated areas, such as Switzerland (Lotter *et al.*, 1997). It should also be considered that errors within such analysis and subsequent modelling tend to be compounded in a factorial as opposed to additive manner. Thus an accurate air temperature model with very low errors would be fundamental to the success of such an approach. Another technique to assess the faunal-temperature relationship may be to investigate it using degree days as a measure as opposed to temperature. Such a technique revealed a statistically significant relationship with taxa in Lotter *et al.*'s (1997) investigation and is advocated in Velle *et al.*, (*in press*). The latter of these papers highlights that the technique may be especially appropriate when there is a notable range in the continentality of the sites as would be the case in Patagonia (Velle *et al.*, *in press*). Thus, to summarise, further investigation of the data presented in this study and future Patagonian midge studies may benefit from employing alternative approaches to assess the impact of temperature on the midge fauna.

8.3 Discussion of down-core records

8.3.1 Chronology

Dating of the two sequences has provided new geochronological data for the region. The basal date from Laguna Boal is particularly useful, as there are no other minimum dates for deglaciation for the Chonos-Taitao area at such an altitude; previous studies in the region had only provided dates from sites at 0 – 50m a.s.l. The dates confirm that deglaciation was underway by c. 16000 cal yr BP, as proposed by Kaplan *et al.* (2004), McCulloch *et al.*, (2000) and Denton *et al.* (1999a). The Laguna Leta site deglaciated later, at c. 13.9 cal ka BP, perhaps as a result of local conditions or delayed melting of the ice in the kettle hole.

One of the notable attractions of undertaking Late-Quaternary research within Patagonia is the potential for harnessing tephrochronology as a relative dating method. It was hoped that tephrochronology would provide tighter chronological constraints on the records in this study than has been the case. Analysis of the tephra deposits has added to the tephrochronological database available to future workers in the area. This is illustrated with the identification and analysis of the macro-tephra in the Laguna Leta core, as there are currently no published EMPA data on the tephra deposits from this previously documented eruption. Together with the relatively high number of associated ^{14}C dates from other Chilean Lake District studies for this eruption, it can now be used as a time-stratigraphic marker. Within the Laguna Boal core, a tephra layer previously undocumented in the literature was encountered and analysed. This basaltic – andesitic macro-tephra was dated to originate from an eruption 4768 ± 33 ^{14}C ka BP (5591-5331 cal yr BP). The production of these data will aid chronological control of future studies within the region.

8.3.2 Palaeoenvironmental records from Laguna Boal and Leta

Statistically significant relationships were present between the taxonomic assemblage and several of the environmental variables conducted. Of these, the correlations with LOI, taken to be a proxy of lake productivity, and lake depth were consistently strong and therefore used in order to produce qualitative reconstructions of Late Quaternary palaeoenvironmental change.

In general there was a good representation of taxa within the modern samples in the down-core record, although some taxa, such as *Smittia* and *Mesosmittia*, were absent from the training set. However, these were present in only minimal abundances within the down-core record. A greater issue was that assemblages quite dissimilar to those encountered within the modern day sites analysed were encountered within the cores. This was more severe in the core from Laguna Boal than Leta, especially directly following deglaciation and between c. 13.3 – 9.4 cal ka BP at the former site. This mismatch may be because (a) current day environmental conditions do not support such an assemblage, or (b) an insufficiently large number of modern sites were visited to include the whole spectrum of modern Patagonian midge assemblages currently existent. Increasing the size and possibly geographical range of the training set may resolve this issue.

The palaeoenvironmental reconstructions from Laguna Leta appear promising within the context of local research. The midge record seems to be recording the general trends of deglaciation to a warm and dry early Holocene before effective precipitation in the area increases from c. 7 cal ka BP up to at least the late Holocene. Links might be made between the fluctuations inferred in the lake level during the LGIT and the inferences of sub-Milankovitch scale change inferred from Chilean and Argentinian Lake District records (Moreno and Leon, *in press*; Moreno, 1997; Moreno *et al.*, 2001; Heusser, 1984; Hajdas *et al.*, 2003). However, such correlations should be viewed with caution since, although a statistically significant relationship was demonstrated to exist between variables such as LOI, lake depth and the taxonomic assemblage, these variables still only explain a relatively small amount of the overall variance. Additionally, inferences regarding lake level depth hinge on the assumption that at any level lower than the present, the lake was a closed system with negligible, if any, drainage through surface or groundwater. Furthermore, the Laguna Leta sedimentary record has fairly low stratigraphic resolution, with the whole LGIT recorded in only 40cm of sediment. However, there are distinct changes in the assemblage indicating some sort of environmental change. Moreover, a good agreement between the timing of such changes and those in these areas (Figure 6.16), adds weight to the argument that the midges are responding to the same forcing mechanisms as the pollen. It also is a further, complimentary line of evidence to suggest that sub-Milankovitch change was experienced in Patagonia.

Results from Laguna Boal are interesting (Figure 7.16). The midge fauna seemed to exhibit a greater sensitivity to changes during the LGIT than previous palynological studies from

the region, detecting high-frequency palaeoenvironmental changes not recorded in the Taitao – Chonos pollen records (Bennett *et al.*, 2000). The midge data from the Boal core argues strongly for LGIT palaeoenvironmental change. These changes are recorded in several proxy records: macrofossil content, sediment geochemistry and the midge assemblage. If one assumes that such changes are climate related, in terms of changes in precipitation or temperature, this offers a new line of evidence to the debate concerning Patagonian, LGIT climate change. The strength of this LGIT instability argument might be bolstered when it is viewed in conjunction with the Laguna Stibnite midge record (Massaferro and Brooks, 2002), which is argued to exhibit evidence of a cooling which happed shortly before the increase in effective precipitation and decrease in productivity indicated in the Boal record (12.3 – 11.1 cal ka BP). Within the restrictions of ^{14}C dating during this period it may be that these events were actually synchronous. In some respects, when modern day relationships are used to infer how climate changed at Boal, the results appear not to correlate well with the existing data in terms of large scale climate trends, especially during the Holocene. This outcome presents an interesting challenge within the scope of palaeoentology, as arguing that the midge record during the LGIT is inferring climate-driven change is problematic when the assemblage during the Holocene appears to be very much decoupled, potentially responding to local, catchment scale changes.

8.3.3 Wider palaeoclimatic implications

One of the major debates that this thesis hoped to contribute towards was the nature of LGIT climate change in Patagonia. The three different hypotheses which currently encapsulate the debate at present, as presented in Chapter 2, are that LGIT climate change in the Southern Hemisphere either (a) led or (b) lagged or (c) was synchronous with Northern Hemisphere LGIT sub-Milankovitch scale change. Assuming that the changes in taxa within the LGIT at both sites are related to climatic forcing or at least environmental changes, it can be proposed that sub-Milankovitch scale climatic changes are recorded in the records during the LGIT. The three "distinctive (warming) steps" discussed in McCulloch *et al.* (2000, 412) are all corroborated by the palaeoclimatic reconstructions at the sites. The first at c. 17,500 – 17,150 cal yr BP is coeval with the initiation of the formation of a limnic system at Laguna Boal whilst the second at 15,650 – 15,350 cal yr BP can be linked to the lake formation at Laguna Leta. The third major warming step c. 11,400 cal yr BP appears to coincide with decreases in effective precipitation or increases in bioproductivity

at both Boal and Leta. This adds weight to the hypothesis that these changes in fauna are in response to climatic changes versus local changes which were purely catchment driven.

Finding broad-scale regionally synchronous changes recorded in both records at a higher temporal scale is more challenging. This may be because such changes did not occur coevally or because incorrect assumptions have been made when chronologies were produced, due, at least in part, to a lack of dating resolution. The latter issue may be particularly relevant with Laguna Boal, where an offset based on the difference between dates from plant-macrofossil and bulk sediment assays was applied to the sedimentation curve. However, the curve based on this method produces interesting results when this record is compared to polar ice cores (Figure 8.2). The longer of the two inferred increases in effective precipitation from 12.3 - 11.1 cal yr BP, which may correlate with the Stibnite cooling (12.8-11.6 cal ka BP), occurs shortly after GS-1. The existence of a shorter climatic deterioration before this event within the Boal core, produces a similar pattern of climatic fluctuations as that shown in the Greenland event stratigraphy, although based on the chronology constructed, it appears to post date GI-1d. This earlier Boal cooling and the LGIT increase in effective precipitation at the site both fall within the ACR window and the time frame for ice advance within the Magellan Straits (advance D) of Clapperton *et al.*, (1995), respectively. Although they both appear significantly shorter in duration than these events, this may be due to the inaccuracies in dating due to ^{14}C plateaus during this period.

When Laguna Leta results are placed in the wider context, it can be seen that the potential cooling event of LET-2 starts and begins slightly before GS-1. However its timing is still more similar to GS-1 than it is to the ACR (Figure 8.2). It is interesting to note that the timing of LET-2 is very similar to that of the Huelmo/Mascardi cooling found in Patagonia which Hajdas *et al.* (2003) propose represents both GS-1 and GI-1b in the GRIP stratigraphy. On these grounds Hajdas *et al.* (2003) support the hypothesis of global synchrony, but arguing that the warming of GI-1a is not reflected in their Patagonian records. It may be that a similar phenomena that is recorded at Laguna Leta.

Overall a major conclusion of this thesis is that it provides strong evidence from two sites that indicates that environmental instability existed during the LGIT, with climate being a probable forcing mechanism. The evidence presented in this thesis is unable to support or reject the three, current, major hypotheses presented in Chapter 2 in terms of the timing of these fluctuations relative to sub-Milankovitch climatic vartaions in the Northern

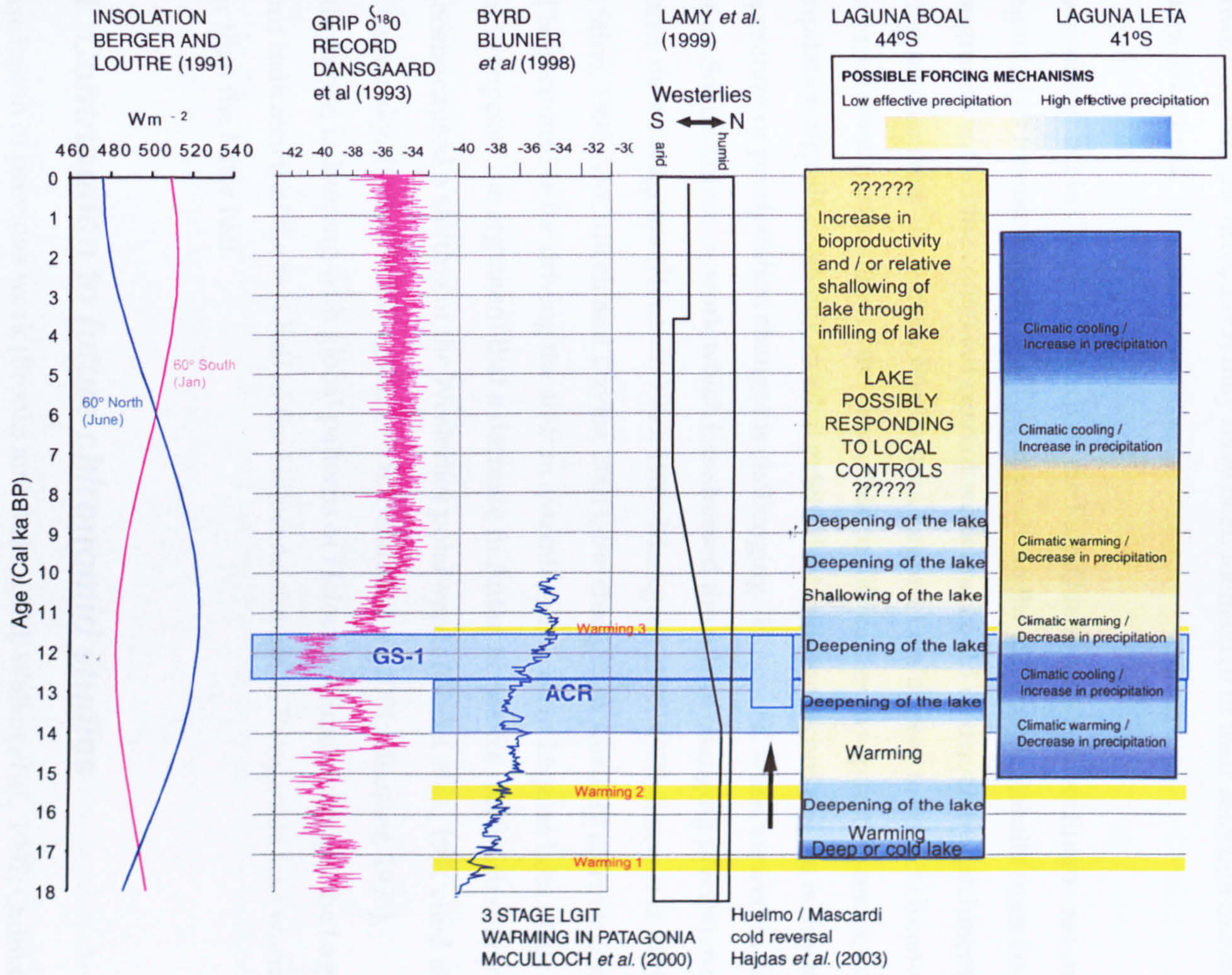

Figure 8.2: Diagram showing suammary of Patagonian palaeoenvironmental reconstructions developed during this study within the context of other regional and global record of Late Quaternary change.

Hemisphere. However, it does appear to support the timing of the three major warming phases indicated by existing geomorphic, palynological and coleopteran research, as summarised in McCulloch *et al.* (2000). Furthermore, it supports the existence of sub-Milankovitch scale climate change within Patagonia during this transition. This latter finding suggests that certain past studies (eg Bennett *et al.*, 2000; Lumley, 1993; Lumley and Switsur, 1993; Haberle and Bennett, 2001, *in press*; Ashworth *et al.*, 1991; Hoganson and Ashworth, 1992; Gilchrist, 1999) may have been ineffective in their selection of sites and/ or proxies examined.

As was discussed in Chapter 2, much of the Late-Quaternary palaeoclimatic research in Patagonia has focussed on the LGIT as opposed to the Holocene. Results from Boal appear incongruous within the context of current work and could be driven by catchment-scale forcing mechanisms. However, results from Laguna Leta appear to reflect climate change as inferred from past studies in the area. Due to difficulties in separating temperature and precipitation signals, assessing to what extent the Holocene record at Leta is due to temperature or precipitation changes is challenging. However, when viewed in the context of other South American work which has stressed the role of changing precipitation regimes over Patagonia (Heusser, 1983, 1989; Markgraf, 1987, 1989; Lamy *et al.*, 1999; Stine and Stine, 1990; McCulloch and Davies, 2001), the changes in westerly storm tracks may well be responsible for driving the shift in assemblages seen in Laguna Leta. This would seem to support the argument that a decrease in Antarctic sea-ice during the early Holocene caused a shifting of the Westerlies polarwards (Garlef *et al.*, 1991 cited in Whatley and Cuminsky, 1999, 237; Villagran, 1990b; Pendall *et al.*, 2001; Heusser, 1995). Furthermore, in keeping with global patterns of Holocene climate change, the Laguna Leta record indicates that the first half of the Holocene climate in Patagaonia was warmer and drier than the latter half.

8.4 Contribution to future chironomid studies

Consultation of previous work (Brooks and Birks, 2000; Walker *et al.*, 1997; Quinlan *et al.*, 1998) prior to embarking on this investigation led to a working hypothesis that a strong environmental - taxonomic relationship would be found during the study of the modern Patagonian fauna. By sampling over such a large latitudinal, and thus temperature, gradient it was hoped that a strong relationship between temperature and taxa could be extracted and harnessed. Conversely, the fact that none of the environmental - taxonomic

relationships were sufficiently robust to allow quantification of records indicates that chironomids may not be as powerful proxy as has been previously advocated (eg Battarbee, 2000). This may be the case if a study is undertaken in a biogeographic region where taxa are more eurytopic than in regions such as the Nearctic and Palaearctic. However, the existence of a more eurytopic Patagonian fauna is, at this stage, purely a hypothesis that has arisen from this study. Further work is required to truly assess the extent to which the Patagonia fauna is or is not more eurytopic than that previously indicated to be the case in Canada and Europe. Nonetheless, it is worth reiterating that significant faunal shifts are recorded in both Boal and Leta records, thus indicating that taxa must exhibit sensitivity to environmental factors of some sort. Improvement of the quality and representivity of the environmental data is paramount in achieving a full understanding of the ecology of the modern fauna.

The study has also highlighted the potential complications that might arise when cores investigated using chironomid analysis contain tephra deposits. Increases in both concentration and relative abundances in *Parapsectrocladius* and *Pseudochironomus* in the Leta and Boal records, respectively, are associated with macro-tephra deposits directly beneath these increases. It has been proposed that a similar effect is seen in the record from Laguna Facil (Massaferro *et al., submitted*), where there is an increase in the relative of abundance of *Parapsectrocladius* above the tephra horizon dated to 11.2 cal ka BP. Significant shifts in midge assemblages above tephra deposits are recorded in several published records (Heirichs *et al.*, 1999; Pellatt *et al.*, 1998, Bianchi *et al.* 1999; Walker and Mathewes, 1989), although the impact on of the tephra on the assemblage is not always invoked as a controlling factor on the assemblage (Pellatt *et al.*, 1998). Care in interpretation is especially important when transfer functions are being used to produce quantitative reconstructions, to ensure that such influences are not overlooked, as this could produce misleading interpretations.

A final contribution that this study may make to future chironomid research is the value that can be added to records by presenting counts in both terms of relative abundance and concentration. Although other proxies such as pollen are often presented using concentration data, this method seems to have been neglected within chironomid studies to date. Presentation of the data in this form allows inferences about the absolute increase and decrease in specific taxa to be made, especially when relative sedimentation rates can be established through a sound chronology. In this study, such an approach proved valuable

several times. A good example was in assessing the manner in which the midge community recovered after the deposition of the macro-tephra in the Laguna Leta record. In this case, analysis of concentration data allowed inferences to be made that changes in the faunal assemblage were driven by changes in absolute abundance in *Parapsectrocladius* as opposed to a shift in the whole assemblage, thus increasing the strength of the link between the increased *Parapsectrocladius* presence and the tephra deposits within the sequence. Furthermore, as it is routine to measure the overall concentration of head capsules per gram to investigate site productivity, individual concentration data could easily be calculated from the existing data.

8.5 Conclusions

This study has added to the small number of chironomid records from Patagonia. Robust quantification of the down-core analysis was not possible due to weak relationships between the environmental variables measured in conjunction with modern analysis of midge ecology. However, these investigations of modern data have provided new and important findings about modern chironomid ecology in Patagonia. In addition, the study has raised important previously unidentified issues associated with taxonomic identification of the Patagonian midge fauna. Thus, the principal findings of the studies can be concluded as the following:

- Further taxonomic research into the Patagonian midge fauna is required to improve the power with which chironomids can be used as a palaeoenvironmental proxy in this region;
- The modern Patagonian chironomid fauna appears to be eurytopic relative to that of the Holarctic. The taxa encountered indicate that vicariance mechanisms have played a notable role in determining the Patagonian midge fauna;
- The proposed eurytopic nature of the fauna means that environmental – taxonomic relationships discovered were insufficiently strong to warrant training set development. However, statistically significant relationships were demonstrated between the fauna and LOI, pH, lake depth and altitude;
- Laguna Boal became deglaciated prior to c. 17.9 cal ka BP, whereas Laguna Leta became ice-free at c. 13.9 cal ka BP. These dates fit well within the proposed local pattern of deglaciation, with Boal becoming ice free during the first of the three

LGIT warming steps proposed by McCulloch *et al.* (2000), and Leta following the second;

- Chironomid analysis of records at these two sites indicated that the LGIT was characterised by high frequency environmental change, whereas climate change during the Holocene appears to be gradual;
- Temporal links can be drawn between the high frequency shifts in lake levels indicated to have occurred during the LGIT and previous studies, both at a local and global level. This evidence indicates that substantial environmental variability during the LGIT was a global phenomenon. This contradicts some of the previous work from the region;
- Whilst the Holocene record from Boal seems to reflect basin specific driven changes, the Laguna Leta record corroborates existing studies indicating a warm, dry early Holocene existed until conditions became more mesic c. 5.5 cal ka BP, probably due to shifts in the position of the Westerlies. This shift in palaeoprecipitation supports the hypothesis that there were notable reorganisations in atmospheric circulation systems during the Holocene.

9 REFERENCES

Aari, T (1981) Climatic and geomorphic influences on lake temperature, Verhandlungen der Internationhlen vereinigung für Limnologie, 21, 130-134,

Abarzúa, A.M., Villagrán, C. and Moreno, P.I. (2004) Deglacial and postglacial climate history in east-central Isal Grande de Chiloé (43°S), Quaternary Research,,62, 49-59

Abbott, M.B., Seltzer, G.O., Kelts,K.R. and Southon, J. (1997) Holocene Palaeohydrology of the tropcial Andes from Lake Levels, Quaternary Research, 47, 70-80

Ahrens, C.D. (1996) Meteorology today: an introducation to weather, climate, and the environment, West Publiching Company, St Paul, Minnesota

Ammann B, Birks HJB, Brooks SJ, Eicher U, von Grafenstein U, Hofmann W, Lemdahl G, Schwander J, Tobolski K, Wick L (2000) Quantification of biotic responses to rapid climatic changes around the Younger Dryas – a synthesis, Palaeogeography, Palaeoclimatology, Palaeoecology, 159 (3-4), 313-347

Anaya, M. (1996) Holocene variations of Ameghino Glacier, south Patagonia, Holocene, 6 (2), 247 - 252

Andersen, B.G., Denton, G.H., Heusser, C.J., Lowell, T.V., Moreno, P.I., Hauser, A., Heusser, L.E., Schlüchter, C., and Marchant, D.R. (1995) Climate, vegetation and glacier fluctuations in Chile, between 40°30'S and 42°30'S Latitude – A short review of preliminary results, Quaternary International, 28, 199-201

Andersen, B.G., Denton, G.H., Lowell, T.V. (1999) Glacial geomorphic maps of Llanquihue drift in the area of the Southern Lake District , Chile, Geographiska Annaler, 81A (2) 155-166

Aniya, M. (1995) Holocene glacial chronology in Patagonia – Tyndall and Upsala Glaciers, Arctic and Alpine Research, 27 (4), 311-322

Ariztegui, D., Bianchi, M. M., Masaferro, J., Lafargue, E. and Niessen. (1997). Interhemispheric synchrony of late-glacial climatic instability as recorded in proglacial Lake Mascardi, Argentina. Journal of Quaternary Science 12(4): 333-338.

Armitage, P. D (1995) Behaviour and ecology of adults, in The Chironomidae: the biology and ecology of non-biting midges. P. Armitage, P. S. Cranston and L. V. Pinder (*eds*). London, Chapman and Hall: 194-224.

Ashworth, A. C., Markgraf, V. and Villigran, C. (1991) Late Quaternary climatic history of the Chilean Channels based on fossil pollen and beetle analyses, with an analysis of the modern vegetation and pollen rain, Journal of Quaternary Science, 6, (4) 279-291

9 REFERENCES

Aari, T (1981) Climatic and geomorphic influences on lake temperature, Verhandlungen der Internationhlen vereinigung für Limnologie, 21, 130-134,

Abarzúa, A.M., Villagrán, C. and Moreno, P.I. (2004) Deglacial and postglacial climate history in east-central Isal Grande de Chiloé (43°S), Quaternary Research,,62, 49-59

Abbott, M.B., Seltzer, G.O., Kelts,K.R. and Southon, J. (1997) Holocene Palaeohydrology of the tropcial Andes from Lake Levels, Quaternary Research, 47, 70-80

Ahrens, C.D. (1996) Meteorology today: an introducation to weather, climate, and the environment, West Publiching Company, St Paul, Minnesota

Ammann B, Birks HJB, Brooks SJ, Eicher U, von Grafenstein U, Hofmann W, Lemdahl G, Schwander J, Tobolski K, Wick L (2000) Quantification of biotic responses to rapid climatic changes around the Younger Dryas – a synthesis, Palaeogeography, Palaeoclimatology, Palaeoecology, 159 (3-4), 313-347

Anaya, M. (1996) Holocene variations of Ameghino Glacier, south Patagonia, Holocene, 6 (2), 247 - 252

Andersen, B.G., Denton, G.H., Heusser, C.J., Lowell, T.V., Moreno, P.I., Hauser, A., Heusser, L.E., Schlüchter, C., and Marchant, D.R. (1995) Climate, vegetation and glacier fluctuations in Chile, between 40°30'S and 42°30'S Latitude – A short review of preliminary results, Quaternary International, 28, 199-201

Andersen, B.G., Denton, G.H., Lowell, T.V. (1999) Glacial geomorphic maps of Llanquihue drift in the area of the Southern Lake District , Chile, Geographiska Annaler, 81A (2) 155-166

Aniya, M. (1995) Holocene glacial chronology in Patagonia – Tyndall and Upsala Glaciers, Arctic and Alpine Research, 27 (4), 311-322

Ariztegui, D., Bianchi, M. M., Masaferro, J., Lafargue, E. and Niessen. (1997). Interhemispheric synchrony of late-glacial climatic instability as recorded in proglacial Lake Mascardi, Argentina. Journal of Quaternary Science 12(4): 333-338.

Armitage, P. D (1995) Behaviour and ecology of adults, in The Chironomidae: the biology and ecology of non-biting midges. P. Armitage, P. S. Cranston and L. V. Pinder (*eds*). London, Chapman and Hall: 194-224.

Ashworth, A. C., Markgraf, V. and Villigran, C. (1991) Late Quaternary climatic history of the Chilean Channels based on fossil pollen and beetle analyses, with an analysis of the modern vegetation and pollen rain, Journal of Quaternary Science, 6, (4) 279-291

Ashworth, A.C. and Markgraf, V (1989) Climate of the Chilean channels between 11,000 to 10,000 yr B.P. based on fossil beetle and pollen analysis, Revista Chilena de Historia Natural, 62, 61-74

Barker, P., Williamson, D., Gasse, F. and Gibert, E. (2003) Climatic and volcanic forcing revealed in a 50,000-year diatom record from Lake Massoko, Tanzania, Quaternary Research, 60 (3), 368-376

Barker, P.A., Street-Perrott, F.A., Leng, M.J., Greenwood, P.B., Swain, D.L., Perrott, R.A., Telford, R.J. and Ficken, K.J., (2001), A 14,000-year oxygen isotope record from diatom silica in two alpine lakes on Mt. Kenya, Science, 292 (5525): 2307-2310

Battarbee, R. W. (2000). Palaeolimnological approaches to climate change, with special regard to the biological record. Quaternary Science Reviews 19, 107-124

Bender, M., Sowers, T. Dickson, M.L., Orchado, J. Grootes, J., Mayewski, P.A., Meese, D.A. (1994) Climate correlations between Greenland and Antarctica during the past 100,000 years, Nature, 372, 663-666

Bengtsson, L. and Enell., (1986) Chemical analysis in Berglund, B.E.., Handbook of Holocene Palaeoecology and Palaeohydrology, John Wiley., Chichester and New York., 423-454

Bennett, K.D. (1996) Determination of the number of zones in a biostratigraphical sequence, New Phytologist, 132 (1), 155-170

Bennett, K.D., Haberle, S.G. and Lumley, S.H. (2000) The last glacial - Holocene transition in southern Chile, Science, 290 (5490) 325-328

Berg, M. B. (1995) Larval food and feeding behaviour.in P. Armitage, P. S. Cranston and L. V. Pinder (*eds*) The Chironomidae: the biology and ecology of non-biting midges.. Chapman and Hall, London, 136-168.

Bianchi, M. M., Massaferro, J., Román Ross, G., del Valle, R., Amos, A. J. and Lami, A. (1999) Late Pleistocene and early Holocene ecological response of Lake el Trébol (Patagonia, Argentina) to environmental changes, Journal of Paleolimnology, 22, 137-148

Bianchi, M. M., Massaferro, J., Román Ross, G., del Valle, R., Tatur, A. and Amos, A. J.(1997) The Pleistocene- Holocene boundary from cores of Lago el Trébol, Patagonia, Argentina : paleolimnological evidence, Verhandlungen der Internationhlen vereinigung für Limnologie, 26, 805-808

Bigler, C., Larocque, I., Peglar, S.M., Birks, H.J.B and Hall , R.I. (2002) Quantitative multiproxy assessment of long-term patterns of Holocene environmental change from a small lake near Abisko, northern Sweden, The Holocene, 12, 4, 481-496

Birks, H and Wright, H.E (2000) Introduction to the reconstruction of the late glacial and early Holocene aquatic ecosystems at Kråkenes Lake, Norway, Journal of Paleolimnology, 23 (1), 1-5

Birks, H. H., Battarbee, R.W. and Birks, H.J.B (2000) The development of the aquatic ecosystem of Kråkenes Lake, western Norway, during the late glacial and early Holocene: a synthesis, Journal of Paleolimnology, 23 (1), 91 -114

Birks, H.J.B. (1986) Numerical zonation, comparison and correlation of Quaternary pollen-stratigraphical data in Chemical analysis in Berglund, B.E. (*ed*), Handbook of Holocene Palaeoecology and Palaeohydrology, John Wiley., Chichester and New York., 743- 774

Birks, H.J.B. (1988) Numerical tools in palaeolimnology – Progress, potentialities and problems, Journal of Paleolimnology, 20, 307-332

Birks, H.J.B. (1994) The importance of pollen and diatom taxonomic precision in quantitative palaeoenvironmental reconstruction, Review of Palaeobotany and Palynology, 83, 107-117

Birks, H.J.B. (1995) Quantitative palaeoenvironmental reconstructions in Maddy, D. and Brew, J.S. (*eds*) Statistical Modelling of Quaternary Science Data, Quaternary Research Association Technical Guide No. 5, Quaternary Research Association, Cambridge, 161-254

Björck, S., Walker, M. J. C., Cwynar, L.C., Johnsen, S., Knudsen, K.L., Lowe, J.J., Wohlfarth, B. (1998). An event stratigraphy for the Last Termination of the North Atlantic region based on the Greenland ice-core record: a proposal by the INTIMATE group. Journal of Quaternary Science, 13(4): 283-292.

Blunier, T., Chappellaz, J., Schwander, J., Dallenbach, A., Stauffer, B., Stocker, T.F., Raynaud, D., Jouzel, J., Clausen, H.B., Hammer, C.U. and Johnsen, S.J. (1998) Asynchrony of Antarctic and Greenland climate change during the last glacial period, Nature, 394, (6995) 739-743

Blunier, T., Schwander, J., Stauffer, B., Stocker, T., Dallenbach. A., Indermuhle, A., Tschumi, J., Chappellaz, J., Raynaud, D., Barnola, J.M. (1997). Timing of the Antarctic Cold Reversal and Atmospheric CO2 increase with respect to the Younger Dryas event, Geophysical Research Letter, 24, 2683-2686.

Bradley, R. S. (1999) Paleoclimatology: reconstructing climates of the Quaternary, San Diego, California: London Harcourt Academic Press, 2nd edition

Bradley, R.S. (2003) Climate Forcing during the Holocene, in Mackay, A., Battarbee, R. Birks, J.J.B., Oldfield, F. (*eds*) Global Change in the Holocene, Arnold, London, 328-341 10-19

Briggs, J.C. (1987) Biogeography and plate tectonics, Elsevier, Amsterdam

Brodersen, K.P. and Anderson, J., (2002) Distribution of chironomids (Diptera) in low arctic West Greenland lakes: trophic conditions, temperature and environmental reconstructions, Freshwater Biology, 47 1137-1157

Brodersen, K.P. and Lindegaard, C. (1999) Classification, assessment and trophic reconstruction of Danish lakes using chironomids, Freshwater Biology, 42 (1) 143-157

Brodersen, K.P., Dall, P.,C. and Lindegaard, C. (1998) The fauna in the upper stony littoral of Danish lakes : macroinvertebrates as trophic indicators, Freshwater Biology, 39 (3) 577-592

Brodin, Y. W. (1982) Paleoecological studies of recent development of the Lake Växjösjön. IV. Interpretation of the eutrophication process through the analysis of subfossil chironomids, Archiv fűr Hydrobiologie, 93, 313-26

Brodin, Y.W. and Gransberg, M (1993) Response of insects, especially Chironomidae (Diptera), and mites to 130 years of acidification in a Scottish lake, Hydrobiologia, 250, 201-212

Broecker, W. S. and Denton, G. H. (1990). The role of ocean-atmosphere reorganisation in glacial cycles. Quaternary Science Review, 9, 305-341.

Broecker, W.S. (1998) Paleocean circulation during the last deglaciation: A bipolar seesaw? Paleoceanography, 13, 2, 119 - 121

Brooks, S. J. (1995) The response of Chironomidae (Diptera) Faunas to Climate Change in Harrington, R. and Stork, N.E. (*ed*) Insects in a changing environment: the 17th symposium of the royal entomological society of London, Academic Press, London

Brooks, S. J. (1997). The response of Chironomidae (Insecta: Diptera) assemblages to late-glacial climatic change in Kråkenes Lake, Western Norway, Quaternary Proceedings, 5, 49-58.

Brooks, S. J. (2000). Late-glacial fossil midge stratigraphies (Insecta: Diptera: Chironomidae) from the Swiss Alps. Palaeogeography, Palaeoclimatology, Palaeoecology, 159, 261-279.

Brooks, S. J. and H. J. B. Birks (2000a). Chironomid-inferred late-glacial and early-Holocene mean July air temperatures for Kråkenes Lake, western Norway, Journal of Paleolimnology, 23, 77-89.

Brooks, S. J., Lowe, J.J. and Mayle, F. E. (1997a) The Late Devensian Lateglacial palaeoenvironment record from Whitrig bog, SE Scotland. 2. Chironomidae (Insecta: Diptera), Boreas, 26, 297-308

Brooks, S. J. Mayle, F. E. and Lowe, J.J. (1997b) Chironomid based Late-glacial climatic reconstruction from southeast Scotland, Journal of Quaternary Science, 12, 161-167

Brooks, S. J and Birks, H. J. B. (2000b) Chironomid-inferred Lateglacial air temperature at Whitrig Bog, south east Scotland, Journal of Quaternary Science, 15, 759-64

Brooks, S.J and Jackson, K.A. (2002) Biodiversity of non-biting midges (Insecta: Diptera: Chironomidae) and other freshwater insects of the Laguna San Rafael National Park, southern Chile, Unpublished report written by members of the Natural History Museum, London for Raleigh International

Brooks, S.J. (2003) Chironomid analysis to interpret and quantify Holocene Climate Change in Mackay, A., Battarbee, R., Birks, J and Oldfield, F. (*eds*) Global change in the Holocene, Arnold, London, 328-341

Brooks, S.J. and Birks, H. J. B. (2001) Chironomid-inferred air temperatures from Lateglacial and Holocene sites in northwest Europe: progress and problems, Quaternary Science Reviews, 20, 1723-41

Brooks, S.J., Bennion, H., and Birks, H.J.B (2001) Tracing lake trophic history with a chironomid-total phosphorous inference model, Freshwater Biology, 46, 413-533

Brundin, L. (1958) The bottom faunistical lake type system and its application to the Southern Hemisphere, Moreover a theory of glacial erosion as a factor of productivity in lakes and oceans, Verhandlungen der internationahlen vereinigung für limnologie. 13, 228-297

Brundin, L., (1966) Transantarctic relationships and their significance, evidenced by chironomid midges, with a monograph of the subfamilies Podonominae and Aphroteniinae and the austral Heptagyiae, Kunglica Svenska Vetenskapsakademiens Handlingar, 11, 1-472

Brundin, L.Z. (1988) Phylogenetic biogeography, in Myers, A. and Giller, P.S. (*eds*) Analytical Biogeography : an integrated approach to the study of animal and plant distributions, Chapman and Hall, London, 343-370

Burbridge, R.E., Mayle, F.E. and Killeen (2004) Fifty-thousand-year vegetation and climate history of Noel Kempff Mercado National Park, Bolivian Amazon, Quaternary Research, 61, 215-230

Caldeniusm C. (1932) Las glaciacones cuarternarias en la Patagonia y Teirra del Fuego, Geografiska Annaler, 14, 1 -64

Carter, C. E. (2001). On the use of instar information in the analysis of subfossil chironomid data, Journal of Paleolimnology, 25, 493 - 501.

Chappellaz, J., Blunier, T., Raynauld, D., Barola, J.M., Schwander, J. and Stauffer, B. (1993) Synchronous changes in atmospheric CH4 and Greenland climate between 40yr and 8kyr BP, Nature, 366, 443-445

Charles, C.D., Lynch-Stieglitz J., Ninnemann, U S. and Fairbanks, R .G. (1996) Climate connections between the hemisphere revealed by deep sea sediment core ice core correlations, Earth and Planetary Science Letters, 142, (1-2),19-27

Chen,F. H., Bloemendal, J., Wang, J.M,, Li, J.J., Oldfield, F. (1997). High-resolution multi-proxy climate records form Chinese loess: evidence for rapid climatic changes over the last 75ka BP. Palaeogeography, Palaeoclimatology, Palaeoecology, 130, 323-335.

Clapperton, C., (1993) Quaternary geology and geomorphology of South America. Amsterdam, Elsevier Science Publishers B.V.

Clapperton, C.M. and Sugden, D. E. (1998) Holocene glacier fluctuations in South America and Antarctica, Quaternary Science Reviews, 7, 185 – 198

Clapperton, C.M., Sugden, D.E., Kaufman, D.S. McCulloch, R.D. (1995) The Last Glaciation in central Magellan-Strait, Southernmost Chile, Quaternary Research, 44(2), 133-148

Coope, G.R.(1977) Fossil coleopteran assemablges as sensitive indicators of climate change during the Devensioan last cold stage, Philosophical Transactions of the Royal Society of London, B., 280, 313-340

Cranston, P.S. and Edward, D.H.D. (1999) Botryocladius gen.n: a new transantarctic genus of orthocladiine midge (Diptera: Chironomidae), Systematic Entomology (24), 305-333

Cranston, P. (1995a) Biogeography in Armitage, P., Cranston, P. S. and Pinder, L. V. (*eds*) The Chironomidae: the biology and ecology of non-biting midges. London, Chapman and Hall, 62-84.

Cranston, P. (1995b). Morphology in Armitage, P., Cranston, P. S. and Pinder, L. V. (*eds*) The Chironomidae: the biology and ecology of non-biting midges. Chapman and Hall, London, 11-30.

Cranston, P. (1995b). Morphology in Armitage, P., Cranston, P. S. and Pinder, L. V. (*eds*) The Chironomidae: the biology and ecology of non-biting midges. Chapman and Hall, London, 11-30.

Cranston, P. (1995c). Systematics, in Armitage, P. S. Cranston and L. V. Pinder (*eds*), The Chironomidae: the biology and ecology of non-biting midges. P. Chapman and Hall, London, 31-61.

Cranston, P. (1997) Identification Guide to the Chironomidae of New South Wales, Australian Water Technologies Pty Ltd, West Ryde, Australia

Cranston, P.S. (1999) Two unusual Chironomini (Diptera: Chironomidae) from Australian rainforest streams: one new genus and a neotropical genus new for the region, Australian Journal of Entomology, 38, 291-299

Cranston, P.S. and Naumann, I.D. (1991) Biogeography in Naumann, I.D. (ed) The insects of Australia: a textbook for students and research workers, Vol. 1., CSIRO, Melbourne Press, 2nd edition, 180-197

Cranston, P.S. and Oliver, D.R. (1987) Problems in Holarctic chironomid biogeography, Entomologica Scandinavica Supplement, 29, 51-56

Cranston, P.S., Oliver, D.R. and Sæther, O.A, (1983) The larvae of Orthocladiinae (Diptera: Chrionomidae) of the Holarcitc region – keys and diagnosis, in Wiederholm, R. (*ed.*) (1983) Chironomidae of the Holarctic Region, Keys and Diagnosis. Part 1: Larvae. Entomologica Scandinavica Suppl., 19. 457 Lund, 149-292

Cranston., P. S., (2000) *Parapsectrocladius*: a new genus of Orthocladiinae Chironomidae (Diptera) from Patagonia, the southern Andes, Insect systematics and evolution, 31(1), 103 – 120

Crisci, J.V., Cigliano, M. M. Morrrone, J.J. Roig-juňent, S. (1991) Historical biogeography of Southern South America, Systematic Zoology, 40 (2), 152-171

Crowley, T.J. (2000) Causes of climatic change over the past 100 years, Science, 289, 270-277

Crowley, P. H. (1992) Resampling methods for computation-intensive data analysis in ecology and evolution, Annual review of ecology and systematics, 23, 405-447

Dahl, S.O. and Nesje, A. (1996)A new approach to calculating Holocene winter precipitation by combining glacier equilibrium-line altitudes and pine-tree limits: A case study from Hardangerjokulen, central southern Norway, Holocene, 6 (4), 381-398

Dansgaard, W. Johnsen, S.J. Clausen, H,B. Dahl-Jensen, D. Gundestrup, N. Hammer, C.U., Hvidberg, C.S., Steffensen, J.P., Sveinbjornsdottir, A.E.>, Jouzel., J. and Bond, G. (1993) Evidence for general instability of past climate from a 250-kyr ice-core record, Nature, 364, 218-220

Davies, I.J. (1975) Selective feeding in some arctic Chironomidae, Verhandlungen der Internationhlen vereinigung für Limnologie, 19, 3149-3154

Davies. S.J., Metcalfe, S.E., Caballero, M.E. and Juggins, S. (2002) Developing diatom-based transfer functions for Central Mexican lakes, Hydrobiologia, 467, 199-213

Davis, M.B, Moeller, R.E. and Fod, J. (1984) Sedimnet focusing and pollen influx Haworth, Y.E. and Lund, J.W.G (eds) Lake seiments and environemtnal history, Leicester University Press, Leicester, UK., 261 - 294

Dearing, J. (1986) Core correlation ad total sediment influx, in Berglund, B.E. (*ed*), Handbook of Holocene Palaeoecology and Palaeohydrology., John Wiley., Chichester and New York., 247-270

Dearing, J. (1999) Magnetic susceptibility, in Walden, J., Oldfield, F. and Smith, J. (*eds*) Environmental magnetism: a practical guide. Technical Guide, No. 6, Quaternary Research Association, London

deMenocal, P., Ortiz, J., Guilderson, T., Adkins, J., Sarnthein, M., Baker, L. and Yarusinsky. M. (2000)Abrupt onset and termination of the African Humid Period: rapid climate responses to gradual insolation forcing, Quaternary Science Reviews, 19 (1-5), 347-361

Denton, G. H. and C. H. Hendy (1994) Younger Dryas age advance of Franz Josef Glacier in the Southern Alps of New Zealand, Science, 264, 1434-1436.

Denton, G. H., Heusser, C.J., Lowell, T. V., Moreno, P. I., Andersen, B.G., Heusser, L. E., Schluchter, C., Marchant, D. R. (1999a) Interhemispheric linkage of palaeoclimate during the last glaciation. Geographiska Annaler, 81 A (2), 107-153.

Denton, G. H., Lowell, T. V., Heusser, C. J., Schluchter, C., Andersen, B.G., Heusser, L. E., Moreno, P. I., Marchant, D. R. (1999b). Geomorphology, stratigraphy, and radiocarbon chronology of the Llanquihue drift in the area of the Southern Lake District, Seno Reloncaví, and Isla Grande de Chiloé, Chile. Geographiska Annaler, 81 A (2), 167-229.

Denton, G.H. (1999) Glacial and vegetational history of the southern Lake District of Chile – Preface, Geographiska Annaler , 81A (2), 105-106

Denton, G.H., Lowell, T.V., Heusser, C.J., Moreno, P.J, Bjørh, G.A., Heusser, L.E., Shclüchter, C. and Marchant, D.R. (2000) Abrupt vegetation and climate changes during the last glacial maximum and last termination in the Interhemispheric linkage of palaeoclimate during the last glaciation, Geographiska Annaler, 81A (2), 107-153

Dimitriadis, S. and Cranston, P. S. (2001) An Australian Holocene climate reconstruction using Chironomidae from a tropical volcanic maar lake, Palaeogeography, Palaeoclimatology, Palaeoecology, 176, 109-131

Dodds, W.K. (2002) Freshwater Ecology: Concepts and Environmental Applications, Academic Press, San Diego

Doner, L. (2003) Late-Holocene paleoenvironments of northwest Iceland from lake sediments, Palaeogeography, Palaeoclimatology, Palaeoecology, 193, 2003, 535 - 560

Dugmore, A.J. and Newton, A.J (1995) 7 Isochrones in Scotland, Holocene, 5(3), 257 - 266

Dugmore, A.J. and Newton, A.J. (1992) Thin tephra layers in peat revealed by X-raydiology, Journal of Archaeological Science, 19, 163-170

Edwards, K.J. and Whittington, G (2001) Lake sediments, erosion and landscape change during the Holocene in Britain and Ireland, Catena, 42, 143-173

Einarsson, T. (1986) Tephrochronology in Berglund, B.E. (*ed*)., Handbook of Holocene Palaeoecology and Palaeohydrology., John Wiley., Chichester and New York., 329-342

Engstrom, D.R., Fritz, S.C., Almemdinger, J.E. and Juggins, S. (1991) Chemical and biological trends during lake evolution in recently deglaciated terrain, Nature, 408, 161-1664

Eriksson, M.G. and Sandgren, P. (1999) Mineral magnetic analyses of sediment cores recording recent soil erosion history in central Tanzania, Palaeogeography, Palaeoclimatology, Palaeoecology, 152, 365 – 383

Fallu, M-A; Peinitz, R., Walker, I.R. and Overpeck, J. (2004) AMS14C dating of tundra lake sediments using chironomid head capsules, Journal of Paleolimnology, 31, 11-22

Feng, X. and Epstein, S. (1995), Climate Implications of an 8000-Year Hydrogen Isotope Time Series from Bristlecone Pine Trees, Science, 265,(5175), 1079 – 1081

Fischer, D.A. and Koerner, R.M. (2003) Holocene Ice-core climate history: a multivariable approach in Mackay, A., Battarbee, R., Birks, J and Oldfield, F. (*eds*) Global change in the Holocene, Arnold, London, 281-293

Forsyth, D. J.(1978) Benthic macroinvertebrates in seven New Zealand lakes, New Zealand, Journal of Marine and Freshwater Research, 12, 42-9

Francis, D. R. (2001). A record of hypolimnetic oxygen conditions in a temperate multi-depression lake from chemical evidence and chironomid remains, Journal of Paleolimnology, 25, 351 - 365.

Francis, D.F. and Foster, D.R. (2001) Response of small New England ponds to historic land use, The Holocene, 11 (3), 301-312

Fritz, S.C., Juggins, S., Battarbee, R.W. and Engstrom, D.R. (1991) Reconstruction of past changes in salinity and climate using a diatom-based transfer-function, Nature, 352 (6337), 706-708

Fritz, S.C., Stevenson, A.C., Patrick, S.T., Appleby, P.G., Oldfield, F., Rippey, B., Natkanski, J. and Battarbee, R.W. (1989) Paleolimnological evidence for the recent acidification of Llyn Hir, Dyfed, Wales, Journal of Paleolimnology, 2, 245-262

Frogatt, P.C. (1992) Standardiizaion of the chemical analysis of tephra deposits, report of the ICCT working group, Quaternary International, 13/14, 93-96

Futa, K. and C. R. Stern (1988). Sr and Nd isotopic trace element compositions of Quaternary volcanic centres of the southern Andes, Earth and Planetary Science Letters, 88(253 - 262).

Gasse, F. (2000) Hydrological changes in the African tropics since the Last glacial Maximum, Quaternary Science Reviews, 19, 189-221

Gauch, H.G. and Whitaker, R.H (1981) Hierarchical classification of community data, Journal of Ecology, 69, 135-152

Gauch, H.G. Jr (1994) Multivariate analysis in community ecology, Cambridge University Press, Cambridge

Gilchrist, S.J.L. (2000) A Palaeoecological reconstruction of climate change at Cerro Ataud, (47°S), Chilean Patagonia during the Last Glacial Interglacial Transition and early Holocene (14.1-7.5 cal ka BP), Unpublished MSc Dissertation, University of London

Gorgoza, G., Sinito, A.M., Lirio, J.M., Nuñez, H., Chaparro, M. and Vilas, J.F. (2002) Paleosecular variations 0-19,000 years recorded by sediments from Escondido Lake (Argentina) , Physics of the Earth and Planetary Interiors, 113, 35-55

Grimm (1987) CONISS: A forran 77 program for stratigraphically constrained cluster analyissi by the method of instrunemantl sum of squares, Computers and Geoscineces, 13. 13-35

Grimm (1991 – 1993), Tilia version 2.0.b.4, Illinois State Museum, Springfield, Illinois

Grimm (1991) Tiliagraph version, 2.0.b.5, Illinois State Museum, Springfield, Illinois

Grootes, P.M., Steig, E.J., Stuiver, M., Waddington, E.D., Morse, D.L. and Nadeau, M (2001) The Taylor Dome Arctic δ18O record and global synchronous changes in climate, Quaternary Research, 56, 289-298

Grosjean, M. (2001) Mid-Holocene climate in the south-central Andes: Humid or dry? Response, Science, 292 (5526)

Grove, J. M. (1988) The Little Ice Age, Methuen, London

Haberle, 1999, http://www.arts.monash.edu.au/ges/who/haberle/chile/tephra.html

Haberle, S. G. and Lumley, S. H. (1998). Age and origin of tephras recorded in postglacial lake sediments to the west of the southern Andes, Journal of vulcanology and geothermal research, 84, 239-256.

Haberle, S.G. and Bennett, K.D. (2001) Modern pollen rain and lake mud-water interface geochemistry along environmental gradients in southern Chile, Review of Paleobotany and Palynology, 117, 93 – 107

Haberle, S.G. and Bennett, K.D. (*in press*), Postglacial Formation and Dynamics of North Patagonian Rainforest in the Chonos Archipelago, Southern Chile, Quaternary Science Reviews,

Hajdas I, Bonani G, Moreno PI, Ariztegui D, (2003)Precise radiocarbon dating of late-glacial cooling in mid-latitude South America, Quaternary Research, 59 (1) , 70-78

Håkanson, L. (1996) A new, simple, general technique to predict seasonal variability of river discharge and lake temperature for lake ecosystem models, Ecological Modelling, 88, 157-188

Hann, B.J., Warner, B. G. and Warwick, W. F (1992) Aquatic invertebrates and climate change: a comment on Walker *et al*, (1991) Canadian Journal of Fisheries and Aquatic Science, 49, 1274-1276

Hays, J.D., Loranzo, J.A., Shackleton, N. and Irving, G, (1976) Reconstruction of the Atlantic Western Indian Ocean Sectors of the 18,000 B.P. Antarctic Ocea, Memoirs of the Geological Society of America, 145, 337-372

Heinrichs, M. L., Walker, I.R. and Mathewes, R.W. (2001). Chironomid based paleosalinity records in southern British Colombia, Canada: a comparison of transfer functions, Journal of Paleolimnology, 25, 147 - 159.

Heinrichs, M.L, Walker, I.R., Mathewes, R.W. and Hebda, R.J. (1999). Holocene chironomid-inferred salinity and paleovegetation reconstruction from Kilpoola Lake, British Columbia. Geographie physique et Quaternaire, 53 (2), 211-221.

Heiri, O. and Lotter, A.F. (2001) Effects of low count sums on quantitative environmental reconstructions: an example using subfossil chironomids, Journal of Paleolimnology, 26, 343-350

Heiri, O., Lotter, A.F. and Lemcke, G. (2001) Loss on ignition as a method for estmating organic and carbonate content in sediments: reproducibility and comparability of results, Journal of Paleolimnology, 25, 101-110

Heiri, O., Birks, H.J.B., Brooks, S.J., Velle, G., Willassen, E., (2003b) Effects of within-lake variability of fossil assemblages on quantitative chironomid inferred temperature reconstruction, Palaeogeography, Palaeoclimatology, Palaeoecology, 199, 95-106

Heiri, O., Lotter, A.F., Hausmann, S. and Kienast, F. (2003a) A chironomid-based Holocene summer air temperature reconstruction from the Swiss Alps, The Holocene, 13 (4), 477-484

Hellstrom, J., McCulloch, M., and Stone, J. (1998) , A detailed 31,000-year record of climate and vegetation change from the Isotope Geochemistry of two New Zealand Speleothems, Quaternary Research, 50, 167-178

Heusser, C. J. (1983). Quaternary record from Laguna de Tagua Tagua, Chile, Science, 219, 1429-1432.

Heusser, C. J., Heusser, L. E., Lowell, T. V. (1999). Paleoecology of the southern Chilean Lake District - Isla Grande de Chiloé during middle-late Llanquihue glaciation and deglaciation. Geographiska Annaler, 81A (2), 167-230.

Heusser, C.J. (1964) Some pollen profiles from the Laguna San Rafael Area, Chile, in Cranwell, L. M. (*ed*) Ancient Pacific Floras: the pollen story, University of Hawaii Press, Honolulu, 95-114

Heusser, C.J. (1984) Late-Glacial-Holocene Climate of the Lake District of Chile, Quaternary Research, 22, 77-90

Heusser, C.J. (1995) Three Late Quaternary pollen diagrams form Southern Patagonia and their palaeoecological implications, Palaeogeography, Palaeoclimatology, Palaeoecology, 118, 1-24

Heusser, C.J. (1999) C-14 age of glaciation in Estrecho de Magallanes-Bahia Inutil, Chile, Radiocarbon, 41 (3), 287-293

Heusser, C.J. (2002) On glaciation of the southern Andes with special reference to the Peninsula de Taitao and adjacent Andean cordillera (~46º 30's), Journal of South American Earth Sciences, 15, 577-589

Heusser, C.J., Heusser, L.E., Lowell, T.V., Moreira, A., Moreira, S. (2000). Deglacial palaeoclimate at Puerto del Hambre, Subantarctic Patagonia, Chile, Journal of Quaternary Science, 15, 101-114

Heusser, C.J., Lowell, T.V., Heusser, L.E. Hauser, A., Andersen, B.G. and Denton, G.H. (1996) Full-glacial-late-glacial palaeoclimate of the Southern Andes: evidence from pollen, beetle and glacial records, Journal of Quaternary Science, 11 (3), 173-184

Heusser, C.J.., Denton, G.H.., Heusser, A., Andersen, B.G. and Lowell, T.V. (1995) Quaternary pollen records from the Archipiélago de Chiloé in the context of glaciation and climate, Revista Geológica de Chile, 22, 1, 25-46

Hill, M.O. (1979) TWINSPAN - A FORTRAN programfor arranging multivariate data in an ordered two-way Table by classification of the individuals and attributes, Cornell University , Ithica, New York

Hoffert, M.I. and Covey, C. (1992) Deriving Global Climate sensitivity from paleoclimate reconstructions, Nature, 360 (6404), 573- 576

Hofmann, W. (1988). The significance of chironomid analysis (Insecta: Diptera) for palaeolimnological research. Palaeogeography, Palaeoclimatology, Palaeoecology 62: 501-509.

Hofmann, W. (1998). Cladocerans and chironomids as indicators of lake level changes in north temperate lakes. Journal of paleolimnology, 19, 55-62.

Hofmann, W. (2001). Late-Glacial/ Holocene succession of the chironomid and cladocera fauna of Soppensee (Central Switzerland). Journal of Paleolimnology, 25, 411 - 420.

Hoganson, J. W. and Ashworth, A.C. (1992). Fossil beetle Evidence for climatic change 18,000-10,000 years B.P. in South-Central Chile. Quaternary Research, 31, 101-116.

Hoffman, W. (1986) Chironlomid analysis, in Berglund, B.E (*ed*) Handbook of Holocene Palaeoecology and Palaeohydrology, John Wiley., Chichester and New York, 715-723

http://www.niwa.cri.nz/rc/prog/freshbiodiversity/chirolist.pdf (Accessed 12/ 02/ 2004)

http://www.ru.ac.za/academic/departments/zooento/Martin/chironomidae.html (Accessed 12/ 02/ 2004)

Hubbard, A.L. (1997)Modelling climate, topography and palaeoglacier fluctuations in the Chilean Andes, Earth Surface Processes and Landforms, 22 (1), 79-92

Hugget, R.J. (1998) Fundamentals of biogeography, Routledge, London

Hulme, M., Barrow, E.M., Arnell, N.W., Harrison, P.A., Johns, T.C., Downing, T.E. (1999)Relative impacts of human-induced climate change and natural climate variability, Nature, 397 (6721), 688-691

Hulton, N.R .J., Purves., R.S., McCulloch., R.D. Sugden., D.E. and Bentley., M.J., (2002) The Last Glacial Maximum and deglaciation in southern South America., Quaternary Science Reviews, 21, 233-241

Hulton, N.R.J., Sugden, D.E.., Payne., A.J., Clapperton, C. (1994) Glacier modelling and the climate of Patagonia during the Last Glacial Maximum, Quaternary Research, 42, 1-19

Humphries, C. J. and Parenti, L.R. (1989) Cladistic Biogeography: Oxford monographs on biogeography No. 2, Oxford University Press, Oxford

Hunt, J. B. and P. G. Hill (1993). Tephra geochemistry: a discussion of some persistent analytical problems, The Holocene, 3(3), 271-278.

Ilyashuk, B. P. and E. A. Ilyashuk (2001). Response of alpine chironomid communities (Lake Chuna, Kola Peninsula, northwestern Russia) to atmospheric contamination, Journal of Paleolimnology, 25, 467-475.

Ivy Ochs, S. I., Schluchter, C., Kubik, P. W., Denton, G. H. (1999). Moraine exposure dates imply synchronous Younger Dryas glacier advances in the European Alps and in the Southern Alps of New Zealand, Geographiska Annaler, 81A (2), 313-323.

Jager, J.C. and Looman, C. (1995) Data Collection in Jongman, R.H.G., ter Braak, C.J.F and van Tongeren, O.F.R., (*eds*) Data analysis in community and landscape ecology, Cambridge University Press, Cambridge, UK, 10 – 28

Jones, V.J., Battarbee, R.W. and Hedges, R.E.M. (1993) The use of chironomid remains for AMS 14C dating of lake sediments, The Holocene, 3, 161-163

Jowsey, P.C. (1966) An improved peat sampler, New Phytologist, 65, 235-248

Kansansen, P. H., Aho, J and Paasivirta, L., (1984) Testing the benthic lake type concept based on chironomid associations in some Finnish lakes using multivariate statistical methods, Ann. Zool. Fennici, 21, 55-76

Kaplan, M.R., Ackert, R.P., Singer, B.S., Douglass, D.C., Kurz, M.D. (2004) Cosmogenic nuclide chronology of millennial-scale glacial advances during O-isotope stage 2 in Patagonia, Geological Society of America Bulletin, 116 (3-4), 308-321

Kaufman, D.S., Ager, T. A., Anderson, N.J., Anderson, P.M., Andrews, J.T., Bartlein, P. J., Brubaker, L.B., Coats, L.L., Cwynar, L.C., Duvall, M.L., Dyke, A.S., Edwards, M.E., Eisner, W.R., Gajewski, K., Geirsdóttir, A., Hu, F.S., Jennings, A.E., Kaplan, M.R., Kerwin, M.W., Lozhkin, A.V., MacDonald, G.M., Miller, G.H., Mock, C.J., Oswald, W.W. Otto-Bliesner, B.L., Porinchu, D.F.., Rűhland, K., Smol, J. P., Steig, E.J. and Woflfe, B.B. (2004) Holocene thermal maximum in the western Arctic (0-180°W), Quaternary Science Reviews, 23 (5-6), 529 - 560

Kim, J.H., Schneider, R.R., Hebbeln, D., Muller, P.J., Wefer, G. (2002) Last deglacial sea-surface temperature evolution in the Southeast Pacific compared to climate changes on the South American continent, Quaternary Science Reviews, 21 (18-19), 2085-2097

Kim, S-J, Crowley, T.J. and Stössel,A (1998) Local orbital forcing of Antarctic climate change during the last interglacial, Science, 280 (5364) 728-730

King, L., Barker, P. and Jones, R.J.(2000) Epilithic algal communities and their relationship to environmental variables in lakes of the English Lake District, Freshwater Biology, 45, 425-442

Kling, G. W., (2000) A lake's life is not its own, Nature, 408 (6809), 149-150

Korhola, A., Olander H., Blom, T. (2000) Cladoceran and chironomid assemblages as quantitative indicators of water depth in subarctic Fennoscandian lakes, Journal of Paleolimnology, 24 , 43-53

Korhola, A.., Vasko, K., Toivonen, H.T.T. and Olander, K. (2002) Holocene temperate changes in northern Fennoscandia reconstructed from chironomids using Bayesian modelling, Quaternary Science Reviews, 21, 1841-1860

Kovach, W.L (1985) Multivariate data analysis in Maddy, D. and Brew, J.S. (*eds*) Statistical Modelling of Quaternary Science Data, Quaternary Research Association Technical Guide No. 5, Quaternary Research Association, Cambridge, 1-38

Lami, A., F. Niessen, *et al.* (1994). Palaeolimnological studies of the eutrophication of volcanic Lake Albano (Central Italy). Journal of paleolimnology 10: 181-197.

Lamy, F., Hebbeln, D., Wefer, G. (1999) High resolution marine record of climatic change in mid-latitude Chile during the last 28,000 years based on terrigenous sediment parameters, Quaternary Research, 51(2), 83-93

Langmuir, D. (1997) Aqueous Environmental Geochemistry, Prentice Hall, New Jersey

Larocque, I. (2001) How many chironomid head capsules are enough? A statistical approach to determining the sample size for palaeoclimatic reconstructions, Palaeogeography, Palaeoclimatology, Palaeoecology, 172, 133-142

Larocque, I., R. I. Hall, Grahn, E. (2001). Chironomids as indicators of climate change: a 100-lake training set from a subarctic region of northern Sweden (Lapland). Journal of Paleolimnology, 26, 307-322.

Larsen, J., Birks, H.J.B. Birks, Raddum, G.G. and Fjellheim, A. (1996) Quantitative relationships of invertebrates to pH in Norwegian river systems, Hydrobiologia, 328, 57-74

Legendre, P and Legendre, L. (1998) Numerical Ecology: Developments in environmental modelling 20, Elsevier, 2nd edition

Lehman, J. T. (1975). Reconstructing the rate of accumulation of lake sediment: The effect of sediment focusing. Quaternary Research, 5, 541-550.

Lepš, J., Šmilauer, P. (2003) Multivariate Analysis of Ecological Data Using CANOCO, Cambridge University Press, Cambridge

Levesque A.J., Cwynar L.C., Walker I.R. (1997) Exceptionally steep north south gradients in lake temperatures during the last deglaciation, Nature, 385 (6615), 423-426

Levesque A.J., Mayle, F.E., Cwynar L.C., Walker I.R. (1993) A previously unrecognised late-glacial cold event in eastern North-America, Nature, 353 (6425), 188-188

Levesque, A.J., Cwynar, L.C. and Walker, I.R. (1996) Richness, diversity and succession of late-glacial chironomid assemblages in New Brunswick, Canada, Journal of Paleolimnology, 16, 257-274

Lindegaard, C. (1992) Zoobenthos ecology of Thingvallavatn : vertical distribution, abundance, population dynamics and production, Okios, 64, 257- 304

Lindegaard, C. (1995) Classification of water-bodies and pollution in Armitage, P., Cranston, P.S. and Pinder, L. V. (*eds*) The Chironomidae: the biology and ecology of non-biting midges, London, Chapman and Hall, 385 -404

Little, J. L. and J. P. Smol (2001). A chironomid-based model for inferring late-summer hypolimnetic oxygen in southeastern Ontario lakes. Journal of Paleolimnology, 26, 259 - 270.

Livingstone, D. M. and A. F. Lotter (1998). The relationship between air and water temperatures in lakes of the Swiss Plateau: a case with palæolimnological implications, Journal of Paleolimnology, 19, 181-198.

Lotter, A. F., Birks, H.J.B., Hofmann, W. and Marchetto, A. (1997a). Modern diatom, cladocera, chironomid and chrysophyte cyst assemblages as quantitative indicators for the reconstruction of past environmental conditions in the Alps. I. Climate, Journal of Paleolimnology, 18, 395-420.

Lotter, A. F., H. J. B. Birks, Hofmann, W and Marchetto, A. (1998). Modern diatom, cladocera, chironomid and chrysophyte cyst assemblages as quantitative indicators for the reconstruction of past environmental conditions in the Alps. II. Nutrients, Journal of Paleolimnology, 19, 443-463.

Lotter, A. F., Walker, I.R., Brooks, S. J. and Hofmann, W. (1999). An intercontinental comparison of chironomid palaeotemperature inference models: Europe vs North America, Quaternary Science Reviews, 18, 717-735.

Lotter, A.F. and Birks, H.J.B. (1993) The impact of the Laacher See tephra on terrestrial and aquatic ecosystems in the Black Forest, southern Germany, Journal of Quaternary Science, 8, 263-276

Lowe, J. J. and Walker, M. J. C. (1986) Flandrian environmental history of the Isle of Mull, Sotland, 2, Pollen data from sites in Western and Northern Mull, New Phytologist, 103 (2): 417 - 436

Lowe, J. J. and Walker, M. J. C. (1997). Reconstructing Quaternary Environments. London, Longman, 2nd Edition

Lowe, J.J. (2001) Abrupt climatic changes in Europe during the last glacial interglacial transition: the potential for testing hypotheses on the synchroneity of climatic events using tephrochronology, Global Planetary Change, 30 (1-2): 73-84

Lowe, J.J. and Walker, M.J.C (2000) Radiocarbon dating the Last Glacial-Interglacial Transition (Ca.14 – 9 14C ka BP) in terrestrial and marine records: the need for new quality assurance protocols, Radiocarbon, 42, 1, 53-68

Lowe, J.J. and Walker, M.J.C. (1980) Problems associated with radiocarbon dating the close of the Lateglacial period in the Rannoch Moor area, Scotland, in Lowe, J.J., Gray, J.M. and Robinson, J.E. (*Eds*) Studies in the Lateglacial of North-West Europe, Pergamon Press, Oxford, UK, 123-138

Lowell, T.V., Heusser, C.J., Anderson, G., Moreno, P.I., Hauser, A., Heusser, L.E., Schlüchter, Marchant., D.R., Denton, G.H. (1995) Interhemispheric Correlation of Late Pleistocene Glacial Events, Science, 269, 1541-1549

Lumley, S. H. and R. Switsur (1993). Late Quaternary chronology of the Taito Peninsula, southern Chile. Journal of Quaternary Science, 8(2): 161-165.

Lumley, S.H. (1993) Late Quaternary vegetational and environmental history of the Taitao Peninsula, Chile. Ph.D. Thesis, Cambridge University.

Mabin, M.C.G., (1996) The age of the Waiho Loop glacial event, Science, 271 (5249),668 - 668

Mackereth, F.J. (1965) Chemical investigations of lake sediments and their interpretation, Proceedings of the Royal Society of London, B161, 295-309

Mancini, M.V. (2002), Vegetation and climate during the Holocene in Southwest Patagonia, Argentina, Review of Palaeobotany and Palynology, 122, 101-115

Mandryk, C.A.S., Josenhans, H., Fedje, D.W., Mathewes, R.W. (2001), Late Quaternary paleoenvironments of Northwestern North America: implications for inland versus coastal migration routes, Quaternary Science Reviews, 20, 301-314

Mangerud, J., Andersen, S.T., Berglund, B.E. and Donner, J.J. (1974). Quaternary stratigraphy of Norden: A proposal for terminology and Classification, Boreas, 3, 109-128

Marden, C. J. (1997), Late-glacial fluctuations of South Patagonian Icefield, Torres del Paine National Park, Southern Chile, Quaternary International, 38/39, 61-68.

Marden, C. J. and Clapperton, C. M. (1995), Fluctuations of the Southern Patagonian ice field during the last glaciation and the Holocene, Journal of Quaternary Science, 10 (3), 197- 210.

Marden, C.J. (1993) Late glacial and Holocene variations of the Grey Glacier, an outlet of the South Patagonian Icefield, Scottish Geographical Magazine, 109, 27-31

Markgaf, V. (1993b), Younger Dryas in Southernmost South-America – an Update, Journal of Quaternary Science, 12, 351 – 355

Markgraf, V. (1989) Reply to C. J. Heusser's "Southern Westerlies during the Last Glacial Maximum", Quaternary Research, 31, 426-432

Markgraf, V. (1991) Younger Dryas in southern South America, Boreas, 20, 63-69

Markgraf, V. (1993a) Paleoenvironments and paleoclimate in Tierra del Fuego and southernmost Patagonia, South America, Palaeogeography, Palaeoclimatology, Palaeoecology, 102, 53-68

Markgraf, V., and Kenny, R. (1997) Character of rapid vegetation and climate change during the late glacial in southernmost South America. In. Huntley, B., Cramer, W., Morgan, A. V., Prentice, H. C. and Allen, J. R. M. (*eds*). Past and Future Rapid Enrivonmental Changes: The Spatial and Evolutionary Responses of Terrestrial Biota, Springer, Berlin, 81–90.

Markgraf, V., Webb, R.S., Anderson, K.H., and Anderson, L. (2002) Modern pollen/climate calibration for southern South America, Palaeogeography, Palaeoclimatology, Palaeoecology , 181, 375-397

Markgraf, V., Bradbury, J.P., Schwalb, A., Burns, S.J., Stern, C., Ariztegui, D., Gilli, A., Anselmetti, F.S., Stine, S., Maidana, N. (2003) Holocene palaeoclimates of southern Patagonia: limnological and environmental history of Lago Cardiel, Argentina, Holocene, 13 (4), 581-591

Massaferro, J. and Brooks, S. J. (2002) Response of chironomids to Late Quaternary environmental change in the Taito Peninsula, southern Chile, Journal of Quaternary Science, 17 (2), 101-111

Massaferro, J., Brooks, S.J. and Haberle, S.G. (*submitted*) The dynamics of chironomid assemblages and vegetation during the Late Quaternary at Laguna Facil, Chonos Archipelago, southern Chile,

Mayewski, P.A., Rohlin, E.E., Stager, J.C., Karlén. W. Maasch, K.A., Meeker, L.D., Meyerson, E.A., Gasse, F., van Kreveld. S., Holmgren, K., Lee-Thorp, J., Rosqvist, G., Rack, F., Staubwasser, R.R., Schneider, R.R. and Steig, E.J. (2004) Holocene Climate Variability, Quaternary Research, 63, 243-255

Mayle, F. E. and L. C. Cwynar (1995). A review of multi-proxy data for the Younger Dryas in Atlantic Canada. Quaternary Science Reviews, 14, 813-821.

McCulloch, R. D. and M. J. Bentley (1998). Late glacial ice advances in the Strait of Magellan, Southernmost Chile, Quaternary Science Reviews 17, 775-787.

McCulloch, R. D. M. (1994). Palaeoenvironmental evidence for the Late Wisconsin / Holocene transition in the Strait of Magellan, southern Patagonia. Geography, Aberdeen.

McCulloch, R. D., Bentley, M.J., Purves, R.S., Hulton, N.R.J., Sugden, D.E., Clapperton, C.M. (2000). Climatic inferences form glacial and palaeoecological evidence at the last glacial termination, southern South America, Journal of Quaternary Science, 15 (4): 409-417.

McCulloch, R.D. and Davies, S.J. (2001) Palaeoenvironmental evidence for the Late-glacial/Holocene transition in the Magellan Region, southernmost Chile. Palaeogeography, Palaeoclimatology, Palaeoecology, 173, (3-4), 143-173

McCulloch, R.D., Clapperton, C.M., Rabassa, J. and Currant, A.P. (1997) The natural setting: the glacial and post-glacial environmental seeing of Fuego Patagonia, in Prieto, A. (*eds*) Patagonia: Natural History, prehistory and ethnography at the uttermost end of the World, Petruzzi, Italy, 12-31

McDonald, G.M., Edwards, T.W.D., Moser, K.A., Pientirtz, R and Smol, J.P. (1993) Rapid resposnse of treeline vegetation and lakes to past climate warming, Nature, 361, 243-346

McGlone, M.S. (1995) Lateglacial landscape and vegetation change and the Younger Dryas climatic oscillation in New Zealand, Quaternary Science Reviews, 14, 867-881

Mercer, J.H. (1982) Holocene glacier variations in southernmost South America, Striae, 18, 35-40

Mercer, J.H. (1976) Glacial history of southernmost South America, Quaternary Research, 6, 125-166

Mercer, J.H. (1984) Late Cainozoic glacial variations of South America south of the equator, in Vogel., J.C. (*ed*) Late Cainozoic Palaeoclimates of the Southern Hemisphere, A.A. Balkema, Rotterdam, 45-58

Moreno, P. I., Jacobson, G.L., Lowell, T.V., Denton, G.H. (2001). Interhemispheric climate links revealed by a late-glacial cooling episode in southern Chile, Nature, 409, 804-808.

Moreno, P.I. and León, A.L. (2003 */in press*) Abrupt vegetation changes during the last glacial to Holocene transition in mid-latitude South America, Journal of Quaternary Science, 18 (0), 1-14

Moreno, P.I.(1997) Vegetation and climate near Lago Llanquihue in the Chilean Lake District between 20200 and 9500 14C yr BP, Journal of Quaternary Science, 12, 485-500

Moreno, P.J., Lowell, T.V., Jacobson, J.R. and Denton, G.H. (1999) Abrupt vegetation and climate changes during the last glacial maximum and last termination in the Chilean Lake District: A case study from Canal de la Puntilla (41°S), Geographiska Annaler, 81A (2), 285-312

Moritz, R. E., Bitz, C.M and Steig, E.J. (2002) Dynamics of Recent Climate Change in the Arctic, Science, 297, 1497-1502

Naranjo, J. A. and C. R. Stern (1998) Holocene explosive activity of Hudson Volcano, southern Andes. Holocene explosive activity of Hudson Volcano, southern Andes, Bulletin of Vulcanology, 59, 291-306.

Newnham, R.M., Lowe, D.J. and Green, J.D. (1989) Palynology, vegetation and climate change in the Waikoto lowlands, North Island, New Zealand, since c. 18,000 years ago, Journal of the Royal Society of New Zealand, 19, 127-150

Newton, A.J. and Metclalfe, S.E (1999) Tephrochronology of the Toluca Basin, central Mexico, Quaternary Science Reviews, 18, (8-9) 1039 - 1059

Nyman, M, Korhola, A. and Brooks, S.J.B., (*submitted*) The diversity and distribution of Chironomidae (Insecta: Diptera) in western Finnish Lapland,

Olander, H., Korhola, A., Blom, T., Birks, H.J.B, (1999) An expanded calibration model for inferring lakewater and air temperatures from fossil chironomid assemblages in northern Fennoscandia, The Holocene, 9 (3), 279-294

Oldfield, F (1999) Environmental Magnetism: the range of applications in Walden, J., Oldfield, F. and Smith, J.P., (*eds*) Environmental Magnetism: a practical guide. Technical Guide, No. 6, Quaternary Research Association, London

Oldfield, F. (2003) Introduction: The Holocene, a special Time, in Mackay, A., Battarbee, R. Birks, J.J.B., Oldfield, F. (*eds*) Global Change in the Holocene, Arnold, London, 1-9

Oliver, D. R. (1981) Chironomidae in Mc Alpine, J.F., Peteoron, B.V., Shewell, H.J., Jeskey, J.R., Vockeroth, J.R. and Wood, D. M (*eds*) Manual of Nearctic Diptera (Vol. 1), Research Branch Agriculture, Canada

Digby, P.G.N. and R.A. Kempton, R.A. (1987) Multivariate analysis of ecological communities, Chapman and Hall, London

Palmer, M. W. (1993) Putting Things in Even Better Order: The advantages of Canonical Correspondence Analysis, Ecology, 74 (8) 2215-2230

Palmer, S., Walker, I., Heinrichs, M., Hedba, R. and Scudder, G. (2002) Postglacial midge community change and Holocene palaeotemperature reconstructions near treeline, southern British Columbia (Canada), Journal of Paleolimnology, 28, 469-490

Pellatt, M., Smith, M.J., Mathewes, R.W., Walker, I.R. (1998). Palaeoecology of postglacial treeline shifts in the northern Cascade Mountains, Canada, Palaeogeography, Palaeoclimatology, Palaeoecology,141, 123-138.

Pendall. E. Markgraf, V., White, J.W.C., Drier, M. and Kenny, R. (2001) Multiproxy record of Late Pleistocene-Holocene climate and vegetation changes from a peat bog in Patagonia, Quaternary Research, 55, 168-178

Pinder, L. V. C. (1995a). Biology of the eggs and first-instar larvae, in P. Armitage, P. S. Cranston and L. V. Pinder (*eds*) The Chironomidae: the biology and ecology of non-biting midges, Chapman and Hall, London, 97-106.

Pinder, L. V. C. (1995b). The habitats of chironomid larvae, in P. Armitage, P. S. Cranston and L. V. Pinder (*eds*) The Chironomidae: the biology and ecology of non-biting midges, Chapman and Hall, London, 107-135.

Pinder, L.C.V and Morley, D.J. (1995) Chrinomidae as indicators of water quality - with a comparison of the chironomid faunas of a series of contrasting Cumbrian Tarns , in Harrington, R. and Stork, N.E. (*eds*) Insects in a changing environment, Academic press. London, 272-290

Pinder, L.C.V. (1986) Biology of freshwater Chironomidae, Annual review of Entomology, 31, 1-23

Pinder, L.C.V. and Reiss F. (1983) The larvae of Chironominae (Diptera: Chironomidae) of the Holarctic region – Keys and diagnoses in Weiderholm, T. (*ed*) Chironomidae of the Holarctic region: Keys and diagnosis: Part 1 – Larvae, Entomologica Scandinavica, Supplement No. 19, Lund

Porch, N. and Elias, S. (2000) Quaternary beetles: A review and issues for Australian studies, Australian Journal of Entomology, 39, 1-9

Porinchu, D. F. and Cwynar, L. C (2000). The distribution of Freshwater Chironomidae (Insecta: Diptera) across Treeline near the Lower Lena River, Northeast Siberia, Russia. Arctic, Antarctic and Alpine Research, 32 (4): 429-437.

Porinchu, D.F. and MacDonald, G. M. (2003) the use and application of freshwater midges (Chironomidae: Insecta: Diptera) in geographical research, Progress in Physical Geography, 27 (3), 378-422

Porter, S.C. (1981) Pleistocene glaciation in the southern lake district of Chile, Quaternary Research, 16, 263-292

Purves, R.S. and Hulton., 2000., Experiments in linking regional climate, ice sheet models and topographies, Journal of Quaternary Science, 15, 369-376

Quinlan, R. and Smol, J.P. (2001) Setting minimum head capsule abundance and taxa deletion criteria in chironomid-base inference models, Journal of Paleolimnology, 26, 327-342

Quinlan, R., J. P. Smol and Hall, R.I. (1998). Quantitative inferences of past hypolimnetic anoxia in south-central Ontario lakes using fossil midges (Diptera: Chironomidae). Canadian Journal of Fisheries and Aquatic Sciences, 55, 587-596.

Rech JA, Quade J, Betancourt JL.(2002), Late Quaternary paleohydrology of the central Atacama Desert (lat 22 degrees-24 degrees S), Chile, Geological Society of America Bulletin, 114 (3), 334-348

Richards, O. W. and Davies, R. G. (1977) Imms' general textbook of entomology: Volume 1 Structure, Physiology and Development, Chapman and Hall, London, 10th Edition.

Rieradevall, M. and S. J. Brooks (2001). An identification guide to subfossil Tanypodinae larvae (Insecta: Diptera: Chironomidae) based on cephalic setation. Journal of Paleolimnology, 25, 81-99.

Roberts, N. (1998) The Holocene: an environmental history, Blackwell Publishers, Oxford, 2nd Edition

Rollison, H., (1993) Using Geochemical Data: Evaluation, Presentation, Interpretation, Addisonn Wesley Longman Ltd, Essex, England.

Rosén, P., Segerström, U., Eriksson, L. and Renberg, I. (2003) Do diatom, chironomid, and pollen records consistently infer Holocene July air temperature? A comparison using sediment cores from four alpine lakes in Northern Sweden, Arctic, Antarctic and Alpine Research, 35 (3), 279-290

Rosén, P., Segerström, U., Eriksson, L., Renberg, I., Birks, H.J.B. Birks. (2001) Holocene climatic change reconstructed from diatoms, chironomids, pollen and near-infrared spectroscopy at an alpine lake (Sjuodjijaure) in northern Sweden, The Holocene, 11 (5), 551-562

Rossaro, B. (1991), Chironomids and water temperature, Aquatic Insects, 13, 87-98.

Rück, A., I. A. Walker, Hebda, R. (1998). A palaeolimnological study of Tigulnuit Lake, British Colombia, Canada, with special emphasis on river influence as recorded by chironomids in the lake's sediments. Journal of Paleolimnology, 19 (1), 63-75.

Sadler, J. P. and Jones, J.C. (1997) Chironomids as indicators of Holocene environmental change in the British Isles, Quaternary Proceedings, 5, 219-232

Saether, O. (1979) Chironomid communities as water quality indicators, 1979. Holarctic Ecology, 2, 65-74

Saether, O.A. (2000) Zoogeographical patterns in Chironomidae (Diptera), Verhandlungender internationalen Vereinigung für theoretische und Andgewandte Limnologie, 27, 290-302

Sandiford, A., Newnham, R.M., Alloway, B.V. and Ogden, J. (2003) A high resolution Southern Hemisphere, mid-latitude LGM to Holocene record of vegetation and climate change from northern New Zealand, Palaeogeography, Palaeoclimatology, Palaeoecology, 201 (3-4): 235-247

Schmäh, A. (1993) Variation among fossil chironomid assemblages in surficial sediments of Bodensee-Untersee (SW-Germany): implications for paleolimnological interpretation, Journal of Paleolimnology, 9, 99-108

Seppa, H. and Birks, H.J.B. (2001) July mean temperature and annual precipitation trends during the Holocene in the Fennoscandian tree-line area: pollen-based climate reconstructions, Holocene, 11 (5), 527-539

Seppa, H. and Birks, H.J.B. (2002) Holocene climate reconstructions from the fennoscandian tree-line area based on pollen data from Toskaijavri, Quaternary Research, 57 (2), 191-199

Severinghaus, J.P., and Brook, E. J., (1999) Abrupt climate change at the end of the Last Glacial Period Inferred from Trapped Air in Polar Ice, Science, 286, 930-934

Severinghaus, J.P., Sowers, T.D., Brook, E.J. Alley, R.B. and Bender, M.L (1998) Timing of abrupt climate change at the end of the Younger Dryas interval from thermally fractionated gasses in polar ice, Nature, 391, 141-146

Singer ,B.S., Ackert, R.P., Guillou, H. (2000) Ar-40/Ar-19 and K-Ar chronology of Pleistocene glaciations in Patagonia, Geological Society of America Bulletin, 116 (3-4), 434-450

Singer, C., Shulmeister, J. and McCLea, B, (1998) Evidence against a significant Younger Dryas Cooling Event in New Zealand, Science, 281, 812 – 814

Sivan, O., Erel, Y., Mandler, D. and Nishri, A (1998) The dynamic redox chemistry of iron in the epilimnion of Lake Kinneret (Sea of Galilee), Geochimica and Cosmochimica Acta, 62 (4), 565-576

Snyder, J.A., Miller, G.H., Werner, A. Jull, A.J.T and Stafford, T.W Jnr. (1994) AMS-radicarbon dating of organic-poor lake sediment, and example from Linnévatnet, Spitsbergen, Svalbard, The Holocene, 4, 413-421

Sowers, T. and Bender, M. (1995) Climate records covering the last deglaciation, Science, 269, 210-213

Speight, M.R., Hunter, M.D. and Watt, A.D. (1999) Ecology of insects: concepts and applications, Blackwell Science, Oxford

Spellerberg, I.F. and Sawyer, J.W.D. (1999) An introduction to applied biogeography, Cambridge University Press, Cambridge

Stager, J.C., Cummong, B.F. and Meeker, L.D. (2003) A 10,000-yar high resolution diatom record from Pilkington Bay, Lake Victoria, East Africa, Quaternary Research, 59, 172-181

Stahl, J.B. (1969) The use of chironomids and other midges in interpreting lake histories, Mitteilugen Internationale Vereinigung fűr Theoretische und Angewandte Limnologie, 17, 111-25

Steig, E.J. (2001) No two latitudes alike, Science, 293, (5537), 2015-2016

Steig, E.J. and Alley, R.B. (2002) Phase relationships between Antarctic and Greenland climate records, Annals of Glaciology, 35, 451 – 456

Steig, E.J., Brook, E. J., White, J.W.C, Sucher, C.M., Bender, M.L., Lehman, S.J., Morse, E.D., Waddington, E.D., Clow, G.D. (1998) Synchronous climate changes in Antarctica and the North Atlantic, Science, 282, 92- 95

Steig, E.J., Morse, D.L., Waddington, E.D., Stuiver, M., Grootes, P.M., Mayewski, P.A., Twickler, M.S., Whitlow, S.I. (2000) Wisconsinan and Holocene climate history from

an ice core at Taylor Dome, western Ross Embayment, Antarctica, Geographiska Annaler, 82 (A) (2-3), 213-235

Stenni, B., Masson-Delmotte, V., Johnsen, S., Jouzel, J., Longinelli, A., Monnin, E., Rothlisberger, R., Selmo, E. (2001), An oceanic cold reversal during the last deglaciation, Science, 293, 5537, 2074-2077

Stern, C. (1992) Tefrocronologia de Magallanes: nuevos datos e implicaciones, Anales de Instituto de la Patagonia, 21, 129-140

Stern, C. R. (1990). Tephrochronology of Southernmost Patagonia, National Geographic Research, 6 (1), 110 - 126.

Stern, C. R. (1991). Mid-Holocene tephra on Tierra del Fuego (54°S) derived form the Hudson Volcano (46°S): Evidence for a large explosive eruption, Revista Geológica de Chile, 18, 139-146.

Stine, S. and Stine, M. (1990) A record from Lake Cardiel of climate change in southern South America, Nature, 345, 705-708

Stocker, T.F., (1998) The seesaw Effect, Science, 282, 61-26

Straškraba, M (1993) Some new data on latitudinal differences in the physical limnology of lakes and reservoirs in Boltovsky, A. and López, H.L. in Conferences in Limnology, UNLP-CONICET, La Plata, Argentina

Street Perrott, F.A. and Harrison, S.P (1985) Lake levels and climate reconstruction in Hecht, A.D. (*ed*) Paleoclimate Analysis and Modelling, Wiley, Chichester, 291-340

Street-Perrott, F.A. and Roberts, R.A. (1993), Holocene vegetation, lake levels and climate of Africa, in Wright, H.E., Kutzbach, J.E., Web III, T., Ruddiman, W.F., Street Perrott, F.A., and Bartlein, P.J. (*eds*) Global Climates Since the Last Glacial Maximum, Minneapolis, University on Minnesota Press, 318-356

Strelin, J.A., Malagnino, E.C. (2000) Late-glacial history of Lago Argentino, Argentina, and age of the Puerto Bandera moraines, Quaternary Research, 54 (3), 339-347

Stuiver, M. and Reimer, P.J. (1993). Extended ^{14}C data base and revised CALIB 3.0 14C age calibration program, Radiocarbon, 35, 215-230, Radiocarbon, 35, 215-230.

Stuiver, M., Reimer, P.J., Bard, E., Beck, J.W., Burr, G.S., Hughen, K.A., Kromer, B., McCormac, G., Van der Plicht, J., Spurk, M. (1998). INTCAL98 radiocarbon age calibration, 24,000-0 cal BP, Radiocarbon 40 (3), 1041-1083.

Stumm, W. and Baccini, P. (1978) Man-Made Chemical Perturbation of Lakes, in Lerman, A. (*ed*) Lakes – Chemistry, Geology, Physics, Springer - Verlag, New York, 363

Sugden, D. E., Bentley, M.J., Fogwill, C.J., Hulton, N.R.J., McCulloch, R.D. and Purves, R.S. (2005) Late-glacial glacier events in southernomost South America: a blend of 'northern; and 'southern' hemispheric signals?, Geographiska Annaler,

Sutherland, D.G. (1980) Problems of radiocarbon dating of deposits from newly deglaciated terrain: Examples from the Scottish Lateglacial, in Lowe, J.J., Gray, J.W. and Robinson, J.E. (*eds*) Studies in the Late-glacial of North-west Europe, 139-149, Pergamon Press, Oxford

Tatur, A., del Valle, R., Bianchi, M., Outes, V., Villarosa, G., Niegodzisz, J. and Debaene, G. (2002) Late Pleistocene palaelolakes in the Andean and Extra-Andean Patagonia at the mid-latitudes of South America, Quaternary International, 89, 135-130

Ter Braak, C.J. F and Prentice, I.C. (1988) A theory of gradient analysis, Advances in ecological research, 18, 271-317

Ter Braak, C.J.F (1986) Canonical Correspondence analysis: a new eigenvector technique for multivariate analysis, Ecology, 67 (5) 1167-1179

Ter Braak, C.J.F. and Juggins, S (1993) Weighted averaging partial least square regression (WA-PLS): an improved method for reconstructing environmental variables from species assemblages, Hydrobiologia, 269/270, 485- 5102

Ter Braak, C.J.F. and Smilauer, P. (1998) CANOCO Reference Manual and Users Guide to Canoco for Windows: Software for Community Ordination (Version 4), Microcomputer Polwer, Ithaca, NY

Thompson, L G. , Davis, M.E., Mosely-Thompson, E., Sowers, T.A., Henderson, K.A., Zagorodnov, V.S.,m Lin, P.-N., Mikhalenko, V.N., Campen, R.K., Bolzan, J.F., Cole-Dai, J. and Francou, B. (1998) a 25, 000-year Tropical climate history form Bolivian Ice Cores, Science, 282,1858-1864

Timms, B.V. (1978) The benthos of seven lakes in Tasmania, Archiv für Hydrobiologie, 81, 422-44

Trumbore, S.E. (2000) Radiocarbon Geochronology, in Stratton Noller, J., Sowers, J.N., Lettis, W.R (*eds*) Quaternary Geochronology: Methods and Applications, American Geophysical Union, Florida, USA

Turney, C.S.M and Lowe, J.J. (2001) Tephrochronology , in Tracking Environmental in Last, W. M. and Smol, J.P., Birks, J.B (*eds*), Change using lake sediments: Volume 1 : Basin Analysis, coring, and chronological techniques, Kluwer Academic Publishers, Dordrecht, The Netherlands, pp 451-472

Turney, C.S.M. (1998) Extraction of rhyolitic component of Vedde microtephra from minerogenic lake sediments, Journal of Paleolimnology, 19 (2), 199-206

Turney, C.S.M., Coope, G.R., Harkness, D.D., Lowe, J.J. and Walker, M.J.C. (2000) Implications for the dating of Wisconsinian (Weichselian) Lateglacial events of systematic radiocarbon age differences between terrestrial plant macrofossils from a site in SW Ireland, Quaternary Research, 53, 114 - 121

van Tongeren, O.F..R. (1995) Cluster analysis in Jongman, R.H.G., ter Braak, C.J.F and van Tongeren, O.F.R., (*eds*) Data analysis in community and landscape ecology, Cambridge University Press, Cambridge, UK, 174-212

Vandergoes, M.J. and Fitzsimons, S.J., (2003) The Last Glacial-Interglacial Transition (LGIT) in south Westland, New Zealand: palaeoecological insight into mid-latitude Southern Hemisphere climate change, Quaternary Science Reviews, 22 (14), 1461- 1476

Velle, G., Brooks, S.J., Birks, H.J.B, & Willassen, E. (*in press*) Chironomids as a tool for inferring Holocene climate: an assessment based on six sites in southern Scandinavia. Quaternary Science Reviews

Verschuren, D. (2003) Lake-based climate reconstruction in Africa: progress and challenges, Hydrobiologia, 500, 315-330

Verschuren, D., Laird, K.R. and Cumming, B.F. (2000a) Rainfall and drought in equatorial east Africa during the past 1,100 years, Nature, 403 , 410-414

Verschuren, D., Tibby, J., Sabbe, K. and Roberts, N. (2000b) Effects of depth, salinity and substrate on the invertebrate community on a fluctuating tropical lake, Ecology, 81 (1) 164-182

Villagran, C. (1988) Expansion of Magellanic moorland during the Late Pleistocene: Palynological evidence from northern Isla Chiloé, Chile, Quaternary Research, 30, 304-314

Villagran, C. (1990a) Glacial climates and their effects on the history of the vegetation of Chile: a synthesis based on palynological evidence from Isla de Chiloé, Review of Palaeoecology and Palynology, 65, 17-24

Villagran, C. (1990b) Late Quaternary Vegetation of Southern Isla Grande de Chiloé, Chile, Quaternary Research, 29, 294-306

Villalba, R., Lara, A./, Boninsegna, J.A., Masiokas, M., Delgado, S., Aravena, J.C.,Roig, F. A., Schmelter, A., Wolodarsky, A. and Ripalta, A., (2003) Large-Scale temperature changes across the southern Andes: 20th Century variations in the context of the past 400 years, Climate Change, 59, 177-232

Villigran, C., (1988) Expansion of Magellanic moorland during the Late Pleistocene: Palynological evidence from northern Isla Chiloé, Quaternary Research, 30, 304-314

Waite, S, (2000) Statistical ecology in Practice : a guide to analysing environmental and ecological field data, Pearson Education Ltd, Harlow, Essex

Walker, I. R. (1995) Chironomids as indicators of past environmental change in P. Armitage, P. S. Cranston and L. V. Pinder (*eds*)The Chironomidae: the biology and ecology of non-biting midges. Chapman and Hall, London, 405-422

Walker, I. R. and MacDonald, G.M. (1995) Distributions of Chironomidae (Insecta: Diptera) and other freshwater midges with respect to treeline, Northwest Territories, Canada, Arctic and Alpine Research, 27, 258 – 263

Walker, I. R. and Mathewes, R. W. (1987). Chironomidae (Diptera) and Postglacial Climate at Marion Lake, British Columbia, Canada, Quaternary Research, 27, 89-102.

Walker, I. R., 2000. The WWW Field Guide to Subfossil Midges. (http://www.ouc.bc.ca/eesc/iwalker/wwwguide/)

Walker, I. R., Fernando, C.H. and Paterson, C. G. (1984) The chironomid fauna of four shallow humic lakes and bog pools in Atlantic Canada and their representation by subfossil assemblages in the surficial sediments, Hydrobiologia, 112, 61-67

Walker, I. R., Levesque, A.J., Cwynar, L.C., Lotter, A.F. (1997). An expanded surface-water palaeotemperature inference model for use with fossil midges from eastern Canada. Journal of Paleolimnology 18, 165-178.

Walker, I. R., Smol, J.P, Engstom, D.R., and Birks, H.J.B. (1991a). An assessment of Chironomidae as quantitative indicator of past climate change. Canadian Journal of Fisheries and Aquatic Science, 48, 975-987

Walker, I.R. (1990) Modern assemblages of arctic and alpine Chironomidae as analogues for late-glacial communities, Hydrobiologia, 214, 223-227

Walker, I.R. and Mathewes, R.W. (1989a) Early postglacial chironomid succession in southwestern British Columbia, Canada, and its palaeoenvironmental significance, Journal of Paleolimnology, 2, 1-14

Walker, I.R. and Mathewes, R.W. (1989b) Chironomidae (Diptera) remains in surficial lake sediments from the Canadian Cordillera: analysis of the fauna across an altitudinal gradient, Journal of Paleolimnology, 2, 61 - 80

Walker, I.R., (2001) Midges: Chironomidae and related Diptera in Last, W. M. and Smol, J.P., Birks, J.B (*eds*) Tracking Environmental Change using lake sediments : Volume 4 : Zoological indicators , Kluwer Publishing, The Netherlands , 43 – 66

Walker, I.R., Wilson, S.E., and Smol, J.P., (1995) Chironomidae (Diptera): Quantitative palaeosalinity indicators for lakes of western Canada, Canadian Journal of Fisheries and Aquatic Science, 52, 950 - 960

Walker, M. J. C., Bjorck. S., Lowe, J.J., Cwynar, L.C., Johnsen, S., Knudsen, K.L., Wohlfarth, B. (1999). Isotopic 'events' in the GRIP ice core: a stratotype for the Late Pleistocene, Quaternary Science Reviews, Quaternary Science Reviews, 18, 1143-1150.

Walker, M.J.C. (*in press*) Radiocarbon dating the age and duration of abrupt climatic oscillations during the last glacial-interglacial transition (ca. 14-9 14C ka BP): the need for new quality assurance protocols (a contribution to the INTIMATE programme of the INQUA Palaeoclimate Commission). Radiocarbon

Walker, M.J.C., Coope, G.R., Sheldrick, C., Turney, C.S.M., Lowe, J.J., Blockley, S.P.E., and Harkness, D.D. (2003), Quaternary Science Reviews, 22, 475-520

Warwick, F.W. (1989) Chironomids, lake development and climate: a commentary, Journal of Paleolimnology, 2, 15-17

Warwick, W. F. (1980) Palaeolimnology of the Bay of Quinte, Lake Ontario: 2800 years of cultural influence, Canadian Bulletin of Fisheries and Aquatic Sciences, 206, 1-117

Watanabe, O., Jouzel, J., Johnsen, S., Parrenin, F., Shoji, H., Yoshida, N. (2003) Homogeneous climate variability across East Antarctica over the past three glacial cycles, Nature, 422, 509

Wetzel, R.G. (2001) Limnology: Lake and river ecosystems, Academic Press, San Diego, 3rd edition

Whatley, R.C., Cuminsky, G.C. (1999) Lacustrine Ostracoda and late Quaternary palaeoenvironments from the Lake Cari-Laufquen region, Rio Negro province, Argentina, Palaeogeography, Palaeoclimatology, Palaeoecology, 172, 133-142

White, J.W.C, and Steig, E.J. (1998) Timing is everything in a game of two hemispheres, Nature, 394, 717-718

Wiederholm, R. (*ed.*) (1983) Chironomidae of the Holarctic Region, Keys and Diagnosis. Part 1: Larvae. Entomologica Scandinavica Suppl., 19. Lund

Wiederholm, T and Eriksson (1979) Subfossil chironomids as evidence of eutrophication in Ekoln bay, Central Sweden, Hydrobiologia, 3, 283-302

Wiederholm, T. (1984) Responses of aquatic insects to environmental pollution in Resh, V.H. and Rosenberg, D.M. (*eds*) The ecology of aquatic insects, Praeger Publishers, New York

Wilson, S. E., I. R. Walker, Mott, R.J. and Smol, J.P. (1993). Climatic and limnological changes associated with the Younger Dryas in Atlantic Canada. Climatic Dynamics, 8, 177-187.

10 APPENDICES

APPENDIX 1:
Tephra results and technical details associated with EMPA analysis

APPENDIX 2:
Plates showing examples of the chironomid taxa encountered in this investigation

APPENDIX 3:
Environmental variables data after normalisation

APPENDIX 4:
Full chironomid raw data sets

APPENDIX 5:
Table of abbreviations used for taxa in diagrams

APPENDIX 6:
Loss on ignition results from Laguna Leta and Laguna Boal

APPENDIX 7:
Magnetic susceptibility data from Laguna Boal

APPENDIX 8:
Macrofossil abundance data from Laguna Boal

APPENDIX 1

Electron Microprobe Analysis (EMPA) results from analyses of shards from Laguna Leta

Data is presented with mean values and standard deviation for the population analysed at each depth. Parameters and settings are stated at the end of the appendix

	SiO_2	TiO_2	Al_2O_3	FeO	MnO	MgO	CaO	Na_2O	K_2O	Total
161cm (lower segment)	68.87	0.89	13.96	4.50	0.13	0.71	2.18	4.49	2.67	98.39
	68.04	1.59	13.73	4.66	0.11	0.71	2.30	4.15	2.66	97.94
	67.67	0.83	14.02	3.98	0.14	1.19	2.98	3.92	1.83	96.56
	66.84	0.77	15.46	3.52	0.16	0.73	1.85	5.09	3.35	97.90
	64.96	0.75	15.46	3.38	0.18	1.06	1.97	7.30	3.09	98.16
	62.45	1.11	15.91	5.32	0.14	1.82	4.20	4.58	2.41	97.94
	61.37	1.12	15.12	6.13	0.21	2.12	3.58	4.84	2.54	97.04
	58.19	1.38	15.76	7.58	0.25	2.80	5.11	4.89	1.69	97.67
	58.00	1.25	16.10	6.97	0.14	2.82	5.68	5.95	1.97	98.86
	53.20	1.35	16.15	7.34	0.17	3.99	7.42	4.17	1.38	95.17
	52.71	0.54	21.54	4.15	0.10	2.46	11.25	3.62	0.37	96.74
	52.42	1.06	16.14	9.26	0.19	5.38	9.39	3.03	0.61	97.48
	74.17	0.06	13.70	0.80	0.10	0.12	1.24	3.91	3.12	97.22
	72.59	0.05	13.06	1.33	0.02	0.20	1.18	3.61	2.86	94.91
	72.37	0.02	13.27	1.23	0.03	0.23	1.12	3.33	3.15	94.74
	72.28	0.07	12.95	1.15	0.03	0.22	1.18	2.92	3.06	93.93
	70.85	0.07	12.96	1.17	0.05	0.18	1.17	2.66	2.62	91.74
	69.79	0.32	13.67	3.31	0.14	0.21	1.48	4.68	3.43	97.05
	69.51	0.20	13.26	2.78	0.09	0.16	1.36	4.46	2.88	94.71
	68.65	0.41	13.56	4.01	0.12	0.29	1.79	4.21	2.49	95.53
	68.26	0.31	13.82	3.34	0.11	0.26	1.31	4.59	3.45	95.46
	66.93	0.59	15.53	3.80	0.12	0.70	2.26	4.46	3.02	97.41
Mean	*65.73*	*0.65*	*14.69*	*3.99*	*0.12*	*1.24*	*3.18*	*4.28*	*2.47*	*96.23*
SD	*6.55*	*0.49*	*1.85*	*2.26*	*0.05*	*1.36*	*2.71*	*1.10*	*0.84*	*1.83*
161cm (lower segment)	74.31	0.06	12.41	0.92	0.08	0.10	0.83	2.07	3.18	93.98
	74.17	0.06	13.70	0.80	0.10	0.12	1.24	3.91	3.12	97.22
	72.59	0.05	13.06	1.33	0.02	0.20	1.18	3.61	2.86	94.91
	72.37	0.02	13.27	1.23	0.03	0.23	1.12	3.33	3.15	94.74
	72.28	0.07	12.95	1.15	0.03	0.22	1.18	2.92	3.06	93.93
	70.85	0.07	12.96	1.17	0.05	0.18	1.17	2.66	2.62	91.74
	69.79	0.32	13.67	3.31	0.14	0.21	1.48	4.68	3.43	97.05
	69.51	0.20	13.26	2.78	0.09	0.16	1.36	4.46	2.88	94.71
	68.65	0.41	13.56	4.01	0.12	0.29	1.79	4.21	2.49	95.53
	68.26	0.31	13.82	3.34	0.11	0.26	1.31	4.59	3.45	95.46
	6.93	0.59	15.53	3.80	0.12	0.70	2.26	4.46	3.02	97.41
	63.00	0.86	14.90	5.05	0.13	1.31	3.58	5.75	1.49	93.06
Mean	*70.23*	*0.25*	*13.59*	*2.41*	*0.09*	*0.33*	*1.54*	*3.89*	*2.90*	*94.98*
SD	*3.13*	*0.25*	*0.83*	*1.41*	*0.04*	*0.33*	*0.71*	*0.98*	*0.50*	*1.64*

194cm	76.95	0.23	11.04	1.17	0.10	0.19	0.53	3.26	2.89	96.36
	69.87	0.73	13.63	2.91	0.10	0.20	1.01	4.71	3.74	96.88
	69.25	0.44	15.29	3.21	0.18	0.82	2.95	4.39	1.33	97.85
	68.84	0.32	15.06	3.44	0.09	0.77	2.94	4.22	1.33	97.00
	68.75	0.39	15.49	2.76	0.22	0.89	3.46	4.03	1.10	97.11
	68.33	0.81	13.91	4.54	0.20	0.77	2.32	4.25	2.64	97.78
	68.03	0.66	12.96	3.67	0.15	0.84	2.44	3.46	1.45	93.65
	67.94	0.55	16.98	1.75	0.04	0.14	4.53	4.94	1.28	98.16
	67.78	0.55	15.72	3.29	0.09	0.67	2.25	4.75	2.73	97.84
	67.10	0.98	14.24	4.82	0.05	0.98	2.75	4.49	2.54	97.96
	66.94	0.49	15.73	3.67	0.12	1.11	3.35	4.47	1.26	97.45
	66.93	0.58	15.53	3.17	0.13	0.76	3.15	4.66	3.09	98.00
	66.87	0.54	15.46	3.56	0.09	0.69	2.00	4.53	3.01	96.75
	66.75	0.39	16.15	2.11	0.09	0.67	3.58	4.33	1.33	95.40
	66.61	0.63	15.48	3.58	0.12	0.68	1.86	4.33	2.86	96.15
	65.79	1.27	14.72	2.80	0.08	0.70	2.77	3.81	1.34	93.26
	64.79	1.57	15.44	4.99	0.12	1.24	3.40	4.67	1.74	97.95
	64.33	0.44	16.97	3.28	0.12	0.98	4.29	4.77	1.15	95.33
	63.27	1.36	14.09	4.98	0.09	0.60	2.82	4.86	1.89	93.97
	60.67	0.68	19.08	4.08	0.14	1.03	6.63	4.57	0.74	97.63
	57.12	1.78	14.86	8.73	0.19	2.54	5.27	3.71	1.75	95.95
	55.78	1.03	18.54	3.55	0.11	0.93	9.48	4.96	1.20	95.57
	52.59	1.34	14.60	11.95	0.24	5.81	8.18	2.96	0.83	98.50
Mean	*65.71*	*0.77*	*15.26*	*4.00*	*0.12*	*1.04*	*3.56*	*4.31*	*1.88*	*96.63*
SD	*5.04*	*0.42*	*1.66*	*2.21*	*0.05*	*1.11*	*2.07*	*0.53*	*0.84*	*1.48*
212-232cm	70.87	0.36	13.67	3.19	0.14	0.22	1.32	4.28	3.73	97.76
	70.03	0.28	13.70	3.37	0.10	0.23	1.39	4.51	3.48	97.08
	69.92	0.29	13.84	3.32	0.12	0.22	1.40	4.81	3.65	97.57
	69.74	0.37	13.88	3.34	0.16	0.27	1.36	4.86	3.52	97.50
	69.44	0.29	13.80	3.65	0.13	0.27	1.37	4.53	3.64	97.13
	69.26	0.47	14.12	3.89	0.18	1.42	1.94	4.61	3.41	98.30
	69.02	0.29	13.85	3.48	0.14	0.28	1.48	4.46	3.45	96.44
	68.88	0.27	13.41	3.14	0.14	0.21	1.27	4.31	3.38	95.02
	68.80	0.30	13.62	3.53	0.16	0.26	1.37	4.35	3.40	95.78
	68.77	0.35	13.63	3.70	0.14	0.22	1.51	4.82	3.64	96.79
	68.69	0.36	13.66	3.42	0.13	0.19	1.35	4.19	3.26	95.25
	68.68	0.30	13.56	3.46	0.13	0.22	1.30	4.69	3.60	95.94
	68.51	0.37	13.77	3.62	0.13	0.26	1.53	4.36	3.58	96.11
	68.41	0.30	13.65	3.53	0.15	0.23	1.50	3.53	3.27	94.57
	67.95	0.28	13.61	3.39	0.16	0.25	1.52	4.13	3.52	94.81
	67.17	0.47	14.41	4.38	0.18	0.66	2.19	4.70	3.29	97.47
	66.82	0.34	14.31	3.94	0.12	0.63	2.54	4.66	3.20	96.56
	66.77	0.60	13.60	3.99	0.16	0.43	1.65	4.17	3.26	94.62
	64.74	0.67	14.42	5.32	0.19	1.31	3.50	4.70	2.66	97.51
Mean	*68.55*	*0.37*	*13.82*	*3.67*	*0.14*	*0.41*	*1.66*	*4.46*	*3.42*	*96.43*
SD	*1.37*	*0.11*	*0.28*	*0.49*	*0.02*	*0.35*	*0.54*	*0.31*	*0.23*	*1.14*

Analysis was performed at the Grant Institute, University of Edinburgh, using a Cambridge Instruments Microsan V with automated wavelength discursive spectrometers.

The probe operated at an accelerating voltage of 20kV, using a 15nA mean current and a 1μm bean and analysed two oxides simultaneously (10 seconds for each pair of elements analysed, leading to a total analysis time of 50s). The shards were not exposed to the beam during the machine's drive time, resulting the sample being exposed to the beam for 50s. 20s background counts were conducted on the first shard of each sample. The element counts for this shard were outwith the minimum of ten shards sampled for each population

Standards used were as follows

Na	Jadite ($NaAlSi_2O_6$)	Mg	Periclase (Mg))
Al	Corundum (Al_2O_3)	Si	Wollastonite ($CaSiO_3$)
K	Orthoclase ($KaSi_3O_8$)	Ca	Wollastonite ($CaSiO_3$)
Ti	Rutile (TiO_2)	Mn	Pure metal (Mn)
Fe	Pure Metal (Fe)		

Electron Microprobe Analysis (EMPA) results from analyses of shards from Laguna Boal

	SiO_2	TiO_2	Al_2O_3	FeO	MnO	MgO	CaO	Na_2O	K_2O	Total
59cm	59.17	1.45	16.10	5.49	0.14	2.14	4.54	5.00	2.23	96.25
	57.36	1.55	14.92	7.23	0.20	2.81	5.10	4.92	2.04	96.12
	56.51	1.41	11.99	9.68	0.33	7.42	6.10	3.59	1.36	98.40
	56.48	1.79	14.44	8.13	0.20	2.96	5.67	4.87	2.07	96.60
	55.62	1.60	16.87	8.10	0.19	3.14	7.84	3.71	1.33	98.38
	54.79	1.42	16.22	7.44	0.20	3.91	7.01	4.61	1.36	96.95
	54.61	1.76	16.07	8.25	0.18	3.04	7.78	4.51	1.34	97.53
	54.37	1.60	15.41	8.43	0.18	4.03	8.14	4.41	1.35	97.92
	54.28	1.45	16.23	7.47	0.18	4.32	7.51	4.55	1.35	97.35
	54.02	1.60	15.17	8.49	0.16	4.61	7.83	4.13	1.38	97.37
	53.88	1.43	16.25	7.80	0.15	4.43	7.87	4.18	1.28	97.25
	53.85	1.57	16.11	6.49	0.14	4.03	7.81	4.63	1.32	95.95
	53.63	1.44	16.04	7.56	0.17	4.31	7.79	4.23	1.29	96.46
Mean	*55.27*	*1.54*	*15.52*	*7.73*	*0.18*	*3.93*	*7.00*	*4.41*	*1.52*	*97.12*
1 s.d.	*1.60*	*0.12*	*1.20*	*0.98*	*0.05*	*1.24*	*1.17*	*0.42*	*0.33*	*0.78*
62cm	67.26	0.69	16.25	3.15	0.14	0.79	1.77	5.20	3.28	98.53
	66.97	0.64	16.08	3.14	0.14	0.80	1.84	5.09	3.33	98.03
	66.93	0.69	15.94	3.24	0.16	0.71	1.71	5.08	3.33	97.78
	66.85	0.72	15.98	3.17	0.12	0.79	1.85	5.06	3.21	97.74
	66.22	0.65	15.70	3.08	0.11	0.80	1.79	5.59	3.28	97.22
	65.79	0.63	15.92	3.28	0.14	0.74	1.69	5.35	3.25	96.78
	65.10	0.76	15.96	3.60	0.09	0.91	2.13	4.81	3.10	96.46
	65.01	0.70	15.64	3.21	0.13	0.79	1.79	5.15	3.11	95.52
	60.69	1.13	16.09	5.11	0.12	2.00	3.94	4.98	2.46	96.52
	56.34	1.32	16.48	7.42	0.18	3.57	6.36	4.76	1.81	98.23
	55.41	1.50	16.00	7.80	0.22	4.31	7.23	4.26	1.49	98.21
	54.43	1.43	16.36	7.69	0.20	4.01	7.26	4.39	1.40	97.17
	54.37	1.42	16.35	7.47	0.20	3.94	7.16	4.59	1.44	96.93
Mean	*62.41*	*0.95*	*16.06*	*4.72*	*0.15*	*1.86*	*3.58*	*4.95*	*2.65*	*97.32*
1 s.d.	*5.13*	*0.34*	*0.24*	*1.98*	*0.04*	*1.44*	*2.36*	*0.36*	*0.78*	*0.84*
67cm	63.42	0.94	16.19	3.67	0.14	1.09	2.14	5.23	2.83	95.63
	62.39	1.12	16.11	4.40	0.12	1.61	3.30	4.94	2.53	96.52
	62.12	1.11	15.84	4.49	0.19	1.62	3.06	5.20	2.42	96.06
	61.98	1.12	15.20	6.26	0.14	1.64	4.06	5.09	1.35	96.83
	59.62	0.96	14.93	7.25	0.17	1.84	5.26	5.00	1.23	96.27
	58.38	1.70	14.72	7.32	0.20	2.10	4.37	4.71	2.37	95.86
	58.24	1.68	15.80	7.07	0.20	1.71	5.09	5.09	2.01	96.90
	56.30	1.50	15.57	7.74	0.20	3.22	6.98	3.89	1.41	96.81
	54.71	2.05	13.71	10.07	0.24	3.33	6.69	4.21	1.81	96.81
	54.63	2.05	11.95	10.08	0.28	6.14	8.99	3.63	1.61	99.35
	54.37	1.79	15.21	8.74	0.17	3.26	7.32	4.15	1.54	96.56
	53.59	1.25	19.77	5.52	0.10	2.07	8.86	4.48	0.95	96.59
	53.55	0.97	10.43	15.36	0.44	11.36	3.13	3.54	0.82	99.57
Mean	*57.95*	*1.40*	*15.03*	*7.54*	*0.20*	*3.15*	*5.33*	*4.55*	*1.76*	*96.91*
1 s.d.	*3.53*	*0.39*	*2.13*	*2.98*	*0.08*	*2.68*	*2.17*	*0.59*	*0.61*	*1.15*

157cm	50.91	1.281	15.38	10.26	0.22	4.84	8.56	3.51	0.74	95 69
	52.06	1.37	15.62	9.51	0.19	4.94	8.53	3.68	0.72	96.61
	52.13	1.40	15.00	9.87	0.20	5.68	8.44	3.39	0.74	96.82
	52.29	1.24	16.09	9.14	0.28	5.18	8.82	3.43	0.68	97.13
	52.80	1.38	15.59	9.13	0.16	4.94	8.63	3.09	0.72	96.44
	52.77	1.43	15.3	9.57	0.13	4.78	8.35	3.64	0.73	96.69
	51.84	1.21	15.56	8.94	0.18	5.18	8.50	3.85	0.75	95.99
	52.53	1.41	18.30	8.55	0.14	3.25	9.71	4.18	0.43	98.49
	52.17	1.30	15.41	9.49	0.24	5.50	8.5	3.63	0.77	97.00
	51.94	1.31	15.73	9.4	0.14	5.35	8.43	3.60	0.73	96.63
Mean	*52.14*	*1.33*	*15.80*	*9.39*	*0.19*	*4.96*	*8.64*	*3.60*	*0.70*	*96.75*
1 s.d.	*0.52*	*0.07*	*0.88*	*0.46*	*0.05*	*0.63*	*0.38*	*0.27*	*0.09*	*3.35*
256cm (upper core segment)	65.81	0.55	14.38	4.15	0.10	0.73	2.42	3.91	3.16	95.20
	64.72	0.46	13.74	3.68	0.08	0.62	2.02	4.30	3.30	92.92
	61.26	1.03	15.38	5.73	0.18	1.10	4.12	4.82	2.13	95.76
	60.82	1.85	13.04	7.62	0.16	1.01	2.91	3.90	3.34	94.65
	54.86	2.03	14.23	10.59	0.24	4.46	6.33	3.51	1.62	97.85
	54.84	2.06	13.30	10.04	0.18	6.35	7.62	3.89	1.34	99.61
	54.15	1.96	14.68	10.17	0.19	3.96	6.85	4.06	1.68	97.68
	54.10	1.81	14.66	8.50	0.22	4.61	8.77	3.79	1.12	97.58
	53.54	3.74	11.80	12.36	1.29	2.99	6.41	3.54	1.63	97.30
	53.45	1.82	16.84	6.87	0.17	2.69	7.25	4.34	1.11	94.55
	53.42	2.08	15.27	10.54	0.24	3.39	7.33	3.84	1.50	97.59
	52.55	2.07	11.99	10.56	0.26	5.29	8.36	2.84	1.51	95.42
	52.32	1.51	16.41	7.20	0.18	3.17	9.37	3.67	1.14	94.97
Mean	*56.60*	*1.77*	*14.28*	*8.31*	*0.27*	*3.10*	*6.13*	*3.88*	*1.89*	*96.24*
1 s.d.	*4.58*	*0.79*	*1.46*	*2.59*	*0.30*	*1.77*	*2.37*	*0.46*	*0.80*	*1.77*
256cm (lower core segment)	68.58	0.33	13.99	3.33	0.13	0.28	1.53	4.36	3.59	96.10
	66.39	0.45	13.95	3.84	0.18	0.42	1.87	4.36	3.37	94.81
	65.68	0.54	15.41	5.05	0.16	0.68	2.94	4.59	3.14	98.18
	58.14	1.57	15.53	6.99	0.14	2.30	5.33	4.34	2.14	96.46
	58.10	1.39	17.66	6.01	0.15	1.49	6.19	4.94	1.49	97.40
	55.66	1.67	14.16	8.79	0.26	2.53	6.27	4.09	2.11	95.54
	54.90	2.55	14.54	10.21	0.24	2.35	5.77	3.96	1.72	96.23
	54.71	1.92	13.71	9.58	0.17	4.46	7.48	2.93	1.77	96.73
	54.57	1.65	15.51	8.13	0.23	4.78	8.97	4.36	0.93	99.14
	54.33	2.12	15.74	8.36	0.15	2.81	7.43	3.98	1.36	96.28
	54.04	2.35	13.24	11.39	0.21	3.44	6.50	3.61	1.43	96.22
	53.81	1.81	14.35	10.59	0.22	3.11	7.31	3.52	1.82	96.52
	53.19	2.16	12.09	9.69	0.32	6.07	10.45	3.09	1.07	98.13
	52.30	1.77	15.77	9.02	0.23	3.50	7.19	3.78	1.31	94.88
	50.88	1.52	14.89	11.37	0.21	5.95	9.68	3.55	0.94	99.00
	50.87	1.82	15.19	11.43	0.23	5.85	8.99	3.67	1.13	99.19
Mean	*56.63*	*1.60*	*14.73*	*8.36*	*0.20*	*3.13*	*6.49*	*3.94*	*1.83*	*97.05*
1 s.d	*5.32*	*0.63*	*1.24*	*2.55*	*0.05*	*1.85*	*2.52*	*0.52*	*0.82*	*1.35*

423cm (upper core segment)	65.72	0.71	16.06	4.09	0.13	0.48	3.43	5.24	2.31	98.18
	65.39	1.00	14.68	5.47	0.12	0.58	3.06	4.22	2.36	96.88
	65.02	0.82	14.04	5.25	0.10	1.08	2.59	4.95	2.41	96.26
	64.79	0.67	15.11	3.78	0.11	0.66	2.90	5.57	2.28	95.87
	64.44	0.61	16.99	3.65	0.08	0.57	3.93	5.76	1.97	98.00
	64.22	0.56	17.46	3.60	0.07	0.53	4.25	5.70	1.79	98.18
	63.87	0.77	14.16	5.94	0.16	1.62	3.09	5.04	2.10	96.73
	63.67	0.85	13.78	5.92	0.14	2.12	3.30	4.89	2.05	96.72
	63.50	0.62	16.92	4.03	0.11	1.05	4.02	5.49	1.72	97.44
	62.79	0.66	16.58	4.57	0.14	0.72	4.23	5.63	1.85	97.16
	61.95	0.52	18.25	3.66	0.11	0.82	4.77	5.83	1.40	97.30
	61.91	0.68	16.34	6.78	0.12	1.39	4.12	5.02	1.78	98.13
	61.60	0.72	17.30	4.35	0.09	0.79	4.74	5.77	1.56	96.90
	59.83	0.47	17.33	5.01	0.18	2.79	5.47	5.53	1.14	97.74
Mean	*63.48*	*0.69*	*16.07*	*4.72*	*0.12*	*1.09*	*3.85*	*5.33*	*1.91*	*97.25*
1 s.d.	*1.62*	*0.13*	*1.40*	*0.99*	*0.03*	*0.65*	*0.79*	*0.44*	*0.36*	*0.71*
423cm (lower core segment)	59.20	0.87	12.70	7.46	0.33	4.28	4.40	3.689	1.645	94.58
	62.64	1.08	14.30	5.34	0.13	1.20	3.22	4.67	2.09	94.66
	62.68	1.27	16.04	6.80	0.15	1.90	3.96	4.61	1.91	99.31
	62.70	0.86	16.75	4.90	0.15	1.02	4.44	5.05	1.67	97.53
	63.10	0.78	15.37	4.81	0.08	1.08	3.50	4.36	2.07	95.15
	63.12	0.81	15.22	4.84	0.14	1.31	3.59	4.60	2.12	95.75
	63.19	0.63	16.44	4.12	0.10	0.77	3.92	5.11	2.03	96.31
	63.45	0.73	15.68	4.23	0.14	1.04	3.78	4.19	1.88	95.11
	63.48	0.76	15.33	4.90	0.10	1.14	3.44	4.49	2.07	95.71
	63.62	0.93	14.48	4.89	0.14	0.84	2.94	4.85	2.39	95.08
	63.92	0.82	15.57	4.88	0.10	1.16	3.45	4.30	2.13	96.33
	64.35	1.07	13.70	5.24	0.16	0.81	2.62	4.59	2.47	95.00
	64.46	0.86	14.47	5.68	0.18	1.75	3.20	4.66	2.12	97.39
	64.68	1.00	12.39	7.75	0.27	2.78	2.79	3.90	2.32	97.87
	64.81	1.01	13.79	4.96	0.12	0.79	2.52	4.16	2.48	94.63
	65.03	0.95	12.77	5.77	0.17	0.77	2.24	4.40	2.73	94.79
	65.33	0.92	13.56	5.02	0.10	0.66	2.23	4.08	2.63	94.54
	66.60	0.85	13.14	4.98	0.17	0.92	2.35	3.80	2.70	95.51
	67.47	0.89	13.69	4.18	0.14	0.54	2.48	4.34	2.53	96.25
Mean	*64.33*	*0.87*	*14.52*	*5.07*	*0.14*	*1.08*	*3.09*	*4.43*	*2.27*	*95.81*
1 s.d.	*1.27*	*0.11*	*1.26*	*0.82*	*0.04*	*0.52*	*0.65*	*0.36*	*0.30*	*1.02*

APPENDIX 2

Plates showing examples of the chironomid taxa encountered in this investigation

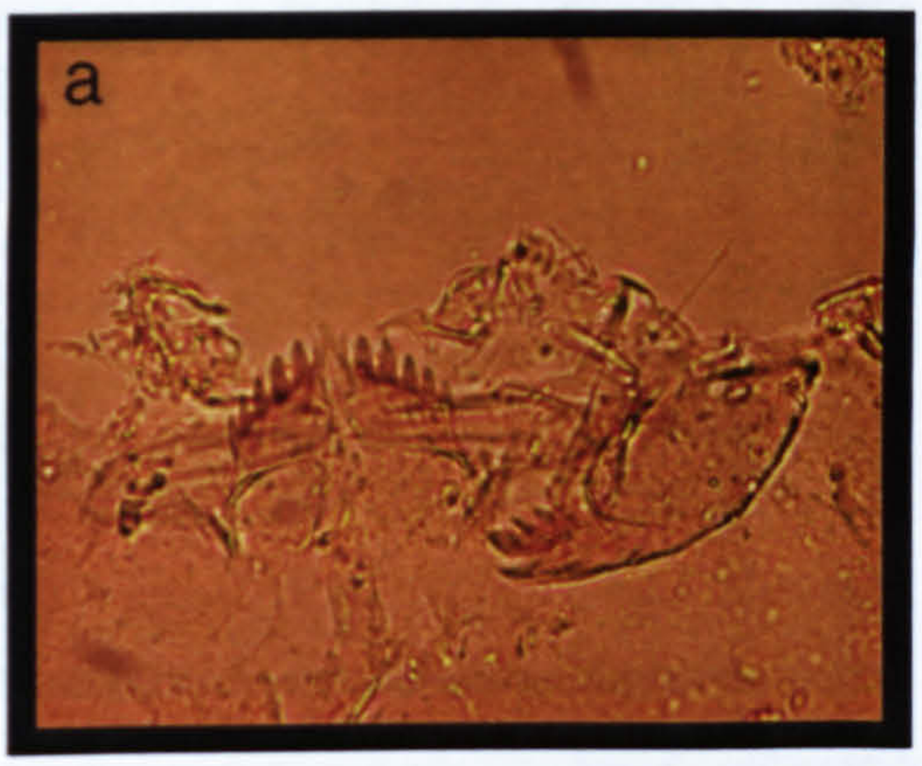

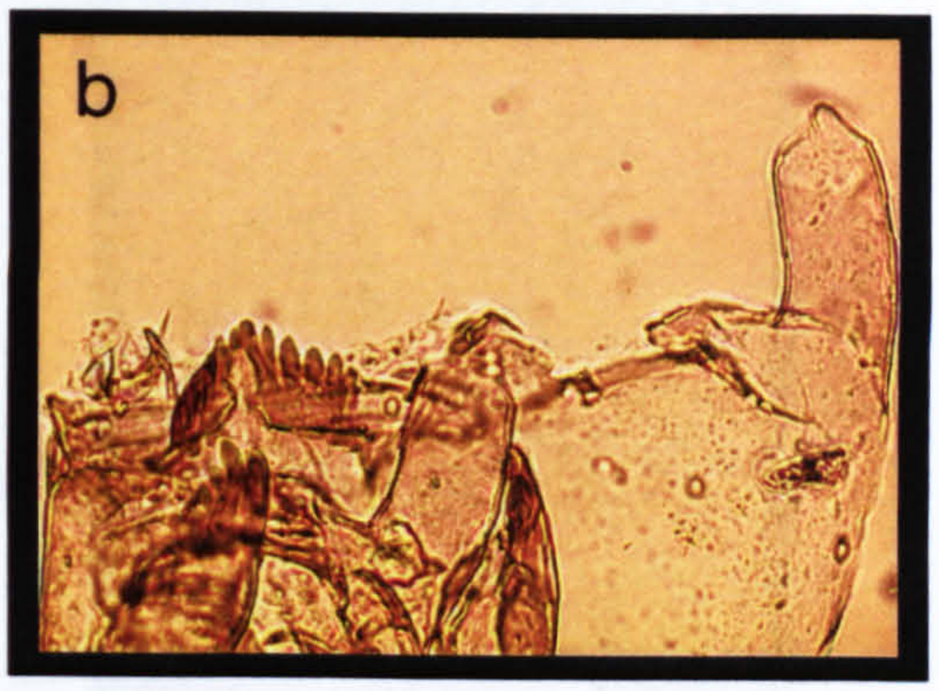

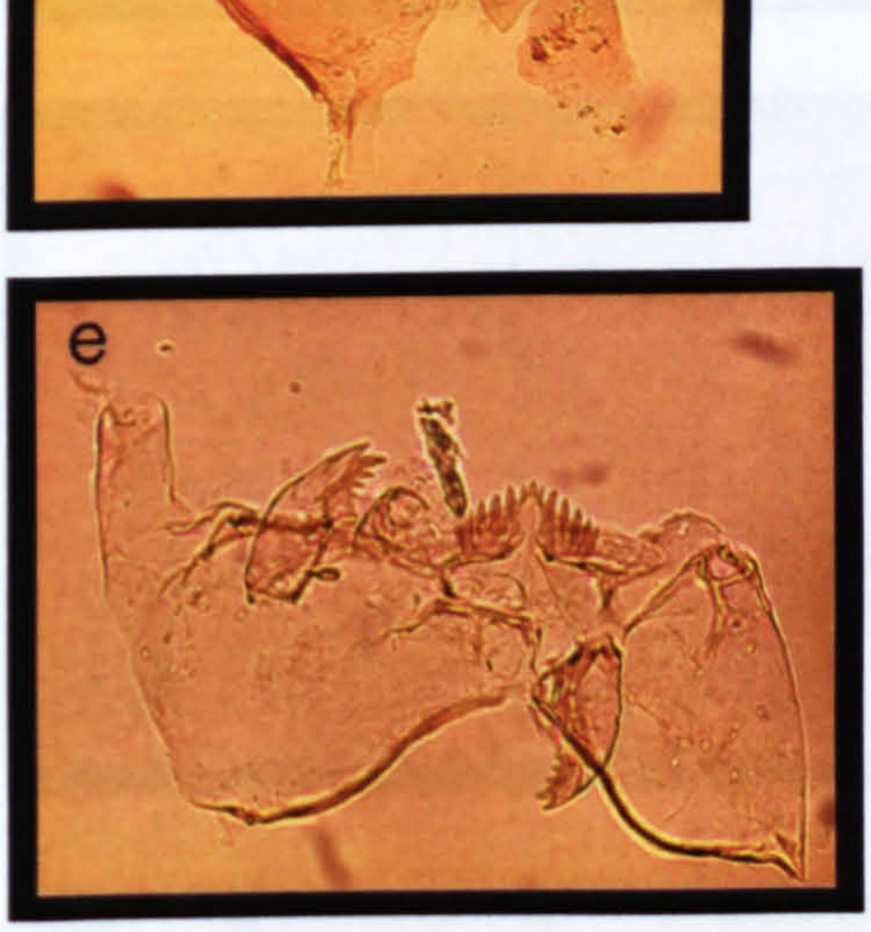

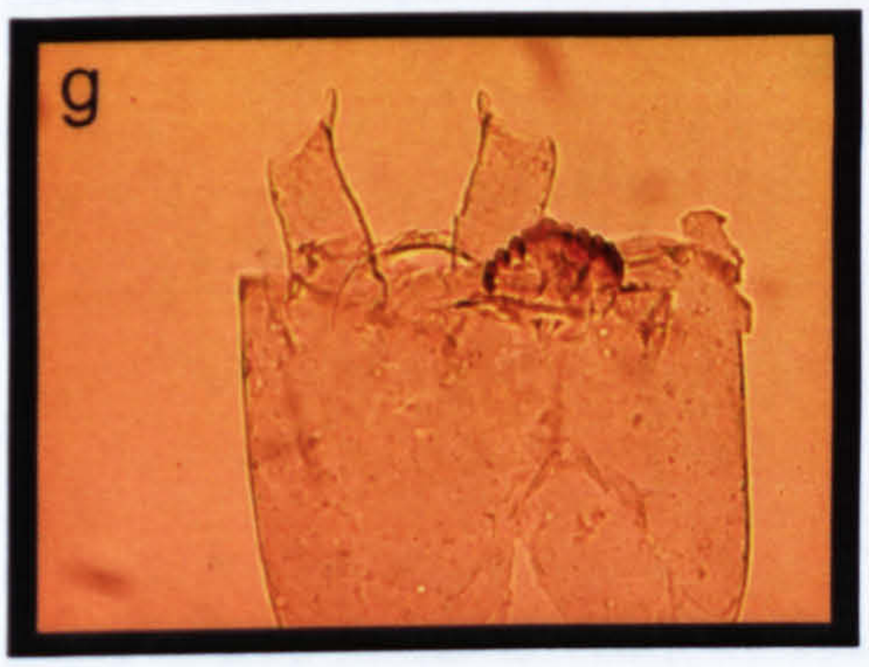

a Tanytarsini Taxon C (showing mentum and mandible), **b** Tanytarsini Taxon B **c** Tanytarsini Taxon C, **d** Tanytarsini Taxon E, **e** Tanytarsini Taxon D, **f** Tanytarsini taxon E, **g & h** Tanytarsini Taxon C (g showing post occipital plate, h showing mentum and mandibles)

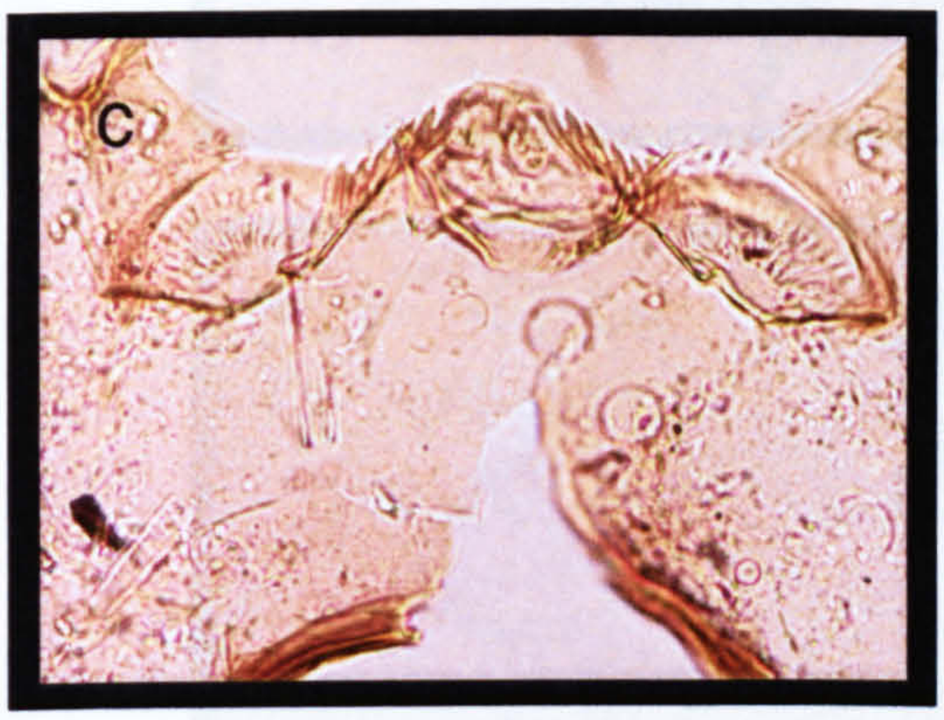

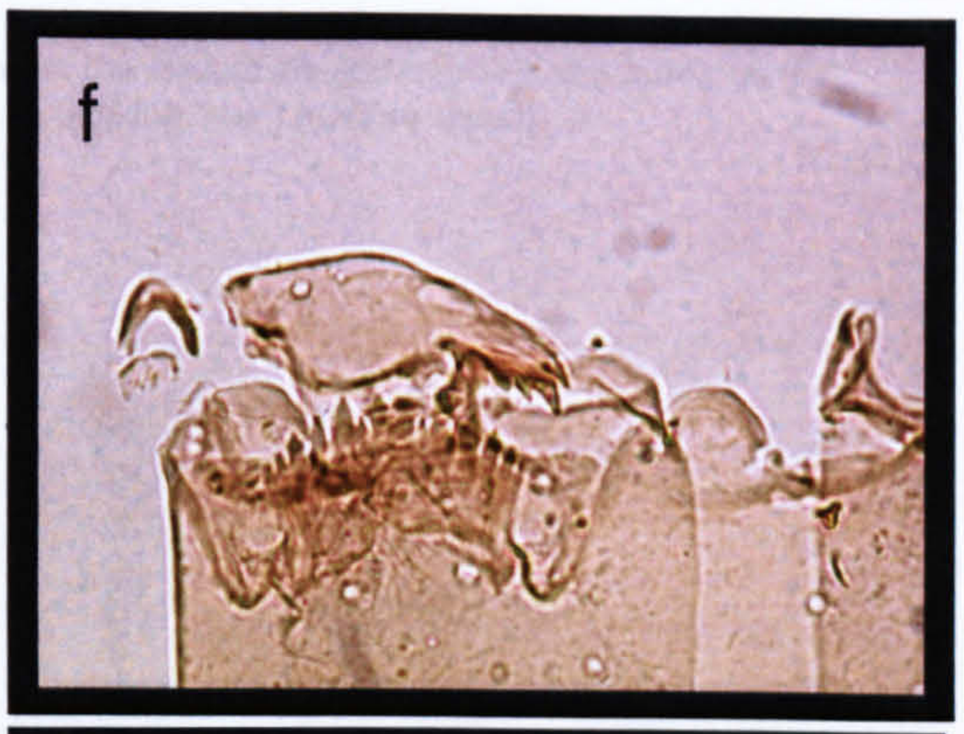

a *Chironomus*, **b** *Cryptochironomus*, **c** *Cryptotendipes*, **d** Chironomini larvula, **e** *Dicrotendipes*, **f & g** *Lauterborniella* (f showing mandible), **h** *Microtendipes* Taxon A

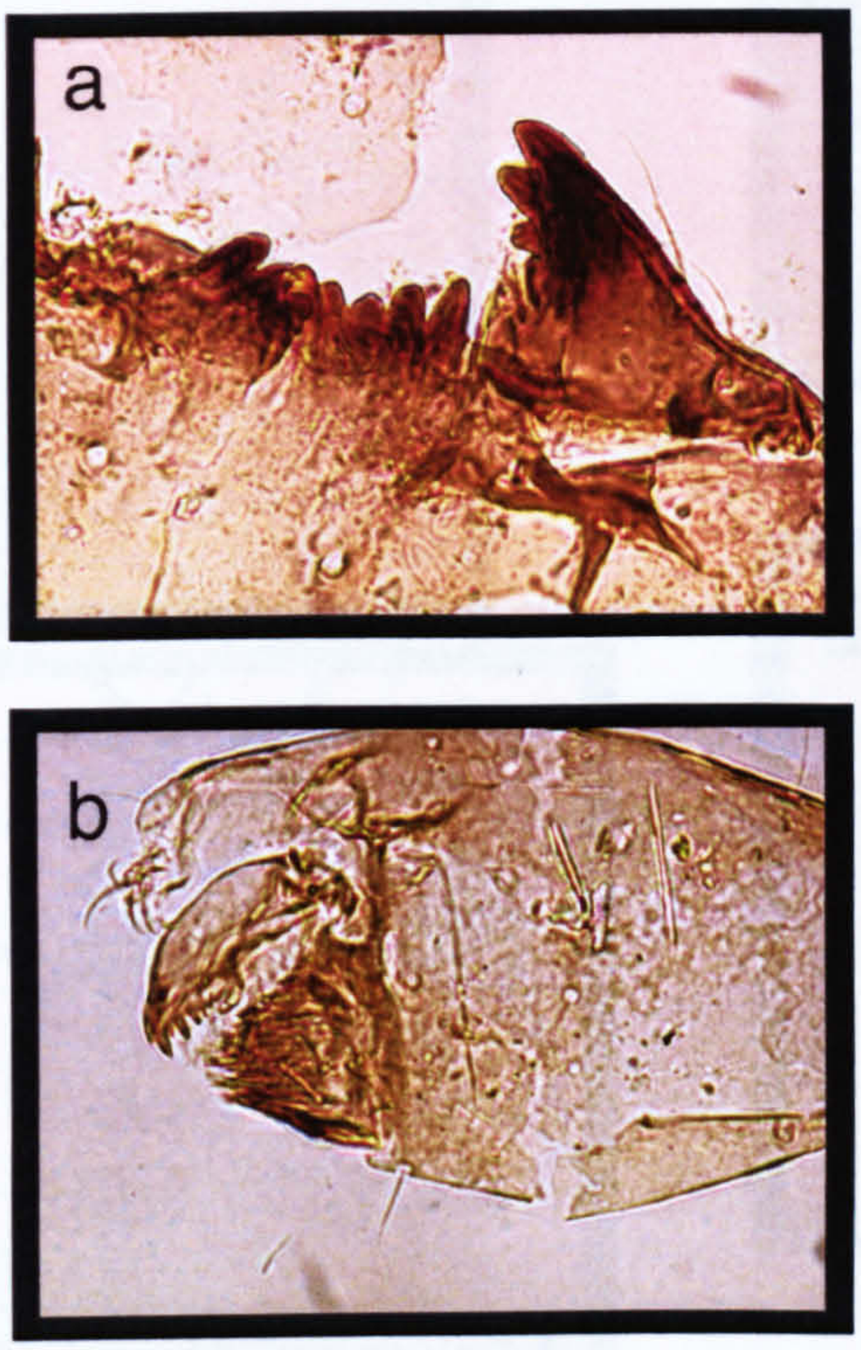

a *Stenochironomus*, **b & c** Podonominae (b shows the mandibles and hair-like structures on the ventral side of the mentum, c shows the mentum (lacking 'hair') in more detail)

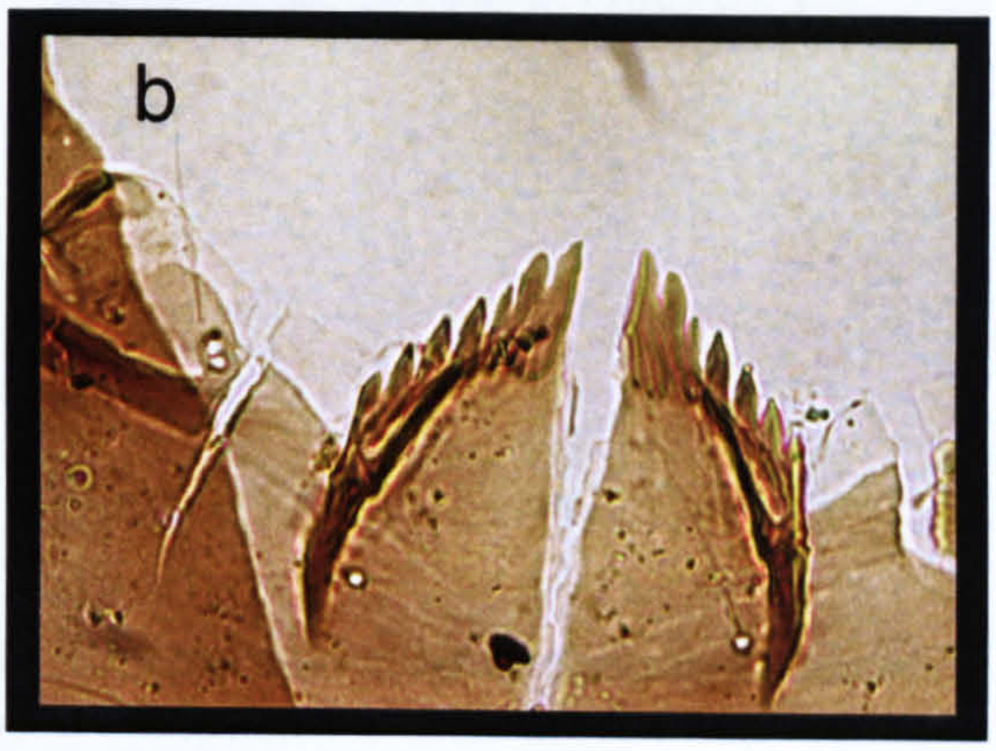

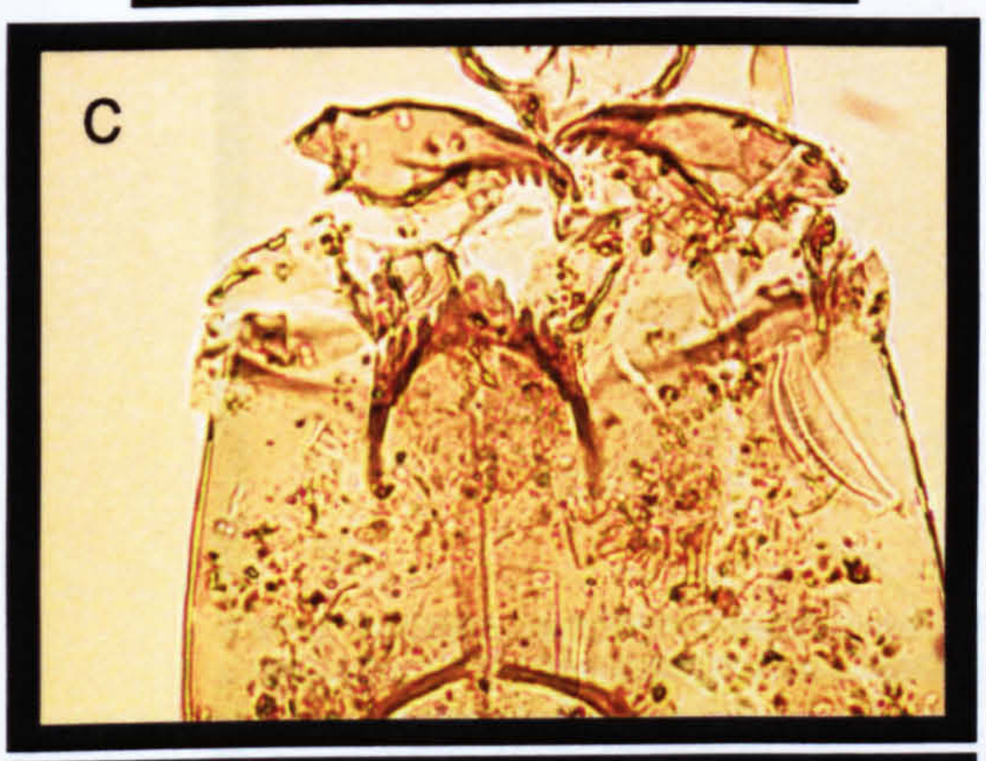

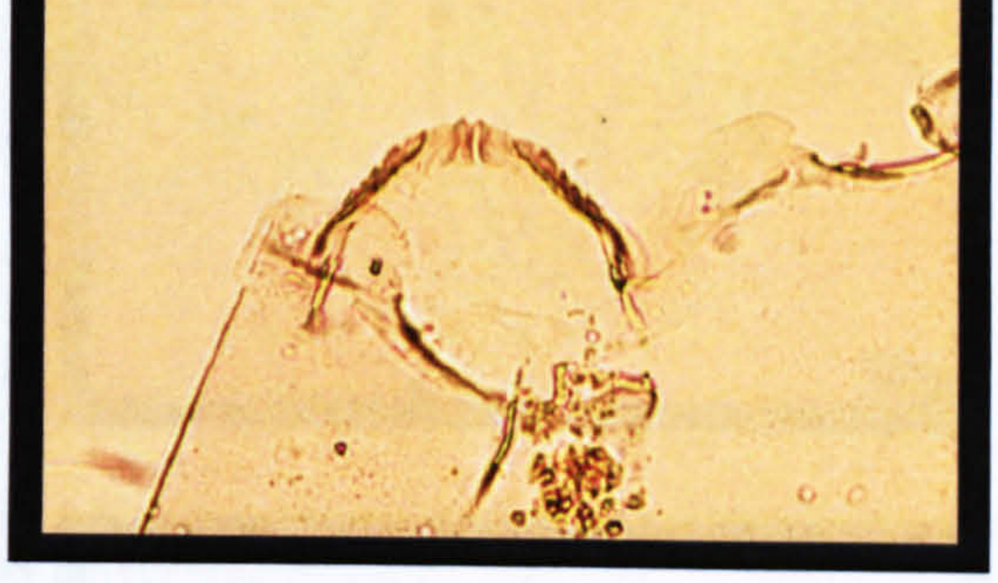

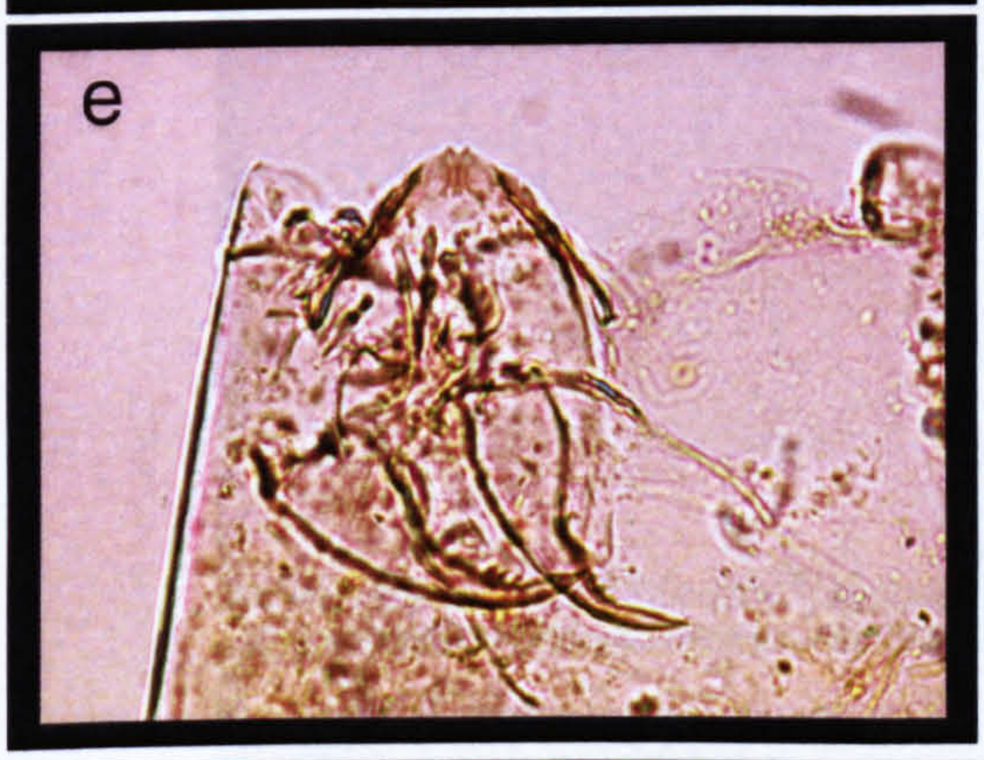

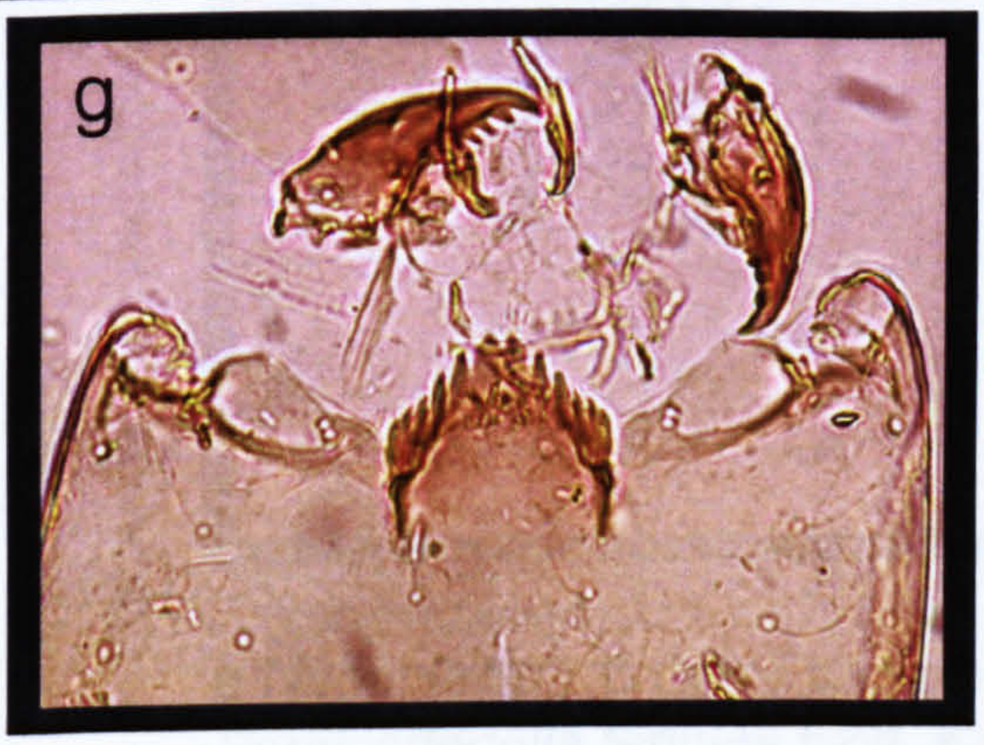

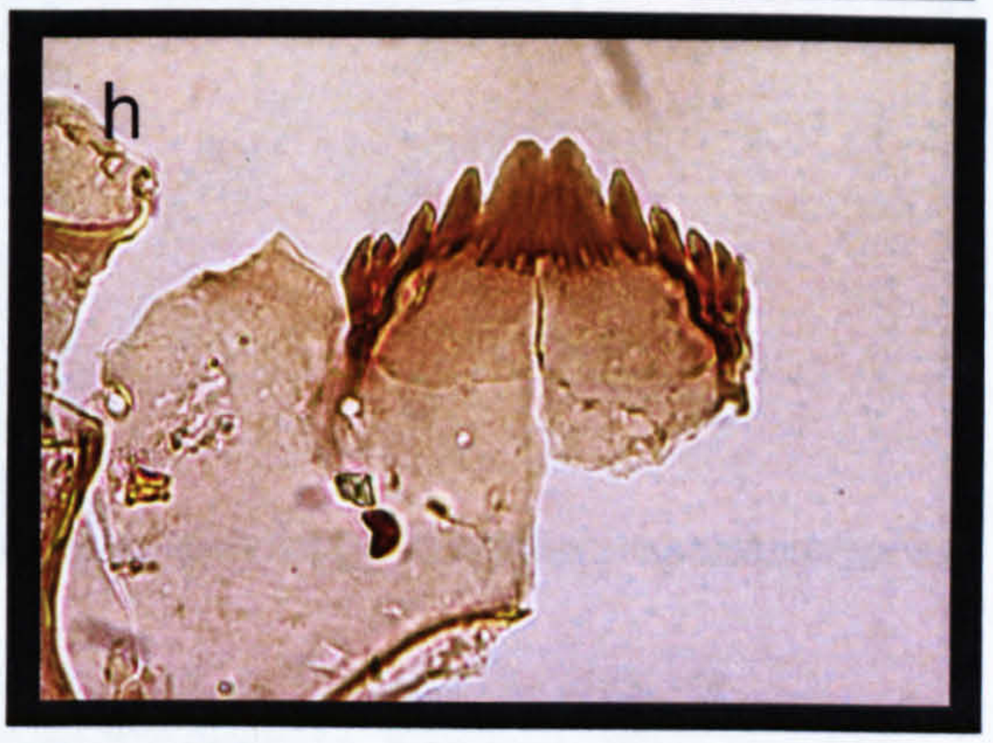

a *Corynoneura* / *Thienemanniella*, **b & c** *Cricotopus* / *Orthocladius* (c. shows mentum in detail), **d & e** *Orthocladius* (Cranston), **f** *Gymnometriocnemus*, **g** *Paralimnophyes* / *Limnophyes* Taxon A, **h** *Paralimnophyes* / Limnophyes Taxon B
NB. *Paralimnophyes* / *Limnophyes* Taxon A and *Paralimnophyes* / *Limnophyes* Taxon B were differentiated by the position of the setation. In Taxon B the seta is located directly at the base of the ventromental plates.

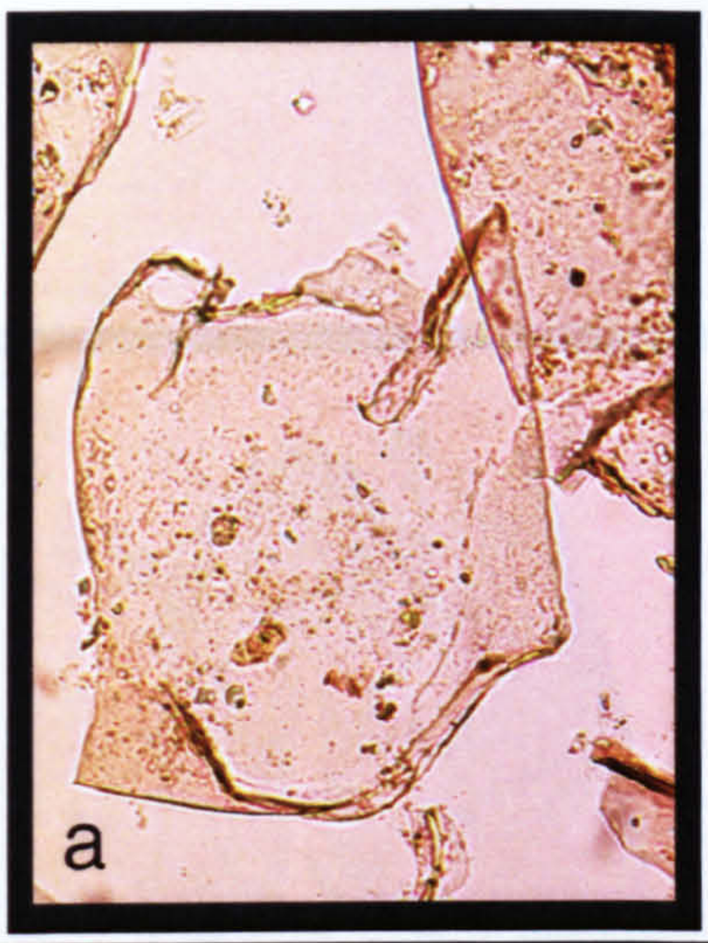

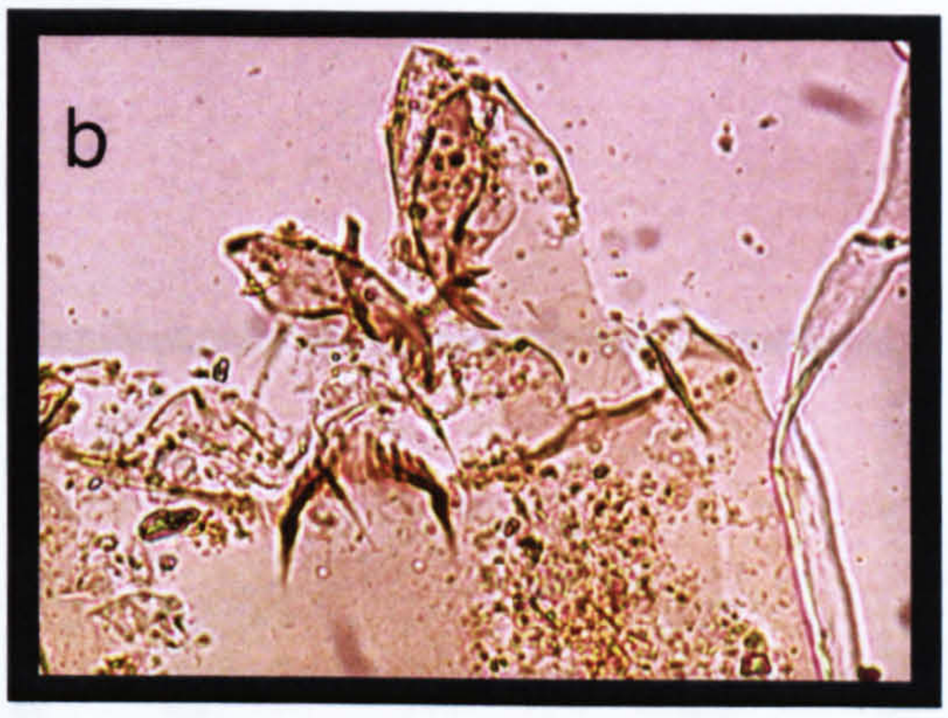

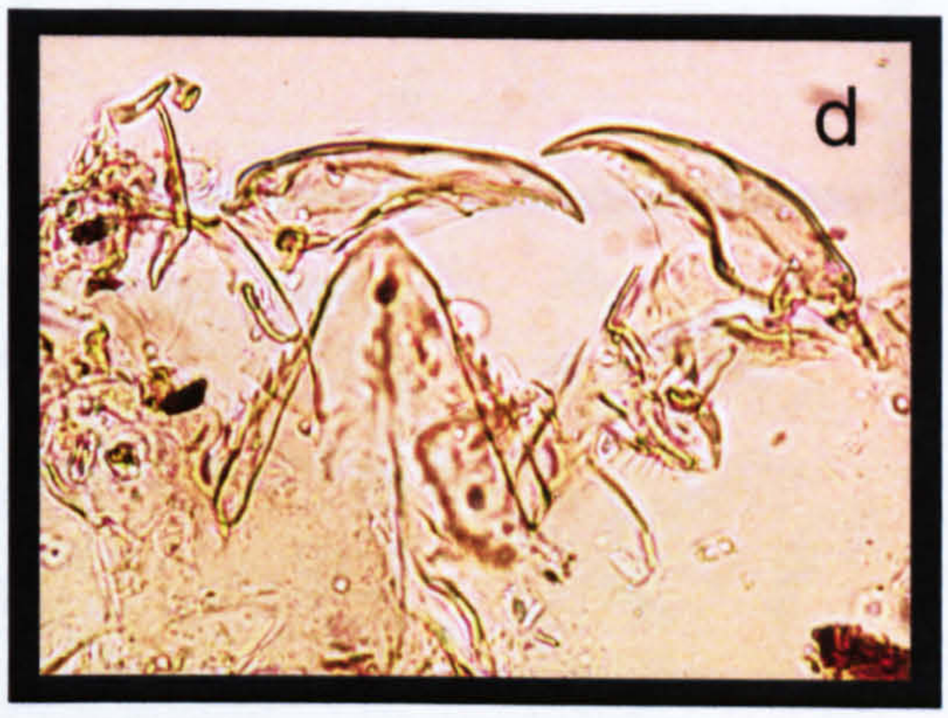

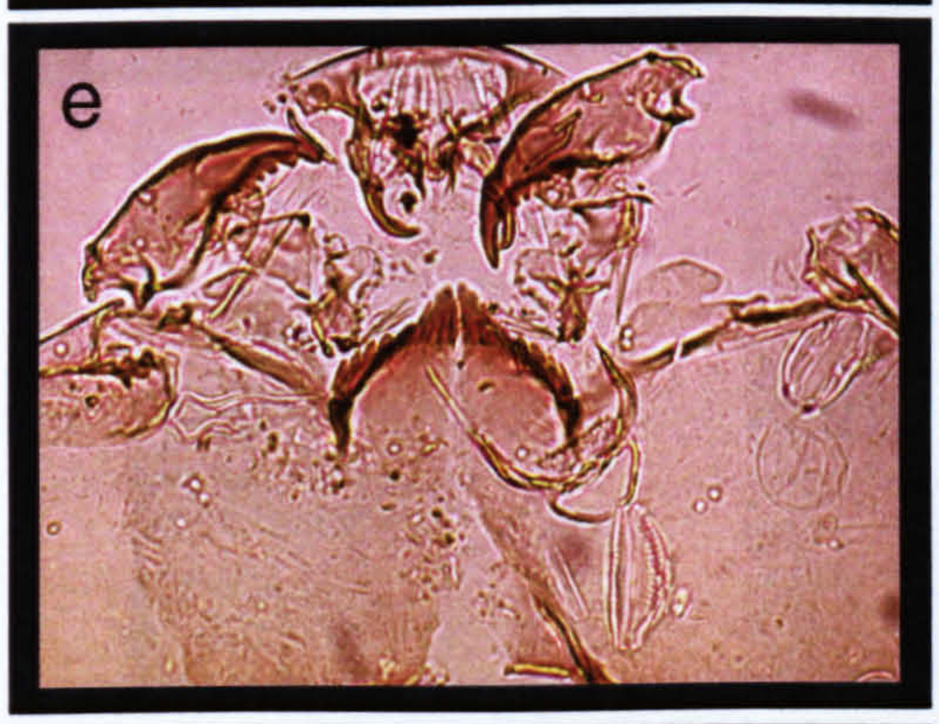

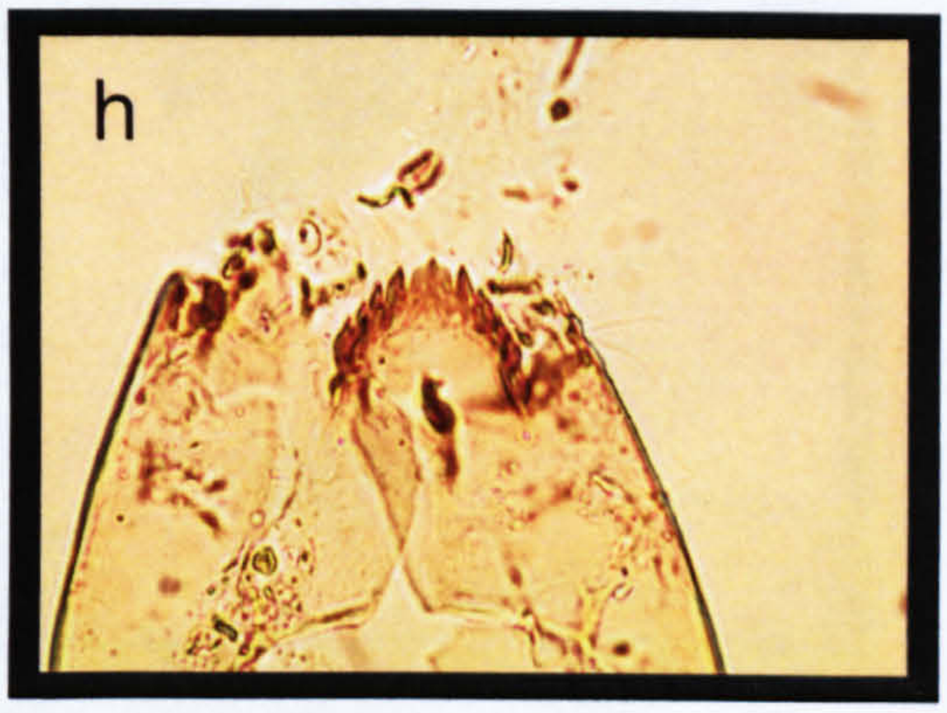

a *Nanocladius,* **b** Orthocladiinae early instar, **c** *Parakiefferiella,* **d** *Parakiefferiella fennica type,* **e** *Parapsectrocladius,* **f** *Parasmittia,* **g** SO4 (Cranston), **h** *Smittia*

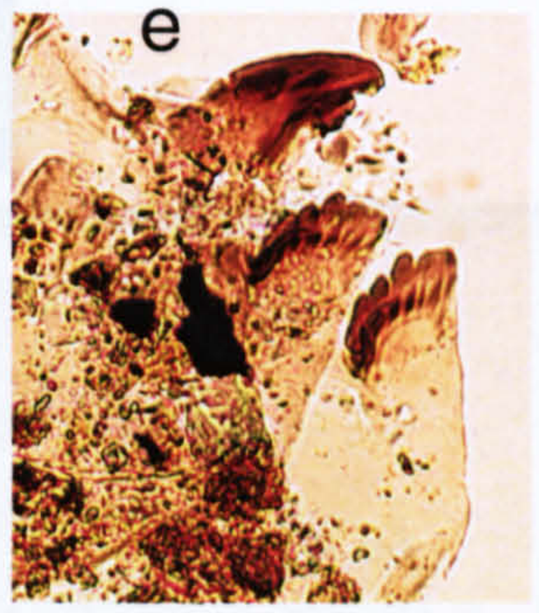

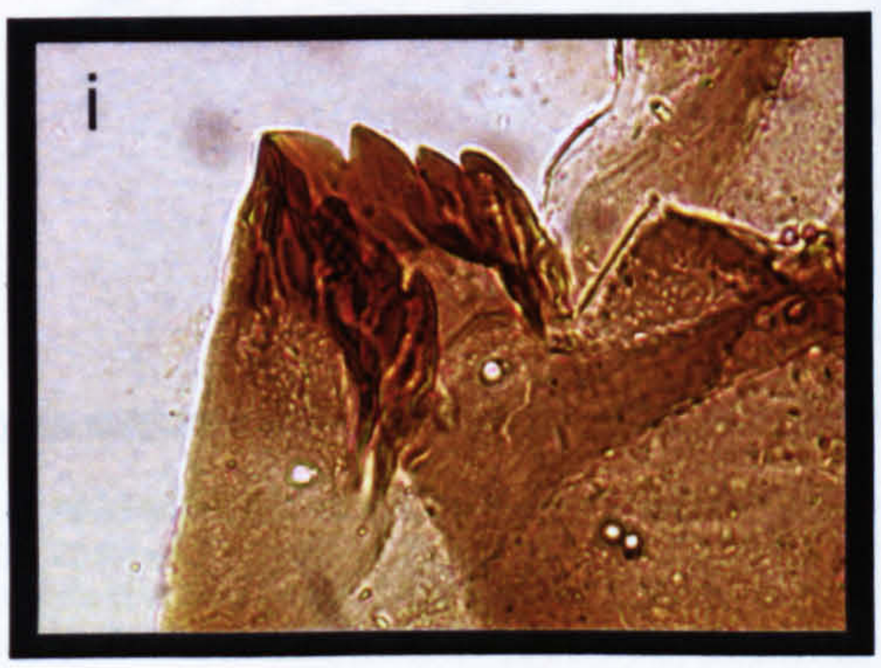

a *Tventia / Eukiefferiella,* **b** Orthocladiinae Taxon A, **c & d** Orthocladiinae Taxon C, **e, f, g, h & i** Orthocladiinae D, **j** Orthocladiinae Taxon B,

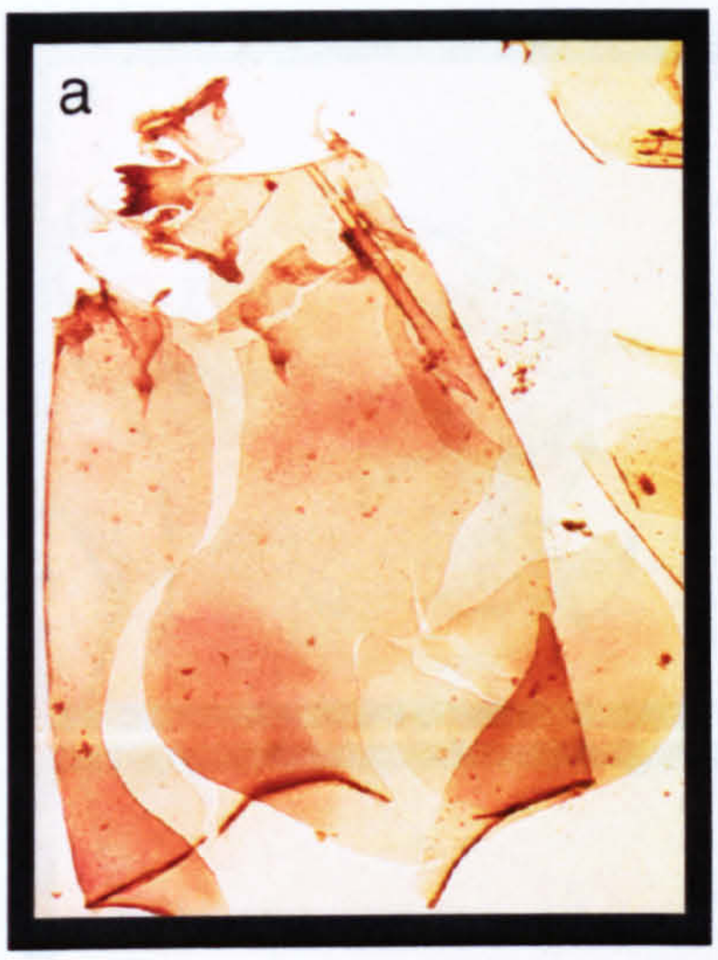

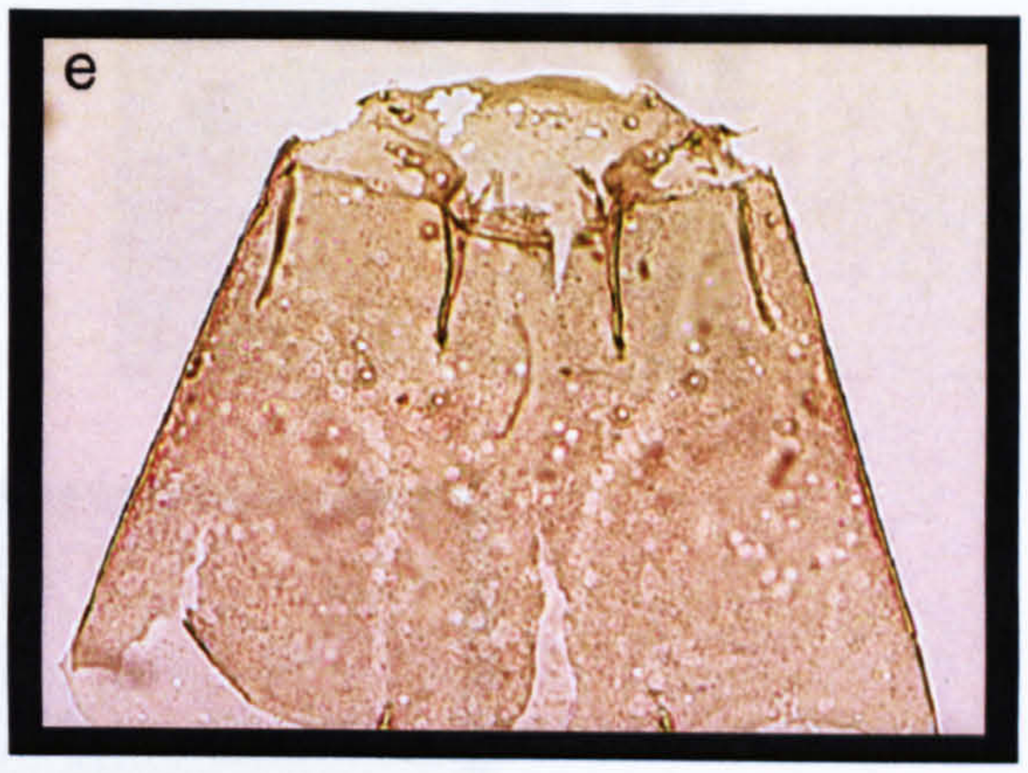

a, b & c *Ablabesmyia* (a shows the full head capsule, b shows ventral setation, **c** shows ligula and paraligula), **d & e** *Clinotanypus* (d shows ligula and paraligula in detail and e shows setation on the head capsule), **f & g** Labrundinia (f shows mouth-parts in detail, g shows the whole head capsule, with teeth-markings towards the base of the head capsule)

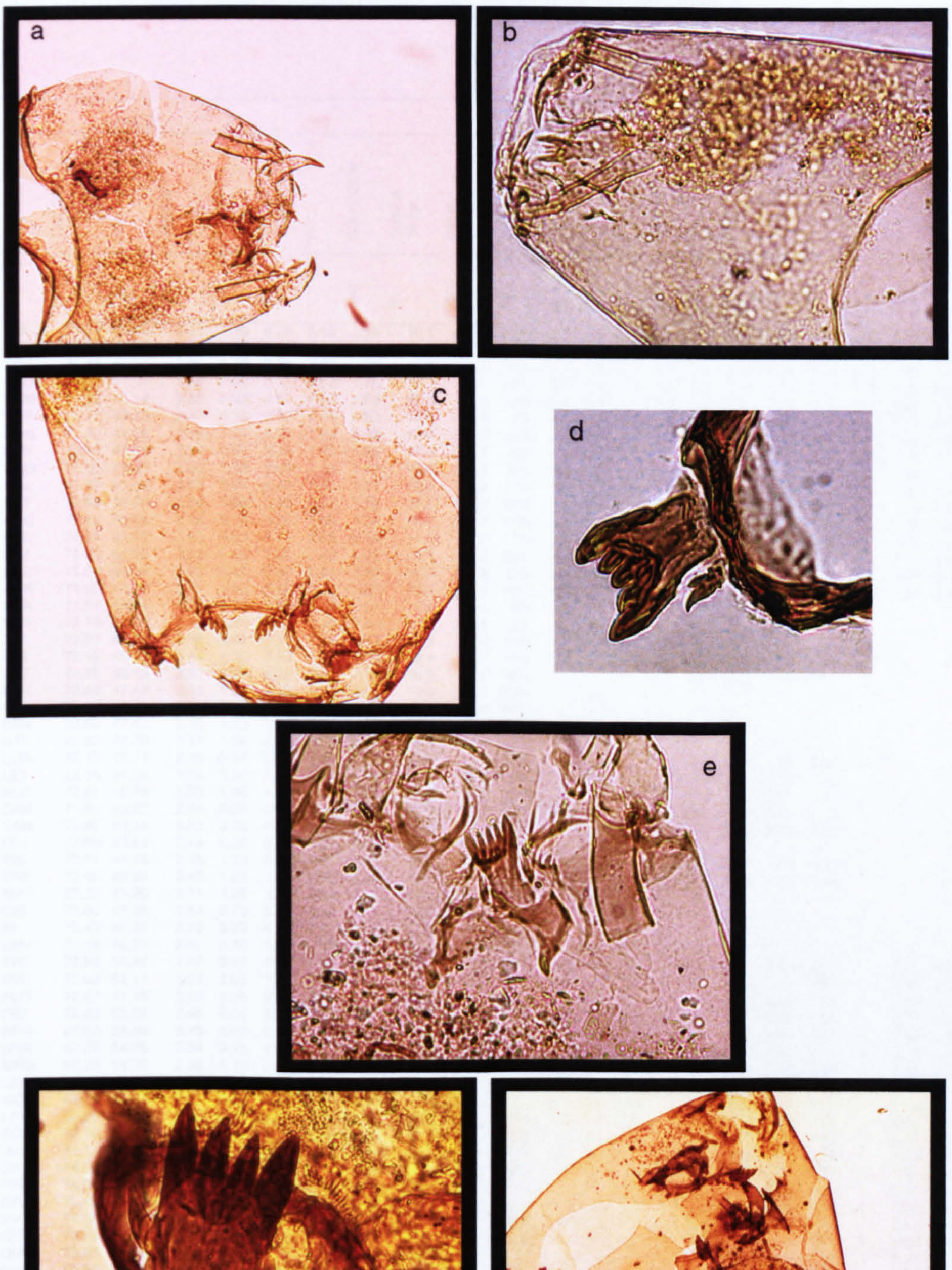

a *Procladius* **b** Chironomini early instar, **c & d** Tanypodinae Taxon B (b & c shows the same specimen, the mouth-parts of which had become detached from the main head capsule, **e** Tanypodinae Taxon C (showing ligula and paraligula), **f & g** Tanypodinae Taxon D (f shows ligula in detail, g shows the whole head capsule of the same specimen)

APPENDIX 3

Modern Environmental variable measurements after logarithmic transformation

		FIELD											WATER											
Site Number	Code	Dec long	Dec Lat	Altitude	Depth	Secchi Depth	pH	Conductivity	Surface temp	Basal temp	LOI		TP	TN	Si	N-NH4	Ca	Mg	Na	K	T Alc	Cl	SO_4	N-NO3
		(° N)	(°E)	(m)	(m)	(m)		(µs)	°C	°C	(%)		µg l-1	mg l-1	mg l-1	µeq l-1	µeq l-1	µeq l-1	µeq l-1	µeq l-1	µeq l-1	µeq l-1	µeq l-1	µeq l-1
1	PIR	71 81	40 79	2 87	1 30	6 20	5 93	1 56	16 1	14 0	12%		3 6	0 7	2 8	0 5	3 5	3 78	2 50	2 27	3.87	2 32	2 18	1 72
2	BW	71.71	40 70	2 90	0 95	2.80	4 05	0.03	20 5	17 9	26%		3 7	1 3	3 2	2 5	3 4	3 22	2.25	1.61	2 79	1.48	0 52	0.00
3	TBL	71 44	41 16	2 88	1 02	3 80	7 75	1.97	18 3	18 5	28%		3 7	1 6	2 7	1 7	3 6	3 41	2 25	1.13	2 88	1 67	1 77	0 00
4	ESC	71.44	41.16	2 88	0 86	5.18	7.53	1.80	19 3	18 3	24%		3 7	1 4	2 8	1 5	3 5	3 18	2.11	1 07	2 76	1 47	1 29	0 00
5	MOR	71.52	41 14	2 88	0 93	4 80	7 67	1.89	18 6	18 5	22%		3 8	1 4	2 7	2 9	3 6	3.30	2 16	1.15	2 78	1 55	2 08	0 00
6	VER	71 72	40 69	3 17	0 18	0 92	7 48	1.53	15.5	15 4	8%		4 2	1 4	1 9	0 8	3 1	2 99	1 92	1.02	2 48	0 91	0 36	0 00
7	FON	71 30	41 36	2 88	1 24	6 10	7 66	0 88	17 6	12 0	28%		3 7	1.1	2 8	2 5	3 2	2 94	1 97	1.11	2 51	1 21	0 85	0 00
8	HES	70.74	41 37	2.86	0 92	8 30	7 39	1.66	17 7	17 7	9%		3 6	1 1	2.7	2 5	3 4	2 95	1 84	1 02	2 58	1 03	1 75	0 00
9	MOS	71.62	41 49	2.90	1 30	7 60	7 56	1.73	18 4	17 4	9%		3 8	1 2	2 6	2 7	3 4	2.94	1 80	1.01	2 58	1 01	1 82	0 00
10	GAL	71 62	41 50	3 00	0 93	6 00	7 02	1 51	13 3	15 2	14%		3 9	0 9	2 8	1 0	3 0	2 90	2.00	1 07	2 44	1.47	0 97	1 76
11	PAT	71 00	40.76	2 99	0 86	5 10	6 97	1 52	16 1	15 1	24%		3 6	0 9	2 9	0 6	3 0	2 90	2 00	1 07	2.45	1.44	0 91	1 15
12	ANG	71 66	40 86	2 89	0.74	2.00	7 55	1 24	19 4	19 7	24%		4 2	1 3	3 2	3 5	3 5	3.56	2.32	1 43	2 95	1 56	1 67	0 00
13	HUL	71 51	41 64	2.92	0 83	6 70	8.85	2 10	14 3	17 7	47%		3 9	1 0	2 7	0 8	3 9	3.32	1 97	0 86	3 05	0 45	1.91	0 00
14	LEZ	71 46	40 99	2 83	0 85	7 00	8 48	2.02	19 1	17 5	29%		4 0	1 1	2 5	0.6	3 6	3 39	2 46	1 47	2 96	1.55	1 35	0 00
15	RED	71 56	40 99	2 92	0 88	1 90	7 04	1.80	16 4	15 8	22%		4 0	0 7	3 2	3 1	3 3	3.15	2.30	1 49	2 74	1 47	0 32	0 00
16	MER	71 57	41.00	2 91	1 30	5 20	7 29	1 69	18 3	9 2	30%		4 4	1 2	2 8	1 2	3 1	3.11	2 26	1.39	2 63	1 61	0 32	0 00
17	LGA	71 57	40 04	2 92	1 23	5 50	7.42	1 69	17.4	16 5	6%		-	-	-	-	-	-	-	-	-	-	-	-
18	COF	72 74	46.21	2 75	1 24	7 00	7 38	1 59	12 8	12 8	6%		-	-	-	-	-	-	-	-	-	-	-	-
19	X-	71 91	45.83	2 86	0 98	3 30	7 82	1 86	12 9	12 8	20%		-	-	-	-	-	-	-	-	-	-	-	-
20	PIG	72 12	45.15	2 44	1 20	7 10	7.23	1 50	12 8	12 2	16%		-	-	-	-	3 3	2 49	1 91	1 04	-	-	-	-
21	FUT	71 86	43 19	2 51	1 00	4.70	7 52	1 70	16 2	14.6	30%		-	-	-	-	3 5	2.75	1.97	1.35	-	-	-	-
22	LAR	72.80	47.48	2 43	1 24	9.60	7 80	1 83	13 5	13 2	15%		-	-	-	-	-	-	-	-	-	-	-	-
23	GUA	72 40	47.11	2 64	0 85	4.00	8 58	2.70	14 8	14 8	59%		-	-	-	-	-	-	-	-	-	-	-	-
24	ESM	72.60	47 43	2 46	1.23	6.30	8 09	1.99	15.1	15 0	10%		-	-	-	-	-	-	-	-	-	-	-	-
25	ATR	72.22	45 79	2 57	1 02	3 30	7 78	1 85	14 3	14 0	22%		-	-	-	-	-	-	-	-	-	-	-	-
26	LOB	72.33	44 77	2.36	0.85	5.65	6.38	1.30	14 0	11 7	26%		-	-	-	-	2.9	2 21	1 82	0 48	-	-	-	-
27	LET	73.16	41 58	1.86	0 40	2.05	6.01	1 29	19 0	18 8	56%		-	-	-	-	2.7	2.35	2 12	1.13	-	-	-	-
28	BLC	72.61	42.75	1.99	1 46	4 82	6 73	1.26	14 2	12 7	33%		-	-	-	-	2 9	2 44	1 97	1.15	-	-	-	-
29	CAS	71 81	45 67	2 84	0 93	8 50	7.99	1 95	12 2	12 1	24%		-	-	-	-	3 6	3.10	2 62	1.72	-	-	-	-
30	TAM	71.90	43 34	2.62	0 70	4 40	6 91	1 73	12 6	12 3	36%		-	-	-	-	3.5	2 78	2.05	1 25	-	-	-	-
31	FOI	72 09	45 64	2.44	0 66	2 60	8 09	1 34	16 3	15 3	33%		-	-	-	-		-	- -	-	-	-	-	-
32	RIS	72 51	44 38	2 15	1 23	6 10	7 22	1 51	13 5	12 5	12%		-	-	-	-	3 3	2 55	1 89	1 31	-	-	-	-
33	TRE	72 48	46.84	2 42	1 08	1 50	8 17	2 49	17 6	17 4	17%		-	-	-	-	4 3	3 56	2.84	2 24	-	-	-	-
34	MAN	72 15	43 30	2 11	1 29	3 60	6 84	1 11	15 0	14 9	28%		-	-	-	-	-	-	-	-	-	-	-	-
35	CIS	72 60	47 28	2 64	0 78	5.50	8 64	2 71	14 6	14 5	25%		-	-	-	-	-	-	-	-	-	-	-	-
36	EI	72 43	47 24	2 76	0 89	4 10	8 31	2 14	13 6	13 7	13%		-	-	-	-	-	-	-	-	-	-	-	-
37	ENV	72 02	46.20	2 67	0 70	1 50	7 89	2 35	13 4	13 1	21%		-	-	-	-	-	-	-	-	-	-	-	-
38	TWI	72 96	51 18	1 97	0 93	1 60	8.20	2 72	11 1	11 3	16%		1 4	1.8	2.8	-	4 3	4 48	3 35	2 11	-	3.01	3 05	1.35
39	AVE	72.92	51 11	2 07	1 02	1.00	8 68	2 65	12 6	12 3	43%		1 4	2.0	2 9	-	4 2	3 46	3 52	1 64	-	2 61	2 56	1 10
40	FLO	72 83	51 18	2 06	1 28	2 20	8.52	2 66	12 1	11 9	33%		1 2	1.8	3 0	-	4 4	3.35	3 38	1 81	-	2.75	3 06	1 29
41	PRI	72.80	51 04	2 46	0 95	1 30	9.04	3 18	11 3	9 3	29%		1 5	2 0	3 0	-	4 3	3 71	3.90	2 86	-	3 12	3 53	0 98
42	BRO	67 50	54 99	0.70	0 60	0 90	8 51	2 06	13 3	11 4	48%		1 3	1 6	2 8	-	4 1	3 15	2.96	1.49	-	2 96	2 38	0 86
43	BNA	67 25	54 76	2.34	0.45	1 40	7 31	1.66	11.8	11.9	69%		1 1	1 6	0 8	-	3 1	3.78	2.48	1 31	-	2 33	1 40	1 30
44	MRG	67 25	54 76	2.08	1 15	4 30	8 05	2 18	12.3	12 3	8%		0 8	1 0	2 4	-	4 1	0.76	2.42	0 89	-	2.15	2.72	1 05
45	LNF	67 19	54 99	1.51	0 85	0 70	7 41	2.28	11 3	11 2	37%		1 4	1 7	1 7	-	3.8	4 19	3 04	1 41	-	3 06	0 72	1 59
46	MOA	66 79	55 04	1 23	0 57	0 65	7.04	2 27	9 5	8 6	53%		1 4	1 9	1 5	-	3.5	3 33	3 05	1 36	-	3 06	0 72	1 24
47	LAV	66 95	54.98	1.53	0 51	1 35	8 32	2 38	10 6	10 2	34%		1 2	1 5	1 6	-	4 2	3 53	2 84	1 25	-	2.68	2 80	0 74
48	TOL	67 19	54 68	1.51	0 51	3 20	7 60	2 02	12 3	11 1	47%		1 0	1 4	1 7	-	3 9	4 05	2 48	1 19	-	2 26	2 32	0 67
49	Vicl	74 11	45 32	0 78	0 76	3 00	5 78	2.03	23 7	-	23%		-	-	-	-	3 5	2.69	2 22	0 78	-	2.14	1 15	-
50	DII	74 22	45 33	1.92	0 69	3 00	6 10	1 62	22 7	14 6	22%		-	-	-	-	0 8	2 59	2 12	0 58	-	1 98	0 82	-
51	PIII	74 07	45 39	1 26	0 21	1 29	6 00	1.79	20 8	20 3	38%		-	-	-	-	3.6	2 72	2.24	0 83	-	2 07	1 12	-
52	GIV	73 81	45 45	1.63	0 52	1 74	6 20	1 79	16 3	12 6	42%		-	-	-	-	3 7	2 62	2 06	0 67	-	1 80	1 24	-
53	VV	74 08	45 48	1 68	0 88	3 32	6 40	1 79	16 7	13 4	28%		-	-	-	-	3.6	2.56	2.08	0.82	-	1 92	2 14	-
54	QVI	73.93	45.52	1.49	0 63	1 10	5 20	1 86	15 3	9.1	48%		-	-	-	-	0 9	2 76	2 16	0 75	-	1 95	1 37	-
55	QVII	73 85	45 38	1 80	0 41	1 22	3 90	2.12	22 3	15 3	52%		-	-	-	-	0 7	2 65	2.16	0 93	-	2 01	1 06	-
56	QVIII	73 85	45 41	0 00	0 13	1.40	4 50	1 86	17.7	13 5	44%		-	-	-	-	3.6	2 75	2 28	0 81	-	2.08	1 05	-
57	EII	72 43	47 24	2 76	0 92	4 10	7.80	2 16	9 0	-	12%		-	-	-	-	3.9	3 50	2 32	1.20	-	1.48	1 77	-
58	ALD	72 48	47.27	3.00	0 60	4 00	7 60	-	10 0	-	11%		-	-	-	-	3 9	2.94	1 97	1 39	-	1.37	2 02	-
59	MEC	72 49	47 15	2 99	1.15	10 0	7.70	2 03	8 0	-	21%		-	-	-	-	3 9	3.46	2 35	1 48	-	1 42	2.04	-
60	NOR	72 50	47 16	3.03	-	7 00	7.50	2 00	9 5	-	10%		-	-	-	-	3 9	2 91	1 82	1 25	-	1.12	2 10	-
61	COM	72 50	47 27	3.03	-	3.00	7.70	1 48	11 0	-	26%		-	-	-	-	-	-	-	-	-	1.35	-	-
62	ERI	72 42	47 13	2 76	1 15	5 15	7 30	2 18	11 0	-	20%		-	-	-	-	4 0	3 51	2 38	1 51	-	1 62	1 80	-
63	CON	72.39	47 88	2 77	0 90	4 25	6 90	2.14	15 0	-	14%		-	-	-	-	4.0	3 68	2 33	1.43	-	1.63	1 84	-
64	HEN	72 38	47 13	2 85	1 16	4 00	7 30	2 20	10 0	-	7%		-	-	-	-	4 0	3.60	2 31	1.30	-	1 62	1 93	-

		FIELD										WATER											
Site Number	Code	Dec long	Dec Lat	Altitude	Depth	Secchi Depth	pH	Conductivity	Surface temp	Basal #temp	LOI	TP	TN	Si	N-NH4	Ca	Mg	Na	K	T Alc	Cl	SO_4	N-NO3
		(° N)	(°E)	(m)	(m)	(m)		(µs)	°C	°C	(%)	µg l-1	mg l-1	mg l-1	µeq l-1	µeq l-1	µeq l-1	µeq l-1	µeq l-1	µeq l-1	µeq l-1	µeq l-1	µeq l-1
65	ADE	72.37	47 22	2 79	1 12	10 2	7 10	2.29	10 5	-	18%	-	-	-	-	3 1	2 69	1 99	1 17	-	1 65	2 08	-
66	CHE	72 42	47 21	2 78	1 47	8 00	7 40	2 46	8.0	-	17%	-	-	-	-	4.1	4 05	2 62	1 60	-	1 85	1 82	-
67	II	72 82	47 22	2 58	1.18	5 05	7.25	1.66	13.4	11 4	50%	-	-	-	-	3 5	2 89	1 77	0 86	-	1 16	0 60	-
68	III	72 75	47 18	2 98	0 49	3 11	7 82	1.66	9 0	8 7	60%	-	-	-	-	3 5	2 96	1 76	0 69	-	0 98	1 40	-
69	IV	72 75	47.27	2 98	0 61	4 11	7 07	1.18	10 1	8.9	34%	-	-	-	-	3 1	2 44	1 66	0 61	-	1 07	1 20	-
70	V	72 77	47 33	3 08	0 10	1 25	7 07	0 70	8.1	7 3	17%	-	-	-	-	2 9	1 92	1 32	0 45	-	0 89	1 21	-
71	VI	72 78	47 29	3 04	0 93	6 71	7 14	0.90	7.1	6 4	32%	-	-	-	-	3 0	2 14	1 51	0 42	-	0 91	1 68	-
72	VII	72 74	47 33	3.02	0 94	7 62	7.07	0.30	7.5	7.8	46%	-	-	-	-	0 8	2 15	1 47	0 36	-	0 87	0 88	-
73	VIII	72 75	47.21	2 86	1 44	7.01	7.07	1.32	8.2	7.7	5%	-	-	-	-	3 2	2 50	1 57	0 59	-	0 94	1 46	-
74	IX	72 73	47 19	2.94	0 81	-	7 07	1 85	8.6	8.2	31%	-	-	-	-	3 5	2 56	1 66	0 40	-	0 80	1 05	-
75	X	73 02	47 24	2 53	1 17	3 15	7 05	1.59	14 7	6 8	59%	-	-	-	-	3 4	3 00	1 66	0 71	-	1 08	1 25	-
76	XI	73 17	47 11	2 87	0 78	6 04	7.01	0.30	15 4	12.2	65%	-	-	-	-	2 5	2 00	1 46	0 52	-	1 06	0 04	-
77	XII	73.17	47.11	2 87	0 96	7 04	7.00	0.60	13.5	9.1	58%	-	-	-	-	0 7	2 01	1 47	0 63	-	1 03	0 15	-
78	XIII	72 84	47 25	2 62	1 23	7 02	7 01	1.73	16 7	7 3	36%	-	-	-	-	3 6	3 08	1 79	0 62	-	1 15	1 41	-

APPENDIX 4

Training set chironomid raw counts

	PIR	BW	TBL	ESC	MOR	VER	FON	HES	MOS	GAL	PAT	ANG	HUL	LEZ	RED	MER
Chironomini	0	0	0	0	0	0	0	0	0	0	1	0	0	0	0	2
Chironomus	0	4	8	0	0	1	1	5	4	25	8	12	17	3	16	3
Cryptochironomus	0	0	0	0	0	0	0	0	1	0	0	0	0	0	0	0
Cryptotendipes	0	0	0	3	1	0	0	0	4	0	0	0	1	0	1	2
Lauterborniella	0	2	0	0	0	0	1	0	0	0	0	0	0	5	0	1
Stenochironomus	1	0	0	0	0	0	0	0	0	0	0	0	0	0	0	1
Parachironomus	4	12	0	0	0	0	1	2	1	8	2	8	8	0	15	3
Polypedilum	1	0	2	0	1	9	1	7	13	0	0	16	0	3	0	5
Phaenopsectra	2	0	0	0	0	0	0	0	0	0	0	0	0	0	0	0
Pseudochironomus	0	1	2	21	7	54	0	16	19	16	5	1	0	0	3	2
Micropsectra Taxon A	2	0	0	0	0	0	0	0	0	1	0	1	0	0	1	1
Micropsectra Taxon B	0	0	3	0	0	6	0	5	3	0	0	0	0	1	0	4
Dicrotendipes	0	0	10	18	33	0	0	2	0	0	0	0	48	35	0	1
Orthocladiinae Undif	1	0	0	0	0	0	0	0	0	0	1	0	0	0	0	0
Corynoneura / Thienemanniella	4	0	0	0	1	0	5	0	0	0	0	0	0	0	0	6
Cricotopus / Orthocladius	9	0	3	0	1	1	2	2	1	0	0	0	0	1	1	10
Orth Cranst	0	0	0	0	0	0	1	1	0	0	0	2	2	0	10	0
Parapsectrocladius	0	6	11	1	0	1	10	30	22	32	54	32	28	4	10	3
Parakiefferiella	3	6	2	2	0	0	4	0	1	1	2	1	0	0	5	24
Parakiefferiella fennica type	0	0	0	0	0	0	0	0	1	0	1	0	0	0	0	0
Limnophyes / Paralimnophyes Taxon A	5	0	0	0	0	0	13	1	0	5	0	1	0	0	0	8
Limnophyes / Paralimnophyes Taxon B	0	0	0	0	0	0	1	0	0	0	0	0	0	0	0	0
Orthocladiinae Taxon B	0	0	0	0	0	0	0	0	0	0	0	0	0	0	0	0
Tvetenia / Eukiefferiella	4	0	0	0	0	0	4	0	1	1	0	0	0	0	0	0
Gymnometriocnemus	0	0	0	0	0	0	0	0	0	0	0	0	0	0	0	0
Nanocladius	0	1	1	0	0	0	3	1	0	0	0	0	0	0	1	0
Orthocladiinae Taxon C	0	0	0	0	0	0	0	0	0	0	0	0	0	0	0	0
SO4 (Cranson)	0	0	0	0	0	0	4	0	0	0	0	0	0	0	0	0
Orthocladiinae early instar	1	0	0	0	0	0	1	0	0	12	2	1	0	0	1	0
Orthocladiinae Taxon A	0	0	0	0	0	0	0	0	0	0	0	0	0	0	0	1
Tanytarsini Undif	0	0	2	0	3	2	1	3	3	0	1	10	1	1	2	0
Tanytarsini Taxon A	0	7	1	1	6	0	2	7	6	0	8	1	1	0	4	1
Tanytarsini Taxon E	11	10	38	17	25	19	4	3	7	1	1	30	11	23	47	1
Tanytarsini Taxon D	17	4	30	10	19	0	6	38	3	0	6	18	3	1	30	7
Tanytarsini Taxon B	10	28	42	19	31	2	5	18	20	0	1	56	11	3	81	4
Tanytarsini Taxon C	0	0	0	0	0	0	0	0	0	0	0	0	0	0	0	0
Paratanytarsus	1	0	0	0	0	0	1	4	1	0	0	0	0	0	0	0
Tanypodinae Undif	0	0	0	0	1	2	0	0	2	0	0	1	0	1	0	0
Tanypodinae Taxon C	2	0	21	1	5	1	1	0	8	0	0	0	0	0	1	0
Tanypodinae Taxon A	0	0	1	1	0	5	2	1	3	2	0	6	3	0	4	0
Ablabesmyia	1	0	9	16	9	0	2	32	29	7	7	2	12	12	5	10
Procladiini / Macropelopiini early instar	2	1	1	0	0	0	4	1	0	21	3	3	1	0	0	0
Procladius	0	0	0	0	0	0	1	2	1	0	0	0	0	0	1	0
Labrundinia	0	10	10	0	0	0	2	7	0	14	26	6	9	0	3	5
Tanypodinae Taxon B	1	3	0	0	1	0	2	0	0	5	1	8	1	0	4	0
Clinotanypus	0	0	0	0	1	0	0	0	0	0	0	0	0	0	0	0
Podonominae	13	0	0	0	0	0	11	0	0	3	0	0	0	0	0	0
Chironomini early instar	1	9	3	0	2	0	1	1	0	27	8	2	5	0	3	0

	LGA	COF	X-667	PIG	FUT	LAR	GUA	ESM	ATR	LOB	LET	BLC	CAS	TAM	FOI	RIS
Chironoms	0	0	0	0	0	0	0	0	0	0	0	0	0	0	0	0
Chironomus	0	0	29	0	18	1	2	0	12	1	35	0	1	12	55	0
Cryptochironomus	0	0	0	1	0	1	0	0	0	0	0	0	0	0	0	0
Cryptotendipes	0	0	0	1	1	0	0	0	0	0	3	1	0	0	0	0
Lauterborniella	0	0	0	0	0	0	0	0	0	1	23	0	0	0	0	0
Stenochironomus	0	0	0	0	0	0	0	0	0	0	0	0	0	0	0	0
Parachironomus	1	0	0	2	0	1	0	3	15	0	8	2	2	11	4	1
Polypedilum	2	0	7	11	0	10	0	9	0	19	6	0	19	0	0	3
Phaenopsectra	0	0	0	1	0	0	0	0	0	0	0	39	0	0	0	3
Pseudochironomus	5	0	24	1	1	1	0	9	1	5	25	0	22	0	1	0
Micropsectra Taxon A	0	0	0	0	0	0	0	0	0	0	0	0	0	0	0	1
Micropsectra Taxon B	2	0	0	2	0	0	0	1	0	0	0	0	0	0	0	0
Dicrotendipes	1	0	5	0	1	1	10	4	0	0	0	0	10	0	0	0
Orthocladiinae Undif	0	0	0	1	0	0	0	0	0	0	0	1	1	0	0	0
Corynoneura / Thienemanniella	3	0	0	1	0	0	1	0	0	1	0	4	0	1	1	3
Cricotopus / Orthocladius	3	3	1	2	0	0	0	0	0	2	0	0	0	5	0	2
Orth Cranst	0	0	0	0	0	0	0	0	2	0	0	0	0	0	0	0
Parapsectrocladius	0	3	7	2	7	0	8	11	10	24	84	0	7	42	33	0
Parakiefferiella	25	13	0	5	0	4	0	0	2	2	1	4	1	0	0	2
Parakiefferiella fennica type	8	0	0	4	0	7	0	4	1	10	0	1	0	0	0	0
Limnophyes / Paralimnophyes Taxon A	0	3	0	3	0	1	0	0	1	5	0	7	1	0	0	12
Limnophyes / Paralimnophyes Taxon B	0	1	0	0	0	0	0	0	0	2	0	1	0	1	0	1
Orthocladiinae Taxon B	0	0	0	0	0	0	0	0	0	0	0	0	0	0	0	0
Tventia / Eukiefferiella	0	0	0	0	0	1	0	0	1	2	0	1	0	2	0	3
Gymnomectrocnemus	0	0	0	0	0	0	0	0	0	1	0	0	0	0	0	3
Nanocladius	0	0	0	1	0	0	0	0	0	0	0	0	1	0	0	2
Orthocladiinae Taxon C	0	0	0	0	0	0	0	0	0	0	0	2	0	0	0	0
SO4 (Cranson)	0	0	0	0	0	0	0	0	0	0	0	0	0	0	0	3
Orthocladiinae early instar	0	1	1	0	0	0	1	0	1	0	0	0	0	0	0	0
Orthocladiinae Taxon A	0	0	0	0	0	0	0	0	0	1	0	0	0	0	0	4
Tanytarsini Undif	2	1	0	1	3	1	0	1	10	4	3	1	2	11	1	0
Tanytarsini Taxon A	2	0	0	12	2	7	0	5	1	16	21	0	0	27	0	0
Tanytarsini Taxon E	8	21	1	11	38	13	40	26	30	4	12	0	2	25	7	6
Tanytarsini Taxon D	4	8	0	5	10	5	6	3	18	8	6	2	3	36	8	1
Tanytarsini Taxon B	3	28	1	7	22	7	19	4	56	3	9	2	2	86	12	8
Tanytarsini Taxon C	0	0	0	0	0	0	0	0	0	15	0	1	0	0	0	6
Paratanytarsus	0	0	0	0	0	0	0	0	0	0	0	1	0	0	0	0
Tanypodinae Undif	2	0	2	1	0	2	0	8	1	1	0	0	2	4	1	0
Tanypodinae Taxon C	7	2	10	2	3	12	2	9	0	0	1	1	9	0	0	1
Tanypodinae Taxon A	5	0	7	5	1	12	0	9	6	2	4	0	2	2	2	1
Ablabesmyia	8	6	18	4	17	9	13	14	2	24	13	8	13	5	1	0
Procladiini / Macropelopiini early instar	3	5	2	2	0	0	0	2	3	2	4	3	0	2	5	0
Procladius	1	0	0	1	0	0	0	0	0	0	0	0	0	0	0	0
Labrundinia	3	0	0	12	0	1	0	4	6	0	24	6	1	2	13	2
Tanypodinae Taxon B	1	1	2	1	3	3	0	1	8	0	7	0	0	16	13	0
Clinotanypus	0	0	0	0	0	0	0	0	0	0	0	0	0	0	0	0
Podonominae	0	1	0	8	0	2	0	0	0	2	0	10	0	0	0	22
Chironomini early instar	3	5	1	0	4	1	1	0	2	1	3	1	0	3	12	0

	TRE	MAN	CIS	EI	ENV	TVI	AVE	FLO	PRI	BRO	BNA	MRT	LNF	MOA	LAV	TOL
Chironomus	0	0	0	0	0	0	0	0	0	0	0	0	0	0	0	0
Chironomus	43	3	12	16	28	2	0	1	0	1	10	0	9	4	3	3
Cryptochironomus	0	0	0	0	0	0	0	0	0	0	0	0	0	0	0	0
Cryptotendipes	0	0	0	0	0	0	0	0	0	0	1	0	0	0	0	0
Lauterborniella	0	5	1	0	0	0	0	0	0	0	1	0	0	0	0	6
Stenochironomus	0	0	0	0	0	0	0	0	0	0	0	0	0	0	0	0
Parachironomus	24	2	3	1	4	1	1	3	0	42	0	0	3	1	0	8
Polypedilum	5	5	0	1	0	14	23	24	66	0	0	0	3	7	0	9
Phaenopsectra	0	0	0	0	0	0	0	0	0	1	0	0	1	3	0	0
Pseudochironomus	7	4	2	7	0	0	0	0	0	0	3	0	0	3	3	0
Micropsectra Taxon A	0	0	0	0	0	0	0	0	0	0	0	0	0	0	0	0
Micropsectra Taxon B	24	0	1	1	0	0	2	0	0	0	0	2	0	0	0	0
Dicrotendipes	0	1	1	2	0	0	5	0	0	0	35	0	0	0	12	0
Orthocladiinae Undif	0	0	1	0	0	0	0	0	0	1	0	0	0	0	0	0
Corynoneura / Thienemanniella	0	0	0	0	0	0	1	2	0	2	0	0	0	0	1	0
Cricotopus / Orthocladius	1	0	0	0	0	1	0	1	0	23	0	4	4	0	11	0
Orth Cranst	0	0	0	0	0	0	0	0	0	0	0	1	0	0	0	0
Parapsectrocladius	89	10	23	5	18	0	4	2	1	34	7	1	6	0	2	39
Parakiefferiella	0	0	0	1	0	1	1	1	0	6	0	41	2	9	4	0
Parakiefferiella fennica type	0	0	0	0	0	0	1	1	0	1	0	7	0	1	0	0
Limnophyes / Paralimnophyes Taxon A	4	2	2	1	0	0	2	1	1	11	0	3	3	3	4	5
Limnophyes / Paralimnophyes Taxon B	0	0	1	0	0	0	0	0	0	1	0	0	0	7	0	0
Orthocladiinae Taxon B	2	0	0	0	0	0	0	1	1	0	0	1	1	0	0	0
Tvetenia / Eukiefferiella	0	0	0	1	0	0	0	0	0	0	0	7	0	0	1	0
Gymnometriocnemus	0	0	0	0	0	0	0	0	0	1	0	0	0	2	0	0
Nanocladius	0	0	0	0	0	0	0	0	0	0	0	0	0	0	0	0
Orthocladiinae Taxon C	0	0	0	0	0	0	0	0	0	0	0	0	0	0	0	0
SO4 (Cranson)	0	0	0	0	0	0	0	0	0	0	0	1	0	0	0	0
Orthocladiinae early instar	10	0	0	1	1	0	0	0	0	7	0	0	0	0	2	9
Orthocladiinae Taxon A	0	1	0	0	0	0	0	0	0	0	0	0	0	2	1	0
Tanytarsini Undif	0	1	1	2	3	1	2	0	0	0	1	2	0	0	2	0
Tanytarsini Taxon A	0	8	0	0	0	0	0	0	0	0	1	12	0	3	0	0
Tanytarsini Taxon E	0	22	35	13	23	51	86	29	27	19	22	0	17	12	39	31
Tanytarsini Taxon D	0	7	1	4	9	5	3	1	0	9	2	3	15	10	13	14
Tanytarsini Taxon B	0	18	7	17	25	25	22	23	7	21	6	7	38	14	44	37
Tanytarsini Taxon C	0	0	0	0	0	0	0	0	0	0	0	0	0	0	0	0
Paratanytarsus	0	0	0	0	0	0	0	0	0	0	0	0	0	0	0	0
Tanypodinae Undif	1	0	0	3	0	0	1	0	0	0	0	4	0	0	0	1
Tanypodinae Taxon C	4	0	1	16	0	1	1	1	0	2	0	14	3	8	18	0
Tanypodinae Taxon A	3	0	3	5	20	1	3	3	0	2	1	6	2	11	11	0
Ablabesmyia	19	23	18	15	1	0	13	0	0	0	22	0	0	9	0	3
Procladiini / Macropelopiini early instar	12	2	2	2	1	0	0	0	2	0	1	1	2	0	0	2
Procladius	0	0	0	0	0	0	0	0	0	0	0	0	0	0	0	0
Labrundinia	3	18	0	3	11	0	2	0	0	8	0	0	3	8	3	3
Tanypodinae Taxon B	7	0	3	3	9	0	0	2	8	0	0	0	1	0	0	2
Clinotanypus	0	0	0	0	0	0	0	0	0	0	0	0	0	0	0	0
Podonominae	0	0	0	0	0	0	0	0	0	0	0	8	0	2	1	1
Chironomini early Instar	21	3	0	2	10	0	0	0	0	5	1	0	2	3	6	1

	VI	DII	PIII	GIV	VV	QVI	QVII	QVIII	EII	ALD	MEC	NOR	COM	ERI	CON	HEN
Chironomus	0	0	1	0	0	0	0	0	0	0	0	0	0	0	0	0
Chironomus	2	1	0	6	0	1	2	19	22	17	0	9	33	0	17	2
Cryptochironomus	0	1	1	1	0	0	0	0	0	0	0	0	0	1	0	0
Cryptotendipes	0	4	1	1	2	0	2	7	0	0	0	0	0	0	0	0
Lauterborniella	1	9	0	1	0	3	0	0	0	0	0	0	0	0	0	0
Stenochironomus	0	0	0	0	1	0	0	0	0	0	0	0	0	0	0	0
Parachironomus	1	0	0	1	0	4	0	3	4	8	0	0	1	1	4	0
Polypedilum	1	7	8	6	21	5	10	1	1	0	2	19	0	5	0	0
Phaenopsectra	1	0	1	1	0	2	0	4	0	0	0	0	0	0	0	0
Pseudochironomus	0	11	0	4	2	4	0	1	6	1	48	0	0	4	11	3
Micropsectra Taxon A	1	0	0	0	1	0	0	0	1	0	0	0	0	0	0	0
Micropsectra Taxon B	0	4	0	0	0	4	0	2	0	1	1	0	0	2	2	1
Dicrotendipes	0	0	0	0	0	1	0	0	3	0	11	0	0	1	0	1
Orthocladiinae Undif	0	0	0	0	0	0	0	0	0	0	0	0	0	0	0	0
Corynoneura / Thienemanniella	0	2	1	0	1	6	0	1	0	0	0	1	0	1	0	0
Cricotopus / Orthocladius	0	0	0	1	0	0	0	10	0	0	1	0	0	0	0	0
Orth Cranst	0	0	0	0	0	0	0	0	0	0	0	0	0	0	0	0
Parapsectrocladius	3	17	1	6	1	14	4	0	3	37	10	52	77	7	17	7
Parakiefferiella	69	17	64	4	30	2	0	2	0	0	0	0	0	0	1	0
Parakiefferiella fennica type	0	1	6	0	0	0	0	0	0	0	1	0	0	0	0	0
Limnophyes / Paralimnophyes Taxon A	9	2	1	6	6	7	11	6	2	0	0	0	0	2	0	0
Limnophyes / Paralimnophyes Taxon B	1	0	1	1	4	2	0	2	3	0	1	1	0	0	0	0
Orthocladiinae Taxon B	0	0	0	0	0	0	0	0	0	0	0	0	0	0	0	0
Tvetenia / Eukiefferiella	1	0	0	2	0	2	0	5	0	1	2	0	0	0	0	0
Gymnometriocnemus	0	1	0	0	0	0	0	2	0	0	0	0	0	0	0	0
Nanocladius	0	1	0	0	0	0	0	0	0	0	0	0	0	0	0	0
Orthocladiinae Taxon C	0	0	0	0	0	0	0	0	0	0	0	0	0	0	0	0
SO4 (Cranson)	0	0	0	0	0	0	0	0	0	0	0	0	0	0	0	0
Orthocladiinae early instar	0	2	0	0	0	2	0	0	0	0	0	0	10	0	0	0
Orthocladiinae Taxon A	1	0	0	0	0	0	0	1	0	0	0	0	0	0	0	0
Tanytarsini Undif	1	2	2	4	1	0	5	0	0	0	0	0	0	2	0	0
Tanytarsini Taxon A	0	27	6	5	5	1	12	0	0	0	0	0	0	1	0	0
Tanytarsini Taxon E	0	9	15	6	6	1	17	1	13	19	2	3	0	24	43	49
Tanytarsini Taxon D	3	1	2	4	0	5	8	1	1	1	2	0	0	7	6	13
Tanytarsini Taxon B	9	16	15	16	4	5	28	0	12	7	2	2	1	22	41	31
Tanytarsini Taxon C	4	0	0	1	5	1	0	7	0	0	0	0	0	0	0	0
Paratanytarsus	0	0	0	0	0	0	0	0	0	0	0	0	0	0	0	0
Tanypodinae Undif	1	1	2	2	1	0	2	0	0	0	2	0	0	0	0	0
Tanypodinae Taxon C	2	10	5	15	0	0	0	14	4	0	8	0	1	6	2	0
Tanypodinae Taxon A	0	9	4	11	4	0	7	2	4	6	11	4	4	4	5	2
Ablabesmyia	0	30	1	1	1	7	0	2	11	1	6	1	0	27	29	9
Procladiini / Macropelopiini early instar	6	0	0	1	0	4	0	0	0	0	0	1	5	0	0	2
Procladius	0	0	2	0	0	0	0	0	0	0	0	0	0	0	0	0
Labrundinia	1	3	0	0	1	8	1	1	3	0	0	0	0	6	1	1
Tanypodinae Taxon B	2	1	6	1	3	2	5	1	3	1	2	4	15	4	2	0
Clinotanypus	0	0	0	0	0	1	0	0	0	0	0	0	0	0	0	0
Podonominae	0	0	0	0	0	2	0	3	0	0	0	0	0	0	0	0
Chironomini early instar	2	2	0	2	0	3	0	0	0	0	0	0	6	0	1	0

	ADE	CHE	II	III	IV	V	VI	VII	VIII	IX	X	XI	XII	XIII	ADE	CHE
Chironomus	0	0	0	0	0	0	0	0	0	0	0	0	0	0	0	0
Chironomus	3	2	4	32	0	0	0	0	0	3	0	1	0	1	3	2
Cryptochironomus	0	0	0	0	0	0	0	0	0	0	0	0	0	0	0	0
Cryptotendipes	0	0	0	0	0	0	0	0	0	0	0	0	0	0	0	0
Lauterborniellaerborniella	0	0	0	0	0	0	0	0	0	0	0	0	0	1	0	0
Stenochironomus	0	0	0	0	0	0	0	0	0	0	0	0	0	0	0	0
Parachironomus	5	2	0	4	0	0	0	0	1	1	0	1	0	16	5	2
Polypedilum	2	0	0	4	13	0	20	0	0	17	11	1	6	7	2	0
Phaenopsectra	0	0	0	0	0	0	0	0	0	0	0	0	0	0	0	0
Pseudochironomus	0	0	2	1	1	0	0	0	7	4	0	0	0	0	0	0
Micropsectra Taxon A	0	0	0	0	0	0	0	0	0	0	0	0	0	0	0	0
Micropsectra Taxon B	0	2	2	4	1	7	4	3	0	2	2	1	0	3	0	2
Dicrotendipes	15	2	11	0	0	0	0	0	0	0	3	0	0	0	15	2
Orthocladiinae Undif	0	0	0	0	0	0	0	0	0	0	0	0	0	0	0	0
Corynoneura / Thienemanniella	0	0	0	1	1	4	2	0	1	0	0	0	0	1	0	0
Cricotopus / Orthocladius	1	0	0	0	0	0	1	0	0	0	0	0	0	0	1	0
Orth Cranst	0	0	0	0	0	0	0	0	0	0	0	0	0	0	0	0
Parapsectrocladius	43	19	29	35	16	1	37	3	3	1	15	85	15	17	43	19
Parakiefferiella	0	0	0	0	0	0	20	0	4	19	0	0	0	0	0	0
Parakiefferiella fennica type	0	0	0	0	0	0	2	0	5	7	0	0	0	0	0	0
Limnophyes / Paralimnophyes Taxon A	0	0	0	0	0	1	0	0	0	2	1	0	1	5	0	0
Limnophyes / Paralimnophyes Taxon B	0	0	0	0	0	0	0	0	0	1	0	0	0	0	0	0
Orthocladiinae Taxon B	0	0	0	0	0	0	0	0	0	0	0	0	0	0	0	0
Tventia / Eukiefferiella	0	0	0	0	0	0	0	0	0	0	0	0	0	0	0	0
Gymnomectriocnemus	0	0	0	0	0	0	0	0	0	0	0	0	0	0	0	0
Nanocladius	0	0	0	0	0	0	0	0	0	0	0	0	0	0	0	0
Orthocladiinae Taxon C	0	0	0	0	0	0	0	0	0	0	0	0	0	0	0	0
SO4 (Cranson)	0	0	0	0	0	0	0	0	0	0	0	0	0	0	0	0
Orthocladiinae early instar	0	0	0	2	4	1	10	0	0	1	0	4	0	3	0	0
Orthocladiinae Taxon A	0	0	0	0	0	0	0	0	0	0	0	0	0	0	0	0
Tanytarsini Undif	0	3	3	0	4	1	0	1	0	0	2	0	2	1	0	3
Tanytarsini Taxon A	0	0	1	0	0	0	0	0	7	0	3	0	0	1	0	0
Tanytarsini Taxon E	12	62	19	18	23	46	0	40	8	9	37	5	17	21	12	62
Tanytarsini Taxon D	1	2	20	3	1	2	0	11	6	1	4	0	1	28	1	2
Tanytarsini Taxon B	3	40	36	19	13	23	0	28	11	4	25	0	19	34	3	40
Tanytarsini Taxon C	0	0	0	0	0	0	0	0	0	0	0	0	0	0	0	0
Paratanytarsus	0	0	0	0	0	0	0	0	0	0	0	0	0	0	0	0
Tanypodinae Undif	1	0	1	0	0	0	1	3	0	2	1	0	0	0	1	0
Tanypodinae Taxon C	17	2	0	0	0	0	2	0	12	12	0	0	0	1	17	2
Tanypodinae Taxon A	7	0	1	4	9	6	0	1	11	3	1	1	0	4	7	0
Ablabesmyia	28	10	45	8	7	1	1	11	12	1	33	6	27	18	28	10
Procladiini / Macropelopiini early instar	2	0	8	3	5	1	3	2	3	1	1	4	1	0	2	0
Procladius	0	0	0	0	0	0	0	0	0	0	0	0	0	0	0	0
Labrundinia	13	5	12	0	1	0	0	0	4	2	11	4	11	14	13	5
Tanypodinae Taxon B	0	2	4	1	6	6	1	1	1	4	4	0	1	2	0	2
Clinotanypus	0	0	0	0	0	0	0	0	0	0	0	0	0	0	0	0
Podonominae	0	0	1	0	0	0	0	0	1	0	0	0	0	1	0	0
Chironomini early Instar	0	0	6	3	0	0	0	0	0	0	2	2	0	4	0	0

Laguna Boal raw counts

	DEPTH / cm															
	3	20	36	52	68	100	116	132	148	164	200	208	216	232	248	264
Chironomus	0	0	0	0	0	1	0	0	0	0	0	0	0	0	0	0
Cryptochironomus	0	0	1	0	0	0	0	0	0	1	0	0	0	0	0	0
Lauterborniella	0	5	1	1	1	4	1	0	0	0	0	0	0	0	1	2
Stenochironomus	0	0	0	0	0	0	0	0	0	0	0	0	0	0	0	2
Parachironomus	0	1	0	0	1	2	0	0	0	0	0	0	0	0	0	3
Polypedilum	3	4	5	2	1	6	15	9	12	20	2	2	0	5	3	0
Phaenopsectra	0	3	0	0	0	1	0	1	0	0	0	0	0	0	0	0
Pseudochironomus	0	1	0	0	23	0	0	0	0	0	0	0	0	0	0	0
Microtendipes Taxon A	0	0	0	0	3	0	0	1	0	5	0	1	0	1	2	4
Micropsectra Taxon B	0	0	0	0	0	0	0	0	0	0	0	0	0	0	0	0
Orthocladiinae Undif	0	1	0	0	0	0	0	0	0	2	0	0	0	0	0	1
Corynoneura / Thienemanniella	0	0	2	0	0	1	1	0	1	0	0	0	0	0	0	2
Cricotopus / Orthocladius	0	0	1	0	0	0	0	0	0	0	1	1	1	0	0	0
Parasmi	0	0	0	0	0	0	0	0	0	0	0	0	0	0	0	0
Parakiefferiella	0	3	0	0	1	7	9	9	8	24	19	21	29	10	12	74
Parakiefferiella fennica type	3	3	3	0	0	1	3	5	3	4	1	1	0	3	4	3
Parapsectrocladius	30	40	50	31	10	54	35	34	96	38	35	34	23	25	21	40
Psorth	0	0	0	0	0	1	0	0	0	0	0	0	0	0	1	0
Limnophyes / Paralimnophyes Taxon A	6	13	2	3	2	7	3	9	2	8	4	4	6	11	2	20
Limnophyes / Paralimnophyes Taxon B	1	2	1	0	2	0	2	1	0	2	3	2	0	2	2	3
Smittia	0	0	0	0	0	1	0	0	0	0	0	0	0	0	0	0
Mesosm	0	0	0	0	0	0	0	0	0	0	0	0	0	0	0	0
Tventia / Eukiefferiella	0	1	2	0	0	1	0	1	0	2	0	0	0	1	1	0
Nanocladius	0	0	0	0	0	0	0	0	0	0	0	0	0	0	0	0
Orthocladiinae early instar	1	0	0	0	1	0	0	1	0	0	0	0	0	0	0	0
Orthocladiinae Taxon At	0	0	0	0	0	0	0	0	0	0	0	0	1	0	0	0
Gymnometriocnemus	1	0	0	0	0	0	0	1	1	0	0	0	0	0	0	1
Orthocladiinae Taxon D	0	0	0	0	2	0	0	0	0	0	1	0	0	0	0	2
Orthocladiinae Taxon C	0	0	0	0	0	0	0	0	1	0	0	0	0	0	0	0
Tanytarsini Undif	8	7	3	1	1	4	6	4	6	9	0	5	2	1	7	7
Tanytarsini Taxon A	7	4	6	5	3	1	6	9	15	12	0	5	7	4	6	3
Tanytarsini Taxon E	14	23	16	5	11	10	7	16	32	12	7	6	4	24	7	17
Tanytarsini Taxon D	2	0	0	0	0	3	2	2	1	2	0	0	0	4	0	0
Tanytarsini Taxon B	16	15	5	0	7	10	10	7	18	8	6	9	4	8	10	17
Tanytarsini Taxon C	1	4	10	0	2	3	0	2	1	4	7	0	12	5	5	23
Tanypodinae Undif	6	11	1	2	2	3	5	2	13	4	1	5	3	2	4	1
Tanypodinae Taxon B	2	5	4	2	3	3	4	2	2	2	4	1	0	3	1	3
Tanypodinae Taxon A	7	6	11	6	4	3	5	2	0	9	5	0	4	7	6	8
Clinotanypus	0	0	0	0	0	0	0	0	0	0	0	0	0	0	0	0
Procladiini / Macropelopiini early instar	2	1	1	0	3	0	0	0	3	1	0	1	2	0	0	1
Ablabesmyia	4	6	4	4	3	4	6	0	2	1	0	2	4	2	0	3
Labrundinia	0	1	2	0	0	1	0	0	2	0	1	0	2	2	2	3
Podonominae	2	1	1	2	3	1	2	1	0	7	2	0	1	4	1	3
Chironomini early Instar	0	0	0	0	0	0	0	0	0	0	0	0	0	0	0	0

	DEPTH / cm															
	280	296	302	304	308	312	320	328	336	344	352	360	362	364	366	368
Chironomus	0	0	0	0	0	0	0	0	0	1	2	0	0	0	0	0
Cryptochironomus	0	0	0	0	0	0	0	0	0	0	0	0	0	0	0	0
Lauterborniella	1	2	6	0	2	0	2	0	0	3	5	3	3	0	1	2
Stenochironomuso	0	0	0	0	0	0	0	0	0	0	0	2	0	1	0	0
Parachironomus	1	0	2	0	0	1	1	0	1	0	0	0	0	0	0	1
Polypedilum	1	1	2	2	4	1	0	1	2	1	0	2	3	0	0	1
Phaenopsectra	0	1	3	1	0	6	1	1	0	3	9	0	0	0	0	0
Pseudochironomus	1	0	0	0	0	0	0	0	0	0	0	0	0	0	0	2
Microtendipes Taxon A	5	2	0	0	1	2	0	1	3	4	0	1	0	1	2	0
Micropsectra Taxon B	0	0	0	0	0	0	0	0	0	0	0	0	0	0	0	0
Orthocladiinae Undif	0	0	0	0	0	0	0	0	0	0	0	0	0	0	0	0
Corynoneura / Thienemanniella	1	2	0	6	0	0	3	0	4	7	0	2	3	2	0	8
Cricotopus / Orthocladius	3	1	0	0	0	0	0	0	0	0	1	0	0	0	0	0
Parasmi	0	0	0	0	0	0	0	0	0	0	0	0	0	0	0	0
Parakiefferiella	125	27	2	4	17	197	49	43	17	6	3	1	6	6	18	2
Parakiefferiella fennica type	1	2	0	2	2	2	0	0	2	1	4	6	2	1	0	1
Parapsectrocladius	18	14	26	43	42	17	36	15	38	53	49	51	48	32	7	43
Psorth	0	0	0	1	0	0	0	0	0	0	0	1	0	0	0	1
Limnophyes / Paralimnophyes Taxon A	16	9	13	1	10	16	4	2	8	7	7	1	3	3	3	9
Limnophyes / Paralimnophyes Taxon B	3	7	4	1	2	15	0	1	10	10	0	1	4	2	14	1
Smittia	0	0	0	0	0	0	0	0	0	0	0	0	0	0	0	0
Mesosm	2	0	0	0	0	0	0	0	0	0	0	0	0	0	0	0
Tventia / Eukiefferiella	0	1	1	0	1	1	1	1	1	0	0	0	0	0	0	0
Nanocladius	0	0	0	0	0	3	0	1	0	0	0	1	0	0	0	0
Orthocladiinae early instar	0	0	0	0	0	0	0	0	0	1	1	1	0	0	0	0
Orthocladiinae Taxon A	0	0	0	0	0	0	0	0	0	0	0	0	0	0	0	0
Gymnomectriocnemus	0	0	0	0	0	0	0	0	0	4	1	0	0	1	0	0
Orthocladiinae Taxon D	0	0	0	0	0	0	0	1	0	0	1	0	0	0	0	0
Orthocladiinae Taxon C	0	0	0	0	0	0	0	0	1	0	0	0	0	0	0	2
Tanytarsini Undif	10	3	2	3	3	0	3	1	4	1	1	2	0	0	0	7
Tanytarsini Taxon A	4	2	3	4	7	3	2	0	3	5	5	1	9	1	1	5
Tanytarsini Taxon E	15	16	22	17	26	13	4	4	8	10	7	7	21	1	2	13
Tanytarsini Taxon D	0	4	1	2	0	3	3	0	2	3	3	0	4	1	0	0
Tanytarsini Taxon B	14	7	7	2	13	10	5	3	7	11	11	12	15	1	0	6
Tanytarsini Taxon C	29	13	4	3	10	38	14	13	19	18	15	3	11	19	15	13
Tanypodinae Undif	9	1	2	2	10	1	4	1	6	1	3	3	0	1	0	6
Tanypodinae Taxon B	3	3	2	0	2	5	2	2	1	0	4	2	3	1	1	4
Tanypodinae Taxon A	3	5	1	3	3	7	2	1	0	0	1	6	10	5	3	11
Clinotanypus	0	0	0	0	0	0	0	0	0	0	0	0	0	0	0	0
Procladiini / Macropelopiini early instar	0	0	0	1	1	0	0	0	1	1	1	0	1	0	0	0
Ablabesmyia	6	2	4	4	1	3	7	1	4	9	6	8	10	1	3	8
Labrundinia	7	3	6	1	1	6	3	0	8	12	26	10	5	6	2	14
Podonominae	7	6	2	0	4	8	1	1	1	3	0	0	0	1	3	2
Chironomini early Instar	0	0	0	0	0	0	0	0	0	0	0	0	0	0	0	0

	DEPTH / cm															
	370	372	374	376	378	380	382	384	386	388	390	392	394	396	398	400
Chironomus	0	0	0	0	3	3	0	1	0	0	0	3	1	2	2	2
Cryptochironomus	0	0	0	0	0	0	0	0	0	0	0	0	0	0	0	0
Lauterborniella	0	3	0	0	2	2	0	0	0	0	0	1	1	1	0	0
Stenochironomus	0	0	0	0	0	0	0	0	0	0	0	0	0	0	0	0
Parachironomus	0	0	1	1	1	1	0	2	0	0	0	4	1	0	2	0
Polypedilum	1	1	2	1	5	0	0	2	1	0	0	1	1	0	1	0
Phaenopsectra	5	0	2	0	3	0	1	4	3	3	3	0	0	0	1	0
Pseudochironomus	0	0	0	0	0	0	0	0	0	0	1	1	0	0	0	0
Microtendipes Taxon A	3	3	0	1	0	1	1	1	2	0	0	3	0	0	0	0
Micropsectra Taxon B	0	0	0	0	0	0	0	0	0	0	0	0	0	0	0	1
Orthocladiinae Undif	0	0	0	1	0	0	0	0	1	0	0	0	0	0	0	0
Corynoneura / Thienemanniella	6	10	5	5	2	6	2	0	0	0	3	1	0	0	1	1
Cricotopus / Orthocladius	1	0	1	1	3	6	0	7	1	0	3	8	1	1	0	0
Parasmi	0	0	0	0	0	0	0	0	0	0	0	0	0	0	0	0
Parakiefferiella	1	2	0	0	0	8	2	34	50	40	16	1	0	2	0	1
Parakiefferiella fennica type	1	1	0	0	1	0	1	4	7	8	4	8	1	0	2	0
Parapsectrocladius	22	22	40	53	106	58	51	59	41	35	37	77	34	53	94	54
Psorth	0	0	0	0	0	0	0	0	0	0	0	0	0	0	0	0
Limnophyes / Paralimnophyes Taxon A	9	6	3	2	5	5	6	5	9	7	5	7	1	1	1	1
Limnophyes / Paralimnophyes Taxon B	15	9	9	3	8	6	7	4	9	2	3	2	1	2	1	0
Smittia	0	0	0	0	0	0	0	0	0	0	0	0	0	0	0	0
Mesosm	0	0	0	0	0	0	0	0	0	0	0	0	0	0	0	0
Tvetia / Eukiefferiella	1	0	1	1	4	1	0	3	2	2	3	2	0	0	1	1
Nanocladius	0	0	0	0	0	0	0	0	0	0	0	0	0	0	0	0
Orthocladiinae early instar	1	0	0	0	2	0	0	0	1	0	0	0	0	2	2	0
Orthocladiinae Taxon A	0	0	0	0	0	0	0	0	0	0	1	0	0	0	0	0
Gymnomectriocnemus	1	0	0	0	1	0	0	0	5	0	0	0	1	0	1	0
Orthocladiiniae Taxon D	0	0	1	0	1	2	0	0	3	2	1	0	0	0	0	0
Orthocladiiniae Taxon C	0	0	0	0	0	0	0	0	0	0	0	1	0	0	0	1
Tanytarsini Undif	0	1	0	1	0	2	0	1	1	0	0	0	0	2	0	1
Tanytarsini Taxon A	0	1	0	0	1	4	1	6	0	3	3	1	0	2	1	1
Tanytarsini Taxon E	1	3	3	0	7	12	3	8	7	0	3	17	15	14	30	9
Tanytarsini Taxon D	0	0	1	0	0	1	0	0	1	1	0	0	0	1	1	0
Tanytarsini Taxon B	2	2	1	3	4	5	2	5	2	3	7	4	13	11	27	7
Tanytarsini Taxon C	23	26	13	21	18	10	9	15	23	0	2	4	0	0	0	0
Tanypodinae Undif	0	0	0	0	0	2	0	0	2	0	0	1	1	0	1	2
Tanypodinae Taxon B	7	1	1	3	5	3	1	4	2	0	2	5	5	4	5	3
Tanypodinae Taxon A	3	1	1	1	3	3	0	6	9	2	2	5	1	2	6	7
Clinotanypus	0	0	0	0	0	0	0	0	0	0	0	0	0	0	0	0
Procladiini / Macropelopiini early instar	2	1	1	0	0	0	1	0	2	0	1	1	0	1	0	0
Ablabesmyia	3	6	7	7	18	21	8	15	7	2	3	8	7	15	19	9
Labrundinia	10	9	15	5	18	13	8	7	9	5	2	7	6	3	6	4
Podonominae	3	4	2	5	6	0	0	4	13	11	9	0	2	2	3	0
Chironomini early Instar	0	0	0	0	0	1	0	0	1	0	0	0	0	3	2	0

	DEPTH / cm															
	402	404	406	408	410	412	414	416	418	420	422	426	428	430	432	434
Chironomus	2	4	1	0	1	4	1	2	0	0	0	1	3	2	1	1
Cryptochironomus	0	0	0	0	0	0	0	0	0	0	0	0	0	0	0	0
Lauterborniella	0	0	0	1	0	0	3	6	0	0	2	2	4	3	1	0
Stenochironomus	0	0	0	0	0	0	0	0	0	0	0	0	0	0	0	0
Parachironomus	1	0	0	0	1	1	0	0	1	2	0	0	1	1	0	0
Polypedilum	1	1	0	1	0	5	2	3	2	3	0	1	4	2	5	4
Phaenopsectra	0	1	1	0	0	0	0	1	1	1	2	0	1	2	0	0
Pseudochironomus	0	0	0	0	0	1	0	0	0	0	0	0	1	0	0	1
Microtendipes Taxon A	2	0	3	0	0	2	1	1	2	1	1	2	5	0	1	3
Micropsectra Taxon B	0	0	1	2	1	0	0	0	0	0	0	0	1	4	0	2
Orthocladiinae Undif	0	0	0	0	0	0	0	0	0	0	0	0	0	0	0	0
Corynoneura / Thienemanniella	0	5	1	2	0	0	2	0	2	3	3	0	6	0	0	3
Cricotopus / Orthocladius	0	8	2	7	0	1	0	0	0	0	0	0	1	1	0	2
Parasmi	0	0	0	0	0	0	0	0	0	0	0	0	0	0	0	0
Parakiefferiella	0	13	4	0	4	11	6	1	10	2	7	0	1	3	10	25
Parakiefferiella fennica type	3	2	4	7	3	0	3	0	1	0	3	0	0	0	0	3
Parapsectrocladius	102	29	184	93	67	61	49	45	89	253	69	79	304	332	117	11
Psorth	0	0	0	0	0	0	0	0	0	0	0	0	1	1	0	0
Limnophyes / Paralimnophyes Taxon A	2	3	1	0	0	3	0	1	1	3	8	0	8	5	6	11
Limnophyes / Paralimnophyes Taxon B	3	6	2	0	1	1	1	1	5	5	3	2	6	7	6	5
Smittia	0	0	0	0	0	0	0	0	0	0	0	0	0	3	0	1
Mesosm	0	0	0	0	0	0	0	0	0	0	0	0	0	10	0	0
Tventia / Eukiefferiella	0	0	1	2	0	1	0	1	2	0	0	1	12	0	8	17
Nanocladius	0	0	0	0	0	0	0	0	0	0	0	0	0	0	0	0
Orthocladiinae early instar	0	0	1	0	1	0	0	0	0	13	2	0	8	5	0	0
Orthocladiinae Taxon A	0	0	0	0	0	0	0	1	0	0	0	0	0	0	0	0
Gymnomectriocnemus	0	0	0	0	0	0	0	0	0	0	0	0	1	1	1	0
Orthocladiiniae Taxon D	0	0	0	0	0	0	0	0	0	0	0	0	0	0	0	0
Orthocladiiniae Taxon C	0	0	0	0	0	0	0	0	0	0	0	0	0	0	3	0
Tanytarsini Undif	0	0	0	0	0	0	0	1	0	1	0	0	2	2	1	1
Tanytarsini Taxon A	0	0	0	1	0	9	0	1	0	4	1	1	7	2	12	0
Tanytarsini Taxon E	10	10	11	12	6	24	11	8	9	11	6	11	45	23	12	5
Tanytarsini Taxon D	3	0	1	1	0	0	3	0	0	3	0	8	1	0	3	0
Tanytarsini Taxon B	14	4	14	1	10	6	3	4	3	19	9	1	32	31	9	0
Tanytarsini Taxon C	0	12	0	2	0	0	0	0	0	0	0	0	4	1	2	3
Tanypodinae Undif	0	0	1	1	0	0	0	2	2	1	1	0	4	1	2	1
Tanypodinae Taxon B	6	0	6	3	1	2	3	2	1	3	4	2	7	9	5	2
Tanypodinae Taxon A	4	4	4	8	2	6	4	6	1	2	2	1	8	13	8	1
Clinotanypus	0	0	1	0	0	0	0	0	0	0	0	0	0	1	0	0
Procladiini / Macropelopiini early instar	0	0	0	0	0	0	1	1	0	1	1	0	4	3	0	0
Ablabesmyia	6	9	9	6	9	5	6	8	3	19	7	6	21	28	10	1
Labrundinia	8	4	14	9	3	7	5	6	7	13	6	4	29	24	6	0
Podonominae	1	2	4	2	0	4	3	6	3	9	6	3	27	28	15	24
Chironomini early Instar	1	0	1	0	1	0	0	0	0	0	0	0	0	0	1	0

	DEPTH / cm						
	442	446	450	454	458	462	466
Chironomus	0	0	0	3	0	1	0
Cryptochironomus	0	0	0	0	0	0	0
Lauterborniella	0	0	0	0	0	0	0
Stenochironomus	0	0	0	0	0	0	0
Parachironomus	0	0	0	1	0	0	1
Polypedilum	4	4	8	9	3	3	1
Phaenopsectra	0	0	0	0	0	1	0
Pseudochironomus	2	1	2	2	0	0	0
Microtendipes Taxon A	2	4	1	2	0	1	1
Micropsectra Taxon B	2	2	1	10	2	31	26
Orthocladiinae Undif	0	0	0	0	0	0	0
Corynoneura / Thienemanniella	5	1	1	4	2	1	1
Cricotopus / Orthocladius	8	5	6	5	1	3	3
Parasmi	0	0	0	0	0	0	1
Parakiefferiella	36	29	11	14	10	86	81
Parakiefferiella fennica type	1	1	0	0	1	1	0
Parapsectrocladius	9	14	14	14	4	4	4
Psorth	0	1	1	0	0	0	0
Limnophyes / Paralimnophyes Taxon A	5	1	3	5	0	0	1
Limnophyes / Paralimnophyes Taxon B	7	2	1	0	3	0	0
Smittia	1	0	0	0	0	1	1
Mesosm	0	0	0	0	0	0	0
Tventia / Eukiefferiella	8	8	3	1	0	0	0
Nanocladius	0	0	0	0	0	0	0
Orthocladiinae early instar	0	0	0	0	0	0	1
Orthocladiinae Taxon A	0	0	0	0	0	0	0
Gymnometriocnemus	0	0	0	0	0	0	0
Orthocladiinae Taxon D	0	0	0	0	0	1	0
Orthocladiinae Taxon C	0	0	1	0	0	1	0
Tanytarsini Undif	0	1	0	0	0	0	0
Tanytarsini Taxon A	0	0	0	0	1	0	0
Tanytarsini Taxon E	0	1	0	1	0	0	11
Tanytarsini Taxon D	1	0	0	0	0	0	0
Tanytarsini Taxon B	2	0	0	0	0	1	12
Tanytarsini Taxon C	0	1	0	0	0	3	0
Tanypodinae Undif	3	2	0	1	1	3	3
Tanypodinae Taxon B	0	1	0	1	0	0	6
Tanypodinae Taxon A	2	1	1	1	0	4	2
Clinotanypus	0	0	0	0	0	0	0
Procladiini / Macropelopiini early instar	0	0	0	0	0	0	0
Ablabesmyia	1	0	0	2	0	1	0
Labrundinia	1	0	0	0	0	1	1
Podonominae	10	20	12	12	4	12	10
Chironomini early instar	0	1	0	0	0	0	0

Laguna Leta raw counts

	DEPTH / cm												
	54	62	70	78	86	92	96	100	104	112	116	120	124
Chironomus	2	3	3	0	0	0	0	2	0	0	0	0	1
Cryptochironomusironomus	1	1	0	0	1	0	0	1	1	0	0	1	0
Cryptotendipes	5	0	1	2	1	1	2	3	0	1	2	0	0
Dicrotendipes	0	0	0	0	1	0	0	0	0	0	0	0	0
Lauterborniella	28	2	0	0	0	2	0	3	0	0	0	0	0
Stenochironomus	0	0	0	0	0	1	0	0	0	1	0	0	0
Parachironomus	1	1	3	1	1	0	2	6	2	1	5	1	2
Polypedilum	6	8	10	2	1	5	0	2	0	0	4	1	0
Phaenopsectra	0	1	2	3	2	0	1	0	1	3	2	1	2
Pseudochironomus	2	2	0	0	2	0	0	1	0	0	0	0	3
Microtendipes Taxon A	0	0	0	0	0	0	0	0	0	0	0	0	0
Micropsectra Taxon B	1	1	0	0	1	2	3	12	2	0	0	1	0
Orthocladiinae Undif	0	0	0	0	0	0	0	0	0	0	0	0	0
Corynoneura / Thienemanniella	0	0	0	1	1	0	0	0	0	0	0	2	1
Cricotopus / Orthocladius	0	0	0	0	0	0	0	0	0	0	0	0	0
Parakiefferiella	6	80	144	55	88	28	49	54	40	48	71	37	55
Parakiefferiella fennica type	9	1	5	1	0	1	0	2	0	0	0	0	0
Parapsectrocladius	3	3	2	2	4	1	4	8	1	1	2	2	2
Limnophyes / Paralimnophyes Taxon A	2	1	22	6	14	6	6	11	6	7	2	10	13
Limnophyes / Paralimnophyes Taxon B	0	1	0	0	0	0	0	0	0	0	0	0	1
Tvetia / Eukiefferiella	0	0	0	0	0	0	0	0	0	0	0	0	0
Orth Cranston	0	0	0	0	0	0	0	1	0	1	0	0	0
Orthocladiinae early instar	0	0	0	0	0	0	0	0	0	0	0	0	0
Orthocladiinae Taxon A	0	0	0	0	0	0	0	0	0	0	0	0	0
Gymnomectriocnemus	0	0	0	0	0	0	0	1	0	0	0	0	0
Orthocladiinae Taxon D	0	0	0	0	0	0	0	0	0	0	0	0	0
Orthocladiinae Taxon A	0	0	0	0	0	0	0	0	0	0	0	0	0
Orthocladiinae Taxon C	0	1	0	0	0	0	0	0	0	0	0	0	0
Tanytarsini Undif	8	3	3	5	4	3	2	6	1	1	2	5	1
Tanytarsini Taxon A	62	33	112	18	50	29	18	24	9	10	18	7	9
Tanytarsini Taxon E	15	8	11	16	20	14	20	13	8	9	17	4	14
Tanytarsini Taxon D	9	23	17	18	32	12	22	27	20	14	21	9	11
Tanytarsini Taxon B	30	52	103	35	51	25	27	30	12	13	24	12	32
Tanytarsini Taxon C	0	0	0	0	0	0	0	0	0	0	0	0	0
Tanypodinae Undif	5	0	1	1	1	1	1	8	0	1	0	1	1
Tanypodinae Taxon C	7	0	1	0	0	0	1	2	0	0	0	0	0
Tanypodinae Taxon B	1	4	8	7	2	1	4	2	0	3	3	1	0
Tanypodinae Taxon A	3	2	2	2	5	1	2	2	1	1	2	1	2
Clinotanypus	2	0	0	0	0	0	0	0	0	0	0	0	0
Procladiini / Macropelopiini early instar	0	1	1	1	2	0	0	3	1	0	4	0	0
Ablabesmyia	28	8	17	9	11	2	1	10	2	2	1	5	1
Labrundinia	3	6	15	3	9	4	2	11	4	1	2	2	1
Tanypodinae Taxon D	0	0	0	0	0	0	0	0	0	0	0	0	0

	DEPTH / cm												
	128	136	140	144	148	152	160	168	172	176	184	186	188
Chironomus	0	0	0	0	0	0	0	1	5	1	0	1	0
Cryptochironomusironomus	1	1	0	0	0	2	0	0	0	0	1	2	0
Cryptotendipes	0	3	1	1	1	3	1	0	0	0	0	0	0
Dicrotendipes	0	0	0	0	0	0	0	0	4	0	0	0	0
Lauterborniella	0	1	0	0	0	0	0	0	5	0	0	1	0
Stenochironomus	0	0	0	0	0	1	0	0	1	0	0	0	0
Parachironomus	2	4	1	2	2	4	10	4	3	1	2	1	1
Polypedilum	3	9	2	4	6	4	1	5	3	2	2	5	3
Phaenopsectra	2	2	1	1	3	0	0	3	0	0	1	2	1
Pseudochironomus	0	0	0	0	1	1	1	0	4	0	0	0	0
Microtendipes Taxon A	0	0	0	0	0	0	0	0	0	0	0	0	0
Micropsectra Taxon B	4	0	0	0	2	2	9	4	5	3	8	6	1
Orthocladiinae Undif	0	1	0	0	1	0	0	0	0	0	0	0	0
Corynoneura / Thienemanniella	0	0	0	1	1	0	0	3	2	3	3	2	1
Cricotopus / Orthocladius	0	0	0	0	0	0	0	0	0	0	0	0	0
Parakiefferiella	37	65	105	70	75	48	62	27	9	21	19	30	28
Parakiefferiella fennica type	0	1	0	0	0	1	0	0	1	0	0	0	0
Parapsectrocladius	1	2	3	1	3	5	3	6	1	4	5	5	2
Limnophyes / Paralimnophyes Taxon A	13	10	16	14	11	8	11	6	4	6	5	8	7
Limnophyes / Paralimnophyes Taxon B	0	1	0	0	0	1	0	0	0	0	0	0	2
Tvetia / Eukiefferiella	0	0	0	0	0	1	0	0	1	1	2	0	0
Orth Cranston	0	1	0	2	0	0	0	0	0	0	0	0	0
Orthocladiinae early instar	0	0	1	0	0	0	0	0	0	0	0	0	0
Orthocladiinae Taxon At	0	0	0	0	0	0	0	0	1	0	0	0	1
Gymnomectriocnemus	0	0	0	0	0	0	0	0	0	0	0	0	0
Orthocladiiniae Taxon D	0	0	0	0	0	0	0	0	0	0	0	0	0
Orthocladiiniae Taxon A	0	0	0	0	0	0	0	0	0	0	0	0	0
Orthocladiiniae Taxon C	0	0	0	0	0	0	0	0	0	0	0	0	0
Tanytarsini Undif	6	3	3	10	7	7	7	8	5	1	2	5	2
Tanytarsini Taxon A	23	40	17	12	19	47	24	14	4	3	12	9	1
Tanytarsini Taxon E	6	27	35	14	26	28	39	29	26	29	12	15	20
Tanytarsini Taxon D	19	22	22	37	25	9	21	7	3	3	9	10	2
Tanytarsini Taxon B	15	19	11	29	18	31	13	10	18	14	10	15	15
Tanytarsini Taxon C	0	1	0	0	1	1	0	0	1	0	0	2	0
Tanypodinae Undif	0	3	4	3	4	3	7	10	6	1	1	5	0
Tanypodinae Taxon C	1	0	0	0	0	0	1	1	0	0	2	0	0
Tanypodinae Taxon B	3	6	6	2	3	5	4	5	2	8	5	2	4
Tanypodinae Taxon A	2	8	1	6	5	11	8	9	10	3	4	5	4
Clinotanypus	3	0	0	0	0	0	1	0	0	0	0	0	0
Procladiini / Macropelopiini early instar	1	1	0	0	0	0	2	1	0	0	0	1	1
Ablabesmyia	1	3	3	3	3	3	11	4	13	0	1	2	2
Labrundinia	0	7	2	6	5	16	8	9	6	9	13	14	9
Tanypodinae Taxon D	0	0	0	0	0	0	0	0	0	1	0	0	1

	DEPTH / cm												
	190	192	196	200	204	206	208	210	212	214	216	218	233
Chironomus	2	0	3	2	14	4	19	12	4	8	9	10	10
Cryptochironomus	0	0	0	0	0	0	0	0	0	0	0	0	1
Cryptotendipes	0	0	0	0	1	1	1	1	0	0	1	2	3
Dicrotendipes	1	0	13	18	5	8	6	5	6	7	1	4	0
Lauterborniella	1	3	6	3	3	3	5	4	3	4	0	0	16
Stenochironomus	0	0	0	0	0	0	0	0	0	0	0	0	5
Parachironomus	1	3	0	1	1	0	0	1	0	0	2	0	0
Polypedilum	2	2	4	3	5	1	9	5	6	4	5	5	3
Phaenopsectra	1	0	0	0	0	0	0	0	0	0	0	0	0
Pseudochironomus	0	1	0	6	0	0	0	1	0	1	1	1	7
Microtendipes Taxon A	0	0	0	0	0	0	1	0	0	0	0	0	0
Micropsectra Taxon B	9	6	1	2	0	1	0	1	12	10	18	2	1
Orthocladiinae Undif	0	0	0	0	0	0	0	0	0	0	0	0	0
Corynoneura / Thienemanniella	3	0	0	0	0	0	0	0	0	0	0	0	0
Cricotopus / Orthocladius	0	0	0	0	0	0	0	0	0	0	0	0	0
Parakiefferiella	8	20	1	0	0	0	0	0	0	0	1	0	0
Parakiefferiella fennica type	0	1	0	0	0	0	0	0	0	0	1	0	9
Parapsectrocladius	5	2	7	7	7	8	14	15	18	22	27	5	0
Limnophyes / Paralimnophyes Taxon A	5	1	0	2	0	0	0	0	6	1	0	0	6
Limnophyes / Paralimnophyes Taxon B	0	0	0	0	0	0	0	0	0	0	0	0	0
Tventia / Eukiefferiella	0	0	0	0	0	0	0	0	0	0	0	0	0
Orth Cranston	0	0	0	0	0	0	0	0	0	0	0	0	0
Orthocladiinae early instar	0	0	0	0	0	0	0	0	0	0	0	0	0
Orthocladiinae Taxon At	0	0	0	0	0	0	0	0	0	0	0	0	0
Gymnomectriocnemus	0	0	0	0	0	0	0	0	0	0	0	0	0
Orthocladiinae Taxon D	0	0	0	0	0	0	0	0	0	0	0	0	0
Orthocladiinae Taxon A	0	0	0	0	0	0	0	0	0	0	0	0	0
Orthocladiinae Taxon C	0	0	0	0	0	0	0	0	0	0	0	0	0
Tanytarsini Undif	7	2	8	3	8	5	10	3	6	0	12	1	11
Tanytarsini Taxon A	11	3	7	12	15	12	14	8	7	1	2	2	46
Tanytarsini Taxon E	13	18	29	40	21	19	25	11	14	6	14	19	5
Tanytarsini Taxon D	2	8	7	2	10	3	1	2	7	2	26	2	18
Tanytarsini Taxon B	17	14	22	12	14	9	9	13	5	8	18	13	12
Tanytarsini Taxon C	2	0	0	1	0	0	0	0	0	0	0	0	0
Tanypodinae Undif	1	2	1	4	2	0	2	3	1	0	0	0	1
Tanypodinae Taxon C	0	0	0	0	0	0	0	0	0	0	0	0	0
Tanypodinae Taxon B	1	4	3	4	2	0	0	3	1	0	0	1	1
Tanypodinae Taxon A	1	0	1	1	1	0	0	2	0	1	0	0	0
Clinotanypus	0	0	0	1	0	2	1	1	0	1	0	0	1
Procladiini / Macropelopiini early instar	0	0	0	0	0	0	0	0	0	0	2	0	1
Ablabesmyia	8	5	24	36	34	19	21	19	11	6	8	11	24
Labrundinia	8	8	4	4	4	3	6	3	8	5	7	0	4
Tanypodinae Taxon D	0	0	0	0	0	0	0	0	0	0	0	0	0

	DEPTH / cm												
	234	235	236	237	238	239	240	241	242	243	244	245	246
Chironomus	10	4	8	5	1	10	0	0	1	0	5	6	1
Cryptochironomus/ronomus	1	1	1	1	2	0	0	0	1	1	1	0	2
Cryptotendipes	3	1	1	1	5	2	2	1	2	1	1	5	3
Dicrotendipes	0	0	0	0	0	1	0	0	0	0	0	0	0
Lauterborniella	16	23	13	13	6	1	1	2	1	2	7	1	9
Stenochironomus	5	0	0	0	0	0	0	0	0	0	0	0	1
Parachironomus	0	1	0	1	0	0	1	0	0	1	0	0	0
Polypedilum	3	12	16	11	8	5	2	0	2	1	2	0	7
Phaenopsectra	0	0	0	0	0	0	0	0	0	0	0	0	0
Pseudochironomus	7	3	18	15	21	6	1	1	3	2	0	1	0
Microtendipes Taxon A	0	0	0	0	0	0	0	0	0	0	0	0	0
Micropsectra Taxon B	1	0	3	2	0	6	0	0	1	0	1	0	1
Orthocladiinae Undif	0	0	0	0	0	0	0	0	0	0	0	0	0
Corynoneura / Thienemanniella	0	0	0	0	0	0	0	0	0	0	1	0	0
Cricotopus / Orthocladius	0	0	0	0	1	0	0	0	0	0	0	0	2
Parakiefferiella	0	1	0	13	1	9	11	16	9	8	10	9	6
Parakiefferiella fennica type	9	4	2	5	2	0	7	3	1	0	1	0	0
Parapsectrocladius	0	2	2	7	7	5	2	0	0	3	0	1	4
Limnophyes / Paralimnophyes Taxon A	6	3	2	4	2	1	0	4	4	5	4	1	2
Limnophyes / Paralimnophyes Taxon B	0	0	0	0	0	0	0	0	0	0	0	0	0
Tvetenia / Eukiefferiella	0	0	0	0	0	1	0	0	0	1	0	0	1
Orth Cranston	0	0	0	1	0	1	0	1	0	0	0	0	0
Orthocladiinae early instar	0	0	0	0	0	0	0	0	0	0	0	0	0
Orthocladiinae Taxon At	0	0	0	0	0	0	0	0	0	0	0	0	0
Gymnomectricnemus	0	0	0	0	0	0	0	0	0	0	0	0	0
Orthocladiinae Taxon D	0	0	0	0	0	0	0	0	0	0	0	0	1
Orthocladiinae Taxon A	0	0	0	0	0	0	0	2	0	0	0	0	0
Orthocladiinae Taxon C	0	0	0	0	0	0	0	0	0	0	0	0	0
Tanytarsini Undif	11	1	16	14	5	14	3	9	2	3	4	5	16
Tanytarsini Taxon A	46	33	34	44	11	11	14	19	22	13	12	9	3
Tanytarsini Taxon E	5	2	5	53	14	25	43	29	31	23	74	52	20
Tanytarsini Taxon D	18	12	8	35	2	5	7	7	7	0	4	6	2
Tanytarsini Taxon B	12	9	4	12	6	10	2	4	12	3	9	6	8
Tanytarsini Taxon C	0	0	0	0	0	0	0	0	0	0	0	0	0
Tanypodinae Undif	1	1	1	4	1	0	4	1	4	6	7	2	6
Tanypodinae Taxon C	0	0	0	8	0	1	1	6	3	2	1	1	3
Tanypodinae Taxon B	1	1	0	0	1	0	3	0	1	7	6	1	6
Tanypodinae Taxon A	0	2	0	7	3	4	2	3	8	0	7	8	0
Clinotanypus	1	0	0	1	1	1	0	1	2	1	0	0	3
Procladiini / Macropelopiini early instar	1	0	0	1	0	0	0	0	0	0	1	0	0
Ablabesmyia	24	25	14	30	31	7	3	10	9	13	16	4	12
Labrundinia	4	1	1	2	2	4	0	1	0	1	0	0	0
Tanypodinae Taxon D	0	0	0	0	1	0	0	0	0	0	0	0	0

	DEPTH / cm								
	247	248	249	250	251	252	253	257	267
Chironomus	0	12	1	1	0	0	1	0	0
Cryptochironomusironomus	0	1	0	0	0	0	1	0	0
Cryptotendipes	1	1	0	1	1	0	1	0	0
Dicrotendipes	0	0	0	0	0	0	0	0	0
Lauterborniella	2	2	7	2	21	11	11	0	0
Stenochironomuso	0	0	0	0	0	0	0	0	0
Parachironomus	0	1	0	0	0	0	0	0	1
Polypedilum	4	6	4	7	7	2	5	2	1
Phaenopsectra	0	0	0	0	0	0	0	0	0
Pseudochironomus	0	0	6	6	9	7	6	1	7
Microtendipes Taxon A	0	0	0	0	0	0	0	0	0
Micropsectra Taxon B	2	2	0	0	1	0	0	0	2
Orthocladiinae Undif	0	0	0	0	0	0	0	0	0
Corynoneura / Thienemanniella	0	0	0	0	0	0	0	0	0
Cricotopus / Orthocladius	1	0	3	1	2	0	0	0	2
Parakiefferiella	8	48	6	2	6	5	0	1	0
Parakiefferiella fennica type	0	4	0	0	0	0	4	1	0
Parapsectrocladius	1	2	0	3	1	0	0	0	1
Limnophyes / Paralimnophyes Taxon A	2	7	2	0	2	0	2	0	0
Limnophyes / Paralimnophyes Taxon B	0	0	0	0	0	0	0	0	0
Tvetenia / Eukiefferiella	0	0	0	0	0	2	0	0	0
Orthocladiinae early instar	0	0	0	0	0	0	0	0	0
Orthocladiinae Taxon A	0	0	0	0	0	0	0	0	0
Gymnomectriocnemus	0	0	0	0	0	0	0	0	0
Orthocladiiniae Taxon D	0	0	0	0	0	0	0	0	0
Orthocladiiniae Taxon A	0	0	0	0	0	0	0	0	0
Orthocladiiniae Taxon C	0	0	0	0	0	0	0	0	0
Tanytarsini Undif	7	10	10	3	3	5	1	0	0
Tanytarsini Taxon A	6	27	10	3	20	1	1	1	1
Tanytarsini Taxon E	46	85	3	6	11	2	2	1	0
Tanytarsini Taxon D	0	13	4	0	8	1	6	0	0
Tanytarsini Taxon B	9	15	4	5	3	3	2	1	1
Tanytarsini Taxon C	0	0	0	0	0	0	0	0	0
Tanypodinae Undif	4	17	2	2	4	1	0	0	1
Tanypodinae Taxon C	0	7	2	2	1	4	2	0	0
Tanypodinae Taxon B	0	8	3	3	4	4	1	1	0
Tanypodinae Taxon A	4	9	4	5	2	4	2	0	0
Clinotanypus	0	2	1	1	1	0	0	0	0
Procladiini / Macropelopiini early instar	0	0	0	0	0	0	0	0	0
Ablabesmyia	5	24	10	9	14	0	2	0	0
Labrundinia	0	0	0	0	0	1	0	0	0
Tanypodinae Taxon D	0	0	0	0	0	1	0	0	0

APPENDIX 5

Codes for chironomid taxa

TAXON / MORPHOTAXON	CODE
Ablabesmyia	ABL
Chironomini early instar	CINST
Chironomus	CHIR
Corynoneura / Thienemanniella	C/T
Cricotopus / Orthocladius	C/O
Cryptotendipes	CRY
Dicrotendipes	DICRO
Labrundinia	LAB
Lauterborniella	LAUT
Limnophyes / Paralimnophyes Taxon A	L/P-A
Limnophyes / Paralimnophyes Taxon B	L/P-B
Microtendipes Taxon B	MIC B
Nanocladius	NANO
Orthocladiinae early instar	OINST
Parachironomus	PARC
Parakiefferiella	PARAK
Parakiefferiella fennica type	FENN
Parapsectrocladius	PARAP
Phaenopsectra	PHAEN
Podonominae	POD
Polypedilum	POLY
Procladiini / Macropelopiini early instar	PINST
Pseudochironomus	PSEUD
Tanypodinae Taxon B	TAP B
Tanypodinae Taxon A	TAP A
Tanypodinae Taxon C	TAP C
Tanypodinae Undif	TANYP
Tanytarsini Taxon A	TAN A
Tanytarsini Taxon B	TAN B
Tanytarsini Taxon C	TAN C
Tanytarsini Taxon D	TAN D
Tanytarsini Taxon E	TAN E
Tanytarsini Undif	TANY
Tventia / Eukiefferiella	TV/EU

APPENDIX 6

Loss on ignition for Laguna Leta

Depth / cm	% LOI	Depth / cm	% LOI	Depth / cm	% LOI
54	35.7	129	87.6	204	77.0
56	19.7	131	89.2	206	75.9
58	35.4	133	89.4	207	71.9
60	43.0	135	88.5	209	69.5
62	33.6	137	88.3	211	66.7
64	41.4	139	88.3	213	59.8
66	46.4	141	88.3	215	48.3
68	56.8	143	88.4	217	25.0
70	47.9	145	89.0	219	37.6
72	62.8	147	90.4	221	27.1
74	84.5	149	88.4	223	8.5
76	50.2	151	88.9	225	7.9
78	83.5	153	87.5	227	10.1
80	84.6	155	87.3	228	6.3
82	82.3	157	89.0	230	8.3
84	82.6	159	83.5	233	41.8
86	83.5	160	84.3	235	50.1
88	85.0	162	72.2	237	54.8
90	76.7	164	77.1	239	56.0
91	80.9	166	89.1	241	55.5
93	85.7	168	85.1	243	54.1
95	87.9	170	86.2	245	52.0
97	88.5	172	86.9	247	50.9
99	90.7	174	87.8	249	44.9
101	95.5	176	88.0	251	42.8
103	87.4	178	88.1	253	35.8
105	88.7	180	88.1	255	21.5
107	88.5	182	86.9	257	23.4
109	88.7	184	85.3	259	18.4
111	87.3	186	84.6	261	17.4
113	87.0	188	86.0	263	16.6
115	88.0	190	85.8	265	12.6
117	89.7	192	83.4	267	15.2
119	90.0	194	70.3	269	19.8
121	89.4	196	74.3	271	19.0
123	88.3	198	78.3	273	19.1
125	87.4	200	77.6		
127	87.6	202	74.2		

Loss on ignition for Laguna Boal

Depth / cm	% LOI	Depth / cm	% LOI	Depth / cm	% LOI	Depth / cm	% LOI
0	37.1	136	32.9	248	33.8	354	18.4
2	39.6	138	33.0	250	33.6	356	12.4
6	36.3	140	33.9	254	27.7	358	26.1
8	40.9	144	31.4	256	36.2	360	39.6
10	36.4	148	34.5	258	31.4	362	37.2
12	29.3	150	39.5	260	30.9	364	32.5
14	49.0	152	40.6	262	35.1	366	28.3
16	41.1	154	36.4	264	35.5	368	37.5
18	41.9	156	28.7	266	33.2	370	37.4
20	41.6	158	35.8	268	33.4	372	41.3
22	34.5	160	33.9	270	32.9	374	35.4
24	38.5	162	36.1	272	26.5	376	40.9
26	35.1	164	36.9	274	39.2	378	35.8
28	32.3	166	35.6	276	39.6	380	37.8
30	35.2	168	36.1	278	33.4	382	38.5
32	34.5	170	37.8	280	31.1	384	37.0
34	41.6	172	39.2	282	27.4	386	34.8
38	39.8	174	37.2	284	22.6	388	33.2
40	39.1	176	36.2	286	23.5	390	32.4
42	35.7	178	36.6	288	35.2	392	35.2
44	37.1	180	33.5	290	23.1	394	33.8
46	40.9	182	37.8	292	38.8	396	41.7
48	38.5	184	38.0	302	32.0	398	43.7
50	39.4	186	41.4	304	40.0	400	39.2
52	41.4	188	34.1	306	35.6	402	39.0
54	33.8	190	29.4	308	31.7	404	40.4
56	28.8	200	32.8	310	27.5	406	34.7
58	27.3	202	33.2	312	26.2	408	30.5
60	27.8	204	31.1	314	31.7	410	26.4
62	24.1	206	30.8	316	26.8	412	18.3
64	27.6	208	31.1	318	32.1	414	14.2
102	35.3	210	32.4	320	41.8	416	29.9
104	42.2	212	28.6	322	26.6	418	39.2
106	43.7	214	30.2	324	39.6	420	25.1
108	38.4	216	29.0	326	31.0	422	28.7
110	27.7	220	28.1	328	36.8	424	7.2
112	27.8	222	30.3	330	26.0	426	33.5
114	34.8	224	30.0	332	43.6	428	34.2
116	35.9	226	33.9	334	44.0	430	27.9
118	34.7	228	37.4	336	35.3	432	34.5
120	33.9	230	24.8	338	36.8	446	33.4
122	33.6	232	32.1	340	34.0	450	28.3
124	35.1	234	32.2	342	45.9	454	20.9
126	35.0	236	33.8	344	44.8	458	19.9
128	33.3	238	20.4	346	29.3	462	17.9
130	33.1	240	37.1	348	43.6	466	16.0
132	30.1	242	32.8	350	34.8		
134	27.4	244	29.8	352	33.0		

APPENDIX 7

Magnetic susceptibility data from Laguna Boal

Depth / m	Magnetic Susceptibility	Depth / m	Magnetic Susceptibility	Depth / m	Magnetic Susceptibility	Depth / m	Magnetic Susceptibility
2.000	7.0	2.102	4.50	2.202	26.0	2.304	2.0
2.002	10.5	2.104	3.50	2.204	26.5	2.306	1.0
2.004	12.0	2.106	4.00	2.206	27.5	2.308	2.0
2.006	12.0	2.108	6.00	2.208	28.5	2.310	1.5
2.008	12.0	2.110	5.00	2.210	30.5	2.312	2.0
2.010	9.0	2.112	4.50	2.212	33.0	2.314	2.0
2.012	6.0	2.114	5.00	2.214	31.5	2.316	2.5
2.014	3.0	2.116	4.50	2.216	29.5	2.318	2.0
2.016	3.0	2.118	5.00	2.218	24.0	2.320	1.5
2.018	2.0	2.120	3.50	2.220	19.0	2.322	1.5
2.020	2.5	2.122	4.50	2.222	14.5	2.324	2.5
2.022	2.0	2.124	4.50	2.224	13.0	2.326	2.0
2.024	3.0	2.126	4.50	2.226	19.5	2.328	3.0
2.026	3.0	2.128	3.50	2.228	24.5	2.330	2.0
2.028	3.5	2.130	3.50	2.230	15.0	2.332	2.0
2.030	4.0	2.132	4.00	2.232	7.5	2.334	3.0
2.032	4.0	2.134	4.00	2.234	3.5	2.336	3.0
2.034	4.0	2.136	3.50	2.236	2.5	2.338	3.0
2.036	3.0	2.138	4.50	2.238	2.5	2.340	4.0
2.038	4.0	2.140	5.00	2.240	2.0	2.342	3.0
2.040	4.0	2.142	4.50	2.242	3.5	2.344	3.0
2.042	4.0	2.144	4.50	2.244	3.5	2.346	2.5
2.044	4.0	2.146	6.00	2.246	6.0	2.348	1.5
2.046	4.0	2.148	4.50	2.248	12.0	2.350	1.5
2.048	4.5	2.150	5.00	2.250	19.0	2.352	1.0
2.050	4.5	2.152	4.50	2.252	17.0	2.354	1.5
2.052	4.5	2.154	4.00	2.254	9.0	2.356	1.5
2.054	3.5	2.156	5.50	2.256	4.0	2.358	1.5
2.056	4.0	2.158	5.00	2.258	3.0	2.360	3.0
2.058	4.0	2.160	7.50	2.260	2.0	2.362	2.5
2.060	3.5	2.162	11.00	2.262	1.0	2.364	1.0
2.062	4.5	2.164	19.50	2.264	1.0	2.366	1.0
2.064	3.0	2.166	28.50	2.266	2.0	2.368	2.0
2.066	3.0	2.168	31.00	2.268	2.0	2.370	2.5
2.068	4.0	2.170	22.50	2.270	1.0	2.372	1.5
2.070	4.0	2.172	16.00	2.272	2.0	2.374	2.0
2.072	4.0	2.174	15.00	2.274	2.0	2.376	2.0
2.074	4.0	2.176	19.00	2.276	2.0	2.378	1.0
2.076	4.0	2.178	21.00	2.278	1.5	2.380	2.5
2.078	4.0	2.180	16.50	2.280	2.5	2.382	2.5
2.080	5.0	2.182	9.50	2.282	2.5	2.384	2.0
2.082	4.0	2.184	7.00	2.284	2.0	2.386	2.0
2.084	3.5	2.186	7.50	2.286	3.5	2.388	1.5
2.086	3.0	2.188	10.50	2.288	3.5	2.390	2.5
2.088	4.5	2.190	11.00	2.290	6.5	2.392	2.5
2.090	5.0	2.192	14.00	2.292	8.0	2.394	2.0
2.092	5.0	2.194	19.00	2.294	5.0	2.396	3.0
2.094	4.5	2.196	19.50	2.296	2.5	2.398	2.5
2.096	3.5	2.198	22.50	2.298	2.5	2.400	1.5
2.098	5.0	2.200	24.00	2.300	1.5	2.402	2.5
2.100	5.0			2.302	2.0		

Depth / m	Magnetic Susceptibility	Depth / m	Magnetic Susceptibility	Depth / m	Magnetic Susceptibility	Depth / m	Magnetic Susceptibility
2.404	3.0	2.506	3.0	2.606	5.0	2.708	4.50
2.406	1.0	2.508	3.0	2.608	6.0	2.710	5.00
2.408	2.0	2.510	2.5	2.610	6.0	2.712	5.00
2.410	3.0	2.512	2.0	2.612	7.0	2.714	6.00
2.412	2.0	2.514	1.0	2.614	4.0	2.716	6.00
2.414	2.0	2.516	2.0	2.616	5.0	2.718	7.00
2.416	3.0	2.518	2.0	2.618	4.5	2.720	6.00
2.418	3.0	2.520	3.0	2.620	4.0	2.722	5.50
2.420	2.0	2.522	2.5	2.622	3.5	2.724	4.50
2.422	2.0	2.524	3.5	2.624	2.0	2.726	3.00
2.424	3.0	2.526	2.0	2.626	3.0	2.728	3.00
2.426	4.0	2.528	3.0	2.628	8.0	2.730	2.00
2.428	4.0	2.530	4.0	2.630	3.0	2.732	3.00
2.430	4.0	2.532	4.0	2.632	2.5	2.734	2.50
2.432	4.0	2.534	5.5	2.634	2.5	2.736	2.50
2.434	4.0	2.536	4.5	2.636	4.0	2.738	2.50
2.436	3.0	2.538	5.5	2.638	4.0	2.740	3.00
2.438	4.0	2.540	6.0	2.640	3.5	2.742	3.00
2.440	3.0	2.542	5.5	2.642	2.5	2.744	3.50
2.442	4.0	2.544	4.0	2.644	2.5	2.746	3.50
2.444	5.0	2.546	4.0	2.646	2.0	2.748	3.00
2.446	4.0	2.548	4.0	2.648	2.5	2.750	3.00
2.448	4.0	2.550	4.0	2.650	1.5	2.752	4.00
2.450	4.0	2.552	4.0	2.652	2.0	2.754	5.50
2.452	4.0	2.554	3.0	2.654	2.5	2.756	4.50
2.454	4.0	2.556	3.0	2.656	2.5	2.758	5.50
2.456	5.0	2.558	2.0	2.658	3.5	2.760	4.50
2.458	5.0	2.560	3.0	2.660	4.0	2.762	4.00
2.460	5.0	2.562	2.5	2.662	2.5	2.764	5.50
2.462	6.0	2.564	3.5	2.664	2.5	2.766	6.00
2.464	6.0	2.566	2.0	2.666	3.0	2.768	5.50
2.466	4.5	2.568	3.5	2.668	3.0	2.770	5.00
2.468	4.5	2.570	3.5	2.670	1.5	2.772	3.00
2.470	5.5	2.572	2.0	2.672	3.0	2.774	4.50
2.472	4.5	2.574	3.5	2.674	1.0	2.776	5.50
2.474	3.0	2.576	3.5	2.676	1.0	2.778	5.50
2.476	4.0	2.578	3.0	2.678	1.0	2.780	7.50
2.478	4.0	2.580	4.0	2.680	1.5	2.782	4.00
2.480	4.0	2.582	3.0	2.682	2.0	2.784	4.50
2.482	6.0	2.584	4.0	2.684	3.0	2.786	3.50
2.484	5.0	2.586	3.0	2.686	3.0	2.788	3.00
2.486	6.0	2.588	4.0	2.688	1.5	2.790	3.00
2.488	4.5	2.590	3.5	2.690	2.5	2.792	2.50
2.490	3.5	2.592	3.5	2.692	3.5	2.794	4.00
2.492	3.5	2.594	4.0	2.694	3.5	2.796	3.00
2.494	3.0	2.596	5.0	2.696	3.5	2.798	2.50
2.496	3.5	2.598	5.0	2.698	2.5	2.800	3.00
2.498	3.5	2.600	5.0	2.700	3.5	2.802	3.00
2.500	3.5	2.602	6.0	2.702	2.5	2.804	3.00
2.502	4.0	2.604	5.0	2.704	4.0	2.806	3.00
2.504	4.0			2.706	3.5		

Depth / m	Magnetic Susceptibility	Depth / m	Magnetic Susceptibility	Depth / m	Magnetic Susceptibility	Depth / m	Magnetic Susceptibility
2.808	4.50	2.910	7.00	3.544	10.5	3.646	19.0
2.81	3.50	2.912	4.50	3.546	13.0	3.648	20.5
2.812	2.50	2.914	4.50	3.548	20.0	3.650	19.0
2.814	3.50	2.916	5.00	3.550	32.5	3.652	19.5
2.816	3.00	2.918	5.50	3.552	50.5	3.654	19.5
2.818	2.50	2.920	6.00	3.554	91.5	3.656	20.0
2.82	3.50	2.922	8.50	3.556	183.0	3.658	21.5
2.822	2.00	2.924	8.50	3.558	338.0	3.660	19.5
2.824	2.50	2.926	9.50	3.560	528.5	3.662	15.5
2.826	3.50	2.928	10.00	3.562	639.0	3.664	10.5
2.828	3.00	2.930	6.00	3.564	599.0	3.666	6.0
2.83	4.00	2.932	4.00	3.566	423.5	3.668	3.0
2.832	4.00	2.934	2.00	3.568	197.5	3.670	3.5
2.834	5.00	2.936	0.50	3.570	77.5	3.672	4.5
2.836	5.00	2.938	0.50	3.572	32.5	3.674	4.0
2.838	6.00	2.940	-0.50	3.574	17.0	3.676	3.5
2.84	6.00	2.942	-1.00	3.576	12.0	3.678	3.5
2.842	5.00	2.944	-0.50	3.578	9.5	3.680	2.5
2.844	5.50	2.946	0.00	3.580	7.0	3.682	2.5
2.846	5.50	2.948	1.00	3.582	7.0	3.684	2.0
2.848	5.00	2.950	-0.50	3.584	9.0	3.686	2.0
2.85	6.00	2.952	0.50	3.586	10.0	3.688	2.0
2.852	9.00	3.488	3.50	3.588	13.0	3.690	3.0
2.854	14.50	3.490	4.50	3.590	17.0	3.692	3.0
2.856	14.50	3.492	6.00	3.592	30.0	3.694	4.0
2.858	12.00	3.494	9.50	3.594	44.0	3.696	3.0
2.86	11.50	3.496	12.50	3.596	47.0	3.698	3.0
2.862	11.50	3.498	13.50	3.598	36.5	3.700	3.0
2.864	12.50	3.500	14.00	3.600	23.5	3.702	3.0
2.866	13.50	3.502	14.00	3.602	13.0	3.704	4.0
2.868	11.00	3.504	14.00	3.604	11.0	3.706	2.0
2.87	8.00	3.506	12.50	3.606	10.0	3.708	2.0
2.872	5.00	3.508	10.50	3.608	8.0	3.710	3.5
2.874	5.00	3.510	7.50	3.610	7.0	3.712	4.0
2.876	6.00	3.512	6.00	3.612	6.0	3.714	3.5
2.878	6.50	3.514	6.50	3.614	5.0	3.716	4.0
2.88	8.50	3.516	7.50	3.616	6.0	3.718	3.0
2.882	11.00	3.518	7.50	3.618	7.0	3.720	2.0
2.884	13.00	3.520	8.00	3.620	7.5	3.722	2.0
2.886	14.00	3.522	9.00	3.622	6.5	3.724	2.0
2.888	13.50	3.524	9.50	3.624	7.0	3.726	3.5
2.89	12.50	3.526	7.00	3.626	6.5	3.728	2.5
2.892	12.50	3.528	7.50	3.628	6.5	3.730	2.0
2.894	14.00	3.530	6.50	3.630	7.0	3.732	2.0
2.896	14.50	3.532	6.00	3.632	7.5	3.734	2.5
2.898	14.00	3.534	6.00	3.634	8.5	3.736	2.0
2.9	13.00	3.536	7.50	3.636	10.0	3.738	1.5
2.902	10.00	3.538	8.00	3.638	12.0	3.740	2.0
2.904	9.00	3.540	7.50	3.640	13.0	3.742	2.5
2.906	9.00	3.542	8.50	3.642	13.0	3.744	2.5
2.908	7.50			3.644	16.5		

Depth / m	Magnetic Susceptibility	Depth / m	Magnetic Susceptibility	Depth / m	Magnetic Susceptibility	Depth / m	Magnetic Susceptibility
3.746	3.0	3.848	2.0	3.948	3.0	4.050	4.0
3.748	4.0	3.850	2.0	3.950	2.0	4.052	4.0
3.750	4.5	3.852	3.5	3.952	2.5	4.054	5.0
3.752	5.0	3.854	2.5	3.954	2.5	4.056	7.0
3.754	5.0	3.856	4.0	3.956	2.0	4.058	10.0
3.756	4.5	3.858	5.5	3.958	2.5	4.060	14.0
3.758	4.0	3.860	5.5	3.960	4.0	4.062	19.0
3.760	5.5	3.862	5.5	3.962	2.5	4.064	26.0
3.762	6.5	3.864	5.0	3.964	2.0	4.066	28.0
3.764	6.0	3.866	6.0	3.966	1.5	4.068	19.0
3.766	5.5	3.868	4.5	3.968	1.5	4.070	14.0
3.768	5.0	3.870	4.0	3.970	2.0	4.072	13.0
3.770	5.0	3.872	4.0	3.972	2.0	4.074	13.5
3.772	3.5	3.874	3.0	3.974	3.5	4.076	13.5
3.774	4.0	3.876	3.0	3.976	2.5	4.078	11.0
3.776	5.0	3.878	3.0	3.978	3.0	4.080	11.0
3.778	6.0	3.880	2.5	3.980	3.0	4.082	15.0
3.780	10.5	3.882	2.5	3.982	3.0	4.084	23.0
3.782	14.5	3.884	2.5	3.984	3.0	4.086	24.5
3.784	14.0	3.886	3.5	3.986	2.0	4.088	22.0
3.786	11.5	3.888	3.0	3.988	2.0	4.090	19.0
3.788	6.5	3.890	3.0	3.990	2.5	4 092	17.5
3.790	5.0	3.892	5.0	3.992	2.5	4.094	16.0
3.792	4.5	3.894	6.0	3.994	2.0	4.096	19.0
3.794	5.5	3.896	7.5	3.996	2.0	4.098	25.0
3.796	6.0	3.898	6.5	3.998	2.0	4.100	29.0
3.798	5.0	3.900	4.0	4.000	2.0	4.102	37.0
3.800	6.0	3.902	3.0	4.002	1.0	4.104	50.5
3.802	5.5	3.904	2.0	4.004	2.5	4.106	61.5
3.804	5.5	3.906	3.0	4.006	2.5	4.108	67.0
3.806	3.0	3.908	4.5	4.008	2.5	4.110	89 0
3.808	2.5	3.910	3.5	4.010	1.5	4.112	140.0
3.810	2.5	3.912	3.5	4.012	1.5	4.114	202.5
3.812	2.0	3.914	5.0	4.014	1.5	4.116	206.5
3.814	3.0	3.916	4.5	4.016	1.5	4.118	141.0
3.816	4.0	3.918	4.5	4.018	0.5	4.120	74.5
3.818	4.0	3.920	5.0	4.020	2.0	4.122	50.5
3.820	6.0	3.922	4.5	4.022	2.0	4.124	50.0
3.822	8.0	3.924	4.0	4.024	2.5	4.126	48.5
3.824	9.0	3.926	4.0	4.026	2.5	4.128	35.5
3.826	9.0	3.928	4.5	4.028	2.0	4.130	21.0
3.828	9.0	3.930	4.5	4.030	2.0	4.132	13.0
3.830	8.0	3.932	4.5	4.032	2.0	4.134	8.5
3.832	7.0	3.934	3.5	4.034	3.0	4.136	7.5
3.834	7.5	3.936	3.0	4.036	2.0	4.138	9.0
3.836	7.5	3.938	3.0	4.038	3.0	4.140	8.5
3.838	7.0	3.940	3.0	4.040	3.0	4.142	12.0
3.840	6.0	3.942	3.0	4.042	3.0	4.144	16.0
3.842	5.0	3.944	1.5	4.044	3.0	4.146	17.5
3.844	3.0	3.946	1.5	4.046	2.0	4.148	20.0
3.846	3.0			4.048	2.0		

Depth / m	Magnetic Susceptibility	Depth / m	Magnetic Susceptibility	Depth / m	Magnetic Susceptibility	Depth / m	Magnetic Susceptibility
4.150	20.0	4.202	51.0	4.252	1.0	4.302	9.5
4.152	20.0	4.204	23.5	4.254	2.0	4.304	7.5
4.154	20.0	4.206	11.5	4.256	1.5	4.306	7.5
4.156	19.5	4.208	7.5	4.258	2.5	4.308	7.0
4.158	21.0	4.210	5.5	4.260	3.0	4.310	7.0
4.160	23.0	4.212	3.5	4.262	3.5	4.312	7.0
4.162	25.5	4.214	3.0	4.264	3.0	4.314	7.0
4.164	24.0	4.216	4.0	4.266	3.5	4.316	8.5
4.166	18.5	4.218	3.0	4.268	2.0	4.318	9.5
4.168	16.5	4.220	4.5	4.270	2.0	4.320	7.0
4.170	15.0	4.222	5.5	4.272	2.5	4.322	5.0
4.172	15.0	4.224	8.0	4.274	2.0	4.324	3.5
4.174	15.0	4.226	11.0	4.276	2.5	4.326	1.5
4.176	14.0	4.228	21.5	4.278	2.5	4.328	1.0
4.178	13.0	4.230	39.5	4.280	3.5	4.330	1.0
4.180	14.0	4.232	67.0	4.282	2.0	4.332	0.5
4.182	14.5	4.234	81.5	4.284	3.0	4.334	1.0
4.184	15.5	4.236	71.0	4.286	2.5	4.336	0.5
4.186	17.0	4.238	43.0	4.288	2.5	4.338	0.5
4.188	18.0	4.240	18.0	4.290	2.0	4 340	0.5
4.190	23.5	4.242	11.5	4.292	3.5	4.342	0.5
4.192	41.5	4.244	7.0	4.294	4.0	4.344	1.0
4.194	75.5	4.246	2.5	4.296	5.5	4.346	1.0
4.196	121.0	4.248	1.5	4.298	7.5	4.348	1.0
4.198	138.0	4.250	1.5	4.300	10.0	4.354	0.5
4.200	101.0						

APPENDIX 8

Macrofossil Presence Analysis for Laguna Boal

Depth / cm	Macrofossil Score	Depth / cm	Macrofossil Score
350	0	388	0
352	0	390	0
354	0	392	0
356	0	394	0.5
358	0	396	0
360	0	398	2
362	0	400	2
364	1	402	2
366	2	404	3
368	1	406	5
370	0	408	2
372	0	410	0
374	0	412	0
376	0.5	414	0
378	2	416	1
380	0	418	3
382	3	420	4
384	3	422	5
386	0	424	1

Scores range from 0 (absent) to 5 (abundant)